# World Journal of Gastroenterology®

Volume 12 Number 6
February 14, 2006

Supported by NSFC
2005-2006

National Journal Award
2005

The WJG Press

The WJG Press, Apartment 1066 Yishou Garden, 58 North
Langxinzhuang Road, PO Box 2345, Beijing 100023, China
Telephone: +86-10-85381901
Fax: +86-10-85381893
E-mail: wjg@wjgnet.com
http: //www.wjgnet.com

ISSN 1007-9327 CN 14-1219/R Local Post Offices Code No. 82-261

World Journal of Gastroenterology www.wjgnet.com Volume 12 Number 06 Feb 14 2006

ISSN 1007-9327
CN 14-1219/R

WJG

World Journal of Gastroenterology®

**Indexed and Abstracted in:**
Index Medicus, MEDLINE, PubMed, Chemical Abstracts, EMBASE/Excerpta Medica, Abstracts Journals, Nature Clinical Practice Gastroenterology and Hepatology, CAB Abstracts and Global Health.

**Volume 12 Number 6**
**February 14, 2006**

*World J Gastroenterol*
2006 February 14; 12(6): 837-1000
**Online Submissions**
www.wjgnet.com/wjg/index.jsp
www.wjgnet.com
Printed on Acid-free Paper

A Weekly Journal of Gastroenterology and Hepatology

# World Journal of Gastroenterology®

## Editorial Board

2004-2006

Published by The WJG Press, PO Box 2345, Beijing 100023, China
Fax: +86-10-85381893 E-mail: wjg@wjgnet.com http://www.wjgnet.com

**HONORARY EDITORS-IN-CHIEF**
Ke-Ji Chen, *Beijing*
Li-Fang Chou, *Taipei*
Dai-Ming Fan, *Xi'an*
Zhi-Qiang Huang, *Beijing*
Shinn-Jang Hwang, *Taipei*
Min-Liang Kuo, *Taipei*
Nicholas F LaRusso, *Rochester*
Jie-Shou Li, *Nanjing*
Geng-Tao Liu, *Beijing*
Lein-Ray Mo, *Tainan*
Fa-Zu Qiu, *Wuhan*
Eamonn M Quigley, *Cork*
David S Rampton, *London*
Rudi Schmid, *California*
Nicholas J Talley, *Rochester*
Guido NJ Tytgat, *Amsterdam*
Jaw-Ching Wu, *Taipei*
Meng-Chao Wu, *Shanghai*
Ming-Shiang Wu, *Taipei*
Jia-Yu Xu, *Shanghai*
Hui Zhuang, *Beijing*

**PRESIDENT AND EDITOR-IN-CHIEF**
Lian-Sheng Ma, *Beijing*

**EDITOR-IN-CHIEF**
Bo-Rong Pan, *Xi'an*

**ASSOCIATE EDITORS-IN-CHIEF**
Gianfranco D Alpini, *Temple*
Bruno Annibale, *Roma*
Jordi Bruix, *Barcelona*
Roger William Chapman, *Oxford*
Alexander L Gerbes, *Munich*
Shou-Dong Lee, *Taipei*
Walter Edwin Longo, *New Haven*
You-Yong Lu, *Beijing*
Masao Omata, *Tokyo*
Harry H-X Xia, *Hong Kong*

**MEMBERS OF THE EDITORIAL BOARD**

Albania
Bashkim Resuli, *Tirana*

Argentina
Julio Horacio Carri, *Córdoba*

Australia
Minoti Vivek Apte, *Liverpool*
Filip Braet, *Sydney*
Andrew D Clouston, *Sydney*
Darrell HG Crawford, *Brisbane*
Michael Anthony Fink, *Melbourne*
Robert JL Fraser, *Daw Park*
Yik-Hong Ho, *Townsville*
Gerald J Holtmann, *Adelaide*
Michael Horowitz, *Adelaide*
Phillip S Oates, *Perth*
Stephen M Riordan, *Sydney*
ICR Thomson, *Woodville South*
Nathan Subramaniam, *Brisbane*
Herbert Tilg, *Innsbruck*
Martin John Veysey, *Gosford*
DL Worthley, *Bedford*

Austria
Alfred Gangl, *Vienna*
Kurt Lenz, *Linz*
MPeck-Radosavljevic, *Vienna*
RE Stauber, *Auenbruggerplatz*
Michael Trauner, *Graz*
Harald Vogelsang, *Vienna*
Guenter Weiss, *Innsbruck*

Belarus
Yury K Marakhouski, *Minsk*

Belgium
Rudi Beyaert, *Gent*
Bart Rik De Geest, *Leuven*
Inge Irma Depoortere, *Leuven*
Olivier Detry, *Liège*
Karel Geboes, *Leuven*
Thierry Gustot, *Brussels*
Yves J Horsmans, *Brussels*
Geert G Leroux-Roels, *Ghent*
Louis Libbrecht, *Leuven*
Yvan Vandenplas, *Brussels*
Eddie Wisse, *Keerbergen*

Brazil
Heitor Rosa, *Goiania*

Bulgaria
Zahariy Krastev, *Sofia*

Canada
Matthew Bjerknes, *Toronto*
Michael F Byrne, *Vancouver*
Wang-Xue Chen, *Ottawa*
Hugh J Freeman, *Vancouver*
Chantal Guillemette , *Québec*
Samuel S Lee, *Calgary*
Gerald Y Minuk, *Manitoba*
Morris Sherman, *Toronto*
Alan BR Thomson, *Edmonton*
Eric M Yoshida, *Vancouver*

China
Henry LY Chan, *Hongkong*
Xiao-Ping Chen, *Wuhan*
Jun Cheng, *Beijing*
Chi-Hin Cho, *Hong Kong*
Zong-Jie Cui, *Beijing*
Da-Jun Deng, *Beijing*
Er-Dan Dong, *Beijng*
Sheung-Tat Fan, *Hong Kong*
Xue-Gong Fan, *Changsha*
Jin Gu, *Beijing*
De-Wu Han, *Taiyuan*
Ming-Liang He, *Hong Kong*
Fu-Lian Hu, *Beijing*
Wayne HC Hu, *Hong Kong*
Guang-Cun Huang, *Shanghai*
Xiao-Long Ji, *Beijing*
Ching Lung Lai, *Hong Kong*
Kam Chuen Lai, *Hong Kong*
Yuk Tong Lee, *Hong Kong*
Suet Yi Leung, *Hong Kong*
Wai-Keung Leung, *Hong Kong*
Zhi-Hua Liu, *Beijing*
Ai-Ping Lu, *Beijing*
Jing-Yun Ma, *Beijing*
Lun-Xiu Qin, *Shanghai*
Yu-Gang Song, *Guangzhou*
Qin Su, *Beijing*
Yuan Wang, *Shanghai*
Benjamin Chun-Yu Wong, *Hong Kong*
Wai-Man Wong, *Hong Kong*
Hong Xiao, *Shanghai*
Dong-Liang Yang, *Wuhan*
Yuan Yuan, *Shenyang*
Man-Fung Yuen, *Hong Kong*
Jian-Zhong Zhang, *Beijing*
Xin-Xin Zhang, *Shanghai*
Zhi-Rong Zhang, *Chengdu*
Shu Zheng, *Hangzhou*

Croatia
Tamara Cacev, *Zagreb*
Marko Duvnjak, *Zagreb*

Czech
Milan Jirsa, *Praha*

Denmark
Peter Bytzer, *Copenhagen*
Hans Gregersen, *Aalborg*
Jens H Henriksen, *Hvidovre*
Fin Stolze Larsen, *Copenhagen*
SØren MØller, *Hvidovre*

Egypt
Abdel-Rahman El-Zayadi, *Giza*
Sanaa Moharram Kamal, *Cairo*
Ayman Yosry, *Cairo*

Finland
Pentti Sipponen, *Espoo*

France
Corlu Anne, *Rennes*
Denis Ardid, *Clermont-Ferrand*
Charles Paul Balabaud, *Bordeaux*
Jacques Belghiti, *Clichy*
Pierre Brissot, *Rennes*
Patrice Philippe Cacoub, *Paris*
Franck Carbonnel, *Besancon*
Laurent Castera, *Pessac*
Bruno Clément, *Rennes*
Jacques Cosnes, *Paris*
Thomas Decaens, *Cedex*
Francoise Lunel Fabiani, *Angers*
Gérard Feldmann, *Paris*
Jean Fioramonti, *Toulouse*
Chantal Housset, *Paris*
Juan Lucio Iovanna, *Marseille*
Rene Lambert, *Lyon*
Francis Mégraud, *Bordeaux*
Richard Moreau, *Clichy*
Thierry Piche, *Nice*
Jean Rosenbaum, *Bordeaux*
Jose Sahel, *Marseille*
Jean-Yves Scoazec, *Lyon*
Khalid Ahnini Tazi, *Clichy*
MC Vozenin-brotons, *Villejuif*
Jean-Pierre Henri Zarski, *Grenoble*
Jessica Zucman-Rossi, *Paris*

Germany
HD Allescher, *Garmisch-Partenkirchen*
Martin Anlauf, *Kiel*
Rudolf Arnold, *Marburg*
Max G Bachem, *Ulm*
Thomas F Baumert ,*Freiburg*
Daniel C Baumgart, *Berlin*
Hubert Blum, *Freiburg*
Katja Breitkopf, *Mannheim*
Markus W Büchler, *Heidelberg*
Reinhard Buettner, *Bonn*
Elke Cario, *Essen*
Uta Dahmen, *Essen*
CF Dietrich, *Bad Mergentheim*
Paul Enck, *Tuebingen*
Fred Fändrich, *Kiel*
Ulrich Robert Fölsch, *Kiel*
Peter R Galle, *Mainz*
Andreas Geier, *Aache*
Dieter Glebe, *Giessen*
Burkhard Göke, *Munich*
Florian Graeple, *Tuebingen*
Axel M Gressner, *Aachen*
Veit Gülberg, *Munich*
Rainer Haas, *Munich*
Eckhart Georg Hahn, *Erlangen*
Stephan Hellmig, *Kiel*
ohannes Herkel, *Hamburg*
Eberhard Hildt, *Berlin*
Joerg C Hoffmann, *Berlin*
Werner Hohenberger, *Erlangen*
RG Jakobs, *Ludwigshafen*
Jutta Keller, *Hamburg*
Stefan Kubicka, *Hannover*
Joachim Labenz, *Siegen*
Michael Peter Manns, *Hannover*
Stephan Miehlke, *Dresden*
Sabine Mihm, *Göttingen*
Silvio Nadalin, *Essen*
Markus F Neurath, *Mainz*
Johann Ockenga, *Berlin*
Gustav Paumgartner, *Munich*
Ulrich Ks Peitz, *Magdeburg*
Steffen Rickes, *Magdeburg*
Gerhard Rogler, *Regensburg*
Tilman Sauerbruch, *Bonn*
Andreas Schäffler, *Regensburg*
Hans Scherubl, *Berlin*
Roland M Schmid, *München*
AG Schreyer, *Regensburg*
Tobias Schroeder, *Essen*
Hans Seifert, *Oldenburg*
J Ruediger Siewert, *Munich*
Manfred V Singer, *Mannheim*
Gisela Sparmann, *Rostock*
Jurgen M Stein, *Frankfurt*
Manfred Stolte, *Bayreuth*
Rainer Straub, *Regensburg*
WR Stremmel, *Heidelberg*
Harald F Teutsch, *Ulm*
HL Tillmann, *Leipzig*
Tung-Yu Tsui, *Regensburg*
Axel Ulsenheimer, *Munich*
Patrick Veit, *Essen*
Siegfried Wagner, *Deggendorf*
Henning Walczak, *Heidelberg*
Fritz von Weizsacker, *Berlin*
Jens Werner, *Heidelberg*
Bertram Wiedenmann, *Berlin*
Reiner Wiest, *Regensburg*
Stefan JP Zeuzem, *Homburg*

Greece
Elias A Kouroumalis, *Heraklion*

Hungary
Peter Laszlo Lakatos, *Budapest*

Iceland
H Gudjonsson, *Reykjavik*

India
Sujit K Bhattacharya, *Kolkata*
Yogesh K Chawla, *Chandigarh*
Radha K Dhiman, *Chandigarh*
Sri Prakash Misra, *Allahabad*
ND Reddy, *Hyderabad*

Iran
Reza Malekzadeh, *Tehran*
Seyed Alireza Taghavi, *Shiraz*

Ireland
Anthony P Moran, *Galway*

Israel
Simon Bar-Meir, *Hashomer*
Abraham Rami Eliakim, *Haifa*
Yaron Ilan , *Jerusalem*
Yaron Niv, *Pardesia*
Ran Oren, *Tel Aviv*

Italy
Giovanni Addolorato, *Roma*
Domenico Alvaro, *Rome*
Annese V, *San Giovanni Rotond*
Adolfo Francesco Attili, *Roma*
Giovanni Barbara, *Bologna*
Gabrio Bassotti, *Perugia*
Franco Bazzoli, *Bologna*
Stefano Bellentani, *Carpi*
Antomio Benedetti, *Ancona*
Mauro Bernardi, *Bologna*
Luigi Bonavina, *Milano*
Giovanni Cammarota, *Roma*
Antonino Cavallari, *Bologna*
Giuseppe Chiarioni, *Valeggio*
Massimo Conio, *Sanremo*
Dario Conte, *Milano*
Gino Roberto Corazza, *Pavia*
Francesco Costa, *Pisa*
Antonio Craxi, *Palermo*
Roberto De Giorgio, *Bologna*

Giovanni D De Palma, *Naples*
Fabio Farinati, *Padua*
Andrea Galli, *Firenze*
Valeria Ghisett , *Turin*
Edoardo G Giannini, *Genoa*
Paolo Gionchetti, *Bologna*
Mario Guslandi, *Milano*
Giacomo Laffi, *Firenze*
Giovanni Maconi, *Milan*
ED Mangoni, *Napoli*
Giulio Marchesini, *Bologna*
Giuseppe Montalto, *Palermo*
Giovanni Monteleone, *Rome*
Gerardo Nardone, *Napoli*
Luisi Pagliaro, *Palermo*
Fabrizio R Parente, *Milan*
F Perri, *San Giovanni Rotondo*
Raffaele Pezzilli, *Bologna*
A Pilotto, *San Giovanni Rotondo*
Paolo Del Poggio, *Treviglio*
Gabriele Bianchi Porro, *Milano*
Piero Portincasa, *Bari*
Bernardino Rampone, *Siena*
Claudio Romano, *Messina*
Mario Del Tacca, *Pisa*
Pier Alberto Testoni, *Milan*
Enrico Roda, *Bologna*
Vincenzo Savarino, *Genova*
Roberto Testa, *Genoa*
Dino Vaira, *Bologna*

Japan
Kyoichi Adachi, *Izumo*
Yasushi Adachi, *Sapporo*
Taiji Akamatsu, *Matsumoto*
Sk Md Fazle Akbar, *Ehime*
Takafumi Ando, *Nagoya*
Akira Andoh, *Otsu*
Taku Aoki, *Tokyo*
Masahiro Arai, *Tokyo*
Tetsuo Arakawa, *Osaka*
Yasuji Arase, *Tokyo*
Masahiro Asaka, *Sapporo*
Hitoshi Asakura, *Tokyo*
Takeshi Azuma, *Fukui*
Yoichi Chida, *Fukuoka*
Takahiro Fujimori, *Tochigi*
Jiro Fujimoto, *Hyogo*
Kazuma Fujimoto, *Saga*
Mitsuhiro Fujishiro, *Tokyo*
Yoshihide Fujiyama, *Otsu*
Hiroyuki Hanai, *Hamamatsu*
Kazuhiro Hanazaki, *Nagano*
Naohiko Harada, *Fukuoka*
Makoto Hashizume, *Fukuoka*
Tetsuo Hayakawa, *Nagoya*
Kazuhide Higuchi, *Osaka*
Keiji Hirata, *Kitakyushu*
Yuji Iimuro, *Nishinomiya*
Kenji Ikeda, *Tokyo*
Fumio Imazeki, *Chiba*
Yasuhiro Inokuchi, *Yokohama*
Haruhiro Inoue, *Yokohama*
Masayasu Inoue, *Osaka*
Hiromi Ishibashi, *Nagasaki*
Shunji Ishihara, *Izumo*
Toru Ishikawa, *Niigata*
Kei Ito, *Sendai*
Masayoshi Ito, *Tokyo*
Hiroaki Itoh, *Akita*
Ryuichi Iwakiri, *Saga*
Hiroshi Kaneko, *Aichi-Gun*
Takashi Kanematsu, *Nagasaki*
Junji Kato, *Sapporo*
Mototsugu Kato, *Sapporo*
Shinzo Kato, *Tokyo*
Sunao Kawano, *Osaka*
Mitsuhiro Kida, *Kanagawa*
Yoshikazu Kinoshita, *Izumo*
Tsuneo Kitamura, *Chiba*
Seigo Kitano, *Oita*
Kazuhiko Koike, *Tokyo*
Norihiro Kokudo, *Tokyo*
Satoshi Kondo, *Sapporo*
Shoji Kubo, *Osaka*
Shigeki Kuriyama, *Kagawa*
Masato Kusunoki, *Tsu Mie*
Katsunori Iijima, *Sendai*
Shin Maeda, *Tokyo*
Masatoshi Makuuchi, *Tokyo*
Osamu Matsui, *Kanazawa*
Yasushi Matsuzaki, *Tsukuba*
Kiyoshi Migita ,*Omura*
Tetsuya Mine, *Kanagawa*
Hiroto Miwa, *Hyogo*
Masashi Mizokami, *Nagoya*
Motowo Mizuno, *Hiroshima*
Morito Monden, *Suita*
Hisataka S Moriwaki, *Gifu*
Yoshiharu Motoo, *Kanazawa*
Akihiro Munakata, *Hirosaki*
Kazunari Murakami, *Oita*
Kunihiko Murase, *Tusima*
Yujl Naito, *Kyoto*
Hisato Nakajima, *Tokyo*
Hiroki Nakamura, *Yamaguchi*
Shotaro Nakamura, *Fukuoka*
Mikio Nishioka, *Niihama*
Susumu Ohmada, *Maebashi*
Masayuki Ohta, *Oita*
Tetsuo Ohta, *Kanazawa*
Kazuichi Okazaki, *Osaka*
Katsuhisa Omagari, *Nagasaki*
Saburo Onishi, *Nankoku*
Morikazu Onji, *Ehime*
Satoshi Osawa, *Hamamatsu*
Yutaka Inagaki , *Kanagawa*
Hiromitsu Saisho, *Chiba*
Isao Sakaida, *Yamaguchi*
Michiie Sakamoto, *Tokyo*
Yasushi Sano, *Chiba*
Iwao Sasaki, *Sendai*
Motoko Sasaki, *Kanazawa*
Chifumi Sato, *Tokyo*
Shuichi Seki, *Osaka*
Hiroshi Shimada, *Yokohama*
Mitsuo Shimada, *Tokushima*
Tomohiko Shimatan, *Hiroshima*
Hiroaki Shimizu, *Chiba*
Ichiro Shimizu, *Tokushima*
Tooru Shimosegawa, *Sendai*
Tadashi Shimoyama, *Hirosaki*
Ken Shirabe, *Iizuka City*
Yoshio Shirai, *Niigata*
Katsuya Shiraki, *Mie*
Yasushi Shiratori, *Okayama*
Yasuhiko Sugawara, *Tokyo*
Hidekazu Suzuki, *Tokyo*
Tadatoshi Takayama, *Tokyo*
Tadashi Takeda, *Osaka*
Kiichi Tamada, *Tochigi*
Akira Tanaka, *Kyoto*
Eiji Tanaka, *Matsumoto*
Noriaki Tanaka, *Okayama*
Shinji Tanaka, *Hiroshima*
Wei Tang, *Tokyo*
Kyuichi Tanikawa, *Kurume*
Akira Terano, *Shimotsugagun*
Hitoshi Togash, *Yamagata*
Kazunari Tominaga, *Osaka*
Minoru Toyota, *Sapporo*
Akihito Tsubota, *Chiba*
Shingo Tsuji, *Osaka*
Takato Ueno, *Kurume*
Shinichi Wada, *Tochigi*
Hiroyuki Watanabe, *Kanazawa*
Toshio Watanabe, *Osaka*
Yuji Watanabe, *Ehime*
Chun-Yang Wen, *Nagasaki*
Koji Yamaguchi, *Fukuoka*
Takayuki Yamamoto, *Yokkaichi*
Takashi Yao, *Fukuoka*
Masashi Yoneda, *Tochigi*
Hiroshi Yoshida, *Tokyo*
Masashi Yoshida, *Tokyo*
Norimasa Yoshida, *Kyoto*
Kentaro Yoshika, *Toyoake*
Masahide Yoshikawa, *Kashihara*

Lebanon
Ala I Sharara, *Beirut*
Joseph Daoud Boujaoude, *Beirut*

Lithuania
Sasa Markovic, *Japljeva*

Macedonia
Vladimir Cirko Serafimoski, *Skopje*

Malaysia
Andrew Seng Boon Chua, *Ipoh*
Khean-Lee Goh, *Kuala Lumpur*
Jayaram Menon, *Sabah*

Mexico
Saúl Villa-Trevio, *México*
JKY Furusho, *Mexico*

Monaco
Patrick Rampal, *Monaco*

Netherlands
Lee Bouwman, *Leiden*
Rick Greupink, *Groningen*
Janine K Kruit, *Groningen*
Ernst Johan Kuipers, *Rotterdam*
Yi Liu, *Amsterdam*
Chris JJ Mulder, *Amsterdam*
Michael Müller, *Wageningen*
Amado Salvador Peña, *Amsterdam*
Robert J Porte, *Groningen*
Andreas Smout, *Utrecht*
RW Stockbrugger, *Maastricht*
Renate G Van der Molen, *Rotterdam*
Karel van Erpecum, *Utrecht*
GV Henegouwen, *Utrecht*

New Zealand
Ian David Wallace, *Auckland*

Nigeria
Samuel Babafemi Olaleye, *Ibadan*

Norway
Trond Berg, *Oslo*
Helge Lyder Waldum, *Trondheim*

Pakistan
Muhammad S Khokhar, *Lahore*

Poland
Tomasz Brzozowski, *Cracow*
Robert Flisiak, *Bialystok*
Hanna Gregorek, *Warsaw*
Hanna Gregorek, *Warsaw*
DM Lebensztejn, *Bialystok*
Wojciech G Polak ,*Wroclaw*

Portugal
Miguel Carneiro De Moura, *Lisbon*

Russia
Vladimir T Ivashkin, *Moscow*
Leonid Lazebnik, *Moscow*
Vasiliy I Reshetnyak, *Moscow*

Singapore
Bow Ho, *Kent Ridge*
Khek-Yu Ho, *Singapor*
Francis Seow-Choen, *Singapore*

Slovakia
Anton Vavrecka, *Bratislava*

South Africa
Michael C Kew, *Parktown*

South Korea
Byung Ihn Choi, *Seoul*
Ho Soon Choi, *Seoul*
Jae J Kim, *Seoul*
Jin-Hong Kim, *Suwon*
Myung-Hwan Kim, *Seoul*
Jong Kyun Lee, *Seoul*
Eun-Yi Moon, *Taejeon City*
Jae-Gahb Park, *Seoul*
Dong Wan Seo, *Seoul*

Spain
Juan G Abraldes, *Barcelona*
Agustin Albillos, *Madrid*
Raul J Andrade, *Málaga*
Luis Aparisi, *Valencia*
Fernando Azpiroz, *Barcelona*
Ramon Bataller, *Barcelona*
Josep M Bordas, *Barcelona*
Xavier Calvet, *Sabadell*
Vicente Carreño, *Madrid*
Antoni Castells, *Barcelona*
Vicente Felipo, *Valencia*
Juan C Garcia-Pagán, *Barcelona*
Jaime Bosch Genover, *Barcelona*
Jaime Guardia, *Barcelona*
Angel Lanas, *Zaragoza*
María Isabel Torres López, *Jaén*
José M Mato, *Derio*
MAM Navas, *Pamplona*
Julian Panes, *Barcelona*
Miguel Minguez Perez, *Valencia*
Miguel Perez-Mateo, *Alicante*
Josep M Pique, *Barcelona*
Jesus M Prieto, *Pamplona*
Sabino Riestra, *Pola De Siero*
Luis Rodrigo, *Oviedo*
Manuel Romero-Gómez, *Sevilla*

Sweden
Curt Einarsson, *Huddinge*
Xupeng Ge, *Stockholm*
Hanns-Ulrich Marschall, *Stockholm*
Lars Christer Olbe, *Molndal*
Xiao-Feng Sun, *Linkoping*
Ervin Tóth, *Malmö*

Switzerland
Chrish Beglinger, *Basel*
Pierre A Clavien, Zurich
Jean-Francois Dufour, *Bern*
Franco Fortunato, *Zürich*
Jean Louis Frossard, *Geneva*
Gerd A Kullak-Ublick, *Zurich*
Bruno Stieger, *Zurich*
Arthur Zimmermann, *Berne*

Turkey
Yusuf Bayraktar, *Ankara*
Figen Gurakan, *Ankara*
Aydin Karabacakoglu, *Konya*
Serdar Karakose, *Konya*
Hizir Kurtel, *Istanbu*
Osman Cavit Ozdogan, *Istanbul*
Cihan Yurdaydin, *Ankara*

United Arab Emirates
Sherif M Karam, *Al-Ain*

United Kingdom
Anthony TR Axon, *Leeds*
Mairi Brittan, *London*
Andrew Kenneth Burroughs, *London*
Paul Jonathan Ciclitira, *London*
Amar Paul Dhillon, *London*
Elizabeth Furrie, *Dundee*
Daniel Richard Gaya, Edinburgh
Subrata Ghosh, *London*
William Greenhalf, *Liverpool*
Peter Clive Hayes, Edinburgh
Gwo-Tzer Ho, *Edinburgh*
Anthony R Hobson, *Salford*
David Paul Hurlstone, *Sheffield*
Brian T Johnston, *Belfast*
David EJ Jones, *Newcastle*
Michael A Kamm, *Harrow*
Patricia F Lalor, *Birmingham*
Hong-Xiang Liu, *Cambridge*
Dermot Patrick Mcgovern, *Oxford*
Giorgina Mieli-Vergani, *London*
Nikolai V Naoumov, *London*
John P Neoptolemos, *Liverpool*
James Neuberger, *Birmingham*
Mark S Pearce, *Newcastle Upon Tyne*
Marco Senzolo, *Padova*
Robert Sutton, *Liverpool*
Simon D Taylor-Robinson, *London*
Ulrich Thalheimer, *London*
Nick Paul Thompson, *Newcastle*
David Tosh, *Bath*
Frank Ivor Tovey, *Basingstoke*
Diego Vergani, *London*
Peter James Whorwell, *Manchester*
Karen Leslie Wright, *Bath*
Min Zhao, *Foresterhill*

United States
Christian Cormac Abnet, *Maryland*
Gary A Abrams, *Birmingham*
Golo Ahlenstiel, *Bethesda*
Gavin Edward Arteel, *Louisville*
Jasmohan Singh Bajaj, *Milwaukee*
Jamie S Barkin, *Miami Beach*
Kim Elaine Barrett, *San Diego*
Jennifer D Black, *Buffalo*
Alan Cahill, *Philadelphia*
David L Carr-Locke, *Boston*
Ravi S Chari, *Nashville*
Jiande Chen, *Galveston*
Xian-Ming Chen, *Rochester*
Parimal Chowdhury, *Arkansas*
Raymond T Chung,Boston
James M Church, *Cleveland*
Vincent Coghlan, *Beaverton*
John Cuppoletti, *Cincinnati*
Peter V Danenberg, *Los Angeles*
Kiron Moy Das, *New Brunswick*
Vincent Paul Doria-Rose, *Seattle*
Bijan Eghtesad, *Cleveland*
Hala El-Zimaity, *Houston*
Michelle Embree-Ku, *Providence*
Ronnie Fass, *Tucson*
Chris E Forsmark, *Gainesville*
Scott L Friedman, *New York*
John Geibel, *New Haven*
Ignacio Gil-Bazo, *New York*
David Y Graham, *Houston*
Anna S Gukovskaya, *Los Angeles*
Stephen B Hanauer, *Chicago*
Gavin Harewood, *Rochester*
Alan W Hemming, *Gainesville*
Jamal A Ibdah, *Columbia*
Atif Iqbal, *Omaha*
Hajime Isomoto, *Rochester*
Hartmut Jaeschke, *Tucson*
Dennis M Jensen, *Los Angeles*
Leonard R Johnson, *Memphis*
Peter James Kahrilas, *Chicago*
AN Kalloo, *Baltimore*
Neil Kaplowitz, Los Angeles
Ali Keshavarzian, *Chicago*
Joseph B Kirsner, *Chicago*
Burton I Korelitz, *New York*
Robert J Korst, *New York*
Richard A Kozarek, *Seattle*
Shiu-Ming Kuo, *Buffalo*
Daryl Tan Yeung Lau, *Galvesto*
Glen A Lehman, *Indianapolis*
Frederick H Leibach, *Augusta*
Alex B Lentsch, *Cincinnati*
Andreas Leodolter, *La Jolla*
Gene LeSage, *Houston*
Ming Li, *New Orleans*
LM Lichtenberger, *Houston*
GR Lichtenstein, *Philadelphia*
Martin Lipkin, *New York*
Josep M Llovet, *New York*
Edward V Loftus, *Rocheste*
Robin G Lorenz, *Birmingham*
JD Luketich, *Pittsburgh*
Henry Thomson Lynch, *Omaha*
John Frank Di Mari, *Texas*
John M Mariadason, *Bronx*
WM Mars, *Pittsburgh*
George W Meyer, *Sacramento*
G Michalopoulos, *Pittsburgh*
S Pal Singh S Monga, *Pittsburgh*
Timothy H Moran, *Baltmore*
Hiroshi Nakagawa, *Philadelphia*
Douglas B Neison, *Minneaplis*
Curtis T Okamoto, *Los Angeles*
Stephen J Pandol, *Los Angeles*
Pankaj Jay Pasricha, *Gaveston*
Zhiheng Pei, *New York*
Michael A Pezzone, *Pittsburgh*
CS Pitchumoni, *New Brunswiuc*
Jay Pravda, *Gainesville*
M Raimondo, *Jacksonville*
Adrian Reuben, *Charleston*
Victor E Reyes, *Galveston*
Richard Rippe, *Chapel Hill*
Marcos Rojkind, *Washington*
Hemant Kumar Roy, *Evanston*
Shawn David Safford, *Norfolk*
NJ Shaheen, *Chapel Hill*
Stuart Sherman, *Indianapolis*
Shivendra Shukla, *Columbia*
Alphonse E Sirica, *Virginia*
Michael Steer, *Boston*
Gary D Stoner, *Columbus*
Yvette Tache, *Los Angeles*
Jayant Talwalkar, *Rochester*
K-M Tchou-Wong, *New York*
PJ Thuluvath, *Baltimore*
Swan Nio Thung, *New York*
RA Travagli, *Baton Rouge*
G Triadafilopoulos, *Stanford*
Chung-Jyi Tsai, *Lexington*
Hugo E Vargas, *Scottsdale*
Jian-Ying Wang, *Baltimore*
Steven David Wexner, *Weston*
Keith Tucker Wilson, *Baltimore*
Jackie Wood, *Ohio*
George Y Wu, *Farmington*
Jian Wu, *Sacramento*

Samuel Wyllie, Houston
Wen Xie, *Pittsburgh*
Yoshio Yamaoka, *Texas*
Liqing Yu, *Winston-Salem*
David Yule, *Rochester*
Ruben Zamora, *Pittsburgh*
Michael Zenilman, *Brooklyn*
Zhi Zhong, *Chapel Hill*

Yugoslavia
DM Jovanovic, *Sremska Kamenica*

World Journal of
# Gastroenterology®

National Journal Award 2005

Volume 12 Number 6
February 14, 2006

Supported by NSFC 2005-2006

## Contents

**EDITORIAL**

837 Cardiac and vascular changes in cirrhosis: Pathogenic mechanisms
*Liu H, Gaskari SA, Lee SS*

843 Cutaneous manifestations in celiac disease
*Abenavoli L, Proietti I, Leggio L, Ferrulli A, Vonghia L, Capizzi R, Rotoli M, Amerio PL, Gasbarrini G, Addolorato G*

853 Probiotics and the gastrointestinal tract: Where are we in 2005?
*Chermesh I, Eliakim R*

**LIVER CANCER**

858 Macrophage inflammatory protein-2 contributes to liver resection-induced acceleration of hepatic metastatic tumor growth
*Kollmar O, Menger MD, Schilling MK*

868 Relationship between therapeutic efficacy of arterial infusion chemotherapy and expression of P-glycoprotein and p53 protein in advanced hepatocellular carcinoma
*Akimoto M, Yoshikawa M, Ebara M, Sato T, Fukuda H, Kondo F, Saisho H*

874 Anti-hepatoma activity and mechanism of ursolic acid and its derivatives isolated from *Aralia decaisneana*
*Tian Z, Lin G, Zheng RX, Huang F, Yang MS, Xiao PG*

880 Role of CD80 in stimulating T lymphocyte activation
*Li DC, Zhu XG, Zhang Y, Fu JX*

**BASIC RESEARCH**

885 Characterization of $H^+$ and $HCO_3^-$ transporters in CFPAC-1 human pancreatic duct cells
*Rakonczay Z Jr, Fearn A, Hegyi P, Boros I, Gray MA, Argent BE*

896 Inhibitory effects of interferons on pancreatic stellate cell activation
*Baumert JT, Sparmann G, Emmrich J, Liebe S, Jaster R*

902 Characterization of human gene encoding SLA/LP autoantigen and its conserved homologs in mouse, fish, fly, and worm
*Wang CX, Teufel A, Cheruti U, Grötzinger J, Galle PR, Lohse AW, Herkel J*

908 Trimetazidine: Is it a promising drug for use in steatotic grafts?
*Ben Mosbah I, Casillas-Ramírez A, Xaus C, Serafín A, Roselló-Catafau J, Peralta C*

915 Epidural anaesthesia restores pancreatic microcirculation and decreases the severity of acute pancreatitis
*Demirag A, Pastor CM, Morel P, Jean-Christophe C, Sielenkämper AW, Güvener N, Mai G, Berney T, Frossard JL, Bühler LH*

921 Expression, purification and characterization of enterovirus-71 virus-like particles
*Chung YC, Huang JH, Lai CW, Sheng HC, Shih SR, Ho MS, Hu YC*

**CLINICAL RESEARCH**

928 Cyclooxygenase-2 and epithelial growth factor receptor up-regulation during progression of Barrett's esophagus to adenocarcinoma
*Li Y, Wo JM, Ray MB, Jones W, Su RR, Ellis S, Martin RCG*

*World Journal of Gastroenterology*
**Volume** 12 **Number** 6 **February** 14, 2006

## Contents

935 Low central venous pressure reduces blood loss in hepatectomy
*Wang WD, Liang LJ, Huang XQ, Yin XY*

**RAPID COMMUNICATION**

940 Removal selectivity of Prometheus: A new extracorporeal liver support device
*Rifai K, Ernst T, Kretschmer U, Haller H, Manns MP, Fliser D*

945 Randomized controlled trial of consensus interferon with or without zinc for chronic hepatitis C patients with genotype 2
*Suzuki H, Sato K, Takagi H, Kanda D, Sohara N, Kakizaki S, Nakajima H, Otsuka T, Nagamine T, Mori M*

951 Absence of *MutY* homologue mutation in patients with multiple sporadic adenomatous polyps in Korea
*Kim H, Kim HJ, Chi SG, Lee SK, Joo GR, Dong SH, Kim BH, Chang YW, Lee JI, Chang R*

956 Risk factors of acute cholecystitis after endoscopic common bile duct stone removal
*Lee JK, Ryu JK, Park JK, Yoon WJ, Lee SH, Lee KH, Kim YT, Yoon YB*

961 Effect of interferon alpha and ribavirin treatment on serum levels of transforming growth factor-β1, vascular endothelial growth factor, and basic fibroblast growth factor in patients with chronic hepatitis C
*Janczewska-Kazek E, Marek B, Kajdaniuk D, Borgiel-Marek H*

966 Conversion of cadherin isoforms in cultured human gastric carcinoma cells
*Wang BJ, Zhang ZQ, Ke Y*

**CASE REPORTS**

971 A case of an intussuscepted neuroendocrine carcinoma of the appendix
*Thomas RE, Maude K, Rotimi O*

974 Subfulminant hepatitis B after infliximab in Crohn's disease: Need for HBV-screening?
*Millonig G, Kern M, Ludwiczek O, Nachbaur K, Vogel W*

977 A case of Crohn's disease involving the gallbladder
*Andoh A, Endo Y, Kushima R, Hata K, Tsujikawa T, Sasaki M, Mekata E, Tani T, Fujiyama Y*

979 Intestinal Behcet's disease with pyoderma gangrenosum: A case report
*Nakamura T, Yagi H, Kurachi K, Suzuki S, Konno H*

982 Spontaneous rupture of a type $IV_A$ choledochal cyst in a young adult during radiological imaging
*Stipsanelli E, Valsamaki P, Tsiouris S, Arka A, Papathanasiou G, Ptohis N, Lahanis S, Papantoniou V, Zerva C*

987 Ultrastructure of Kupffer cells and hepatocytes in the Dubin-Johnson syndrome: A case report
*Sobaniec-Lotowska ME, Lebensztejn DM*

990 Pyogenic liver abscess associated with large colonic tubulovillous adenoma
*Lai HC, Chan CY, Peng CY, Chen CB, Huang WH*

993 Delayed ischemic gangrene change of distal limb despite optimal decompressed colostomy constructed in obstructed sigmoid colon cancer: A case report
*Huang WS, Liu KW, Lin PY, Hsieh CC, Wang JY*

**ACKNOWLEDGMENTS**

996 Acknowledgments to Reviewers of *World Journal of Gastroenterology*

**APPENDIX**

997 Meetings

998 Instructions to authors

*World Journal of Gastroenterology*
**Volume** 12 **Number** 6 **February** 14, 2006

## Contents

| | | |
|---|---|---|
| | **1000** | *World Journal of Gastroenterology* standard of quantities and units |
| **FLYLEAF** | I-V | Editorial Board |
| **INSIDE FRONT COVER** | | Online Submissions |
| **INSIDE BACK COVER** | | International Subscription |

**RESPONSIBLE EDITOR FOR THIS ISSUE** Zhu LH

*World Journal of Gastroenterology* ( *World J Gastroenterol* , *WJG* ), a leading international journal in gastroenterology and hepatology, has an established reputation for publishing first class research on esophageal cancer, gastric cancer, liver cancer, viral hepatitis, colorectal cancer, and *Helicobacter pylori* infection, providing a forum for both clinicians and scientists, and has been indexed and abstracted in *Index Medicus*, MEDLINE, PubMed, Chemical Abstracts, EMBASE, Abstracts Journals, Nature Clinical Practice Gastroenterology and Hepatology, CAB Abstracts and Global Health. *WJG* is a weekly journal published by The *WJG* Press. The publication date is on 7th, 14th, 21st, and 28th every month. The *WJG* is supported by The National Natural Science Foundation of China, No. 30224801 and No.30424812, which was founded with a name of *China National Journal of New Gastroenterology* on October 1,1995, and renamed as *WJG* on January 25, 1998.

HONORARY EDITORS-IN-CHIEF
Ke-Ji Chen, *Beijing*
Li-Fang Chou, *Taipei*
Dai-Ming Fan, *Xi'an*
Zhi-Qiang Huang, *Beijing*
Shinn-Jang Hwang, *Taipei*
Min-Liang Kuo, *Taipei*
Nicholas F LaRusso, *Rochester*
Jie-Shou Li, *Nanjing*
Geng-Tao Liu, *Beijing*
Lein-Ray Mo, *Tainan*
Fa-Zu Qiu, *Wuhan*
Eamonn M Quigley, *Cork*
David S Rampton, *London*
Rudi Schmid, *California*
Nicholas J Talley, *Rochester*
Guido NJ Tytgat, *Amsterdam*
Jaw-Ching Wu, *Taipei*
Meng-Chao Wu, *Shanghai*
Ming-Shiang Wu, *Taipei*
Jia-Yu Xu, *Shanghai*
Hui Zhuang, *Beijing*

PRESIDENT AND EDITOR-IN-CHIEF
Lian-Sheng Ma, *Beijing*

EDITOR-IN-CHIEF
Bo-Rong Pan, *Xi'an*

ASSOCIATE EDITORS-IN-CHIEF
Gianfranco D Alpini, *Temple*
Bruno Annibale, *Roma*
Jordi Bruix, *Barcelona*
Roger William Chapman, *Oxford*
Alexander L Gerbes, *Munich*
Shou-Dong Lee, *Taipei*
Walter Edwin Longo, *New Haven*
You-Yong Lu, *Beijing*
Masao Omata, *Tokyo*
Harry H-X Xia, *Hong Kong*

SCIENCE EDITORS
Director: Jing Wang
Deputy Director: Jian-Zhong Zhang

COPY EDITORS
Director: Jing-Yun Ma
Deputy Director: Xian-Lin Wang

ELECTRONICAL EDITORS
Director: Li Cao
Deputy Director: Hong-Yan Li

EDITORIAL ASSISTANT
Yan Jiang

PUBLISHED BY
The WJG Press

PRINTED BY
Printed in Beijing on acid-free paper by Beijing Kexin Printing House

COPYRIGHT
© 2006 Published by The WJG Press. All rights reserved; no part of this publication may be reproduced, stored in a retrieval system, or transmitted in any form or by any means, electronic, mechanical, photocopying, recording, or otherwise without the prior permission of The *WJG* Press. Author are required to grant *WJG* an exclusive licence to publish.
Print ISSN 1007-9327 CN 14-1219/R.

SPECIAL STATEMENT
All articles published in this journal represent the viewpoints of the authors except where indicated otherwise.

EDITORIAL OFFICE
*World Journal of Gastroenterology*,
The WJG Press, Apartment 1066 Yishou Garden, 58 North Langxinzhuang Road, PO Box 2345, Beijing 100023, China
Telephone: +86-10-85381901
Fax: +86-10-85381893
E-mail: wjg@wjgnet.com
http://www.wjgnet.com

SUBSCRIOTION AND AUTHOR REPRINTS
Jing Wang
The WJG Press, Apartment 1066 Yishou Garden, 58 North Langxinzhuang Road, PO Box 2345, Beijing 100023, China
Telephone: +86-10-85381901
Fax: +86-10-85381893
E-mail: j.wang@wjgnet.com
http://www.wjgnet.com

**Institutional Rates**
2006 rates: USD 1500.00

**Personal Rates**
2006 rates: USD 700.00

INSTRUCTIONS TO AUTHORS
Full instructions are available online at http://www.wjgnet.com/wjg/help/instructions.jsp. If you do not have web access please contact the editorial office.

PO Box 2345, Beijing 100023, China
www.wjgnet.com
wjg@wjgnet.com

*World J Gastroenterol* 2006 February 14; 12(6): 837-842
***World Journal of Gastroenterology*** ISSN 1007-9327
© 2006 The WJG Press. All rights reserved.

*EDITORIAL*

# Cardiac and vascular changes in cirrhosis: Pathogenic mechanisms

HongQun Liu, Seyed Ali Gaskari, Samuel S Lee

HongQun Liu, Seyed Ali Gaskari, Samuel S Lee, Liver Unit, University of Calgary, Calgary, Alberta, Canada
Co-first authors: HongQun Liu and Seyed Ali Gaskari
Supported by SAG, Canadian Heart and Stroke Foundation studentship award; SSL, Alberta Heritage Foundation for Medical Research Senior Scholarship award. Most of our studies mentioned in this paper were funded by research operating grants from the Canadian Institutes of Health Research
Correspondence to: Samuel S Lee, MD, Professor of Medicine, Department of Medicine, University of Calgary. 3330 Hospital Drive NW, Calgary, AB, T2N 4N1, Canada. samlee@ucalgary.ca
Telephone: +1-403-220-8457 Fax: +1-403-270-0995
Received: 2005-08-23 Accepted: 2005-09-12

## Abstract

Cardiovascular abnormalities accompany both portal hypertension and cirrhosis. These consist of hyperdynamic circulation, defined as reduced mean arterial pressure and systemic vascular resistance, and increased cardiac output. Despite the baseline increased cardiac output, ventricular inotropic and chronotropic responses to stimuli are blunted, a condition known as cirrhotic cardiomyopathy. Both conditions may play an initiating or aggravating pathogenic role in many of the complications of liver failure or portal hypertension including ascites, variceal bleeding, hepatorenal syndrome and increased postoperative mortality after major surgery or liver transplantation. This review briefly examines the major mechanisms that may underlie these cardiovascular abnormalities, concentrating on nitric oxide, endogenous cannabinoids, central neural activation and adrenergic receptor changes. Future work should address the complex interrelationships between these systems.

© 2006 The WJG Press. All rights reserved.

**Key words:** Hyperdynamic circulation; Portal hypertension; Cirrhotic cardiomyopathy; Hemodynamics; Nitric oxide; Endocannabinoid; cGMP

Liu H, Gaskari SA, Lee SS. Cardiac and vascular changes in cirrhosis: Pathogenic mechanisms. *World J Gastroenterol* 2006; 12(6): 837-842

http://www.wjgnet.com/1007-9327/12/837.asp

## INTRODUCTION

The cardiovascular system in patients with cirrhosis or portal hypertension is abnormal. The circulation becomes hyperdynamic, characterized by increased cardiac output and decreased peripheral vascular resistance and arterial pressure. Moreover, despite the increased cardiac output at rest, with stressful stimuli such as hemorrhage, surgery or vasoactive drug administration, the ventricular response is blunted, a condition known as cirrhotic cardiomyopathy. These cardiovascular abnormalities have been suggested to induce or aggravate several complications of cirrhosis such as renal salt and water retention, variceal bleeding, hepatopulmonary syndrome, and increased cardiovascular fragility under stress. Recent reviews have detailed the clinical aspects of hyperdynamic circulation[1,2] and cirrhotic cardiomyopathy[3-5]. This review will summarize the recent work on pathogenic mechanisms underlying these two conditions.

## HYPERDYNAMIC CIRCULATION

Peripheral vasodilatation is central to hyperdynamic circulation and portal hypertension in cirrhosis. However, the factors directly initiating vasodilatation remain obscure. A hypothesis that has received much attention over the past three decades is the "humoral factor" theory. In cirrhosis, increased intrahepatic resistance induces portosystemic collateral formation, allowing gut-derived humoral substances to directly enter the systemic circulation without detoxification by the liver. The following gut-derived or locally-produced humoral factors have been implicated as possible mediators of peripheral vasodilatation in cirrhosis or portal hypertension.

### *Endocannabinoids*

Endocannabinoids are lipid-like substances that act on two inhibitory G protein-coupled receptors, CB1 and CB2. The vasodilatory effect of endogenous cannabinoids in cirrhosis was first reported in 2001[6]. Anandamide, an endogenous cannabinoid or endocannabinoid, is increased in monocytes of cirrhotic rats[6,7], and its receptor CB1 is also upregulated in the vascular endothelium of patients with cirrhosis[6]. Infusing monocytes isolated from cirrhotic rats into normal rats decreases the mean arterial pressure in the recipients. Furthermore, administering a CB1 receptor antagonist SR141716A to cirrhotic rats increases the total peripheral resistance[6,7], both studies demonstrated that SR141716A significantly increases the reduced arterial pressure in cirrhosis, and blocks the hypotension induced by the infusion of isolated cirrhotic monocytes into normal rats[6,7]. Batkai and colleagues also

found that SR141716A decreases mesenteric blood flow and portal venous pressure in cirrhotic rats[6]. All of these data indicate that the vascular tone in cirrhosis is regulated by CB1 receptors in both the splanchnic and systemic circulations.

Besides vasodilatation, anandamide rapidly and dose-dependently induces apoptosis in primary culture-activated and *in vivo*-activated hepatic stellate cells, with over 70% cell death after 4 h at 25 μmol/L[8]. This effect could alter the hepatic sinusoidal microcirculation and enhance the development of portal hypertension that leads to hyperdynamic circulation.

How does cirrhosis leads to increased endocannabinoids? Varga and co-workers found that bacterial endotoxin stimulates endocannabinoid production in cirrhosis[9]. The upregulation of CB1 receptors in cirrhotic vascular endothelium and thus increased end-organ sensitivity may also enhance endocannabinoid vasodilator tone[6].

### Nitric oxide

NO has been extensively studied. It is now clear that in cirrhosis, changes in NO activity affect different vascular beds in variable ways. In the liver microcirculation, endothelial-constitutive NO synthase (eNOS or NOS3) expression is decreased in a cirrhotic rat model[10]. Simvastatin enhances hepatic nitric oxide production and decreases the hepatic vascular tone in patients with cirrhosis[11]. An NO donor[12] or NOS3 gene transfection[10], which compensates for the decreased hepatic NOS3 expression, significantly lowers the increased portal pressure in cirrhosis.

In contrast, systemic NO production is increased in cirrhotic patients and animal models[13-15]. Moreover, normalization of NO production in cirrhotic rats, by achieving normal concentrations of aortic cGMP with small doses of the NOS inhibitor L-NAME, normalizes the decreased peripheral vascular resistance and the increased cardiac output[16]. *In vitro,* an NO inhibitor reverses the hyporeactivity of blood vessels from cirrhotic rats to vasoconstrictors[17].

All these results strongly support the hypothesis that increased NO production is a major factor in the peripheral arterial vasodilation of cirrhosis. Agents promoting nitric oxide production include inflammatory cytokines and endotoxin. In that regard, selective intestinal decontamination with norfloxacin partially reverses the hyperdynamic circulatory state in cirrhotic patients, suggesting a role for the endotoxin-NO pathway[18]. Where does this endotoxin come from in cirrhosis? First, alcohol is a major cause of cirrhosis in Western countries, and alcoholic gastrointestinal mucosal damage[19], could potentially facilitate transfer of bacteria into the circulation. Second, portosystemic shunting allows gut-derived bacterial endotoxins passage to the systemic circulation. Third, cirrhotic patients with portal hypertension show intestinal structural abnormalities characterized by vascular congestion and edema, which leads to increased intestinal permeability to bacterial toxins[20]. Fourth, intestinal bacterial overgrowth and bacterial translocation are increased in cirrhosis[21]. Besides endotoxins, the other possible factors stimulating NO production include cytokines such as TNF-α, IL-1, IL-6, and IFN-γ[22-24] Among these, TNF-α has been studied the most. Lopez-Talavera *et al* found that anti-TNF-α antibody increases mean arterial pressure and systemic vascular resistance, and decreases cardiac index and portal pressure[25]. In our 4-week BDL rats, in parallel with increased serum TNF-α, aortic NOS3 expression and serum nitrate/nitrite concentrations were increased[26].

Although the evidence is strong that the increased NOS activity in cirrhosis plays an important role in hyperdynamic circulation in cirrhosis, it remains obscure which NOS isoform is involved. The majority of previous studies have used a nonspecific NOS inhibitor to diminish NO production. However, a recent study used aminoguanidine, a preferential inhibitor of NOS2 (inducible NOS), and showed that *in vivo,* the hyperdynamic circulation in portal hypertensive rats is reversed[27]. But in another study aminoguanidine had no *in vitro* effect on the hyporeactivity of aortic rings from cirrhotic rats[28]. We have recently evaluated the activity of the L-arginine-NO pathway at different levels[26]. Although NOS2 mRNA was detectable in the cirrhotic aorta, no NOS2 protein was observed in our Western blots. It is unclear why the mRNA was not expressed as a protein. It might have been degraded or not been transcribed. It is also possible that our method of Western blotting did not allow the detection of small amounts of NOS2 protein.

A consistent augmentation in the expression of NOS3 mRNA and protein levels is observed in cirrhotic rats. Because NOS3 can be upregulated by stimuli such as shear stress and mechanical deformation, some have suggested that hyperdynamic circulation is the cause rather than the consequence of the activation of the NO pathway[14,29,30]. In addition, there may be other reasons for the increased NOS3. Cirrhosis is associated with increased levels of estrogens[31,32], and these compounds have been shown to upregulate NOS3 activity[33]. Other factors which may stimulate NOS3 expression need further investigation.

What is the role of another isoform of NOS, neuronal NOS (nNOS or NOS1)? Xu and his colleagues have demonstrated that nNOS expression is significantly increased in rat cirrhotic aortae[34]. Furthermore, an nNOS-specific inhibitor, 7-nitroindazole (7-NI), significantly decreased the sodium and water retention and normalized the hyperdynamic indices such as cardiac index, mean arterial pressure, and systemic vascular resistance in these rats[34]. Biecker *et al* also showed that nNOS partially compensates for the absence of eNOS in producing hyperdynamic circulation in eNOS-gene knockout mice[35]. These data indicate that the nNOS isoform plays a major pathogenic role in hyperdynamic circulation, and perhaps even in renal salt and water retention in cirrhosis.

It seems that endocannabinoids and nitric oxide may both play an important role in hyperdynamic circulation, but what is the relationship between them? The literature remains inconclusive. In a kidney study, Deutsch *et al* found that the vasodilatation of anandamide is NO dependent, because the NOS inhibitor L-NAME completely blocked the vasodilatory effect of anandamide, similar to a CB1 antagonist[36]. However, another study showed no effect

of L-NAME infusion on the hypotensive effects of anandamide[7].

Some studies suggest the possible involvement of other humoral vasodilators, but a definitive pathogenic role for any of these substances remains elusive. This list includes: glucagons[37], prostaglandins[38], GABA[39], VIP[40], bile acids[41], endotoxin, histamine[42] and adenosine [43].

### *Central neural mechanisms*

Although most research has focused on the humoral mediators, in recent years we and others have shown an important mechanistic role of central nervous system (CNS) activation. A decade ago, our laboratory demonstrated that primary afferent denervation by capsaicin reversed the hyperdynamic circulation in rats with cirrhosis or portal hypertension due to portal vein stenosis (PVS)[44]. What is the relationship between the CNS and hyperdynamic circulation in portal hypertension? Using *c-fos*, an immediate-early gene (whose protein product can be detected by immunohistochemistry as Fos), as a marker of central neuronal activation, we have showed that the brainstem and hypothalamic cardiovascular-regulatory nuclei are activated at the first day after PVS, whereas the hyperdynamic circulation does not start up until 3-5 days after PVS. This time sequence suggests that central neural activation is the initiating signal in the pathogenesis of hyperdynamic circulation.

Subsequently, in portal hypertensive rats, we microinjected *c-fos* antisense oligonucleotide into one of the major cardiovascular-regulatory brainstem nuclei, the nucleus tractus solitarius (NTS), to block local Fos expression. This treatment completely blocked the development of the hyperdynamic circulation, i.e., abnormalities in cardiac output, mean arterial pressure and systemic vascular resistance were completely eliminated[45]. In normal control rats, *c-fos* antisense oligonucleotides had no effect [45]. These results indicate that central neural activation is a *sine qua non* for the development of the hyperdynamic circulation in portal hypertension.

The CNS, as the controller of the circulation, presumably would not arbitrarily activate the cardiovascular system without reason. This raises the question of what the initiating signal is? Likely, it is somehow related to the portal hypertension *per se*. Moreover, the exact route of signaling from the periphery to the CNS remains unclear. The aforementioned capsaicin study suggests that primary afferent nerves may be the signaling pathway from the periphery to the CNS[44]. Our subsequent study showed that capsaicin-treated BDL rats improve the renal function and do not develop ascites[46]. Moreover, both BDL-cirrhotic and portal hypertensive rats show diminished Fos expression in NTS after capsaicin-induced denervation of the afferent nerves as neonates[46]. These observations indicate that intact primary afferent innervation is necessary for the central neuronal activation and development or maintenance of hyperdynamic circulation. Additionally, sodium retention and ascites formation is also dependent on either the presence of hyperdynamic circulation or intact afferent innervation, or both. The complex relationship between CNS activation, local or neurohormonal humoral factor stimulation, and cardiovascular disturbances in cirrhosis/portal hypertension continues to be studied in several labs.

## CIRRHOTIC CARDIOMYOPATHY

This syndrome was first described in the late 1960s, although for many years, it was mistakenly attributed to latent or subclinical alcoholic cardiomyopathy[47-49]. However, studies in human and animal models with nonalcoholic cirrhosis, dating from the mid-1980s showed a similar pattern of increased baseline cardiac output with blunted response to stress[4]. The clinical features of cirrhotic cardiomyopathy include blunted systolic and diastolic contractile responses to stress, in conjunction with evidence of ventricular hypertrophy or chamber dilatation and electrophysiological abnormalities including prolonged QT interval. Recent studies suggest the presence of cirrhotic cardiomyopathy may contribute to the pathogenesis of hepatorenal syndrome precipitated by spontaneous bacterial peritonitis[50], acute heart failure after insertion of transjugular intrahepatic portosystemic shunts (TIPS)[51,52], and increased cardiovascular morbidity and mortality after liver transplantation[53]. Therefore this syndrome is more than an academic curiosity, but rather an important clinical entity. We herein review possible pathogenic mechanisms reported by our laboratory and others.

### *Endocannabinoids*

Endocannabinoids are known to have a negative inotropic effect on cardiac contractility in both human[54] and rats[55]. The plasma level of an endogenous cannabinoid, anandamide, is known to be increased in cirrhosis[6]. We recently demonstrated a major role for increased local cardiac production of endocannabinoids in cirrhotic cardiomyopathy[56]. This conclusion is based on the restoration of blunted contractile response of isolated left ventricular papillary muscles from BDL-cirrhotic rats after preincubation with a CB1 antagonist, AM251. Additionally, endocannabinoid reuptake blockers (VDM11 and AM404) enhance the relaxant response of cirrhotic papillary muscle to higher frequencies of contraction in an AM251-sensitive fashion, suggesting an increase in the local production of endocannabinoids acting through CB1 receptors. Other *in vitro* evidence suggest a main neuronal source for the increase in local production of endocannabinoids, as these effects were mostly abolished by pretreatment with the neurotoxin tetrodotoxin[56].

### *β-adrenergic signaling*

Cardiac-adrenergic signaling is one of the main regulators of cardiac contractility. Adrenergic receptors increase adenylyl cyclase activity through stimulatory G proteins. Increased production of cAMP in turn results in an increase in calcium influx and contractile force mainly through activation of protein kinase A (PKA). We have previously shown that expression and responsiveness of β-adrenergic receptors[57] as well as its post receptor signaling pathway is blunted in cardiac tissue of cirrhotic rats. Post receptor impairment was found at different levels including content and function of stimulatory Gs-proteins[58], uncoupling of the β-adrenoceptor-ligand

complex from G protein[59], and responsiveness of adenylyl cyclase to stimuli[58,60].

### Membrane fluidity

Biochemical and biophysical properties of the cell membrane determines the mobility of membrane-bound protein moieties. This mobility is known as membrane fluidity[61], which is shown to be an important factor in the function of a number of membrane-bound receptors including β-adrenergic receptors[62]. We have shown that membrane fluidity in cardiomyocytes from bile duct-ligated rats is decreased in association with an increase in membrane cholesterol content and cholesterol/phospholipid ratio[58]. Restoration of these abnormalities *in vitro* results in normalization of blunted response of β-adrenergic receptors[58]. Alterations in membrane fluidity may also play a role in abnormal function of other membrane-bound components in cirrhotic cardiomyocytes including ion channels. The significant decrease in $K^+$ currents through $Ca^{2+}$-independent transient outward $K^+$ channel and the delayed rectifier current reported by Ward *et al* is an example that requires further investigation[63].

### Nitric oxide

Nitric oxide is known to negatively regulate cardiac contractile function. It has been shown to be involved in some types of cardiac dysfunction including ischemic heart disease[64]. Balligand *et al* have reported that non-selective blockade of NOS augments the contractile response of rat ventricular myocytes to the β-agonist isoproterenol without affecting the baseline contractility[65]. Whether this effect is mediated by the inhibition of adenylyl cyclase activity by NO[66] or through the second messenger, cyclic guanosine monophosphate (cGMP), remains to be elucidated. Possible effects of NO on cardiac function in physiological and some pathophysiological states were extensively reviewed previously[67,68].

As noted previously, cirrhosis is known to be associated with NO overproduction[29]. Involvement of NO overproduction in the development of cirrhotic cardiomyopathy was first reported in 1996 by Van Obbergh *et al* in the BDL rat. They showed that a nonselective NOS inhibitor, L-NMMA, restored the blunted contractile function of isolated heart from cirrhotic rats while it had no significant effect in control animals[69]. We have reported a similar effect in isolated left ventricular papillary muscles of cirrhotic rats. Furthermore, we observed that iNOS and not eNOS mRNA and protein expression were significantly increased in the heart of a cirrhotic rat[22]. Increased levels of cGMP in cirrhotic ventricles and elevated serum and cardiac levels of cytokines like TNF-α suggest a cytokine/iNOS/cGMP pathway for this effect[22].

### Carbon monoxide

Carbon monoxide (CO) is mainly produced in the body through the action of heme oxygenases. These enzymes are responsible for converting heme to biliverdin and CO. Like NO, CO activates soluble guanylate cyclase resulting in increased levels of cGMP[70,71]. Expression of inducible heme oxygenase (HO-1) mRNA was increased in the right ventricle in a canine model of congestive heart failure[72]. We previously reported an increase in mRNA and protein expression of HO-1 in left ventricle of bile duct-ligated rats, which was associated with an increase in left ventricular cGMP levels[73]. Furthermore, treatment of cirrhotic heart with an HO inhibitor, zinc protoporphyrin IX, restored the elevated cGMP levels[73]. These findings suggest the involvement of an HO-CO-cGMP pathway in the development of cirrhotic cardiomyopathy.

## CONCLUSION

Cardiovascular abnormalities consisting of hyperdynamic circulation and cardiomyopathy are frequent complications in cirrhotic patients and may contribute to significant morbidity and mortality, especially under stressful conditions. Underlying mechanisms of cardiac dysfunction and vascular abnormalities in cirrhosis have been separately explored in recent years, but a number of vasoactive mediator systems may be common to the genesis of both conditions. We believe that central neural activation plays an important initiating role in the genesis of hyperdynamic circulation, eventually leading to an imbalance between the tonic vasodilator *vs* vasoconstrictor tone, with a predominance of the former. Predominant among these peripheral vasodilator pathways are NO and endocannabinoids. The mechanisms of cirrhotic cardiomyopathy include altered cardiomyocyte plasma membrane physicochemical properties, impairment of β-adrenergic receptor signaling pathways, and overactivity of NO, carbon monoxide and endocannabinoid systems. Considering the undeniable interrelation of these systems, further studies are required to elucidate the complex interactions between these mechanisms.

## REFERENCES


1 **Garcia-Tsao G**. Portal hypertension. *Curr Opin Gastroenterol* 2003; **19**: 250-258

2 **Groszmann RJ**. Hyperdynamic circulation of liver disease 40 years later: pathophysiology and clinical consequences. *Hepatology* 1994; **20**: 1359-1363

3 **Liu H,** Song D, Lee SS. Cirrhotic cardiomyopathy. *Gastroenterol Clin Biol* 2002; **26**: 842-847

4 **Ma Z,** Lee SS. Cirrhotic cardiomyopathy: getting to the heart of the matter. *Hepatology* 1996; **24**: 451-459

5 **Moller S,** Henriksen JH. Cirrhotic cardiomyopathy: a pathophysiological review of circulatory dysfunction in liver disease. *Heart* 2002; **87**: 9-15

6 **Batkai S,** Jarai Z, Wagner JA, Goparaju SK, Varga K, Liu J, Wang L, Mirshahi F, Khanolkar AD, Makriyannis A, Urbaschek R, Garcia N Jr, Sanyal AJ, Kunos G. Endocannabinoids acting at vascular CB1 receptors mediate the vasodilated state in advanced liver cirrhosis. *Nat Med* 2001; **7**: 827-832

7 **Ros J,** Claria J, To-Figueras J, Planaguma A, Cejudo-Martin P, Fernandez-Varo G, Martin-Ruiz R, Arroyo V, Rivera F, Rodes J, Jimenez W. Endogenous cannabinoids: a new system involved in the homeostasis of arterial pressure in experimental cirrhosis in the rat. *Gastroenterology* 2002; **122**: 85-93

8 **Siegmund SV,** Uchinami H, Osawa Y, Brenner DA, Schwabe RF. Anandamide induces necrosis in primary hepatic stellate cells. *Hepatology* 2005; **41**: 1085-1095

9 **Varga K,** Wagner JA, Bridgen DT, Kunos G. Platelet- and macrophage-derived endogenous cannabinoids are involved in endotoxin-induced hypotension. *FASEB J* 1998; **12**: 1035-1044

10 **Van de Casteele M,** Omasta A, Janssens S, Roskams T, Desmet V, Nevens F, Fevery J. In vivo gene transfer of endothelial ni-

tric oxide synthase decreases portal pressure in anaesthetised carbon tetrachloride cirrhotic rats. *Gut* 2002; **51**: 440-445
11 **Zafra C,** Abraldes JG, Turnes J, Berzigotti A, Fernandez M, Garca-Pagan JC, Rodes J, Bosch J. Simvastatin enhances hepatic nitric oxide production and decreases the hepatic vascular tone in patients with cirrhosis. *Gastroenterology* 2004; **126**: 749-755
12 **Bhathal PS,** Grossman HJ. Reduction of the increased portal vascular resistance of the isolated perfused cirrhotic rat liver by vasodilators. *J Hepatol* 1985; **1**: 325-337
13 **Guarner C,** Soriano G, Tomas A, Bulbena O, Novella MT, Balanzo J, Vilardell F, Mourelle M, Moncada S. Increased serum nitrite and nitrate levels in patients with cirrhosis: relationship to endotoxemia. *Hepatology* 1993; **18**: 1139-1143
14 **Morales-Ruiz M,** Jimenez W, Perez-Sala D, Ros J, Leivas A, Lamas S, Rivera F, Arroyo V. Increased nitric oxide synthase expression in arterial vessels of cirrhotic rats with ascites. *Hepatology* 1996; **24**: 1481-1486
15 **Garcia-Estan J,** Ortiz MC, Lee SS. Nitric oxide and renal and cardiac dysfunction in cirrhosis. *Clin Sci (Lond)* 2002; **102**: 213-222
16 **Niederberger M,** Martin PY, Gines P, Morris K, Tsai P, Xu DL, McMurtry I, Schrier RW. Normalization of nitric oxide production corrects arterial vasodilation and hyperdynamic circulation in cirrhotic rats. *Gastroenterology* 1995; **109**: 1624-1630
17 **Claria J,** Jimenez W, Ros J, Rigol M, Angeli P, Arroyo V, Rivera F, Rodes J. Increased nitric oxide-dependent vasorelaxation in aortic rings of cirrhotic rats with ascites. *Hepatology* 1994; **20**: 1615-1621
18 **Rasaratnam B,** Kaye D, Jennings G, Dudley F, Chin-Dusting J. The effect of selective intestinal decontamination on the hyperdynamic circulatory state in cirrhosis. A randomized trial. *Ann Intern Med* 2003; **139**: 186-193
19 **Dinda PK,** Leddin DJ, Beck IT. Histamine is involved in ethanol-induced jejunal microvascular injury in rabbits. *Gastroenterology* 1988; **95**: 1227-1233
20 **Bode C,** Kugler V, Bode JC. Endotoxemia in patients with alcoholic and non-alcoholic cirrhosis and in subjects with no evidence of chronic liver disease following acute alcohol excess. *J Hepatol* 1987; **4**: 8-14
21 **Garcia-Tsao G.** Bacterial translocation: Cause or consequence of decompensation in cirrhosis? *J Hepatol* 2001; **34**: 150-155
22 **Liu H,** Ma Z, Lee SS. Contribution of nitric oxide to the pathogenesis of cirrhotic cardiomyopathy in bile duct-ligated rats. *Gastroenterology* 2000; **118**: 937-944
23 **Nagano T,** Yamamoto K, Matsumoto S, Okamoto R, Tagashira M, Ibuki N, Matsumura S, Yabushita K, Okano N, Tsuji T. Cytokine profile in the liver of primary biliary cirrhosis. *J Clin Immunol* 1999; **19**: 422-427
24 **Odeh M,** Sabo E, Srugo I, Oliven A. Serum levels of tumor necrosis factor-alpha correlate with severity of hepatic encephalopathy due to chronic liver failure. *Liver Int* 2004; **24**: 110-116
25 **Lopez-Talavera JC,** Merrill WW, Groszmann RJ. Tumor necrosis factor alpha: a major contributor to the hyperdynamic circulation in prehepatic portal-hypertensive rats. *Gastroenterology* 1995; **108**: 761-767
26 **Liu H,** Song D, Lee SS. Increased nitric oxide synthase expression in aorta of cirrhotic rats. *Life Sci* 1999; **64**: 1753-1759
27 **Lee FY,** Wang SS, Tsai YT, Lin HJ, Lin HC, Chu CJ, Wu SL, Tai CC, Lee SD. Aminoguanidine corrects hyperdynamic circulation without ameliorating portal hypertension and portal hypertensive gastropathy in anesthetized portal hypertensive rats. *J Hepatol* 1997; **26**: 687-693
28 **Weigert AL,** Martin PY, Niederberger M, Higa EM, McMurtry IF, Gines P, Schrier RW. Endothelium-dependent vascular hyporesponsiveness without detection of nitric oxide synthase induction in aortas of cirrhotic rats. *Hepatology* 1995; **22**: 1856-1862
29 **Bomzon A,** Blendis LM. The nitric oxide hypothesis and the hyperdynamic circulation in cirrhosis. *Hepatology* 1994; **20**: 1343-1350
30 **Martin PY,** Xu DL, Niederberger M, Weigert A, Tsai P, St John J, Gines P, Schrier RW. Upregulation of endothelial constitutive NOS: a major role in the increased NO production in cirrhotic rats. *Am J Physiol* 1996; **270**: F494-F499
31 **Gordon GG,** Olivo J, Rafil F, Southren AL. Conversion of androgens to estrogens in cirrhosis of the liver. *J Clin Endocrinol Metab* 1975; **40**: 1018-1026
32 **Longcope C,** Pratt JH, Schneider S, Fineberg E. Estrogen and androgen dynamics in liver disease. *J Endocrinol Invest* 1984; **7**: 629-634
33 **Weiner CP,** Lizasoain I, Baylis SA, Knowles RG, Charles IG, Moncada S. Induction of calcium-dependent nitric oxide synthases by sex hormones. *Proc Natl Acad Sci U S A* 1994; **91**: 5212-5216
34 **Xu L,** Carter EP, Ohara M, Martin PY, Rogachev B, Morris K, Cadnapaphornchai M, Knotek M, Schrier RW. Neuronal nitric oxide synthase and systemic vasodilation in rats with cirrhosis. *Am J Physiol Renal Physiol* 2000; **279**: F1110-F1115
35 **Biecker E,** Neef M, Sagesser H, Shaw S, Koshy A, Reichen J. Nitric oxide synthase 1 is partly compensating for nitric oxide synthase 3 deficiency in nitric oxide synthase 3 knock-out mice and is elevated in murine and human cirrhosis. *Liver Int* 2004; **24**: 345-353
36 **Deutsch DG,** Goligorsky MS, Schmid PC, Krebsbach RJ, Schmid HH, Das SK, Dey SK, Arreaza G, Thorup C, Stefano G, Moore LC. Production and physiological actions of anandamide in the vasculature of the rat kidney. *J Clin Invest* 1997; **100**: 1538-1546
37 **Pak JM,** Lee SS. Glucagon in portal hypertension. *J Hepatol* 1994; **20**: 825-832
38 **Lee FY,** Chu CJ, Wang SS, Chang FY, Lin HC, Hou MC, Chan CC, Wu SL, Chen CT, Huang HC, Lee SD. Inhibition of prostacyclin by indomethacin ameliorates the splanchnic hyposensitivity to glypressin in haemorrhage-transfused common bile duct-ligated rats. *Eur J Clin Invest* 2001; **31**: 145-153
39 **Minuk GY,** MacCannell KL. Is the hypotension of cirrhosis a GABA-mediated process? *Hepatology* 1988; **8**: 73-77
40 **Hunt S,** Vaamonde CA, Rattassi T, Berian G, Said SI, Papper S. Circulating levels of vasoactive intestinal polypeptide in liver disease. *Arch Intern Med* 1979; **139**: 994-996
41 **Pak JM**, Lee SS. Vasoactive effects of bile salts in cirrhotic rats: In vivo and in vitro studies. *Hepatology* 1993; **18**: 1175-1181
42 **Tarnoky K,** Tutsek L, Nagy S. The role of histamine in the increased cardiac output in hyperdynamic endotoxemia. *Shock* 1994; **1**: 153-157
43 **Lee SS,** Chilton EL, Pak JM. Adenosine receptor blockade reduces splanchnic hyperemia in cirrhotic rats. *Hepatology* 1992; **15**: 1107-1111
44 **Lee SS,** Sharkey KA. Capsaicin treatment blocks development of hyperkinetic circulation in portal hypertensive and cirrhotic rats. *Am J Physiol* 1993; **264**: G868-G873
45 **Song D,** Liu H, Sharkey KA, Lee SS. Hyperdynamic circulation in portal-hypertensive rats is dependent on central c-fos gene expression. *Hepatology* 2002; **35**: 159-166
46 **Li Y,** Song D, Zhang Y, Lee SS. Effect of neonatal capsaicin treatment on haemodynamics and renal function in cirrhotic rats. *Gut* 2003; **52**: 293-299
47 **Kowalski HJ,** Abelmann WH. The cardiac output at rest in Laennec's cirrhosis. *J Clin Invest* 1953; **32**: 1025-1033
48 **Murray JF,** Dawson AM, Sherlock S. Circulatory changes in chronic liver disease. *Am J Med* 1958; **24**: 358-367
49 **Abelmann WH.** Hyperdynamic circulation in cirrhosis: a historical perspective. *Hepatology* 1994; **20**: 1356-1358
50 **Ruiz-del-Arbol L,** Urman J, Fernandez J, Gonzalez M, Navasa M, Monescillo A, Albillos A, Jimenez W, Arroyo V. Systemic, renal, and hepatic hemodynamic derangement in cirrhotic patients with spontaneous bacterial peritonitis. *Hepatology* 2003; **38**: 1210-1218
51 **Braverman AC,** Steiner MA, Picus D, White H. High-output congestive heart failure following transjugular intrahepatic portal-systemic shunting. *Chest* 1995; **107**: 1467-1469
52 **Naritaka Y,** Ogawa K, Shimakawa T, Wagatsuma Y, Konno S, Katsube T, Hamaguchi K, Hosokawa T. Clinical experience of transjugular intrahepatic portosystemic shunt (TIPS) and its effects on systemic hemodynamics. *Hepatogastroenterology*

2004; **51**: 1470-1472
53 **Rayes N,** Bechstein WO, Keck H, Blumhardt G, Lohmann R, Neuhaus P. [Cause of death after liver transplantation: an analysis of 41 cases in 382 patients]. *Zentralbl Chir* 1995; **120**: 435-438
54 **Bonz A,** Laser M, Kullmer S, Kniesch S, Babin-Ebell J, Popp V, Ertl G, Wagner JA. Cannabinoids acting on CB1 receptors decrease contractile performance in human atrial muscle. *J Cardiovasc Pharmacol* 2003; **41**: 657-664
55 **Ford WR,** Honan SA, White R, Hiley CR. Evidence of a novel site mediating anandamide-induced negative inotropic and coronary vasodilatator responses in rat isolated hearts. *Br J Pharmacol* 2002; **135**: 1191-1198
56 **Gaskari SA,** Liu H, Moezi L, Li Y, Baik SK, Lee SS. Role of endocannabinoids in the pathogenesis of cirrhotic cardiomyopathy in bile duct-ligated rats. *Br J Pharmacol* 2005; **146:** 315-323
57 **Lee SS,** Marty J, Mantz J, Samain E, Braillon A, Lebrec D. Desensitization of myocardial beta-adrenergic receptors in cirrhotic rats. *Hepatology* 1990; **12**: 481-485
58 **Ma Z,** Meddings JB, Lee SS. Membrane physical properties determine cardiac beta-adrenergic receptor function in cirrhotic rats. *Am J Physiol* 1994; **267**: G87-G93
59 **Ma Z,** Miyamoto A, Lee SS. Role of altered beta-adrenoceptor signal transduction in the pathogenesis of cirrhotic cardiomyopathy in rats. *Gastroenterology* 1996; **110**: 1191-1198
60 **Ma Z,** Lee SS, Meddings JB. Effects of altered cardiac membrane fluidity on beta-adrenergic receptor signalling in rats with cirrhotic cardiomyopathy. *J Hepatol* 1997; **26**: 904-912
61 **Le Grimellec C,** Friedlander G, el Yandouzi EH, Zlatkine P, Giocondi MC. Membrane fluidity and transport properties in epithelia. *Kidney Int* 1992; **42**: 825-836
62 **Ladbrooke BD,** Chapman D. Thermal analysis of lipids, proteins and biological membranes. A review and summary of some recent studies. *Chem Phys Lipids* 1969; **3**: 304-356
63 **Ward CA,** Ma Z, Lee SS, Giles WR. Potassium currents in atrial and ventricular myocytes from a rat model of cirrhosis. *Am J Physiol Gastrointest Liver Physiol* 1997; **273**: G537-G544
64 **Smith TW,** Balligand JL, Kaye DM, Wiviott SD, Simmons WW, Han X, Michel T, Singh K, Kelly RA. The role of the NO pathway in the control of cardiac function. *J Card Fail* 1996; **2:** S141-S147
65 **Balligand JL,** Kelly RA, Marsden PA, Smith TW, Michel T. Control of cardiac muscle cell function by an endogenous nitric oxide signaling system. *Proc Natl Acad Sci U S A* 1993; 90: 347-351
66 **Chung MK,** Gulick TS, Rotondo RE, Schreiner GF, Lange LG. Mechanism of cytokine inhibition of beta-adrenergic agonist stimulation of cyclic AMP in rat cardiac myocytes. Impairment of signal transduction. *Circ Res* 1990; **67**: 753-763
67 **Balligand JL.** Regulation of cardiac beta-adrenergic response by nitric oxide. *Cardiovasc Res* 1999; **43**: 607-620
68 **Paulus WJ,** Shah AM. NO and cardiac diastolic function. *Cardiovasc Res* 1999; **43**: 595-606
69 **van Obbergh L,** Vallieres Y, Blaise G. Cardiac modifications occurring in the ascitic rat with biliary cirrhosis are nitric oxide related. *J Hepatol* 1996; **24**: 747-752
70 **Ewing JF,** Raju VS, Maines MD. Induction of heart heme oxygenase-1 (HSP32) by hyperthermia: possible role in stress-mediated elevation of cyclic 3':5'-guanosine monophosphate. *J Pharmacol Exp Ther* 1994; **271**: 408-414
71 **Tohse N,** Nakaya H, Takeda Y, Kanno M. Cyclic GMP-mediated inhibition of L-type Ca2+ channel activity by human natriuretic peptide in rabbit heart cells. *Br J Pharmacol* 1995; **114**: 1076-1082
72 **Raju VS,** Imai N, Liang CS. Chamber-specific regulation of heme oxygenase-1 (heat shock protein 32) in right-sided congestive heart failure. *J Mol Cell Cardiol* 1999; **31**: 1581-1589
73 **Liu H,** Song D, Lee SS. Role of heme oxygenase-carbon monoxide pathway in pathogenesis of cirrhotic cardiomyopathy in the rat. *Am J Physiol Gastrointest Liver*

**S- Editor** Xu XQ and Guo SY **L- Editor** Elsevier HK **E- Editor** Bi L

PO Box 2345, Beijing 100023, China
www.wjgnet.com
wjg@wjgnet.com

*World J Gastroenterol* 2006 February 14; 12(6): 843-852
***World Journal of Gastroenterology*** ISSN 1007-9327
© 2006 The WJG Press. All rights reserved.

*EDITORIAL*

# Cutaneous manifestations in celiac disease

L Abenavoli, I Proietti, L Leggio, A Ferrulli, L Vonghia, R Capizzi, M Rotoli, PL Amerio, G Gasbarrini, G Addolorato

L Abenavoli, L Leggio, A Ferrulli, L Vonghia, G Gasbarrini, G Addolorato, Institute of Internal Medicine, Università Cattolica del Sacro Cuore, Rome, Italy
I Proietti, R Capizzi, M Rotoli, PL Amerio, Institute of Dermatology, Università Cattolica del Sacro Cuore, Rome, Italy
Correspondence to: Giovanni Addolorato, MD, Institute of Internal Medicine, Catholic University, L.go Gemelli 8, 00168 Rome, Italy. g.addolorato@rm.unicatt.it
Telephone: +39-06-30154334 Fax: +39-06-35502775
Received: 2005-05-06 Accepted: 2005-07-28

## Abstract

Celiac disease (CD) is an autoimmune gluten-dependent enteropathy characterized by atrophy of intestinal villi that improves after gluten-free diet (GFD). CD is often associated with extra-intestinal manifestations; among them, several skin diseases are described in CD patients. The present review reports all CD-associated skin manifestations described in the literature and tries to analyze the possible mechanisms involved in this association. The opportunity to evaluate the possible presence of CD in patients affected by skin disorders is discussed.

© 2006 The WJG Press. All rights reserved.

**Key words:** Celiac disease; Dermatological disease; AGA; EmA; TTG

Abenavoli L, Proietti I, Leggio L, Ferrulli A, Vonghia L, Capizzi R, Rotoli M, Amerio PL, Gasbarrini G, Addolorato G. Cutaneous manifestations in celiac disease. *World J Gastroenterol* 2006; 12(6): 843-852

http://www.wjgnet.com/1007-9327/12/843.asp

## INTRODUCTION

Celiac disease (CD) can be defined as a chronic immune-mediated gluten-dependent enteropathy, resulting from an inappropriate T-cell-mediated immune response, against ingested gluten in genetically predisposed people[1]. Epidemiological studies have shown that CD is very common and affects about 1 in 250 people[2]. CD is a multigenic disorder associated with HLA-DQ2 (DQA1*/DQB1*2) expressed in more than 90% of patients, or HLA-DQ8 (DQA1*0301/DQB1*0302)[3]. The expression of these molecules is necessary, but not sufficient, to develop the disease[4]. The immune response to gluten takes place in two compartments: the lamina propria and the epithelium. While lamina propria CD4 T cells have a recognized role in the pathogenesis of CD, the role of CD8 T cells in the intestinal epithelium is controversial[5].

CD is characterized by intestinal malabsorption and subtotal or total atrophy of intestinal villi which improves after gluten-free diet (GFD)[6]. The classic form of CD presents several symptoms such as diarrhea, abdominal pain, weight loss and nutritional deficiencies, particularly of iron, folate, calcium, and vitamin D[7]. However, there is a large variety of clinical presentations characterized by the presence of extra-intestinal manifestations, including anemia[8], persistent hypertransaminasemia[9], osteopenia[10], neurological[11], psychiatric and affective disorders[12-14], features of hyposplenism (Howell-Jolly bodies and thrombocytosis)[15] and autoimmune diseases[6]. In the last years, growing evidence has documented the involvement of skin diseases among the extra-intestinal manifestations of CD[17]. The aim of this review is to report all CD associated skin manifestations described in the English literature and to analyze the possible mechanisms involved in this association.

### *Dermatitis herpetiformis*

Dermatitis herpetiformis (DH) is a well-described entity, presenting as an itchy, chronic, papulovesicular eruption which may leave pigmentation and scarring[18]. Classically, skin lesions are characterized by a symmetrical eruption on the extensor surfaces of the body such as the knees, elbows, buttocks, and back. DH tends to occur more in the adult male (M/F ratio 2:1) who may also present with the involvement of oral and genital membranes. However this pattern is reversed in children who may simply have purpura over the palmar surfaces. The age of onset varies with geographical location and the incidence is highest in Ireland and Sweden and rare in Asia[19]. Histology of lesional skin shows micro abscesses consisting of neutrophils and eosinophils within the dermal papillae. Sub-epidermal vesicles and bullae are produced within the lamina lucida as a result of collagen degradation. Furthermore there is an increased number of activated T cells. Direct immunofluorescence of the normal skin shows the pathogenomic granular IgA deposits in the papillary dermis but the exact target antigen is still unknown[19-21]. These deposits are often associated with C3 to support the suggestion that the complement is activated via the alternative pathway and C5[22,23]. The activated fraction, C5a, is highly chemotactic for neutrophils and may contribute to the inflammatory change at the papillary tip.

HLA studies in patients, who have DH based on

clinical and immunological criteria, have shown that 85-90% are HLA B8-positive and that there is an even stronger association with HLA DW3 and DRW3. Interestingly, patients with a GSE without DH show a similar high incidence of these antigens[24]. Specific B cell/ macrophage antigens have been noted in patients with DH and the gluten-sensitive enteropathy[25]. Family studies have shown that these B cell antigens segregated independently of HLA antigens[26]. One hypothesis is that both HLA and non-HLA disease genes are necessary for the development of lymphoid cell surface receptors that recognize gluten.

Antigluten, antiendomysium, antigliadin and tissue transglutaminase antibodies have been detected in patients with DH[27-29]. These gluten-specific cells migrate to the gut mucosa where they mediate cytotoxic reactions involving the epithelial cells[30]. There is an immunogenetic association with HLA DR3 DQW2 (HLA class II alleles DQAI 0501 and DQBI 0201), which is very much more common in Caucasians than in Orientals and may be important for the different incidences of DH in different ethnic populations. Gluten must be present in the diet for the development of DH; however, a genetic susceptibility to gluten has been proposed as an etiological mechanism. This observation could explain why DH is very common in some Asian populations, which have a low daily gluten intake (e.g., 7-8 g/d in Korea) compared with Western populations which have higher daily gluten intake (e.g., 15-20 g/d in Scandinavia)[19].

As CD and DH may seem to be vastly different, they both share a unique intestinal sensitivity to gluten, with the rash of DH thought to be an external marker of the underlying intestinal sensitivity that is likely to be the result of molecular mimicry between the auto antigen tissue transglutaminase resident in the gut and the skin derived epidermal transglutaminase.

Although patients with DH are unlikely to have gastrointestinal symptoms or features of malabsorption, they have small intestinal histopathologic changes, with either a classical atrophic appearance with complete villous atrophy, or more commonly a more subtle infiltrative pattern with partial or no villous atrophy. When there is a suspicion of DH with a negative skin biopsy but serologic evidence of CD, a skin biopsy should be repeated given the patchy nature of the lesions, and referral to a gastroenterologist for small bowel biopsy should be pursued. Interestingly, topical skin application of gluten-containing products does not produce the rash of DH in susceptible patients; however, oral or rectal introduction of gluten has been found to result in the classic DH rash[31,32].

The DH rash is often treated with dapsone in conjunction with the gluten withdrawal. In addition to improving the histological changes of the small intestine, the gluten-free diet may also allow a reduction of suppressive medication[32]. Just as patients with CD are at a higher risk of malignancies such as lymphomas, so are those patients with DH not compliant with GFD, which should motivate patients with DH to follow the diet regardless of the absence of other symptoms[31].

### Linear IgA bullous dermatosis

Linear IgA bullous dermatosis (LABD) is a rare disease characterized by erythematous papules or groups of small vesicles. The onset may be acute or gradual and the predominant symptom is usually pruritus. Immunoelectron microscopic studies have shown a linear deposition of IgA along the lamina lucida or in the sub-basal lamina area of stratified squamous epithelium[32]. At the moment, it is considered as a distinct entity from DH and Bullous pemphigoid[32,33]. The incidence of gluten sensitivity enteropathy (GSE) in LABD has been described in the literature to range from 0% to 24%[33-36]. The HLA haplotype (A1, B8, DR3) of LABD patients is often that found in classic DH which is in >85% of CD patients[37,38]. Although the prevalence of CD is low in LABD, some authors have suggested a diagnosis of GSE in these patients[34-36,39].

### Urticaria

Urticaria is an eruption of transient erythematous or edematous swellings of the dermis or sub-cutaneous tissue and is due to a local increase of permeability of capillaries and small venules. Hautekeete *et al*[40] first described the association between CD and chronic urticaria, although this association is still debated[41]. Adults with CD also often have an increase of atopic or immunologic disorders[42,43]. Scala *et al* reported that a GFD eliminated both skin and intestinal symptoms in patients with concomitant CD and chronic urticaria[44]. The passage of antigens and immune-complex formation may be facilitated by an increased mucosal permeability. Theoretically, this mechanism might cause urticarial lesions and so, by restoring the integrity of the mucosa, a gluten-free diet might resolve skin symptomatology.

### Hereditary angioneurotic edema

Hereditary angioneurotic edema (HANE) is characterized by recurrent edematous attacks in the sub-cutis and sub-mucous due to C1-esterase inhibitor (C1-INH) deficiency[45]. Brickman *et al*[46,47] described HANE in association with inflammatory bowel diseases (IBD). In 2002, Farkas *et al*[48] first described the simultaneous occurrence of HANE and CD. The classic activation pathway of the complement system plays a potential role in the immune regulation of both disorders: it is deficient in HANE and gluten is a potent activator of the alternative pathway in CD[49]. There might also be a genetically determined etiology of both diseases[50]. Complement testing is justified whenever the GI symptoms of CD persist despite restoration of damaged mucous. Conversely HANE unresponsive to adequate prophylaxis should prompt for complete GI group tests[48].

### Cutaneous vasculitis

CD may give rise to many skin manifestations but vasculitic skin lesions have rarely been encountered[51,52]. Leucocytoclastic vasculitis is characterized by the involvement of postcapillary venules. The skin is the most common organ involved with the usual clinical appearance of a palpable purpura. In most cases, leucocytoclastic vasculitis is mediated by immunocomplex deposition and the antigen being either exogenous or endogenous[53]. The coexistence of cutaneous vasculitis and CD might be related to in-

creased intestinal permeability[54], and immune complexes, originating from exogenous or endogenous antigens, might circulate because of the impaired phagocytic function of reticular endothelium system and be deposited in the skin[55]. As in inflammatory bowel disease (IBD), exogenous antigens may permeate the damaged CD mucous in larger quantities than normal[54,56]. This is reflected by significant serum milk and gluten fraction antibody titers[57,58]. Alternatively, an autoimmune sensitization may result because of the release of endogenous antigens from damaged small bowel mucosa[59]. Meyers *et al*[60] described a case of cutaneous vasculitis complicating CD and the remission of skin lesions after the treatment with a strict GFD. Treatment of leucocytoclastic vasculitis has generally been difficult, but corticosteroids and a gluten-free diet may improve the dermatosis in cases associated with CD[52].

### Erythema nodosum

Erythema nodosum (EN) is a chronic panniculitis characterized by inflammation of the fat septa and its etiology seems to involve an allergic or immune complex-mediated reaction to many antigens. Triggers include infections, sarcoidosis, adverse drug reaction, IBD, and lymphomas[61]. EN generally resolves in 5-8 weeks but if antigenic stimulus persists, the disease may last for a long period[62]. In 1991, Durand *et al* first observed a causal linkage between CD and EN[63]. CD can be a triggering factor of EN because an altered intestinal permeability to endogenous or exogenous antigens may provoke the immunologic response. EN is also a common finding in sarcoidosis which frequently coincides with CD[62-65]. When EN skin lesions are chronically recurrent or persistent, it is advisable to search for an underlying CD even if it is difficult to estimate the true incidence of the coexistence of both diseases.

### Erythema elevatum diutinum

Erythema elevatum diutinum (EED) is a rare variation of cutaneous leucocytoclastic vasculitis, originally described in 1894[66]. Its lesions appear as soft erythematous papule-plaques and become hard nodules mainly symmetrically affecting the backs of the hands and other extensor surfaces overlying the joints[67]. Ulceration, arthralgia and pain can be other features of this disease[67,68]. Even if it is presumed to be an immune reaction by bacterial antigens, the etiology of EED is unknown[69]. EED has been described in association with several other immunological diseases, especially paraproteinemias (i.e., monoclonal IgA gammopathy)[70]. Tasanen *et al*[70] detected dermo-epidermal IgA and complement deposits in lesional skin of a patient affected by CD; the histopathology was suggestive of EED[71]. The EED skin lesions appear to result from an immune complex reaction, as suggested by the association of various infections or autoimmune diseases. Joint pains are often present in patients affected by autoimmune disease such as EED but are also often found in association with CD[72]. Some authors have therefore suggested that it is important to warrant consideration of underlying CD in at least some patients with EED[71-73].

### Necrolytic migratory erythema

The features of necrolytic migratory erythema (NME) have been reviewed by several authors. Becker *et al*[74] first described a cutaneous reaction pattern with specific histopathologic features in association with a pancreatic islet cell carcinoma. NME is a term used by Wilkinson[75] to describe the characteristic skin disease related with glucagonoma. Typically lesions start with figurate areas of erythema followed by erosions mainly over the trunk, perineum, lower extremities and perioral area. Eventual shedding is caused by superficial necrosis[76]. Most patients have angular cheilitis, stomatitis, glossitis, diffuse alopecia and brittle nails. Gastrointestinal symptoms such as weight loss and diarrhea are common[77]. Most cases of NME were part of the glucagonoma syndrome[76-77]. NME occasionally occurs with chronic liver disease or malabsorption with villous atrophy[78,79]. Kelly *et al*[80], Goodenberg *et al*[79] and Thorisdottir *et al*[81] described the association between CD and NME. The etiology of NME is uncertain, although deficiencies of zinc, amino acids, or essentially fatty acids could play an important role[77,78,82,83]. It must be stressed that in CD patients with NME, this latter disorder seems to have an excellent response to GFD[79,81].

### Psoriasis

Psoriasis is a chronic, relapsing dermatosis characterized by scaling, erythema, and less commonly pustulation[84]. It has been demonstrated that psoriasis is an immunological disease with hyperproliferation of T-cell mediated keratocytes[85]. Recent data indicate that HLA-Cw*0602 may play an important pathogenetic role in the majority of psoriasis patients[86]. Immune mechanisms have an important role in the pathogenesis of this disease. In particular, an overexpression of T helper cell type 1 (Th1) cytokines and a relative under-expression of Th 2 cytokines have been shown in psoriatic patients[87]. The treatment is often difficult; all currently available effective remedies are retinoids or immunosuppressant drugs such as steroids or cyclosporin[84], other than topical treatment[88], photochemotherapy (PUVA)[89] and biological treatment such as infliximab or etanercept[90]. Recent studies have showed an association between CD and psoriasis[91,92,93] and an improvement of skin lesions after 3-6 mo of GFD, without other pharmacological approaches, was described[91]. However at present the relationship between CD and psoriasis remains controversial since there are few data on this topic and other authors sustain that this association seems to be coincidental[94].

In one study, 10 out of 32 (31%) subjects affected by different clinical forms of psoriasis had positive antireticulin antibodies with a variability of titers, related to the extent of the disease[95]. Subsequently, in a first screening study conducted by Michaelsson *et al*[96] 16% of 302 subjects with psoriasis had IgA and/or IgG AGA. Only in 1 of 11 IgA AGA-positive patients from this group screened for antibodies to reticulin/EMA was this positive. An increase of EG2-positive eosinophils in duodenal mucosa associated with elevated serum levels of eosinophil cation protein (ECP) has been documented in psoriatic subjects with AGA, but no tendency to higher

ECP values has been detected in those with AGA[97]. The same authors reported that the increase in the number of eosinophils in the gastrointestinal tract is explained as being part of some unknown process that may be related to the development of skin psoriatic lesions. Cardinali and co-workers[92] performed a study to verify whether gluten intolerance is more frequent in Mediterranean subjects with psoriasis than in healthy controls. The sera of 39 psoriatic patients and 39 controls were screened for AGA, EMA, antibodies anti-transglutaminase (TgA), ECP, serum total IgE levels and number of eosinophils. The results showed positivity for IgG AGA in two psoriatic patients, one borderline for TgA, and none was positive for EMA or IgA AGA. In these subjects the authors found high serum levels of ECP and IgE, but a normal number of eosinophils; on the contrary eosinophil count and serum IgE levels were within the normal range in the controls. Michaelsson *et al*[91] evaluated the effect of GFD in 33 AGA positive patients and six AGA negative patients with psoriasis in an open study. Of the 33 AGA-positive patients, 2 had IgA EMA, and at the duodenal biopsy 15 showed an increased number of lymphocytes in the epithelium, but in some this increase was only slight. GFD was for 3 mo. Thirty out of thirty-three patients strictly complied with GFD, after which they showed a significant decrease of psoriatic lesions. This included a significant decrease in the 16 AGA positive patients with normal routine histology in duodenal biopsy. The AGA negative patients did not improve. There was also a significant decrease in the serum of eosinophil cation protein in patients with elevated AGA. In conclusion, the positive effects of GFD were observed not only in patients with an increased number of lymphocytes in the duodenal epithelium, but also in some patients with seemingly normal epithelium[91,98].

Our group recently reported a case of severe psoriasis in a CD patient, not responding to specific therapies for psoriasis and in whom the regression of skin lesions after GFD was very rapid[99,100]. The association between psoriasis and CD was subsequently confirmed by Ojetti *et al*[101]. The authors evaluated the prevalence of CD in patients affected by psoriasis, showing a high frequency of CD (4.34%) in psoriatic patients.

At present the mechanisms implicated in the possible association between CD and psoriasis, and the effect of GFD on psoriatic skin lesions are not known. There are some hypotheses:

Hypothesis 1: Abnormal small intestinal permeability, frequently present both in psoriasis[102] and in CD patients[103], could be a triggering factor between CD and psoriasis.

Hypothesis 2: T cells play an important role in the pathogenesis of both psoriasis and CD. An increased number of T cells in the blood, in the dermis and in the epidermis of psoriatic patients has been documented[87]. In CD patients, gliadin induces a sensitization of T cells[104] and this may play a role in the pathogenesis of psoriatic skin lesions[99].

Hypothesis 3: Psoriatic lesions in CD patients could be related to vitamin D deficiency, which is present both in CD[105] and in psoriasis[106-107].

### *Vitiligo disease*

Vitiligo is a specific, common, often heritable acquired disorder characterized by well-circumscribed milky white cutaneous macules devoid of identifiable melanocytes[108]. This disease appears to be more commonly observed in parts of the body exposed to the sun and in darker skin types and may develop at any age. The etiology is complex: there appears to be a certain genetic predisposition and a number of potential precipitating causes (i.e. crisis, illness, physical injury, etc.). Numerous attempts to identify HLA markers have revealed certain ethnic-specific markers: HLA-DR4 (blacks), B13 (Jews) and BW-35 (Yemenites). Theiligore[108] has proposed three prevailing theories to explain vitiligo: the neural hypothesis, the self-destruct hypothesis and the immune hypothesis. It carries a risk for ocular abnormalities, particularly iritis, and a significant risk for thyroid disease, diabetes mellitus, Addison's disease and pernicious anemia.

The relationship between CD and vitiligo is controversial. Although some authors have described some cases of vitiligo in patients affected by CD[94,109], a serological screening study for CD in patients with vitiligo did not show any correlation between these two immunological disorders[110]. This implies that the sporadic associated cases must be considered as coincidental.

### *Behçet's disease*

A history of oral ulceration has been described in 25% of patients with CD and about 2-4% of patients with recurrent oral ulceration also have CD[111]. Behçet's disease (BD) is characterized by recurrent ulceration of the mouth and genitalia associated with iritis. Males are affected 5-10 times more frequently than females and the onset is usually between the ages of 10 and 30. The oral ulcers usually show only non-specific inflammatory changes, although there may be infiltration of the grossly thickened walls of thrombosed arterioles. Some authors have suggested that BD may be caused by a virus[112] and antibodies against mucous membrane were demonstrated in 17 of 40 patients[113] but their significance has not yet been evaluated. Triolo and co-workers[114] described 3 cases of coexistence of BD and symptomless CD in 11 patients with BD (defined according to International Study Group-ISG criteria). IgA and IgG class AGA and EMA were found in one patient, another two had IgG AGA alone. There is suggestive but as yet inconclusive evidence of a probable association between CD and autoimmune diseases such as BD. It could be supposed that both diseases are likely the result of molecular mimicry between two undefined auto antigens or virus trigger action. In patients affected by BD, it may therefore be important to search for underlying undiagnosed CD, but future studies are needed to shed light on this point.

### *Oral lichen planus*

The associations between CD and recurrent oral ulceration, glossitis, angular cheilitis and burning mouth are common[111]. Three to six percent of patients with these oral manifestations may have underlying undiagnosed CD[111,115]. Fortune *et al*[116] described the erosive type

of oral lichen planus (OLP) in a patient with gluten enteropathy. OLP is not rare and frequently involves the buccal mucosa, gingiva and tongue. In both the diseases, the lesions had a mucosal T-cell infiltrate and the relief from eating a gluten-free diet was surprising. It is not clear whether the oral lesions are a direct manifestation of CD or due to the effect of malabsorption on the rapidly dividing mucosal cells already predisposed to soreness by a pre-existing disease; because palliative medication of chronic ulcerative stomatitis is often ineffective, it is important to detect the underlying nutritional deficiencies for the patient's general well-being also.

### Dermatomyositis

Dermatomyositis is a disorder mainly of the skin, muscle and blood vessels in which characteristic erythematous and edematous changes in the skin are associated with muscle weakness and inflammation. An underlying carcinoma is commonly described in adults. Juvenile dermatomyositis (JDM) has a more favorable prognosis for life but functional disability is usually severe. Its pathogenesis is probably due to cell-mediated immunity to muscle antigens, humoral immunity and immune complex deposition[117].

Some authors have described an association with CD[118-121]. Both diseases have a strong association with DQA1 0501 heterodimer because a linkage disequilibrium with HLA-DR3 haplotype or alternatively DR5/DR7 heterozygosity in CD[122,123] DQA1 0501 may lead to the activation of CD4-positive T cells by presentation of a still unidentified peptide that may induce CD or JDM. Evron *et al*[124] and Marie *et al*[120] have also described the association between dermatomyositis (DM) and polymyositis (PM) and CD in adults. For these authors CD may be included within the spectrum of gastrointestinal manifestations of DM/PM and they showed that GFD may resolve clinical and laboratory abnormalities.

### Porphyria

Mustajoki *et al*[125] and subsequently Twaddle *et al*[126] reported the coincidental diagnosis of CD in porphyrics. Patients with CD and porphyria present particular problems in terms of management[127]. The porphyrias are a group of rare diseases affecting the enzymes of the heme biosynthetic pathway with subsequent accumulation of porphyrins in the tissues. These substances are photosensitizers and their accumulation in the skin can cause bullae, erosions, increased fragility, scarring, hirsutism and pigmentation on photo-exposed areas. CD is often associated with DH which has some features in common with skin lesions of porphyrias. In one type of porphyria, variegate porphyria (VP), accumulation of porphobilinogen and 5-aminolevulinic acid is associated with gastrointestinal symptoms and an acute neuropsychiatric syndrome. Some drugs such as dapsone are precipitants of these acute attacks[127]. It is essential that patients with bullous skin lesions are adequately investigated to distinguish VP from DH because the administration of dapsone could have a potentially fatal outcome. Furthermore, symptomatic control of CD (e.g., malabsorption, anorexia, calorie restriction) can prevent precipitation of acute attacks of VP and because gluten sensitivity itself may be associated with neurological and psychiatric disorders[12,15], neuropsychiatric porphyria could be one of the differential diagnoses[128].

### Alopecia areata

Alopecia areata (AA) is a chronic autoimmune disease characterized by non-scarring alopecia. Histologically it is possible to find perifollicular lymphocyte infiltration, pointing to an immunologic etiology such as CD. In both the diseases there is the presence of organ-specific autoantibodies[109,129-131], T-lymphocyte infiltration at the site of lesion[132,133], association with HLA genes[134,135] and possible etiologic importance of viral co-factors[136,137]

In the general population the prevalence of CD is 1 in 305[138] and of AA is 1 in 819[139]. Corazza and co-workers[140] found that the prevalence of CD in patients with AA was 1 in 85. Although remission and recurrence may be observed during the clinical course of AA[141], many patients on gluten-free diet showed complete regrowth of scalp and other body hair and no further recurrence of AA at follow-up[140,142]. The positive effects of gluten-free diet on the pattern of autoimmune conditions, such as AA, associated with CD have been attributed to a normalization of the immune response. This study suggests that AA patients constitute a novel risk group of CD. Because AA may be the only clinical manifestation of CD, some authors suggest GSE serological screening tests in alopecia universalis[140].

### Acquired hypertrichosis lanuginosa

Acquired hypertrichosis lanuginosa (AHL) is a rare disease and there are less than 40 cases in the literature[143,144]. This type of hypertrichosis is characterized in its extreme by the rapid growth of fine, down-like hair all over the body, occasionally associated with glossites and loss of taste. A lesser degree of hypertrichosis in which lanugo hair occurs only on the face is more common. It is three times more common in females than in males and most commonly associated with malignancy[145]. Lymphomas, carcinoid tumors, and the Zollinger-Ellison syndrome have also been associated with this pathology[145,146].

In 1988, Corazza *et al*[147] described the only case reported in the literature of acquired hypertrichosis lanuginosa associated with CD. This case report confirms the paraneoplastic features of AHL. CD is often reported as being associated with tumors and can precede clinical presentation of the tumors[148].

### Pyoderma gangrenosum

The pyoderma gangrenosum (PG) is a neutrophilic dermatosis, with destructive, necrotizing and non infectious ulcera, involving face and inferior limbs. The association between PG and CD has been described in some case reports and the importance of GFD in the resolution of PG has been suggested[149].

### Ichthyosiform dermatoses

The ichthyosiform dermatoses consist of a heterogeneous

group of hereditary disorders, all of which are characterized by the accumulation of large amounts of scale on the cutaneous surface. The earliest reports of ichthyosis have been traced to the Indian and Chinese literatures several hundred years B.C. and a dermatology text by Willian first discussed the problem. Kinetic studies of the epidermis in the major forms of ichthyosis have shown increased germinative cell hyperplasia and increased transit rate through the epidermis in lamellar ichthyosis[150]. Menni *et al*[151] first reported a case of ichthyosis revealing CD but the reason for this association is still unknown.

### Pellagra

Pellagra is a disease characterized by lesions of the skin usually proceeded by prodromal symptoms, especially of digestive and nervous systems. The dermatosis begins as erythema and edema on the back of the hands, with pruritus and burnings, determined especially by exposure to the sun and by localized pressure. In some patients, several days after the onset of erythema, blisters appear; these run together to form bullae and then break. In the second stage, the dermatosis becomes hard and brittle. The skin may look like a goose. The usual sites are the face, neck, dorsal surfaces of the hands, arms, and feet. The cause of pellagra is still not entirely clear. It may arise from a diet deficient in niacin or tryptophan, or more commonly both, and aminoacid imbalance may also play a part[152]. In 1999, Schattner[152] described a case of a man with a pellagra-like syndrome due to CD.

### Generalized acquired cutis laxa

Cutis laxa (CL) is a heterogeneous group of inherited and acquired (generalized or localized) diseases characterized by looseness of the skin with the development of inelastic folds that gives the affected person a prematurely senile appearance[153-155]. CL presents a destructive phenomenon of previously apparently normal elastic fibers, with cephalocaudal progression[156]. It occurs mainly in adults and the etiology is unknown. Immunological abnormality has been postulated to explain the destruction of elastic tissue[157]. Generalized acquired cutis laxa (GACL) has been reported in association with infectious disorders, drugs and autoimmune diseases[153,157,159-163]. Many authors have described a dermal deposit of immunoglobulins (IgA) in various diseases, suggesting that destruction of elastic tissue may be immunologically mediated[159]. Cases of association between GACL and CD have been reported[159,164]. Bodvarsson *et al*[164] proposed that dietary intake of glutenin may induce the production of antibodies to elastin and mediate adherence of neutrophils[165,166]. A cross-reaction is possible between gluten and some components of elastic fibers, since glutenin presents a 22.3% amino acid sequence similar to elastin[164,167]. Garcia-Patos and co-workers[163] described a case of GACL associated with CD, evidence of IgA deposits on the dermal elastic fibers and moderate improvement of eruption after treatment with GFD.

### Atypical mole syndrome and congenital giant naevus

Montalto *et al*[168] first described the association between CD, atypical mole syndrome and congenital giant naevus.

**Table 1 Skin disorders in celiac disease**

| | |
|---|---|
| Dermatitis herpetiformis | Seah *et al*[20] |
| | Mann *et al*[25] |
| | Katz *et al*[22] |
| | Porter *et al*[28] |
| Linear IgA bullous dermatosis | Leonard *et al*[36] |
| | Egan *et al*[39] |
| Urticaria | Hautekeete *et al*[40] |
| | Scala *et al*[44] |
| Hereditary angioneurotic edema | Farkas *et al*[48] |
| Cutaneous vasculitis | Holdstock and Oleesky[52] |
| | Jones[51] |
| | Meyers *et al*[60] |
| Erythema nodosum | Durand *et al*[63] |
| | Crieber *et al*[61] |
| | Bartyik *et al*[64] |
| Erythema elevatum diutinum | Collin *et al*[72] |
| | Rodriguez-Serna *et al*[73] |
| | Tasanen *et al*[71] |
| Necrolytic migratory erythema | Goodenberger *et al*[79] |
| | Kelly *et al*[80] |
| | Thorisdottir *et al*[81] |
| Psoriasis | Michaelsson *et al*[96] |
| | Cardinali *et al*[92] |
| | Addolorato *et al*[99] |
| | Ojetti *et al*[101] |
| | Woo *et al*[93] |
| Vitiligo disease | Reunala and Collin[110] |
| | Collin and Reunala[109] |
| Behçet's disease | Triolo *et al*[115] |
| Oral lichen planus | Fortune and Buchanan[117] |
| Dermatomyositis | Evron *et al*[125] |
| | Buderus *et al*[119] |
| | Falcini *et al*[120] |
| | Marie *et al*[121] |
| | Iannone and Lapadula[122] |
| Porphyria | Mustajoki *et al*[126] |
| | Twaddle *et al*[127] |
| Alopecia areata | Corazza *et al*[141] |
| | Naveh *et al*[143] |
| Acquired hypertrichosis lanuginosa | Corazza *et al*[148] |
| Ichthyosiform dermatoses | Menni *et al*[152] |
| Pellagra | Schattner[153] |
| Generalized acquired cutis laxa | Lewis *et al*[160] |
| | Garcia-Patos *et al*[165] |
| Atypical mole syndrome and congenital giant nevus | Montalto *et al*[170] |
| Pyoderma gangrenosum | Gasbarrini and Corazza[150] |

They reported a case of a patient affected by a rare multiple disorder of the cutaneous pigmentary system, which increased the risk of melanoma, and by CD which is frequently associated with some neoplasms[169-172]. Some authors have therefore suggested a more careful objective examination in all the patients with CD[168].

## CONCLUSION

CD is an enteropathy associated with various extra-intestinal manifestations, including several skin diseases. Several hypotheses have been proposed regarding the possible mechanisms involved in this association. In particular, an abnormal small intestinal permeability appears to be implicated, which may allow the crossing of endogenous or exogenous antigens and may provoke the immunological response, common immune mechanisms, vascular alterations and, lastly, vitamin and aminoacid deficiency secondary to malabsorption in patients with CD. However at present the data are not homogeneous and most of the evidence for the association between CD

and skin disorders is based on "case-reports", making it difficult to draw definitive conclusions on this topic; future controlled studies are consequently needed to verify the real involvement of the cutaneous district in CD (Table 1). Nevertheless, despite these limitations, the opportunity to investigate the possible presence of CD in some dermatological patients seems at present justified.

## ACKNOWLEDGMENTS

We express our gratitude to Dr Cristina D'Angelo, Dr Antonio Mirijello, Dr Silvia Cardone, Dr Veruscka Leso (*Università Cattolica del Sacro Cuore*, Rome, Italy) for their cooperation in this paper. The study was partially supported by grants from the "Associazione Ricerca in Medicina", Bologna-Rome, Italy.

## REFERENCES

1 **Schuppan D.** Current concepts of celiac disease pathogenesis. *Gastroenterology* 2000; **119**: 234-242
2 **Fasano A,** Catassi C. Current approaches to diagnosis and treatment of celiac disease: an evolving spectrum. *Gastroenterology* 2001; **120**: 636-651
3 **Green PH,** Jabri B. Coeliac disease. *Lancet* 2003; **362**: 383-391
4 **Greco L,** Romino R, Coto I, Di Cosmo N, Percopo S, Maglio M, Paparo F, Gasperi V, Limongelli MG, Cotichini R, D'Agate C, Tinto N, Sacchetti L, Tosi R, Stazi MA. The first large population based twin study of coeliac disease. *Gut* 2002; **50**: 624-628
5 **Sollid LM.** Coeliac disease: dissecting a complex inflammatory disorder. *Nat Rev Immunol* 2002; **2**: 647-655
6 **Corazza GR,** Gasbarrini G. Coeliac disease in adults. *Baillieres Clin Gastroenterol* 1995; **9**: 329-350
7 **Capristo E,** Addolorato G, Mingrone G, De Gaetano A, Greco AV, Tataranni PA, Gasbarrini G. Changes in body composition, substrate oxidation, and resting metabolic rate in adult celiac disease patients after a 1-y gluten-free diet treatment. *Am J Clin Nutr* 2000; **72**: 76-81
8 **Howard MR,** Turnbull AJ, Morley P, Hollier P, Webb R, Clarke A. A prospective study of the prevalence of undiagnosed coeliac disease in laboratory defined iron and folate deficiency. *J Clin Pathol* 2002; **55**: 754-757
9 **Volta U,** De Franceschi L, Lari F, Molinaro N, Zoli M, Bianchi FB. Coeliac disease hidden by cryptogenic hypertransaminasaemia. *Lancet* 1998; **352**: 26-29
10 **Corazza GR,** Di Sario A, Cecchetti L, Jorizzo RA, Di Stefano M, Minguzzi L, Brusco G, Bernardi M, Gasbarrini G. Influence of pattern of clinical presentation and of gluten-free diet on bone mass and metabolism in adult coeliac disease. *Bone* 1996; **18**: 525-530
11 **Addolorato G,** Di Giuda D, De Rossi G, Valenza V, Domenicali M, Caputo F, Gasbarrini A, Capristo E, Gasbarrini G. Regional cerebral hypoperfusion in patients with celiac disease. *Am J Med* 2004; **116**: 312-317
12 **De Santis A,** Addolorato G, Romito A, Caputo S, Giordano A, Gambassi G, Taranto C, Manna R, Gasbarrini G. Schizophrenic symptoms and SPECT abnormalities in a coeliac patient: regression after a gluten-free diet. *J Intern Med* 1997; **242**: 421-423
13 **Addolorato G,** Capristo E, Ghittoni G, Valeri C, Masciana R, Ancona C, Gasbarrini G. Anxiety but not depression decreases in coeliac patients after one-year gluten-free diet: a longitudinal study. *Scand J Gastroenterol* 2001; **36**: 502-506
14 **Addolorato G,** De Lorenzi G, Abenavoli L, Leggio L, Capristo E, Gasbarrini G. Psychological support counselling improves gluten-free diet compliance in coeliac patients with affective disorders. *Aliment Pharmacol Ther* 2004; **20**: 777-782
15 **Corazza GR,** Frisoni M, Vaira D, Gasbarrini G. Effect of gluten-free diet on splenic hypofunction of adult coeliac disease. *Gut* 1983; **24**: 228-230
16 **Cardenas A,** Kelly CP. Celiac sprue. *Semin Gastrointest Dis* 2002; **13**: 232-244
17 **Zone JJ,** Skin manifestations of celiac disease. *Gastroenterol* 2005; **128**: S87-S91
18 **Farrell RJ,** Kelly CP. Celiac sprue. *N Engl J Med* 2002; **346**: 180-188
19 **Katsambas AD,** Lotti TM. European Handbook of dermatological treatments 2nd ed. 123
20 **Seah PP,** Fry L, Holborow EJ, Rossiter MA, Doe WF, Magalhaes AF, Hoffbrand AV. Antireticulin antibody: incidence and diagnostic significance. *Gut* 1973; **14**: 311-315
21 **van der Meer JB.** Granular deposits of immunoglobulins in the skin of patients with dermatitis herpetiformis. An immunofluorescent study. *Br J Dermatol* 1969; **81**: 493-503
22 **Katz SI,** Hertz KC, Crawford PS, Gazze LA, Frank MM, Lawley TJ. Effect of sulfones on complement deposition in dermatitis herpetiformis and on complement-mediated guinea-pig reactions. *J Invest Dermatol* 1976; **67**: 688-690
23 **Mustakallio KK,** Blomqvist K, Laiho K. Papillary deposition of fibrin, a characteristic of initial lesions of dermatitis herpetiformis. *Ann Clin Res* 1970; **2**: 13-18
24 **Dahl MV.** In Year Book of Dermatology Eds. Dobson RI and Thiers BU. Chicago, 1980 Year Book Medical Pub.Inc.
25 **Mann DL,** Katz SI, Nelson DL, Abelson LD. Specific B-cell antigens associated with gluten-sensitive enteropathy and dermatitis herpetiformis. *Lancet* 1976; **1**: 110-111
26 **Eterman KP,** Feltkamp TE. Antibodies to gluten and reticulin in gastrointestinal diseases. *Clin Exp Immunol* 1978; **31**: 92-99
27 **Seah PP,** Fry L, Hoffbrand AV, Holborow EJ. Tissue antibodies in dermatitis herpetiformis and adult coeliac disease. *Lancet* 1971; **1**: 834-846
28 **Porter WM,** Unsworth DJ, Lock RJ, Hardman CM, Baker BS, Fry L. Tissue transglutaminase antibodies in dermatitis herpetiformis. *Gastroenterology* 1999; **117**: 749-750
29 **Katz SI,** Hall RP 3rd, Lawley TJ, Strober W. Dermatitis herpetiformis: the skin and the gut. *Ann Intern Med* 1980; **93**: 857-874
30 **Marks J,** Shuster S, Watson AJ. Small-bowel changes in dermatitis herpetiformis. *Lancet* 1966; **2**: 1280-1282
31 **Zone JJ**, Taylor TB, Kadunce DP, Meyer LJ. Identification of the cutaneous basement membrane zone antigen and isolation of antibody in linear immunoglobulin A bullous dermatosis. *J Clin Invest* 1990; **85**: 812-820
32 **Oxentenko AS,** Murray JA. Celiac disease and dermatitis herpetiformis: the spectrum of gluten-sensitive enteropathy. *Int J Dermatol* 2003; **42**: 585-587
33 **Wojnarowska F,** Marsden RA, Bhogal B, Black MM. Chronic bullous disease of childhood, childhood cicatricial pemphigoid, and linear IgA disease of adults. A comparative study demonstrating clinical and immunopathologic overlap. *J Am Acad Dermatol* 1988; **19**: 792-805
34 **Lawley TJ,** Strober W, Yaoita H, Katz SI. Small intestinal biopsies and HLA types in dermatitis herpetiformis patients with granular and linear IgA skin deposits. *J Invest Dermatol* 1980; **74**: 9-12
35 **Chorzelski TP,** Jablonska S. Diagnostic significance of the immunofluorescent pattern in dermatitis herpetiformis. *Int J Dermatol* 1975; **14**: 429-436
36 **Leonard JN,** Griffiths CE, Powles AV, Haffenden GP, Fry L. Experience with a gluten free diet in the treatment of linear IgA disease. *Acta Derm Venereol* 1987; **67**: 145-148
37 **Sachs JA,** Awad J, McCloskey D, Navarrete C, Festenstein H, Elliot E, Walker-Smith JA, Griffiths CE, Leonard JN, Fry L. Different HLA associated gene combinations contribute to susceptibility for coeliac disease and dermatitis herpetiformis. *Gut* 1986; **27**: 515-520
38 **Hall RP,** Sanders ME, Duquesnoy RJ, Katz SI, Shaw S. Alterations in HLA-DP and HLA-DQ antigen frequency in patients with dermatitis herpetiformis. *J Invest Dermatol* 1989; **93**: 501-505
39 **Egan CA,** Smith EP, Taylor TB, Meyer LJ, Samowitz WS, Zone JJ. Linear IgA bullous dermatosis responsive to a gluten-free diet. *Am J Gastroenterol* 2001; **96**: 1927-1929
40 **Hautekeete ML,** DeClerck LS, Stevens WJ. Chronic urticaria

associated with coeliac disease. *Lancet* 1987; **1**: 157
41 **Gabrielli M,** Candelli M, Cremonini F, Ojetti V, Santarelli L, Nista EC, Nucera E, Schiavino D, Patriarca G, Gasbarrini G, Pola P, Gasbarrini A. Idiopathic chronic urticaria and celiac disease. *Dig Dis Sci* 2005; **50**: 1702-1704
42 **Hodgson HJ,** Davies RJ, Gent AE, Hodson ME. Atopic disorders and adult coeliac disease presenting with symptoms of worsening astma. *Lancet* 1986; **2**: 1157-1158
43 **Cooper BT,** Holmes GK, Cooke WT. Coeliac disease and immunological disorders. *Br Med J* 1978; **1**: 537-539
44 **Scala E,** Giani M, Pirrotta L, Guerra EC, De Pita O, Puddu P. Urticaria and adult celiac disease. *Allergy* 1999; **54**: 1008-1009
45 **Agostoni A,** Cicardi M. Hereditary and acquired C1-inhibitor deficiency: biological and clinical characteristics in 235 patients. *Medicine* 1992; **71**: 206-215
46 **Brickman CM,** Tsokos GC, Chused TM, Balow JE, Lawley TJ, Santaella M, Hammer CH, Linton GF, Frank MM. Immunoregulatory disorders associated with hereditary angioedema. II. Serologic and cellular abnormalities. *J Allergy Clin Immunol* 1986; **77**: 758-767
47 **Farkas H,** Gyeney L, Nemesanszky E, Kaldi G, Kukan F, Masszi I, Soos J, Bely M, Farkas E, Fust G, Varga L. Coincidence of hereditary angioedema (HAE) with Crohn's disease. *Immunol Invest* 1999; **28**: 43-53
48 **Farkas H,** Visy B, Fekete B, Karadi I, Kovacs JB, Kovacs IB, Kalmar L, Tordai A, Varga L. Association of celiac disease and hereditary angioneurotic edema. *Am J Gastroenterol* 2002; **97**: 2682-2683
49 **Unsworth DJ,** Wurzner R, Brown DL, Lachmann PJ. Extracts of wheat gluten activate complement via the alternative pathway. *Clin Exp Immunol* 1993; **94**: 539-543
50 **Dawkins R,** Leelayuwat C, Gaudieri S, Tay G, Hui J, Cattley S, Martinez P, Kulski J. Genomics of the major histocompatibility complex: haplotypes, duplication, reteroviruses and disease. *Immunol Rev* 1999; **167**: 275-304
51 **Jones FA.** The skin: a mirror of the gut. *Geriatrics* 1973; **28**: 75-81
52 **Holdstock DJ,** Oleesky S. Vasculitis in coeliac diseases. *Br Med J* 1970; **4**: 369
53 **Alarcon-Segovia D.** The necrotizing vasculitides. A new pathogenetic classification. *Med Clin North Am* 1977; **61**: 241-260
54 **Menzies IS,** Laker MF, Pounder R, Bull J, Heyer S, Wheeler PG, Creamer B. Abnormal intestinal permeability to sugars in villous atrophy. *Lancet* 1979; **2**: 1107-1109
55 **Marsh GW,** Stewart JS. Splenic function in adult celiac disease. *Br J Haematol* 1970; **19**: 445-447
56 **Wands JR,** LaMont JT, Mann E, Isselbacher KJ. Arthritis associated with intestinal-bypass procedure for morbid obesity. Complement activation and characterization of circulating cryoproteins. *N Engl J Med* 1976; **294**: 121-124
57 **Taylor KB,** Truelove SC, Thomson DL, Wright R. An immunological study of coeliac disease and idiopathic steatorrhoea. Serological reactions to gluten and milk proteins. *Br Med J* 1961; **5269**: 1727-1731
58 **Falchuk ZM,** Strober W. Gluten-sensitive enteropathy: synthesis of antigliadin antibody in vitro. *Gut* 1974; **15**: 947-952
59 **Scott BB,** Losowsky MS. Coeliac disease: a cause of various associated diseases? *Lancet* 1975; **2**: 956-957
60 **Meyers S,** Dikman S, Spiera H, Schultz N, Janowitz HD. Cutaneous vasculitis complicating coeliac disease. *Gut* 1981; **22**: 61-64
61 **Cribier B,** Caille A, Heid E, Grosshans E. Erythema nodosum and associated diseases. A study of 129 cases. *Int J Dermatol* 1998; **37**: 667-672
62 **Bohn S,** Buchner S, Itin P. Erythema nodosum: 112 cases. Epidemiology, clinical aspects and histopathology. *Schweiz Med Wochenschr* 1997; **127**: 1168-1176
63 **Durand JM,** Lefevre P, Weiller C. Erythema nodosum and coeliac disease. *Br J Dermatol* 1991; **125**: 291-292
64 **Bartyik K,** Varkonyi A, Kirschner A, Endreffy E, Turi S, Karg E. Erythema nodosum in association with celiac disease. *Pediatr Dermatol* 2004; **21**: 227-230
65 **Douglas JG,** Gillon J, Logan RF, Grant IW, Crompton GK. Sarcoidosis and coeliac disease: an association? *Lancet* 1984; **2**: 13-15
66 **Barriere H,** Bureau B, LeRoux P. Erythema elevatum diutinum. *Ann Dermatol Venereol* 1977; **104**: 75-76
67 **Haber H.** Erythema elevatum diutinum. *Br J Dermatol* 1955; **67**: 121-145
68 **Fort SL,** Rodman OG. Erythema elevatum diutinum. Response to dapsone. *Arch Dermatol* 1977; **113**: 819-822
69 **Wolff HH,** Scherer R, Maciejewski W, Braun-Falco O. Erythema elevatum diutinum: immunoelectron microscopical study of leucocytoclastic vasculitis within the intracutaneous test reaction induced by streptococcal antigen. *Arch Dermatol Res* 1978; **26**: 17-26
70 **Archimandritis AJ,** Fertakis A, Alegakis G, Bartsokas S, Melissinos K. Erythema elevatum diutinum and IgA myeloma: an interesting association. *Br Med J* 1977; **2**: 613-614
71 **Tasanen K,** Raudasoja R, Kallioinen M, Ranki A. Erythema elevatum diutinum in association with coeliac disease. *Br J Dermatol* 1997; **136**: 624-627
72 **Collin P,** Korpela M, Hallstrom O, Viander M, Keyrilainen O, Maki M. Rheumatic complaints as a presenting symptom in patients with coeliac disease. *Scand J Rheumatol* 1992; **21**: 20-23
73 **Rodriguez-Serna M,** Fortea JM, Perez A, Febrer I, Ribes C, Aliaga A. Erythema elevatum diutinum associated with celiac disease: response to a gluten-free diet. *Pediatr Dermatol* 1993; **10**: 125-128
74 **Becker SW,** Kahn D, Rothman S. Cutaneous manifestation of internal malignant tumors. *Arch Dermatol Syph* 1942; **45**: 1069-1080
75 **Wilkinson DS.** Necrolytic migratory erythema with carcinoma of the pancreas. *Trans St Johns Hosp Dermatol Soc* 1973; **59**: 244-250
76 **Vandersteen PR,** Scheithauer BW. Glucagonoma syndrome. A clinicopathologic, immunocytochemical, and ultrastructural study. *J Am Acad Dermatol* 1985; **12**: 1032-1039
77 **Mallinson CN,** Bloom SR, Warin AP, Salmon PR, Cox B. A glucagonoma syndrome. *Lancet* 1974; **2**: 1-5
78 **Blackford S,** Wright S, Roberts DL. Necrolytic migratory erythema without glucagonoma: the role of dietary essential fatty acids. *Br J Dermatol* 1991; **125**: 460-462
79 **Goodenberger DM,** Lawley TJ, Strober W, Wyatt L, Sangree MH Jr, Sherwin R, Rosenbaum H, Braverman I, Katz SI. Necrolytic Migratory Erythema without glucagonoma: report of two cases. *Arch Dermatol* 1979; **115**: 1429-1432
80 **Kelly CP,** Johnston CF, Nolan N, Keeling PW, Weir DG. Necrolytic migratory erythema with elevated plasma enteroglucagon in celiac disease. *Gastroenterology* 1989; **96**: 1350-1353
81 **Thorisdottir K,** Camisa C, Tomecki KJ, Bergfeld WF. Necrolytic migratory erythema: a report of three cases. *J Am Acad Dermatol* 1994; **30**: 324-329
82 **Parker CM,** Hanke CW, Madura JA, Liss EC. Glucagonoma syndrome: case report and literature review. *J Dermatol Surg Oncol* 1984; **10**: 884-889
83 **Masri-Friding GD,** Turner MLC. Necrolytic Migratory Erythema without glucagonoma (letter). *J Am Acad Dermatol* 1992; **27**: 486
84 **Kirby B,** Griffiths CE. Novel immune-based therapies for psoriasis. *Br J Dermatol* 2002; **146**: 546-551
85 **Baker BS,** Swain AF, Griffiths CE, Leonard JN, Fry L, Valdimarsson H. Epidermal T lymphocytes and dendritic cells in chronic plaque psoriasis: the effects of PUVA treatment. *Clin Exp Immunol* 1985; **61**: 526-534
86 **Veal CD,** Capon F, Allen MH, Heath EK, Evans JC, Jones A, Patel S, Burden D, Tillman D, Barker JN, Trembath RC. Family-based analysis using a dense single-nucleotide polymorphism-based map defines genetic variation at PSORS1, the major psoriasis-susceptibility locus. *Am J Hum Genet* 2002; **71**: 554-564
87 **Mailliard RB,** Egawa S, Cai Q, Kalinska A, Bykovskaya SN, Lotze MT, Kapsenberg ML, Storkus WJ, Kalinski P. Complementary dendritic cell-activating function of CD8+ and CD4+ T cells: helper role of CD8+ T cells in the development of T helper type 1 responses. *J Exp Med* 2002; **195**: 473-483

88 **van de Kerkhof PC,** Vissers WH. The topical treatment of psoriasis. *Skin Pharmacol Appl Skin Physiol* 2003; **16**: 69-83
89 **Tzaneva S,** Honigsmann H, Tanew A, Seeber A. A comparison of psoralen plus ultraviolet A (PUVA) monotherapy, tacalcitol plus PUVA and tazarotene plus PUVA in patients with chronic plaque-type psoriasis. *Br J Dermatol* 2002; **147**: 748-753
90 **Rich SJ,** Bello-Quintero CE. Advancements in the treatment of psoriasis: role of biologic agents. *J Manag Care Pharm* 2004; 10: 318-325
91 **Michaelsson G,** Gerden B, Hagforsen E, Nilsson B, Pihl-Lundin I, Kraaz W, Hjelmquist G, Loof L. Psoriasis patients with antibodies to gliadin can be improved by a gluten-free diet. *Br J Dermatol* 2000; **142**: 44-51
92 **Cardinali C,** Degl'innocenti D, Caproni M, Fabbri P. Is the search for serum antibodies to gliadin, endomysium and tissue transglutaminase meaningful in psoriatic patients? Relationship between the pathogenesis of psoriasis and coeliac disease. *Br J Dermatol* 2002; **147**: 187-188
93 **Woo WK,** McMillan SA, Watson RG, McCluggage WG, Sloan JM, McMillan JC. Coeliac disease-associated antibodies correlate with psoriasis activity. *Br J Dermatol* 2004; **151**: 891-894
94 **Collin P,** Reunala T. Recognition and management of the cutaneous manifestations of celiac disease: a guide for dermatologists. *Am J Clin Dermatol* 2003; **4**: 13-20
95 **Siri A,** Lozano W, Vignale RA. Antireticulin antibodies in psoriasis. *Acta Derm Venereol* 1980; **60**: 348-351
96 **Michaelsson G,** Gerden B, Ottosson M, Parra A, Sjoberg O, Hjelmquist G, Loof L. Patients with psoriasis often have increased serum levels of IgA antibodies to gliadin. *Br J Dermatol* 1993; **129**: 667-673
97 **Michaelsson G,** Kraaz W, Gerden B, Hagforsen E, Lundin IP, Loof L, Sj-oberg O, Scheynius A. Patients with psoriasis have elevated levels of serum eosinophil cationic protein and increased numbers of EG2 positive eosinophils in the duodenal stroma. *Br J Dermatol* 1996; **135**: 371-378
98 **Kakar S,** Nehra V, Murray JA, Dayharsh GA, Burgart LJ. Significance of intraepithelial lymphocytosis in small bowel biopsy samples with normal mucosal architecture. *Am J Gastroenterol* 2003; **98**: 2027-2033
99 **Addolorato G,** Parente A, de Lorenzi G, D'angelo Di Paola ME, Abenavoli L, Leggio L, Capristo E, De Simone C, Rotoli M, Rapaccini GL, Gasbarrini G. Rapid regression of psoriasis in a coeliac patient after gluten-free diet. A case report and review of the literature. *Digestion* 2003; **68**: 9-12
100 **Abenavoli L,** Leggio L, Ferrulli A, Vonghia L, Gasbarrini G, Addolorato G. Association between psoriasis and coeliac disease. *Br J Dermatol* 2005; **152**: 1393-1394
101 **Ojetti V,** Aguilar Sanchez J, Guerriero C, Fossati B, Capizzi R, De Simone C, Migneco A, Amerio P, Gasbarrini G, Gasbarrini A. High prevalence of celiac disease in psoriasis. *Am J Gastroenterol* 2003; **98**: 2574-2575
102 **Humbert P,** Bidet A, Treffel P, Drobacheff C, Agache P. Intestinal permeability in patients with psoriasis. *J Dermatol Sci* 1991; **2**: 324-326
103 **Montalto M,** Cuoco L, Ricci R, Maggiano N, Vecchio FM, Gasbarrini G. Immunohistochemical analysis of ZO-1 in the duodenal mucosa of patients with untreated and treated celiac disease. *Digestion* 2002; **65**: 227-233
104 **Molberg O,** Mcadam SN, Korner R, Quarsten H, Kristiansen C, Madsen L, Fugger L, Scott H, Noren O, Roepstorff P, Lundin KE, Sjostrom H, Sollid LM. Tissue transglutaminase selectively modifies gliadin peptides that are recognized by gut-derived T cells in celiac disease. *Nat Med* 1998; **4**: 713-717
105 **Cellier C,** Flobert C, Cormier C, Roux C, Schmitz J. Severe osteopenia in symptom-free adults with a childhood diagnosis of coeliac disease. *Lancet* 2000; **355**: 806
106 **Hein G,** Abendroth K, Muller A, Wessel G. Studies on psoriatic osteopathy. *Clin Rheumatol* 1991; **10**: 13-17
107 **Holick MF.** Vitamin D: A millenium perspective. *J Cell Biochem* 2003; **88**: 296-307
108 **Grimes PE.** New insights and new therapies in vitiligo. *JAMA* 2005; **293**: 730-735
109 **Reunala T,** Collin P. Diseases associated with dermatitis herpetiformis. *Br J Dermatol* 1997; **136**: 315-318
110 **Volta U,** Bardazzi F, Zauli D, DeFranceschi L, Tosti A, Molinaro N, Ghetti S, Tetta C, Grassi A, Bianchi FB. Serological screening for coeliac disease in vitiligo and alopecia areata. *Br J Dermatol* 1997; **136**: 801-802
111 **Jones HJ,** Mason DH. Oral manifestation of systemic disease. 2nd ed. London: Baillier Tindall, 1990.
112 **Evans AD,** Pallis CA, Spillane JD. Involvement of the nervous system in Behcet's syndrome; report of three cases and isolation of virus. *Lancet* 1957; **273**: 349-353
113 **Shimizu T,** Katsuta Y, Oshima Y. Immunological studies on Behcet's syndrome. *Ann Rheum Dis* 1965; **24**: 494-500
114 **Triolo G,** Triolo G, Accardo-Palumbo A, Carbone MC, Giardina E, La Rocca G. Behcet's disease and coeliac disease. *Lancet* 1995; **346**: 1495
115 **Ferguson R,** Basu MK, Asquith P, Cooke WT. Jejunal mucosal abnormalities in patients with recurrent aphthous ulceration. *Br Med J* 1976; **1**: 11-13
116 **Fortune F,** Buchanan JA. Oral lichen planus and coeliac disease. *Lancet* 1993; **341**: 1154-1155
117 **Volta U,** De Franceschi L, Molinaro N, Tetta C, Bianchi FB. Organ-specific autoantibodies in coeliac disease: do they represent an epiphenomenon or the expression of associated autoimmune disorders? *Ital J Gastroenterol Hepatol* 1997; **29**: 18-21
118 **Buderus S,** Wagner N, Lentze MJ. Concurrence of celiac disease and juvenile dermatomyositis: result of a specific immunogenetic susceptibility? *J Pediatr Gastroenterol Nutr* 1997; **25**: 101-103
119 **Falcini F,** Porfirio B, Lionetti P. Juvenile dermatomyositis and celiac disease. *J Rheumatol* 1999; **26**: 1419-1420
120 **Marie I,** Lecomte F, Hachulla E, Antonietti M, Francois A, Levesque H, Courtois H. An uncommon association: celiac disease and dermatomyositis in adults. *Clin Exp Rheumatol* 2001; **19**: 201-203
121 **Iannone F,** Lapadula G. Dermatomyositis and celiac disease association: a further case. *Clin Exp Rheumatol* 2001; **19**: 757-758
122 **Reed AM,** Pachman L, Ober C. Molecular genetic studies of major histocompatibility complex genes in children with juvenile dermatomyositis: increased risk associated with HLA-DQA1 *0501. *Hum Immunol* 1991; **32**: 235-240
123 **Lundin KE,** Sollid LM, Qvigstad E, Markussen G, Gjertsen HA, Ek J, Thorsby E. T lymphocyte recognition of a celiac disease-associated cis- or trans-encoded HLA-DQ alpha/beta-heterodimer. *J Immunol* 1990; **145**: 136-139
124 **Evron E,** Abarbanel JM, Branski D, Sthoeger ZM. Polymyositis, arthritis, and proteinuria in a patient with adult celiac disease. *J Rheumatol* 1996; **23**: 782-783
125 **Mustajoki P,** Vuoristo M, Reunala T. Celiac disease or dermatitis herpetiformis in three patients with porphyria. *Dig Dis Sci* 1981; **26**: 618-621
126 **Twaddle S,** Wassif WS, Deacon AC, Peters TJ. Celiac disease in patients with variegate porphyria. *Dig Dis Sci* 2001; **46**: 1506-1508
127 **Moore MR,** Disler PB. Drug sensitive diseases-I-acute porphyrias. *Adverse Drug React Bull* 1988; **129**: 484-487
128 **Hadjivassiliou M,** Gibson A, Davies-Jones GA, Lobo AJ, Stephenson TJ, Milford-Ward A. Does cryptic gluten sensitivity play a part in neurological illness? *Lancet* 1996; **347**: 369-371
129 **Karpati S,** Burgin-Wolff A, Krieg T, Meurer M, Stolz W, Braun-Falco O. Binding to human jejunum of serum IgA antibody from children with coeliac disease. *Lancet* 1990; **336**: 1335-1338
130 **Nunzi E,** Hamerlinck F, Cormane RH. Immunopathological studies on alopecia areata. *Arch Dermatol Res* 1980; **269**: 1-11
131 **Volta U,** Lenzi M, Lazzari R, Cassani F, Collina A, Bianchi FB, Pisi E. Antibodies to gliadin detected by immunofluorescence and a micro-ELISA method: markers of active childhood and adult coeliac disease. *Gut* 1985; **26**: 667-671
132 **Brandtzaeg P,** Halstensen TS, Kett K, Krajci P, Kvale D, Rognum TO, Scott H, Sollid LM. Immunobiology and immunopathology of human gut mucosa: humoral immunity and intraepithelial lymphocytes. *Gastroenterology* 1989; **97**: 1562-1584
133 **Perret C,** Brocker EB, Wiesner-Menzel L, Happle R. In situ

demonstration of T cells in alopecia areata. *Arch Dermatol Res* 1982; **273**: 155-158
134 **Corazza GR,** Tabacchi P, Frisoni M, Prati C, Gasbarrini G. DR and non-DR Ia allotypes are associated with susceptibility to coeliac disease. *Gut* 1985; **26**: 1210-1213
135 **Zhang L,** Weetman AP, Friedmann PS, Oliveira DB. HLA associations with alopecia areata. *Tissue Antigens* 1991; **38**: 89-91
136 **Kagnoff MF,** Austin RK, Hubert JJ, Bernardin JE, Kasarda DD. Possible role for a human adenovirus in the pathogenesis of celiac disease. *J Exp Med* 1984; **160**: 1544-1557
137 **Stankler L.** Synchronous alopecia areata in two siblings: a possible viral aetiology. *Lancet* 1979; **1**: 1303-1304
138 **Catassi C,** Ratsch IM, Fabiani E, Rossini M, Bordicchia F, Candela F, Coppa GV, Giorgi PL. Coeliac disease in the year 2000: exploring the iceberg. *Lancet* 1994; **343**: 200-203
139 **Safavi K.** Prevalence of alopecia areata in the First National Health and Nutrition Examination Survey. *Arch Dermatol* 1992; **128**: 702
140 **Corazza GR,** Andreani ML, Venturo N, Bernardi M, Tosti A, Gasbarrini G. Celiac disease and alopecia areata: report of a new association. *Gastroenterology* 1995; **109**: 1333-1337
141 **Mitchell AJ,** Krull EA. Alopecia areata: pathogenesis and treatment. *J Am Acad Dermatol* 1984; **11**: 763-775
142 **Naveh Y,** Rosenthal E, Ben-Arieh Y, Etzioni A. Celiac disease-associated alopecia in childhood. *J Pediatr* 1999; **134**: 362-364
143 **Hovenden AL.** Acquired hypertrichosis lanuginosa associated with malignancy. *Arch Intern Med* 1987; **147**: 2013-2018
144 **Jemec GB.** Hypertrichosis lanuginosa acquisita. Report of a case and review of the literature. *Arch Dermatol* 1986; **122**: 805-808
145 **Ikeya T,** Izumi A, Suzuki M. Acquired hypertrichosis lanuginosa. *Dermatologica* 1978; **156**: 274-282
146 **Fretzin DF.** Malignant down. *Arch Dermatol* 1967; **95**: 294-297
147 **Corazza GR,** Masina M, Passarini B, Neri I, Varotti C. Ipetricosi lanuginosa acquisita associata a sindrome celiaca. *G Ital Dermatol Venereol* 1988; **123**: 611-612
148 **Lowosky MS.** Malasorption. In: Wetherall DJ, Lendicham JGG, Warrel DA. Oxford text book of medicine. ed. *Oxford* 1983; **1**: 1290
149 **Gasbarrini G,** Corazza GR. L'eterogenicità clinica della malattia celiaca. In: Il malassorbimento intestinale e sindromi cliniche ad esso correlate. ed. Luigi Pozzi, 1992; 220-244.
150 **Shwayder T.** Disorders of keratinization: diagnosis and management. *Am J Clin Dermatol* 2004; **5**: 17-29
151 **Menni S,** Boccardi D, Brusasco A. Ichthyosis revealing coeliac disease. *Eur J Dermatol* 2000; **10**: 398-399
152 **Schattner A.** A 70-year-old man with isolated weight loss and a pellagra-like syndrome due to celiac disease. *Yale J Biol Med* 1999; **72**: 15-18
153 **Koch SE,** Williams ML. Acquired cutis laxa: case report and review of disorders of elastolysis. *Pediatr Dermatol* 1985; **2**: 282-288
154 **Schreiber MM,** Tilley JC. Cutis laxa. *Arch Dermatol* 1961; **84**: 266-272
155 **Goltz RW,** Hult AM, Goldfarb M, Gorlin RJ. Cutis laxa. A manifestation of generalized elastolysis. *Arch Dermatol* 1965; **92**: 373-387
156 **Fisher BK,** Page E, Hanna W. Acral localized acquired cutis laxa. *J Am Acad Dermatol* 1989; **21**: 33-40
157 **Nanko H,** Jepsen LV, Zachariae H, Sogaard H. Acquired cutis laxa (generalized elastolysis): light and electron microscopic studies. *Acta Derm Venereol* 1979; **59**: 315-324
158 **Tsuji T,** Imajo Y, Sawabe M, Kuniyuki S, Ishii M, Hamada T, Ishimura E, Hamada N, Nishisawa Y, Morii H. Acquired cutis laxa concomitant with nephrotic syndrome. *Arch Dermatol* 1987; **123**: 1211-1216
159 **Lewis FM,** Lewis-Jones S, Gipson M. Acquired cutis laxa with dermatitis herpetiformis and sarcoidosis. *J Am Acad Dermatol* 1993; **29**: 846-848
160 **Randle HW,** Muller S. Generalized elastolysis associated with systemic lupus erythematosus. *J Am Acad Dermatol* 1983; **8**: 869-873
161 **Mascarò JM Jr,** Torras H, Lecha V. Lupus Eritematoso Cutàneo Chalazodérmico Asossociado ag Nefropatia IgA Mesangial, Enfermedad de Berger, Case no.28. XII° International Meeting of Clinical Dermatology, Barcelona, 1993.
162 **Linares A,** Zarranz JJ, Rodriguez-Alarcon J, Diaz-Perez JL. Reversible cutis laxa due to maternal D-penicillamine treatment. *Lancet* 1979; **2**: 43
163 **Harpey JP,** Jaudon MC, Clavel JP, Galli A, Darbois Y. Cutis laxa and low serum zinc after antenatal exposure to penicillamine. *Lancet* 1983; **2**: 858
164 **Bodvarsson S,** Jonsdottir I, Freysdottir J, Leonard JN, Fry L, Valdimarsson H. Dermatitis herpetiformis--an autoimmune disease due to cross-reaction between dietary glutenin and dermal elastin? *Scand J Immunol* 1993; **38**: 546-550
165 **Hendrix JD,** Mangum KL, Zone JJ, Gammon WR. Cutaneous IgA deposits in bullous diseases function as ligands to mediate adherence of activated neutrophils. *J Invest Dermatol* 1990; **94**: 667-672
166 **Tatham AS,** Shewry PR. Elastomeric proteins: biological roles, structures and mechanisms. *Trends Biochem Sci* 2000; **25**: 567-571
167 **McFadden JP,** Leonard JN, Powles AV, Rutman AJ, Fry L. Sulphamethoxypyridazine for dermatitis herpetiformis, linear IgA disease and cicatricial pemphigoid. *Br J Dermatol* 1989; **121**: 759-762
168 **Montalto M,** Diociaiuti A, Alvaro G, Manna R, Amerio PL, Gasbarrini G. Atypical mole syndrome and congenital giant naevus in a patient with celiac disease. *Panminerva Med* 2003; **45**: 219-221
169 **Wright DH.** The major complications of coeliac disease. *Baillieres Clin Gastroenterol* 1995; **9**: 351-369
170 **Marghoob AA,** Schoenbach SP, Kopf AW, Orlow SJ, Nossa R, Bart RS. Large congenital melanocytic nevi and the risk for the development of malignant melanoma. A prospective study. *Arch Dermatol* 1996; **132**: 170-175
171 **Marghoob AA,** Kopf AW, Rigel DS, Bart RS, Friedman RJ, Yadav S, Abadir M, Sanfilippo L, Silverman MK, Vossaert KA. Risk of cutaneous malignant melanoma in patients with 'classic' atypical-mole syndrome. A case-control study. *Arch Dermatol* 1994; **130**: 993-998
172 **Ackerman AB,** Sood R, Koenig M. Primary acquired melanosis of the conjunctiva is melanoma in situ. *Mod Pathol* 1991; **4**: 253-263

**S- Editor** Guo SY **L- Editor** Elsevier HK **E- Editor** Liu WF

PO Box 2345, Beijing 100023, China
www.wjgnet.com
wjg@wjgnet.com

*World J Gastroenterol* 2006 February 14; 12(6): 853-857
***World Journal of Gastroenterology*** ISSN 1007-9327
© 2006 The WJG Press. All rights reserved.

*EDITORIAL*

# Probiotics and the gastrointestinal tract: Where are we in 2005?

Irit Chermesh, Rami Eliakim

Irit Chermesh, Rami Eliakim, Gastroenterology Department, Rambam Medical Center, Haifa, Israel
Correspondence to: Professor Rami Eliakim, Gastroenterology Department, Rambam Medical Center, P.O.B 9602, Haifa 31096, Israel. r_eliakim@rambam.health.gov.il
Telephone: 972-4-8541912 ( Mobile: 972-50-2062323)
Fax: 972-4-8543058
Received: 2005-08-15 Accepted: 2005-09-12

## Abstract

Probiotic agents are live microbes or components of microbes that have a positive effect on the host. They exert their action through interplay with the immune system of the host. Some of this effect is local and some is systemic. The full story is yet to be discovered. Probiotics have a definite positive effect on rotavirus diarrhea, post antibiotic diarrhea and pouchitis. Their exact role in inflammatory bowel disease, irritable bowel syndrome, other forms of infectious diarrhea, and prevention of cancer is yet to be determined. This review summarizes the data about probiotics in these conditions.

© 2006 The WJG Press. All rights reserved.

**Keywords**: Probiotics; Inflammatory bowel disease; Crohn's disease; Lactose intolerance; Antibiotic associated diarrhea; Rotavirus; Pseudomembranous colitis; Clostridium dificile; Irritable bowel syndrome; Toll like receptor 9

Chermesh I, Eliakim R. Probiotics and the gastrointestinal tract: Where are we in 2005? *World J Gastroenterol* 2006; 12(6): 853-857

http://www.wjgnet.com/1007-9327/12/853.asp

## INTRODUCTION

The modern term 'probiotic' was first used by Fuller [1], describing a live microbial feed supplement which beneficially affects the host animal by improving its microbial balance. Later it was demonstrated that heat-inactivated bacteria or fragments of bacterial DNA have positive effects as well. Marteau *et al* [2] in 2002 defined probiotics as 'microbial cell preparations or components of microbial cells that have a beneficial effect on the health and well-being'. The mechanisms by which probiotics beneficially affect the host are multiple. Probiotics can prevent or ameliorate diarrhea and inflammation through their local effects and/or their effect on the immune system. In the gut, probiotic bacteria are thought to occupy binding sites on the gut mucosa, preventing pathogenic bacteria from adhering to the mucosa [3, 4]. Lactobacilli produce proteinaceous compounds, namely bacteriocins, that act as local antibiotics against more pathogenic organisms [5, 6] and decrease production of pro-inflammatory cytokines such as IFN-γ, TNF-α and IL-12 [7-9]. Probiotics stimulate IgA production [10]. Lactobacilli produce acetic and lactic acid and inhibit the growth of bacterial pathogens [3]. It has been postulated that probiotics compete with pathogens for nutrients and modify toxins produced by pathogens or toxin receptors found in the gut wall. Rachmilewitz *et al* [11] have shown that specific DNA repeats isolated from probiotics (VSL #3) can attenuate experimental colitis in various animal models. This is true even with inactivated bacteria. By using toll-like receptor 9 (TLR-9) deficient mice, they have proved that TLR9 signaling is essential in mediating the anti-inflammatory effect of probiotics [12].

Prerequisites for probiotics are to be effective and safe. The characteristics of an effective probiotic as defined by Saavedra [11] are resistance to digestion by enteric or pancreatic enzymes, gastric acid and bile, ability to prevent the adherence, establishment and/or replication of pathogens in the gastrointestinal tract.

Examples of probiotic bacteria are members of the Lactobacilli family such as Lactobacillus rhamnosus GG, bifidobacteria and the yeast saccharomyces boulardii. There are many candidate bacteria which can be qualified as probiotics, but different bacteria have different actions in different disease states, taking into account that some disease states are better treated with a combination of bacteria and that there is an issue of dosing and viable vs. non viable components of the bacteria. Treatment with probiotics is relatively safe, but not risk free. Probiotics are potentially pathogenic [13]. A recent report describes 3 patients with fungemia in whom the probiotic origin was proven by DNA fingerprinting [14]. Reports of infections of probiotic origin emphasize the fact that these patients are usually immunosupressed with multiple ports of entry, such as venous and urinary catheter.

This article reviews the use of various probiotics in the treatment of infectious diarrhea, inflammatory bowel disease and lactose intolerance.

## PROBIOTICS AND DIARRHEAL DISEASE

Probiotics have been proved to be beneficial to four types of diarrhea: rotavirus diarrhea, antibiotic-associated diarrhea, clostridium difficile diarrhea, and traveler's diarrhea.

Trials of probiotics for other infectious diarrhea diseases have not been consistent in terms of efficacy so far. Paton *et al* [15] have produced toxin binding probiotics in a breakthrough study using a toxin-binding recombinant probiotic for the treatment and prevention of enterotoxigenic Escherichia coli diarrhea. If these probiotics can be proved effective, it might open a whole new era in the treatment of different kinds of diarrhea.

## ACUTE VIRAL DIARRHEA

One of the established benefits of probiotics is that they are effective in the treatment of children with acute viral enteritis [16,17] . Lactobacillus reuteri can shorten the course of acute diarrhea in infants from 2.5 days to 1.5 days [18]. Lactobacillus casei GG is effective in treating acute diarrhea as well [19]. Different strains of probiotics exhibit different efficacy. Kaila *et al* [20] studied different lactic acid bacteria for their effect on the immune response to rotavirus in children with acute rotavirus gastroenteritis and found that Lactobacillus casei subsp. casei strain GG (LGG) is most effective on disease duration and produces the highest titers of IgA antibodies. It has been postulated that IgA specific Ab confers immunity against future infectious diarrhea, a higher level of such Ab is desired. Allan *et el* [21] systematically reviewed 23 papers concerning probiotic treatment of infectious diarrhea and concluded that probiotics appear to be a useful adjunct to rehydration therapy in treating acute infectious diarrhea in adults and children.

## ANTIBIOTIC-ASSOCIATED DIARRHEA AND PSEUDOMEMBRANOUS COLITIS

Antibiotic-associated diarrhea (AAD) is seen in up to 39% of hospitalized patients treated with antibiotics [22] and varies from uncomplicated diarrhea to colitis and pseudomembranous colitis. The pathogenic factors include any one or all the followings: use of antibiotics causing changes in the normal gut flora, pathogenic bacteria taking advantage of the situation and causing inflammation and diarrhea, change in bacterial flora causing changes in carbohydrate metabolism and changes in short chain fatty acid metabolism and absorption. The latter is interfered and osmotic diarrhea ensues. The well-known syndrome of pseudomembranous colitis characterized by high levels of toxin forming Clostridium difficile may take a fulminate course with a high recurrence and mortality rate. AAD can be prevented or treated with probiotics. A meta-analysis summing the results of nine controlled trials indicates that both Lactobacilli and S boulardii are effective in preventing AAD [23]. Various probiotics have been used to prevent and treat Clostidium difficile-associated pseudomembranous colitis, including S. boulardii, Lactobacillus GG, B. longum and B. longum with L. acidophilus. S. boulardii and fecal transplantation can be used through a naso-enteric tube or as an enema [24]. S. boulardii seems to be a choice in prevention and treatment of recurrent Clostridium difficile pseudomembranous colitis [24].

## INFLAMMATORY BOWEL DISEASE

Inflammatory bowel disease (IBD) has a complex etiology. Environmental as well as genetic factors play a role. It has been established that microbes play a crucial role in IBD though search for an infectious agent has been futile so far. It was reported that Lactobacillus and bifidobacteria counts are significantly reduced in feces of patients with Crohn's disease compared to those with ulcerative colitis and controls and continuous interplay exists between the immune system and intestinal flora, suggesting that normalization of gut flora is a logical means of treatment [25, 26]. Venturi *et al* [25] treated 20 ulcerative colitis patients with VSL#3 and it is able to change the gut microflora because the faecal concentrations of Streptococcus salivarius ssp. thermophilus, Lactobacilli and bifidobacteria were significantly increased in all patients, compared to their basal level which remained stable throughout study. As mentioned before, probiotics have local and systemic effects. Lactobacillus casei strain GG given to pediatric Crohn's patients results in increased serum titers of IgA [27]. It was also reported that murine colitis was successfully treated with Lactococcus lactis secreting interleukin-10 [28].

Probiotics can achieve and maintain remission, prevent post surgical recurrence of Crohn's disease and pouchitis, and treat pouchitis, but an established role of probiotics exists only in the latter two indications. Gosselink *et al* [29] treated 39 patients with L. rhamnosus GG and proved that it had a better effect on these patients than on those not treated with it. Gionchetti *et al* [30, 32] demonstrated that pouchitis episode was reduced by 30% using VSL#3 in a double blind placebo-controlled study. Mirura *et al* [31] and kuisma *et al* [33] showed that remission of chronic pouchitis can be achieved with antibiotics. S. boulardii has no efficacy on ulcerative colitis [34].

Treatment of active ulcerative colitis has been extensively investigated in clinical trials [34-37]. All the studies proved that probiotics are effective at least on one of the followings: clinical and endoscopic improvement or decrease in proinflammatory cytokine expression. One additional report described six active refractory patients treated with human probiotic infusions and symptoms were abolished in all within four months [38]. These data support using probiotics in mild to moderate active disease. Three trials showed probiotics can be used as a maintenance treatment of UC [39-41].

Clinical trials have also been conducted in Crohn's disease patients [42-45]. Campieri *et al* [45] compared mesalazine with VSL#3 in 40 patients and found that endoscopic recurrence was significantly reduced noted in probiotic-treated patients, but Lactobacillus GG and L. Jonhsonii effect cannot prevent post surgical recurrence of Crohn's disease. Treatment of active Crohn's disease has been assessed in some studies [46, 47], no definite conclusion could be reached due to methodological drawbacks.

## LACTOSE MALABSORPTION

Lactase deficiency is a frequent condition causing intolerance to lactose due to maldigestion. Kolars *et al* [48] and Savaiano *et al* [49] in 1984 showed that absorption of lactose from yogurt is improved compared with milk, presumably due to digestion of lactose by lactase released from the yogurt microorganisms [50]. Shermak *et al* [51] examined the effect of yogurt or milk on symptoms and hydrogen breath concentration in children with lactose intolerance and found that symptoms as well as exhaled hydrogen concentration were lower in children challenged with yogurt.

## IRRITABLE BOWEL SYNDROME

Evidence for benefit of probiotic treatment in irritable bowel syndrome (IBS) has not been consistent. Nobaek *et al* [52] conducted a double-blind, randomized placebo-controlled study in 60 unselected patients with IBS, and found that probiotic treatment resulted in improvement of flatulence only. Recently, O'Mahony *et al* [53] reported patients taking B infantis had improvement in their symptoms, but no difference was observed between patients treated with L. salivarius and those treated with placebo. An interesting finding was that the basal ratio of IL-10/IL-12 was lower in IBS patients than in matched healthy controls. Treatment with B. infantis but not L. salivarius or placebo led to normalization of the ratio, suggesting that inflammation plays a role in the pathogenesis of IBS.

## PROBIOTICS AND CANCER

It is assumed that cancer is the outcome of genetic and environmental conditions. In each individual the interplay between the two is different. Cancer is the endpoint of a series of events. Various studies have shown the effect of probiotics on some of the enzymatic pathways and intermediates assumed to precede cancer [54-56]. Brady *et al* [54] have summarized the data concerning the use of probiotics in the prevention of cancer in their review. Other studies reported that the use of probiotics is inversely related with aberrant crypts or tumor development [55, 56]

## POTENTIAL BENEFIT OF PROBIOTICS

Treatment of constipation with probiotics has yielded confusing results [57, 58]. Probiotic *E. coli* strain has been found to be effective on collagenous colitis [59].

## CONCLUSION

Probiotics are a large group of microbes. Different microbes have different actions in different situations. Probiotics play a definite role in a number of clinical situations, namely rotavirus diarrhea, post antibiotic diarrhea and pouchitis. Their role in other clinical situations is yet to be defined.

## REFERENCES


1 **Fuller R**. Probiotics in man and animals. *J Appl Bacteriol* 1989; **66:** 365-378

2 **Marteau P**, Cuillerier E, Meance S, Gerhardt MF, Myara A, Bouvier M, Bouley C, Tondu F, Bommelaer G, Grimaud JC. Bifidobacterium animalis strain DN-173 010 shortens the colonic transit time in healthy women: a double-blind, randomized, controlled study. *Aliment Pharmacol Ther* 2002; **16:** 587-593

3 **Resta-Lenert S**, Barrett KE. Live probiotics protect intestinal epithelial cells from the effects of infection with enteroinvasive Escherichia coli (EIEC). *Gut* 2003; **52:** 988-997

4 **Servin AL**, Coconnier MH. Adhesion of probiotic strains to the intestinal mucosa and interaction with pathogens. *Best Pract Res Clin Gastroenterol* 2003; **17:** 741-754

5 **Dembele T**, Obdrzalek V, Votava M. Inhibition of bacterial pathogens by lactobacilli. *Zentralbl Bakteriol* 1998; **288:** 395-401

6 **Ocana VS**, Elena Nader-Macias M. Production of antimicrobial substances by lactic acid bacteria II: screening bacteriocin-producing strains with probiotic purposes and characterization of a Lactobacillus bacteriocin. *Methods Mol Biol* 2004; **268:** 347-353

7 **Yan F**, Polk DB. Probiotic bacterium prevents cytokine-induced apoptosis in intestinal epithelial cells. *J Biol Chem* 2002; **277:** 50959-50965

8 **Di Caro S**, Tao H, Grillo A, Elia C, Gasbarrini G, Sepulveda AR, Gasbarrini A. Effects of Lactobacillus GG on genes expression pattern in small bowel mucosa. *Dig Liver Dis* 2005; **37:** 320-329

9 **Dotan I**, Rachmilewitz D. Probiotics in inflammatory bowel disease: possible mechanisms of action. *Curr Opin Gastroenterol* 2005; **21:** 426-430

10 **Kaila M**, Isolauri E, Soppi E, Virtanen E, Laine S, Arvilommi H. Enhancement of the circulating antibody secreting cell response in human diarrhea by a human Lactobacillus strain. *Pediatr Res* 1992; **32:** 141-144

11 **Saavedra JM**. Microbes to fight microbes: a not so novel approach to controlling diarrheal disease. *J Pediatr Gastroenterol Nutr* 1995; **21:** 125–129

12 **Rachmilewitz D**, Katakura K, Karmeli F, Hayashi T, Reinus C, Rudensky B, Akira S, Takeda K, Lee J, Takabayashi K, Raz E. Toll-like receptor 9 signaling mediates the anti-inflammatory effects of probiotics in murine experimental colitis. *Gastroenterology* 2004; **126:** 520-528

13 **Ishibashi N**, Yamazaki S. Probiotics and safety. *Am J Clin Nutr* 2001; **73:** 465S-470S

14 **Munoz P**, Bouza E, Cuenca-Estrella M, Eiros JM, Perez MJ, Sanchez-Somolinos M, Rincon C, Hortal J, Pelaez T. Saccharomyces cerevisiae fungemia: an emerging infectious disease. *Clin Infect Dis* 2005; **40:** 1625-1634

15 **Paton AW**, Jennings MP, Morona R, Wang H, Focareta A, Roddam LF, Paton JC. Recombinant probiotics for treatment and prevention of enterotoxigenic Escherichia coli diarrhea. *Gastroenterology* 2005; **128:** 1219-1228

16 **Pearce JL**, Hamilton JR. Controlled trial of orally administered lactobacilli in acute infantile diarrhea. *J Pediatr* 1974; **84:** 261-262

17 **Pene P**, Linhard J, Bernou JC. [The colibacillus-lactobacillus combination in the treatment of diarrhea in adults, children and infants] *Sem Hop* 1966; **42:** 241-244

18 **Shornikova AV**, Casas IA, Mykkanen H, Salo E, Vesikari T. Bacteriotherapy with Lactobacillus reuteri in rotavirus gastroenteritis. *Pediatr Infect Dis J* 1997; **16:** 1103-1107

19 **Isolauri E**, Juntunen M, Rautanen T, Sillanaukee P, Koivula T. A human Lactobacillus strain (Lactobacillus casei sp strain GG) promotes recovery from acute diarrhea in children. *Pediatrics* 1991; **88:** 90-97

20 **Kaila M**, Isolauri E, Saxelin M, Arvilommi H, Vesikari T. Viable versus inactivated lactobacillus strain GG in acute rotavirus diarrhoea. *Arch Dis Child* 1995; **72:** 51-53

21 **Allen SJ**, Okoko B, Martinez E, Gregorio G, Dans LF. Probiotics for treating infectious diarrhoea. *Cochrane Database Syst Rev* 2004; **2:** CD003048

22 **McFarland LV**. Epidemiology, risk factors and treatments for antibiotic-associated diarrhea. *Dig Dis* 1998; **16:** 292-307

23 **D'Souza AL**, Rajkumar C, Cooke J, Bulpitt CJ. Probiotics in prevention of antibiotic associated diarrhoea: meta-analysis.

*BMJ* 2002; **324:** 1361
24 **Surawicz CM**. Probiotics, antibiotic-associated diarrhoea and Clostridium difficile diarrhoea in humans. *Best Pract Res Clin Gastroenterol* 2003; **17:** 775-783
25 **Venturi A**, Gionchetti P, Rizzello F, Johansson R, Zucconi E, Brigidi P, Matteuzzi D, Campieri M. Impact on the composition of the faecal flora by a new probiotic preparation: preliminary data on maintenance treatment of patients with ulcerative colitis. *Aliment Pharmacol Ther* 1999; **13:** 1103-1108
26 **Laake KO**, Bjorneklett A, Aamodt G, Aabakken L, Jacobsen M, Bakka A, Vatn MH. Outcome of four weeks' intervention with probiotics on symptoms and endoscopic appearance after surgical reconstruction with a J-configurated ileal-pouch-anal-anastomosis in ulcerative colitis. *Scand J Gastroenterol* 2005; **40:** 43-51
27 **Malin M**, Suomalainen H, Saxelin M, Isolauri E. Promotion of IgA immune response in patients with Crohn's disease by oral bacteriotherapy with Lactobacillus GG. *Ann Nutr Metab* 1996; **40:** 137-145
28 **Steidler L**, Hans W, Schotte L, Neirynck S, Obermeier F, Falk W, Fiers W, Remaut E. Treatment of murine colitis by Lactococcus lactis secreting interleukin-10. *Science* 2000; **289:** 1352-1355
29 **Gosselink MP**, Schouten WR, van Lieshout LM, Hop WC, Laman JD, Ruseler-van Embden JG. Delay of the first onset of pouchitis by oral intake of the probiotic strain Lactobacillus rhamnosus GG. *Dis Colon Rectum* 2004; **47:** 876-884
30 **Gionchetti P**, Rizzello F, Helwig U, Venturi A, Lammers KM, Brigidi P, Vitali B, Poggioli G, Miglioli M, Campieri M. Prophylaxis of pouchitis onset with probiotic therapy: a double-blind, placebo-controlled trial. *Gastroenterology* 2003; **124:** 1202-1209
31 **Mimura T**, Rizzello F, Helwig U, Poggioli G, Schreiber S, Talbot IC, Nicholls RJ, Gionchetti P, Campieri M, Kamm MA. Once daily high dose probiotic therapy (VSL#3) for maintaining remission in recurrent or refractory pouchitis. *Gut* 2004; 53: 108-114
32 **Gionchetti P**, Rizzello F, Venturi A, Brigidi P, Matteuzzi D, Bazzocchi G, Poggioli G, Miglioli M, Campieri M. Oral bacteriotherapy as maintenance treatment in patients with chronic pouchitis: a double-blind, placebo-controlled trial. *Gastroenterology* 2000; **119:** 305-309
33 **Kuisma J**, Mentula S, Jarvinen H, Kahri A, Saxelin M, Farkkila M. Effect of Lactobacillus rhamnosus GG on ileal pouch inflammation and microbial flora. *Aliment Pharmacol Ther* 2003; **17:** 509-515
34 **Guslandi M**, Giollo P, Testoni PA. A pilot trial of Saccharomyces boulardii in ulcerative colitis. *Eur J Gastroenterol Hepatol* 2003; **15:** 697-698
35 **Furrie E**, Macfarlane S, Kennedy A, Cummings JH, Walsh SV, O'neil DA, Macfarlane GT. Synbiotic therapy (Bifidobacterium longum/Synergy 1) initiates resolution of inflammation in patients with active ulcerative colitis: a randomised controlled pilot trial. *Gut* 2005; **54:** 242-249
36 **Kato K**, Mizuno S, Umesaki Y, Ishii Y, Sugitani M, Imaoka A, Otsuka M, Hasunuma O, Kurihara R, Iwasaki A, Arakawa Y. Randomized placebo-controlled trial assessing the effect of bifidobacteria-fermented milk on active ulcerative colitis. *Aliment Pharmacol Ther* 2004; **20:** 1133-1141
37 **Tursi A**, Brandimarte G, Giorgetti GM, Forti G, Modeo ME, Gigliobianco A. Low-dose balsalazide plus a high-potency probiotic preparation is more effective than balsalazide alone or mesalazine in the treatment of acute mild-to-moderate ulcerative colitis. *Med Sci Monit* 2004; **10:** PI126-PI131
38 **Borody TJ**, Warren EF, Leis S, Surace R, Ashman O. Treatment of ulcerative colitis using fecal bacteriotherapy. *J Clin Gastroenterol* 2003; **37:** 42-47
39 **Kruis W**, Fric P, Pokrotnieks J, Lukas M, Fixa B, Kascak M, Kamm MA, Weismueller J, Beglinger C, Stolte M, Wolff C, Schulze J. Maintaining remission of ulcerative colitis with the probiotic Escherichia coli Nissle 1917 is as effective as with standard mesalazine. *Gut* 2004; **53:** 1617-1623
40 **Rembacken BJ**, Snelling AM, Hawkey PM, Chalmers DM, Axon AT. Non-pathogenic Escherichia coli versus mesalazine for the treatment of ulcerative colitis: a randomised trial. *Lancet* 1999; **354:** 635-639
41 **Ishikawa H**, Akedo I, Umesaki Y, Tanaka R, Imaoka A, Otani T. Randomized controlled trial of the effect of bifidobacteria-fermented milk on ulcerative colitis. *J Am Coll Nutr* 2003; **22:** 56-63
42 **Prantera C**, Scribano ML, Falasco G, Andreoli A, Luzi C. Ineffectiveness of probiotics in preventing recurrence after curative resection for Crohn's disease: a randomised controlled trial with Lactobacillus GG. *Gut* 2002; **51:** 405-409
43 **Van Gossum A**, Geboes KD, De Vos MB, Louis E, Enslen M, Paintin M, Franchimont D. A randomized Placebo-Controlled Trial of Probiotics (L. Jonhsonii, Lal) on Early Endoscopic Recurrence of Crohn's Disease After Ileo- Caecal Resection. Abstract DDW 2005 #: 98
44 **Philippe MR**, Marc L, Philippe S, David L, Jean Fredreric, Yoram B, Guillaume C, Jean Claude S, Arnaud B, Etienne M, Eric L, Franck C, Jean Louis D, Michel V, Jean Yves M. Ineffectiveness of the Probiotic Strain Lactobacillus Johnsonii Lal in Preventing Recurrence After Curative Resection for Crohn's Disease- a Randomized Double- Blind Placebo Controlled Trial. Abstract DDW2005 # 97
45 **Campieri M**, Rizzello F, Venturi A et al. Combination of antibiotic and probiotic treatment is efficacious in prophylaxis of post-operative recurrence of Crohn's disease: a randomised controlled study vs mesalazine. *Gastroenterology* 2000; **118:** A781.
46 **Malchow HA**. Crohn's disease and Escherichia coli. A new approach in therapy to maintain remission of colonic Crohn's disease? *J Clin Gastroenterol* 1997; **25:** 653-658
47 **Gupta P**, Andrew H, Kirschner BS, Guandalini S. Is lactobacillus GG helpful in children with Crohn's disease? Results of a preliminary, open-label study. *J Pediatr Gastroenterol Nutr* 2000; **31:** 453-457
48 **Kolars JC**, Levitt MD, Aouji M, Savaiano DA. Yogurt--an autodigesting source of lactose. *N Engl J Med* 1984; **310:** 1-3
49 **Savaiano DA**, AbouElAnouar A, Smith DE, Levitt MD. Lactose malabsorption from yogurt, pasteurized yogurt, sweet acidophilus milk, and cultured milk in lactase-deficient individuals. *Am J Clin Nutr* 1984; **40:** 1219–1223
50 **Saavedra JM**. Clinical applications of probiotic agents. *Am J Clin Nutr* 2001; **73:** 1147S-1151S
51 **Shermak MA**, Saavedra JM, Jackson TL, Huang SS, Bayless TM, Perman JA. Effect of yogurt on symptoms and kinetics of hydrogen production in lactose-malabsorbing children. *Am J Clin Nutr* 1995; **62:** 1003-1006
52 **Nobaek S**, Johansson ML, Molin G, Ahrne S, Jeppsson B. Alteration of intestinal microflora is associated with reduction in abdominal bloating and pain in patients with irritable bowel syndrome. *Am J Gastroenterol* 2000; **95:** 1231-1238
53 **O'Mahony L**, McCarthy J, Kelly P, Hurley G, Luo F, Chen K, O'Sullivan GC, Kiely B, Collins JK, Shanahan F, Quigley EM. Lactobacillus and bifidobacterium in irritable bowel syndrome: symptom responses and relationship to cytokine profiles. *Gastroenterology* 2005; **128:** 541-551
54 **Brady LJ**, Gallaher DD, Busta FF. The role of probiotic cultures in the prevention of colon cancer. *J Nutr* 2000; **130:** 410S-414S
55 **Marotta F**, Naito Y, Minelli E, Tajiri H, Bertuccelli J, Wu CC, Min CH, Hotten P, Fesce E.Chemopreventive effect of a probiotic preparation on the development of preneoplastic and neoplastic colonic lesions: an experimental study. *Hepatogastroenterology* 2003; **50:** 1914-1918
56 **Yamazaki K**, Tsunoda A, Sibusawa M, Tsunoda Y, Kusano M, Fukuchi K, Yamanaka M, Kushima M, Nomoto K, Morotomi M. The effect of an oral administration of Lactobacillus casei strain shirota on azoxymethane-induced colonic aberrant crypt foci and colon cancer in the rat. *Oncol Rep* 2000; **7:** 977-982
57 **Koebnick C**, Wagner I, Leitzmann P, Stern U, Zunft HJ. Probiotic beverage containing Lactobacillus casei Shirota improves gastrointestinal symptoms in patients with chronic constipation. *Can J Gastroenterol* 2003; **17:** 655-659

58 **Banaszkiewicz A**, Szajewska H. Ineffectiveness of Lactobacillus GG as an adjunct to lactulose for the treatment of constipation in children: a double-blind, placebo-controlled randomized trial. *J Pediatr* 2005; **146:** 364-369

59 **Tromm A**, Niewerth U, Khoury M, Baestlein E, Wilhelms G, Schulze J, Stolte M. The probiotic E. coli strain Nissle 1917 for the treatment of collagenous colitis: first results of an open-label trial. *Z Gastroenterol* 2004; **42:** 365-369

**S- Editor** Wang XL and Guo SY **L- Editor** Elsevier HK **E- Editor** Bai SH

PO Box 2345, Beijing 100023, China
www.wjgnet.com
wjg@wjgnet.com

*World J Gastroenterol* 2006 February 14; 12(6): 858-867
***World Journal of Gastroenterology*** ISSN 1007-9327
© 2006 The WJG Press. All rights reserved.

*LIVER CANCER*

# Macrophage inflammatory protein-2 contributes to liver resection-induced acceleration of hepatic metastatic tumor growth

Otto Kollmar, Michael D Menger, Martin K Schilling

Otto Kollmar, Martin K Schilling, Department of General, Visceral, Vascular and Pediatric Surgery, University of the Saarland, D-66421 Homburg/Saar, Germany
Michael D Menger, Institute for Clinical and Experimental Surgery, University of the Saarland, D-66421 Homburg/Saar, Germany
Supported by the grants of the Research Committee and the Medical Faculty of the University of Saarland, No. HOMFOR-A/2003/1
Correspondence to: Otto Kollmar, MD, Department of General, Visceral, Vascular and Pediatric Surgery, University of the Saarland, D-66421 Homburg/Saar, Germany. chokol@uniklinik-saarland.de
Telephone: +49-6841-1622611 Fax: +49-6841-1622697
Received: 2005-07-22 Accepted: 2005-08-26

## Abstract

**AIM:** To study the role of macrophage inflammatory protein (MIP)-2 in liver resection-induced acceleration of tumor growth in a mouse model of hepatic metastasis.

**METHODS:** After a 50% hepatectomy, $1\times10^5$ CT26.WT cells were implanted into the left liver lobe of syngeneic balb/c mice (PHx). Additional animals were treated with a monoclonal antibody (MAB452) neutralizing MIP-2 (PHx+mAB). Non-resected and non-mAB-treated mice (Con) served as controls. After 7 d, tumor angiogenesis and microcirculation as well as cell proliferation, tumor growth, and CXCR-2 expression were analyzed using intravital fluorescence microscopy, histology, immunohistochemistry, and flow cytometry.

**RESULTS:** Partial hepatectomy increased ($P<0.05$) the expression of the MIP-2 receptor CXCR-2 on tumor cells when compared with non-resected controls, and markedly accelerated ($P<0.05$) angiogenesis and metastatic tumor growth. Neutralization of MIP-2 by MAB452 treatment significantly ($P<0.05$) depressed CXCR-2 expression. Further, the blockade of MIP-2 reduced the angiogenic response ($P<0.05$) and inhibited tumor growth ($P<0.05$). Of interest, liver resection-induced hepatocyte proliferation was not effected by anti-MIP-2 treatment.

**CONCLUSION:** MIP-2 significantly contributes to liver resection-induced acceleration of colorectal CT26.WT hepatic metastasis growth.

© 2006 The WJG Press. All rights reserved.

**Key words:** Chemokines; MIP-2; Liver resection; Partial hepatectomy; Liver regeneration; Metastatic tumor growth; Angiogenesis; Microcirculation

Kollmar O, Menger MD, Schilling MK. Macrophage inflammatory protein-2 contributes to liver resection-induced acceleration of hepatic metastatic tumor growth. *World J Gastroenterol* 2006; 12(6): 858-867

http://www.wjgnet.com/1007-9327/12/858.asp

## INTRODUCTION

Major liver resection initiates rapid regeneration and growth of the remaining liver to restore the functional hepatic capacity[1]. The cellular changes which provoke liver regeneration are orchestrated by a complex network of different growth factors, cytokines[1-3] and chemokines[4-6]. The latter include macrophage inflammatory protein (MIP)-2, ENA-78, and IL-8, which all may act through the CXCR-2 receptor. The role of this receptor has been shown in that blockade with antibodies or deletion in gene-targeted animals significantly reduced the regeneration after hepatectomy[4,6]. The role of the individual chemokines in regeneration after hepatectomy, however, may be redundant. The murine CXC chemokine MIP-2 is a functional analog of human IL-8[7]. Similar to IL-8, it acts as a potent neutrophil chemoattractant, contributing to wound healing[8] and inflammation[9]. While blockade of the chemokine receptor CXCR-2 decreases regeneration of the residual liver, neutralization of MIP-2 through the use of anti-MIP-2 antibodies did not affect the process of regeneration as indicated by the unchanged liver weight to body weight (BW) ratios[4]. These findings indicate that other chemokines may replace or act via the CXCR-2 receptor in case of MIP-2 deletion for liver regeneration[4,6].

Besides parenchymal regeneration, hepatectomy also accelerates tumor growth in the remaining liver[10-14] as well as in remote organ sites[15]. Slooter and co-workers showed that a 70% liver resection provokes excessive growth of liver metastases when compared to non-resected controls. Of interest, the intravenous application of TNF-α was effective to significantly reduce these outgrowths of tumor masses[11]. In fact, the acceleration of tumor growth seems to be proportional to the volume of the resected

liver tissue[10,11,13]. The cause of enhanced tumor growth in the liver after hepatectomy is likely to be multifactorial. It has been suggested that, besides mechanisms of liver regeneration, residual "dormant" micrometastases or tumor cells in the remnant liver are stimulated through distinct pro-tumorigenic factors[13,14]. In addition, a depression of local defense mechanisms due to a decrease of Kupffer cell tumoricidal activity and systemic immune paralysis may also contribute to the enhancement of tumor growth[16]. The role of chemokines, such as MIP-2, in the hepatectomy-induced acceleration of tumor growth, however, has not been elucidated yet.

By use of a murine colorectal hepatic metastasis model, we studied whether the accelerated metastatic growth after hepatectomy is mediated by the CXC chemokine MIP-2, and whether the inhibition of tumor growth by blockade of MIP-2 is associated with a downregulation of angiogenesis and tumor blood vessel formation.

## MATERIALS AND METHODS

Experiments were performed after approval by the local governmental ethic committee, and were in accordance with the UKCCCR Guidelines for the Welfare of Animals in Experimental Neoplasia (*Br J Cancer* 1998; 77: 1-10) and the Interdisciplinary Principles and Guidelines for the Use of Animals in Research (New York Academy of Sciences Ad Hoc Committee on Animal Research, NY, USA).

### *Tumor cell line and culture conditions*

The CT26 cell line is an *N*-nitroso-*N*-methylurethane-induced undifferentiated adenocarcinoma of the colon, syngeneic with the BALB/c mouse. For our studies, the CT26.WT cell line (ATCC CRL-2638®, LGC Promochem GmbH, Wesel, Germany) was grown in cell culture as monolayers in RPMI-1640 medium with 2 mmol/L L-glutamine (Sigma Aldrich Chemie GmbH, Taufkirchen, Germany) supplemented with 10% fetal calf serum (FCS Gold, PAA Laboratories GmbH, Cölbe, Germany), 100 U/mL penicillin and 100 μg/mL streptomycin (PAA Laboratories GmbH). The cells were incubated at 37 °C in a humidified atmosphere containing 50 mL/L $CO_2$ in air. Only cells of the first two serial passages after cryo-storage were used. At the day of implantation, CT26.WT cells were harvested from sub-confluent cultures (70%-85%) by trypsinization (0.5 g/L trypsin and 0.2 g/L EDTA, PAA Laboratories GmbH), and washed twice in phosphate-buffered saline solution (PBS, PAA Laboratories GmbH) before being resuspended in PBS at $1\times10^7$ cells/L.

### *Flow cytometric analysis of CT26.WT cells*

FACScan (Becton Dickinson, Mountain View, CA, USA) analysis was performed to assess the expression of the chemokine receptor CXCR-2 of the CT26.WT cells. After trypsinization, the cells were fixed in 1 mL Cytofix/Cytoperm (BD Biosciences, Heidelberg, Germany) for 20 min at 4 °C, washed twice with Perm Wash (BD Biosciences) and incubated at room temperature for 40 min with a polyclonal rabbit anti-mouse CXCR-2 antibody (Santa Cruz, Heidelberg, Germany) or an isotype-matched control antibody (Dianova, Hamburg, Germany). A goat anti-rabbit Cy3-conjugated antibody (1:25; Dianova) was used for fluorescence labeling. To remove excess of antibody, cells were washed again and were then maintained in 10 g/L paraformaldehyde in PBS. Flow cytometry was performed within the next 3 h. The FACScan flow cytometer was calibrated with fluorescent standard microbeads (CaliBRITE Beads, BD Biosciences) for accurate instrument setting. Tumor cells were selectively analyzed for their fluorescence properties using the CellQuest data handling program (BD Biosciences) with the assessment of 5 000 events per sample.

### *Hepatectomy and tumor cell implantation*

Eight to twelve weeks old female BALB/c mice with a BW of 18-20 g, kept in a temperature and humidity controlled 12-h light/dark cycle environment, were used. The animals were anesthetized by intraperitoneal injection of 25 mg/kg BW xylazin hydrochloride (Rompun®, Bayer, Leverkusen, Germany) and 125 mg/kg BW ketamine hydrochloride (Ketavet®, Pharmacia GmbH, Erlangen, Germany). The anesthetized animals were placed in supine position. After laparotomy through a midline incision, a 50% hepatectomy was performed. After ligature of the supplying and draining blood vessels with PDS 5-0 (Ethicon, Johnson & Johnson Company, Norderstedt, Germany), the right lateral lobes (ventral and dorsal), the right medial lobe and a part of the left medial lobe were resected. The weight of the resected tissue was 0.35±0.01 g. The procedure of intrahepatic implantation of CT26.WT tumor cells was performed as described previously[17]. The left liver lobe was gently mobilized and $1\times10^5$ tumor cells in 10 μL PBS were implanted under the capsule of the lower surface using a 25-μL syringe with a 32-G needle (Gastight® #1702, Hamilton Bonaduz AG, Bonaduz, Switzerland). The puncture site was sealed with acrylic glue (Histoacryl®, B. Braun, Aesculap AG, Tuttlingen, Germany), and the left liver lobe was repositioned anatomically into the peritoneal cavity. The abdominal wall was closed by a one layer technique with a polypropylene suture (Prolene® 5-0).

### *Intravital fluorescence microscopy*

At d 7 after tumor cell implantation, the animals were again anesthetized and laparotomized. The left liver lobe with the tumor was exteriorized and placed on an adjustable stage, so that the lower surface of the lobe was positioned horizontally to the microscope. This guaranteed adequate focus levels for the *in vivo* fluorescence microscopy procedure. The surface of the lobe was covered with a cover slip to avoid drying of the tissue and influences of the ambient oxygen[17]. *In vivo* fluorescence microscopy was performed by epi-illumination technique using a modified Zeiss Axiotech microscope (Zeiss, Oberkochen, Germany)[18]. Microscopic images were monitored by a charge-coupled device video camera (FK 6990, Prospective Measurements Inc., San Diego, CA, USA) and were transferred to a video system (VO-5800 PS, Sony, München, Germany) for subsequent off-line analysis. Angioarchitecture and microvascular perfusion were analyzed after intravenous contrast enhancement with sodium fluorescein (2 μmol/kg; Merck, Darmstadt,

Germany) using blue light epi-illumination (450 to 490 nm > 520nm, excitation and emission wavelengths).

### Microcirculation analysis

Assessment of hepatic microcirculatory parameters was performed off-line by frame-to-frame analysis of the videotaped images using a computer-assisted image analysis system (CapImage; Zeintl, Heidelberg, Germany). Sinusoidal, capillary and venular diameters (μm) were measured perpendicularly to the vessel path. Sinusoidal density within the liver and capillary density within the tumors ($cm/cm^2$) were determined by measuring the length of red cell perfused capillary per area of observation. The number of venules draining the blood flow from the tumor was counted and was given per tumor margin. The angiogenic front neighboring the tumor margin, characterized by newly developed, chaotically arranged capillaries, was measured in $mm^2$ surface area.

### Morphological examinations

At the end of the experiment, the left liver lobe was harvested and cut into slices with a diameter of 1 mm using a Tissue Slicer (McIlwain Tissue Shopper, Saur Laborbedarf, Reutlingen, Germany). Slices were documented with the use of a stereo-microscope (Leica M651, Leica Microsystems AG, Heerbrugg, Switzerland) and a video system, and the size of the tumor was measured with CapImage according to: tumor volume ($mm^3$) = $4/3\pi \times a/2 \times b/2 \times c/2$ ($a$, $b$, and $c$ represent the three perpendicularly orientated diameters of the tumor).

### Histochemistry and immunohistochemistry

For light microscopy, formalin-fixed biopsies were embedded in paraffin. Five micrometer thick sections were cut and stained with hematoxylin and eosin for routine histology according to standard procedures.

Proliferating cell nuclear antigen (PCNA) staining was performed using indirect immunoperoxidase techniques. Therefore, deparaffinized sections were incubated with 30 mL/L $H_2O_2$ to block endogenous peroxidases and with 20 mL/L goat normal serum for blocking unspecific binding sites. A monoclonal mouse anti-pan PCNA antibody (PC10, 1:50; DakoCytomation, Hamburg, Germany) was used as primary antibody. A biotinylated goat anti-mouse rabbit IgG antibody was used as secondary antibody for streptavidin-biotin-complex peroxidase staining (1:200, LSAB 2 System HRP, DakoCytomation). 3,3'-Diaminobenzidine (DakoCytomation) was used as a chromogen. Sections were counterstained with hemalaun according to Mayer and examined by light microscopy.

For CXCR-2 immunohistochemistry tumor slices were embedded in Tissue Freezing Medium (Jung; Leica Microsystems, Nussloch, Germany), snap-frozen in liquid nitrogen and stored at -80 °C. Five micrometer thick cryostat sections were cut, fixed in 4 °C cold acetone for 5 s followed by fixation in 16 g/L formaldehyde for 10 min and blocked with 2% normal donkey serum. Tissue sections were then incubated with the polyclonal rabbit anti-mouse CXCR-2 antibody (1:100; Santa Cruz, CA, USA). A donkey anti-rabbit IgG HRP conjugated antibody (1:500; Amersham, Freiburg, Germany) was used as secondary antibody. 3,3'-Diaminobenzidine was used as chromogen. Sections were counterstained with hemalaun according to Mayer and examined by light microscopy. As a negative control, additional slices from each specimen were exposed to appropriate IgG isotype-matched antibody (Sigma Aldrich Chemie GmbH) in place of primary antibody under the same conditions to determine the specificity of antibody binding. All of the control stainings were found negative.

### Experimental protocol

A total of 21 animals received tumor cell implantation and were assigned to three different groups. Animals without liver resection and without further treatment received tumor cell implantation in the left liver lobe and served as controls (Con; $n = 7$). In the additional two groups ($n = 7$ each), a 50% hepatectomy was performed before the tumor cells were implanted into the left liver lobe. One group of animals (PHx+mAB) received 1 mg/kg BW of the monoclonal rat anti-mouse MIP-2 antibody (MAB452, R&D Systems, Wiesbaden, Germany) at the day of operation and every second day thereafter. Untreated animals with 50% liver resection served as hepatectomy controls (PHx). Seven days after tumor cell implantation and treatment, all animals underwent intravital microscopic examination and the liver and tumor tissue were harvested for histology and immunohistochemistry.

### Statistical analysis

All values were expressed as mean ± SE. After proving the assumption of normality and homogeneity of variance across groups, differences between groups were calculated by a one-way analysis of variance (ANOVA) followed by a *post hoc* Student-Newman-Keuls test, including correction of the alpha error to compensate for multiple comparisons. Overall statistical significance was set at $P < 0.05$. Statistical analysis was performed with the use of the software package SigmaStat (SPSS Inc., Chicago, IL, USA).

## RESULTS

### Tumor growth

Tumor cell implantation, hepatectomy and treatment with the anti-mouse MIP-2 antibody did not affect the general conditions of the animals. All animals had an uneventful postoperative recovery, and, regardless of the group, animals did not show significant changes of BW during the 7-d experimental period. Intravital fluorescence microscopy at d 7 after tumor cell implantation showed that hepatectomy (PHx) provoked a significant ($P < 0.05$) acceleration of tumor growth, as indicated by an increased tumor area at the surface of the liver when compared with that of controls (Figure 1). Analysis of the tumor volume confirmed the significantly ($P < 0.05$) increased tumor growth, demonstrating a tumor mass which was 18-fold greater than that of controls (Figure 1). Treatment with the MIP-2 antibody (PHx+mAB) was capable of significantly ($P < 0.05$) reducing the hepatectomy-induced acceleration of tumor growth, resulting in a tumor volume which was only 6-fold of that of non-resected controls (Figure 1).

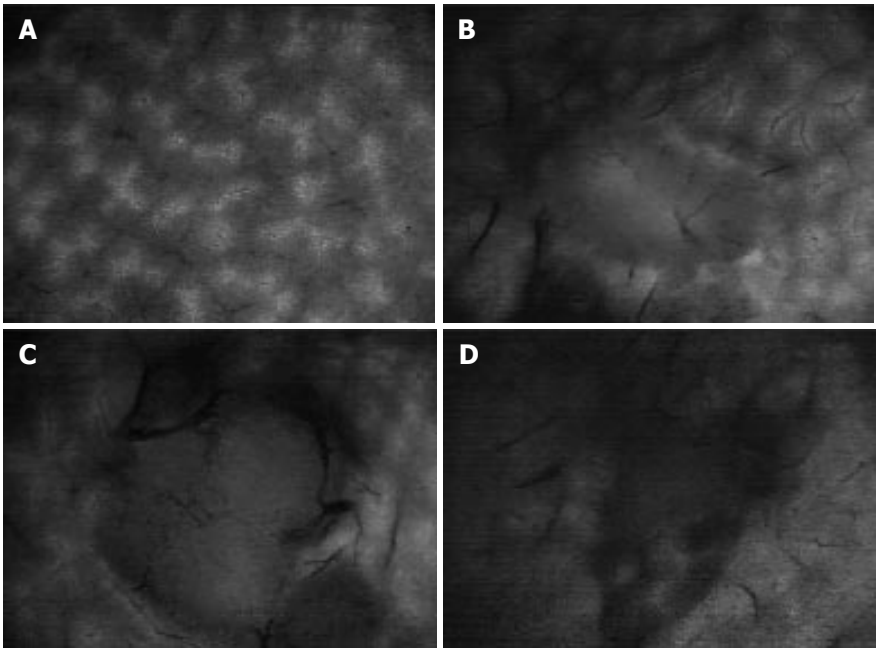


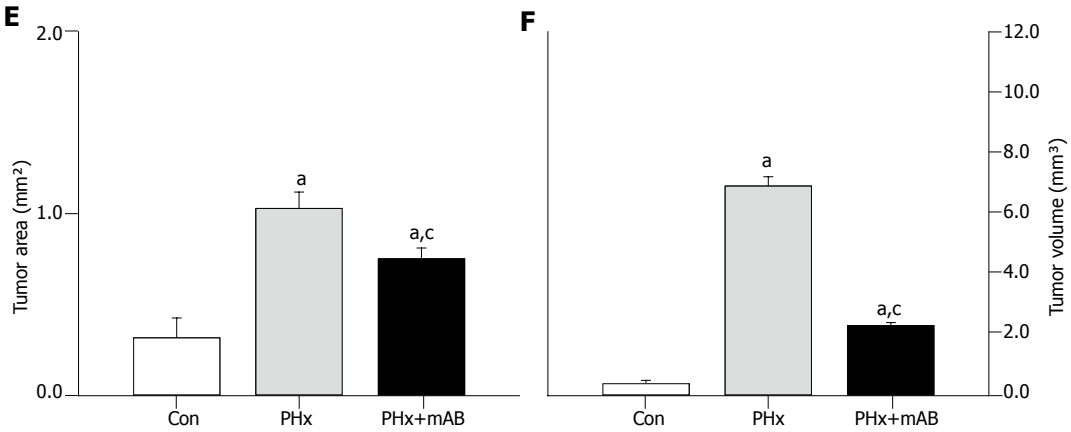


**Figure 1** Intravital fluorescence microscopy at d 7 after tumor cell implantation. **A:** Displays the normal liver microvasculature; **B:** shows the microvasculature of the tumor of a non-resected control animal (Con); **C:** displays a 7-day tumor and its microvasculature of an animal which underwent hepatectomy (PHx); **D:** shows the tumor microvasculature after additional anti-MIP-2 treatment (PHx+mAB). Quantitative analysis of tumor area (**E**) and tumor volume (**F**) showed that hepatectomy (PHx) markedly accelerated tumor growth when compared with controls (Con), and that additional anti-MIP-2 treatment (PHx+mAB) was capable of significantly reducing this liver resection-induced tumor growth. Mean ± SE; $^{a}P<0.05$ *vs* Con; $^{c}P<0.05$ *vs* PHx. Magnifications (**A-D**) ×16.

### *Angiogenesis and microangioarchitecture*

Intravital fluorescence microscopy revealed that normal liver presents with a regularly arranged architecture of sinusoids and homogeneous staining of parenchymal cell nuclei (Figure 1A). In contrast, the center of the tumor showed a density of capillaries which was markedly lower than that of the sinusoids in the normal liver (Figure 1 and 2). The margin of the tumor showed an angiogenic front with newly developed, chaotically arranged capillaries (Figure 2) and large draining venules (Figure 3). In control animals, the implantation of CT26.WT cells induced an area of the tumor surrounding angiogenic front of 0.33 mm² at day 7 (Figure 2). Hepatectomy (PHx) significantly increased the area of the angiogenic front by 3-fold ($P<0.05$) when compared with that of controls. Blockade of MIP-2 (PHx+mAB) was capable of inhibiting angiogenesis, as indicated by a significantly ($P<0.05$) reduced area at the tumor margin which showed new blood vessel development (Figure 2D).

Because angiogenesis is regularly associated with vasodilation, we analyzed the capillary diameters within the angiogenic front. Within the tumor margin, hepatectomy (PHx) induced a significant dilation of the newly formed capillaries ($P<0.05$) when compared with that of controls. Additional anti-MIP-2 treatment (PHx+mAB) further pronounced ($P<0.05$) this dilatory effect (Figure 2E). Of interest, the enlargement of the newly formed capillaries within the angiogenic front after hepatectomy and MIP-2 treatment was a homogeneous response, as indicated by the fact that the coefficient of variance of capillary diameters did not differ when compared with untreated controls (Figure 2F). Further, hepatectomy (PHx) also significantly ($P<0.05$) increased the density of venules draining the tumor, as indicated by a 6.5-fold increase of the number of venules within the tumor margin when compared to controls (Figure 3). These venules were also found enlarged in diameter (Figure 3E), however, without increased heterogeneity when compared with controls (Figure 3F). Interestingly, blockade of MIP-2 significantly ($P<0.05$) reduced the number of draining tumor venules when compared with animals undergoing only hepatectomy (Figure 3D).

### *Tumor morphology*

Hematoxylin-eosin-stained sections revealed solid growth of the colorectal CT26.WT hepatic metastasis in all the animals (Figure 4). Satellite metastases were not observed in the left liver lobe. In the control group, tumors were

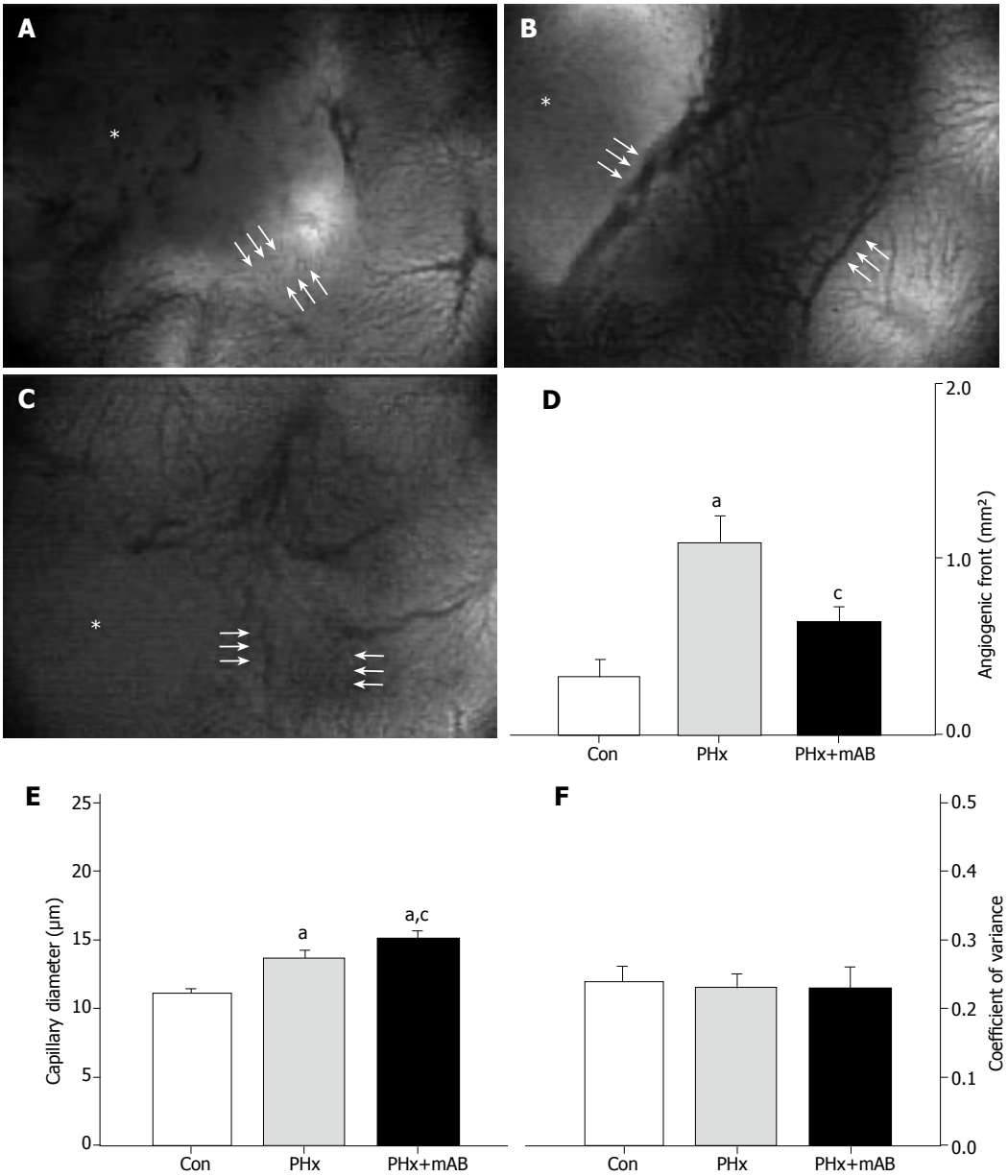


**Figure 2** Analysis of the size of the angiogenic front (area between the triple arrows) at the margin of tumors (asterisks) in control mice (**A**, Con), after hepatectomy (**B**, PHx) and after hepatectomy and additional anti-MIP-2 treatment (**C**, PHx+mAB). Quantitative analysis of the area of the angiogenic front (**D**) indicated a significant increase after hepatectomy (PHx) when compared with that of controls (Con). Additional anti-MIP-2 treatment (PHx+mAB) was capable of reducing the angiogenic process. Further, hepatectomy (PHx) significantly increased capillary dilation within the angiogenic front (**E**) compared to controls (Con), which was even more pronounced after additional anti-MIP-2 treatment (PHx+mAB). The heterogeneity of capillary diameters, as given by the coefficient of variance, was not affected in either of the treatment groups (**F**). Mean ± SE; $^{a}P<0.05$ *vs* Con; $^{c}P<0.05$ *vs* PHx. Magnifications (**A-C**) ×40.

round in nature with a homogeneous appearance, however, with aggressive growth characteristics (Figures 4A and B). Hepatectomy (PHx) accelerated tumor growth, resulting in enlarged tumors with a dense arrangement of tumor cells in the center (Figures 4C and D). In two of the seven animals, lung metastases could be detected macroscopically, although no additional metastases could be found in the abdominal cavity. In contrast, tumors of animals, which additionally were treated with anti-MIP-2 showed central cell death via either necrotic or apoptotic pathways (Figures 4E and F). In this group tumor growth at distant sites was not observed.

In vitro FACScan analysis and CXCR-2 expression *in vivo*

FACScan analysis showed that 98.8% of the CT26.WT cells were CXCR-2 receptor positive *in vitro* (Figure 5). *In vivo*, CXCR-2 immunohistochemistry revealed that - 40% of the tumor cells were receptor-positive. The majority of these CXCR-2 expressing cells were located within the tumor margin (Figure 6). Quantitative analysis of CXCR-2 expression indicated that hepatectomy (PHx) significantly increased ($P<0.05$) CXCR-2 expression to -60% of tumor cells (Figure 6). Blockade of MIP-2 (PHx +mAB) not only abolished the hepatectomy-induced increase of CXCR-2 expression, but further reduced ($P<0.05$) CXCR-2 expression on tumor cells to only -10% (Figure 6).

### *Proliferation of tumor cells and normal liver*

PCNA as an indicator of cell proliferation showed that >90% of tumor cells displayed strong PCNA staining (Figure 7). By this, the tumor sharply demarcated from the surrounding liver tissue. Notably, neutralization of MIP-2 (PHx+mAB) decreased the rate of PCNA-positive cells to -60% (Figures 7C and D), indicating a reduction of proliferation by deletion of MIP-2 function. Normal liver tissue only occasionally showed single PCNA-positive cells (Figure 8). Hepatectomy (PHx) resulted in a significant ($P<0.05$) increase of the number of PCNA-stained cells when compared with that of non-resected controls (Figure 8). Of interest, additional blockade of MIP-2 induced

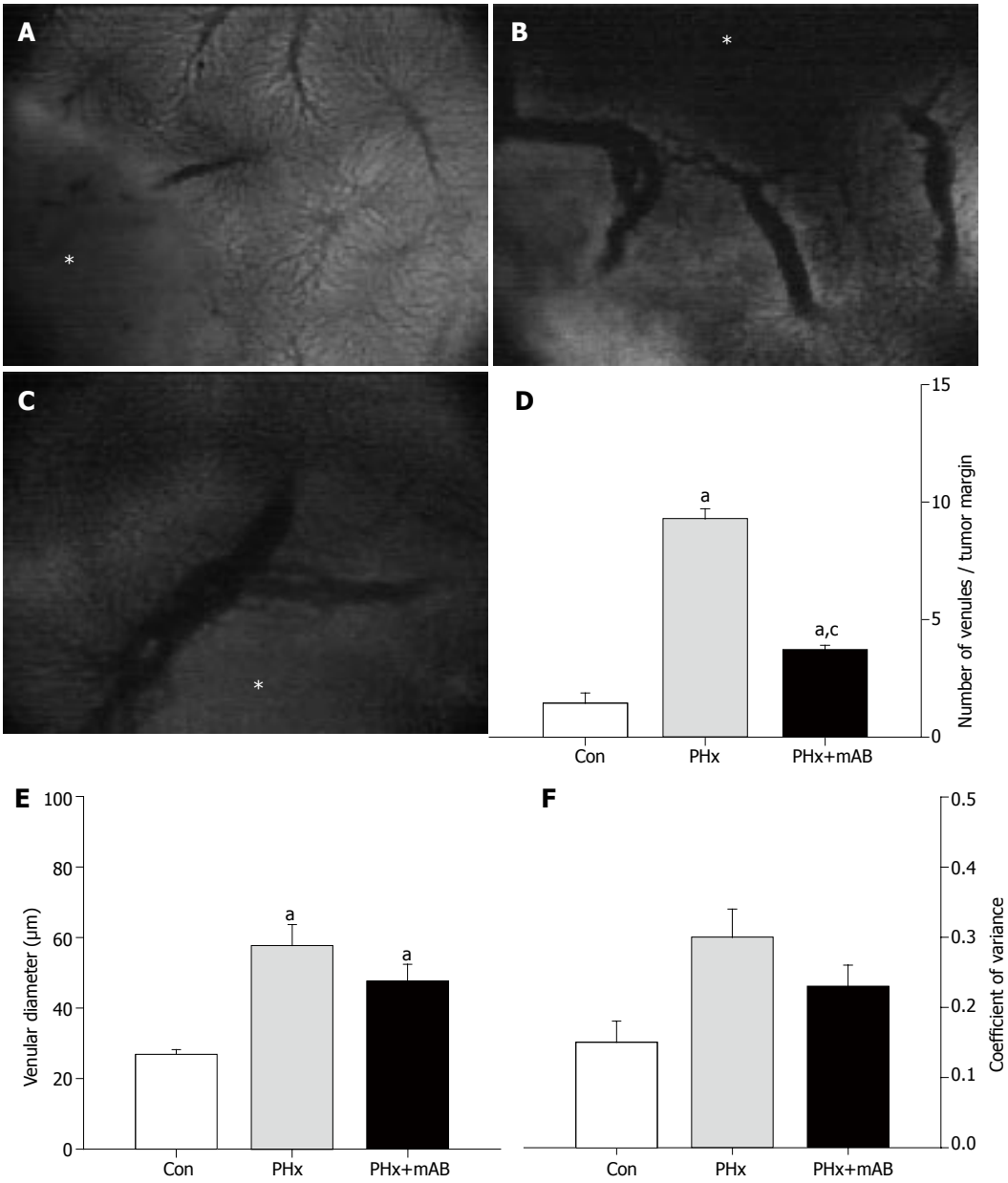


**Figure 3** Analysis of the number of venules within the margin of tumors (**A-C**, asterisk) of control mice (A, Con), after hepatectomy (**B**, PHx) and after hepatectomy and additional anti-MIP-2 treatment (**C**, PHx+mAB). Quantitative analysis showed that hepatectomy significantly increases the number of venules (**D**), and causes a marked dilation of the draining venules within the margin of the tumors (**E**). Additional anti-MIP-2 treatment was capable of significantly reducing the liver resection-induced increase of the number of tumor venules (**D**). The heterogeneity of venular diameters, as given by the coefficient of variance, was not affected in either of the treatment groups (**F**). Mean ± SE; $^{a}P<0.05$ *vs* Con; $^{c}P<0.05$ *vs* PHx. Magnifications (**A-C**) ×40.

a further increase ($P<0.05$) of the fraction of PCNA-positive cells in the normal liver (Figure 8).

## DISCUSSION

The major findings of the present study are that (1) MIP-2 significantly promotes liver resection-induced expression of the chemokine receptor CXCR-2, and (2) blockade of MIP-2 blunts the augmentation of angiogenesis and metastatic tumor growth after hepatectomy. This indicates for the first time a significant role of this chemokine in the acceleration of tumor growth after hepatectomy. The rodent liver fully regenerates within 8 d after resection[19,20]. The setpoint for growth regulation is the ratio between liver mass and body mass rather than liver mass *per se*[1]. Using a 70% liver resection model in mice, Drixler *et al.* demonstrated that liver regeneration is accompanied by intrahepatic angiogenesis[20]. Liver resection has also been shown to affect the immune system in the early phase of liver regeneration[3]. The MIP-2-CXCR-2 system is thought to be involved in the hepatic regenerative processes after extended resection[4,6]. While blockade of the chemokine receptor CXCR-2 decreases regeneration of the residual liver, selective neutralization of MIP-2 through the use of anti-MIP-2 antibodies is not affecting the liver-to-BW ratio[4]. Of interest, CXCR-2 seems to be pivotal, because other chemokines may replace or act via the CXCR-2 receptor in case of MIP-2 deletion for liver regeneration[4,6].

After resection of colorectal liver metastases, diseases recur in over two-thirds of the patients[21]. This observation indicates that undetected residual microscopic tumors remain in the majority of patients undergoing curative hepatectomy[22]. The locally released factors which trigger the process of regeneration after hepatectomy may even augment the outgrowth of these residual microtumors, thus, additionally contributing to the high rate of recurrences. This view is supported by experimental studies, demonstrating that liver resection enhances tumor growth during regeneration[11,13,14,16]. Using different rat hepatectomy models, these authors suggested

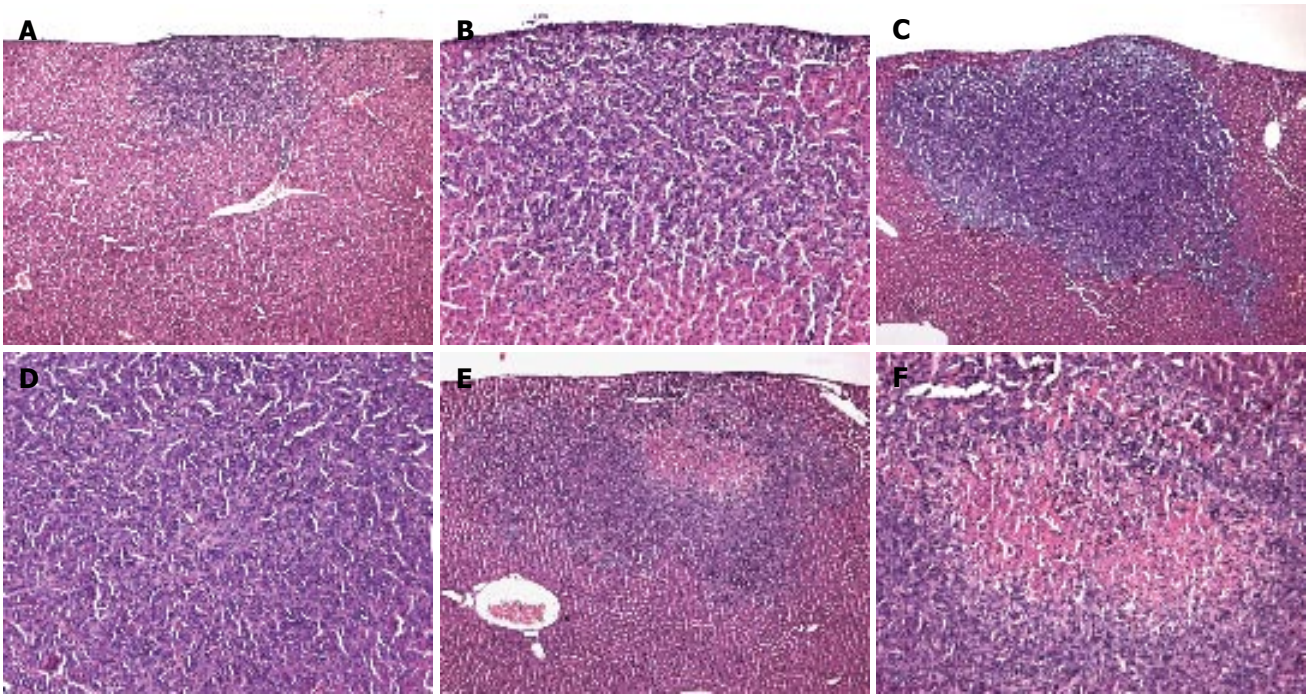


**Figure 4** Hematoxylin–eosin-staining of tumors of a control mouse (**A** and **B**), a mouse which underwent hepatectomy (PHx) (**C** and **D**), and a mouse which additionally received anti-MIP-2 treatment (**E** and **F**). Sections revealed solid growth of the colorectal CT26.WT hepatic metastasis in all the animals. Tumors were round in nature, however, showed aggressive growth characteristics. Anti-MIP-2 treatment provoked an area of necrosis within the tumor center (**E** and **F**). Magnifications (**A**, **C** and **E**) ×18, (**B**, **D** and **F**) ×88.

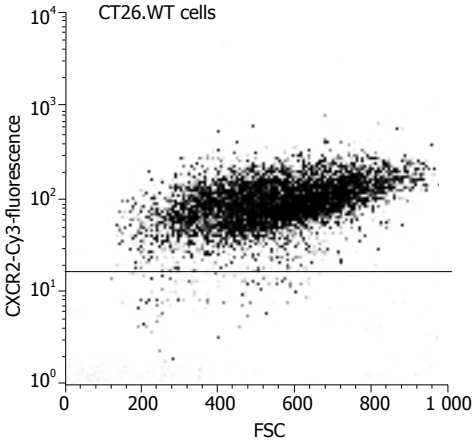


**Figure 5** FACScan analysis of CT26.WT cells, demonstrating positive staining and thus expression of the chemokine receptor CXCR-2 by almost all of the tumors cells studied.

that immunoparalysis with lack of Kupffer cell function and TNF-α response as well as overproduction of growth factors, such as TGF-α, TGF-β and bFGF, contribute to the acceleration of tumor growth.

For the first time, we have herein demonstrated that MIP-2 is involved in hepatectomy-induced metastatic tumor growth. So far, little is known about the role of MIP-2 in tumorigenesis. A recent study indicated that the reduction of fibrosarcoma growth by inhibiting lymphotoxin-β receptor can be reconstituted through co-transfection with MIP-2[23]. The mechanism how MIP-2 is involved in the herein observed liver resection-induced acceleration of tumor growth seems to be the pro-proliferative action of this chemokine, because neutralization of MIP-2 significantly reduced PCNA expression on the tumor cells. Of interest, regeneration of the normal liver was not affected by the anti-MIP-2 treatment, inasmuch as hepatocyte PCNA expression after resection was found even increased when compared with that of untreated hepatectomized controls. This is in line with other experimental studies, which demonstrate that blockade of MIP-2 alone did not affect the process of regeneration[4].

In the present study, we have shown that *in vitro* almost all CT26.WT cells expressed the CXC receptor CXCR-2. *In vivo*, approximately 40% of the cells of non-treated CT26 tumors showed positive CXCR-2 staining 7 days after tumor cell implantation. The reduction of the number of CXCR-2 positive cells is probably due to the fact that solid tumors *in vivo* consist besides the CT26.WT clone of a variety of other cells, including endothelia, fibroblasts and stromal cells, which do not necessarily express CXCR-2. Furthermore, we have demonstrated for the first time that over a 7-d period partial hepatectomy increased the expression of CXCR-2 to -60%. Because receptor expression seems to be required for the proliferative action of chemokines on tumors[24], the increased *in vivo* expression of CXCR-2 may represent the mechanism of action of the MIP-2-associated acceleration of tumor growth after hepatectomy. The neutralization of MIP-2 by MAB452 significantly reduced CXCR-2 expression within the tumor. Although we cannot exclude that neutralization of MIP-2 directly alters the CXCR-2 expression of tumor cells, the histological findings may additionally suggest a relative increase of CXCR-2-negative stromal cells.

The progressive growth of a malignant solid tumor depends on the development of new blood vessels. The

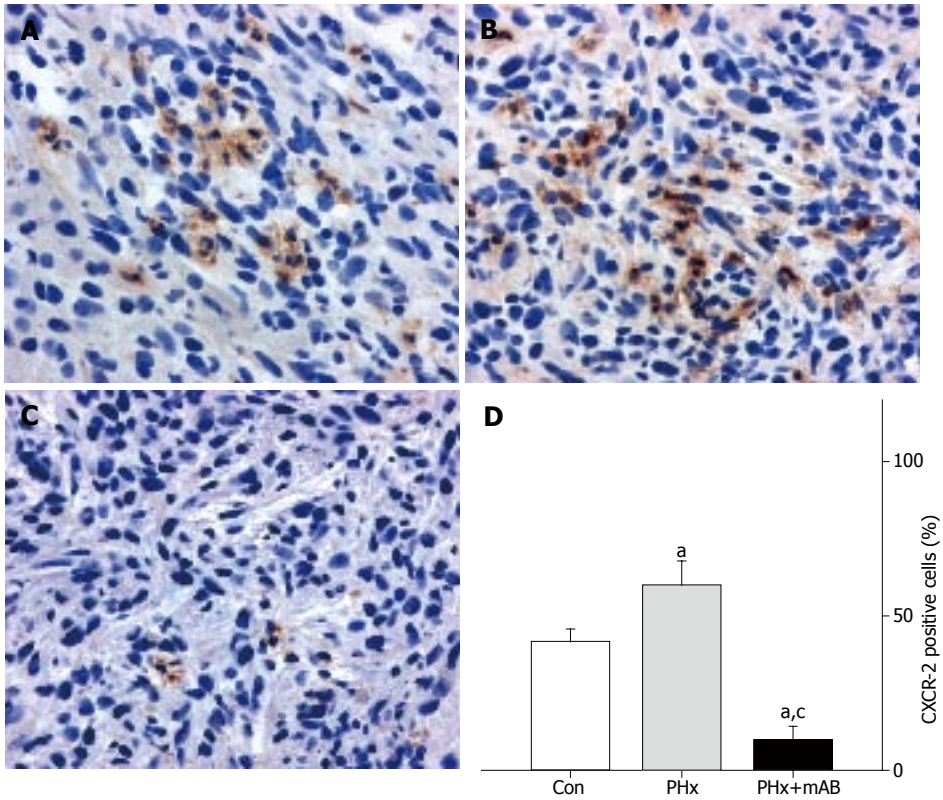


**Figure 6** CXCR-2 immunohistochemistry and quantitative analysis of the number of receptor-positive cells (given in percent of all cells) revealed that within tumors of control animals (Con) ~40% of the cells express CXCR-2 (**A** and **D**). Hepatectomy (PHx) significantly increased CXCR-2 expression to ~60% (**B** and **D**). Of interest, additional blockade of MIP-2 (PHx+mAB) significantly reduced tumor cell CXCR-2 expression and inhibits significantly the liver resection-induced increase of CXCR-2 expression (**C** and **D**). Mean ± SE; $^{a}P<0.05$ *vs* Con; $^{c}P<0.05$ *vs* PHx. Magnifications (**A-C**) ×175.

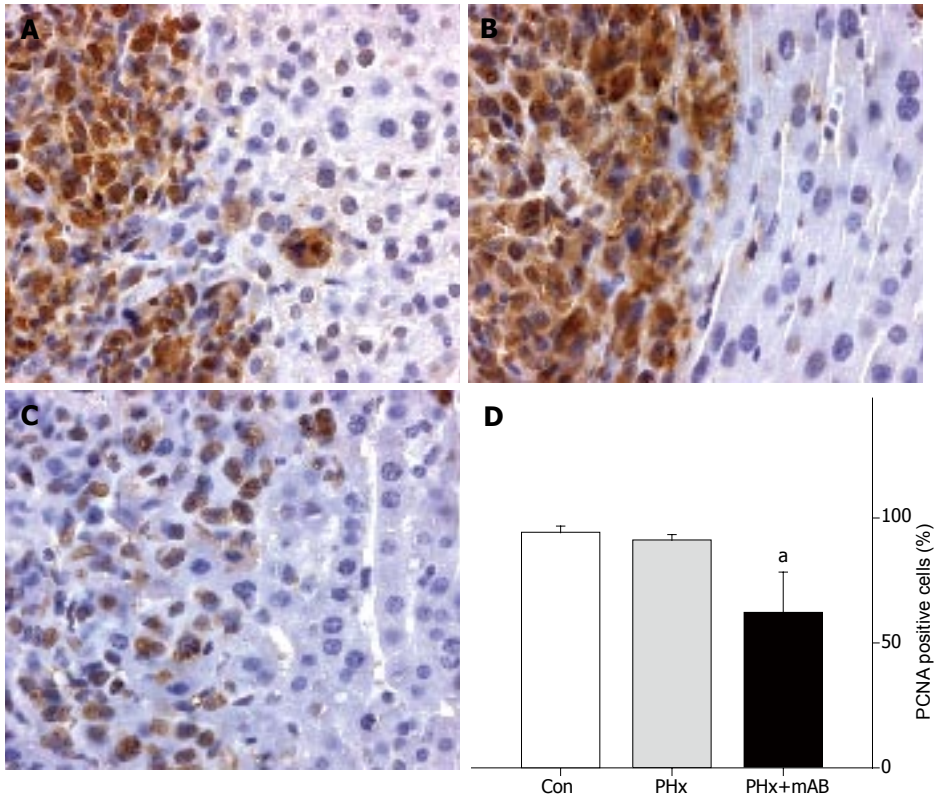


**Figure 7** PCNA immunohistochemistry and quantitative analysis of the number of PCNA-positive cells (given in percent of all cells) in liver tumors of control mice (**A**, Con), after hepatectomy (**B**, PHx), and after hepatectomy and additional anti-MIP-2 treatment (**C**, PHx+mAB). Tumor cells display massive PCNA staining, in particular to those located within the tumor margin. By this, these positive cells sharply demarcate the tumor from the surrounding liver tissue (**A, B,** and **C**). Quantitative analysis revealed that neutralization of MIP-2 significantly reduces the number of PCNA-positive tumor cells (**D**). Mean ± SE; $^{a}P<0.05$ *vs* Con. Magnifications (**A-C**) ×175.

tumor vasculature is chaotically organized and does not follow a hierarchical branching pattern of normal vascular networks[25]. As a result of this abnormal organization, the diameters of those tumor vessels are irregular, the blood flow is heterogeneous, and the endothelial lining is leaky[25]. In the present study, the tumor microvasculature presented with a marked heterogeneity, as indicated by a relatively high coefficient of variance of capillary and venular diameter within the angiogenic front. This is in line with the results of previous reports, which also demonstrated markedly irregular vessel diameters of tumors grown from other colon cancer cell lines at ectopic sites different from that of the liver[26].

CXC chemokines with the three amino acids Glu-

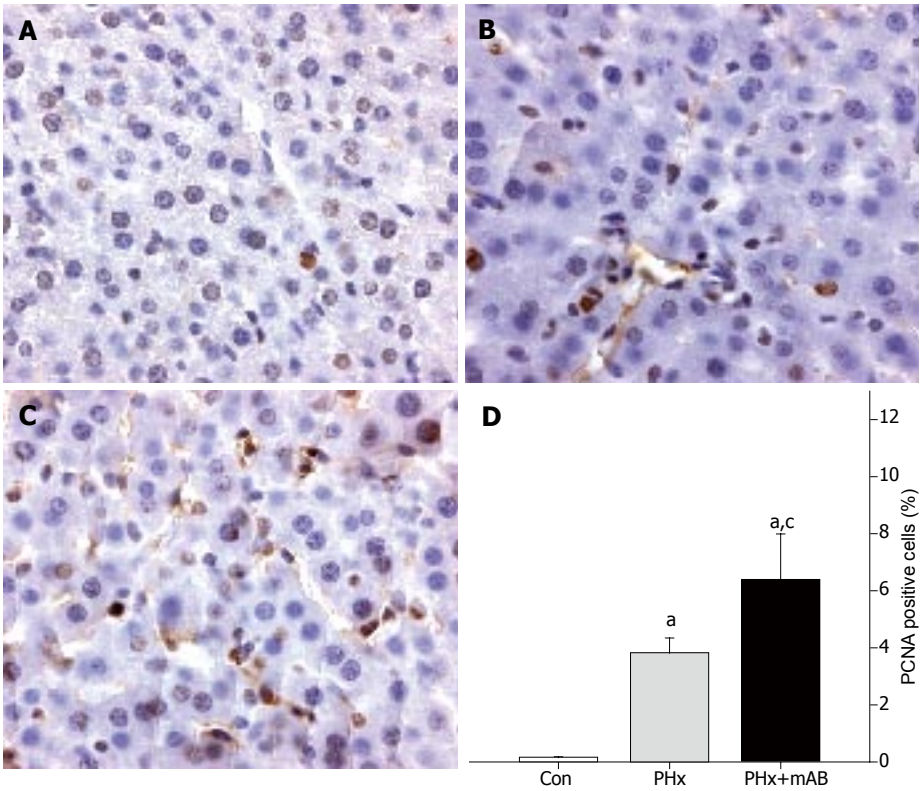


**Figure 8** PCNA immunohistochemistry of normal liver tissue of control mice (**A**, Con), after hepatectomy (**B**, PHx), and after hepatectomy and additional anti-MIP-2 treatment (**C**, PHx+mAB). Quantitative analysis revealed that hepatectomy increases the number of PCNA-positive stained cells when compared to controls (**D**). Additional neutralization of MIP-2 further enhanced the number of PCNA-positive cells (**D**). Mean ± SE; $^{a}P<0.05$ *vs* Con; $^{c}P<0.05$ *vs* PHx. Magnifications (**A-C**) ×175.

Leu-Arg immediately amino-terminal to the CXC motif (ELR+) are thought to be angiogenic, while CXC (ELR –) chemokines are angiostatic[27]. There is no information, however, on whether the CXC (ELR+) chemokine MIP-2 is involved in angiogenesis of tumors. In inflammation, Scapini *et al*[28] demonstrated that MIP-2 induces angiogenesis *in vivo* and that this is mediated by the neutrophil-derived vascular endothelial growth factor-A. In addition, Keane *et al*[29] showed that neutralization of MIP-2 by monoclonal antibodies inhibits the bleomycin-induced angiogenic activity in lung specimens. The present study provides evidence that MIP-2 is also involved in tumor angiogenesis, because the inhibition of the chemokine blunted the liver resection-induced acceleration of new blood vessel formation.

The mechanisms of inhibition of angiogenesis by blockade of MIP-2 are not clarified yet. Our intravital microscopic studies demonstrate that the hepatectomy-mediated increase in angiogenesis is associated with pronounced dilation of the newly formed microvessels. Although we have not studied the mechanism of this dilatory response, it may be speculated that it is caused by the action of VEGF, which is capable of inducing distinct vasodilation, in particular in ischemic tissue[30]. VEGF is known as the predominant inductor of tumor angiogenesis and its promoter is preferentially activated within the angiogenic front of the tumor margin[31]. This effect, however, cannot be attributed to the action of MIP-2, because anti-MIP-2 treatment could not abolish the liver-resection-induced dilation of the newly formed microvessels.

In the present study we found that inhibition of MIP-2 induced central cell death within the tumors. Previous studies on inflammation have demonstrated that apoptotic cells are capable of enhancing secretion of MIP-2 by macrophages, triggering an inflammatory response to remove cell debris[32,33]. Accordingly, the functional inhibition of MIP-2 in our experiments may have prevented the recruitment of inflammatory cells, and, thus avoided the removal of the cell debris from the center of the tumors.

In conclusion, we have demonstrated that MIP-2 significantly promotes liver resection-induced acceleration of angiogenesis and metastatic tumor growth. Our results therefore indicate that the neutralization of MIP-2 may be a potential strategy for additional anti-tumor therapy in patients undergoing liver resection.

## ACKNOWLEDGMENTS

We thank C. Marx, R. M. Nickels, and J. Becker for their excellent technical assistance.

## REFERENCES

1 **Fausto N.** Liver regeneration. *J Hepatol* 2000; **32:** 19-31
2 **Kren BT,** Trembley JH, Fan G, Steer CJ. Molecular regulation of liver regeneration. *Ann N Y Acad Sci* 1997; **831:** 361-381
3 **Sato Y,** Farges O, Buffello D, Bismuth H. Intra- and extrahepatic leukocytes and cytokine mRNA expression during liver regeneration after partial hepatectomy in rats. *Dig Dis Sci* 1999; **44:** 806-816
4 **Ren X,** Carpenter A, Hogaboam C, Colletti L. Mitogenic properties of endogenous and pharmacological doses of macrophage inflammatory protein-2 after 70% hepatectomy in the mouse. *Am J Pathol* 2003; **163:** 563-570
5 **Hogaboam CM,** Bone-Larson CL, Steinhauser ML, Lukacs NW, Colletti LM, Simpson KJ, Strieter RM, Kunkel SL. Novel CXCR2-dependent liver regenerative qualities of ELR-containing CXC chemokines. *FASEB J* 1999; **13:** 1565-1574
6 **Colletti LM,** Green M, Burdick MD, Kunkel SL, Strieter RM.

Proliferative effects of CXC chemokines in rat hepatocytes in vitro and in vivo. *Shock* 1998; **10:** 248-257
7 **Oppenheim JJ,** Zachariae CO, Mukaida N, Matsushima K. Properties of the novel proinflammatory supergene "intercrine" cytokine family. *Annu Rev Immunol* 1991; **9:** 617-648
8 **Fahey TJ 3rd,** Sherry B, Tracey KJ, van Deventer S, Jones WG 2nd, Minei JP, Morgello S, Shires GT, Cerami A. Cytokine production in a model of wound healing: the appearance of MIP-1, MIP-2, cachectin/TNF and IL-1. *Cytokine* 1990; **2:** 92-99
9 **Schramm R,** Thorlacius H. Neutrophil recruitment in mast cell-dependent inflammation: inhibitory mechanisms of glucocorticoids. *Inflamm Res* 2004; **53:** 644-652
10 **Mizutani J,** Hiraoka T, Yamashita R, Miyauchi Y. Promotion of hepatic metastases by liver resection in the rat. *Br J Cancer* 1992; **65:** 794-797
11 **Slooter GD,** Marquet RL, Jeekel J, Ijzermans JN. Tumour growth stimulation after partial hepatectomy can be reduced by treatment with tumour necrosis factor alpha. *Br J Surg* 1995; **82:** 129-132
12 **Drixler TA,** Borel Rinkes IH, Ritchie ED, van Vroonhoven TJ, Gebbink MF, Voest EE. Continuous administration of angiostatin inhibits accelerated growth of colorectal liver metastases after partial hepatectomy. *Cancer Res* 2000; **60:** 1761-1765
13 **Picardo A,** Karpoff HM, Ng B, Lee J, Brennan MF, Fong Y. Partial hepatectomy accelerates local tumor growth: potential roles of local cytokine activation. *Surgery* 1998; **124:** 57-64
14 **Panis Y,** Ribeiro J, Chretien Y, Nordlinger B. Dormant liver metastases: an experimental study. *Br J Surg* 1992; **79:** 221-223
15 **Schindel DT,** Grosfeld JL. Hepatic resection enhances growth of residual intrahepatic and subcutaneous hepatoma, which is inhibited by octreotide. *J Pediatr Surg* 1997; **32:** 995-997; discussion 997-998
16 **Karpoff HM,** Jarnagin W, Delman K, Fong Y. Regional muramyl tripeptide phosphatidylethanolamine administration enhances hepatic immune function and tumor surveillance. *Surgery* 2000; **128:** 213-218
17 **Kollmar O,** Schilling MK, Menger MD. Experimental liver metastasis: standards for local cell implantation to study isolated tumor growth in mice. *Clin Exp Metastasis* 2004; **21:** 453-460
18 **Menger MD,** Marzi I, Messmer K. In vivo fluorescence microscopy for quantitative analysis of the hepatic microcirculation in hamsters and rats. *Eur Surg Res* 1991; **23:** 158-169
19 **Michalopoulos GK,** DeFrances MC. Liver regeneration. *Science* 1997; **276:** 60-66
20 **Drixler TA,** Vogten MJ, Ritchie ED, van Vroonhoven TJ, Gebbink MF, Voest EE, Borel Rinkes IH. Liver regeneration is an angiogenesis- associated phenomenon. *Ann Surg* 2002; **236:** 703-711; discussion 711-712
21 **Fong Y,** Fortner J, Sun RL, Brennan MF, Blumgart LH. Clinical score for predicting recurrence after hepatic resection for metastatic colorectal cancer: analysis of 1001 consecutive cases. *Ann Surg* 1999; **230:** 309-318; discussion 318-321
22 **Delman KA,** Zager JS, Bennett JJ, Malhotra S, Ebright MI, McAuliffe PF, Halterman MW, Federoff HJ, Fong Y. Efficacy of multiagent herpes simplex virus amplicon-mediated immunotherapy as adjuvant treatment for experimental hepatic cancer. *Ann Surg* 2002; **236:** 337-342; discussion 342-343
23 **Hehlgans T,** Stoelcker B, Stopfer P, Muller P, Cernaianu G, Guba M, Steinbauer M, Nedospasov SA, Pfeffer K, Mannel DN. Lymphotoxin-beta receptor immune interaction promotes tumor growth by inducing angiogenesis. *Cancer Res* 2002; **62:** 4034-4040
24 **Zeelenberg IS,** Ruuls-Van Stalle L, Roos E. The chemokine receptor CXCR4 is required for outgrowth of colon carcinoma micrometastases. *Cancer Res* 2003; **63:** 3833-3839
25 **Jain RK.** Molecular regulation of vessel maturation. *Nat Med* 2003; **9:** 685-693
26 **Leunig M,** Yuan F, Menger MD, Boucher Y, Goetz AE, Messmer K, Jain RK. Angiogenesis, microvascular architecture, microhemodynamics, and interstitial fluid pressure during early growth of human adenocarcinoma LS174T in SCID mice. *Cancer Res* 1992; **52:** 6553-6560
27 **Homey B,** Muller A, Zlotnik A. Chemokines: agents for the immunotherapy of cancer? *Nat Rev Immunol* 2002; **2:** 175-184
28 **Scapini P,** Morini M, Tecchio C, Minghelli S, Di Carlo E, Tanghetti E, Albini A, Lowell C, Berton G, Noonan DM, Cassatella MA. CXCL1/macrophage inflammatory protein-2-induced angiogenesis in vivo is mediated by neutrophil-derived vascular endothelial growth factor-A. *J Immunol* 2004; **172:** 5034-5040
29 **Keane MP,** Belperio JA, Moore TA, Moore BB, Arenberg DA, Smith RE, Burdick MD, Kunkel SL, Strieter RM. Neutralization of the CXC chemokine, macrophage inflammatory protein-2, attenuates bleomycin-induced pulmonary fibrosis. *J Immunol* 1999; **162:** 5511-5518
30 **Takeshita S,** Isshiki T, Ochiai M, Eto K, Mori H, Tanaka E, Umetani K, Sato T. Endothelium-dependent relaxation of collateral microvessels after intramuscular gene transfer of vascular endothelial growth factor in a rat model of hindlimb ischemia. *Circulation* 1998; **98:** 1261-1263
31 **Fukumura D,** Xavier R, Sugiura T, Chen Y, Park EC, Lu N, Selig M, Nielsen G, Taksir T, Jain RK, Seed B. Tumor induction of VEGF promoter activity in stromal cells. *Cell* 1998; **94:** 715-725
32 **Lucas M,** Stuart LM, Savill J, Lacy-Hulbert A. Apoptotic cells and innate immune stimuli combine to regulate macrophage cytokine secretion. *J Immunol* 2003; **171:** 2610-2615
33 **Hohlbaum AM,** Gregory MS, Ju ST, Marshak-Rothstein A. Fas ligand engagement of resident peritoneal macrophages in vivo induces apoptosis and the production of neutrophil chemotactic factors. *J Immunol* 2001; **167:** 6217-6224

**S- Editor** Guo SY **L- Editor** Elsevier HK **E- Editor** Kong LH

PO Box 2345, Beijing 100023, China
www.wjgnet.com
wjg@wjgnet.com

*World J Gastroenterol* 2006 February 14; 12(6): 868-873
***World Journal of Gastroenterology*** ISSN 1007-9327
© 2006 The WJG Press. All rights reserved.

*LIVER CANCER*

# Relationship between therapeutic efficacy of arterial infusion chemotherapy and expression of P-glycoprotein and p53 protein in advanced hepatocellular carcinoma

Masahide Akimoto, Masaharu Yoshikawa, Masaaki Ebara, Tsunenobu Sato, Hiroyuki Fukuda, Fukuo Kondo, Hiromitsu Saisho

Masahide Akimoto, Masaharu Yoshikawa, Masaaki Ebara, Tsunenobu Sato, Hiroyuki Fukuda, Hiromitsu Saisho, Department of Medicine and Clinical Oncology, Chiba University, School of Medicine, 1-8-1 Inohana, Chuo-ku, Chiba City, Chiba 260-0856, Japan
Fukuo Kondo, Department of Molecular Pathology, Chiba University, School of Medicine, Chiba, Japan
Correspondence to: Masahide Akimoto, Department of Medicine and Clinical Oncology, School of Medicine, Chiba University, 1-8-1, Inohana, Chuo-ku, Chiba City, Chiba 260-0856, Japan. khikyoku@mb.infoweb.ne.jp
Telephone: +81-43-226-2083 Fax: +81-43-226-2088
Received: 2005-06-20 Accepted: 2005-07-28

## Abstract

**AIM:** To investigate the relationship between the chemotherapeutic drug efficacy and the expression of P-glycoprotein (PGP) and p53 protein in advanced hepatocellular carcinoma (HCC).

**METHODS:** The study was conducted on 41 patients with advanced HCC who were treated by repeated arterial infusion chemotherapy. Biopsy specimens from the tumor were collected before the start of treatment in all the patients, and the specimens were stored frozen until immunohistochemical staining, which was performed after the start of treatment, to detect PGP and p53 protein expressions. Twenty of the forty-one patients were treated with an anthracycline drug (epirubicin hydrochloride; anthracycline group), and the remaining 21 were treated with a non-anthracycline drug (mitoxantrone hydrochloride in 11 patients and carboplatin in 10 patients; non-anthracycline group). The relationship between the chemotherapeutic efficacy and the results of immunostaining were compared between the two groups.

**RESULTS:** Before the start of the treatment, PGP-positive rate was 90.2% (strongly-positive, 36.6%) and p53 protein-positive rate was 34.1% (strongly-positive, 19.5%). In the anthracycline group, the response rate was 40.0%. The number of patients showing poor response to the treatment was significantly larger in the patients with strongly positive PGP expression ($P = 0.005$), and their prognoses were poor ($P = 0.001$). In the non-anthracycline group, the response rate was 42.9%, and there was no significant relationship between the chemotherapeutic drug efficacy and the PGP or p53 protein expression. When only the data from the 11 patients treated with anthraquinone drug, mitoxantrone, were analyzed, however, the number of patients who showed poor response to treatment was significantly higher among the p53-positive patients ($P = 0.012$), irrespective of the survival outcome.

**CONCLUSION:** The chemotherapeutic efficacy with an anthracycline drug for advanced HCC can be predicted by immunohistochemical analysis of PGP expression. Similarly, immunostaining to evaluate p53 protein may be useful to predict the response in patients treated with an anthraquinone drug.

© 2006 The WJG Press. All rights reserved.

**Key words**: Arterial infusion chemotherapy; Hepatocellular carcinoma; P-glycoprotein; p53 protein

Akimoto M, Yoshikawa M, Ebara M, Sato T, Fukuda H, Kondo F, Saisho H. Relationship between therapeutic efficacy of arterial infusion chemotherapy and expression of P-glycoprotein and p53 protein in advanced hepatocellular carcinoma. *World J Gastroenterol* 2006; 12(6): 868-873

http://www.wjgnet.com/1007-9327/12/868.asp

## INTRODUCTION

Transcatheter hepatic arterial embolization (TAE) is widely employed for the treatment of inoperable advanced hepatocellular carcinoma (HCC). However, TAE is unsuitable for the cases with a tumor embolus in the main trunk or the first branch of the portal vein, or for those with severe hepatic injury. For these cases, repeated arterial infusion chemotherapy (RAIC) with a reservoir may be useful, although it is still difficult, at present, to assert that RAIC would provide satisfactory therapeutic results.

Drug resistance is a serious problem in the treatment of HCC, and is mediated by various mechanisms, including those mediated by P-glycoprotein (PGP) and p53 protein expressions. PGP is known to act as an ATP-dependent pump that facilitates transport of substances,

including anticancer drugs, from within to outside the cells, facilitating the development of multidrug resistance, including that to anthracyclines[1]. Moreover, resistance to apoptosis conferred by p53 protein expression is also thought to be a potential factor in the development of multidrug resistance in cancer cells[2]. It has been reported that a mutant-type p53 protein may emerge in various types of cancers due to gene deletion, recombination, or point mutations. This mutant type of p53 protein has been reported to have a considerably longer half life as compared with its wild-type counterpart[3], and it is thought to act as a dominant-negative inhibitor against the wild-type protein, influencing the anti-tumor effects of anticancer drugs[4].

While PGP and p53 protein expressions have been reported in HCC, mainly from the examination of surgically resected specimens, only a few reports have discussed the relationship between the efficacy of chemotherapeutic agents and the expression of PGP in cases of HCC[5,6]; the relationship between the outcome of arterial infusion chemotherapy and the expression of PGP and p53 protein remains particularly obscure. In this study, immunohistochemical analysis was conducted on frozen biopsy specimens obtained from patients with advanced HCC before the treatment to evaluate PGP and p53 protein expressions, and the therapeutic outcomes of RAIC in relation to the expression of these proteins were compared by the type of drugs that were administered.

## MATERIALS AND METHODS

### Patients

One hundred and thirty patients were diagnosed to have an unresectable advanced HCC and treated by RAIC at the Department of Medicine and Clinical Oncology, School of Medicine, Chiba University, and its affiliated institutes between April 1995 and June 1997. We could obtain tumor biopsy specimens before the initiation of RAIC from 41 of these patients, and stored these specimens at -80 °C until the assay. Immunohistochemical staining for PGP and p53 expressions was performed on these specimens and the results were analyzed in relation to the therapeutic outcome in the patients.

### Immunohistochemical staining for PGP and p53 protein

Immediately before the start of RAIC, two or three biopsy specimens were obtained percutaneously using a 21G biopsy needle under ultrasound guidance from 41 patients. The tissue specimens were embedded in OCT compound and immediately stored at -80 °C.

For the immunohistochemical staining, frozen sections (5 μm thick) were prepared and fixed with acetone for 5 min. After pretreatment to prevent non-specific staining, the sections were allowed to react overnight at 4 °C with mdr (Ab-1, diluted 1:250) (Oncogene Research Products, Cambridge, MA, USA) as the primary antibody for PGP. For p53 protein staining, the sections were allowed to react at room temperature for 1 h with DO-7 (diluted 1:40, DAKO, Denmark). The sections were then successively treated with the secondary antibody, and then stained by the avidin-biotinylated peroxidase complex method for PGP, and the streptavidin-biotin method for p53 protein. Color development was conducted by DAB staining, and nuclear staining was conducted with Mayer's hematoxylin for PGP and methyl green for the p53 protein.

Light-microscopic examinations of the stained sections were conducted to detect positive staining for PGP on the cytoplasmic membranes or for p53 protein within the nuclei of the cells in the cancerous areas. At least 300 cells were examined, and the staining intensity was classified based on the percentage of positively stained cells as follows: negative (0-5%); weakly positive (6%-30%); and strongly positive (31% or more).

### Arterial infusion chemotherapy

A 6F indwelling catheter (Anthron PU®; Toray, Tokyo) was introduced percutaneously through the left subaxillary artery (16 patients) or right femoral artery (25 patients) up to the level of the proper hepatic artery or common hepatic artery. The catheter was connected at the other end to a subcutaneously implanted reservoir (Port-A-Cath®, Pharmacia Deltec, St. Paul, MN, USA; or Cersite®, Toray, Tokyo)[7,8].

An anticancer drug was administered over a period of 15 min once in every 4 wk at the outpatient clinic, after first confirming the patency of the catheter by fluoroscopy. Twenty, eleven, and ten of the forty-one patients received epirubicin hydrochloride, mitoxantrone hydrochloride, and carboplatin, respectively. The doses for each administration were set as follows: 70 mg/body surface area for epirubicin hydrochloride, 12 mg/body surface area for mitoxantrone hydrochloride, and 300 mg/body surface area for carboplatin. No other therapy was administered concomitantly in any of the patients. All the patients had underlying liver cirrhosis, and the diagnosis of HCC was confirmed histopathologically in all of them. Fifteen of the forty-one patients had received TAE prior to the RAIC with epirubicin hydrochloride at 40-70 mg/body surface area, while in the remaining 26 patients, RAIC was administered as the initial therapy. Informed consent was obtained from all the patients prior to tissue biopsy and RAIC. In this study, these patients were divided into anthracycline group (20 patients) treated with the anthracycline drugs, epirubicin hydrochloride and non-anthracycline group (remaining 21 patients) treated with the other drugs. No significant differences in the background characteristics were observed between the anthracycline group and the non-anthracycline group (Table 1). The therapeutic efficacies of the drugs were evaluated according to WHO guidelines. The anticancer drug administration was discontinued in the event of detection of any serious side effects, such as leucopenia, thrombocytopenia, or hepatic dysfunction. Observation of the patients was continued until September 30, 2003, by which date, all of the patients died.

### Statistical analysis

The data were statistically analyzed using $\chi^2$ test or Mann–Whitney's *U*-test. Differences at a *P* value of 5% or lower were considered to be statistically significant. The survival rate from the start of the RAIC was calculated by the Kaplan-Meier method and analyzed using the log rank test.

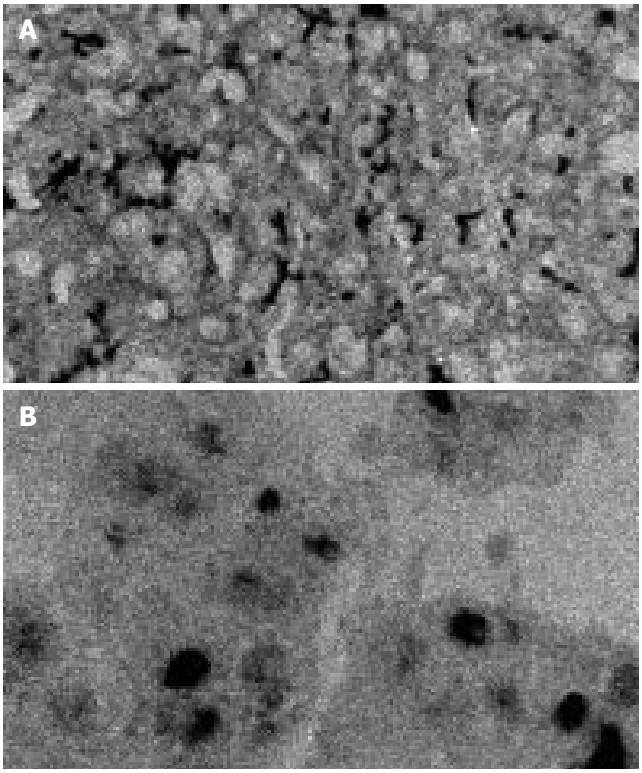


**Figure 1** Immunohistochemical staining of PGP and p53 protein (×100). **A**: Strongly positive staining for PGP; **B**: Strongly positive staining for p53.

**Table 1 Patient characteristics**

| | | Anthracycline group | Non-anthracycline group |
|---|---|---|---|
| Age (yr) | Mean | 60.5±7.2 | 62.1±8.8 |
| Gender[1] | Male | 18 | 19 |
| | Female | 2 | 2 |
| Tumor stage[1,2] | III | 1 | 1 |
| | IV | 19 | 20 |
| Child's class[1] | A | 12 | 11 |
| | B | 6 | 9 |
| | C | 2 | 1 |
| Hepatitis virus[1] | B(–) C(+) | 15 | 14 |
| | B(+) C(+) | 3 | 5 |
| | B(+) C(–) | 0 | 1 |
| | B(–) C(–) | 2 | 1 |
| Chemotherapy[1,3] | (–) | 13 | 13 |
| | (+) | 7 | 8 |
| HCC differentiation[1] | Well | 1 | 2 |
| | Moderately | 14 | 15 |
| | Poorly | 5 | 4 |

Not significant (Mann-Whitney U-test). [1]Number of patients. [2]According to the criteria for tumor stage according to TNM classification (UICC). [3]Chemoembolization with epirubicin hydrochloride.

**Table 2 Correlation between positivity of PGP and that of p53 protein**

| | PGP positivity | | |
|---|---|---|---|
| Positivity | Strongly-positive | Weakly-positive | Negative |
| p53 strongly-positive | 5 | 2 | 1 |
| p53 weakly-positive | 2 | 4 | 0 |
| p53 negative | 8 | 16 | 3 |
| | | | Not significant ($\chi^2$) |

## RESULTS

### *Immunohistochemical analysis for PGP and p53 protein expressions*

Strongly-positive, weakly-positive, and negative PGP expressions were observed in 15 (36.6%), 22 (53.7%), and 4 patients (9.8%), respectively. Strongly-positive, weakly-positive, and negative p53 protein expressions were observed in 8 (19.5%), 6 (14.6%), and 27 patients (65.9%), respectively. Sections showing strong positivity for PGP and p53 protein expressions on immunohistochemical staining are shown in Figures 1A and B, respectively.

Of the 15 patients who had received TAE with anthracycline, 9 (60%) and 6 (40%) were found to be strongly and weakly positive for PGP, respectively, and none of the cases showed negative staining for PGP. Of the 26 patients who had not undergone TAE prior to the RAIC, 6 (23.1%), 16 (61.5%), and 4 (15.4%) patients were found to have strongly positive, weakly positive, and negative PGP expressions, respectively. Thus, the number of cases showing strong positivity for PGP expression was significantly higher among those who had a previous history of treatment with an anthracycline drug than those without such history ($P=0.036$). The percentage of cases showing p53 protein expression did not differ significantly among the patients with or without a history of treatment with an anthracycline drug.

No significant relationship was observed between the expression of PGP and that of the p53 protein (Table 2).

### *Relationship between therapeutic outcomes and immunohistochemical findings*

Of the 41 patients, the 20 belonging to the anthracycline group received average arterial infusions of 11.4±8.1 (range, 3-34) times during a mean follow-up period of 14.5 (range, 3-43) mo; 95%CI=0.00-30.3. Of these 20 patients, 2, 6, 7, and 5 patients showed CR, PR, NC, and PD, respectively, yielding a response rate of 40.0% (95%CI=18.5-61.5). In the 21 patients belonging to the non-anthracycline group, the mean number of arterial infusions and the mean duration of follow-up were 13.3±9.5 (range, 3-38) times and 18.7 (range, 3-78) mo; 95%CI=8.1-29.4, respectively. In this group, 3, 6, 8, and 4 patients showed CR, PR, NC, and PD, respectively, yielding a response rate of 42.9% (95%CI=21.7-64.0).

The expression rate of PGP and p53 protein did not differ significantly between the anthracycline group and the non-anthracycline group (Table 3). Since the positive rate of PGP expression was very high in cases of HCC, the patients were further divided into those showing strongly positive expression (positive group) and those showing weakly positive or negative expression (non-positive group); a similar classification of the patients was conducted for p53 protein expression, into those showing strongly or weakly positive expression (positive group) and

**Table 3 Correlation between PGP or p53 protein positivity and therapeutic efficacy by anticancer drugs**

| Positivity | Anthracycline group ($n$ = 20) | | | | Response rate (%) (95%CI) | Non-anthracycline group ($n$ = 21) | | | | Response rate (%) (95%CI) |
|---|---|---|---|---|---|---|---|---|---|---|
| | CR | PR | NC | PD | | CR | PR | NC | PD | |
| PGP[1,2] | | | | | | | | | | |
| Non-positive group | 2 | 6 | 3 | 0 | 72.7 (46.4-99.1)[b] | 3 | 5 | 5 | 2 | 53.3 (28.1-78.6) |
| Positive group | 0 | 0 | 4 | 5 | 0.0 (0.0-0.0) | 0 | 1 | 3 | 2 | 16.7 (-13.2-46.5) |
| p53[1,3] | | | | | | | | | | |
| Non-positive group | 2 | 4 | 2 | 4 | 50.0 (21.7-78.3) | 3 | 6 | 6 | 2 | 52.9 (29.2-76.7) |
| Positive group | 0 | 2 | 5 | 1 | 25.0 (-5.0-55.0) | 0 | 0 | 2 | 2 | 0.0 (0.0-0.0) |

[b]$P<0.01$ *vs* positive group ($\chi^2$). [1]Number of patients. [2]Non-positive group: negative and weakly positive. Positive group: strongly positive. [3]Non-positive group: negative. Positive group: weakly positive and strongly positive.

**Table 4 Correlation between PGP or p53 protein positivity and cumulative survival rates**

| Positivity | Number of patients | Survival rates (%) | | | Median survival time (mo) | 95%CI |
|---|---|---|---|---|---|---|
| | | 12 mo | 24 mo | 36 mo | | |
| Anthracycline group | | | | | | |
| PGP | | | | | | |
| Non-positive | 11 | 90.9 | 54.6 | 9.1 | 26.5 | 15.8-37.2[b] |
| Positive | 9 | 11.1 | 0.0 | 0.0 | 6.6 | 6.4-6.8 |
| P53 | | | | | | |
| Non-positive | 12 | 58.3 | 41.7 | 8.3 | 18.3 | 0.0-41.4 |
| Positive | 8 | 50.0 | 12.5 | 0.0 | 9.7 | 0.0-20.7 |
| Non-anthracycline group | | | | | | |
| PGP | | | | | | |
| Non-positive | 15 | 80.0 | 53.3 | 33.3 | 24.5 | 13.3-35.8 |
| Positive | 6 | 50.0 | 16.7 | 16.7 | 9.3 | 0.0-21.2 |
| P53 | | | | | | |
| Non-positive | 15 | 80.0 | 46.7 | 33.3 | 18.7 | 5.7-31.8 |
| Positive | 6 | 50.0 | 33.3 | 16.7 | 9.3 | 0.0-25.2 |

[b]$P<0.01$ *vs* positive group (log rank test).

those showing negative expression (non-positive group). As for the relationship of the therapeutic outcome to PGP expression in the anthracycline group, the number of non-responders was significantly higher in the positive group ($P=0.005$); on the other hand, no such difference regarding PGP expression was found in the non-anthracycline group. In regard to the correlation of the therapeutic outcome with the expression of p53 protein, no significant differences between the positive and non-positive patients were found in either the anthracycline group or in the non-anthracycline group. But when only the data of the 11 mitoxantrone-treated patients of the non-anthracycline group were analyzed, 2 and 4 patients in the non-p53-positive group showed CR and PR, respectively, while 4 and 1 patients in the p53-positive group showed NC and PD, respectively, demonstrating the significant correlation between therapeutic outcome and the expression status of the p53 protein ($P=0.012$). On the other hand, in the remaining 10 carboplatin-treated patients in this group, 1, 2, 4, and 2 patients in the non-p53-positive group showed CR, PR, NC, and PD, respectively, and the remaining one p53-positive patient showed PD, revealing the absence of any significant correlation between the therapeutic outcome and the p53 protein expression status.

The relationships between the positive rates for PGP or p53 protein and the survival rate are shown in Table 4. With regard to the PGP expression status in the anthracycline group, the survival rate was significantly lower in the positive group compared to non-positive group ($P=0.001$); on the other hand, in the non-anthracycline group, no significant difference was observed between patients in the positive and non-positive group. As for the p53 protein expression status, no significant correlation was observed between the expression and the survival rate in either the anthracycline or the non-anthracycline group, including the 11 mitoxantrone-treated patients.

## DISCUSSION

In conventional studies, the PGP-positive rate has been determined, mainly based on the examination of surgically resected specimens, to range from 52% to 92%[5,9]. It has also been suggested that the expression of PGP decreases with decreasing degree of differentiation[10]. In the present study, our patients had a relatively high PGP-positive rate of 90.2%, when weakly positive cases were

also included. It has been suggested that PGP expression might be induced by previously administered anthracycline chemotherapy in some cases[11], and that following therapy, only the PGP-positive cells survived, resulting in the high overall positivity rate. However, further studies are required because the study population was small and we could not perform biopsies of the tumors for the duration of chemotherapy or after chemotherapy. On the other hand, the p53-positivity rate in patients with HCC has been reported to range from 12.5% to 51.2%[6,10]. Consistent with these reports, the p53-positivity rate in our present study was 34.1%.

As to the relationship between the p53 tumor suppressor gene expression and the MDR1 gene expression, while some reported that the wild-type p53 protein represses the MDR1 promoter and the mutant-type p53 protein stimulates it, other investigators have suggested that the wild-type p53 stimulates the expression of this promoter[12,13]. In our patients, no significant correlation was observed between the expression of PGP and that of the mutant-type p53 protein, suggesting that mutation of p53 may not regulate the expression of PGP, consistent with recently reported studies[6,9,10]. In the present study, p53 protein was examined only by immunostaining using DO-7 which indicates the expressions of p53 protein variants. Therefore, a relationship between wild-type p53 protein and expressions of PGP could not be identified.

A relationship between PGP expression and the therapeutic efficacy of chemotherapeutic agents has been reported in cases of osteosarcoma and neuroblastoma[14,15]. On the other hand, while no significant correlation was observed between the therapeutic outcome and the expression of PGP in 13 patients with HCC treated with hepatic arterial infusion of doxorubicin[5], a significant correlation between the two was observed in 25 patients with advanced HCC treated by oral or intravenous administration of VP-16 or doxorubicin[6]. In the present study on RAIC, the expression of PGP was significantly correlated with the therapeutic outcome and prognosis of the patients with advanced HCC, but only in the group treated with an anthracycline drug. These results, obtained from actually treated clinical cases of HCC, provide important evidence supporting the involvement of PGP in anthracycline resistance which was demonstrated in basic scientific studies[1]. In addition, resistance mediated by alteration of nuclear topoisomerase, rather than PGP, has also been reported in patients receiving anthracycline drugs[16], necessitating further studies on this issue. No significant correlation was found in this study between the expression of PGP and the therapeutic outcome or prognosis in patients treated with non-anthracycline drugs, such as an anthraquinone or a platinum-based drug. It is speculated that canalicular multispecific organic anion transporter (cMOAT) is involved in the excretion of cisplatin, and over-expression of cMOAT has been observed in an HCC cell line[17].

As for the p53 protein, expression of a mutant-type of p53 protein has been reported to be associated with a poor prognosis[10,18], and it has been suggested that apoptosis induced by anti-cancer drugs, such as doxorubicin, mitoxantrone, cisplatin and bleomycin, is mediated, at least in part, by p53-dependent stimulation of the CD95 receptor/ligand system[19,20]. However, no relationship between the chemotherapeutic drug efficacy and expression of the p53 protein has been reported until now in patients with HCC. In our present study, expression of p53 protein was not correlated with the chemotherapeutic drug efficacy or prognosis in patients treated with the anthracycline drug, suggesting a lesser importance of the expression of a mutant-type p53 protein, as compared with that of PGP, in the evaluation of the sensitivity of advanced HCC to anthracyclines. As for the anthraquinones among the non-anthracycline drugs, a fundamental study in a mitoxantrone-resistant cell line revealed that the expression of wild-type p53 protein induced cellular apoptosis[21]; on the other hand, in relation to platinum-based drugs, expression of an abnormal type of p53 protein was reported to be associated with resistance to chemotherapy in cases of lung cancer[22]. In our patients, treated with an anthraquinone, a significant correlation was observed between the expression of the p53 protein and the chemotherapeutic drug efficacy, but not the prognosis of patients with advanced HCC. On the other hand, no such correlation of the p53 expression was observed with either the chemotherapeutic drug efficacy or the prognosis in HCC patients treated with the platinum-based drug, carboplatin. Although further studies are required, these results indicate the possibility that evaluation of the expression of a mutant-type p53 protein may be useful for predicting the sensitivity of HCC to anthraquinone drugs.

In conclusion, our study demonstrates the existence of a correlation between the outcome of arterial infusion chemotherapy and the expression of PGP and p53 protein in patients with advanced HCC. Therefore, it is suggested that immunostaining for PGP may be useful for predicting the effectiveness of RAIC in cases treated with an anthracycline drug, and that p53 protein expression may be useful for predicting the outcome in cases treated with an anthraquinone drug.

## ACKNOWLEDGMENTS

The staff of the Department of Medicine and Clinical Oncology and Department of Molecular Pathology, School of Medicine, Chiba University generously supported the completion of this study.

## REFERENCES

1 **Leveille-Webster CR**, Arias IM. The biology of the P-glycoproteins. *J Membr Biol* 1995; **143**: 89-102
2 **Kataoka S**, Naito M, Tomida A, Tsuruo T. Resistance to anti-tumor agent-induced apoptosis in a mutant of human myeloid leukemia U937 cells. *Exp Cell Res* 1994; **215:** 199-205
3 **Harris CC**, Hollstein M. Clinical implications of the p53 tumor-suppressor gene. *N Engl J Med* 1993; **329**: 1318-1327
4 **Lowe SW**, Ruley HE, Jacks T, Housman DE. p53-dependent apoptosis modulates the cytotoxicity of anticancer agents. *Cell* 1993; **74**: 957-967
5 **Itsubo M**, Ishikawa T, Toda G, Tanaka M. Immunohistochemical study of expression and cellular localization of the multidrug resistance gene product P-glycoprotein in primary liver carcinoma. *Cancer* 1994; **73**: 298-303
6 **Chou YY**, Cheng AL, Hsu HC. Expression of P-glycoprotein

and p53 in advanced hepatocellular carcinoma treated by single agent chemotherapy: clinical correlation. *J Gastroenterol Hepatol* 1997; **12**: 569-575

7 **Yoshikawa M**, Ebara M, Nakano T, Minoyama A, Sugiura N, Ohto M. Percutaneous transaxillary catheter insertion for hepatic artery infusion chemotherapy. *AJR Am J Roentgenol* 1992; **158**: 885-886

8 **Yoshikawa M**, Ebara M, Saisho H, Hatano R, Morimoto N, Sanada M, Fukuda H, Sugiura N, Ohto M. Long-term outcome of percutaneously implanted port and catheter for hepatic arterial chemoinfusion. *J Int Radiol* 1997; **12**: 137-142

9 **Ng IO**, Liu CL, Fan ST, Ng M. Expression of P-glycoprotein in hepatocellular carcinoma. A determinant of chemotherapy response. *Am J Clin Pathol* 2000; **113**: 355-363

10 **Nakano A**, Watanabe N, Nishizaki Y, Takashimizu S, Matsuzaki S. Immunohistochemical studies on the expression of P-glycoprotein and p53 in relation to histological differentiation and cell proliferation in hepatocellular carcinoma. *Hepatol Res* 2003; **25**: 158-165

11 **Goldstein LJ**, Galski H, Fojo A, Willingham M, Lai SL, Gazdar A, Pirker R, Green A, Crist W, Brodeur GM. Expression of a multidrug resistance gene in human cancers. *J Natl Cancer Inst* 1989; **81:** 116-124

12 **Chin KV**, Ueda K, Pastan I, Gottesman MM. Modulation of activity of the promoter of the human MDR1 gene by Ras and p53. *Science* 1992; **255**: 459-462

13 **Goldsmith ME**, Gudas JM, Schneider E, Cowan KH. Wild type p53 stimulates expression from the human multidrug resistance promoter in a p53-negative cell line. *J Biol Chem* 1995; **270**: 1894-1898

14 **Baldini N**, Scotlandi K, Barbanti-Brodano G, Manara MC, Maurici D, Bacci G, Bertoni F, Picci P, Sottili S, Campanacci M. Expression of P-glycoprotein in high-grade osteosarcomas in relation to clinical outcome. *N Engl J Med* 1995; **333:** 1380-1385

15 **Chan HS**, Haddad G, Thorner PS, DeBoer G, Lin YP, Ondrusek N, Yeger H, Ling V. P-glycoprotein expression as a predictor of the outcome of therapy for neuroblastoma. *N Engl J Med* 1991; **325**: 1608-1614

16 **Cole SP**, Chanda ER, Dicke FP, Gerlach JH, Mirski SE. Non-P-glycoprotein-mediated multidrug resistance in a small cell lung cancer cell line: evidence for decreased susceptibility to drug-induced DNA damage and reduced levels of topoisomerase II. *Cancer Res* 1991; **51:** 3345-3352

17 **Minemura M,** Tanimura H, Tabor E. Overexpression of multidrug resistance genes MDR1 and cMOAT in human hepatocellular carcinoma and hepatoblastoma cell lines. *Int J Oncol* 1999; **15**: 559-563

18 **Nishio M**, Koshikawa T, Kuroishi T, Suyama M, Uchida K, Takagi Y, Washimi O, Sugiura T, Ariyoshi Y, Takahashi T, Ueda R, Takahashi T. Prognostic significance of abnormal p53 accumulation in primary, resected non-small-cell lung cancers. *J Clin Oncol* 1996; **14**: 497-502

19 **Muller M**, Strand S, Hug H, Heinemann EM, Walczak H, Hofmann WJ, Stremmel W, Krammer PH, Galle PR. Drug-induced apoptosis in hepatoma cells is mediated by the CD95 (APO-1/Fas) receptor/ligand system and involves activation of wild-type p53. *J Clin Invest* 1997; **99**: 403-413

20 **Muller M**, Wilder S, Bannasch D, Israeli D, Lehlbach K, Li-Weber M, Friedman SL, Galle PR, Stremmel W, Oren M, Krammer PH. p53 activates the CD95 (APO-1/Fas) gene in response to DNA damage by anticancer drugs. *J Exp Med* 1998; **188**: 2033-2045

21 **Seth P**, Katayose D, Li Z, Kim M, Wersto R, Craig C, Shanmugam N, Ohri E, Mudahar B, Rakkar AN, Kodali P, Cowan K. A recombinant adenovirus expressing wild type p53 induces apoptosis in drug-resistant human breast cancer cells: a gene therapy approach for drug-resistant cancers. *Cancer Gene Ther* 1997; **4**: 383-390

22 **Rusch V**, Klimstra D, Venkatraman E, Oliver J, Martini N, Gralla R, Kris M, Dmitrovsky E. Aberrant p53 expression predicts clinical resistance to cisplatin-based chemotherapy in locally advanced non-small cell lung cancer. *Cancer Res* 1995; **55**: 5038-5042

**S- Editor** Kumar M and Guo SY **L- Editor** Elsevier HK **E- Editor** Kong LH

PO Box 2345, Beijing 100023, China
www.wjgnet.com
wjg@wjgnet.com

World J Gastroenterol 2006 February 14; 12(6): 874-879
World Journal of Gastroenterology ISSN 1007-9327
© 2006 The WJG Press. All rights reserved.

LIVER CANCER

# Anti-hepatoma activity and mechanism of ursolic acid and its derivatives isolated from *Aralia decaisneana*

Ze Tian, Geng Lin, Rui-Xia Zheng, Feng Huang, Meng-Su Yang, Pei-Gen Xiao

Ze Tian, Geng Lin, Rui-Xia Zheng, Feng Huang, Pei-Gen Xiao, Department of Pharmacology, Institute of Medicinal Plant Development, Chinese Academy of Medical Sciences, Peking Union Medical College, Beijing 100094, China
Meng-Su Yang, Department of Biology and Chemistry, City University of Hong Kong, Kowloon, Hong Kong, China
Supported by the National Natural Science Foundation of China, No. 30470195
Co-correspondence: Pei-Gen Xiao
Correspondence to: Ze Tian, Associate Professor of Institute of Medicinal Plant Development, Chinese Academy of Medical Sciences, Peking Union Medical College, Beijing 100094, China. zetian603@hotmail.com
Telephone: +86-10-62894597 Fax: +86-10-62894597
Received: 2005-07-17 Accepted: 2005-07-29

## Abstract

**AIM:** To investigate the anti-tumor activity of ursolic acid (UA) and its derivatives isolated from *Aralia decaisneana* on hepatocellular carcinoma both *in vitro* and *in vivo*.

**METHODS:** *In vivo* cytotoxicity was first screened by 3-[4,5-dimethylthiazol-2-yl]-2, 5-diphenyltetrazolium bromide (MTT) assay. Morphological observation, DNA ladder, flow cytometry analysis, Western blot and real time PCR were employed to elucidate the cytotoxic mechanism of UA. Implanted mouse hepatoma $H_{22}$ was used to evaluate the growth inhibitory effect of UA *in vivo*.

**RESULTS:** UA could significantly inhibit the proliferation of HepG2 and its drug-resistance strain, R-HepG2 cells, but had no inhibitory effect on primarily cultured normal mouse hepatocytes whereas all the six derivatives of UA could not inhibit the growth of all tested cell lines. Further study on mechanism demonstrated that apoptosis and $G_0/G_1$ arrest were involved in the cytotoxicity and cleavage of poly-(ADP-ribose)-polymerase (PARP). Downregulation of cyclooxygenase-2 (COX-2) protein and upregulation of heat shock protein (HSP) 105 mRNA correlated to the apoptosis of HepG2 cells treated with UA. In addition, UA also could inhibit the growth of $H_{22}$ hepatoma *in vivo*.

**CONCLUSION:** UA is a promising anti-tumor agent, but further work needs to be done to improve its solubility.

© 2006 The WJG Press. All rights reserved.

**Key words:** *Aralia decaisneana*; Ursolic acid; Hepatoma

Tian Z, Lin G, Zheng RX, Huang F, Yang MS, Xiao PG. Anti-hepatoma activity and mechanism of ursolic acid and its derivatives isolated from *Aralia decaisneana*. *World J Gastroenterol* 2006; 12(6): 874-879

http://www.wjgnet.com/1007-9327/12/874.asp

## INTRODUCTION

Hepatocellular carcinoma is one of the most common malignant neoplasms worldwide and one of the leading causes of malignancy-related death in China[1,2]. Its therapy in clinic is still a big challenge.

Ursolic acid (UA) is a versatile compound, which possesses anti-cancer[3,4], anti-inflammatory[5,6], anti-HIV[7] and immunomodulatory effects[8]. There is a growing interest in the anti-tumor activities of UA. UA could act on almost all steps in the whole cancer process: initiation, promotion, progression, and metastasis. Multiple lines of evidence indicate that UA is a promising chemo-preventive agent both *in vivo* and *in vitro*. UA could inhibit Epstein-Barr virus activation induced by 12-*O*-tetradecanoylphorbol-13-acetate in Raji cells and two-stage mouse skin tumor promotion[9,10]. The mechanism involved might associate with the inhibition of AP-1-mediated induction of COX-2 by disrupting PKC signal transduction pathway[11]. UA could inhibit the proliferation of various cancerous cell lines by inhibiting DNA polymerase and topoisomerase[12], inducing apoptosis through proteolytic activation of caspase-3 and/or other similar caspases[3]. It was also reported that UA has anti-invasion and anti-metastasis activity by inhibiting nuclear factor-kappa B (NF-$\kappa$B) activation, down-regulating COX-2 and matrix metalloproteinase 9[13].

Besides its cytotoxicity to hepatoma, it was reported that UA can exert its hepatoprotective action in mice and rats[14–16]. The reason for the phenomenon is worth studying. Moreover, the growth inhibitory activity of UA on hepatocellular carcinoma *in vivo* is still unknown.

In the present study, UA and its six derivatives isolated from the bark of *Aralia decaisneana* were used to treat rheumatism, lumbago, hepatitis, nephritis, and diabetes mellitus in Chinese folk medicine. The cytotoxicity of these UA compounds to HepG2, its drug-resistance strain R-HepG2 and primarily cultured normal mouse and rat hepatocytes were examined in order to find their anti-hepatoma efficiency on both parental and drug-resistant hepatocellular carcinoma as well as their low toxicity.

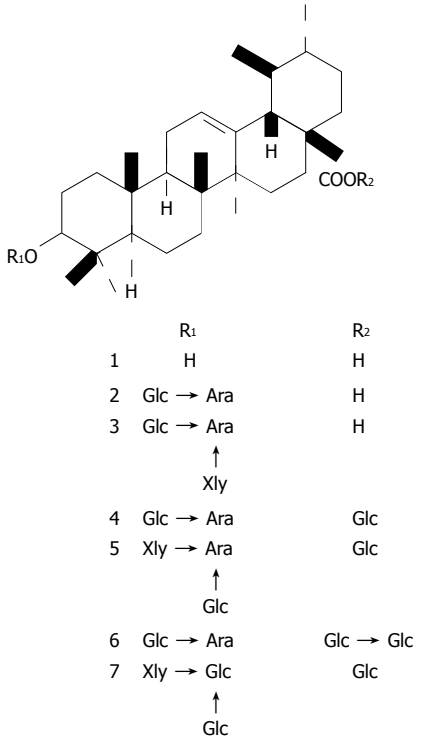


**Figure 1** Structures of UA and its derivatives.
1. UA
2. UA-3-O-β-D-glucopyranosyl-(1→3)-α-L-arabinopyranoside,
3. UA-3-O-[β-D-xylopyranosyl-(1→2)][β-D-glucopyranosyl-(1→3)]-α-L-arabinopyranoside,
4. UA-3-O-β-D-glucopyranosyl-(1→3)-α-L-arabinopyranosyl-28-O-β-D-glucopyranoside,
5. UA-3-O-[β-D-glucopyranosyl-(1→2)][β-D-xylopyranosyl-(1→3)]-α-L-arabinopyranosyl-28-O-β-D-glucopyranoside,
6. UA-3-O-β-D-glucopyranosyl-(1→3)-α-L-arabinopyranosyl-28-O-β-D-glucopyranosyl-(1→6)-O-β-D-glucopyranoside,
7. UA-3-O-[β-D-glucopyranosyl-(1→2)][β-D-xylopyranosyl-(1→3)]-β-D-xylopyranosyl-28-O-β-D-glucopyranoside.

Morphological observation, DNA ladder, cell cycle analysis, Western blot and real time PCR were performed to elucidate the cytotoxic mechanism of UA on HepG2 cells. Mice bearing murine hepatoma $H_{22}$ were used to investigate the growth inhibitory effect of UA *in vivo*.

## MATERIALS AND METHODS

### Tissue culture and drug treatment

HepG2 (ATCC) cells were maintained in RPMI 1640 (Gibco) containing 10% FBS (Gibco), 2 mg/mL sodium bicarbonate, 100 μg/mL penicillin sodium salt and 100 μg/mL streptomycin sulfate. R-HepG2 (City University of Hong Kong) was maintained in the presence of 1.2 μmol/L doxorubicin (Sigma). Hepatocytes were isolated from normal Kunming mice (Experimental Animal Centre of Zhongshan Medical University) and SD rats (Experimental Animal Centre of Zoology, Chinese Academy of Sciences) with enzymatic perfusion technique as previously described[17]. Logarithmically growing cells were used for all the experiments.

UA and its derivatives (Figure 1) were isolated from the bark of *Aralia decaisneana* by silica gel column chromatography and their structures were identified by spectral analysis[18]. UA was dissolved in DMSO at the concentration of 100 and 10 mmol/L in cellular and *in vivo* experiments, respectively and diluted in tissue culture medium and saline before use. Six UA derivatives were directly dissolved in tissue culture medium.

### Cytotoxicity assay

HepG2 and R-HepG2 cells ($1.5\times10^4$) as well as mouse and rat hepatocytes ($8\times10^3$) were seeded in 96-well plates and treated with the compounds at various concentrations (3.125-100 μmol/L). Then the cells were incubated at 37 °C in an atmosphere containing 50 mL/L $CO_2$ for 48 h followed by MTT assay. $IC_{50}$ of the tested compounds on different cell lines were obtained from the concentration–effect curves.

### Morphology observation

HepG2 cells were cultured in 3.5-cm dishes. UA was added to the medium at 20 μmol/L for 6, 12, and 24 h. A harringtonin-(20 μmol/L, 24 h) and vehicle-(0.1% DMSO) treated sample was regarded as a positive and negative control, respectively. After the treatment, all the cultures were incubated at 37 °C in an atmosphere containing 50 mL/L $CO_2$ for the indicated time. Photographs were taken under an inverted Leica fluorescence 40×10 microscope after acridine orange (AO)/ethidium bromide (EB) staining.

### DNA ladder analysis

HepG2 cells were grown to 70–80% confluence and exposed to 20 μmol/L UA or harringtonin. Then the cultures were incubated at 37 °C in an atmosphere containing 50 mL/L $CO_2$ and collected at 0, 6, 12, and 24 h. Their genomic DNA was extracted and analyzed by gel electrophoresis[19].

### Flow cytometry analysis

Flow cytometry analysis was used to evaluate cell cycle distribution of HepG2 cells. HepG2 cells were treated with 20 μmol/L UA for 0, 6, 12, and 24 h, respectively, collected and fixed in 70% cold ethanol (–20 °C) overnight. After being washed twice with PBS, the cells were resuspended in PBS. RNA in the fixed cells was digested using RNase A (0.5 mg/mL) at 37 °C for 1 h. Finally, the cells were stained with 2.5 μg/mL propidium iodide (PI). The DNA content of the cells was then analyzed with an FACSCalibur instrument (Becton-Dickinson) at excitation 488/emission 600 nm. Data were analyzed by cell cycle distribution software (ModFit LT version 2.0, Verity Software House, USA).

### Western blotting

After the treatment, cells were washed thrice with ice-cold PBS and collected with lysis buffer. Protein determination, SDS-PAGE and transfer were performed as previously described[17]. Nitrocellulose membranes were then incubated with a monoclonal anti-PARP or polyclonal anti-COX-2 antiserum. Secondary antibody to IgG conjugated to horseradish peroxidase was used. The blots were probed with the ECL Western blot detection system according to the manufacturer's instructions.

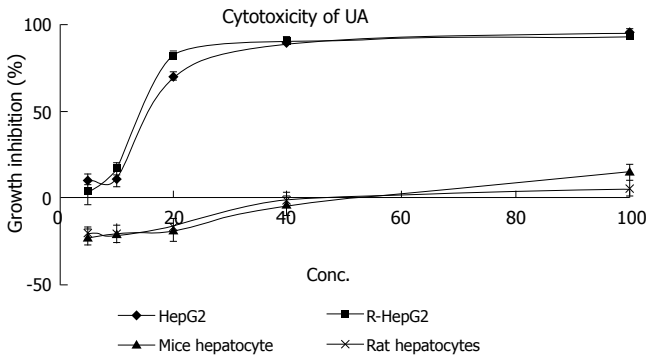


**Figure 2** Cytotoxicity of UA to a panel of hepatocytes.

### RT-PCR and real time PCR analysis

Total RNA was isolated from HepG2 cells using Trizol reagent according to the standard protocol and used to generate cDNA in each sample using the SuperScript II reverse transcriptase with oligo (dT) primers. Aliquots of total cDNA were diluted and added into each PCR reaction mixture together with 0.5 μmol/L of forward and reverse primers of HSP 105 (F: CAGGATCCAGTTGTACGTGCTC; R: TGATGTGGAGGTTCAGCACC, 197 bp) and glyceraldehyde-3-phosphate dehydrogenase (GAPDH, F: ATCAGCAATGCCTCCTGCA; R: CCTGCTTCACCACCTTCTTGA, 355 bp) (Shanghai Biotech Engineering Service Limited Company). PCR amplification was performed on a GeneAmp 9700 PCR System (ABI). After denaturation of cDNA at 94 °C for 3 min, the cycling conditions were as follows: 32 cycles consisting of denaturation at 94 °C for 30 s, annealing at 59 °C for 30 s, and extension at 72 °C for 1 min. The PCR products were analyzed by agarose gel electrophoresis and Bio-Rad Chemi Doc. The mRNA expression levels were normalized to the expression of a housekeeping gene GAPDH. SYBR-Green-I fluorescence labeling method was used in real-time quantitative RT-PCR amplification on an ABI Prism 7000 SDS and analyzed with its software according to the standard protocol and manufacturer's instructions[20]. The $2^{-\Delta\Delta CT}$ method was used in data analysis based on similar (<10%) amplification efficiency of the target and reference genes, which was achieved by the determination of $\Delta CT$ variations with template dilution[21]. GAPDH was used as a reference gene for internal control.

### Anti-tumor evaluation on implanted mouse $H_{22}$

Male CD-1 (ICR) mice (Beijing Vital Laboratory Animal Technology Company) weighing 20–22 g were used for the implantation of hepatoma $H_{22}$ (s.c.) which was maintained by weekly i.p. passages in CD-1 (ICR) mice, 0.2 mL ascites of 1:6 dilution from tumor-bearing mice 7 days after the tumor inoculation was implanted (s.c.) into the armpit region of the mice. Eight mice were treated i.p. with either UA or vehicle (1% DMSO in saline) once a day for 10 days 24 h after the tumor inoculation. Cyclophosphamide (10 mg/kg b.w.) was used as positive control. Tumor inhibition rate (TIR) was derived from $(1-T/C)\times100$, where $T$ is the mean tumor weight of the UA-treated group and $C$ is the mean tumor weight of the negative control group.

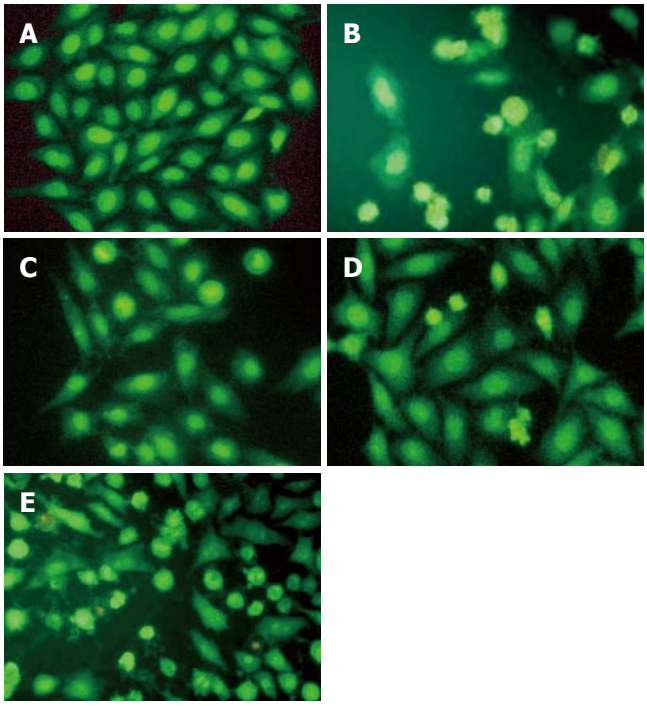


**Figure 3** Morphological changes of HepG2 cells in response to harringtonin and UA. Cells were stained with AO/EB and observed under an inverted Leica fluorescence 40×10 microscope. **A**: Normal HepG2 cells; **B**: harringtonin (20 μmol/L) for 24 h; **C-E**: UA (20 μmol/L) for 6, 12, and 24 h, respectively.

### Statistical analysis

Student's *t*-test was used in all the experiments. $P<0.05$ was considered statistically significant.

## RESULTS

### Selective cytotoxicity

Cytotoxicity of UA and its derivatives was determined by MTT assay. UA was demonstrated to have similar anti-proliferation activity on HepG2 and R-HepG2 cells in a concentration-dependent manner (Figure 2) with its $IC_{50}$ value being 18 and 15 μmol/L, respectively, whereas it exhibited less growth inhibitory activity on primarily cultured normal mouse and rat hepatocytes and the $IC_{50}$ value could not be detected at the tested concentration. On the contrary, six UA derivatives did not show any cytotoxicity to all the tested cells, while they possessed better solubility in water than UA.

### Morphological changes of HepG2 cells

HepG2 cells treated with harringtonin and 20 μmol/L UA showed similar and significant changes (Figure 3). Chromatin aggregation, nuclear, and cytoplasmic condensation only could be seen in a few cells after being treated with UA for 6 and 12 h. Partition of cytoplasm and nuclei into the membrane bound-vesicles (apoptotic bodies) was observed in the cells treated with harringtonin and UA for 24 h. At the same time, apoptotic cells were found at this time point.

### DNA ladder analysis of HepG2 cells

DNA ladder was used to prove the apoptosis of HepG2 cells induced by UA. After treatment with 20 μmol/L

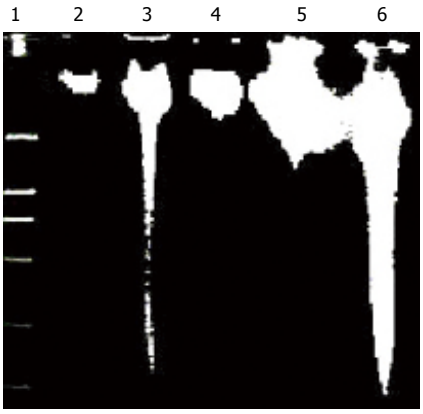


**Figure 4** Induction of time-dependent fragmentation of nuclear DNA by harringtonin and UA. Genomic DNA of the treated cells was collected at different time points during the incubation. Lane 1: DNA marker (DL-2000); lane 3: harringtonin (20 μmol/L) for 24 h; lanes 2, 4–6: UA (20 μmol/L) for 0, 6, 12, and 24 h, respectively.

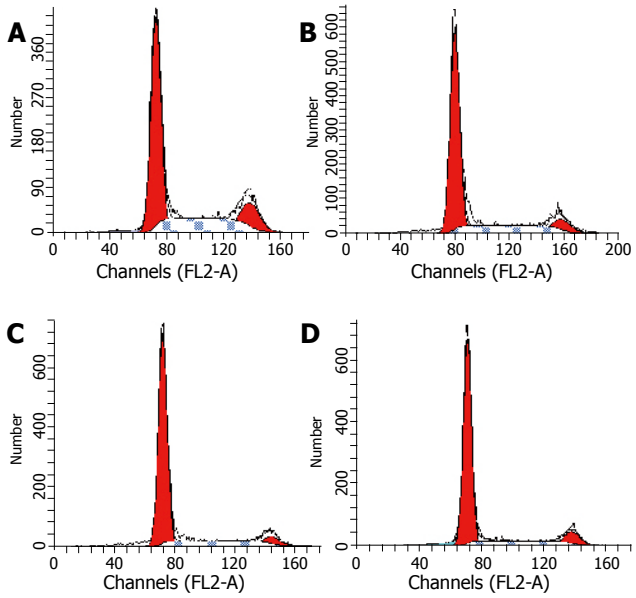


**Figure 5** Cell cycle analysis of HepG2 cells treated with UA (20 μmol/L) for 0 (**A**), 6 (**B**), 12 (**C**), and 24 h (**D**), respectively. Cells were stained with PI and analyzed by flow cytometry.

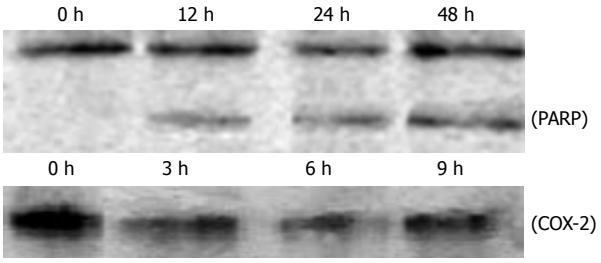


**Figure 6** Cleavage of PARP and downregulation of COX-2 protein expression in HepG2 cells treated with UA. Cellular lysate protein (23 μg/lane) was loaded for 10% SDS-polyacrylamide gel electrophoresis, and subsequently transferred onto nitrocellulose. Immunoblots were probed with antibody specific for PARP and COX-2 protein. Lysates were from HepG2 cells treated with 20 μmol/L UA for indicated times.

UA for different time points, evident DNA ladder was detected at 24 h on HepG2 cells treated with UA and harringtonin (Figure 4), indicating the apoptosis observed in morphological inspection.

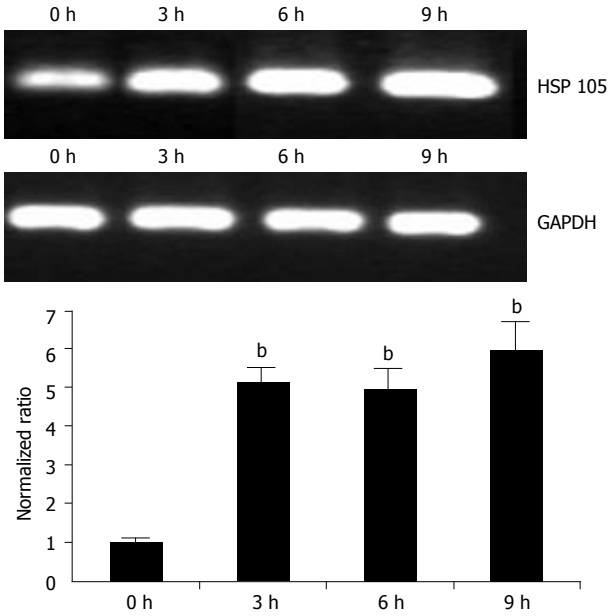


**Figure 7** RT-PCR and real time PCR analysis of up-regulated HSP 105 gene in HepG2 cells in response to treatment with UA. HepG2 cells were treated with 20 μmol/L UA for 0, 3, 6, and 9 h. Total RNA was isolated and subjected to semi-quantitative and quantitative RT-PCR analysis. GAPDH was used as a control. For quantitative analysis, data shown are mean±SD. $^{b}P<0.001$ *vs* control, $n=3$.

### *Cell cycle distributions in HepG2 cells*

After being exposed to 20 μmol/L UA for 0, 6, 12, and 24 h, respectively, the cell cycle progression of HepG2 cells showed evident changes (Figure 5). UA caused significant $G_0/G_1$ arrest with a concomitant decrease of cell population in S and $G_2/M$ phases. The distribution of cell cycle in $G_0/G_1$, S and $G_2/M$ phases was 57.80%, 27.24%, and 14.96% at 0 h; 67.78%, 22.92%, and 9.3% at 6 h; 73.73%, 19.59%, and 6.69% at 12 h; 74.31%, 15.69%, and 10.0% at 24 h, respectively. When treated with UA for 12 and 24 h, higher percentage of cell cycle distribution in $G_0/G_1$ phase was detected than that at 6 h.

### *Cleavage of PARP protein and downregulation of COX-2*

Exposure to 20 μmol/L UA for 0, 12, 24, and 48 h, respectively, PARP was cleaved into 89- and 24-ku fragments, indicating that the apoptosis of HepG2 cells induced by UA was involved in caspase activation. After HepG2 cells were treated with UA for 0, 3, 6, and 9 h, respectively, COX-2 expression was significantly inhibited (Figure 6).

### *Upregulation of HSP 105 mRNA expression*

HSP 105 belongs to HSP 70 super family and is closely related with apoptosis. The amplification efficiency of target and reference genes HSP 105 and GAPDH was quite similar (data not shown). The $2^{-\Delta\Delta Ct}$ method was used in data analysis. After being treated with 20 μmol/L UA for 3, 6, and 9 h, respectively, HSP 105 mRNA expression was upregulated in a time-dependent manner both in RT-PCR and real time PCR (Figure 7).

**Table 1 Tumor growth inhibition effect of UA in mice bearing $H_{22}$ (mean±SD, $n$ = 8)**

| Samples | Dosage (mg/kg) | Tumor weight (g) | Growth inhibition (%) |
|---|---|---|---|
| Control | | 2.8±1.22 | |
| C.P. | 10 | 1.07±0.55b | 61.1 |
| UA | 30 | 1.27±0.90a | 54.6 |
| UA | 15 | 1.55±0.91a | 44.6 |

[a]$P$<0.05, [b]$P$<0.01 *vs* control.

### *Tumor growth inhibitory effect*

Twenty-four hours after tumor implantation, administration of UA (30 and 15 mg/kg b.w.) and cyclophosphamide (10 mg/kg b.w.) once a day for 10 days, could significantly suppress the growth of $H_{22}$ (Table 1). Significant body weight loss was observed in cyclophosphamide-treated group compared to the control group, whereas only slight body weight loss was observed in UA-treated group, suggesting that UA might possess anti-hepatoma effect *in vivo* with low toxicity.

## DISCUSSION

In terms of cancer treatment, chemotherapy has serious limitations, namely the lack of selectivity of active ingredients and resistance of cancer cells to these chemicals[22]. Thus, it is urgent to find new compounds that can kill both parental cancer cells and drug resistant cells and differentiate between normal and cancer cells in order to selectively kill cancerous cells with reduced toxicity. UA possesses good cytotoxicity on HepG2 and R-HepG2 cells, but no cytotoxicity to primarily cultured normal mouse and rat hepatocytes has been detected at corresponding concentrations. These results indicate that UA is a promising anti-tumor agent to parental and drug resistant HepG2 cells with low toxicity and could partially explain why UA inhibits the proliferation of hepatoma while possesses hepatoprotective activity. In addition, UA can lead to apoptosis, DNA ladder and PARP protein cleavage as well as $G_0/G_1$ cell-cycle arrest.

However, the cytotoxic mechanisms of HepG2 cells induced by UA are not completely understood. PARP is a substrate of apoptosis specific protease from the ICE-family (caspases). The 113 ku PARP is cleaved during apoptosis into 89- and 24-ku fragments which could serve as an early hallmark of apoptosis. In our study, cleaved PARP protein not only further proved apoptosis, but also it was implied that activation of caspases was involved in apoptosis of HepG2 cells treated with UA. COX-2 is an early-response gene that is highly inducible by mitogenic and inflammatory stimuli[23–25]. Multiple lines of evidence suggest that COX-2 is important in carcinogenesis and overexpressed in cancer cells[26,27]. NS-398, a representative of non-selective COX inhibitors can induce $G_0/G_1$ cell cycle arrest through inhibition of CDK2 and induction of p21 and p27[28,29]. Upregulation of p21 could further stimulate mRNA transcription of cytochrome *C* and caspase 3 which induces apoptosis in the end[30]. In the light of our study, UA could significantly inhibit COX-2 protein expression, suggesting that inhibition of COX-2 may correlate with increased p21 expression and subsequent activation of cytochrome *C* and caspase-3 in HepG2 cells treated with UA[31].

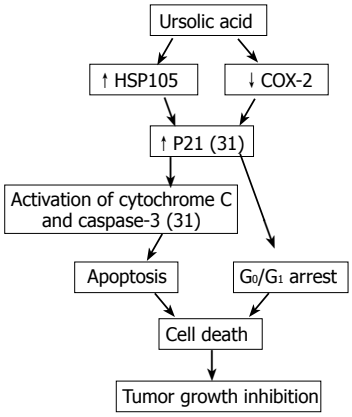


**Figure 8** Summary of current understanding of cytotoxicity of UA to hepatoma cells. Functions with reference number represent known mechanism and bold words without reference number represent the mechanism revealed in our study.

HSP 105 belonging to heat shock protein (HSP) 70 super family acts as a chaperone and plays a role in control of cell proliferation and cellular aging. It was reported that overexpression of HSP105α could enhance stress-induced apoptosis, but not necrosis in mouse embryonal F9 cells[32,33]. Some HSPs purified from murine tumors and used as vaccine are prophylactically and therapeutically effective in cancer immunotherapy models[34]. Further more, MKT-077, a cationic rhodacyanine dye analog exerts its selective toxicity to cancer cells by binding to the HSP 70 family protein mot-2 and reactivating p53 function, thus resulting in increased p53 downstream gene p21 expression[35]. Upregulation of HSP 105 and increase of p21 expression[31] may contribute to apoptosis and $G_0/G_1$ cell-cycle arrest induced by UA, which are at least partially responsible for the selectivity of UA for cancer cells.

Tumor growth inhibitory effect in mice bearing hepatoma could predict the activity of corresponding tumors in human beings. Accordingly, the anti-neoplasm action of UA on mouse hepatoma $H_{22}$ indicates that it can be used to treat human hepatoma. However, few researches have been done on the pharmacokinetics of UA. We also did not monitor the concentration of UA in the blood of mice. Therefore, more attention should be paid to the active plasma concentration of UA in future.

In conclusion, UA is a potential anti-hepatoma agent with reduced toxicity both *in vitro* and *in vivo*. Summary of current understanding of anti-tumor activity of UA on hepatoma is shown in Figure 8. However, poor water solubility of UA has confined its use. Although its derivatives have good water solubility, these derivatives possess no anti-neoplasm activity. More work should be done to solve this problem.

## REFERENCES

1 **Zhu ZZ**, Cong WM, Liu SF, Dong H, Zhu GS, Wu MC. Homozygosity for Pro of p53 Arg72Pro as a potential risk factor for hepatocellular carcinoma in Chinese population. *World J Gastroenterol* 2005; **11**: 289-292

2 **Yuan SL,** Wei YQ, Wang XJ, Xiao F, Li SF, Zhang J. Growth inhibition and apoptosis induction of tanshinone II-A on human hepatocellular carcinoma cells. *World J Gastroenterol* 2004; **10**: 2024-2028

3 **Hollosy F**, Meszaros G, Bokonyi G, Idei M, Seprodi A, Szende B, Keri G. Cytostatic, cytotoxic and protein tyrosine kinase inhibitory activity of ursolic acid in A431 human tumor cells. *Anticancer Res* 2000; **20**: 4563-4570

4 **Hsu HY,** Yang JJ, Lin CC. Effects of oleanolic acid and ursolic acid on inhibiting tumor growth and enhancing the recovery of hematopoietic system postirradiation in mice. *Cancer Lett* 1997; **111**: 7-13

5 **Diaz AM,** Abad MJ, Fernandez L, Recuero C, Villaescusa L, Silvan AM, Bermejo P. In vitro anti-inflammatory activity of iridoids and triterpenoid compounds isolated from Phillyrea latifolia L. *Biol Pharm Bull* 2000; **23**:1307-1313

6 **Baricevic D,** Sosa S, Della Loggia R, Tubaro A, Simonovska B, Krasna A, Zupancic A. Topical anti-inflammatory activity of Salvia officinalis L. leaves: the relevance of ursolic acid. *J Ethnopharmacol* 2001; **75**: 125-132

7 **Min BS,** Jung HJ, Lee JS, Kim YH, Bok SH, Ma CM, Nakamura N, Hattori M, Bae K. Inhibitory effect of triterpenes from Crataegus pinatifida on HIV-I protease. *Planta Med* 1999; **65**: 374-375

8 **Raphael TJ,** Kuttan G. Effect of naturally occurring triterpenoids glycyrrhizic acid, ursolic acid, oleanolic acid and nomilin on the immune system. *Phytomedicine* 2003; **10**: 483-489

9 **Banno N,** Akihisa T, Tokuda H, Yasukawa K, Higashihara H, Ukiya M, Watanabe K, Kimura Y, Hasegawa J, Nishino H. Triterpene acids from the leaves of Perilla frutescens and their anti-inflammatory and antitumor-promoting effects. *Biosci Biotechnol Biochem* 2004; **68**: 85-90

10 **Tokuda H,** Ohigashi H, Koshimizu K, Ito Y. Inhibitory effects of ursolic and oleanolic acid on skin tumor promotion by 12-O-tetradecanoylphorbol-13-acetate. *Cancer Lett* 1986; **33**: 279-285

11 **Subbaramaiah K,** Michaluart P, Sporn MB, Dannenberg AJ. Ursolic acid inhibits cyclooxygenase-2 transcription in human mammary epithelial cells. *Cancer Res* 2000; **60**: 2399-2404

12 **Mizushina Y,** Iida A, Ohta K, Sugawara F, Sakaguchi K. Novel triterpenoids inhibit both DNA polymerase and DNA topoisomerase. *Biochem J* 2000; **350 Pt 3**: 757-763

13 **Shishodia S,** Majumdar S, Banerjee S, Aggarwal BB. Ursolic acid inhibits nuclear factor-kappaB activation induced by carcinogenic agents through suppression of IkappaBalpha kinase and p65 phosphorylation: correlation with down-regulation of cyclooxygenase 2, matrix metalloproteinase 9, and cyclin D1. *Cancer Res* 2003; **63**: 4375-4383

14 **Liu J,** Liu Y, Mao Q, Klaassen CD. The effects of 10 triterpenoid compounds on experimental liver injury in mice. *Fundam Appl Toxicol* 1994; **22**: 34-40

15 **Saraswat B,** Visen PK, Agarwal DP. Ursolic acid isolated from Eucalyptus tereticornis protects against ethanol toxicity in isolated rat hepatocytes. *Phytother Res* 2000; **14**: 163-166

16 **Ovesna Z,** Vachalkova A, Horvathova K, Tothova D. Pentacyclic triterpenoic acids: new chemoprotective compounds. Minireview. *Neoplasma* 2004; **51**: 327-333

17 **Tian Z,** Yang M, Huang F, Li K, Si J, Shi L, Chen S, Xiao P. Cytotoxicity of three cycloartane triterpenoids from Cimicifuga dahurica. *Cancer Lett* 2005; **226**: 65-75

18 **Miyase T,** Shiokawa KI, Zhang DM, Ueno A. Araliasaponins I-XI, triterpene saponins from the roots of Aralia decaisneana. *Phytochemistry* 1996; **41**: 1411-1418

19 **Sambrook J,** Fritsch E F, Maniatis T, In Molecular cloning, A Laboratory Manual, 2nd ED.; Cold Spring Harbor Laboratory press: New York, 1989

20 **Chen WF,** Huang MH, Tzang CH, Yang M, Wong MS. Inhibitory actions of genistein in human breast cancer (MCF-7) cells. Biochim Biophys Acta 2003; 1638: 187-196

21 **Livak KJ,** Schmittgen TD. Analysis of relative gene expression data using real-time quantitative PCR and the 2(-Delta Delta C(T)) Method. *Methods* 2001; **25**: 402-408

22 **Setzer WN,** Setzer MC. Plant-derived triterpenoids as potential antineoplastic agents. *Mini Rev Med Chem* 2003; **3**: 540-556

23 **Kujubu DA,** Fletcher BS, Varnum BC, Lim RW, Herschman HR. TIS10, a phorbol ester tumor promoter-inducible mRNA from Swiss 3T3 cells, encodes a novel prostaglandin synthase/cyclooxygenase homologue. *J Biol Chem* 1991; **266**: 12866-12872

24 **Jones DA,** Carlton DP, McIntyre TM, Zimmerman GA, Prescott SM. Molecular cloning of human prostaglandin endoperoxide synthase type II and demonstration of expression in response to cytokines. *J Biol Chem* 1993; **268**: 9049–9054

25 **DuBois RN,** Awad J, Morrow J, Roberts LJ 2nd, Bishop PR. Regulation of eicosanoid production and mitogenesis in rat intestinal epithelial cells by transforming growth factor-alpha and phorbol ester. *J Clin Invest* 1994; **93**: 493-498

26 **Eberhart CE,** Coffey RJ, Radhika A, Giardiello FM, Ferrenbach S, DuBois RN. Up-regulation of cyclooxygenase 2 gene expression in human colorectal adenomas and adenocarcinomas. *Gastroenterology* 1994; **107**: 1183-1188

27 **Tucker ON,** Dannenberg AJ, Yang EK, Zhang F, Teng L, Daly JM, Soslow RA, Masferrer JL, Woerner BM, Koki AT, Fahey TJ 3rd. Cyclooxygenase-2 expression is up-regulated in human pancreatic cancer. *Cancer Res* 1999; **59**: 987-990

28 **Buecher B,** Broquet A, Bouancheau D, Heymann MF, Jany A, Denis MG, Bonnet C, Galmiche JP, Blottiere HM. Molecular mechanisms involved in the antiproliferative effect of two COX-2 inhibitors, nimesulide and NS-398, on colorectal cancer cell lines. *Dig Liver Dis* 2003; **35**: 557-565

29 **Detjen KM,** Welzel M, Wiedenmann B, Rosewicz S. Nonsteroidal anti-inflammatory drugs inhibit growth of human neuroendocrine tumor cells via G1 cell-cycle arrest. *Int J Cancer* 2003; **107**: 844-853

30 **Narayanan BA,** Condon MS, Bosland MC, Narayanan NK, Reddy BS. Suppression of N-methyl-N-nitrosourea/testosterone-induced rat prostate cancer growth by celecoxib: effects on cyclooxygenase-2, cell cycle regulation, and apoptosis mechanism(s). *Clin Cancer Res* 2003; **9**: 3503-3513

31 **Kim DK,** Baek JH, Kang CM, Yoo MA, Sung JW, Chung HY, Kim ND, Choi YH, Lee SH, Kim KW. Apoptotic activity of ursolic acid may correlate with the inhibition of initiation of DNA replication. *Int J Cancer* 2000; **87**: 629-636

32 **Yamagishi N,** Saito Y, Ishihara K, Hatayama T. Enhancement of oxidative stress-induced apoptosis by Hsp105alpha in mouse embryonal F9 cells. *Eur J Biochem* 2002; **269**: 4143-4151

33 **Yamagishi N,** Ishihara K, Saito Y, Hatayama T. Hsp105alpha enhances stress-induced apoptosis but not necrosis in mouse embryonal f9 cells. *J Biochem* 2002; **132**: 271-278

34 **Castelli C,** Rivoltini L, Rini F, Belli F, Testori A, Maio M, Mazzaferro V, Coppa J, Srivastava PK, Parmiani G. Heat shock proteins: biological functions and clinical application as personalized vaccines for human cancer. *Cancer Immunol Immunother* 2004; **53**: 227-233

35 **Wadhwa R,** Sugihara T, Yoshida A, Nomura H, Reddel RR, Simpson R, Maruta H, Kaul SC. Selective toxicity of MKT-077 to cancer cells is mediated by its binding to the hsp70 family protein mot-2 and reactivation of p53 function. *Cancer Res* 2000; **60**: 6818-6821


**S- Editor** Wang XL and Guo SY **L- Editor** Elsevier HK **E- Editor** Liu WF

PO Box 2345, Beijing 100023, China
www.wjgnet.com
wjg@wjgnet.com

World J Gastroenterol 2006 February 14; 12(6): 880-884
World Journal of Gastroenterology ISSN 1007-9327
© 2006 The WJG Press. All rights reserved.

LIVER CANCER

# Role of CD80 in stimulating T lymphocyte activation

De-Chun Li, Xing-Guo Zhu, Yong Zhang, Jian-Xin Fu

De-Chun Li, Xing-Guo Zhu, Yong Zhang, Jian-Xin Fu, Department of General Surgery, the First Affiliated Hospital of Soochow University, Suzhou 215006, Jiangsu Province, China
Correspondence to: Xing-Guo Zhu, Department of General Surgery, the First Affiliated Hospital of Soochow University, 96 Shizi Road, Suzhou 215006, Jiangsu Province, China. zxg45@hotmail.com
Telephone: +86-512-62003650 Fax: +86-512-65223637
Received: 2005-03-15 Accepted: 2005-04-02

## Abstract

**AIM:** To observe biological characteristics of hepatocarcinoma cells before and after CD80 transfection and to compare the effect of CD80-transfected hepatocarcinoma cells on T lymphocyte activation.

**METHODS:** Retro virus vector carrying CD80 gene was transfected into HepG2 cells to establish CD80-transfected hepatocarcinoma cells (HepG2/hCD80). Flow cytometry (FCM) was performed to detect CD80 expression in the transfected cells. RT-PCR was used to evaluate CD80 expression at mRNA level. In the presence of anti-CD3 mAb, the proliferation of T lymphocyte was observed by MTT. Meanwhile, the expression of activated molecule marker CD25 was analyzed through FCM.

**RESULTS:** A stable cell line HepG2/hCD80 expressing the human CD80 was established. Growth curve showed that the molecule CD80 could obviously decrease the growth of tumor cells. HepG2/hCD80 was evidenced to have a potency to enhance T cell proliferation and up-regulate CD25 expression.

**CONCLUSION:** CD80 transfection can lower malignant phenotype of hepatocarcinoma cells. CD80 transfection has a down-regulatory effect to activated T cells *in vitro*.

© 2006 The WJG Press. All rights reserved.

**Key words:** Hepatocarcinoma cells; CD80; Transfection; T lymphocyte activation

Li DC, Zhu XG, Zhang Y, Fu JX. Role of CD80 in stimulating T lymphocyte activation. *World J Gastroenterol* 2006; 12(6): 880-884

http://www.wjgnet.com/1007-9327/12/880.asp

## INTRODUCTION

It has been widely accepted that T cell activation in the course of anti-tumor immunity requires two distinct signals for T helper precursor cell expansion[1,2]. Optimal activation of antigen-specific T cells requires not only the engagement of T-cell receptor (TCR) with Ag/major histocompatibility complex (MHC), but also co-stimulatory signals provided by antigen-presenting cells[3,4]. Among the interactions of these co-stimulatory molecules, ligation of CD28/CTLA-4 and CD86 or CD80 is regarded as a major signal transduction pathway[5]. As the first identified B7 family member, CD80 is widely expressed in a broad spectrum of tissues, even on some malignant tumor cells, thereby suggesting the potential mechanism of immune evasion of tumor cells[6]. Cancer of the liver is regarded as a tumor of low immunogenicity. Although there is a high level of HLA I expression on the surface of hepatocarcinoma cells, it still has a low immunogenicity due to the absence or low expression of CD80[7]. In this study, we established a CD80-transfected hepatocarcinoma cell line to observe the characteristic of HepG2/hCD80 and make further investigation on the role it plays in T cell activation.

## MATERIALS AND METHODS

### Materials

Retro virus vector pLNShB7 carrying hCD80 was presented by Professor Lu Daru of Fudan University. Package cell (singlephilic GP+E86, doublephilic GP+envAm12) and fibroblast cell NIH3T3 were kept by Jiangsu Hematological Research Institute and cultured in DMEM supplemented with 150 mL/L new born calf serum (NCS), and incubated at 37 °C in a humidified atmosphere containing 50 mL/L $CO_2$ in air. Hepatocarcinoma cell line HepG2 was purchased from Shanghai Zhongshang Hospital, cultured in RPMI 1640 medium supplemented with 150 mL/L NCS, and incubated at 37 °C in a humidified atmosphere containing 50 mL/L $CO_2$ in air. ELISA kit was purchased from Shanghai Senxiong Biological Co., Ltd. Mouse *Ig*G-PE or *Ig*G-FITC was purchased from Immunotech Company. MTT kit was purchased from Sigma Company. The mouse anti-human CD80 mAb was kindly gifted by Dr. Qiu Yuhua, Immunology Research Institute of Suzhou University.

### Vector transduction and production of envAm12/CD80

Plasmid pLNShCD80 was transfected into *E. coli* JM109 and was confirmed by *Eco*RI. Purified vector DNA was transfected into GP+E86 cells using Lipofectamine. Singlephilic GP+E86/CD80 cells were selected by G418

(0.6 g/L) and then Ping-pong transfection strategy was adopted to produce doublephilic GP+envAm12/CD80. Supernatant of GP+envAm12/CD80 was collected and stored at –80 °C.

### CD80 virus transduction into HepG2 cells

HepG2 cells were incubated in Petri dish until they grew to 60% confluence. Then, the culture medium was replaced with 1:1 mixed virus supernatant and culture medium containing Polybrene at the final concentration of 4 mg/L. Such transduction process was repeated after a 3-h incubation at 37 °C. After 24 h, the cells were digested and adjusted to proper concentration for selective culture in medium with G418 (0.6 g/L). The empty vector-transfected HepG2 (HepG2/mock) cells were prepared as a negative control in the following experiment.

### Integration of CD80 gene

PCR was adopted to integrate NeoR gene in target cells and hCD80 gene. Primers for NeoR gene: 5'-CGTTG TCACT GAAGC GGGAA GG-3'. Primers for hCD80: 5'-ATTTT CTTCT CCTTT TGCCA GTAG-3'. Samples were initially denatured for 5 min at 95 °C. Gene amplification was conducted for 32 cycles, each cycle consisted of denaturation at 94 °C for 45 s, annealing at 58 °C for 45 s, and polymerization at 72 °C for 2 min, followed by an extra incubation at 72 °C for 7 min to ensure full extension of the products. Products of amplification were analyzed on 12 g/L agarose gels in Tris –borate–EDTA, and stained with ethidium bromide.

### Detection of CD80 expression by FCM

CD80-transfected HepG2 cells were cultured with anti-CD80 mAb (2 mg/L) at 4 °C for 30 min. After being washed twice, the FITC-goat anti-mouse *Ig*G as secondary antibody was added, followed by incubation at 4 °C for 30 min. Then flow cytometry (FCM) was performed to detect the expression of CD80 after washes.

### CD80 expression analysis by RT-PCR

Total RNA was isolated from $10^6$ transfected cells with TRIzol reagents (Takara, Dalian, China) following the manufacturer's instructions. Using the total RNA as template, the first-strand cDNA of CD80 was obtained with oligo (dT) as a reverse primer following the manufacturer's protocol. Then the PCR amplification was carried out under the similar PCR conditions with the primers mentioned above.

### Proliferation analysis of HepG2 and HepG2/hCD80 cells

The HepG2/hCD80 or HepG2/mock cells were seeded onto a 24-well plate with $1\times10^5$/well. During the 8-day culture, cells' status was detected every day for an average value. According to the results, curves of cell growth were drawn and multiple proliferation time was calculated by the following formula: times of growth=maximum living cell number/living cell number of inoculation; multiple proliferation time=time from inoculation to the maximum cell number/time of growth.

### Isolation of T lymphocytes

Two milliliters fresh peripheral blood was diluted with Hanks' balanced salt solution at a ratio of 1:3 and subjected to separation by 10 mL Ficoll density-gradient centrifugation at 2 000 r/min for 20 min. Then turbid fluid containing T cells was collected and subjected to another 10 mL Ficoll. After being washed twice with Hanks' balanced salt solution and separated by density-gradient centrifugation at 1 500 r/min for 15 min, the isolated T cells were cultured in RPMI 1640 at 37 °C in a humidified atmosphere containing 50 mL/L $CO_2$ in air. Through the detection by FCM with PE-labeled anti-CD3 mAb, the T cell purification was about 70%.

### Preparation of tumor vaccine

About $1\times10^6$ HepG2/CD80 or HepG2/mock cells were collected separately for Co-60 radiation (100 Gy) and then cultured in RPMI 1640 at 37 °C in a humidified atmosphere containing 50 mL/L $CO_2$ in air for further usage.

### Detection of proliferation index (PI)

HepG2/CD80 or HepG2/mock cells were seeded onto 96-well plates with 200 μL/well. Each was divided into two groups, and three double wells were set for each group. Lymphocytes were added into each well according to E:T ratio of 1:10. The mixture of lymphocytes and tumor cells was cultured in RPMI 1640 at 37 °C in a humidified atmosphere containing 50 mL/L $CO_2$ in air. After a 3-day culture, MTT solution was added to each well to the final concentration of 10 g/L and the cells were further incubated for 5 h. Then 100 μL of isopropylalcohol was added to dissolve the crystal after the supernatant was removed by centrifugation at 3 000 r/min for 5 min and the wells were washed thrice with PBS. Then the absorbance of solution of each well was measured at 570 nm by a microplate reader (Bio-Rad). All the measurements were separately performed in triplicate. PI was calculated using the formula: PI=($A_{570}$ nm of HepG2/hCD80–$A_{570}$ nm of HepG2/mock well)/$A_{570}$ nm of lymphocytes in each well.

### Analysis of surface antigen expression

HepG2/CD80 or HepG2/mock cells were seeded onto 24-well plates. Lymphocytes were added into each well according to E:T ratio of 1:10. The mixture of lymphocytes and tumor cells was cultured in RPMI 1640 at 37 °C in a humidified atmosphere containing 50 mL/L $CO_2$ in air. After 2-, 5- and 7-day co-cultures, the lymphocytes, respectively, were stained with FITC-CD4 mAb, FITC-CD8 mAb, and FITC-CD25 mAb and incubated for 30 min, washed again with PBS. FCM was performed to detect the expressions of CD4, CD8, and CD25 on the surface of T cells.

### Statistical analysis

The data was statistically analyzed by two-sided *t*-test, and $P\leqslant0.01$ was considered statistically significant. Values were expressed as mean±SD.

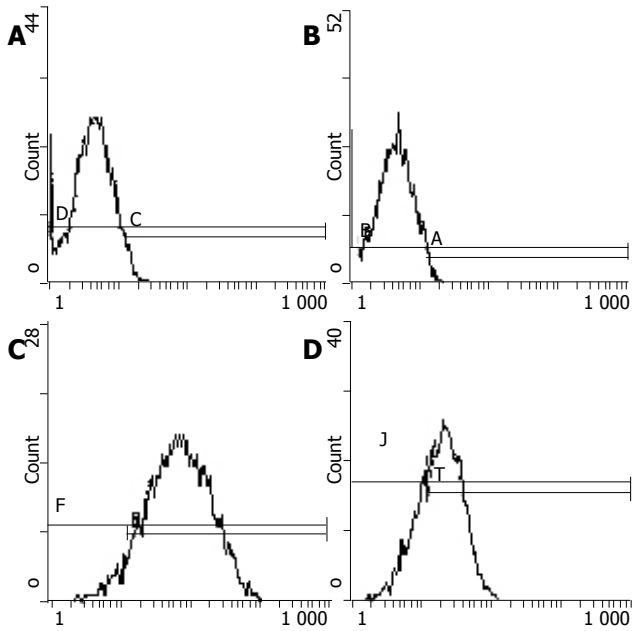


**Figure 1** Flow cytometric analysis of CD80 expression in cells of different groups. **A**: HepG2/mock; **B**: negative control; **C**: HepG2/hCD80; **D**: positive control.

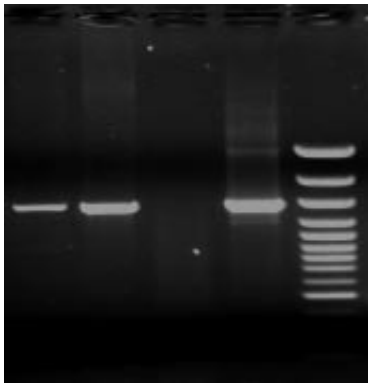

**Figure 2** RT-PCR analysis of CD80 mRNA expression in different group cells. M: DL1000 molecule marker; lane 1: β-action; lane 2: positive control; lane 3: HepG2/mock; lane 4: HepG2/hCD80 cells.

## RESULTS

### *Stable expression of CD80 in HepG2 cells*

Retro virus vector pLNShB7 was transfected into HepG2 cells with the help of GP+envAm12 package cell. Drug resistant strains were selected by G418 to obtain doublephilic GP+envAm12/CD80 clones. FCM analysis showed that the expression of CD80 reached a rather high level (Figure 1). RT-PCR result further confirmed the expression of CD80 in the transfected cells at mRNA level (Figure 2).

### *Curve of cell growth and time of multiple proliferations*

During 8 d of culture, the cells were counted each day for an average value. Curve of cell growth was drawn according to the results (Figure 3), which showed that the curve of HepG2/hCD80 cells was rising up very slowly, indicating that the growth ratio of HepG2/hCD80 cells was obviously lower compared to HepG2/mock cells. Multiple proliferation time of HepG2 cells was 13.86 h, while that of HepG2/hCD80 was 25.09 h.

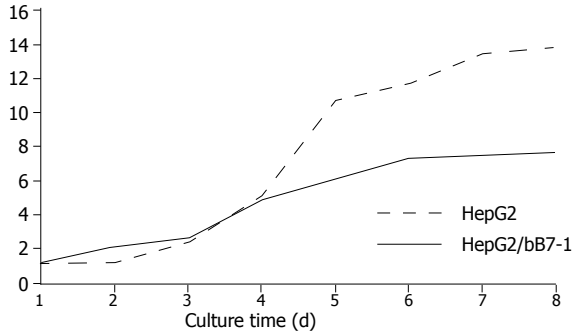


**Figure 3** Curve of cell growth and time of multiple proliferation.

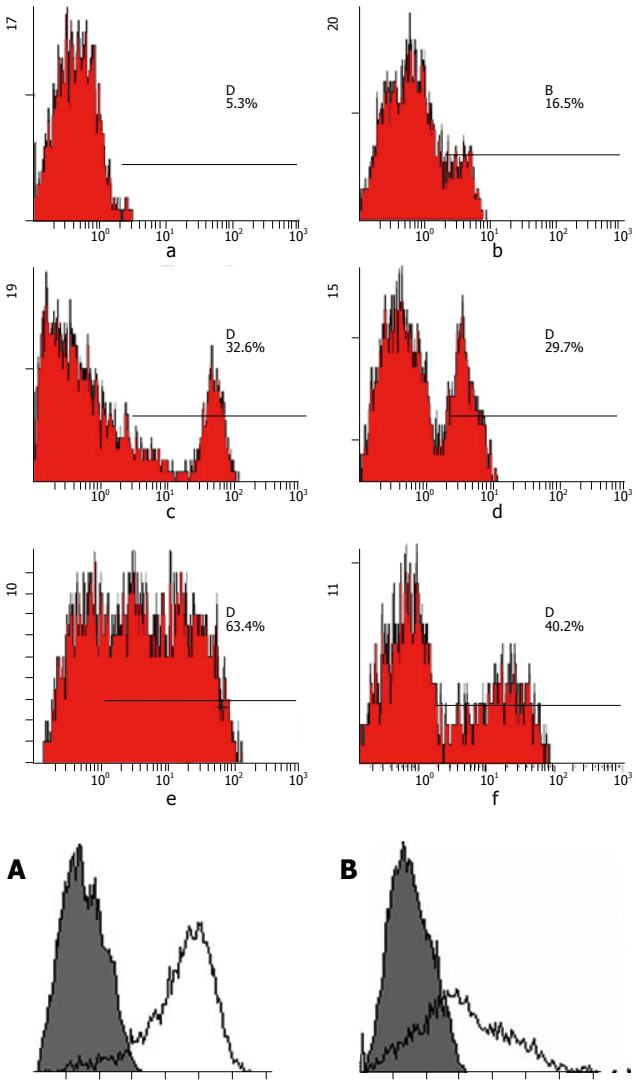


**Figure 4** CD25 expression on T cells stimulated by HepG2/mock cells or HepG2/hCD80 cells. **A**: T cells stimulated by HepG2/hCD80 cells; **B**: T cells stimulated by HepG2/mock cells. Shaded histograms show reactivity with the isotype control. Each figure is representative of at least three experiments.

### *Surface molecular expression of T cells stimulated by HepG2/hCD80*

After Co-60 radiation, HepG2/mock or HepG2/hCD80 cells were mixed with lymphocytes and cultured together. FCM was used to detect surface molecular expression in T cells on days 2, 5, and 7. The results showed that CD4,

CD8, and CD25 expressions were obviously higher in HepG2/hCD80 group than in HepG2/mock group on day 5 (Figure 4).

### *T cell proliferation stimulated by HepG2/hCD80*

HepG2/CD80 or HepG2/mock cells were mixed with lymphocytes and cultured together as described above. After a 3-day co-culture, lymphocyte proliferation was examined by MTT. The results showed that PI of HepG2/hCD80 group (1.25±0.12) was obviously higher than that of HepG2 group (0.43±0.07, $P<0.01$).

## DISCUSSION

Immune response of solid tumor is mainly cell immunity whose major effector cells are T lymphocytes. An optimal initiation of antigen-specific lymphocytes requires a combination of signals 1 and 2 (co-stimulatory signals). Hepatocarcinoma was regarded as a tumor of absent or low immunogenicity. Through testing different hepatocarcinoma cell lines, Tatsumi *et al.*[8] discovered that only high level MHC-II molecules were expressed on the surface of hepatocarcinoma cells, while the expression levels of CD80 and CD86 turned to be very low. Although mRNA of both CD80 and CD86 was detected, the concentration was very low. Using FCM, we also examined CD80 expression level on the surface of HepG2 cells, which showed that only a few HepG2 cells expressed CD80 molecule with a percentage of only 3.66%. Obvious differentiation was found compared with positive control group. RT-PCR showed that human CD80 mRNA was about 605-bp in length (Figure 2), which was consistent with that of FCM results. Taken together the present and previous studies, we speculated that absence of CD80 expression contributed to the low immunogenicity of HepG2 cells.

CD80, a glycoprotein of 44/45 ku, is mainly expressed on activated B lymphocytes, macrophages and dendritic cells as well as tissues of chronic infection and tumor cells[9]. Our experiment demonstrated that only a low level of CD80 expression was detected on the surface of HepG2 cells. Researches showed that some cytokines could upregulate CD80 expression on many kinds of cells. For example, IL-2 and IL-4 are able to enhance CD80 expression on B lymphocytes[2]. But, generally speaking CD80 expression, even under above stimulation, is yet relatively low and unable to stimulate effective anti-tumor immune response. Therefore, by means of highly effective CD80 gene transfection to enhance B7 molecule expression at gene level, signal 2 was regained so as to effectively trigger anti-tumor immune response.

To effectively transfect CD80 gene, a vector of high efficiency and fewer side effects is necessary. Retro virus vector, at present, is a vector most widely used in the study of gene therapy. With this kind of vector, IL-2, p53 and other therapeutic genes could be transferred with high efficiency into hepatocarcinoma cells[10]. So, we adopted retro virus as a carrier of CD80 gene. After selection by G418, FCM analysis showed that the positive ratio of HepG2/hCD80 group was about 92.2%, 28 times higher than the control group. Thus, a clone stably expressing CD80 molecule was established, host cell HepG2 regained the ability of transducting the second signal, which is necessary to trigger T cell immune response.

By CD80 transfection, we not only established positive clones highly expressing CD80 molecules but also found that the growth curve of HepG2/hCD80 cells was rising up very slowly with the growth ratio obviously lower than that of HepG2 cells. Multiple proliferation time of HepG2/hCD80 was markedly longer than that of HepG2 ($P<0.01$). So, CD80 transfection might change the status of tumor cells, while there is still a long way to go before clarifying its underlying molecular mechanisms.

T cell activation is crucial to immune response. After activation, a series of biochemical reactions occur, including signal transduction, gene activation and transcription, new molecule expression on cell surface, cytokine secretion and cells entering proliferation cycles[11]. Following activation, interaction between IL-2 and IL-2R plays an important role in T cell proliferation[12]. Absence of co-stimulatory signals might lead to T cell anergy, which could be explained by IL-2 decrease or no-response on IL-2 stimulation. On the surface of T cells, there are two IL-2 receptors, one is p55 (CD25) the other is p75 which has a relatively higher affinity, both have low affinity to IL-2[13]. Resting T cells just express p75 and not p55, so it could only be activated by highly concentrated IL-2[14]. A study showed that by the positive-feedback regulation of IL-2, CD25 could rapidly express and form complex with p75 to enhance the affinity of IL-2 and T cells[15]. In this way, biological effects could be fully exerted with low level of IL-2 stimulation. After CD80 transfection, our experiment showed that CD25 expression on T cell surface was greatly improved and was obviously higher compared to control group, which may be explained by cascade effects of immune system[16].

Enhancement of CD4 and CD8 expressions on T cell surface means the improvement of combined ability between TCR and MHC-I or MHC-II molecules[17]. Compared with HepG2 group, HepG2/hCD80 group showed markedly increased CD4 and CD8 molecules and actively proliferated T cells, suggesting that the malignant status of hepatocarcinoma cells might be changed and enhancement of co-stimulatory signal could effectively stimulate T cell activation so as to exert strong anti-tumor effects.

## REFERENCES


1 **Zhang H**, Haasch D, Idler KB, Okasinski GF. Isolation and promoter mapping of the gene encoding murine co-stimulatory factor B7-1. *Gene* 1996; **183:** 1-6

2 **Ranheim EA,** Kipps TJ. Tumor necrosis factor-alpha facilitates induction of CD80 (B7-1) and CD54 on human B cells by activated T cells: complex regulation by IL-4, IL-10, and CD40L. *Cell Immunol* 1995; **161**: 226-235

3 **Chambers CA.** The expanding world of co-stimulation: the two-signal model revisited. *Trends Immunol* 2001; **22**: 217-223

4 **Gause WC,** Halvorson MJ, Lu P, Greenwald R, Linsley P, Urban JF, Finkelman FD. The function of costimulatory molecules and the development of IL-4-producing T cells. *Immunol Today* 1997; **18**: 115-120

5 **Gerstmayer B,** Pessara U, Wels W. Construction and expression in the yeast Pichia pastoris of functionally active soluble

forms of the human costimulatory molecules B7-1 and B7-2 and the B7 counter-receptor CTLA-4. *FEBS Lett* 1997; **407**: 63-68

6 **Yeh KY,** Pulaski BA, Woods ML, McAdam AJ, Gaspari AA, Frelinger JG, Lord EM. B7-1 enhances natural killer cell-mediated cytotoxicity and inhibits tumor growth of a poorly immunogenic murine carcinoma. *Cell Immunol* 1995; **165**: 217-224

7 **Dessureault S**, Gallinger S. Allogeneic lymphocyte responses to B7-1 expressing human cancer cell lines. *J Surg Res* 1996; **64:** 42-48

8 **Tatsumi T,** Takehara T, Katayama K, Mochizuki K, Yamamoto M, Kanto T, Sasaki Y, Kasahara A, Hayashi N. Expression of costimulatory molecules B7-1 (CD80) and B7-2 (CD86) on human hepatocellular carcinoma. *Hepatology* 1997; **25**: 1108-1114

9 **Wang SD,** Chen LP. Immune regulation of B7-CD28. *Shanghai Mianyixue Zazhi* 2003; **23**: 1-5

10 **Felzmann T,** Ramsey WJ, Blaese RM. Anti-tumor immunity generated by tumor cells engineered to express B7-1 via retroviral or adenoviral gene transfer. *Cancer Lett* 1999; **135**: 1-10

11 **Xu P**, Qian M. A new mechanism of T cell activation-synapse. *Guowai Yixue Mianyixue Fence* 2001; **24:** 225-227

12 **Chen Y**, Yan MS, Wei Q. Calcieurin and NFAT in T cell activation. *Guowai Yixue Mianyixue Fence* 1999; **22:** 225-228

13 **Linsley PS,** Brady W, Grosmaire L, Aruffo A, Damle NK, Ledbetter JA. Binding of the B cell activation antigen B7 to CD28 costimulates T cell proliferation and interleukin 2 mRNA accumulation. *J Exp Med* 1991; **173**: 721-730

14 **Phillips JH,** Takeshita T, Sugamura K, Lanier LL. Activation of natural killer cells via the p75 interleukin 2 receptor. *J Exp Med* 1989; **170**: 291-296

15 **Schulz O,** Sewell HF, Shakib F. Proteolytic cleavage of CD25, the alpha subunit of the human T cell interleukin 2 receptor, by Der p 1, a major mite allergen with cysteine protease activity. *J Exp Med* 1998; **187**: 271-275

16 **Tanaka Y,** Albelda SM, Horgan KJ, van Seventer GA, Shimizu Y, Newman W, Hallam J, Newman PJ, Buck CA, Shaw S. CD31 expressed on distinctive T cell subsets is a preferential amplifier of beta 1 integrin-mediated adhesion. *J Exp Med* 1992; **176**: 245-253

17 **Rabinowitz R**, Hadar R, Schlesinger M. The appearance of the CD4+CD8+ phenotype on activated T cells: possible role of antigen transfer. *Hum Immunol* 1997; **55:** 1-10

**S- Editor** Kumar M and Guo SY **L- Editor** Elsevier HK **E- Editor** Liu WF

PO Box 2345, Beijing 100023, China
www.wjgnet.com
wjg@wjgnet.com

*World J Gastroenterol* 2006 February 14; 12(6): 885-895
***World Journal of Gastroenterology*** ISSN 1007-9327
© 2006 The WJG Press. All rights reserved.

*BASIC RESEARCH*

# Characterization of $H^+$ and $HCO_3^-$ transporters in CFPAC-1 human pancreatic duct cells

Zoltán Rakonczay Jr, Amy Fearn, Péter Hegyi, Imre Boros, Michael A Gray, Barry E Argent

Zoltán Rakonczay Jr, Amy Fearn, Péter Hegyi, Michael A Gray, Barry E Argent, Institute for Cell and Molecular Biosciences, University of Newcastle upon Tyne, Medical School, Newcastle upon Tyne NE2 4HH, United Kingdom
Zoltán Rakonczay Jr, Péter Hegyi, First Department of Medicine, Faculty of Medicine, University of Szeged, H-6720 Szeged, Hungary
Imre Boros, Hungarian Academy of Sciences, Biological Research Center, Institute of Biochemistry, H-6726 Szeged, Hungary
Supported by a Wellcome Trust Travelling Fellowship to Z.R., No. 069470, and a Wellcome Trust IRDA Grant to P.H., No. 068096
Correspondence to: Professor Barry E Argent, Institute for Cell and Molecular Biosciences, University of Newcastle upon Tyne, Medical School, Framlington Place, Newcastle upon Tyne NE2 4HH, United Kingdom. b.e.argent@ncl.ac.uk
Telephone: +44-191-222-7009 Fax: +44-191-222-7424
Received: 2005-07-18 Accepted: 2005-08-03

## Abstract

**AIM:** To characterize $H^+$ and $HCO_3^-$ transporters in polarized CFPAC-1 human pancreatic duct cells, which were derived from a cystic fibrosis patient with the ΔF508 CFTR mutation.

**METHODS:** CFPAC-1 cells were seeded at high density onto permeable supports and grown to confluence. The cells were loaded with the pH-sensitive fluorescent dye BCECF, and mounted into a perfusion chamber, which allowed the simultaneous perfusion of the basolateral and apical membranes. Transmembrane base flux was calculated from the changes in intracellular pH and the buffering capacity of the cells.

**RESULTS:** Our results showed differential permeability to $HCO_3^-/CO_2$ at the apical and basolateral membranes of CFPAC-1 cells. $Na^+/HCO_3^-$ co-transporters (NBCs) and $Cl^-/HCO_3^-$ exchangers (AEs) were present on the basolateral membrane, and $Na^+/H^+$ exchangers (NHEs) on both the apical and basolateral membranes of the cells. Basolateral $HCO_3^-$ uptake was sensitive to variations of extracellular $K^+$ concentration, the membrane permeable carbonic anhydrase (CA) inhibitors acetazolamide (100 μmol/L) and ethoxyzolamide (100 μmol/L), and was partially inhibited by $H_2$-DIDS (600 μmol/L). The membrane-impermeable CA inhibitor 1-*N*-(4-sulfamoylphenylethyl)-2,4,6-trimethylpyridine perchlorate did not have any effect on $HCO_3^-$ uptake. The basolateral AE had a much higher activity than that in the apical membrane, whereas there was no such difference with the NHE under resting conditions. Also, 10 μmol/L forskolin did not significantly influence $Cl^-/HCO_3^-$ exchange on the apical and basolateral membranes. The administration of 250 μmol/L $H_2$-DIDS significantly inhibited the basolateral AE. Amiloride (300 μmol/L) completely inhibited NHEs on both membranes of the cells. RT-PCR revealed the expression of pNBC1, AE2, and NHE1 mRNA.

**CONCLUSION:** These data suggest that apart from the lack of CFTR and apical $Cl^-/HCO_3^-$ exchanger activity, CFPAC-1 cells express similar $H^+$ and $HCO_3^-$ transporters to those observed in native animal tissue.

© 2006 The WJG Press. All rights reserved.

**Key words:** CFPAC-1; Pancreatic duct cells; $HCO_3^-$; Intracellular pH

Rakonczay Z Jr, Fearn A, Hegyi P, Boros I, Gray MA, Argent BE. Characterization of $H^+$ and $HCO_3^-$ transporters in CFPAC-1 human pancreatic duct cells. *World J Gastroenterol* 2006; 12(6): 885-895

http://www.wjgnet.com/1007-9327/12/885.asp

## INTRODUCTION

There are two $HCO_3^-$ transport processes in the pancreatic ductal epithelium. The first is the secretion, mainly by the smaller ducts, of $HCO_3^-$ rich isotonic fluid that serves to flush digestive enzymes down the ductal tree and to neutralize gastric acid entering the duodenum[1,2]. The second $HCO_3^-$ transport process is the flow-dependent exchange of luminal $HCO_3^-$ for blood $Cl^-$ that is generally considered to occur in the larger ducts, including the main duct[1,2]. The physiological function of ductal $HCO_3^-$ absorption (or salvage) may be protective as it will lower luminal $HCO_3^-$ (and therefore luminal pH) during interdigestive periods when the flow is low or absent. A fall in luminal pH would reduce the activity of digestive enzymes within the static column of fluid in the ductal tree, thereby preventing damage to the ductal epithelium.

The initial step of $HCO_3^-$ secretion is the accumulation of $HCO_3^-$ within the duct cell[1,2]. This can occur by two

mechanisms: (1) the forward transport of $HCO_3^-$ by the $Na^+/HCO_3^-$ co-transporter (NBC); and (2) diffusion of $CO_2$ into the duct cell which is then hydrated to carbonic acid by carbonic anhydrase (CA), followed by the backward transport of protons via the $Na^+/H^+$ exchangers and $H^+$-pumps. The $HCO_3^-$ ions are then secreted across the apical membrane via $Cl^-/HCO_3^-$ exchangers (SLC26A3, DRA and SLC26A6, PAT1)[3] and/or cystic fibrosis transmembrane conductance regulator (CFTR) $Cl^-$ channels, which exhibit a finite permeability to $HCO_3^-$[4,5]. The exact mechanism how the SLC26 exchangers and apical $Cl^-$ channels produce a high $HCO_3^-$ secretion is controversial[1,2]. Nevertheless, the key role of CFTR in $HCO_3^-$ secretion is emphasized by the fact that the severity of the pancreatic phenotype in cystic fibrosis correlates best with the ability of mutant CFTRs to activate SLC26 exchangers, rather than their ability to conduct $Cl^-$ ions[6].

Rather less is known about the secondary, flow- and $Cl^-$-dependent absorption of $HCO_3^-$ that occurs in the larger ducts. A luminal $Na^+/H^+$ exchanger (NHE3) and an electroneutral NBC (SLC4A7, NBCn1, NBC3) have been identified in the main duct of the mouse pancreas and probably explain $HCO_3^-$ absorption across the apical membrane[7-9]. There is a clear evidence that activity of these luminal $HCO_3^-$ salvage transporters is downregulated following stimulation of $HCO_3^-$ secretion by a rise in intracellular cyclic AMP[7-9]. How the absorbed $HCO_3^-$ exits the duct cell at the basolateral membrane is uncertain, but a candidate pathway is the basolateral $Cl^-/HCO_3^-$ exchanger (possibly AE2)[10]. The AE2 must be switched off during stimulation as the prevailing ion gradients would favor $Cl^-$ uptake and $HCO_3^-$ efflux across the basolateral membrane.

Our current understanding of pancreatic ductal $HCO_3^-$ secretion/salvage is mainly based on the experiments performed in animal tissues[1]. Studies in human tissue have been largely confined to adenocarcinoma duct cell lines; however, with the exception of CAPAN-1, human duct cell lines do not express CFTR to any significant degree[11]. An alternative approach is to use CFPAC-1 cells, which were derived from a 26-year-old cystic fibrosis (CF) patient with the ΔF508 mutation[12]. The utility of CFPAC-1 cells is that they allow us to examine $HCO_3^-$ transport not only in the diseased state, but also in the corrected state by transfecting the cells with wild-type CFTR. A number of previous studies have shown that wild-type CFPAC-1 cells express some of the key transporters involved in $HCO_3^-$ secretion; e.g. the basolateral NBC[13], anion exchanger-2 and the apical $Cl^-/HCO_3^-$ exchangers DRA and PAT-1[14]. Moreover, the expression of apical $Cl^-/HCO_3^-$ exchangers was significantly increased in CFPAC-1 cells expressing functional CFTR, as was the stimulatory effect of ATP on luminal $Cl^-/HCO_3^-$ exchange[15]. CFPAC-1 cells can also be reconstituted as polarized monolayers on permeable supports and the effects of various agents, such as angiotensin II[16,17] and PKC[18], have been studied using the short circuit current technique. Finally, in one study a stimulatory effect of ATP on $HCO_3^-$ secretion from CFPAC cells was demonstrated by measuring the extracellular pH at the apical cell surface[19].

A number of issues regarding the mechanism of pancreatic ductal $HCO_3^-$ secretion remain controversial. For instance, how much of the secreted $HCO_3^-$ enters the lumen via CFTR and how much via SLC26 anion exchangers? How is coordinate regulation of apical and basolateral acid base transporters achieved during secretion and salvage? How do luminal signals regulate apical $HCO_3^-$ and $H^+$ transporters? What is the molecular explanation for the strong outward rectification of $HCO_3^-$ permeability exhibited by the apical membrane of the duct cell? A human pancreatic duct cell line, which reconstituted as a polarized monolayer allowing easy access to the luminal membrane, would be a very useful resource for answering these questions. An added bonus would be a model system that facilitates investigation of how CFTR expression affects duct cell transporters. Therefore, in this study, we aimed to establish whether polarized CFPAC-1 cells grown on permeable supports could fulfill these requirements. To do this, we investigated the $HCO_3^-$ permeability characteristics of the basolateral and apical membranes of CFPAC-1 cells, and the spatial distribution of acid/base transporters.

## MATERIALS AND METHODS

### *Materials and solutions*

All laboratory chemicals were purchased from Sigma (Poole, Dorset, UK). 2',7'-Bis-(2-carboxyethyl)-5(6)-carboxyfluorescein-acetoxymethyl ester (BCECF-AM) and dihydro-4,4'-diisothiocyanostilbene-2,2'-disulfonic acid ($H_2$-DIDS) were from Molecular Probes Inc. (Eugene, OR, USA); 1-*N*-(4-sulfamoylphenylethyl)-2,4,6-trimethylpyridine perchlorate (STP) was kindly provided by Prof. C Supuran. Stock solutions of BCECF (2 mmol/L), acetazolamide (0.4 mol/L), ethoxyzolamide (0.4 mol/L), amiloride (0.8 mol/L) and STP (10 mmol/L) were prepared in dimethyl sulfoxide (DMSO). Nigericin (10 mmol/L) and forskolin (50 mmol/L) were dissolved in ethanol and stored at -20 ℃. Polyester Transwells were supplied by Corning-Costar (Buckinghamshire, UK). The standard HEPES-buffered solution contained 130 mmol/L NaCl, 5 mmol/L KCl, 1 mmol/L $MgCl_2$, 1 mmol/L $CaCl_2$, 10 mmol/L Na-HEPES, and 10 mmol/L D-glucose (pH 7.4 with HCl). In the $Na^+$-free HEPES solution, NaCl was replaced by 140 mmol/L *N*-methyl-D-glucamine (NMDG)-Cl and the Na-HEPES was replaced by equimolar HEPES-acid. The $Cl^-$-free HEPES solution contained 140 mmol/L Na-gluconate, 2.5 mmol/L $K_2SO_4$, 6 mmol/L Ca-gluconate, 1 mmol/L Mg-gluconate, 10 mmol/L HEPES-acid, 10 mmol/L D-glucose (pH 7.4 with NaOH). The $Na^+/Cl^-$-free HEPES solution contained 130 mmol/L NMDG-gluconate, 2.5 mmol/L $K_2SO_4$, 1 mmol/L $MgSO_4$, 1 mmol/L $CaSO_4$, 10 mmol/L HEPES-acid, 10 mmol/L D-glucose (pH 7.4 with gluconate). The standard $HCO_3^-$ solution contained 115 mmol/L NaCl, 5 mmol/L KCl, 1 mmol/L $MgCl_2$, 1 mmol/L $CaCl_2$, 25 mmol/L Na-$HCO_3$, 10 mmol/L D-glucose. In the $K^+$-free $HCO_3^-$ solution, KCl was replaced with equimolar NaCl. The high $K^+$ $HCO_3^-$ solution contained the same ingredients as the standard $HCO_3^-$ solution but the KCl and NaCl concentrations were 115 and 5 mmol/L, respectively. The $Na^+$-free $HCO_3^-$ solution contained NMDG-Cl instead of NaCl and choline $HCO_3^-$ in place of $NaHCO_3$. $Cl^-$-free

$HCO_3^-$ solution contained 115 mmol/L sodium gluconate, 2.5 mmol/L $K_2SO_4$, 6 mmol/L Ca-gluconate, 1 mmol/L Mg-gluconate, 25 mmol/L Na-$HCO_3$, 10 mmol/L D-glucose. The $Na^+/Cl^-$-free $HCO_3^-$ solution contained 115 mmol/L NMDG-gluconate, 2.5 mmol/L $K_2SO_4$, 1 mmol/L $MgSO_4$, 1 mmol/L $CaSO_4$, 25 mmol/L choline-$HCO_3^-$, 10 mmol/L D-glucose (pH 7.4 with gluconate). 10 μmol/L atropine was added to the solutions containing choline to prevent the possible activation of muscarinic receptors. In solutions containing $NH_4^+$, the concentration of $Na^+$ or NMDG was replaced to maintain osmolarity. All the solutions containing $HCO_3^-$ were continuously equilibrated with 5% $CO_2$-95% $O_2$ to maintain pH at 7.4.

### Culture of CFPAC-1 cells

CFPAC-1 cells (passage number 27-60) were obtained from Prof. RA Frizzell (University of Pittsburgh, Pittsburgh, PA, USA) and were grown in Iscove's modified Dulbecco's medium supplemented with 100 mL/L fetal calf serum, 2 mmol/L glutamine, 100 units/mL penicillin and 0.1 mg/mL streptomycin and were cultured as described previously[12]. The media was changed every 1-2 d. Cells were maintained at 37 ℃ in a humidified atmosphere containing 5% $CO_2$. Cell monolayers were prepared by seeding at high density (300-350 cells/$cm^2$) onto polyester permeable supports (12 mm diameter, 0.4 μm pore size Transwells). Cell confluence was checked by microscopy and determination of transepithelial electrical resistance using an EVOM-G voltohmmeter (World Precision Instruments, Sarasota, FL, USA). Experiments were performed 4-6 d after seeding.

### Measurement of intracellular pH

Intracellular $pH_i$ was estimated with the pH-sensitive dye BCECF[20,21]. CFPAC-1 cells were loaded with 2 μmol/L BCECF-AM in both the apical and basal chambers in standard HEPES for 30-45 min at 37 ℃. After loading, the Transwells were transferred to a perfusion chamber mounted on an inverted Nikon Diaphot microscope (Nikon UK, Kingston upon Thames, UK). Apical and basal bath volumes were 0.5 and 1 mL and the perfusion rates were 3 and 6 mL/min, respectively. All the experiments started and ended with standard HEPES solution perfusing both sides of the cells. Experiments were performed at 37 ℃. $pH_i$ was measured using a Life Sciences Microfluorimeter System (Life Sciences Resources, Cambridge, UK). About 10-15 cells were alternately excited with wavelengths of 440 and 490 nm, and the 490/440 fluorescence emission ratio was recorded at 535 nm over a sampling period of 256 ms. The resting $pH_i$ of CFPAC-1 cells in standard HEPES solution was determined using the method described by Hegyi *et al.*[21]. Calibration of 490/440 ratio to $pH_i$ was obtained using the high-$K^+$/nigericin method. Extracellular pH was stepped between 5.94 and 8.46.

### Determination of buffering capacity

The intrinsic buffering capacity ($\beta_i$) of CFPAC-1 cells was estimated according to the $NH_4^+$ prepulse technique[22]. Briefly, the cells were exposed to varying concentrations of $NH_4Cl$ (0-30 mmol/L) while $Na^+$ and $HCO_3^-$ were omitted from the bath solution to block the $Na^+$- and $HCO_3^-$-dependent pH regulatory mechanisms. $\beta_i$ was estimated by the Henderson-Hasselbalch equation. The total buffering capacity ($\beta_{total}$) was calculated as $\beta_{total}=\beta_i+\beta_{HCO3^-}$, where $\beta_{HCO3^-}$ is the buffering capacity of the $HCO_3^-/CO_2$ system. $\beta_{HCO3^-}=2.3\times[HCO_3^-]_i$. $[HCO_3^-]_i$ is the intracellular concentration of $HCO_3^-$.

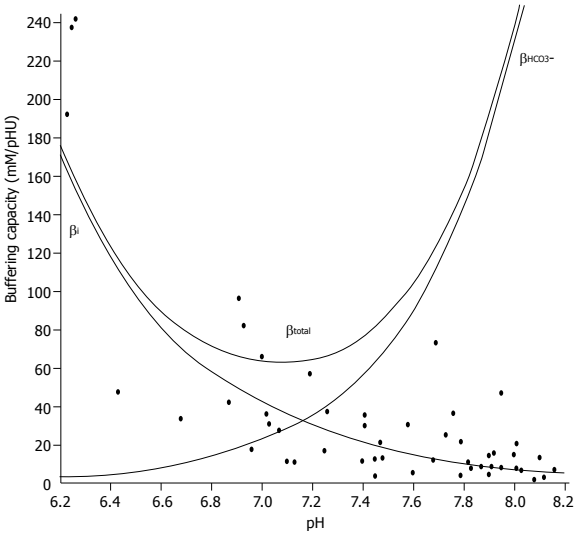


**Figure 1** Buffering capacity of CFPAC-1 human pancreatic duct cells at different $pH_i$ values. Polarized CFPAC-1 cells were exposed to varying concentrations of $NH_4Cl$ (0–30 mmol/L), while $Na^+$ and $HCO_3^-$ were omitted from the bath solution to block the $Na^+$ and $HCO_3^-$-dependent pH regulatory mechanisms. $\beta_i$ was estimated by the Henderson–Hasselbalch equation (n=50). The total buffering capacity ($\beta_{total}$) was calculated as $\beta_{total}=\beta_i+\beta_{HCO3^-}$, where $\beta_{HCO3^-}$ is the buffering capacity of the $HCO_3^-/CO_2$ system. $\beta_{HCO3^-}=2.3\times[HCO_3^-]_i$. $[HCO_3^-]_i$ is the intracellular concentration of $HCO_3^-$.

### Overall $\Delta pH_i$, base flux

The overall $\Delta pH_i$ was measured by determining the $pH_i$ immediately before and at the peak level during the administration of solutions containing $HCO_3^-/CO_2$ by averaging the values of 80 data points. The initial rates of $\Delta pH_i$ (over 30 s) were used to calculate transmembrane base flux $J$(B) using the equation $J(B)=\Delta pH_i/\Delta t*\beta_i$. The $\beta_i$ value used in the calculation of $J$(B)s was obtained from Figure 1 by using the average $pH_i$ value over a 30-s period immediately before the administration of $HCO_3^-/CO_2$ (virtually no $HCO_3^-$ in the cells). Therefore, we were most likely underestimating $J$(B) because of the increase in buffering capacity as $HCO_3^-$ fluxes into the cell during the administration of the basolateral $HCO_3^-/CO_2$ solution. The only time we used $\beta_{total}$ to calculate $J$(B) was when we administered basolateral standard $HCO_3^-/CO_2$ solution during perfusion with apical standard $HCO_3^-/CO_2$. We denote base influx as $J$(B) and base efflux as -$J$(B).

### RT-PCR

Total RNA was extracted from CFPAC-1 cells grown in tissue culture flasks using RNAzol solution (Gibco-BRL) according to the manufacturer's instructions. For reverse transcriptase (RT)-PCR, 2 μg of RNA was reverse transcribed with 50 ng of random hexamer primers (GIBCO-BRL) in a final volume

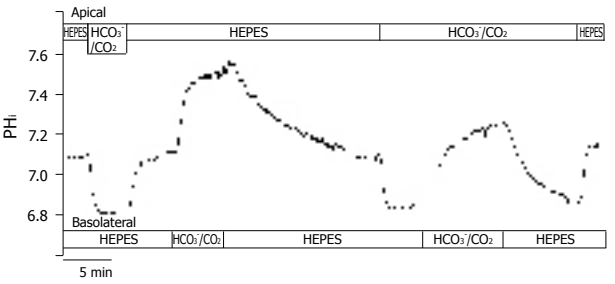


**Figure 2** Functional polarities of CFPAC-1 cells. CFPAC-1 cells were grown to confluence on permeable supports, loaded with the pH-sensitive fluorescent dye BCECF-AM (2 μmol/L) and mounted into a perfusion chamber, which allowed the simultaneous perfusion of different solutions to the basolateral and apical membranes. The figure shows representative $pH_i$ traces demonstrating cell polarity. The administration of standard $HCO_3^-/CO_2$ solution to the apical and the basolateral sides of the cells showed a marked difference in response ($n$ = 12–20).

of 20 μL using 50 U of Moloney murine leukemia virus RT (Fermentas) at 37 ℃ for 1 h, following the manufacturer's instructions. The primers used for PCR amplification were previously described[23-25]. NHE1: 5'-CCAGCTCATTGCCTTCTACC-3' (sense) and 5'-TGTGTCTGTTGTAGGACCGC-3' (antisense) (length of amplified region 245 residues); AE2: 5'-GAAGATTCCTGAGAATGCCG-3' (sense) and 5'-GTCCATGTTGGCACTACTCG-3' (antisense) (length of amplified region 181 residues); pancreatic NBC1 (pNBC): 5'-ATGTGTGTGATGAAGAAGAAGTAGAAG-3' (sense) and 5'-GACCGAAGGTTGGATTTCTTG-3' (antisense) (length of amplified region 621 residues); glyceraldehyde-3-phosphate dehydrogenase (GAPDH): 5'-ATGGCACCGTCAAGGCTGAGA-3' (sense) and 5'-GGCATGGACTGTGGTCATGAG-3' (antisense) (length of amplified region 371 residues). The PCR reaction was started with a 3-min 94 ℃ step and was followed by standard step-cycling conditions with 30 cycles of amplification utilizing *Taq* DNA polymerase (Fermentas); the reaction was ended by a 10-min 72℃ step. The cycling conditions for NHE1, AE2, and GAPDH were 94 ℃ for 30 s, 58 ℃ for 30 s and 72 ℃ for 30 s; and for pNBC1 were 94 ℃ for 30 s, 58 ℃ for 30 s and 68 ℃ for 3 min. RT-PCR products were separated by electrophoresis on a 20 g/L agarose gel containing ethidium bromide (0.5 μg/mL) and were visualized under ultraviolet light.

### Statistical analyses

In agreement with Zsembery *et al*[26], we noticed a variation in the rate and magnitude of $HCO_3^-$ uptake between the different set of monolayers that we could not attribute to the passage number or time after seeding. To avoid errors arising from this fact, we (1) performed a particular experimental protocol on the same day using one set of cell cultures, (2) randomized the order in which monolayers in the same group were exposed to experimental maneuvers (i.e., exposure to inhibitors), and (3) always included internal controls where possible. Summary data in the figures are expressed as percent change from control and statistical analyses were performed using either Student's paired or unpaired $t$ test or the analysis of variance as appropriate. $P$ values <0.05 were considered statistically significant.

## RESULTS

### Transepithelial electrical resistance, resting $pH_i$ and buffering capacity

The CFPAC-1 cells grown on polyester Transwells became confluent in 2-3 d as judged by visual observation. The net transepithelial resistance increased steadily over 4-5 d after seeding when it reached a plateau of 100±4 Ω/cm$^2$ ($n$ = 88). The resting $pH_i$ of the cells in standard HEPES solution was 7.11±0.08 ($n$ = 6).

### Apical administration of $HCO_3^-/CO_2$

After perfusing both the apical and basolateral sides of the CFPAC-1 cells with standard HEPES solution, apical perfusion was switched to the standard $HCO_3^-/CO_2$ solution (Figure 2). We then observed a rapid acidification (-17.5 ± 1.5 mmol/L B/min, $n$ = 20) of $pH_i$, most likely caused by the diffusion of $CO_2$ into the cells. Following this, the $pH_i$ reached a new approximate steady state value (6.82 ± 0.02, $n$ = 20) and remained at this level until the standard HEPES solution was restored to the apical membrane. Restoration of standard HEPES solution induced a rapid alkalinization of $pH_i$ towards the resting $pH_i$ value probably brought about by the diffusion of $CO_2$ from the cells. These observations suggested that $CO_2$ influx was very fast across the apical membrane of CFPAC-1 cells, and that significant $HCO_3^-$ influx did not occur.

### Basolateral administration of $HCO_3^-/CO_2$

After perfusion of both the apical and basolateral membranes of CFPAC-1 cells with standard HEPES solution, the basolateral perfusion was switched to standard $HCO_3^-/CO_2$ (Figure 2). Upon changing the basolateral perfusate, there was a rapid alkalinization of $pH_i$ ($\Delta pH_i$ = 0.48 ± 0.03, $J$(B) = 15.0±2.3 mmol/L B/min, $n$ = 12), most likely induced by the transport of $HCO_3^-$ into the cells. Removal of the standard $HCO_3^-/CO_2$ solution from the basolateral side induced a further small transient increase in $pH_i$ consistent with efflux of $CO_2$, followed by a slow acidification towards the resting $pH_i$ value brought about by the extrusion of $HCO_3^-$ (Figure 2). These observations suggested that $HCO_3^-$ might cross the basolateral membrane of CFPAC-1 cells much faster than $CO_2$. To rule out the possibility that basolateral $HCO_3^-$ entry was at least partly due to $CO_2$ influx, followed by its rapid hydration to $HCO_3^-$ ions, we perfused the apical side of CFPAC-1 cells with a standard $HCO_3^-/CO_2$ solution for 4 min (intracellular $pCO_2$ was increased) and then the same solution was added to the basolateral side (Figure 2). Under these conditions we still observed a rapid alkalinization of $pH_i$, ($\Delta pH_i$ = 0.40 ± 0.05, $J$(B) = 14.1 ± 1.9 mmol/L B/min, $n$ = 6) which was not significantly different compared to the absence of apical $HCO_3^-/CO_2$.

Taken together with the effects of apical $HCO_3^-/CO_2$ administration, these data showed that CFPAC-1 monolayers exhibited functional polarity with respect to $HCO_3^-$ transport. Subsequently, we used the apical administration of $HCO_3^-/CO_2$ to check the functional polarity of monolayers at the beginning of each experiment. The cells were considered to be polarized, if

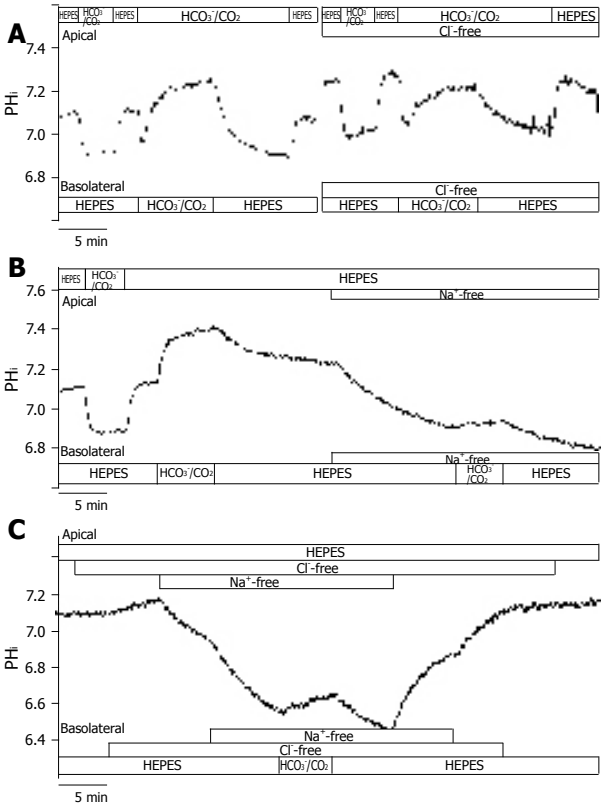


**Figure 3** Basolateral $HCO_3^-$ uptake – effects of $Cl^-$ and/or $Na^+$ withdrawal. The figure shows representative $pH_i$ traces. **A**: The rate of $HCO_3^-$ uptake was significantly decreased in Cl-free conditions compared to standard conditions (J(B) = 73.1 ± 7.2% and 100 ± 8.5%, respectively, $n$ = 5); **B**: The administration of basolateral $HCO_3^-/CO_2$ in $Na^+$-free conditions ($n$ = 6) greatly decreased $\Delta pH_i$ and J(B) compared to standard conditions, suggesting that a large proportion of the $HCO_3^-$ uptake was due to a $Na^+$-sensitive process, most likely NBC; **C**: Interestingly, the decrease in the rate of $HCO_3^-$ uptake was obviously ameliorated in the absence of both $Na^+$ and $Cl^-$ ($n$ = 6) compared to the $Na^+$-free condition.

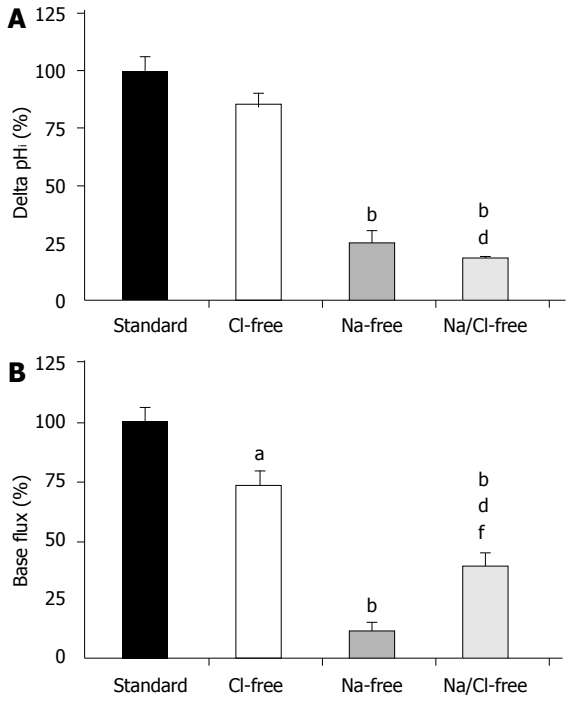


**Figure 4** Basolateral $HCO_3^-$ uptake – changes in (**A**) $\Delta pH_i$ and (**B**) $J$(B) caused by the withdrawal of $Cl^-$ and/or $Na^+$. SE of the control groups (standard, black bar) is somewhat different for each of the respective ion-withdrawal groups. The SEs depicted on the standard bars are the maximum values observed. $^aP$<0.05 and $^bP$<0.01 *vs* control group $^dP$<0.01 *vs* $Cl^-$-free group and/or $^fP$<0.01 *vs* $Na^+$-free group.

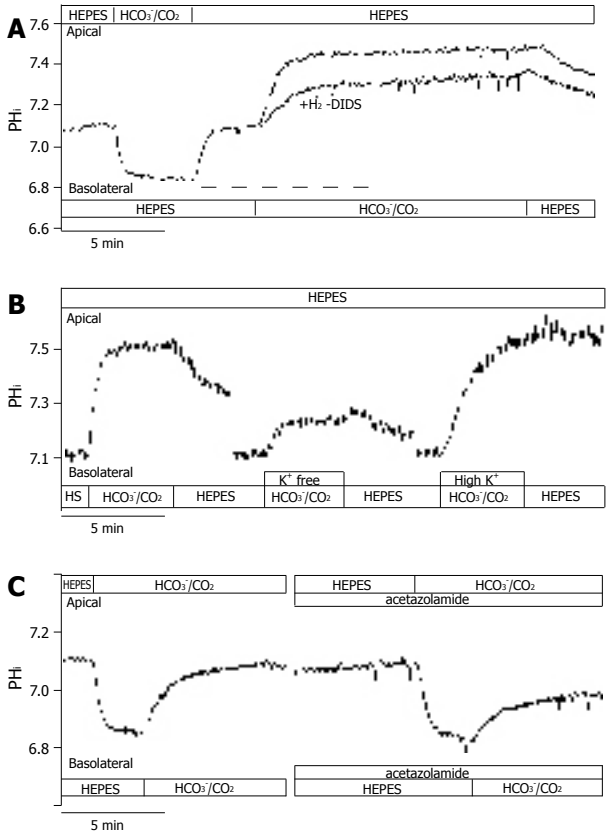


**Figure 5** Basolateral $HCO_3^-$ uptake – effects of $H_2$-DIDS, acetazolamide and varying extracellular $K^+$ concentration. The figure shows representative $pH_i$ traces. **A**: The anion transport inhibitor 600 μmol/L $H_2$-DIDS (added to the basolateral membrane of cells for 2 min before and during the administration of basolateral $HCO_3^-/CO_2$, dashed line, n=6) significantly decreased the extent of alkalinization ($\Delta pH_i$) and rate of J(B) (n=6); **B**: Varying extracellular [$K^+$] caused significant differences in $\Delta pH_i$ and J(B) (n=9–11); **C**: The application of the membrane-permeable carbonic anhydrase inhibitor acetazolamide (100 μmol/L, $n$ = 6) significantly decreased the overall $\Delta pH_i$ and J(B). HS: HEPES.

the $pH_i$ remained constant after the initial decrease in $pH_i$ caused by the diffusion of $CO_2$ into the cells.

### *Investigation of basolateral $HCO_3^-$ uptake*

In theory, the alkalinization observed after the administration of basolateral standard $HCO_3^-/CO_2$ could be explained by the action of the NBC and the reversal of $Cl^-/HCO_3^-$ anion exchanger. The initial rate of $HCO_3^-$ uptake was significantly decreased in $Cl^-$-free *vs* standard conditions ($J$(B)=73.1±7.2% and 100±8.5%, respectively, $n$=5, Figures 3A and 4); however, no significant difference was noted for the overall $\Delta pH_i$ for the two groups (85.5 ±6.0% and 100±6.3%, respectively). The administration of basolateral $HCO_3^-/CO_2$ greatly decreased $\Delta pH_i$ (25.6 ±5.1%) and $J$(B) (11.7±2.3%) in $Na^+$-free conditions ($n$=6) compared to those (100±7.5% and, 100±10.7%, respectively) in standard conditions, suggesting that a large proportion of the $HCO_3^-$ uptake was due to a $Na^+$-sensitive process, most likely via an NBC (Figures 3B and 4). Interestingly, the decrease in the rate of $HCO_3^-$ uptake was somewhat attenuated in the absence of both $Na^+$ and $Cl^-$ [$n$=6, $J$(B) changed to 38.4±6.9%, Figures 3C and 4].

To further confirm the presence of NBC on the basolateral membrane of CFPAC-1 cells, we examined the recovery from a $Na^+$-free acid load in the presence

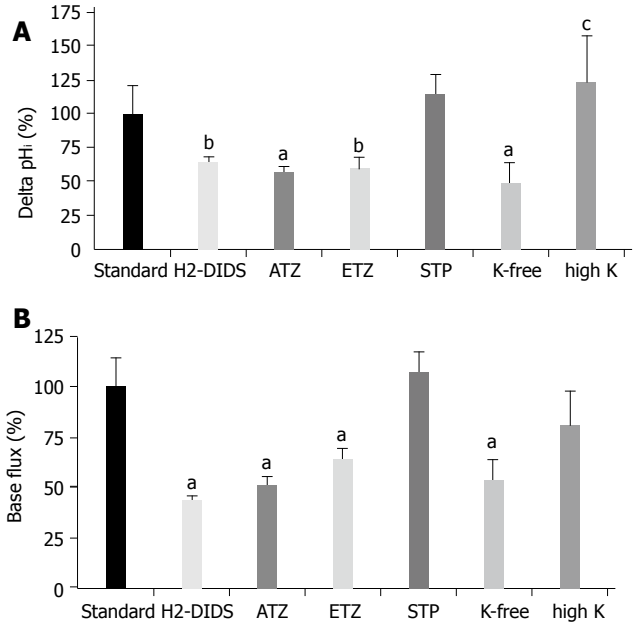


**Figure 6** Basolateral $HCO_3^-$ uptake – changes in (**A**) $\Delta pH_i$ (**B**) $J$(B) caused by application of $H_2$-DIDS, acetazolamide, ethoxyzolamide, STP and varying extracellular $K^+$ concentration. Data are shown as mean ± SE ($n$ = 6–11). SE of the control groups (standard, black bar) is somewhat different for each of the respective ion-withdrawal groups. The SE depicted on the control bar was the maximum values observed. $^aP$<0.05 and $^bP$<0.01 *vs* control group or $^cP$<0.05 vs $K^+$-free group. ATZ: acetazolamide; ETZ: ethoxyzolamide; STP: 1-*N*-(4-sulfamoylphenylethyl)-2,4,6-trimethylpyridine perchlorate. The SE depicted on the standard bars was the maximum values observed.

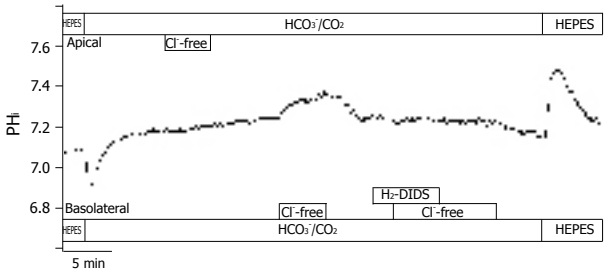


**Figure 7** Localization of $Cl^-/HCO_3^-$ exchangers in CFPAC-1 cells. The figure shows representative $pH_i$ traces ($n$ = 6). The localization of $Cl^-/HCO_3^-$ exchangers was performed by measuring the effect of changes in $Cl^-$ gradient across the luminal or basolateral membranes on $pH_i$. In the presence of $HCO_3^-$, the removal of $Cl^-$ from the apical membrane did not result in changes of $pH_i$. The removal of $Cl^-$ from the basolateral membrane caused a $\Delta pH_i$ of 0.08 ± 0.01 and a $J$(B) of 4.37 ± 0.46 mmol/L B/min. Furthermore, the basolateral administration of 250 μmol/L $H_2$-DIDS completely blocked $pH_i$ changes caused by the withdrawal of $Cl^-$.

of $HCO_3^-/CO_2$ by adding basolateral $Na^+$ with/without 300 μmol/L amiloride (to block basolateral $Na^+/H^+$ exchange, $n$ = 6). After acid loading of cells, the basolateral addition of $Na^+$ stimulated a $J$(B) of 39.0±4.4 mmol/L B/min (please see below the much lower values in HEPES solution). In contrast, the basolateral addition of $Na^+$ in the presence of amiloride decreased this value to 22.2± 3.6 mmol/L B/min, suggesting that a third pathway of acid transport is due to a basolateral NHE. The anion transport inhibitor $H_2$-DIDS (600 μmol/L, added to the basolateral membrane of cells for 2 min before and during the administration of basolateral $HCO_3^-/CO_2$, $n$ = 6), significantly decreased the extent of alkalinization ($\Delta pH_i$) to 63.2±4.7% and rates of $J$(B) to 43.9±5.1% ($n$ = 6, Figures 5A and 6). Varying the extracellular $K^+$ concentrations ($K^+$-free, high $K^+$, $n$ = 9-11) of the basolateral standard $HCO_3^-/CO_2$ solution induced significant differences between the $\Delta pH_i$ values *vs* the standard $HCO_3^-/CO_2$ solution (41.5±24.5%, 139.6±15.0% and 100 ± 11.1%, respectively; Figures 5B and 6). The $J$(B) significantly decreased when $K^+$-free $HCO_3^-/CO_2$ (73.9 ±6.4%) was administered to the basolateral membrane, but was not affected by high $K^+$, $HCO_3^-/CO_2$ (96.6 ± 11.0%) *vs* the standard $HCO_3^-/CO_2$ solution (100.0 ± 15.8%). Thus, our experiments showed that alteration of the membrane potential of CFPAC-1 cells, by varying basolateral extracellular $K^+$ concentration, modified the extent of $HCO_3^-$ uptake. The application of the membrane permeable CA inhibitors acetazolamide (100 μmol/L, $n$ = 6, Figures 5C and 6) or ethoxyzolamide (100 μmol/L, $n$ = 6) in the apical (standard $HCO_3^-/CO_2$ solution) and basolateral (standard HEPES solution) perfusions, 10 min before and during the administration of basolateral standard $HCO_3^-/CO_2$ solution, significantly decreased the overall $\Delta pH_i$ to 56.8±4.2% or 59.0±9.8%, and $J$(B) to 50.5±4.6% or 63.7±8.3%, respectively. The basolateral addition of the membrane impermeable CA inhibitor STP (10 μmol/L, $n$ = 6) in standard HEPES solution (the apical side of the cells was perfused with standard $HCO_3^-/CO_2$ solution), 5 min before and during the administration of basolateral standard $HCO_3^-/CO_2$ solution, did not significantly influence overall $\Delta pH_i$ (114.3±14.3%) and $J$(B) (106.7±17.9%, Figure 6).

### *Localization of $Cl^-/HCO_3^-$ exchangers in CFPAC-1 cells*

The localization of $Cl^-/HCO_3^-$ exchangers was performed by measuring the effect of changes in $Cl^-$ gradient across the luminal and/or basolateral membranes on $pH_i$. In the presence of $HCO_3^-$, the removal of $Cl^-$ from the apical membrane did not result in changes of $pH_i$. The removal of $Cl^-$ from the basolateral membrane caused a $\Delta pH_i$ of 0.08±0.01 and a $J$(B) of 4.4±0.5 mmol/L B/min ($n$ = 6, Figure 7). Furthermore, the basolateral administration of 250 μmol/L $H_2$-DIDS (from 2 min before changing the solution to $Cl^-$-free $HCO_3^-/CO_2$) completely blocked $pH_i$ changes caused by the withdrawal of $Cl^-$. However, 10 μmol/L forskolin, 100 μmol/L acetazolamide or 100 μmol/L ethoxyzolamide (from 10 min before changing the solution to $Cl^-$-free $HCO_3^-/CO_2$) did not significantly influence $Cl^-/HCO_3^-$ exchange on the apical and basolateral membranes ($n$ = 6-8, data not shown).

### *Localization of $Na^+/H^+$ exchangers in CFPAC-1 cells*

In HEPES-buffered solutions, the removal of $Na^+$ from the perfusing solutions had a small acidifying effect on $pH_i$ [$J$(B)=1.00±0.13 mmol/L B/min, $n$=12]. After exposure and then removal of the $NH_4^+$ in the absence of $Na^+$ on both sides of the duct cells, $pH_i$ reduced to 6.73±0.03 ($n$ = 12), and stabilized at this level (Figure 8A). We could not detect any active $H^+$-pumps in CFPAC-1 cells, since $pH_i$ did not increase in the absence of extracellular $Na^+$. Re-addition of $Na^+$ to the apical or the basolateral side caused $pH_i$ recovery towards the resting values [$J$(B) = -6.6

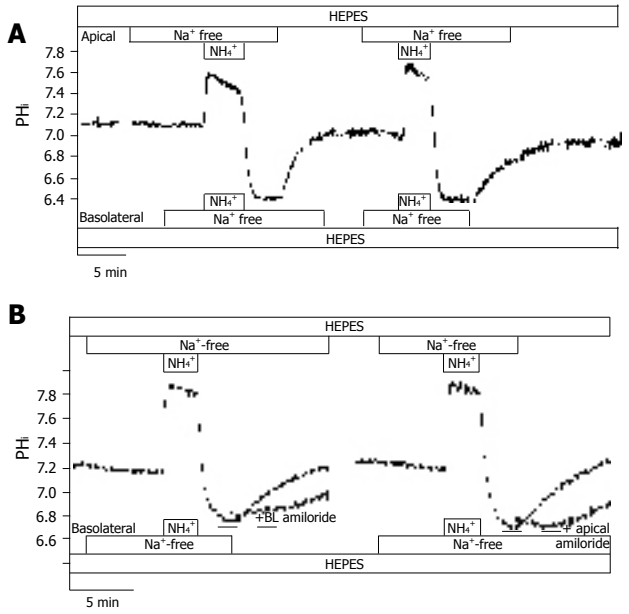


**Figure 8** Localization of $Na^+/H^+$ exchangers in CFPAC-1 cells. The figure shows representative $pH_i$ traces. **A**: After exposure to $NH_4^+$ in the absence of $Na^+$ on both sides of the duct cells, $pH_i$ reduced to 6.73±0.03 ($n$=12), and stabilized at this level. We could not detect any active $H^+$-pumps in CFPAC-1 cells, since $pH_i$ did not increase in the absence of extracellular $Na^+$. Upon addition of $Na^+$ to the apical or the basolateral side prompted the $pH_i$ to recover towards the resting values ($n$=6-10); **B**: The administration of 300 μmol/L amiloride (dashed line) to the $Na^+$-free (from 2 min before the addition of $Na^+$) and $Na^+$-containing HEPES solutions prevented the recovery of $pH_i$ in the presence of $Na^+$ ($n$=6). Removal of amiloride resulted in the recovery of $pH_i$ to resting values.

±2.6 mmol/L B/min and -7.5±1.3 mmol/L B/min, respectively, $n$=6-10]. The administration of 300 μmol/L amiloride to the $Na^+$-free (from 2 min before the addition of $Na^+$) and $Na^+$-containing HEPES solutions prevented the recovery of $pH_i$ in the presence of $Na^+$ ($n$=6, Figure 8B). Removing amiloride resulted in the recovery of $pH_i$ to resting values. Interestingly, the removal of apical $Na^+$ from the standard $HCO_3^-/CO_2$ solution perfusing CFPAC-1 cells caused a sudden but small acidification of $pH_i$ ($\Delta pH_i$=0.14±0.01 and $J$(B)=-10.8±0.8 mmol/L B/min, $n$=6), whereas we did not see any change in $pH_i$ when we removed $Na^+$ from the basolateral side of the cells ($n$=6). Taken together, our experiments showed that there are $Na^+/H^+$ exchangers on both the apical and the basolateral membranes. Finding a $Na^+/H^+$ exchanger on the apical side was somewhat unexpected. A possible explanation for this would be that the cells were leaky to $Na^+$ ions. However, despite the great difference in $Na^+$ concentration (0 mmol/L *vs* 140 mmol/L) of the apical and basolateral perfusates, analysis of the $Na^+$ concentration of the solutions by mass spectrometry showed no contamination during perfusion.

### *Molecular identification of $H^+$ and $HCO_3^-$ transporters*

To further investigate the presence of different $H^+$ and $HCO_3^-$ transporters in CFPAC-1 cells, we undertook RT-PCR analysis. We could detect mRNA expressions for pNBC1, AE2, and NHE1; the housekeeping gene GAPDH was used to normalize mRNA levels (Figure 9).

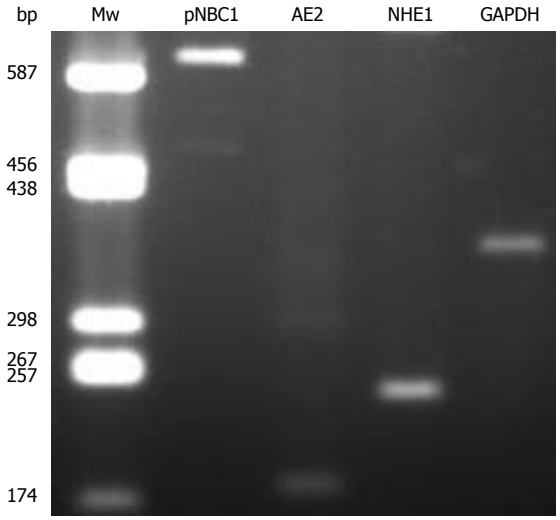


**Figure 9** Expression of pNBC1, AE2, NHE1, and GAPDH mRNA in CFPAC-1 cells. Mw: molecular weight ladder (bp indicates number of base pairs).

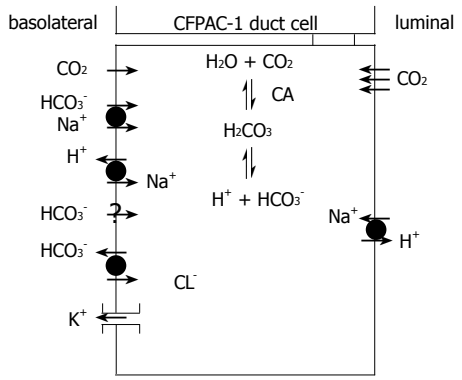


**Figure 10** $H^+$ and $HCO_3^-$ transport mechanisms in CFPAC-1 human pancreatic duct cells. The basolateral membrane expresses $Na^+/HCO_3^-$ co-transporters, $Na^+/H^+$ exchangers and $Cl^-/HCO_3^-$ exchangers plus an unidentified $Na^+$-independent $HCO_3^-$ entry pathway. These transporters facilitate the rapid flux of $HCO_3^-$ ions into the cell. $K^+$ channels are also likely to be expressed on the basolateral membrane because altering extracellular $K^+$ concentration affects $HCO_3^-$ influx. The apical membrane expresses $Na^+/H^+$ exchangers, but not CFTR and $Cl^-/HCO_3^-$ exchangers found in normal pancreatic duct cells. The apical membrane is an effective barrier to $HCO_3^-$ influx from the lumen, but is freely permeable to $CO_2$. CA: Carbonic anhydrase.

## DISCUSSION

Our results showed the functional presence of the NBC and $Cl^-/HCO_3^-$ exchanger on the basolateral membrane, together with $Na^+/H^+$ exchangers on both the apical and basolateral membranes of CFPAC-1 cells (Figure 10). That there was no detectable $Cl^-/HCO_3^-$ exchange activity on the apical membrane was not a surprise as CFTR is known to be required for its activation[3,27]. RT-PCR revealed the expression of pNBC1, AE2, and NHE1 mRNA.

CFPAC-1 cells clearly demonstrated a differential permeability to $HCO_3^-$ at the apical and basolateral membranes. We found that the addition of 25 mmol/L $HCO_3^-/CO_2$ to the basolateral side of the cells caused a marked alkalinization of $pH_i$, whereas exposing the apical membrane to the same solution caused a sustained acidification. These data suggest that the basolateral membrane of CFPAC-1 cells is much more permeable

to $HCO_3^-$ than the apical membrane. Plasma membrane $HCO_3^-$ and $CO_2$ permeabilities have been reported to vary in different species and tissues. In perfused rabbit gastric glands, the luminal membranes of parietal and chief cells were impermeable to $HCO_3^-$ and $CO_2$, while the basolateral membranes were permeable to both[28]. Apical $HCO_3^-$ permeability is relatively low in cultured bovine corneal endothelial cells[29]. In contrast, $HCO_3^-$ permeability of the apical side of intact colonic mucosa of guinea pig is markedly higher[30]. Our results are in accordance with similar observations made by Ishiguro *et al.*[31] using guinea pig ducts. Administration of 25 mmol/L $HCO_3^-/CO_2$ to the lumen of microperfused guinea pig pancreatic ducts decreased $pH_i$ rapidly. Following this, no subsequent increase in $pH_i$ was observed, indicating that little $HCO_3^-$ was able to enter the cell from the lumen. $HCO_3^-$ entry was detected only when the luminal $HCO_3^-$ concentration was raised above 125 mmol/L. A low apical $HCO_3^-$ permeability would make physiological sense in species, such as man and guinea pig, which can secrete near isotonic $NaHCO_3^-$. Our work is the first demonstration of $HCO_3^-/CO_2$ asymmetry in polarized human pancreatic duct cells. Finally, it seems that CFPAC-1 cells, which express ΔF508 CFTR, exhibit the same resistance to $HCO_3^-$ influx across the apical membrane as native guinea pig duct cells. This suggests that the presence of functional CFTR in the apical membrane is not required for this membrane to act as an effective barrier to $HCO_3^-$ influx from the lumen.

A large proportion of the basolateral $HCO_3^-$ uptake was $Na^+$-dependent and was partially inhibited by $H_2$-DIDS, therefore, it is most likely due to the action of pNBC1. However, we also detected a novel $Na^+$-independent $HCO_3^-$ influx mechanism that was significantly increased in $Cl^-$-free conditions, the identity of which remains unknown. NBCs have been detected in the guinea pig[32,33], rat[34,35] and mouse[36]. In contrast, Novak *et al.*[37,38] could not detect any $HCO_3^-$ uptake by NBC in freshly prepared rat pancreatic ducts using electrophysiological and $pH_i$ measurements. Extracellular $HCO_3^-/CO_2$ did not increase the rate of $pH_i$ recovery in experimental acidosis. The expressions of NBC mRNA and protein have been noted in the human pancreas[39]. Immunofluorescence localized the transporter to the basolateral but not the apical membrane of the pancreatic duct cells. Interestingly, immunohistological studies have shown the NBC in both the apical and basolateral membranes of rat pancreatic duct cells[35]. NBC1 mRNA was also detected in CFPAC-1 cells by Northern hybridization[13]. In accordance with our findings, expression of NBC1 was also found in non-polarized cells by recovery from acidosis in the presence of $HCO_3^-$, $Na^+$ and amiloride and its sensitivity to the administration of 200 μmol/L DIDS[13]. cAMP had no effect on NBC activity in CFPAC-1 cells, whereas NBC activity was stimulated in CAPAN-1 cells expressing wild-type CFTR[13]. The basolateral localization of the NBC was shown by $^{22}Na^+$ flux studies in CFPAC-1 cells stably transfected with wild-type CFTR grown on permeable supports (no data was reported for untransfected CFPAC-1 cells)[13].

The application of the membrane permeable CA inhibitor acetazolamide or ethoxyzolamide partially inhibited the rate of basolateral base flux in CFPAC-1 cells, whereas the membrane-impermeable CA inhibitor STP[40] had no such effect. Carbonic anhydrases are known to be coupled to $HCO_3^-$ transporters, such as $Cl^-/HCO_3^-$ anion exchangers[41-44], DRA[45] and NBC[46]. There are at least 14 different isoenzymes in the α-CA gene family present in vertebrates[47]. CA I-III and VII are cytosolic, while CA IV, IX, XII and XIII are membrane-associated, V is mitochondrial and VI is secreted. Of the 14 different isoforms, CA II, IV, IX and XII were shown to be expressed in the human pancreas and cultured pancreatic tumor cells[48]. Interestingly, CA II and IV expressions were found to be associated with apical $HCO_3^-$ channels in human pancreatic duct cells CAPAN-1[49], although the targeting of CA IV to the apical plasma membrane was impaired in the CFPAC-1 cells[50]. Kivela *et al.*[51] have clearly detected the transmembrane CA isoenzymes IX and XII on the basolateral membrane of the normal and pathological pancreas by immunohistochemistry. However, it is unlikely that the latter isoenzymes are associated with NBC as STP had no inhibitory effect on $HCO_3^-$ uptake. Furthermore, in accordance with our results, Cheng *et al.*[52] have shown in CAPAN-1 cells that $HCO_3^-$-dependent forskolin-induced $I_{sc}$ could be significantly reduced by acetazolamide. Moreover, the CA inhibitor also had an inhibitory effect on dome formation, which was thought to be due to exchange of water and electrolytes[49]. Taken together, intracellular CAs may be involved in the rapid basolateral transport of $HCO_3^-$ by NBC. The enzyme converts $HCO_3^-$ to carbonic acid and possibly maintains a concentration gradient for $HCO_3^-$ across the basolateral membrane of CFPAC-1 cells.

Alteration of extracellular $K^+$ concentration significantly influenced $HCO_3^-$ uptake in our experiments. The presence of $K^+$ channels in the basolateral membranes of CFPAC-1 cells is highly likely, and one report has identified ATP-sensitive $K^+$ channels[53] in these cells. A basolateral $K^+$ conductance will influence the rate of $HCO_3^-$ secretion by altering the cells membrane potential. In our experiments, high extracellular $K^+$ concentrations increased $HCO_3^-$ entry, which was likely due to basolateral membrane depolarization, and a consequent increase in the electrochemical driving force for $HCO_3^-$ entry on the electrogenic NBC. In contrast, low extracellular $K^+$ concentration inhibited $HCO_3^-$ uptake, probably due to membrane hyperpolarization.

Novak and Greger[37] demonstrated that the basolateral membrane of rat intra- and inter-lobular pancreatic ducts had a relatively large $K^+$ conductance, which could be decreased by the $K^+$ channel blocker $Ba^{2+}$. The luminal membrane had no significant $K^+$ conductance. Interestingly, Fong *et al.*[54] detected $K^+$ conductances not only on the basolateral but also on the apical sides of HPAF human pancreatic duct cells.

CFPAC-1 cells exhibited $Na^+/H^+$ exchange activity on both the apical and basolateral membranes (the latter is most likely to be due to NHE1). $Na^+/H^+$ exchangers were identified in guinea pig[10,28-30], rat[55,56] and mouse[8] pancreatic ducts. These exchangers were localized to the basolateral membrane of intra/interlobular duct cells.

However, the main and common segments of the rat pancreatic ducts also showed $Na^+/H^+$ exchange activity in the apical membrane[10]. There is also evidence for an apical $Na^+/H^+$ exchanger in bovine main pancreatic duct segments[57]. Furthermore, the main pancreatic duct of mice expressed NHE1 in the basolateral membrane, and NHE2 and NHE3 in the luminal membrane[8]. Disruption of the NHE2 gene had no effect on luminal $H^+$ transport, while disruption of the NHE3 gene reduced luminal $Na^+$-dependent $H^+$ efflux by 45%. The remaining 55% of the luminal $Na^+$-dependent $H^+$ efflux from NHE3-knockout mice was inhibited by 50 μmol/L HOE694. $Na^+$-dependent $H^+$ transport mechanisms were inhibited by cAMP, therefore, they are thought to be inhibited during stimulated secretion and are most likely to be active during the resting state[8]. CFTR in the pancreatic duct not only affected the activity, but also the expression of NHE3 protein[7]. NHE3 expression was reduced by about 50%, luminal $Na^+$-dependent and HOE694-sensitive recovery from acid load was reduced by 60% in the ducts of Δ508 CFTR mice[7]. To our knowledge, we are the first to detect NHEs on both the apical and basolateral membranes of human pancreatic duct cells. The presence of NHE on the apical membrane was unexpected, since it acted against $HCO_3^-$ secretion. We do not know which section of the pancreatic duct CFPAC-1 cells originate from, but they might be from the main region where the expression of the apical NHEs was noted in animal studies. In accordance with our results, failure of $pH_i$ to recover from acid loading in the absence of extracellular $Na^+$ suggests that there is little $H^+$-pump activity in the unstimulated guinea pig ducts[32]. This is in contrast with the observations made in rat[10] and pig[58] pancreatic ducts, which showed $H^+$-pump activity.

The role of apical $Cl^-/HCO_3^-$ exchangers in pancreatic ductal $HCO_3^-$ secretion is a controversial issue. One hypothesis is that all of the $HCO_3^-$ is secreted on an anion exchanger and that CFTR's role is to activate the exchangers and to provide a route for the recycling of $Cl^-$ across the apical membrane[59]. An alternative proposal is that $HCO_3^-$ secretion occurs on the exchanger until the luminal concentration reaches about 70 mmol/L after which $HCO_3^-$ exits the duct cell via CFTR[60]. Previously, it has been shown that CFPAC-1 cells express AE2 on their basolateral membrane (which was also confirmed in our study) and SLC26A3 (DRA) and SLC26A6 (PAT1) on their apical membrane, and that expression of the apical SLC26 exchangers is upregulated by CFTR[14]. In accordance with these data, we observed basolateral $Cl^-/HCO_3^-$ exchange activity (which was inhibited by $H_2$-DIDS) in wild-type CFPAC-1 cells, but no apical activity, presumably due to the lack of CFTR. We also found that forskolin had no effect on either the basolateral or apical anion exchange in CFPAC-1 cells.

In conclusion, apart from the lack of CFTR and apical $Cl^-/HCO_3^-$ exchange activity, CFPAC-1 cells have similar $H^+$ and $HCO_3^-$ transporters to those observed in native animal tissue. Moreover, intracellular CAs appear to play a role in the basolateral uptake of $HCO_3^-$. Taken together, polarized CFPAC-1 human pancreatic duct cells are likely to be a useful model to study $H^+$ and $HCO_3^-$ transporters, and their dependence on CFTR, in human pancreatic duct cells.

## ACKNOWLEDGMENTS

We thank Professor RA Frizzell for kindly providing us with the CFPAC-1 cells, and Professor C Supuran for providing the 1-*N*-(4-sulfamoylphenylethyl)-2,4,6-trimethylpyridine perchlorate.

## REFERENCES

1 **Steward MC**, Ishiguro H, Case RM. Mechanisms of bicarbonate secretion in the pancreatic duct. *Annu Rev Physiol* 2005; **67**: 377-409

2 **Argent BE**, Gray MA, Steward MC, Case RM Cell physiology of pancreatic ducts. In: Johnson LR eds Physiology of the Gastrointestinal Tract, 4th edn. Elsevier, San Diego, 2005 (in press)

3 **Ko SB**, Shcheynikov N, Choi JY, Luo X, Ishibashi K, Thomas PJ, Kim JY, Kim KH, Lee MG, Naruse S, Muallem S. A molecular mechanism for aberrant CFTR-dependent $HCO_{(3)}^{(-)}$ transport in cystic fibrosis. *EMBO J* 2002; **21**: 5662-5672

4 **Gray MA**, Pollard CE, Harris A, Coleman L, Greenwell JR, Argent BE. Anion selectivity and block of the small-conductance chloride channel on pancreatic duct cells. *Am J Physiol* 1990; **259**: C752-C761

5 **Linsdell P**, Tabcharani JA, Rommens JM, Hou YX, Chang XB, Tsui LC, Riordan JR, Hanrahan JW. Permeability of wild-type and mutant cystic fibrosis transmembrane conductance regulator chloride channels to polyatomic anions. *J Gen Physiol* 1997; **110**: 355-364

6 **Choi JY**, Muallem D, Kiselyov K, Lee MG, Thomas PJ, Muallem S. Aberrant CFTR-dependent $HCO_3^-$ transport in mutations associated with cystic fibrosis. *Nature* 2001; **410**: 94-97

7 **Ahn W**, Kim KH, Lee JA, Kim JY, Choi JY, Moe OW, Milgram SL, Muallem S, Lee MG. Regulatory interaction between the cystic fibrosis transmembrane conductance regulator and $HCO_3^-$ salvage mechanisms in model systems and the mouse pancreatic duct. *J Biol Chem* 2001; **276**: 17236-17243

8 **Lee MG**, Ahn W, Choi JY, Luo X, Seo JT, Schultheis PJ, Shull GE, Kim KH, Muallem S. $Na^{(+)}$-dependent transporters mediate $HCO_{(3)}^{(-)}$ salvage across the luminal membrane of the main pancreatic duct. *J Clin Invest* 2000; **105**: 1651-1658

9 **Park M**, Ko SB, Choi JY, Muallem G, Thomas PJ, Pushkin A, Lee MS, Kim JY, Lee MG, Muallem S, Kurtz I. The cystic fibrosis transmembrane conductance regulator interacts with and regulates the activity of the $HCO_3^-$ salvage transporter human $Na^+$-$HCO_3^-$ cotransport isoform 3. *J Biol Chem* 2002; **277**: 50503-50509

10 **Zhao H**, Star RA, Muallem S. Membrane localization of $H^+$ and $HCO_3^-$ transporters in the rat pancreatic duct. *J Gen Physiol* 1994; **104**: 57-85

11 **Chambers JA**, Harris A. Expression of the cystic fibrosis gene and the major pancreatic mucin gene, MUC1, in human ductal epithelial cells. *J Cell Sci* 1993; **105 ( Pt 2)**: 417-422

12 **Schoumacher RA,** Ram J, Iannuzzi MC, Bradbury NA, Wallace RW, Hon CT, Kelly DR, Schmid SM, Gelder FB, Rado TA. A cystic fibrosis pancreatic adenocarcinoma cell line. *Proc Natl Acad Sci U S A* 1990; **87**: 4012-4016

13 **Shumaker H**, Amlal H, Frizzell R, Ulrich CD, Soleimani M. CFTR drives $Na^+$-*n*$HCO_3^-$ cotransport in pancreatic duct cells: a basis for defective $HCO_3^-$ secretion in CF. *Am J Physiol* 1999; **276**: C16-C25

14 **Greeley T,** Shumaker H, Wang Z, Schweinfest CW, Soleimani M. Downregulated in adenoma and putative anion transporter are regulated by CFTR in cultured pancreatic duct cells. *Am J Physiol Gastrointest Liver Physiol* 2001; **281**: G1301-G1308

15 **Namkung W**, Lee JA, Ahn W, Han W, Kwon SW, Ahn DS, Kim KH, Lee MG. $Ca^{2+}$ activates cystic fibrosis transmembrane

conductance regulator- and $Cl^-$-dependent $HCO_3$ transport in pancreatic duct cells. *J Biol Chem* 2003; **278**: 200-207
16 **Chan HC**, Law SH, Leung PS, Fu LX, Wong PY. Angiotensin II receptor type I-regulated anion secretion in cystic fibrosis pancreatic duct cells. *J Membr Biol* 1997; **156**: 241-249
17 **Cheng HS,** So SC, Law SH, Chan HC. Angiotensin II-mediated signal transduction events in cystic fibrosis pancreatic duct cells. *Biochim Biophys Acta* 1999; **1449**: 254-260
18 **Cheng HS,** Wong WS, Chan KT, Wang XF, Wang ZD, Chan HC. Modulation of Ca2+-dependent anion secretion by protein kinase C in normal and cystic fibrosis pancreatic duct cells. *Biochim Biophys Acta* 1999; **1418**: 31-38
19 **Cheung CY**, Wang XF, Chan HC. Stimulation of $HCO_3^-$ secretion across cystic fibrosis pancreatic duct cells by extracellular ATP. *Biol Signals Recept* 1998; **7**: 321-327
20 **Thomas JA**, Buchsbaum RN, Zimniak A, Racker E. Intracellular pH measurements in Ehrlich ascites tumor cells utilizing spectroscopic probes generated in situ. *Biochemistry* 1979; **18**: 2210-2218
21 **Hegyi P**, Rakonczay Z Jr, Gray MA, Argent BE. Measurement of intracellular pH in pancreatic duct cells: a new method for calibrating the fluorescence data. *Pancreas* 2004; **28**: 427-434
22 **Weintraub WH**, Machen TE. pH regulation in hepatoma cells: roles for Na-H exchange, Cl-HCO3 exchange, and Na-HCO3 cotransport. *Am J Physiol* 1989; **257**: G317-G327
23 **Inglis SK**, Finlay L, Ramminger SJ, Richard K, Ward MR, Wilson SM, Olver RE. Regulation of intracellular pH in Calu-3 human airway cells. *J Physiol* 2002; **538**: 527-539
24 **Dudeja PK,** Hafez N, Tyagi S, Gailey CA, Toofanfard M, Alrefai WA, Nazir TM, Ramaswamy K, Al-Bazzaz FJ. Expression of the Na+/H+ and Cl-/HCO-3 exchanger isoforms in proximal and distal human airways. *Am J Physiol* 1999; **276**: L971-L978
25 **Dudeja PK**, Rao DD, Syed I, Joshi V, Dahdal RY, Gardner C, Risk MC, Schmidt L, Bavishi D, Kim KE, Harig JM, Goldstein JL, Layden TJ, Ramaswamy K. Intestinal distribution of human $Na^+/H^+$ exchanger isoforms NHE-1, NHE-2, and NHE-3 mRNA. *Am J Physiol* 1996; **271**: G483-G493
26 **Zsembery A**, Strazzabosco M, Graf J. $Ca^{2+}$-activated $Cl^-$ channels can substitute for CFTR in stimulation of pancreatic duct bicarbonate secretion. *FASEB J* 2000; **14**: 2345-2356
27 **Lee MG**, Choi JY, Luo X, Strickland E, Thomas PJ, Muallem S. Cystic fibrosis transmembrane conductance regulator regulates luminal $Cl^-/HCO_3^-$ exchange in mouse submandibular and pancreatic ducts. *J Biol Chem* 1999; **274**: 14670-14677
28 **Waisbren SJ**, Geibel JP, Modlin IM, Boron WF. Unusual permeability properties of gastric gland cells. *Nature* 1994; **368**: 332-335
29 **Bonanno JA**, Guan Y, Jelamskii S, Kang XJ. Apical and basolateral $CO_2$-$HCO_3^-$ permeability in cultured bovine corneal endothelial cells. *Am J Physiol* 1999; **277**: C545-C553
30 **Bollert P,** Peters T, von Engelhardt W, Gros G. Mass spectrometric determination of HCO3- permeability and carbonic anhydrase activity in intact guinea-pig colon epithelium. *J Physiol* 1997; **502 ( Pt 3)**: 679-691
31 **Ishiguro H,** Naruse S, Kitagawa M, Suzuki A, Yamamoto A, Hayakawa T, Case RM, Steward MC. CO2 permeability and bicarbonate transport in microperfused interlobular ducts isolated from guinea-pig pancreas. *J Physiol* 2000; **528 Pt 2**: 305-315
32 **Ishiguro H,** Steward MC, Lindsay AR, Case RM. Accumulation of intracellular HCO3- by Na(+)-HCO3- cotransport in interlobular ducts from guinea-pig pancreas. *J Physiol* 1996; **495 ( Pt 1)**: 169-178
33 **de Ondarza J**, Hootman SR. Confocal microscopic analysis of intracellular pH regulation in isolated guinea pig pancreatic ducts. *Am J Physiol* 1997; **272**: G124-G134
34 **Satoh H,** Moriyama N, Hara C, Yamada H, Horita S, Kunimi M, Tsukamoto K, Iso-O N, Inatomi J, Kawakami H, Kudo A, Endou H, Igarashi T, Goto A, Fujita T, Seki G. Localization of Na+-HCO-3 cotransporter (NBC-1) variants in rat and human pancreas. *Am J Physiol Cell Physiol* 2003; **284**: C729-C737
35 **Thevenod F**, Roussa E, Schmitt BM, Romero MF. Cloning and immunolocalization of a rat pancreatic $Na^{(+)}$ bicarbonate cotransporter. *Biochem Biophys Res Commun* 1999; **264**: 291-298
36 **Gross E**, Abuladze N, Pushkin A, Kurtz I, Cotton CU. The stoichiometry of the electrogenic sodium bicarbonate cotransporter pNBC1 in mouse pancreatic duct cells is 2 $HCO_{(3)}^{(-)}$:1 $Na^{(+)}$. *J Physiol* 2001; **531**: 375-382
37 **Novak I**, Greger R. Electrophysiological study of transport systems in isolated perfused pancreatic ducts: properties of the basolateral membrane. *Pflugers Arch* 1988; **411**: 58-68
38 **Novak I**, Christoffersen BC. Secretin stimulates $HCO_{(3)}^-$ and acetate efflux but not $Na^+/HCO_{(3)}^-$ uptake in rat pancreatic ducts. *Pflugers Arch* 2001; **441**: 761-771
39 **Marino CR**, Jeanes V, Boron WF, Schmitt BM. Expression and distribution of the $Na^{(+)}$-$HCO^{(-)}_{(3)}$ cotransporter in human pancreas. *Am J Physiol* 1999; **277**: G487-G494
40 **Scozzafava A,** Briganti F, Ilies MA, Supuran CT. Carbonic anhydrase inhibitors: synthesis of membrane-impermeant low molecular weight sulfonamides possessing in vivo selectivity for the membrane-bound versus cytosolic isozymes. *J Med Chem* 2000; **43**: 292-300
41 **Dahl NK**, Jiang L, Chernova MN, Stuart-Tilley AK, Shmukler BE, Alper SL. Deficient $HCO_3^-$ transport in an AE1 mutant with normal $Cl^-$ transport can be rescued by carbonic anhydrase II presented on an adjacent AE1 protomer. *J Biol Chem* 2003; **278**: 44949-44958
42 **Sterling D**, Reithmeier RA, Casey JR. A transport metabolon. Functional interaction of carbonic anhydrase II and chloride/bicarbonate exchangers. *J Biol Chem* 2001; **276**: 47886-47894
43 **Sterling D**, Alvarez BV, Casey JR. The extracellular component of a transport metabolon. Extracellular loop 4 of the human AE1 $Cl^-/HCO_3^-$ exchanger binds carbonic anhydrase IV. *J Biol Chem* 2002; **277**: 25239-25246
44 **Vince JW**, Reithmeier RA. Carbonic anhydrase II binds to the carboxyl terminus of human band 3, the erythrocyte $C1^-/HCO_3^-$ exchanger. *J Biol Chem* 1998; **273**: 28430-28437
45 **Sterling D,** Brown NJ, Supuran CT, Casey JR. The functional and physical relationship between the DRA bicarbonate transporter and carbonic anhydrase II. *Am J Physiol Cell Physiol* 2002; **283**: C1522-C1529
46 **Alvarez BV**, Loiselle FB, Supuran CT, Schwartz GJ, Casey JR. Direct extracellular interaction between carbonic anhydrase IV and the human NBC1 sodium/bicarbonate co-transporter. *Biochemistry* 2003; **42**: 12321-12329
47 **Hewett-Emmett D**. Evolution and distribution of the carbonic anhydrase gene families. EXS 2000; 29-76
48 **Nishimori I**, FujikawaAdachi K, Onishi S, Hollingsworth MA. Carbonic anhydrase in human pancreas: hypotheses for the pathophysiological roles of CA isozymes. *Ann N Y Acad Sci* 1999; **880**: 5-16
49 **Mahieu I**, Becq F, Wolfensberger T, Gola M, Carter N, Hollande E. The expression of carbonic anhydrases II and IV in the human pancreatic cancer cell line (Capan 1) is associated with bicarbonate ion channels. *Biol Cell* 1994; **81**: 131-141
50 **Fanjul M**, Salvador C, Alvarez L, Cantet S, Hollande E. Targeting of carbonic anhydrase IV to plasma membranes is altered in cultured human pancreatic duct cells expressing a mutated (deltaF508) CFTR. *Eur J Cell Biol* 2002; **81**: 437-447
51 **Kivela AJ**, Parkkila S, Saarnio J, Karttunen TJ, Kivela J, Parkkila AK, Pastorekova S, Pastorek J, Waheed A, Sly WS, Rajaniemi H. Expression of transmembrane carbonic anhydrase isoenzymes IX and XII in normal human pancreas and pancreatic tumours. *Histochem Cell Biol* 2000; **114**: 197-204
52 **Cheng HS**, Leung PY, Cheng Chew SB, Leung PS, Lam SY, Wong WS, Wang ZD, Chan HC. Concurrent and independent $HCO_3^-$ and $Cl^-$ secretion in a human pancreatic duct cell line (CAPAN-1). *J Membr Biol* 1998; **164**: 155-167
53 **Roch B**, Baro I, Hongre AS, Escande D. ATP-sensitive $K^+$ channels regulated by intracellular $Ca^{2+}$ and phosphorylation in normal (T84) and cystic fibrosis (CFPAC-1) epithelial cells. *Pflugers Arch* 1995; **429**: 355-363
54 **Fong P,** Argent BE, Guggino WB, Gray MA. Characterization of vectorial chloride transport pathways in the human pancreatic duct adenocarcinoma cell line HPAF. *Am J Physiol Cell*

*Physiol* 2003; **285**: C433-C445
55 **Stuenkel EL**, Machen TE, Williams JA. pH regulatory mechanisms in rat pancreatic ductal cells. *Am J Physiol* 1988; **254**: G925-G930
56 **Novak I**, Hug M, Greger R. Intracellular pH in rat pancreatic ducts. *Comp Biochem Physiol A Physiol* 1997; **118**: 409-411
57 **Marteau C**, Silviani V, Ducroc R, Crotte C, Gerolami A. Evidence for apical $Na^+/H^+$ exchanger in bovine main pancreatic duct. *Dig Dis Sci* 1995; **40**: 2336-2340
58 **Villanger O**, Veel T, Raeder MG. Secretin causes $H^+/HCO_3^-$ secretion from pig pancreatic ductules by vacuolar-type $H^{(+)}$-adenosine triphosphatase. *Gastroenterology* 1995; **108**: 850-859
59 **Ko SB**, Zeng W, Dorwart MR, Luo X, Kim KH, Millen L, Goto H, Naruse S, Soyombo A, Thomas PJ, Muallem S. Gating of CFTR by the STAS domain of SLC26 transporters. *Nat Cell Biol* 2004; **6**: 343-350
60 **Ishiguro H**, Steward MC, Sohma Y, Kubota T, Kitagawa M, Kondo T, Case RM, Hayakawa T, Naruse S. Membrane potential and bicarbonate secretion in isolated interlobular ducts from guinea-pig pancreas. *J Gen Physiol* 2002; **120**: 617-628

**S- Editor** Kumar M and Guo SY **L- Editor** Elsevier HK **E- Editor** Liu WF

PO Box 2345, Beijing 100023, China
www.wjgnet.com
wjg@wjgnet.com

*World J Gastroenterol* 2006 February 14; 12(6): 896-901
***World Journal of Gastroenterology*** ISSN 1007-9327
© 2006 The WJG Press. All rights reserved.

*BASIC RESEARCH*

# Inhibitory effects of interferons on pancreatic stellate cell activation

Jan-Tido Baumert, Gisela Sparmann, Jörg Emmrich, Stefan Liebe, Robert Jaster

Jan-Tido Baumert, Gisela Sparmann, Jörg Emmrich, Stefan Liebe, Robert Jaster, Department of Medicine, Division of Gastroenterology, Medical Faculty, University of Rostock, E-Heydemann-Str. 6, 18057 Rostock, Germany
Supported by a grant from the Bundesministerium für Bildung und Forschung, No. FKZ 01ZZ0108
Correspondence to: Robert Jaster, MD, Department of Medicine, Division of Gastroenterology, Medical Faculty, University of Rostock, 18057 Rostock, Germany. jaster@med.uni-rostock.de
Telephone: +49-381-4947349 Fax: +49-381-4947482
Received: 2005-07-11 Accepted: 2005-07-28

## Abstract

**AIM:** To analyze and to compare the effects of interferon (IFN)-α, IFN-β, and IFN-γ on pancreatic stellate cell (PSC) activation *in vitro* and to elucidate the molecular basis of IFN action.

**METHODS:** PSCs were isolated from rat's pancreatic tissue, cultured and stimulated with recombinant rat IFNs. Cell proliferation and collagen synthesis were assessed by measuring the incorporation of 5-bromo-2'-deoxyuridine (BrdU) into DNA and [$^3$H]-proline into acetic acid-soluble proteins, respectively. Apoptotic cells were determined by FACS analysis (sub-$G_1$ peak method). Exhibition of the myofibroblastic PSC phenotype was monitored by immunoblot analysis of α-smooth muscle actin (α-SMA) expression. To assess the activation of signal transducer and activator of transcription (STAT), Western blots using phospho-STAT-specific antibodies were performed. In studies on STAT1 function, expression of the protein was inhibited by siRNA.

**RESULTS:** IFN-β and IFN-γ, but not IFN-α significantly diminished PSC proliferation and collagen synthesis. IFN-γ was the only IFN that clearly inhibited α-SMA expression. Under the experimental conditions used, no enhanced rate of apoptotic cell death was observed in response to any IFN treatment. IFN-β and IFN-γ induced a strong increase of STAT1 and STAT3 tyrosine phosphorylation, while the effect of IFN-α was much weaker. Inhibition of STAT1 expression with siRNA was associated with a significantly reduced growth-inhibitory effect of IFN-γ.

**CONCLUSION:** IFN-β and particularly IFN-γ display inhibitory effects on PSC activation *in vitro* and should be tested regarding their *in vitro* efficiency. Growth inhibition by IFN-γ action requires STAT1.

© 2006 The WJG Press. All rights reserved.

**Key words:** Interferons; Pancreatic stellate cell; Apoptosis

Baumert JT, Sparmann G, Emmrich J, Liebe S, Jaster R. Inhibitory effects of interferons on pancreatic stellate cell activation. *World J Gastroenterol* 2006; 12(6): 896-901

http://www.wjgnet.com/1007-9327/12/896.asp

## INTRODUCTION

Pancreatic stellate cells (PSCs) are the main source of extracellular matrix (ECM) proteins in pancreatic fibrosis[1-3], a common feature of chronic pancreatitis and pancreatic cancer[4,5]. They are closely related with hepatic stellate cells (HSCs), the key effector cells in liver fibrosis[6]. In response to pro-fibrogenic cytokines and ethanol metabolites, PSCs exhibit a myofibroblastic phenotype that is characterized by the expression of α-smooth muscle actin (α-SMA), proliferative activity, a loss of the typical retinoid-containing fat droplets, and enhanced ECM synthesis[3,7]. Similar phenotypic changes, considered as PSC activation, are induced when isolated PSCs are plated on cell-culture dishes[1,2,8-10]. The molecular principles of PSC activation *in vivo* and *in vitro* have been extensively analyzed in the past few years. Studies indicate that platelet-derived growth factor (PDGF) exerts strong mitogenic effects on PSCs, while transforming growth factor-beta (TGF-β) has been suggested as the most potent stimulator of ECM synthesis[11,12]. Furthermore, intracellular signal transduction pathways mediating PSC activation have, in part, been deciphered. Thus, we and others have recently shown that mitogen-activated protein kinases are key mediators of activation signals[13-17]. In contrast, natural antagonists of PSC activation have not been systematically studied so far. Their elucidation, however, may be helpful for the development of antifibrotic therapies.

Interferons (IFNs) are multifunctional cytokines that block viral infection, modulate immune as well as inflammatory responses, and inhibit cell proliferation[18]. IFN-α is an effective drug for the treatment of patients with chronic hepatitis B or C associated with liver fibrosis[19,20]. Recent studies suggest that IFNs not only block virus replication but also directly affect key functions

of activated HSCs. Thus, IFN-γ inhibits HSC survival, cell proliferation and collagen synthesis[21-23]. The effects of IFNs on PSCs are largely unknown.

IFNs exert their biological effects on target cells by binding to cell surface receptors with specificity for either type I interferons (IFN-α, -β, and -ω) or type II interferon IFN-γ[18,24]. In the transduction of signals from activated IFN-receptors to the nuclei, tyrosine kinases of the Janus family (JAKs) and signal transducer and activator of transcription (STAT) transcription factors play a key role[18,25]. IFN-α activates the JAK family proteins (JAK1 and TYK2) as well as the ISGF3 complex (consisting of STAT1, 2 and the IFN regulatory family protein p48)[26]. Although tremendous progress has been made, the molecular mechanisms underlying the growth-inhibitory action of these cytokines are only partially characterized so far.

This study was to analyze the biological effects of IFN-α, -β and -γ on PSCs and to study the molecular determinants of IFN efficiency.

## MATERIALS AND METHODS

### Materials

The enhanced chemiluminescence (ECL) plus kit, horseradish-peroxidase labeled antibodies and [$^3$H]-proline were purchased from Amersham Biosciences (Freiburg, Germany), the phospho-STAT1 and STAT3 antibodies from New England Biolabs (Frankfurt, Germany), and anti-STAT1 and STAT3 protein antibodies from Santa Cruz Biotechnologies (Santa Cruz, CA, USA). Hank's buffered salt solution (HBSS), Iscove's modified Dulbecco's medium (IMDM) and all supplements for cell culture were obtained from Biochrom (Berlin, Germany), Nycodenz from Nycomed (Oslo, Norway), simvastatin from Merck Biosciences (Schwalbach, Germany) and the recombinant rat interferons from R&D Systems (Minneapolis, MN, USA). Ascorbat, β-aminoproprionitrile and the α-SMA antibody as well as standard laboratory chemicals were from Sigma-Aldrich (St. Louis, MO, USA).

### Cell culture

PSCs were isolated from the pancreas of male LEW.1W inbred rats by collagenase digestion of the organ and Nycodenz (120 g/L) density gradient centrifugation as previously described[13]. PSCs collected from the top of the gradient were washed and resuspended in IMDM supplemented with 170 g/L fetal calf serum (FCS), 10 mL/L non-essential amino acids (dilution of a 100 × stock solution), $10^5$ U/L penicillin and 100 mg/L streptomycin. The cells were cultured at 37°C in a 50 mL/L $CO_2$ humidified atmosphere. All experiments were performed with cells growing in primary culture, or depending on the experimental settings, with cells of the first passage. If replating of the cells was required, PSCs were harvested by trypzination on d 7 after isolation and recultured at equal seeding densities.

### Quantification of DNA synthesis

To quantitate cell proliferation, incorporation of 5-bromo-2'-deoxyuridine (BrdU) into newly synthesized DNA was measured using the BrdU labeling and enzyme-linked immunosorbent assay kit (Roche Diagnostics). Therefore, cells were plated in 96-well plates in complete culture medium supplemented with IFN as indicated. After 48 h, BrdU labeling was initiated by adding labeling solution at a final concentration of 20 mL/L. After another 16 h, labeling was stopped, and BrdU uptake was measured according to the manufacturer's instructions.

### Analysis of cellular DNA content by flow cytometry (sub-$G_1$-peak)

Cells were grown to about 80% confluency and then incubated for 48 h in complete culture medium with or without IFN as indicated. Then the cells were harvested by trypzination, washed twice with PBS and resuspended in 2 mL ice-cold 70% ethanol for at least 12 h at -20°C, washed again twice with PBS and incubated for 1 h in 400 μL PBS containing 1 mL/L Tween 20 and 1 g/L RNase at room temperature. After the addition of 50 μg propidium iodide/$10^6$ cells, samples were subjected to cytofluorometric analysis using an FACScan (Becton Dickinson) and the CellQuest program. Ten thousand events were measured for each sample and the data were stored in list mode for further analysis.

### Quantification of collagen synthesis

Collagen synthesis was assessed through the quantification of [$^3$H]-proline incorporation into acetic acid-soluble proteins. Therefore, cells were plated in 12-well plates and grown to subconfluency. Afterwards, they were cultured for 48 h in complete culture medium supplemented with 2.5 mCi/L [$^3$H]-proline (48 Ci/mmol), 50 mg/L ascorbate, 50 mg/L β-aminoproprionitrile and IFN as indicated. All further steps were performed essentially as previously described[27]. Raw data of [$^3$H]-proline incorporation were normalized on the basis of absolute cell counts determined by trypan blue staining of PSCs cultured in parallel under identical conditions, except that no [$^3$H]-proline was added.

### Immunoblotting

Protein extracts of PSCs (pretreated as indicated) were prepared, adjusted to identical protein concentrations and subjected to immunoblot analysis as previously described[13]. Briefly, proteins (15 μg/sample) were separated by SDS-polyacrylamide gel electrophoresis and blotted onto nitrocellulose membrane. Next, the filters were blocked with 1% bovine serum albumin (Sigma-Aldrich) and incubated with the indicated antibodies (diluted according to the manufacturer's instructions) overnight at 4°C. After a final incubation with a horseradish-peroxidase labeled anti-rabbit or anti-mouse Ig antibody for 2 h at room temperature, blots were developed using ECL. For reprobing with additional antibodies, membranes were stripped by incubation in stripping buffer (62.5 mmol/L Tris-HCl, pH 6.7, 20 g/L SDS, 100 mmol/L 2-mercaptoethanol) at 50°C for 30 min.

### Inhibition of STAT1 expression using siRNA

STAT1 siRNA was purchased from Qiagen (Hilden,

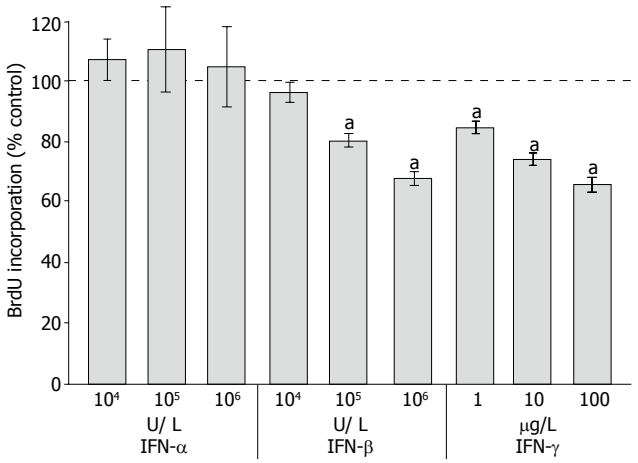


**Figure 1** Effects of interferons on PSC proliferation. PSCs growing in primary culture were harvested, replated at equal seeding densities in 96-well plates and treated with IFN-α, IFN-β and IFN-γ at the indicated concentrations for 48 h, the time when the fastest-growing cultures were almost confluent. Cell proliferation was assessed with the BrdU DNA-incorporation assay. One hundred percent cell proliferation corresponds to untreated PSCs. Data are presented as mean ± SE ($n$ = 6 separate cell preparations from one rat). $^aP < 0.05$ *vs* control cultures. The results shown are representative of three experiments using cells from different rats.

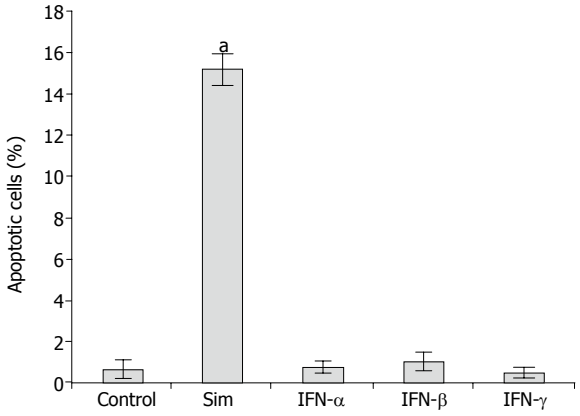


**Figure 2** Effects of IFN and simvastatin on PSC survival. PSCs growing in 12-well plates were cultured with IFN-α ($10^6$ U/L), IFN-β ($10^6$ U/L), IFN-γ (100 μg/L) and simvastatin (Sim; 5 μmol/L) as indicated. To determine the percentage of cell death by flow cytometry analysis, cells with DNA content lower than the $G_1$ peak (sub-$G_1$) were considered apoptotic. Data are indicated as mean ± SE ($n$ = 6 separate cell preparations from one rat). $^aP < 0.05$ *vs* control cultures. Three experiments using cells from different rats yielded qualitatively identical results.

Germany) and applied according to the manufacturer's protocol for the transfection of adherent cells, using a 1:6 ratio of siRNA to RNAsFect Reagent. Efficiency of siRNA treatment was monitored by analyzing the STAT1 protein level at different times after siRNA application. To study the effects of STAT1 siRNA on PSC growth, cells growing in 96-well plates were pretreated with siRNA at 100 nmol/L for 24 h before IFN-γ was added as indicated. After 48 h of incubation, DNA synthesis was quantitated by the determination of BrdU incorporation into DNA as described above. In all the experiments, a non-silencing siRNA oligonucleotide was included as a negative control.

### *Statistical analysis*

Results were expressed as mean±SE for the indicated number of separate cultures per experimental protocol. Statistical significance was checked using Wilcoxon's rank sum test. $P < 0.05$ was considered statistically significant.

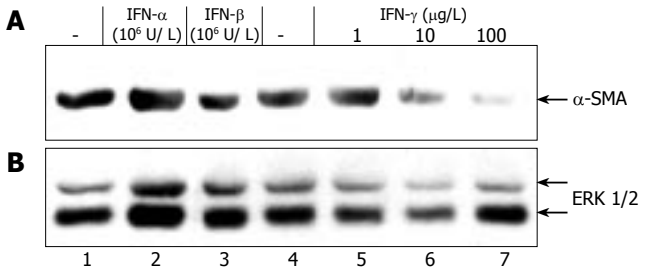


**Figure 3** IFN-γ inhibits expression of α-SMA in PSCs. Freshly isolated PSCs growing in 6-well plates were treated with IFN for 9 d as indicated. Cell lysates were normalized for protein concentration and resolved by SDS-PAGE. **A:** Expression of α SMA assayed by immunoblotting; **B:** Blot stripped and reprobed with an anti-ERK 1/2 protein-specific antibody to control loading. Results are representative of three independent experiments.

## RESULTS

### *Effects of IFNs on PSC functions*

To analyze the effects of IFN-α, IFN-β and IFN-γ on PSC proliferation, DNA synthesis after IFN-pretreatment for 48 h was measured (Figure 1). Both IFN-β and IFN-γ inhibited DNA synthesis significantly and in a dose-dependent manner, causing more than 30% reduction at the highest concentration tested. In contrast, IFN-α even at the concentration of $10^6$ U/L had no effect on PSC growth. To study if the inhibition of DNA synthesis was in fact due to the induction of apoptosis, an FACS analysis was performed (Figure 2). Under the experimental conditions tested, none of IFN-α, IFN-β or IFN-γ induced a significant increase of the sub-$G_1$ fraction (representing apoptotic cells). In contrast, PSCs treated with simvastatin significantly accumulated in the sub-$G_1$ fraction, confirming our previous results of pro-apoptotic effects of hydroxymethylglutaryl coenzyme A reductase inhibitors[28].

Next, we asked how IFNs affect the myofibroblastic phenotype of activated PSCs. IFN-γ incubation for 9 d (starting immediately after isolation) was associated with a dose-dependent reduction of α-SMA protein expression (Figure 3), while the effect of IFN-β (at $10^6$ U/L) remained questionable and IFN-α did not display any inhibitory effect at all. Further studies revealed that IFN-γ (at ⩾1 μg/L) and IFN-β (at ⩾$10^4$ U/L), but not IFN-α (at $10^6$ U/L) significantly diminished collagen synthesis by PSCs (Figure 4). A further increase of IFN-γ and IFN-β concentrations had no additional effect (data not shown).

To correlate the biological effects of the three IFNs with their molecular action, we analyzed STAT protein activation in IFN-stimulated PSCs (Figure 5). IFN-β and IFN-γ induced a rapid and strong increase of STAT1 and STAT3 tyrosine phosphorylation, while IFN-α was much less effective.

In subsequent experiments, we further studied the role of STAT1 in the mediation of IFN-γ effects on

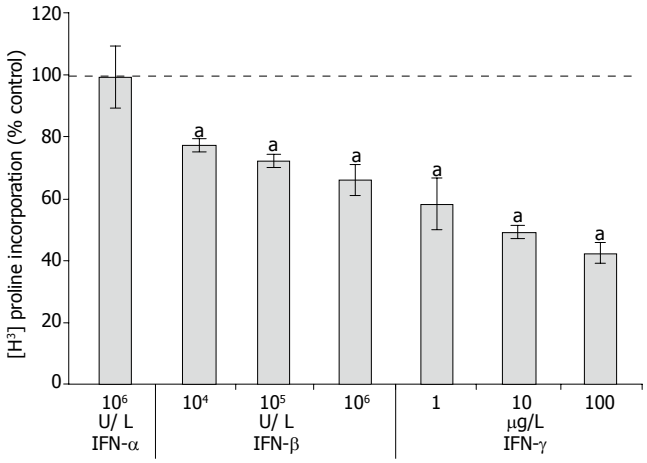


**Figure 4** Effects of IFNs on [$^3$H]-proline incorporation in PSCs. PSCs growing in 12-well plates (one passage) were exposed for 48 h to IFNs as indicated. Collagen synthesis was analyzed through the quantification of [$^3$H]-proline incorporation into acetic acid-soluble proteins, and raw data were normalized for differences in cell growth rates as described under "Materials and methods". One hundred percent [$^3$H]-proline incorporation corresponds to untreated PSCs. Data are presented as mean ± SE ($n$ = 6 separate cell preparations from one rat). $^aP < 0.05$ *vs* control cultures. The results shown are representative of three experiments using cells from different rats.

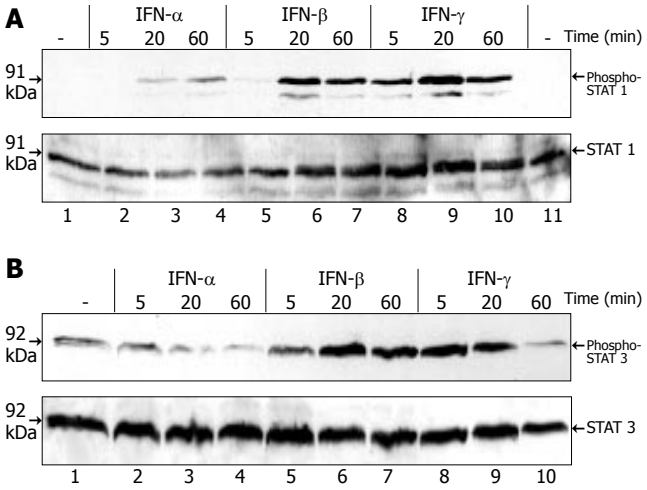


**Figure 5** Tyrosine phosphorylation of STAT1 and STAT3 in PSCs induced by IFN. PSCs growing in 6-well plates (one passage) were treated with IFN-α ($10^6$ U/L), IFN-β ($10^6$ U/L) and IFN-γ (100 μg/L) as indicated. Cell lysates were normalized for protein concentration and resolved by SDS-PAGE. **A:** Tyrosine phosphorylation of STAT1 assayed by immunoblotting using an antibody specific for the tyrosine-phosphorylated protein (upper panel). To control loading, the blot was stripped and reprobed with an anti-STAT1 protein-specific antibody (lower panel); **B:** Immunoblot analysis performed using an antibody specific for tyrosine-phosphorylated STAT3 (upper panel) and the blot stripped and reprobed with an anti-STAT3 protein-specific antibody (lower panel). Results are representative of three independent experiments.

PSC growth. As shown in Figure 6A (upper panel), STAT1 siRNA treatment caused a marked decrease of the STAT1 protein level. Expression of ERK 1 and 2 remained unchanged (lower panel), suggesting that the siRNA inhibited STAT1 expression in a specific manner. Downregulation of the STAT1 protein level was associated with a significant attenuation of the growth-inhibitory effect of IFN-γ (Figure 6B).

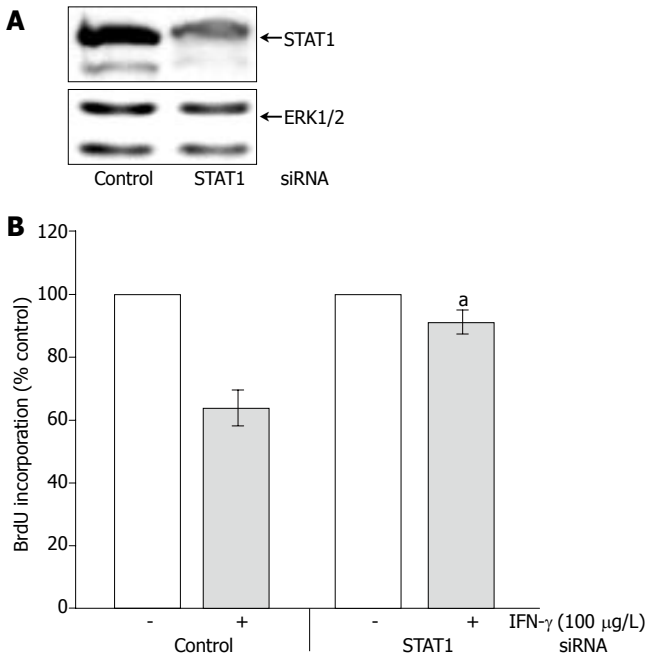


**Figure 6** Effects of STAT1 siRNA on PSC growth. **A:** Expression of STAT1 in PSCs 5 d after STAT1 siRNA application determined by immunoblot analysis as well as ERK 1 and 2 expression analyzed using an anti-ERK 1/2 protein-specific antibody; **B:** PSCs treated with STAT1 siRNA and IFN-γ as indicated and control cultures were exposed to a non-silencing control oligonucleotide at the same concentration. PSC proliferation was analyzed through the determination of BrdU incorporation into newly synthesized DNA as described in the section "Materials and methods". One hundred percent cell proliferation corresponds to PSCs treated with control oligonucleotide (left two columns) or STAT 1 siRNA (right two columns) in the absence of IFN-γ Data are presented as mean ± SE ($n$ = 7 separate cell preparations from one rat). $^aP<0.05$ *vs* IFN-γ-treated control cultures. The results shown are representative of three experiments using cells from different rats.

## DISCUSSION

Chronic pancreatitis is associated with an extended fibrosis that contributes to the development of an exocrine and endocrine insufficiency of the gland. Excessive deposition of connective tissue is also typical of pancreatic cancer and has been implicated in the acceleration of tumor progression[29]. In both cases, activated PSCs have been identified as the principle ECM-producing cell type[3,7,30]. PSCs are therefore considered as a promising target for the development of adjuvant therapies aimed at inhibiting pancreatic fibrogenesis.

The results of this study showed that IFNs displayed direct inhibitory effects on key effector functions of activated PSCs. While both IFN-γ and IFN-β diminished PSC proliferation and collagen synthesis, only IFN-γ efficiently reduced the expression of α-SMA, an indicator of myofibroblastic transdifferentiation. The effects of IFN-α remained insignificant. Whether the latter observation could reflect a peculiarity of the *in vitro* model used in this study, or a general phenomenon of PSC biology, is currently unclear.

The findings described here are largely in agreement with the results of studies on hepatic stellate cells which also showed direct, but distinct inhibitory effects of different IFNs on stellate cell activation. Shen *et al*[21] observed that HSC proliferation is attenuated by IFN-β

and IFN-γ, but not by IFN-α. On the other hand, under the experimental conditions used in this study no significant effects of IFNs on cell survival were detected, while in HSCs pro-apoptotic effects of IFN-γ and an anti-apoptotic action of IFN-α have been reported[23].

Targeted gene disruption studies have shown that the transcription factor STAT1 plays an essential, non-redundant role in IFN-mediated innate immunity to viral diseases[31,32]. Analyzing possible functions of STAT proteins in PSCs, we found a correlation between the efficiency of the different IFNs to inhibit stellate cell functions and their potential to activate STAT1 (as well as STAT3). Further experiments using an siRNA approach to block STAT1 expression revealed a direct involvement of the transcription factor in PSC growth inhibition by IFN-γ. The precise functions of STAT3 in PSCs remain to be characterized.

Previous studies in our laboratory have shown that IFN-γ in PSCs stimulates the expression of interleukin (IL)-15. In a co-culture model of rat PSCs and lymphocytes, a suppression of spontaneous lymphocyte apoptosis has been observed, which is at least in part mediated by IL-15[33]. Together, these data and the results of this study suggest a complex role of IFN-γ in the modulation of pancreatic inflammation and fibrosis. It is conceivable that IFN-γ displays distinct net effects on the progression of chronic pancreatitis, depending on the activation of auto-reactive lymphocytes and possibly the stage of the disease. To further elucidate the effects of IFN-γ on pancreatic fibrogenesis, *in vivo* studies using animal models of pancreatic fibrosis are required.

In summary, the discovery of direct inhibitory IFN-effects on PSC activation encourages further studies with respect to IFN efficiency in chronic pancreatitis. Currently, we are also focusing on a systematic evaluation of IFN target genes in stellate cells.

## ACKNOWLEDGMENTS

We gratefully acknowledge the excellent technical assistance of Mrs. Helga Schulze and Mrs. Katja Bergmann.

## REFERENCES

1 **Bachem MG,** Schneider E, Gross H, Weidenbach H, Schmid RM, Menke A, Siech M, Beger H, Grunert A, Adler G. Identification, culture, and characterization of pancreatic stellate cells in rats and humans. *Gastroenterology* 1998; **115:** 421-432

2 **Apte MV**, Haber PS, Applegate TL, Norton ID, McCaughan GW, Korsten MA, Pirola RC, Wilson JS. Periacinar stellate shaped cells in rat pancreas: identification, isolation, and culture. *Gut* 1998; **43**: 128-133

3 **Haber PS**, Keogh GW, Apte MV, Moran CS, Stewart NL, Crawford DH, Pirola RC, McCaughan GW, Ramm GA, Wilson JS. Activation of pancreatic stellate cells in human and experimental pancreatic fibrosis. *Am J Pathol* 1999; **155**: 1087-1095

4 **Longnecker DS**. Pathology and pathogenesis of diseases of the pancreas. *Am J Pathol* 1982; **107**: 103-121

5 **Etemad B**, Whitcomb DC. Chronic pancreatitis: diagnosis, classification, and new genetic developments. *Gastroenterology* 2001; **120**: 682-707

6 **Gressner AM**, Bachem MG. Molecular mechanisms of liver fibrogenesis--a homage to the role of activated fat-storing cells. *Digestion* 1995; **56**: 335-346

7 **Apte MV**, Wilson JS. Stellate cell activation in alcoholic pancreatitis. *Pancreas* 2003; **27**: 316-320

8 **Apte MV**, Haber PS, Darby SJ, Rodgers SC, McCaughan GW, Korsten MA, Pirola RC, Wilson JS. Pancreatic stellate cells are activated by proinflammatory cytokines: implications for pancreatic fibrogenesis. *Gut* 1999; **44**: 534-541

9 **Mews P**, Phillips P, Fahmy R, Korsten M, Pirola R, Wilson J, Apte M. Pancreatic stellate cells respond to inflammatory cytokines: potential role in chronic pancreatitis. *Gut* 2002; **50**: 535-541

10 **Apte MV**, Phillips PA, Fahmy RG, Darby SJ, Rodgers SC, McCaughan GW, Korsten MA, Pirola RC, Naidoo D, Wilson JS. Does alcohol directly stimulate pancreatic fibrogenesis? Studies with rat pancreatic stellate cells. *Gastroenterology* 2000; **118**: 780-794

11 **Luttenberger T,** Schmid-Kotsas A, Menke A, Siech M, Beger H, Adler G, Grunert A, Bachem MG. Platelet-derived growth factors stimulate proliferation and extracellular matrix synthesis of pancreatic stellate cells: implications in pathogenesis of pancreas fibrosis. *Lab Invest* 2000; **80:** 47-55

12 **Kruse ML**, Hildebrand PB, Timke C, Folsch UR, Schmidt WE. TGFbeta1 autocrine growth control in isolated pancreatic fibroblastoid cells/stellate cells in vitro. *Regul Pept* 2000; **90:** 47-52

13 **Jaster R**, Sparmann G, Emmrich J, Liebe S. Extracellular signal regulated kinases are key mediators of mitogenic signals in rat pancreatic stellate cells. *Gut* 2002; **51**: 579-584

14 **Masamune A**, Kikuta K, Satoh M, Satoh A, Shimosegawa T. Alcohol activates activator protein-1 and mitogen-activated protein kinases in rat pancreatic stellate cells. *J Pharmacol Exp Ther* 2002; **302**: 36-42

15 **McCarroll JA**, Phillips PA, Park S, Doherty E, Pirola RC, Wilson JS, Apte MV. Pancreatic stellate cell activation by ethanol and acetaldehyde: is it mediated by the mitogen-activated protein kinase signaling pathway? *Pancreas* 2003; **27**: 150-160

16 **Masamune A**, Satoh M, Kikuta K, Sakai Y, Satoh A, Shimosegawa T. Inhibition of p38 mitogen-activated protein kinase blocks activation of rat pancreatic stellate cells. *J Pharmacol Exp Ther* 2003; **304**: 8-14

17 **Masamune A**, Kikuta K, Suzuki N, Satoh M, Satoh K, Shimosegawa T. A c-Jun NH2-terminal kinase inhibitor SP600125 (anthra[1,9-cd]pyrazole-6 (2H)-one) blocks activation of pancreatic stellate cells. *J Pharmacol Exp Ther* 2004; **310**: 520-527

18 **Stark GR**, Kerr IM, Williams BR, Silverman RH, Schreiber RD. How cells respond to interferons. *Annu Rev Biochem* 1998; **67**: 227-264

19 **Nguyen MH**, Wright TL. Therapeutic advances in the management of hepatitis B and hepatitis C. *Curr Opin Infect Dis* 2001; **14**: 593-601

20 **Schuppan D**, Krebs A, Bauer M, Hahn EG. Hepatitis C and liver fibrosis. *Cell Death Differ* 2003; **10** Suppl 1: S59-S67

21 **Shen H**, Zhang M, Minuk GY, Gong Y. Different effects of rat interferon alpha, beta and gamma on rat hepatic stellate cell proliferation and activation. *BMC Cell Biol* 2002; **3**: 9

22 **Baroni GS**, D'Ambrosio L, Curto P, Casini A, Mancini R, Jezequel AM, Benedetti A. Interferon gamma decreases hepatic stellate cell activation and extracellular matrix deposition in rat liver fibrosis. *Hepatology* 1996; **23**: 1189-1199

23 **Saile B**, Eisenbach C, Dudas J, El-Armouche H, Ramadori G. Interferon-gamma acts proapoptotic on hepatic stellate cells (HSC) and abrogates the antiapoptotic effect of interferon-alpha by an HSP70-dependant pathway. *Eur J Cell Biol* 2004; **83**: 469-476

24 **Uze G**, Lutfalla G, Mogensen KE. Alpha and beta interferons and their receptor and their friends and relations. *J Interferon Cytokine Res* 1995; **15**: 3-26

25 **Rane SG**, Reddy EP. Janus kinases: components of multiple signaling pathways. *Oncogene* 2000; **19**: 5662-5679

26 **Ihle JN**. Cytokine receptor signalling. *Nature* 1995; **377**: 591-594

27 **Jaster R**, Hilgendorf I, Fitzner B, Brock P, Sparmann G,

Emmrich J, Liebe S. Regulation of pancreatic stellate cell function *in vitro*: biological and molecular effects of all-trans retinoic acid. *Biochem Pharmacol* 2003; **66**: 633-641

28 **Jaster R**, Brock P, Sparmann G, Emmrich J, Liebe S. Inhibition of pancreatic stellate cell activation by the hydroxymethylglutaryl coenzyme A reductase inhibitor lovastatin. *Biochem Pharmacol* 2003; **65**: 1295-1303

29 **Bachem MG**, Schunemann M, Ramadani M, Siech M, Beger H, Buck A, Zhou S, Schmid-Kotsas A, Adler G. Pancreatic carcinoma cells induce fibrosis by stimulating proliferation and matrix synthesis of stellate cells. *Gastroenterology* 2005; **128**: 907-921

30 **Apte MV**, Park S, Phillips PA, Santucci N, Goldstein D, Kumar RK, Ramm GA, Buchler M, Friess H, McCarroll JA, Keogh G, Merrett N, Pirola R, Wilson JS. Desmoplastic reaction in pancreatic cancer: role of pancreatic stellate cells. *Pancreas* 2004; **29**: 179-187

31 **Meraz MA**, White JM, Sheehan KC, Bach EA, Rodig SJ, Dighe AS, Kaplan DH, Riley JK, Greenlund AC, Campbell D, Carver-Moore K, DuBois RN, Clark R, Aguet M, Schreiber RD. Targeted disruption of the Stat1 gene in mice reveals unexpected physiologic specificity in the JAK-STAT signaling pathway. *Cell* 1996; **84**: 431-442

32 **Durbin JE**, Hackenmiller R, Simon MC, Levy DE. Targeted disruption of the mouse Stat1 gene results in compromised innate immunity to viral disease. *Cell* 1996; **84**: 443-450

33 **Sparmann G,** Glass A, Brock P, Jaster R, Koczan D, Thiesen HJ, Liebe S, Emmrich J. Inhibition of lymphocyte apoptosis by pancreatic stellate cells: impact of interleukin-15. *Am J Physiol Gastrointest Liver Physiol* 2005; **289:** G842-G851

**S- Editor** Wang XL and Guo SY **L- Editor** Elsevier HK **E- Editor** Kong LH

PO Box 2345, Beijing 100023, China
www.wjgnet.com
wjg@wjgnet.com

*World J Gastroenterol* 2006 February 14; 12(6): 902-907
***World Journal of Gastroenterology*** ISSN 1007-9327
© 2006 The WJG Press. All rights reserved.

*BASIC RESEARCH*

# Characterization of human gene encoding SLA/LP autoantigen and its conserved homologs in mouse, fish, fly, and worm

Chun-Xia Wang, Andreas Teufel, Uta Cheruti, Joachim Grötzinger, Peter R Galle, Ansgar W Lohse, Johannes Herkel

Chun-Xia Wang, Ansgar W Lohse, Johannes Herkel, I. Department of Medicine, University Medical Centre Hamburg-Eppendorf, Hamburg, Germany
Chun-Xia Wang, Shandong University Shandong Provincial Hospital, Jinan, Shandong Province, China
Andreas Teufel, Uta Cheruti, Peter R Galle, I. Department of Medicine, Johannes Gutenberg University, Mainz, Germany
Joachim Grötzinger, Institute of Biochemistry, Christian-Albrechts-University, Kiel, Germany
Supported by the Deutsche Forschungsgemeinschaft (SFB 548)
Co-first-authors: Chun-Xia Wang and Andreas Teufel
Correspondence to: Johannes Herkel, I. Department of Medicine, University Medical Centre Hamburg-Eppendorf, Martinistr. 52, 20246 Hamburg, Germany. jherkel@uke.uni-mainz.de
Telephone: +49-40-42803-3910 Fax: +49-40-42803-8531
Received: 2005-05-20 Accepted: 2005-08-26

## Abstract

**AIM:** To approach the elusive function of the SLA/LP molecule, we have characterized genomic organization and conservation of the major antigenic and functional properties of the SLA/LP molecule in various species.

**METHODS:** By means of computational biology, we have characterized the complete SLA/LP gene, mRNA and deduced protein sequences in man, mouse, zebrafish, fly, and worm.

**RESULTS:** The human SLA/LP gene sequence of approximately 39 kb, which maps to chromosome 4p15.2, is organized in 11 exons, of which 10 or 11 are translated, depending on the splice variant. Homologous molecules were identified in several biological model organisms. The various homologous protein sequences showed a high degree of similarity or homology, notably at those residues that are of functional importance. The only domain of the human protein sequence that lacks significant homology with homologous sequences is the major antigenic epitope recognized by autoantibodies from autoimmune hepatitis (AIH) patients.

**CONCLUSION:** The SLA/LP molecule and its functionally relevant residues have been highly conserved throughout the evolution, suggesting an indispensable function of the molecule. The finding that the only non-conserved domain is the dominant antigenic epitope of the human SLA/LP sequence, suggests that SLA/LP autoimmunity is autoantigen-driven rather than being driven by molecular mimicry.

© 2006 The WJG Press. All rights reserved.

**Key words:** Autoimmune hepatitis; Autoantigen; Genomics; Bioinformatics

Wang CX, Teufel A, Cheruti U, Grötzinger J, Galle PR, Lohse AW, Herkel J. Characterization of human gene encoding SLA/LP autoantigen and its conserved homologs in mouse, fish, fly, and worm. *World J Gastroenterol* 2006; 12(6): 902-907

http://www.wjgnet.com/1007-9327/12/902.asp

## INTRODUCTION

Autoantibodies to soluble liver antigen (SLA)[1] and to liver/pancreas (LP)[2] have been described as specific markers for autoimmune hepatitis[3]. Recently, identity of the SLA and LP antigens has been demonstrated, and the target antigen of SLA/LP autoantibodies has been cloned[4]. Using the recombinant SLA/LP molecule, the strict specificity of SLA/LP autoantibodies as markers for AIH has been confirmed[5].

The primary biological function of SLA/LP remains unclear. Because the SLA/LP molecule was found to be associated with the UGA tRNP(Ser)Sec complex[6,7], which facilitates the co-translational incorporation of selenocysteine into proteins, it has been speculated that the SLA/LP molecule may have a role in selenoprotein metabolism; the specialized UGA tRNA is initially charged with serine to form seryl-tRNA, which then is enzymatically converted to selenocysteine-tRNA$^{Sec}$. However, there is no direct experimental evidence for such a role of the SLA/LP molecule so far. Nevertheless, a fold recognition study predicted the SLA/LP tertiary structure by comparison to known protein structures to be that of a pyridoxal phosphate (PLP)-dependent transferase[8], which is compatible with a role in selenoprotein metabolism. The active site was proposed to be a cavity with a channel, formed by dimerization of two SLA/LP molecules[8,9]. In the three-dimensional model, five amino acids of monomer A (L88, T89, F92, T94, and S118) as well as two amino acids of monomer B (P251 and G252) were involved in dimerization and the amino acids critical for binding and orientation of the co-enzyme PLP were

identified to be G50, S51, S165, D186, H189, K224[8] (residue numbering according to GenBank accession number NP_722547).

The immune mechanisms that drive SLA/LP autoimmunity and the pathogenetic relevance of autoimmunity to SLA/LP are currently not clear. The main antigenic region crucial for the recognition of SLA/LP autoantibodies was identified to locate between amino acids 390 and 428[4,10], thus being easily accessible by antibodies[8]. This region contains sequence homologies with various microbial antigens, including proteins of Rickettsia species, human herpesvirus 6, and cytomegalovirus[4]; however, the homologous microbial sequences are only poorly recognized by SLA/LP autoantibodies[10]. Nevertheless, molecular mimicry of homologous proteins from other species, such as parasites, may be a trigger of SLA/LP autoimmunity.

Due to the human genome project and other genomic sequencing groups, sequences of many different species are now publicly available. While some chromosomes are completely assembled, most genomic fragments are currently still preliminary and await characterization. To approach the elusive biological function of the SLA/LP molecule, we have characterized here the human SLA/LP gene and homologous sequences of other species by means of computational biology. The obtained results support the hypothesis that SLA/LP autoimmunity is autoantigen-driven rather than being driven by molecular mimicry[10].

## MATERIALS AND METHODS

### Identification of the human SLA/LP gene

We have previously identified the human SLA/LP protein and deposited the corresponding mRNA sequence into the GenBank[11] with the accession numbers NM_016955 and NM_153825. BLASTing the human mRNA sequence against the human genome draft sequence revealed the genomic localization[12,13].

### Identification of SLA/LP homologs in other species

Homologs corresponding to the human SLA/LP were identified by BLAST query with the human SLA/LP protein sequence (NP_722547) against the non-redundant databases of mouse (*Mus musculus*), zebrafish (*Danio rerio*), fruit fly (*Drosophila melanogaster*) and the nematode worm (*Caenorhabditis elegans*).

### Exon/intron structure and chromosomal localization

Exon/intron structure and chromosomal localization were identified by BLASTing the SLA/LP mRNA sequences of each homolog against the corresponding genome draft sequences of the particular species.

### Locus analysis

Data regarding the genomic loci analysis were obtained from the GenBank[11].

### Analysis of protein structure and conservation

The amino acid sequence was deduced from the obtained mRNA sequences. The alignment of SLA/LP homologous sequences was initially performed using the ClustalW algorithm[14]. The sequence alignments in Figure 3 were performed using the longer human SLA/LP variant (CAB89517). The theoretical isoelectric point and molecular weight was calculated with the pI/Mw tool on the ExPASy server[15,16]. Protein structures and domains were analyzed using two independent algorithms, Pfam[17] and NCBI Conserved Domain Search[18].

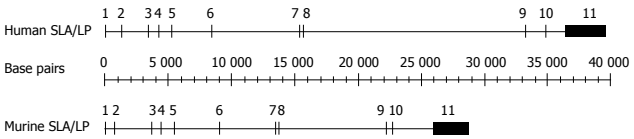


**Figure 1** Organization of SLA/LP genes in man and mouse. The exon/intron structure of the human and mouse SLA/LP gene is represented schematically. Exon sequences (numbered boxes) are highly conserved and of similar size and number in man and mouse. Intron sequences, marked as lines, differ in both species.

## RESULTS

### Human SLA gene and corresponding mRNA and protein sequences

We have previously submitted the human mRNA sequences of two alternative splice variants of SLA/LP to GenBank with the accession numbers NM_016955 and NM_153825. Using the human SLA/LP protein sequence as a query for BLAST searches against the human mRNA database, additional matching mRNA sequences (splice variants) were not identified. Matching the human mRNA sequence to the available human genomic draft sequence (htgs), the corresponding gene was mapped to chromosome 4p15.2. The gene was found to span a genomic region of approximately 39 kb and to be organized in 11 exons (Figure 1). Most exon sizes were rather small, ranging between 91 and 187 bp, with the exception of exon 11 at the 3' end, which covered 3 224 bp. The two splice variants were fully identical, except for the absence of exon 2 (149 bp) in the shorter variant. Both variants have a large 2 930 bp 3' untranslated region; the 5' untranslated region of the two variants is relatively short with 155 and 174 bp, respectively. The amino acid sequences of the two splice variants, as deduced from their mRNA sequence, differ only in their amino-terminal residues (Figure 2). The theoretical molecular weight and isoelectric point of the longer splice variants is 48.84 kDa and 8.64, respectively; that of the shorter variant is 46.85 kDa and 8.52, respectively.

### Mouse SLA gene and corresponding mRNA and protein sequences

The SLA/LP gene and genomic organization was highly conserved in mouse. BLASTing the human SLA/LP protein sequence against the mouse protein database, revealed a mouse homolog with the accession number NP_766078. The human and mouse SLA/LP protein sequences are identical at 85% of the residues (Figure 2). Both, the NCBI and Pfam conserved protein domain

```
Human short   MS-TSYGCFWRR 11
Mouse short   MNPESFAAGERR 12
              *.  *:.    **

Human long    MDSNNFLGNCGVGEREGRVASALVARRHYR 30
Mouse long    MDSNNFLGNCGVGEREGRVASALVARRHYR 30
              ******************************

Human SLA/LP  FIHGIGRSGDISAVQPKAAGSSLLNKITNSLVLDIIKLAGVHTVANCFVVPMAT   65/84
Mouse SLA/LP  FIHGIGRSGDISAVQPKAAGSSLLNKITNSLVLNVIKLAGVHSVASCFVVPMAT   66/84
              ********************************:*********:*******:**.********

Human SLA/LP  GMSLTLCFLTLRHKRPKAKYIIWPRIDQKSCFKSMITAGFEPVVIENVLEGDEL   119/138
Mouse SLA/LP  GMSLTLCFLTLRHKRPKAKYIIWPRIDQKSCFKSMVTAGFEPVVIENVLEGDEL   120/138
              ***********************************:************

Human SLA/LP  RTDLKAVEAKVQELGPDCILCIHSTTSCFAPRVPDRLEELAVICANYDIPHIVN   173/192
Mouse SLA/LP  RTDLKAVEAKIQELGPEHILCLHSTTACFAPRVPDRLEELAVICANYDIPHVVN   174/192
              **********:*****: ***:****:*****************:*******:**

Human SLA/LP  NAYGVQSSKCMHLIQQGARVGRIDAFVQSLDKNFMVPVGGAIIAGFNDSFIQEI   227/246
Mouse SLA/LP  NAYGLQSSKCMHLIQQGARVGRIDAFVQSLDKNFMVPVGGAIIAGFNEPFIQDI   228/246
              ****:******* ******************************************:.***:*

Human SLA/LP  SKMYPGRASASPSLDVLITLLSLGSNGYKKLLKERKEMFSYLSNQIKKLSEAYN   281/300
Mouse SLA/LP  SKMYPGRASASPSLDVLITLLSLGCSGYRKLLKERKEMFVYLSTQLKKLAEAHN   282/300
              **********************..**:**********  ***.*:***:**:*

Human SLA/LP  ERLLHTPHNPISLAMTLKTLDEHRDKAVTQLGSMLFTKQVSGARVVPLGSMQTV   335/354
Mouse SLA/LP  ERLLQTPHNPISLAMTLKTIDGHHDKAVTQLGSMLFTRQVSGARAVPLGNVQTV   336/354
              ****:*****************:*  *:**************:*******.****.:***

Human SLA/LP  SGYTFRGFMSHTNNYPCAYLNAASAIGMKMQDVDLFINRLDRCLKAVRKERSKE   389/408
Mouse SLA/LP  SGHTFRGFMSHADNYPCAYLNAAAAIGMKMQDVDLFIKRLDKCLNIVRKEQTRA   390/408
              **:********::**********:*****************:***:**:  ****:::

Human SLA/LP  ---SDDNYDKTEDVDIEEMALKLDNVLLDTYQDASS                     422/441
Mouse SLA/LP  SVVSGADRNKAEDADIEEMALKLDDVLGDVGQGPAL                     426/444
                 *.  :  :*:**.*********:**  *.  *..:
```

**Figure 2** SLA/LP splice variants in man and mouse. The amino acid sequences of the long and short SLA/LP splice variants in humans and their putative homologs in mouse are aligned. The protein variants differ only in their amino-terminal sequence, 11 or 30 residues in the human protein and 12 or 30 residues in the murine protein, as depicted in the upper panel. The other residues (lower panel) are identical in the respective splice variants within each species.

```
Homo sapiens   ----MDSNNFLGNCGVGEREGRVASALVARRHYRFIHGIGRSGDISAVQPKAAGSSLLNK   56
Mus musculus   ----MDSNNFLGNCGVGEREGRVASALVARRHYRFIHGIGRSGDISAVQPKAAGSSLLNK   56
Danio rerio    ----MDSNNFLGNCGVGEREGRVASSLVARRHYRLIHGIGRSGDIAAVQPKAAGSSLLNK   56
Drosophila m.  MLASLDSNNYPHKVGLGEREARIACKLVARRHYNFGHGIGRSGDLLEAQPKAAGSTLLAR   60
C. elegans     ---------MIPVGAGEREGRVLTPLVQRLHSNLTHGIGRSGNLLEIQPKALGSSMLAC   50
                         *  ****.*:    **  *  *  .:  *******::   ****  **::*

Homo sapiens   ITNSLVLD I IKLAGVHTVANCFVVPMATGMSLTLCFLTL RHKRPKAKYIIWPRIDQKSCF   116
Mus musculus   ITNSLVLN VIKLAGVHSVASCFVVPMATGMSLTLCFLTL RHKRPKAKYIIWPRIDQKSCF   116
Danio rerio    ITNSVVLD VLKLTGVRSVSSCFVVPMATGMSLTLCFLTL RHRRPKARYILWPRIDQKSCF   116
Drosophila m.  LTNALILDLIRGIGLPSCAGCFLVPMCTGMTLTLCLQSLRKRRPGARYVLWSRIDQKSCF   120
C. elegans     LSNEFAKHALHLLGL HAVKSCIVVPLCTGMSLSLCMTSWRRRRPKAKYVVWLRIDQKSSL   110
               ::*  .  .  ::  *:  :  .*:::**:.***:*:**:  :*:::**  *:*::*  ******.:

Homo sapiens   KSMITAGFEPVVIENVLEGDELRTDLKAVEAKVQELGPDCILCIHSTTSCFAPRVPDRLE   176
Mus musculus   KSMVTAGFEPVVIENVLEGDELRTDLKAVEAKIQELGPEHILCLHSTTACFAPRVPDRLE   176
Danio rerio    KSMVTAGFEPVVIENVLEGDELRTNLEEVERKIEEFGAENTLCVHSTTSCFAPRVPDRLE   176
Drosophila m.  KAITATGLVPVVIPCL IKGESLNTNVDLFREKIKSLGVDSILCLYTTTSCFAPRNSDDIA   180
C. elegans     KSIYHAGFEPIIVEPIRDRDSLITDVETVNRIIEQRGEE-ILCVMTTTSCFAPRSPDNVE   169
               *::   :*: *:::  :  .  :.* *::.  ..   ::.*  :   **:  :**:*****  .*  :

Homo sapiens   ELAVICANYDIPHIVNNAYGVQSSKCMHLIQQGARVGRIDAFVQSLDKNFMVPVGGAIIA   236
Mus musculus   ELAVICANYDIPHVVNNAYGLQSSKCMHLIQQGARVGRIDAFVQSLDKNFMVPVGGAIIA   236
Danio rerio    ELSVLCAKHDIPHIVNNAYGVQPSKCMHLIQQGARVGRIDAFVQSLDKNFVVPVGGAIIA   236
Drosophila m.  EVSKLSKQWQIPHLVNNAYGLQAKEIVNQLECANRVGRIDYFVQSSDKNLLVPVGSAIVA   240
C. elegans     AISAICAAHDVPHLVNNAYGLQSEETIRKIAAAHECGRVDAVVQSLDKNFQVPVGGAVIA   229
                 :: :.    ::**:*******:*..:  :.  :  .  .  **:*.***  ***:  ****.*::*

Homo sapiens   GFNDSFIQEISKMYPGRASASPSLDVLI TLLSLGSNGYKKLLKERKEMFSYLSNQIKKLS   296
Mus musculus   GFNEPFIQDISKMYPGRASASPSLDVLI TLLSLGCSGYRKLLKERKEMFVYLSTQLKKLA   296
Danio rerio    GFDENFIQEISKIYPGRASASPSLDVLI TLLTLGANGYKKLLADRKELYGHLAQELSALA   296
Drosophila m.  SFNESVLHDVASTYAGRASGSQSLDVLMTLLSLGRNGFRLLFDQRGENFNYLRENLRKFA   300
C. elegans     AFKQNHIQSIAQSYPGRASSVPSRDLVL TLLYQGQSAFLEPFGKQKQMFLKMRRKLI SFA   289
               .*.:   ::.::.  *.****.  *  *:::***   *  ..:    :  .:  :  :  :   ::   ::

Homo sapiens   EAYNERLLHTPHNPISLAMTLKTLDEHRDKAVTQLGSMLFTRQVSGARVVPLGSMQ-TVS   355
Mus musculus   EAHNERLLQTPHNPISLAMTLKTIDGHHDKAVTQLGSMLFTRQVSGARAVPLGNVQ-TVS   355
Danio rerio    ARHGERLLKTPHNPISLAMSLNHLEAHSSSAVTQLGSMLFTRQVSGARVVPLGVQQ-TVS   355
Drosophila m.  EPRGEIVIDSRFNSISLAITLATLAGDQMKSITKLGSMLHMRGVSGARVIVPGQNK-TID   359
C. elegans     ENIGECVYEVPENEISSAMTLSTI PPAKQ---TLFGSILFAKGITGARVVTSSQSKTTIE   346
                    .*  :  .    *  **  *::*  :            *:**:*.  :  ::***.:  .   :  *:.

Homo sapiens   GYTFRGFMSHTNNYPCAYLNAASAIGMKMQDVDLFI KRLDRCLKAVRKERSKE---SDDN   412
Mus musculus   GHTFRGFMSHADNYPCAYLNAAAAIGMKMQDVDLFI KRLDKCLNIVRKEQTRASVVSGAD   415
Danio rerio    GHTFSGFMSHSEAYPCPYLNAASAIGI TKGDVTVCMKRLGKCLKILKKEKSDP----  --A   409
Drosophila m.  GHEFLGK-----------------------------------------------------   366
C. elegans     GCEFINFGSHTTEQHGGYLNIACSVGMTDHELEELFTRLTSSYAKFVRELAKE---DERI   403
                *   *.

Homo sapiens   YDKTEDVDIEEMALKLDNVLLDTYQDASS          441
Mus musculus   RNKAEDADIEEMALKLDDVLGDVGQGPAL          444
Danio rerio    DLEAEDGELEESPQRSTELRV--------          430
Drosophila m.  ----------------------------
C. elegans     NSSGRRIPINESFDMEND----------          421
```

**Figure 3** Alignment of SLA/LP protein sequences. The SLA/LP amino acid sequences of various eukaryotic species were aligned by ClustalW. The presumed residues that mediate binding to the cofactor pyridoxal phosphate are highlighted in bold and underlined; residues that function in dimerization are highlighted in bold and italic. The immunodominant epitope sequence (390-428) of the human SLA/LP protein is marked in bold.

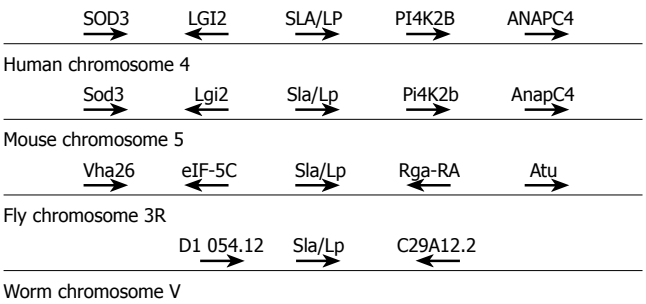


**Figure 4** Chromosomal localization of SLA/LP genes. The genes adjacent to the SLA/LP loci on human chromosome 4, mouse chromosome 5, fly chromosome 3R, and worm chromosome V are represented schematically.

algorithms, predicted the existence of SLA/LP structure between amino acids 61 and 458 and amino acids 61 and 459, respectively. BLASTing the protein sequence against the translated mouse genome database revealed the corresponding mRNA NM_172490.1. BLASTing the mRNA sequence against the draft sequence of the mouse genome, the corresponding SLA/LP gene was mapped to mouse chromosome 5qC1. The genomic region spanned 28.5 kb and the mouse SLA/LP gene was organized into 11 exons like the human homolog (Figure 1). Exon sizes ranged between 91 and 2 927 bp with exon 11 being by far the largest exon. The 3' untranslated region was 2 629 bp and the 5' untranslated region was 19 bp. Although not filed in the GenBank, two murine splice variants are very likely; the mouse genomic organization and exon sequences are very similar to the human gene and a splicing signature similar to that in human beings is present in the homologous mouse sequence. The presumed splice variants in the mouse are shown in Figure 2, aligned to the corresponding human proteins. The theoretical molecular weight and isoelectric point of the longer splice variants is 48.48 ku and 8.86, respectively; that of the shorter variant is 46.5 ku and 8.71, respectively.

### *Zebrafish SLA gene sequence and corresponding mRNA*

The SLA gene and genomic organization was highly conserved in fish. BLASTing the human SLA/LP protein sequence against the zebrafish protein database, revealed a homolog with the accession number NP_956448. The zebrafish sequence was identical to the human protein sequence in 69% of the residues. Both, the NCBI and Pfam conserved protein domain algorithms, predicted the existence of SLA/LP structure between amino acids 61 and 459. BLASTing the protein sequence against the translated zebrafish genome database revealed the corresponding mRNA NM_200154. Chromosomal mapping was not possible, since the genomic fragment containing the SLA/LP sequence was not yet assembled into the genomic context. The corresponding gene could only be mapped to the fragment scaffold Zv4_NA8411.1. Thus a complete exon/intron structure was not yet available, and potential splice variants could not be identified.

### *Drosophila SLA gene sequence and corresponding mRNA*

The SLA gene and genomic organization were also conserved in Drosophila. BLASTing the human SLA/LP protein sequence against the Drosophila protein database revealed a Drosophila homolog (two isoforms) with the accession numbers AAF51994 and AAS65099. The Drosophila protein sequence has 42% identity compared to the human protein sequence. However, this may be an underestimation, as it remains unclear whether the recently annotated Drosophila SLA/LP sequence is complete. Both, the NCBI and Pfam conserved protein domain algorithms predicted the existence of SLA/LP structure between amino acids 61 and 413 and amino acids 61 and 428, respectively. BLASTing the protein sequence against the translated Drosophila genome database revealed the corresponding mRNA NM_141299.1. BLASTing the mRNA sequence against the draft sequence of the fruit fly genome, the corresponding SLA/LP gene was mapped to Drosophila chromosome 3R. The genomic region of the currently annotated Drosophila SLA/LP gene spanning approximately 1.6 kb was found to be organized into (at least) 4 exons. Exon sizes ranged between 114 and 1 021 bp with exon 3 being by far the largest exon. A short 3' UTR was shown to consist of 115 bp. Thus far, a 5' UTR was not identified.

### *C. elegans SLA/LP gene sequence and corresponding mRNA*

The SLA/LP gene and genomic organization were also conserved in *C. elegans*. BLASTing the human SLA/LP protein sequence against the *C. elegans* protein database revealed similarity to *C. elegans* protein D1054.13 with the accession number CAA98446. The *C. elegans* protein sequence had 42% identity compared to the human protein sequence. Again, both the NCBI and Pfam conserved protein domain algorithms predicted the existence of SLA/LP structure between amino acids 53 and 450. BLASTing the protein sequence against the translated *C. elegans* genome database revealed the corresponding mRNA NM_073360. BLASTing the mRNA sequence against the draft sequence of the *C. elegans* genome, the corresponding SLA/LP gene was mapped to *C. elegans* chromosome V. The genomic region spanned 1.8 kb and the *C. elegans* SLA/LP gene was organized in 7 exons. Exon sizes ranged between 67 bp for exon 3 and 636 bp for exon 5. A rather short 5' UTR contained 43 bp, a 3' UTR could not be found in the currently available sequence. Thus, it remains unclear, whether the currently available sequence represents the complete protein sequence of *C. elegans*.

### *Conservation of SLA/LP homologs*

We aligned the protein sequences of the SLA/LP homologs in human, mouse, fish, fly, and worm (Figure 3). The mammalian sequences were the two closest related sequences. The invertebrate sequences of Drosophila and *C. elegans* sequence were most closely related to each other; the zebrafish sequence was equally related to the mammalian and invertebrate sequences.

### *Chromosomal localization of the human, mouse, fly, and worm SLA/LP genes*

We then studied the neighboring genes in man, mouse, fly, and worm (Figure 4). Upstream of the human SLA/

LP sequence on human chromosome 4 was the gene for extracellular-superoxide dismutase 3[19] and the Leucine rich gene, glioma-inactivated 2[20]. Downstream of the SLA/LP locus was the phosphatidylinositol 4-kinase type-II beta (PI4K2B)[21] and anaphase promoting complex, subunit 4[22]. The same structure was found for mouse chromosome 5 that contains the murine SLA/LP locus. The genomic structure of SLA/LP loci in fly and worm did not share these similarities to the mammalian genomes. The fly SLA/LP homolog was flanked by the gene *eIF-5C*, which is involved in long-term memory[23] and the gene for a 26 ku E-subunit of the vacuolar ATPase[24], upstream of the SLA/LP locus. Two currently uncharacterized genes, Rga-RA (account number AAF51992) and Atu (account number AAF51991), are located downstream of the fly SLA/LP gene. The worm SLA/LP sequence was flanked by a gene (5L286) encoding protein of unknown function, upstream, and the serpentine receptor class H (srh-184)[25], downstream of the SLA/LP locus.

### *Conservation of the main antigenic region and main structural features of folding and dimerization*

The dominant autoepitope of SLA/LP autoantibodies had been identified to locate between amino acids 390 and 428 of the longer human SLA/LP protein sequence variant (NP_722547)[4,10]. After aligning the homologous protein sequences (Figure 3), we studied the degree of sequence conservation in the immunodominant antigenic region. Human and mouse sequences showed 57% identity and 71% similarity. All other sequences did not display a considerable level of similarity compared to the human epitope sequence.

We then studied the conservation of the residues that seem to function in protein folding and dimerization[8] (Figure 3). The lysine residue at position 224, which is crucial for covalent binding of the coenzyme PLP (pyridoxal-5'-phosphate) was conserved in all homologous sequences investigated. Of the other five residues directly in contact with PLP, G50, S51, and H189 were identical in all the homologs, whereas S165 was replaced by alanine in mouse and D186 was replaced by glutamine in Drosophila and aspartic acid in *C. elegans*. Of the residues of monomer A involved in dimerization, only L88 was conserved in all homologous sequences. T89 was conserved in most species, but replaced by serine in *C. elegans*. F92 was replaced by leucine in Drosophila and by methionine in *C. elegans*, and otherwise conserved. T94 was conserved in vertebrates, but replaced by serine in non-vertebrates. S118 was replaced by arginine in Drosophila. The contact residues of monomer B, P251 and G252, which mediate dimerization, were conserved in all the species.

## DISCUSSION

SLA/LP autoantibodies have been demonstrated to be highly specific markers of autoimmune hepatitis[4,5]. A role of SLA/LP autoimmunity in the pathogenesis of AIH is likely, at least in a subgroup of AIH patients. However, our current understanding of both, immunogenicity and biological function of the SLA/LP molecule is rather limited. To approach the elusive function and immunogenicity of SLA/LP, we have characterized the genomic organization and sequence conservation of the human SLA/LP molecule and homologous proteins in other eukaryotic species.

For all homologs, mRNA and genomic sequences were available from the GenBank[12]. However, in contrast to human and mouse protein and mRNA sequences, which seemed to be complete, some genomic sequences have yet to be completely assembled, and thus did not allow for complete and final characterization of the genomic organization. This was especially the case for fish, where no chromosomal assignment could be made. Nevertheless, genomic characterization in man, mouse, fly, and worm was possible.

The two mammalian SLA/LP genes were similar in organization of the exon/intron structure (Figure 1) and genomic localization (Figure 4); exon/intron structure and genomic localization in fish, fly, and worm was clearly different from the mammalian sequences. Nevertheless, all homologs displayed a high degree of similarity and identity in their amino acid sequences (Figure 3). The similarity between the most distant species - man and worm - was as high as 42%. The highest degree of similarity was found between the human and the mouse amino acid sequences (Figure 2); both species also have a highly similar exon/intron structure in the SLA/LP gene (Figure 1). Moreover, both mammalian species seem to generate similar variant proteins (Figure 2) by differential splicing of exon 2. Whether splice variants exist in non-mammalian species is currently not clear. Previously, the residues, which seem to mediate dimerization and binding of PLP, have been identified by molecular modeling[8]. These residues are highly conserved among the various species studied (Figure 3). Four of six residues that are crucial for PLP-binding are identical in all the species (G50, S51, H189, K224); the other two residues are homologous (S/A165, D/Q185). Two of the seven residues that mediate dimerization were identical in all the studied species (L88, G252), the other residues were equivalent (T/S89, T/S94, S/A118, P/A251), except for F92, which was conserved in man, mouse and fish, but substituted by leucine in fly and methionine in worm.

The query of human protein databases with the human SLA/LP sequence did not reveal any functional homologies to other proteins and the primary biological function of the SLA/LP protein remains unclear. However, the extraordinary degree of conservation, notably of the presumed functional residues, suggests that the SLA/LP protein has an important biological function that relies on PLP binding. The possible role of the smaller splice variant remains obscure. It may be speculated that the smaller protein variant may act as an inhibitor of the elusive function of the larger variant; the molecular signature of the smaller variant is not compatible with a PLP-dependent transferase, as predicted for the larger variant[8].

The autoimmune response to SLA/LP is not random, but displays a remarkable degree of uniformity: SLA/LP autoantibodies are of a preferred dominant subtype (IgG1) and recognize the same dominant antigenic region, which was mapped to a carboxy-terminal domain between residues 399 and 428 of the longer splice variant (accession

number NP_722547)[10]. Thus, SLA/LP autoimmunity has features of a highly selected immune response and seems to be driven by the same mechanism in all the patients. Of note, the antigenic region is located within the only domain of the molecule that was not conserved among the various species (Figure 3). Thus, it appears that SLA/LP autoimmunity is specific for the self-antigen and not for homologous sequences from other eukaryotic species. The possibility that SLA/LP autoimmunity might be driven by homologous proteins from parasites is hence quite unlikely. SLA/LP-homologous proteins are only found in eukaryotes and archaebacteria, but not in eubacteria[10]. Nevertheless, a few homologous sequences from bacterial or viral proteins with some degree of similarity to the antigenic epitope of the SLA/LP protein do exist; however, these are not recognized by SLA/LP autoantibodies[10]. Likewise, the corresponding sequence of an archaebacterial SLA/LP-homolog is also not recognized by SLA/LP autoantibodies[10]. Therefore, SLA/LP autoimmunity in patients is very likely driven by the self-SLA/LP molecule rather than by a mechanism that involves molecular mimicry.

## ACKNOWLEDGMENTS

Chun-Xia Wang and Andreas Teufel contributed equally. The authors thank A. Schindler for her comments on the manuscript.

## REFERENCES

1 **Manns M**, Gerken G, Kyriatsoulis A, Staritz M, Meyer zum Buschenfelde KH. Characterisation of a new subgroup of autoimmune chronic active hepatitis by autoantibodies against a soluble liver antigen. *Lancet* 1987; **1**: 292-294

2 **Stechemesser E**, Klein R, Berg PA. Characterization and clinical relevance of liver-pancreas antibodies in autoimmune hepatitis. *Hepatology* 1993; **18**: 1-9

3 **Kanzler S,** Weidemann C, Gerken G, Lohr HF, Galle PR, Meyer zum Buschenfelde KH, Lohse AW. Clinical significance of autoantibodies to soluble liver antigen in autoimmune hepatitis. *J Hepatol* 1999; **31**: 635-640

4 **Wies I**, Brunner S, Henninger J, Herkel J, Kanzler S, Meyer zum Buschenfelde KH, Lohse AW. Identification of target antigen for SLA/LP autoantibodies in autoimmune hepatitis. *Lancet* 2000; **355**: 1510-1515

5 **Baeres M,** Herkel J, Czaja AJ, Wies I, Kanzler S, Cancado EL, Porta G, Nishioka M, Simon T, Daehnrich C, Schlumberger W, Galle PR, Lohse AW. Establishment of standardised SLA/LP immunoassays: specificity for autoimmune hepatitis, worldwide occurrence, and clinical characteristics. *Gut* 2002; **51**: 259-264

6 **Gelpi C**, Sontheimer EJ, Rodriguez-Sanchez JL. Autoantibodies against a serine tRNA-protein complex implicated in cotranslational selenocysteine insertion. *Proc Natl Acad Sci U S A* 1992; **89**: 9739-9743

7 **Costa M**, Rodriguez-Sanchez JL, Czaja AJ, Gelpi C. Isolation and characterization of cDNA encoding the antigenic protein of the human tRNP(Ser)Sec complex recognized by autoantibodies from patients withtype-1 autoimmune hepatitis. *Clin Exp Immunol* 2000; **121**: 364-374

8 **Kernebeck T**, Lohse AW, Grotzinger J. A bioinformatical approach suggests the function of the autoimmune hepatitis target antigen soluble liver antigen/liver pancreas. *Hepatology* 2001; **34**: 230-233

9 **Scarsdale JN**, Kazanina G, Radaev S, Schirch V, Wright HT. Crystal structure of rabbit cytosolic serine hydroxymethyltransferase at 2.8 A resolution: mechanistic implications. *Biochemistry* 1999; **38**: 8347-8358

10 **Herkel J,** Heidrich B, Nieraad N, Wies I, Rother M, Lohse AW. Fine specificity of autoantibodies to soluble liver antigen and liver/pancreas. *Hepatology* 2002; **35**: 403-408

11 GenBank website: http://www.ncbi.nlm.nih.gov

12 **Altschul SF**, Gish W, Miller W, Myers EW, Lipman DJ. Basic local alignment search tool. *J Mol Biol* 1990; **215**: 403-410

13 **Altschul SF**, Madden TL, Schäffer AA, Zhang J, Zhang Z, Miller W, Lipman DJ. Gapped BLAST and PSI-BLAST: a new generation of protein database search programs. *Nucleic Acids Res* 1997; **25**: 3389-3402

14 **Thompson JD,** Higgins DG, Gibson TJ. CLUSTAL W: improving the sensitivity of progressive multiple sequence alignment through sequence weighting, position-specific gap penalties and weight matrix choice. *Nucleic Acids Res* 1994; **22**: 4673-4680

15 **Bjellqvist B**, Hughes GJ, Pasquali C, Paquet N, Ravier F, Sanchez JC, Frutiger S, Hochstrasser D. The focusing positions of polypeptides in immobilized pH gradients can be predicted from their amino acid sequences. *Electrophoresis* 1993; **14**: 1023-1031

16 **Bjellqvist B**, Basse B, Olsen E, Celis JE. Reference points for comparisons of two-dimensional maps of proteins from different human cell types defined in a pH scale where isoelectric points correlate with polypeptide compositions. *Electrophoresis* 1994; **15**: 529-539

17 **Bateman A,** Coin L, Durbin R, Finn RD, Hollich V, Griffiths-Jones S, Khanna A, Marshall M, Moxon S, Sonnhammer EL, Studholme DJ, Yeats C, Eddy SR. The Pfam protein families database. *Nucleic Acids Res* 2004; **32**: D138-D141

18 **Marchler-Bauer A**, Anderson JB, DeWeese-Scott C, Fedorova ND, Geer LY, He S, Hurwitz DI, Jackson JD, Jacobs AR, Lanczycki CJ, Liebert CA, Liu C, Madej T, Marchler GH, Mazumder R, Nikolskaya AN, Panchenko AR, Rao BS, Shoemaker BA, Simonyan V, Song JS, Thiessen PA, Vasudevan S, Wang Y, Yamashita RA, Yin JJ, Bryant SH. CDD: a curated Entrez database of conserved domain alignments. *Nucleic Acids Res* 2003; **31**: 383-387

19 **Stern LF,** Chapman NH, Wijsman EM, Altherr MR, Rosen DR. Assignment of SOD3 to human chromosome band 4p15.3-->p15.1 with somatic cell and radiation hybrid mapping, linkage mapping, and fluorescent in-situ hybridization. *Cytogenet Genome Res* 2003; **101**: 178

20 **Nagase T,** Kikuno R, Ohara O. Prediction of the coding sequences of unidentified human genes. XXI. The complete sequences of 60 new cDNA clones from brain which code for large proteins. *DNA Res* 2001; **8**: 179-187

21 **Balla A,** Tuymetova G, Barshishat M, Geiszt M, Balla T. Characterization of type II phosphatidylinositol 4-kinase isoforms reveals association of the enzymes with endosomal vesicular compartments. *J Biol Chem* 2002; **277**: 20041-20050

22 **Yu H,** Peters JM, King RW, Page AM, Hieter P, Kirschner MW. Identification of a cullin homology region in a subunit of the anaphase-promoting complex. *Science* 1998; **279**: 1219-1222

23 **Dubnau J**, Chiang AS, Grady L, Barditch J, Gossweiler S, McNeil J, Smith P, Buldoc F, Scott R, Certa U, Broger C, Tully T. The staufen/pumilio pathway is involved in Drosophila long-term memory. *Curr Biol* 2003; **13**: 286-296

24 **Guo Y**, Wang Z, Carter A, Kaiser K, Dow JA. Characterisation of vha26, the Drosophila gene for a 26 kDa E-subunit of the vacuolar ATPase. *Biochim Biophys Acta* 1996; **1283**: 4-9

25 **Robertson HM.** The large srh family of chemoreceptor genes in Caenorhabditis nematodes reveals processes of genome evolution involving large duplications and deletions and intron gains and losses. *Genome Res* 2000; **10**: 192-203

**S- Editor** Guo SY **L- Editor** Elsevier HK **E- Editor** Liu WF

PO Box 2345, Beijing 100023, China
www.wjgnet.com
wjg@wjgnet.com

*World J Gastroenterol* 2006 February 14; 12(6): 908-914
***World Journal of Gastroenterology*** ISSN 1007-9327
© 2006 The WJG Press. All rights reserved.

*BASIC RESEARCH*

# Trimetazidine: Is it a promising drug for use in steatotic grafts?

Ismail Ben Mosbah, Araní Casillas-Ramírez, Carme Xaus, Anna Serafín, Joan Roselló-Catafau, Carmen Peralta

Ismail Ben Mosbah, Araní Casillas-Ramírez, Carme Xaus, Anna Serafín, Joan Roselló-Catafau, Carmen Peralta, Department of Experimental Pathology; Instituto de Investigaciones Biomédicas de Barcelona-Consejo Superior de Investigaciones Científicas, Instituto de Investigaciones Biomédicas de Barcelona August Pi i Sunyer, Barcelona, Spain
supported by the Ministerio de Ciencia y Tecnología (project grants HP 2003-0051, BFI 2002-00704 and BFI 2003-00912) and the Agencia Española de Cooperación Internacional (AECI, project grant 25/03/P) (Madrid, Spain
Correspondence to: Dr Joan Roselló-Catafau, Experimental Hepatology Unit, IDIBAPS, C/ Rosellón 161, 7ª planta, 08036 Barcelona, Spain. jrcbam@iibb.csic.es
Telephone: +34-933638333 Fax: +34-933638301
Received: 2005-07-12 Accepted:2005-08-03

## Abstract

**AIM:** Chronic organ-donor shortage has led to the acceptance of steatotic livers for transplantation, despite the higher risk of graft dysfunction or nonfunction associated with the ischemic preservation period of these organs. The present study evaluates the effects of trimetazidine (TMZ) on an isolated perfused liver model.

**METHODS:** Steatotic and non-steatotic livers were preserved for 24 h in the University of Wisconsin (UW) solution with or without TMZ. Hepatic injury and function (transaminases, bile production and sulfobromophthalein (BSP) clearance) and factors potentially involved in the susceptibility of steatotic livers to ischemia–reperfusion (I/R) injury, including oxidative stress, mitochondrial damage, microcirculatory diseases, and ATP depletion were evaluated.

**RESULTS:** Steatotic livers preserved in UW solution showed higher transaminase levels, lower bile production and BSP clearance compared with non-steatotic livers. Alterations in perfusion flow rate and vascular resistance, mitochondrial damage, and reduced ATP content were more evident in steatotic livers. TMZ addition to UW solution reduced hepatic injury and ameliorated hepatic functionality in both types of the liver and protected against the mechanisms potentially responsible for the poor tolerance of steatotic livers to I/R.

**CONCLUSION:** TMZ may constitute a useful approach in fatty liver surgery, limiting the inherent risk of steatotic liver failure following transplantation.

© 2006 The WJG Press. All rights reserved.

**Keywords**: Steatotic liver, Ischemia–reperfusion, UW preservation solution

Ben Mosbah I, Casillas-Ramírez A, Xaus C, Serafín A, Roselló-Catafau J, Peralta C. Trimetazidine: Is it a promising drug for use in steatotic grafts? *World J Gastroenterol* 2006; 12(6): 908-914

http://www.wjgnet.com/1007-9327/12/908.asp

## INTRODUCTION

The mounting number of patients awaiting liver transplantation and the limited pool of donor organs have led to the acceptance of marginal livers such as steatotic livers, for transplantation, despite the higher risk of graft dysfunction or nonfunction which is associated with their ischemic preservation[1-3].

There is evidence indicating that the composition of preservation solutions is critical for the quality of livers kept for prolonged ischemic periods. University of Wisconsin (UW) preservation solution, considered as the gold standard of such solutions, has proved itself effective in preventing liver damage during cold ischemia and has extended storage time limits[4,5]. However, irreversible injury occurring after prolonged cold periods (between 16 and 24 h) has also been reported. The main aims of organ preservation, therefore, are striving to prolong organ tolerance[6,7].

Trimetazidine (TMZ), introduced as an anti-ischemic drug into the heart for over 35 years[8,9], has also been used to protect kidneys exposed to the prolonged cold ischemia (48 h)[10,11] and is reported to protect liver against the deleterious effects of warm ischemia[12,13]. In addition, recently, it has been demonstrated that TMZ pre-treatment reduces liver injury and improves liver regeneration and survival rate in an experimental model of partial hepatectomy under hepatic blood inflow occlusion[14]. Studies examining the underlying protective mechanisms of TMZ suggest that this drug protects mitochondria in cardiomyocytes and isolated perfused heart by releasing the calcium accumulated in the matrix and by restoring mitochondrial membrane impermeability[8,15]. TMZ improves energy recovery *in vitro* and *ex vivo* in models of myocardial ischemia[8,15] and reduces oxidative stress

in the liver under warm ischemia[12]. Additionally, TMZ improves microcirculatory alterations in isolated perfused rat kidneys[10]. Taken together, these findings suggest that mitochondria, energy metabolism, oxidative stress, and microcirculation might be important targets through which TMZ exerts its cytoprotective effect. Interestingly, severe mitochondrial damage[16,17], decreased ATP level[16,18], increased reactive oxygen species (ROS) production[19,20], and impaired microcirculation[21,22] have also been proposed as factors that might leave steatotic livers vulnerable to ischemia–reperfusion (I/R) injury. Taking these previous observations into account, here we report the results of a study aimed at investigating whether the addition of TMZ to the standard preservation solution (UW) protects steatotic liver grafts against the deleterious effects of I/R injury.

## MATERIALS AND METHODS

Homozygous (obese, Ob) and heterozygous (lean, Ln) Zucker rats (used as reference group), aged 16-18 wk, were purchased from Iffa-Credo (L'Arbresle, France)[19,20]. In this study we used isolated perfused rat liver. It is a useful experimental system for evaluating hepatic function, isolated from the influence of other organ systems, undefined plasma constituents, and neural-hormonal effects. Hepatic architectures, microcirculation, and bile production were preserved in this experimental model[23,24]. All procedures were performed under isofluorane inhalation anesthesia. This study respected the European Union regulations (Directive 86/609 EEC) for animal experiments.

### *Liver procurement and experimental groups*

The surgical technique was performed as described elsewhere[25]. After cannulation of the common bile duct, the portal vein was isolated, and the splenic and gastroduodenal veins were ligated. The steatotic and non-steatotic livers were flushed and preserved in cold UW solution for 24 h with or without the addition of TMZ ($10^{-6}$ mol/L). This dose of TMZ has been shown to be beneficial in various experimental models of I/R[10,26,27]. At higher concentration, TMZ exerted no protective effect[28]. TMZ was kindly supplied by the Institut de Recherches Internationales Servier (Courbevoie, France).

### *Protocol 1: Effect of TMZ on steatotic liver injury after cold ischemia*

After 24 h of cold storage, livers from 16 Zucker rats (8 Ln and 8 Ob) preserved in UW solution (UW) and livers from 16 Zucker rats (8 Ln and 8 Ob) preserved in UW solution with TMZ (UW+TMZ) were flushed with Ringer's lactate solution. The aliquots of the effluent flush were sampled for the measurements of cumulative ALT and AST after prolonged ischemia.

### *Protocol 2: Effect of TMZ on steatotic liver injury after normothermic reperfusion*

After 24 h of cold preservation, and in order to account for the period of rewarming during surgical implantation *in vivo*[29,30], livers from 16 Zucker rats (8 Ln and 8 Ob) preserved in UW solution and livers from 16 Zucker rats (8 Ln and 8 Ob) preserved in UW+TMZ solution were exposed at 22 ℃ for 30 min prior to reperfusion. Livers were then connected via the portal vein to a recirculating perfusion system for 120 min at 37 ℃[6,25]. Time 0 was the point at which the portal catheter was satisfactorily connected to the circuit. As previously reported[25,31], during the first 15 min of perfusion (initial equilibration period), the flow was progressively increased in order to stabilize the portal pressure at 12 mmHg (Pressure Monitor BP-1, Instruments, Inc., Sarasota, FL, USA). The flow was controlled using a peristaltic pump (Minipuls 3, Gilson, France)[6,25]. The reperfusion liquid consisted of a cell culture medium (William's medium E, BioWhittaker, Spain) with a Krebs-Henseleit-like electrolyte composition enriched with 5% albumin, as oncotic supply. The buffer was continuously ventilated with 95% $O_2$ and 50 mL/L $CO_2$ gas mixture. The buffer was subsequently passed through a heat-exchanger (37 ℃) and a bubble trap prior to entering the liver[25,30]. During 120 min of normothermic reperfusion, the effluent fluid was collected at 30 min intervals to measure transaminases. After the initial equilibration period of 15 min, flow rate and vascular resistance were assessed continuously throughout the reperfusion period. Bile output and hepatic clearance (expressed as percentage of BSP in bile samples) were determined at 120 min of reperfusion. ATP, adenine nucleotides, and lipid peroxidation were evaluated in the liver samples at 120 min of reperfusion. Light/electron microscopy analysis of the liver was also performed at 120 min of reperfusion.

### *Biochemical determinations*

**Transaminase assay** Hepatic injury was evaluated according to transaminase levels using commercial kit from Boehringer Mannheim (Munich, Germany).

**Nucleotide analysis** Livers were homogenized in perchloric acid solution, and the adenine nucleotides pool was measured by high-performance liquid chromatography[32].

**Bile output** Liver function was assessed by measuring bile production[33,34]. Bile was collected through the cannulated bile duct and output reported as μL/g liver.

**Hepatic clearance** As with bile output, hepatic clearance was considered as another parameter of hepatic function[35,36]. Thirty minutes after the onset of the perfusion ($t_{30}$), 1 mg of BSP (Sigma, Spain) was added to the perfusate. The concentration of BSP in bile samples ($t_{120}$) was measured at 580 nm with an UV-visible spectrometer. Bile BSP excretion was expressed as a percentage of perfusate content ($t_{120}$ bile/$t_{30}$ perfusate×100)[35,36].

**Flow rate and vascular resistance** Liver circulation was assessed by measuring perfusion flow rate and vascular resistance[34,37]. Perfusion flow rate was assessed continuously throughout the reperfusion period and expressed as mL/min·g. Vascular resistance was defined as the ratio of portal venous pressure to flow rate and expressed in mmHg·min·g/mL[34,37].

**Lipid peroxidation assay** Lipid peroxidation was used as an indirect measure of the oxidative injury induced by ROS[19,38]. Lipid peroxidation was determined by measuring

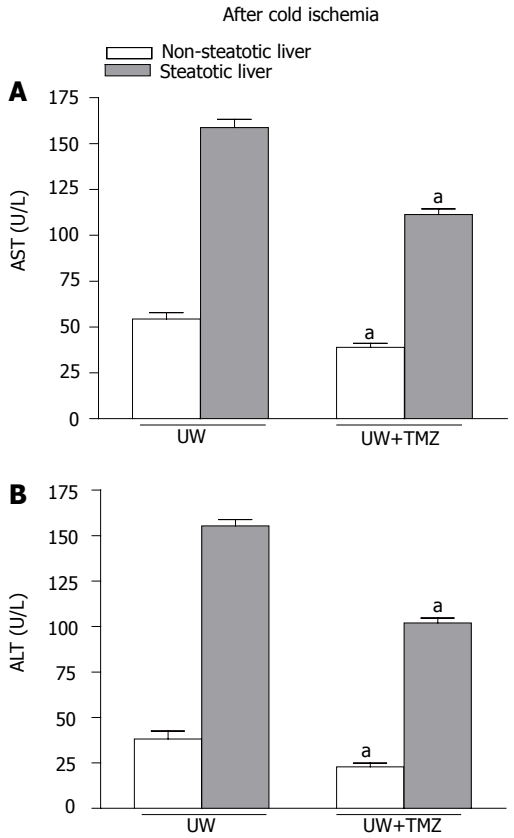


**Figure 1** AST (**A**) and ALT (**B**) levels in flushing effluent after 24-h cold storage. UW: liver preserved in UW solution; UW+TMZ: liver preserved in UW with TMZ. $^{a}P<0.05$ *vs* UW.

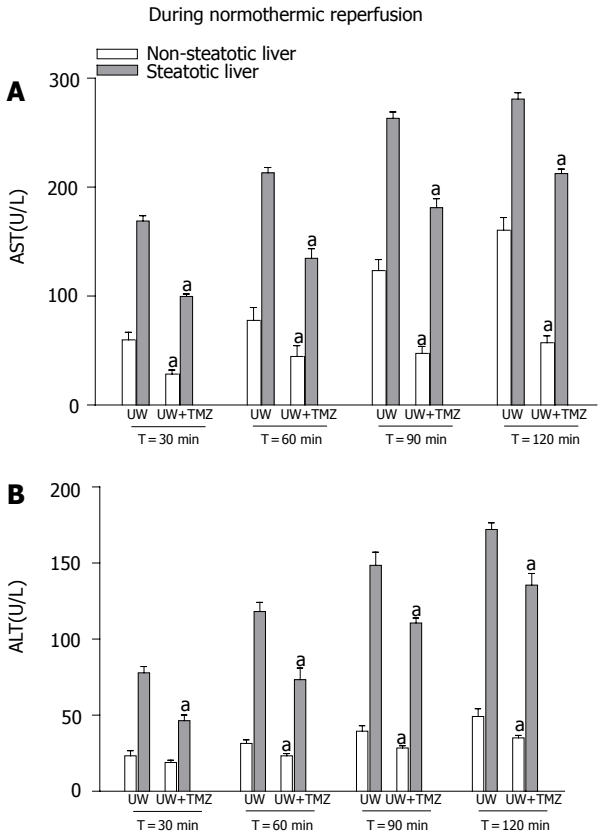


**Figure 2** AST (**A**) and ALT (**B**) levels in perfusate after 30, 60, 90, and 120 min of normothermic reperfusion. UW: liver preserved in UW solution; UW+TMZ: liver preserved in UW with TMZ. $^{a}P<0.05$ *vs* UW.

the formation of malondialdehyde (MDA) with the thiobarbiturate reaction[19].

### *Light/electron microscopy*

For light microscopy examinations, liver samples were fixed in 10% neutral buffered formalin and embedded in Paraplast, and 5-μm sections were stained with hematoxylin and eosin according to standard procedures[19]. For electron microscopy, the fixation of hepatic tissue was performed using a 2.5% glutaraldehyde/2% paraformaldehyde. These samples were post-fixed with osmium tetroxide and potassium ferrocyanide, dehydrated in acetone, and embedded in Spurr's medium. Ultrathin sections were prepared with an ultracut-E ultramicrotome and contrasted with uranyl acetate and lead citrate. Stained sections were reviewed under an H 600-AB Hitachi electron microscope[39].

### *Statistics*

Data were expressed as mean±SE, and were compared statistically by variance analysis, followed by Student-Newman-Keuls test. $P<0.05$ was considered significant.

## RESULTS

### *Protocol 1: Effect of TMZ on steatotic liver injury after 24 h of cold ischemia*

Flushing of livers before reperfusion allowed effluent fluid to collect for the determination of transaminases[6,40]. This measure proved to be a valuable tool for predicting organ damage after cold preservation[6,40]. As shown in Figure 1, the higher levels of transaminases released by steatotic livers after cold preservation in UW solution confirm the increased sensitivity of this type of liver to cold ischemia. The addition of TMZ to UW solution (UW+TMZ) reduced transaminase levels in the flushing effluent of non-steatotic livers and, in particular in that of steatotic livers.

### *Protocol 2: Effect of TMZ on steatotic liver injury after 24 h of cold ischemia followed by 2 h of normothermic reperfusion*

Higher perfusate transaminase levels were observed in steatotic livers as the reperfusion period progressed compared with those found in non-steatotic livers (Figure 2). The addition of TMZ to UW solution reduced the perfusate transaminase release in both types of liver, but especially in steatotic livers. The histological light microscopic study showed a marked disintegration of hepatic architecture in both types of liver preserved in UW solution (Figures 3A and B), but especially in steatotic livers (Figure 3B), whereas in the UW+TMZ group hepatocyte integrity was maintained (Figures 3C and D).

Liver function was assessed by measuring bile production and BSP clearance. Bile output and the percentage of BSP in bile were lower in steatotic livers preserved in UW solution than in non-steatotic livers (Figure 4). Both liver function parameters improved significantly in the two liver types following the addition

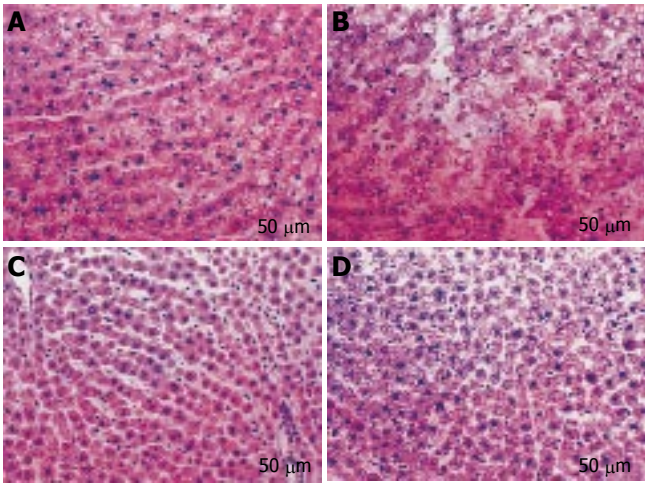


**Figure 3** Histological change in steatotic and non-steatotic livers after 120 min of normothermic reperfusion. Non-steatotic (**A**) and steatotic (**B**) livers preserved in UW solution: Cell swelling and disintegration of hepatic architecture were more evident in steatotic livers. Non-steatotic (**C**) and steatotic (**D**) livers preserved in UW solution with TMZ: Hepatic morphology was better preserved in both types of the liver compared to that recorded in UW solution.

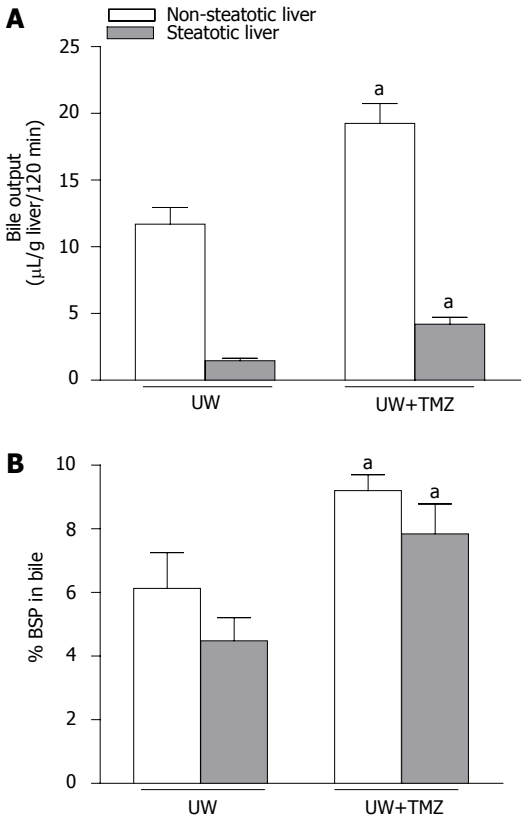


**Figure 4** Bile output (**A**) and percentage of sulfobromophthalein (BSP) in bile (**B**) of steatotic and non-steatotic livers after 120 min of normothermic reperfusion. UW: livers were preserved in UW solution; UW+TMZ: liver preserved in UW with TMZ. $^{a}P<0.05$ *vs* UW.

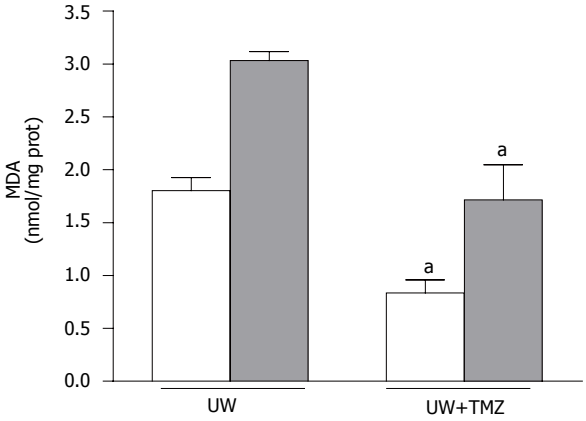


**Figure 5** Hepatic malondialdehyde (MDA) levels after 120 min of normothermic reperfusion. UW: liver preserved in UW solution; UW+TMZ: liver preserved in UW with TMZ. $^{a}P<0.05$ *vs* UW.

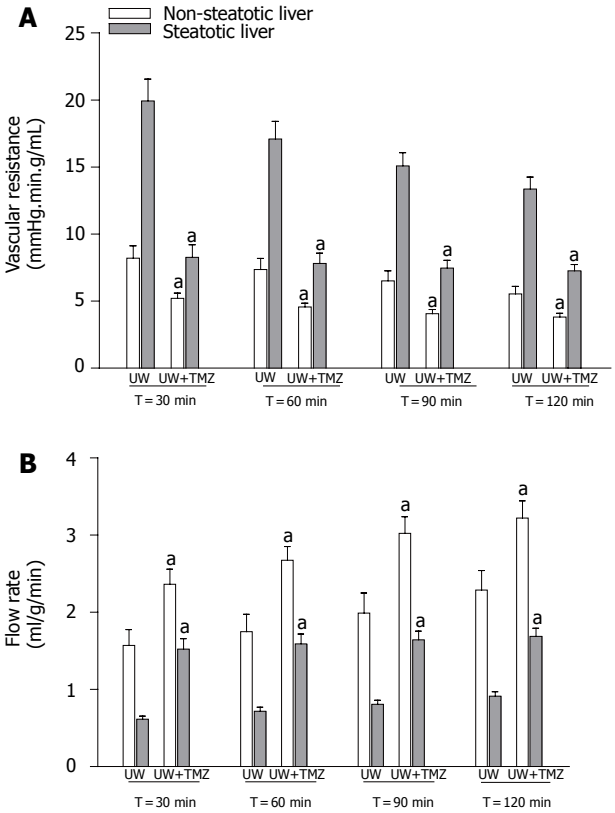


**Figure 6** Vascular resistance (**A**) and perfusion flow rate (**B**) of steatotic and non-steatotic livers after 120 min of normothermic reperfusion. UW: livers were preserved in UW solution; UW+TMZ: liver preserved in UW with TMZ. $^{a}P<0.05$ *vs* UW.

of TMZ to UW solution (UW+TMZ).

The mechanisms by which TMZ was able to protect steatotic livers against the deleterious effects of I/R injury were also evaluated. As shown in Figure 5, MDA levels during reperfusion increased, particularly in the case of steatotic livers. The addition of TMZ to UW solution (UW+TMZ) brought about a reduction in these levels of increase. Marked increases in the vascular resistance and lower perfusion flow rate were observed in steatotic livers preserved in UW solution during the reperfusion period ($t_{30,60,90,120}$) compared with the rates in non-steatotic livers (Figure 6). The liver weight was not statistically significant in both liver types. Vascular resistance was lower and perfusion flow rate was higher in both types of liver following the addition of TMZ to UW preservation solution (UW+TMZ). The beneficial

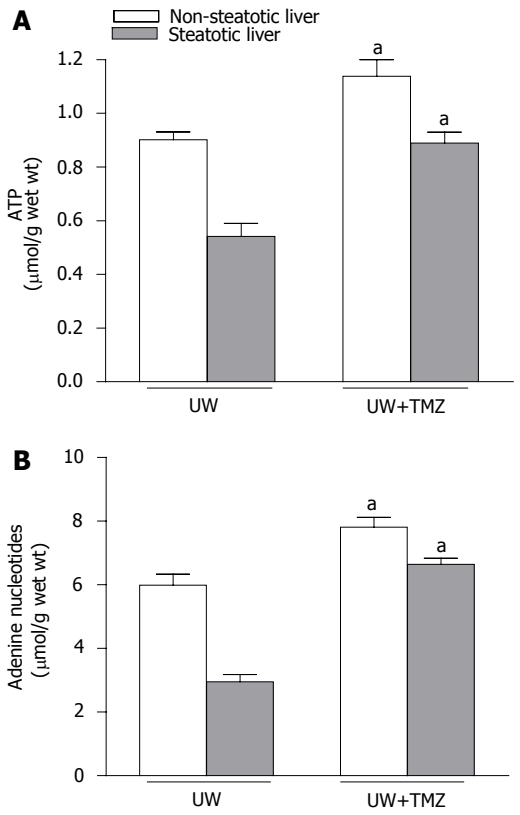


**Figure 7** ATP (**A**) and adenine nucleotide (**B**) levels of steatotic and non-steatotic livers after 120 min of normothermic reperfusion. UW: livers were preserved in UW solution; UW+TMZ: liver preserved in UW with TMZ. $^{a}P<0.05$ *vs* UW.

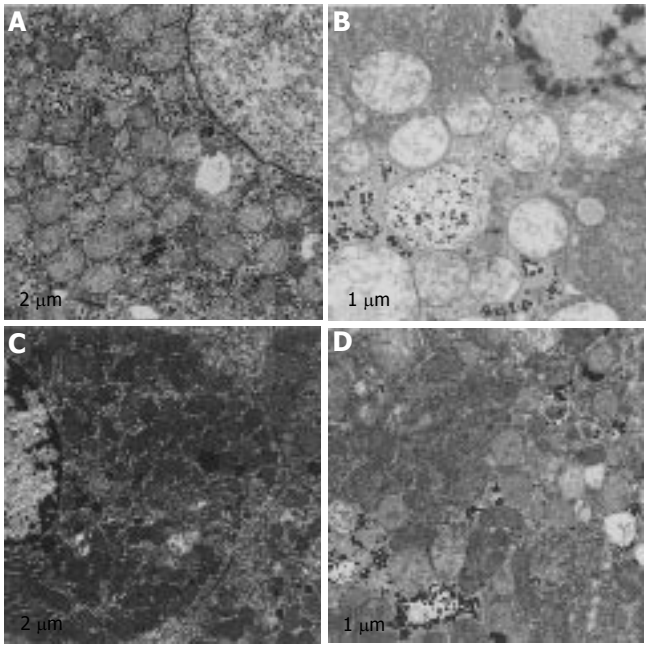


**Figure 8** Electron microscopy analysis of structural integrity of the mitochondria. Non-steatotic (**A**) and steatotic (**B**) livers preserved in UW solution: mitochondria swelling and the alterations in the electron density of their matrices were more evident in steatotic livers. Cristae are only seldom visible in steatotic livers. Non-steatotic (**C**) and steatotic (**D**) livers preserved in UW solution with TMZ. Mitochondrial integrity was better preserved in both types of liver compared to that recorded in UW solution.

effect of TMZ on the vascular resistance and perfusion flow rate were more evident in the steatotic livers (Figure 6). Lower ATP and adenine nucleotides levels during reperfusion were observed in steatotic livers preserved in UW solution than those recorded for non-steatotic livers (Figure 7). The results reported here show that TMZ led to the preservation of more ATP and adenine nucleotides content in both types of liver.

Mitochondrial damage was evaluated by electron microscopy. Ultra-structural analysis after reperfusion in both types of liver preserved in UW solution revealed swelling of mitochondria, a significant decrease in the electron density of their matrices, while cristae were only seldom visible (Figures 8A and B). These morphological alterations were more evident in steatotic livers (Figure 8B). Following the addition of TMZ to UW preservation (UW+TMZ) a greater degree of mitochondrial preservation in both types of liver was recorded (Figures 8C and D) compared to the results obtained for the livers in UW solution.

## DISCUSSION

The results of the present study indicate that the addition of TMZ to UW solution improved the capacity of this standard preservation solution in both types of liver subjected to prolonged ischemic period especially in steatotic livers.

It is widely accepted that bile analysis is a useful means for assessing the integrity of biliary epithelial cells after cold ischemia. If cold storage time exceeds 10-12 h, complications in biliary structures occur in more than 25% of liver transplant recipients[41-43]. Several factors, including poor recovery after ATP depletion appear to contribute to bile duct cell damage after liver transplantation. Furthermore, isolated rat bile duct epithelial cells are noticeably sensitive to oxidative stress, possibly because their cellular stores of reduced glutathione are seven times lower than those of hepatocytes[44]. Taking these observations into account, bile production failure in steatotic livers could be explained, at least partially, by the lower ATP and increased oxidative stress presented by this type of liver compared with non-steatotic liver. Liver transplantation may benefit from strategies such as the addition of TMZ to the preservation solution as this seems to help maintain appropriate bile duct cell functions. Here, this strategy increased ATP recovery and reduced oxidative stress. This was also associated with better bile production.

The lower perfusate flow rate and the higher resistance to flow in steatotic, as opposed to non-steatotic livers indicate that steatotic livers offer greater impediments to perfusion. Fat accumulation in the cytoplasm of the hepatocytes is associated with an increase in cell volume, which may result in the partial or complete obstruction of the hepatic sinusoidal space[3,21]. Our results indicate the beneficial effects of TMZ on the flow rate and vascular resistance especially in the steatotic livers which were preserved during prolonged cold ischemia. Various hypotheses could be forwarded in an attempt at explaining the underlying protective mechanisms. In fact, according

to the literature, TMZ reduces the leakage of intracellular potassium, which is a vasoconstrictor; it affects vasoactive mediators including prostaglandins; and it reduces tissue edema, which has been related to the disturbance of microvascular circulation[10,45,46].

Fatty degeneration, which induces a series of ultrastructural and biochemical alterations both in human and animal mitochondria[17,47] may render these organelles intrinsically more susceptible to I/R injury. Given that mitochondria are the main sites for ATP and ROS production in I/R[16], the lower ATP and adenine nucleotides content and the increased oxidative stress observed in steatotic livers preserved in UW solution could be attributed to mitochondrial damage. Thus, the identification of new strategies to prevent mitochondrial injury should represent an important research goal in attempts to optimize the use of donor steatotic organs for liver transplantation. Our result indicates that the addition of TMZ to UW preservation solution protects against mitochondrial damage caused by I/R, preserves more ATP and adenine nucleotide content during reperfusion and decreases oxidative stress, thus showing a protective effect against I/R injury. Taken together, these data suggest that mitochondria might be an important target through which TMZ exerts its cytoprotective effect. However, the underlying mechanisms are still far from being defined and other possibilities should not be ruled out. Thus, another possible reason for the higher ATP levels that are induced by TMZ might be improved microcirculation at the time of reperfusion. This could increase the availability of oxygen and, therefore, facilitate ATP production. It is well known that failure of liver perfusion can impair the ability of the steatotic liver to restore ATP levels[16,22,48]. Similarly, in addition to mitochondria, the beneficial effects of TMZ on oxidative stress could be exerted on other sources of ROS, including endothelial cells[10].

The addition of TMZ to UW solution ensured that steatotic grafts were less susceptible to the mechanisms involved in I/R injury including microcirculatory diseases, ATP and adenine content, oxidative stress and mitochondrial damage. In addition to allopurinol and glutathione, TMZ could be another antioxidant that should be added to UW solution, considering the benefits of TMZ in terms of oxidative stress and the difficulties for preventing oxidative stress damage in steatotic liver by other pharmacological treatments[19,33,49]. The ability of TMZ to protect both types of the liver is particularly attractive since some strategies that are effective in non-steatotic livers may not be useful in the presence of steatosis[19,20,50].

In conclusion, TMZ protected against hepatic injury and ameliorated liver function in steatotic and non-steatotic livers preserved in UW solution. Further studies will be required to elucidate whether TMZ is such a promising drug for the field of liver transplantation, and if this pharmacological substance can reduce the inherent risk of steatotic liver grafts for transplantation.

## ACKNOWLEDGMENTS

I. Ben Mosbah holds a fellowship from the AECI and A. Casillas-Ramírez holds one from José E. González Hospital-UANL. We would like to thank Robin Rycroft at the Language Advisory Service of the University of Barcelona for revising the English text.

## REFERENCES

1 **Todo S**, Demetris AJ, Makowka L, Teperman L, Podesta L, Shaver T, Tzakis A, Starzl TE. Primary nonfunction of hepatic allografts with preexisting fatty infiltration. *Transplantation* 1989; **47**: 903-905
2 **Imber CJ**, St Peter SD, Handa A, Friend PJ. Hepatic steatosis and its relationship to transplantation. *Liver Transpl* 2002; **8:** 415-423
3 **Selzner M**, Clavien PA. Fatty liver in liver transplantation and surgery. *Semin Liver Dis* 2001; **21**: 105-113
4 **Todo S**, Nery J, Yanaga K, Podesta L, Gordon RD, Starzl TE. Extended preservation of human liver grafts with UW solution. *JAMA* 1989; **261**: 711-714
5 **Stratta RJ**, Wood RP, Langnas AN, Duckworth RM, Markin RS, Marujo W, Grazi GL, Saito S, Dawidson I, Rikkers LF. The impact of extended preservation on clinical liver transplantation. *Transplantation* 1990; **50**: 438-443
6 **El-Gibaly AM**, Scheuer C, Menger MD, Vollmar B. Improvement of rat liver graft quality by pifithrin-alpha-mediated inhibition of hepatocyte necrapoptosis. *Hepatology* 2004; **39:** 1553-1562
7 **Klar E**, Angelescu M, Zapletal C, Kraus T, Bredt M, Herfarth C. Definition of maximum cold ischemia time without reduction of graft quality in clinical liver transplantation. *Transplant Proc* 1998; **30**: 3683-3685
8 **Ikizler M**, Dernek S, Sevin B, Kural T. Trimetazidine improves recovery during reperfusion in isolated rat hearts after prolonged ischemia. *Anadolu Kardiyol Derg* 2003; **3**: 303-308
9 **Veitch K**, Maisin L, Hue L. Trimetazidine effects on the damage to mitochondrial functions caused by ischemia and reperfusion. *Am J Cardiol* 1995; **76**: 25B-30B
10 **Hauet T**, Bauza G, Goujon JM, Caritez JC, Carretier M, Eugene M, Tillement JP. Effects of trimetazidine on lipid peroxidation and phosphorus metabolites during cold storage and reperfusion of isolated perfused rat kidneys. *J Pharmacol Exp Ther* 1998; **285:** 1061-1067
11 **Hauet T**, Baumert H, Amor IB, Gibelin H, Tallineau C, Eugene M, Tillement JP, Carretier M. Pharmacological limitation of damage to renal medulla after cold storage and transplantation by trimetazidine. *J Pharmacol Exp Ther* 2000; **292**: 254-260
12 **Elimadi A**, Sapena R, Settaf A, Le Louet H, Tillement J, Morin D. Attenuation of liver normothermic ischemia--reperfusion injury by preservation of mitochondrial functions with S-15176, a potent trimetazidine derivative. *Biochem Pharmacol* 2001; **62:** 509-516
13 **Settaf A**, Morin D, Lamchouri F, Elimadi A, Cherrah Y, Tillement JP. Trimetazidine ameliorates the hepatic injury associated with ischaemia-reperfusion in rats. *Pharmacol Res* 1999; **39:** 211-216
14 **Kaya Y**, Coskun T, Aral E, Erkasap N, Var A. The effect of trimetazidine on liver regeneration after partial hepatectomy under hepatic blood inflow occlusion. *Hepatogastroenterology* 2003; **50:** 651-655
15 **Guarnieri C**, Muscari C. Effect of trimetazidine on mitochondrial function and oxidative damage during reperfusion of ischemic hypertrophied rat myocardium. *Pharmacology* 1993; **46**: 324-331
16 **Caraceni P**, Bianchi C, Domenicali M, Maria Pertosa A, Maiolini E, Parenti Castelli G, Nardo B, Trevisani F, Lenaz G, Bernardi M. Impairment of mitochondrial oxidative phosphorylation in rat fatty liver exposed to preservation-reperfusion injury. *J Hepatol* 2004; **41**: 82-88
17 **Rashid A**, Wu TC, Huang CC, Chen CH, Lin HZ, Yang SQ, Lee FY, Diehl AM. Mitochondrial proteins that regulate apoptosis and necrosis are induced in mouse fatty liver. *Hepatology* 1999; **29**: 1131-1138
18 **Selzner N**, Selzner M, Jochum W, Clavien PA. Ischemic pre-

conditioning protects the steatotic mouse liver against reperfusion injury: an ATP dependent mechanism. *J Hepatol* 2003; **39**: 55-61

19 **Serafin A**, Rosello-Catafau J, Prats N, Xaus C, Gelpi E, Peralta C. Ischemic preconditioning increases the tolerance of Fatty liver to hepatic ischemia-reperfusion injury in the rat. *Am J Pathol* 2002; **161**: 587-601

20 **Serafin A**, Rosello-Catafau J, Prats N, Gelpi E, Rodes J, Peralta C. Ischemic preconditioning affects interleukin release in fatty livers of rats undergoing ischemia/reperfusion. *Hepatology* 2004; **39**: 688-698

21 **Teramoto K**, Bowers JL, Kruskal JB, Clouse ME. Hepatic microcirculatory changes after reperfusion in fatty and normal liver transplantation in the rat. *Transplantation* 1993; **56**: 1076-1082

22 **Hakamada K**, Sasaki M, Takahashi K, Umehara Y, Konn M. Sinusoidal flow block after warm ischemia in rats with diet-induced fatty liver. *J Surg Res* 1997; **70**: 12-20

23 **Gores GJ**, Kost LJ, LaRusso NF. The isolated perfused rat liver: conceptual and practical considerations. *Hepatology* 1986; **6**: 511-517

24 **Ahmed I**, Attia MS, Ahmad N, Lodge JP, Potts DJ. Use of isolated perfused rat liver model for testing liver preservation solutions. *Transplant Proc* 2001; **33**: 3709-3711

25 **Ben Abdennebi H**, Steghens JP, Margonari J, Ramella-Virieux S, Barbieux A, Boillot O. High-$Na^+$ low-$K^+$ UW cold storage solution reduces reperfusion injuries of the rat liver graft. *Transpl Int* 1998; **11**: 223-230

26 **Hauet T**, Goujon JM, Vandewalle A, Baumert H, Lacoste L, Tillement JP, Eugene M, Carretier M. Trimetazidine reduces renal dysfunction by limiting the cold ischemia/reperfusion injury in autotransplanted pig kidneys. *J Am Soc Nephrol* 2000; **11**: 138-148

27 **Faure JP**, Petit I, Zhang K, Dutheil D, Doucet C, Favreau F, Eugene M, Goujon JM, Tillement JP, Mauco G, Vandewalle A, Hauet T. Protective roles of polyethylene glycol and trimetazidine against cold ischemia and reperfusion injuries of pig kidney graft. *Am J Transplant* 2004; **4:** 495-504

28 **Boucher FR**, Hearse DJ, Opie LH. Effects of trimetazidine on ischemic contracture in isolated perfused rat hearts. *J Cardiovasc Pharmacol* 1994; **24**: 45-49

29 **Minor T**, Yamaguchi T, Isselhard W. Effects of taurine on liver preservation in UW solution with consecutive ischemic rewarming in the isolated perfused rat liver. *Transpl Int* 1995; **8:** 174-179

30 **Minor T**, Akbar S, Tolba R, Dombrowski F. Cold preservation of fatty liver grafts: prevention of functional and ultrastructural impairments by venous oxygen persufflation. *J Hepatol* 2000; **32**: 105-111

31 **Ben Abdennebi H**, Steghens JP, Hadj-Aissa A, Barbieux A, Ramella-Virieux S, Gharib C, Boillot O. A preservation solution with polyethylene glycol and calcium: a possible multiorgan liquid. *Transpl Int* 2002; **15:** 348-354

32 **Peralta C**, Bartrons R, Serafin A, Blazquez C, Guzman M, Prats N, Xaus C, Cutillas B, Gelpi E, Rosello-Catafau J. Adenosine monophosphate-activated protein kinase mediates the protective effects of ischemic preconditioning on hepatic ischemia-reperfusion injury in the rat. *Hepatology* 2001; **34**: 1164-1173

33 **Nakano H**, Nagasaki H, Barama A, Boudjema K, Jaeck D, Kumada K, Tatsuno M, Baek Y, Kitamura N, Suzuki T, Yamaguchi M. The effects of N-acetylcysteine and anti-intercellular adhesion molecule-1 monoclonal antibody against ischemia-reperfusion injury of the rat steatotic liver produced by a choline-methionine-deficient diet. *Hepatology* 1997; **26**: 670-678

34 **Taneja C**, Prescott L, Koneru B. Critical preservation injury in rat fatty liver is to hepatocytes, not sinusoidal lining cells. *Transplantation* 1998; **65**: 167-172

35 **Soto A**, Foy BD, Frazier JM. Effect of cadmium on bromosulfophthalein kinetics in the isolated perfused rat liver system. *Toxicol Sci* 2002; **69**: 460-469

36 **Cespedes JM**, Rodriguez Garay EA. Sulfobromophthalein metabolism in isolated perfused rat liver. Factors determining the applicability of the model. *Acta Physiol Lat Am* 1979; **29**: 207-215

37 **Arnault I**, Bao YM, Sebagh M, Anjo A, Dimicoli JL, Lemoine A, Delvart V, Adam R. Beneficial effect of pentoxifylline on microvesicular steatotic livers submitted to a prolonged cold ischemia. *Transplantation* 2003; **76**: 77-83

38 **Peralta C**, Bulbena O, Xaus C, Prats N, Cutrin JC, Poli G, Gelpi E, Rosello-Catafau J. Ischemic preconditioning: a defense mechanism against the reactive oxygen species generated after hepatic ischemia reperfusion. *Transplantation* 2002; **73**: 1203-1211

39 **Peralta C**, Bulbena O, Bargallo R, Prats N, Gelpi E, Rosello-Catafau J. Strategies to modulate the deleterious effects of endothelin in hepatic ischemia-reperfusion. *Transplantation* 2000; **70**: 1761-1770

40 **Chimalakonda AP**, Mehvar R. Effects of duration of ischemia and donor pretreatment with methylprednisolone or its macromolecular prodrug on the disposition of indocyanine green in cold-preserved rat livers. *Pharm Res* 2004; **21**: 1000-1008

41 **Sanchez-Urdazpal L**, Gores GJ, Ward EM, Maus TP, Wahlstrom HE, Moore SB, Wiesner RH, Krom RA. Ischemic-type biliary complications after orthotopic liver transplantation. *Hepatology* 1992; **16:** 49-53

42 **Kukan M**, Haddad PS. Role of hepatocytes and bile duct cells in preservation-reperfusion injury of liver grafts. *Liver Transpl* 2001; **7**: 381-400

43 **Popescu I**, Sheiner P, Mor E, Forman W, Borcich A, Emre S, Kishikawa K, Schwartz M, Miller C. Biliary complications in 400 cases of liver transplantation. *Mt Sinai J Med* 1994; **61**: 57-62

44 **Noack K**, Bronk SF, Kato A, Gores GJ. The greater vulnerability of bile duct cells to reoxygenation injury than to anoxia. Implications for the pathogenesis of biliary strictures after liver transplantation. *Transplantation* 1993; **56**: 495-500

45 **Maridonneau-Parini I**, Harpey C. Effect of trimetazidine on membrane damage induced by oxygen free radicals in human red cells. *Br J Clin Pharmacol* 1985; **20**: 148-151

46 **Tsimoyiannis EC**, Moutesidou KJ, Moschos CM, Karayianni M, Karkabounas S, Kotoulas OB. Trimetazidine for prevention of hepatic injury induced by ischaemia and reperfusion in rats. *Eur J Surg* 1993; **159:** 89-93

47 **Caldwell SH**, Swerdlow RH, Khan EM, Iezzoni JC, Hespenheide EE, Parks JK, Parker WD Jr. Mitochondrial abnormalities in non-alcoholic steatohepatitis. *J Hepatol* 1999; **31**: 430-434

48 **Hui AM**, Kawasaki S, Makuuchi M, Nakayama J, Ikegami T, Miyagawa S. Liver injury following normothermic ischemia in steatotic rat liver. *Hepatology* 1994; **20**: 1287-1293

49 **Gao W**, Connor HD, Lemasters JJ, Mason RP, Thurman RG. Primary nonfunction of fatty livers produced by alcohol is associated with a new, antioxidant-insensitive free radical species. *Transplantation* 1995; **59:** 674-679

50 **Selzner M**, Rudiger HA, Sindram D, Madden J, Clavien PA. Mechanisms of ischemic injury are different in the steatotic and normal rat liver. *Hepatology* 2000; **32**: 1280-1288

**S- Editor** Guo SY **L- Editor** Elsevier HK **E- Editor** Bai SH

PO Box 2345, Beijing 100023, China
www.wjgnet.com
wjg@wjgnet.com

*World J Gastroenterol* 2006 February 14; 12(6): 915-920
***World Journal of Gastroenterology*** ISSN 1007-9327
© 2006 The WJG Press. All rights reserved.

*BASIC RESEARCH*

# Epidural anaesthesia restores pancreatic microcirculation and decreases the severity of acute pancreatitis

Alp Demirag, Catherine M Pastor, Philippe Morel, Copin Jean-Christophe, Andreas W Sielenkämper, Nilgun Güvener, Gang Mai, Thierry Berney, Jean-Louis Frossard, Leo H Bühler

Alp Demirag, Catherine M Pastor, Philippe Morel, Nilgun Güvener, Gang Mai, Thierry Berney, Leo H Bühler, Surgical Research Unit, Department of Surgery, University Hospital Geneva, 24, Rue Micheli-du-Crest, 1211, Geneva 14, Switzerland
Catherine M Pastor, Copin Jean-Christophe, Jean-Louis Frossard, Division of Gastroenterology, Department of Internal Medicine, University Hospital Geneva, 24, Rue Micheli-du-Crest, 1211, Geneva 14, Switzerland
Andreas W. Sielenkämper, Department of Anaesthesiology and Intensive Care Medicine, Münster, Germany
Gang Mai, Department of General Surgery, West China Hospital, Sichuan University, Chengdu 610041, Sichuan Province, China
Co-correspondence: Jean-Louis Frossard
Correspondence to: Leo H Bühler, MD, Surgical Research Unit, Department of Surgery, University Hospital Geneva, 24, Rue Micheli-du-Crest, 1211, Geneva 14,
Switzerland. leo.buhler@hcuge.ch
Telephone: +41-22-3727698 Fax: +41-22-3727689
Received: 2005-02-21 Accepted: 2005-04-30

## Abstract

**AIM:** To investigate the effect of epidural anaesthesia (EA) on pancreatic microcirculation during acute pancreatitis (AP).

**METHODS:** AP was induced by injection of sodium taurocholate into the pancreatic duct of Sprague-Dawley rats. To realize EA, a catheter was introduced into the epidural space between T7 and T9 and bupivacaine was injected. Microcirculatory flow was measured by laser Doppler flowmetry. Arterial blood gas analyses were performed. At the end of the experiment (≤5 h), pancreas was removed for histology. The animals were divided into three groups: Group 1 ($n=9$), AP without EA; Group 2 ($n=4$), EA without AP; and Group 3 ($n=6$), AP treated by EA.

**RESULTS:** In Group 1, pancreatic microcirculatory flow prior to AP was 141±39 perfusion units (PU). After AP, microcirculatory flow obviously decreased to 9±6 PU ($P<0.05$). Metabolic acidosis developed with base excess (BE) of - 14±3 mmol/L. Histology revealed extensive edema and tissue necrosis. In Group 2, EA did not significantly modify microcirculatory flow. BE remained unchanged and histological analysis showed normal pancreatic tissue. In Group 3, AP initially caused a significant decrease in microcirculatory flow from 155±25 to 11±7 PU ($P<0.05$). After initiation of EA, microcirculatory flow obviously increased again to 81±31 PU ($P<0.05$). BE was -6±4 mmol/L, which was significantly different compared to Group 1 ($P<0.05$). Furthermore, histology revealed less extensive edema and necrosis in pancreatic tissue in Group 3 than that in Group 1.

**CONCLUSION:** AP caused dramatic microcirculatory changes within the pancreas, with development of metabolic acidosis and tissue necrosis. EA allowed partial restoration of microcirculatory flow and prevented development of tissue necrosis and systemic complications. Therefore, EA should be considered as therapeutic option to prevent evolution from edematous to necrotic AP.

© 2006 The WJG Press. All rights reserved.

**Key words:** Acute pancreatitis; Epidural anaesthesia; Pancreatic blood flow; Microcirculation; Taurocholic acid

Demirag A, Pastor CM, Morel P, Jean-Christophe C, Sielenkämper AW, Güvener N, Mai G, Berney T, Frossard JL, Bühler LH. Epidural anaesthesia restores pancreatic microcirculation and decreases the severity of acute pancreatitis. *World J Gastroenterol* 2006; 12(6): 915-920

http://www.wjgnet.com/1007-9327/12/915.asp

## INTRODUCTION

Among patients suffering from acute pancreatitis (AP), 80% have a favorable evolution and approximately 20% develop a severe disease with significant morbidity and mortality[1]. Severe AP is associated with the development of local complications, such as pancreatic and peripancreatic necrosis, abscesses or pseudocysts, and systemic complications, such as adult respiratory distress syndrome or renal failure with a mortality close to 15%[2].

The pathophysiology of AP is incompletely understood but alteration in the pancreatic microcirculatory blood flow has been involved. Thus, a decrease in pancreatic blood flow occurs early in the course of AP and has been suggested to play a role in the conversion of edematous to necrotizing AP[3-7]. The microcirculatory dysfunction includes arterial vasoconstriction with hypoperfusion, ischemia-reperfusion injury, and obstruction of the venous outflow[8-11]. Other factors that participate in the development of microcirculatory

dysfunction are hemoconcentration, hypercoagulability, and increase in microvascular permeability[8-11]. Besides perfusion abnormalities, AP is also characterized by local and systemic inflammatory responses, including leukocyte activation as well as release of free radicals and cytokines[12-14].

Many therapeutic agents, such as dextran, heparin, procaine, L-arginine, antioxidants, or cytokine antagonists, have been tested experimentally and/or clinically to improve pancreatic tissue perfusion during AP, however, no significantly successful result has been achieved[1,4,15-18].

Epidural anesthesia (EA) that is used to induce analgesia in the perioperative period might be an interesting treatment of the microcirculatory blood flow abnormalities. Thus, EA can reduce the incidence of post-operative pulmonary complications, and shorten the duration of the post-operative intestinal paralysis[19,20]. In addition, experimental studies have shown that EA increases gut mucosal blood flow and delays the metabolic acidosis due to intestinal ischemia in the presence of a decreased perfusion pressure[21-22]. The beneficial effect of EA has been attributed to a sympathetic nerve blockade, which redistributes blood flow to the non-perfused regions of the gut[21]. Additionally, EA is useful to decrease pain in patients with AP[23], but no study has investigated the effects of EA on the pancreatic microcirculatory blood flow during AP.

Because we postulated that EA might improve the pancreatic hypoperfusion induced by AP and concomitantly decrease the severity of the disease, we measured the pancreatic microcirculatory blood flow and the severity of the disease in rats injected with taurocholic acid in the biliopancreatic duct, in the presence or in the absence of EA.

## MATERIALS AND METHODS

### Animals

Adult male Wistar rats (275-300 g) were provided by Charles River (L'Arbresle, France). Animals were bred and housed in standard cages and maintained in climate-controlled rooms. Animals were fed with standard laboratory chow, given water *ad libitum*, and randomly assigned to control or treated groups. The protocol was approved by the Animal Ethical Committee of the Geneva University Medical School and by the Geneva Veterinary Authorities.

### Epidural anaesthesia

Epidural catheters were placed in rats under isoflurane anesthesia. A polyethylene catheter (PE10, Portex, Kent, UK) was introduced in the lumbar region and positioned into the epidural region between T7 and T9 according to the technique previously described by Grouls *et al*[24]. The external end of the catheter was tunneled subcutaneously and fixed to the occiput.

The animals were allowed to recover from anesthesia and 1 h after epidural catheterization, bupivacaine (4 g/L, 20 μL) was injected to test anaesthesia. Hind limb muscle tone was scored by manual inspection and visual observation as previously described during 30 min[21,24]. A normal tone with free movement of the hind limbs was scored 0; weak hypotonia of the hind limbs and of the body was scored 1; moderate hypotonia of the hind limbs and of the body was scored 2; and inability to support the body on the hind limbs and flat body posture was scored 3. After scoring, rats were allowed to recover for 2 h. Animals showing signs of neurologic damage were discarded. To verify the position of the catheter, after rat sacrifice, Evans blue solution was injected in the catheter and the spinal column exposed. Animals that had the catheter tip located intrathecally or outside the region between T7 - T9 were excluded from the study.

### Surgical preparation

Anaesthesia was induced by pentobarbital sodium (50 mg/kg intraperitoneally) and isoflurane inhalation. Rats had tracheotomy under isoflurane anesthesia and were mechanically ventilated (Harvard apparatus, model 683, South Natick, MA) with a Fio2 = 0.5. The left femoral vein was cannulated and continuously perfused with saline solution (2.5 mL/100 g/h). The left femoral artery was cannulated for continuous monitoring of arterial blood pressure and blood gas analysis (ABL 505 Analyzer, Radiometer, Copenhagen, Denmark). Body temperature was kept constant with a warm pad.

Blood samples were harvested every 30 min for blood gas analysis and ventilation was adjusted to obtain $pCO_2$ between 35 and 45 mmHg. The blood samples were also analyzed for serum amylase concentrations using 4,6-ethylidene (G1)-p-nitrophenyl (G1)-αaD-malto-heptoside (Sigma Chemical Co, Zurich, Switzerland) as substrate. Mean arterial pressure was continuously recorded and stored via an analog-digital interface converter (Biopac, Santa Barbara, CA) on an AST microcomputer (AST, Limerick, Ireland).

### Induction of acute pancreatitis

After laparotomy, the pancreatic duct was cannulated with a 22-gauge catheter (Abott, Sligo, Ireland)[25]. A clip was placed on the pancreatic duct close to the liver and taurocholic acid (5%, 500 μL, Sigma, Saint-Louis, MO) was infused over 4 min with a micropump[25].

### Pancreatic microcirculatory blood flow

Pancreatic microcirculatory blood flow was measured with a laser Doppler flowmetry (Periflux system 5000, Perimed AB, Järfälla, Sweden). To position the probe, a latex adhesive probe miniholder (model PH07, Perimed, Järfälla, Sweden) and a special articulated laboratory stand were used. The Doppler probe was placed under the pancreatic surface with the light directed upward. After a 10 to 15 min stabilization period, the effect of AP and/or EA on the pancreatic microcirculatory blood flow was measured over time. The pancreatic microcirculatory blood flow was continuously recorded and stored via an analog-digital interface converter (Biopac, Santa Barbara, CA) on an AST microcomputer (AST, Limerick, Ireland).

### Tissue samples

After the rats were sacrificed, pancreatic samples were rapidly collected, fixed in formalin, embedded in paraffin,

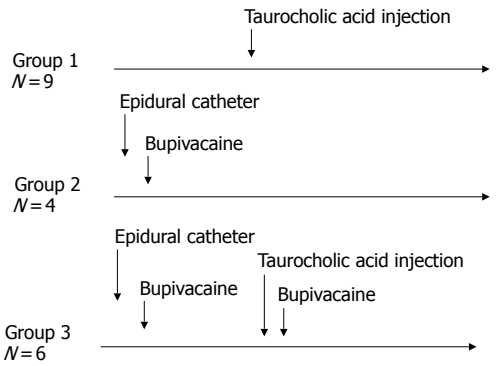


**Figure 1** Experimental design. Acute pancreatitis was induced in Groups 1 and 3 by injection of taurocholic acid (5%, 500 μL) into the biliopancreatic duct. Epidural anesthesia was induced in Groups 2 and 3 by epidural injection of bupivacaine (4 g/L, 20 μL).

and cut into 5-μm thick sections. After staining with hematoxylin-eosin, the sections were examined by two experienced morphologists who were not aware of the sample identity. The extent of acinar cell necrosis was quantified by computer assisted morphometry as previously described[26] and expressed as a percent of total acinar tissue.

### Experimental design

Three experimental groups were studied (Figure 1). In Group 1 ($n=9$), rats had AP induction and no EA. Pancreatic microcirculatory blood flow was measured before taurocholic acid injection and continued after the induction of AP. In Group 2 ($n=4$), the pancreatic microcirculatory blood flow was determined before and continued after the induction of EA. In Group 3 ($n=6$), 30 min after taurocholic acid injection, bupivacaine was injected via the epidural catheter and the pancreatic microcirculatory blood flow measured over time.

### Statistical analysis

Results were expressed as mean ± SD. Nonparametric Wilcoxon Signed ranks test and Kruskal-Walis tests for comparison between groups were used as appropriate. $P<0.05$ was considered statistically significant.

## RESULTS

### Epidural anesthesia in rats

EA was tested by bupivacaine injection in Groups 2 and 3. In all rats, hind limb blockade was complete within 2 min and the motility completely recovered within 25-30 min after the injection. In Group 3, rats had taurocholic acid injection to induce AP and were treated with bupivacaine (Figure 1).

### Pancreatic microcirculatory blood flow

In Group 1, induction of AP caused a significant decrease of mean pancreatic microcirculatory blood flow from 141 ± 40 units to 9 ± 6 units (96%, $P=0.008$) within 30 min (Figure 2). The decreased blood flow remained unchanged until the end of the experiment. In Group 2, EA slightly increased microcirculatory blood flow, but the modification did not reach statistical significance ($P=0.7$, Figure 2). In Group 3, induction of AP caused a similar decrease in pancreatic microcirculatory flow as in Group 1, *i.e.*, from 155 ± 25 units to 11 ± 7 units (93%, $P=0.004$). After induction of EA, mean pancreatic microcirculatory blood flow increased again significantly to 81 ± 31 units within 45 min, reaching 52% of baseline values ($P=0.028$, Figures 2 and 3).

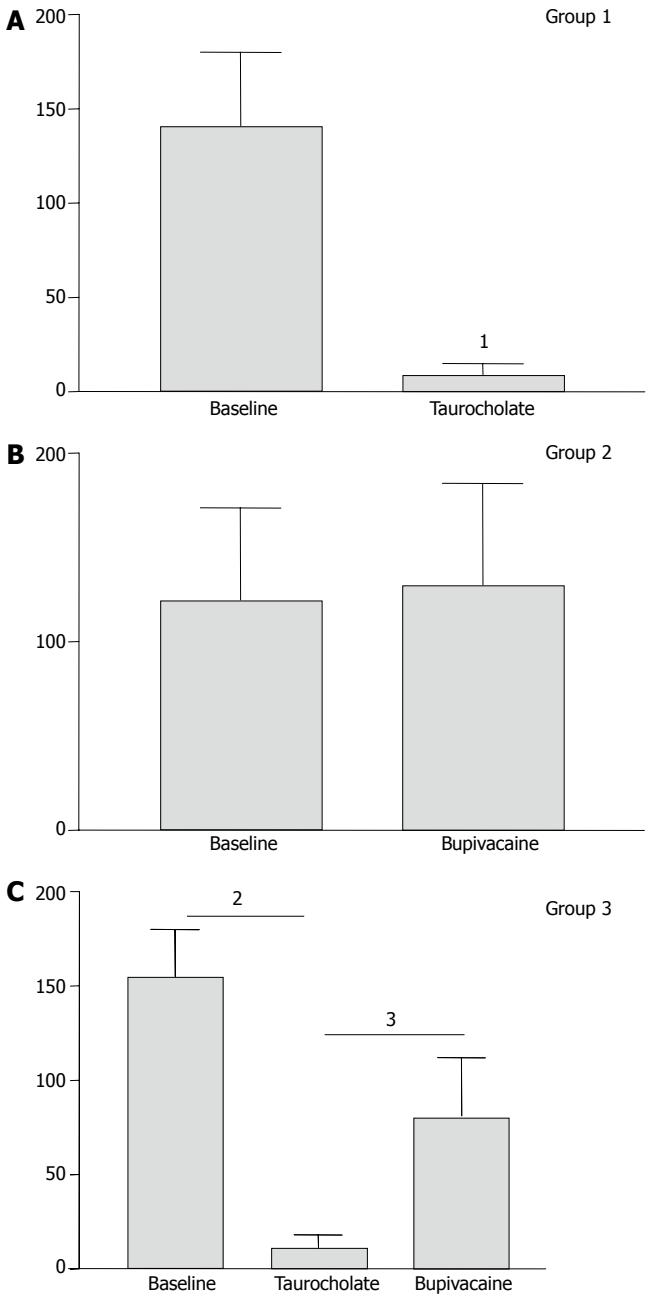


**Figure 2** Pancreatic microcirculatory blood flow (arbitrary units). In Group 1, the mean value of pancreatic blood flow measured prior to and after induction of AP showed a significant decrease of perfusion from 141 ± 40 units to 9 ± 6 units (96%) ($^1P=0.008$) within 30 min. In Group 2, the mean value of pancreatic blood flow measured prior to and after induction of epidural anaesthesia showed no significant modification of perfusion. In Group 3, mean value of pancreatic blood flow measured prior to and after induction of AP, and epidural anaesthesia, respectively. Induction of AP caused a significant decrease in pancreatic microcirculatory flow from 155 ± 25 units to 11 ± 7 units (93%) ($^2P=0.004$). After induction of epidural anesthesia, mean pancreatic microcirculatory blood flow increased again significantly to 81 ± 31 units within 45 min, reaching 52% of base line values ($^3P=0.028$).

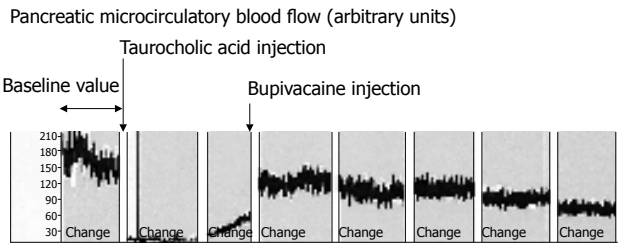


**Figure 3** Recording of pancreatic microcirculatory blood flow in Group 3. Rats were injected with taurocholic acid and treated 30 min later with bupivacaine (0.4%, 20 μL) in the epidural catheter. Induction of AP caused a significant decrease in pancreatic microcirculatory blood flow. After induction of epidural anesthesia, mean pancreatic microcirculatory blood flow increased again significantly within 45 min, reaching approximately 50% of baseline values.

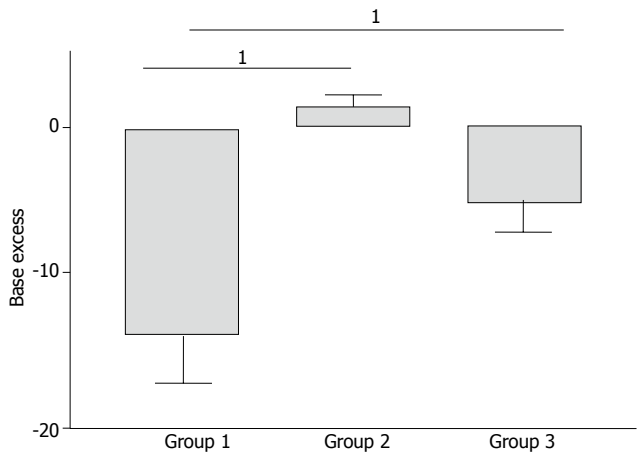


**Figure 4** Arterial blood gas analyses. In Group 1, severe metabolic acidosis developed progressively reaching a maximum base excess (BE) value of -14±3 mmol/L at the end of the experiment. In Group 2, BE values remained unchanged compared to baseline values. In Group 3, a mild metabolic acidosis developed reaching a maximum BE value of -6±4 mmol/L at the end of the experiment. This result was significantly improved compared to Group 1 ($^1P$=0.007).

### *Arterial blood gas and serum amylase analyses*

In Group 1, severe metabolic acidosis developed progressively reaching a maximum base excess (BE) value of -14±3 mmol / L at the end of the experiment (Figure 4). In Group 2, BE values remained unchanged compared to the baseline values during experiment (Figure 4). In Group 3, a mild metabolic acidosis developed reaching a maximum BE value of -6±4 mmol/L at the end of the experiment (Figure 4). This result was significantly improved compared to Group 1 ($P$=0.007).

In Group 1, serum amylase levels increased from 694±419 units/L prior to AP to 2178±561 units/L ($P$<0.05) after 2 h of induction of AP (Figure 5). In Group 2, EA did not modify serum amylase level significantly during the experiment. In Group 3, serum amylase levels increased to a maximum of 1829±641 units/L 2 h after initiation of AP and EA (Figure 5). Although this result was lower compared to Group 1, but did not reach statistical significance.

### *Histopathology*

In Group 1, histopathology revealed a severe form of AP with extensive edema and tissue necrosis (Figure 6C). In Group 2, almost normal pancreatic tissue was observed at the end of the experiment (Figure 6B). In Group 3, edema and necrosis were less extensive compared to animals in Group 1 (Figure 6D).

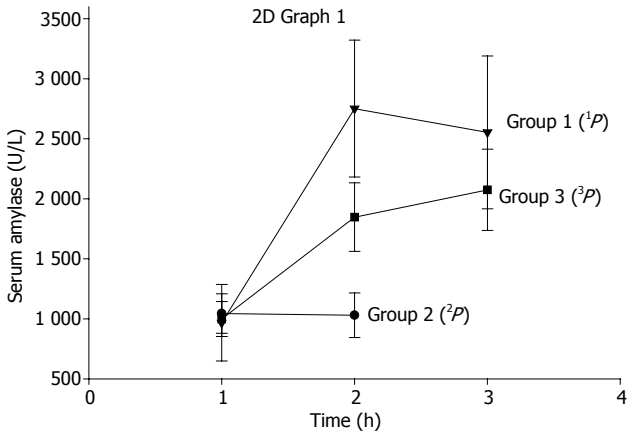


**Figure 5** Serum amylase levels. In Group 1, serum amylase levels increased from 694±units/L 419 prior to AP to 2178±561 units/L ($^1P$<0.05, *vs* serum amylase levels before induction of AP) after 2 h of induction of AP. In Group 2, epidural anaesthesia did not modify serum amylase levels significantly ($P$=0.9). In Group 3, serum amylase levels increased to a maximum of 1829±641 units/L after 2 h of initiation of AP and epidural anesthesia. Although this result was lower compared to Group 1, but did not reach statistical significance ($^3P$=0.08).

The extent of acinar cell necrosis measured as percentage of total surface at high power field (HPF) showed that Group 2 animals had similar cell necrosis as the controls (<10%) (Figure7). Group 1 animals demonstrated over 40% of acinar cell necrosis at HPF, whereas acinar cell necrosis was below 30% in Group 3 animals (Figure 7).

## DISCUSSION

In our study, taurocholic acid injection in the biliopancreatic duct induced a pancreatic hypoperfusion as reported by previous studies[3,7,16,25]. The decrease was -96% within 15 min and pancreatic microcirculatory blood flow remained low until the end of the experiment. The microcirculatory blood flow has been accurately measured by laser Doppler flowmetry. The technique is ideal for monitoring changes in tissue perfusion over time and has successfully been applied to numerous organs in experimental and human studies[4,6,24,27]. However, several factors, such as artifacts induced by respiration, external light exposure and temperature, can affect the interpretation of the laser Doppler signals[4]. In addition, microcirculatory flow can vary widely over short distances, and small changes in probe angle during measurement can alter the measured values. To prevent these technical problems, we used a new type of probe holder, which allows the tissue to be maintained by gravity, avoiding repeated repositioning of the probe.

More importantly, we showed that after induction of AP, bupivacaine injection in the epidural catheter increased pancreatic microcirculatory blood flow. Concomitantly, the improved microcirculatory blood flow within the pancreas decreased the severity of AP. Serum amylase

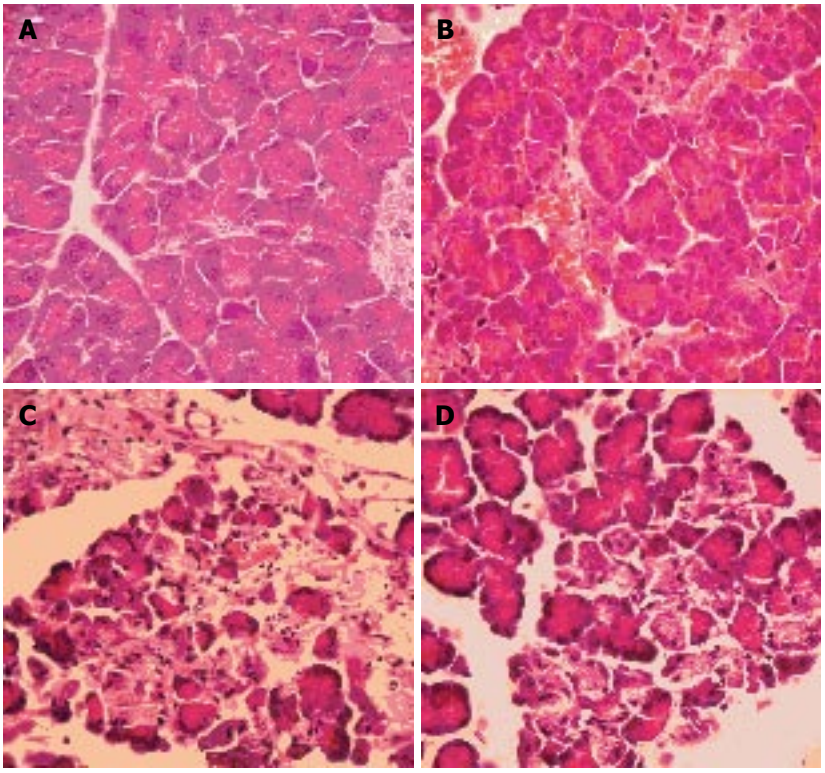


**Figure 6** Histopathological features of pancreatic tissue. **A:** A control animal was sacrificed and histopathology showed normal pancreas; **B:** Group 2 animals showing normal pancreatic tissue with minor modifications, possibly related to vasodilatation and surgical manipulations; **C:** Group 1 animals showing a severe form of AP with extensive edema and tissue necrosis; and **D:** Group 3 animals demonstrating less extensive pancreatic edema and necrosis compared to Group 1 animals.

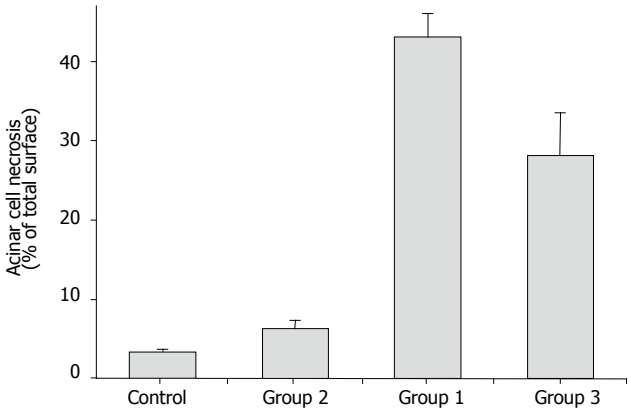


**Figure 7** Acinar cell necrosis (percentage of total pancreatic surface). The measure of acinar cell necrosis by percentage of total surface at high power field (HPF) showed that Group 2 animals had similar cell necrosis as the controls (<10%). Group 1 animals demonstrated over 40% acinar cell necrosis at HPF, whereas acinar cell necrosis was below 30% in Group 3 animals.

concentrations and metabolic acidosis were less severe and the histopathologic scores were improved in comparison to rats with AP and no treatment. These results emphasize the importance of a decreased microcirculatory blood flow in inducing severe AP.

To our best of knowledge, this is the first experimental study showing the beneficial effects of EA on the severity of AP. Previous reports already showed that EA increased splanchnic venous capacitance and decreased arterial tone by blocking sympathetic nerve activity[21,22,28-30]. It was also reported that EA might increase sympathetic activity and vasoconstriction in organs distant from the anesthetized area and redistributes blood flow towards splanchnic organs[21].

It has been postulated that several factors, such as local metabolic acidosis which activates various proteases, oxygen-free radical that injures endothelium and parenchyma, or the incapacity of plasma protease inhibitors to circulate through acinar cells, participate in the modifications of pancreatic microcirculation during AP[3]. These modifications result in diminished intravascular volume, chemically-induced vasoconstriction, intravascular coagulation, and increased endothelial permeability[31]. Finally, pancreatic ischemia, as a consequence of all these local effects, may convert a mild disease to a severe AP with parenchymal necrosis[31]. This has been demonstrated by Klar *et al* [5] who have shown in anesthetized rabbits that pancreatic blood flow increases when AP is edematous (cerulein injection), whereas pancreatic blood flow decreases when AP is severe (necrotizing form induced by taurocholate injection).

In our study, EA decreased serum amylase concentrations, metabolic acidosis, and the severity of pancreatic necrosis score in comparison to rats that had similar taurocholic acid injection and no treatment. Similar benefit of peridural anaesthesia has been shown on metabolic acidosis during hypoxia in dogs[29].

In conclusion, the current study has shown that EA improves the pancreatic hypoperfusion induced by AP with a concomitant decrease in the severity of metabolic acidosis and a diminished tissue injury. EA should therefore be considered a new therapeutic approach to prevent the progression from an edematous disease to a necrotizing AP.

## ACKNOWLEDGEMENTS

The authors thank Martha Jordan for excellent technical assistance.

## REFERENCES


1 **Beger HG,** Rau B, Isenmann R. Prevention of severe change in acute pancreatitis: prediction and prevention. *J Hepatobiliary Pancreat Surg* 2001; **8**: 140-147

2 **Bradley EL 3rd.** A clinically based classification system for acute pancreatitis. Summary of the International Symposium on Acute Pancreatitis, Atlanta, Ga, September 11 through 13, 1992. *Arch Surg* 1993; **128:** 586-590

3 **Plusczyk T**, Westermann S, Rathgeb D, Feifel G. Acute pancreatitis in rats: effects of sodium taurocholate, CCK-8, and Sec on pancreatic microcirculation. *Am J Physiol* 1997; **272**: G310-G320

4 **Dobosz M,** Hac S, Mionskowska L, Dobrowolski S, Wajda Z. Microcirculatory disturbances of the pancreas in cerulein-induced acute pancreatitis in rats with reference to L-arginine, heparin, and procaine treatment. *Pharmacol Res* 1997; **36**: 123-128

5 **Klar E**, Schratt W, Foitzik T, Buhr H, Herfarth C, Messmer K. Impact of microcirculatory flow pattern changes on the development of acute edematous and necrotizing pancreatitis in rabbit pancreas. *Dig Dis Sci* 1994; **39**: 2639-2644

6 **Schilling MK**, Redaelli C, Reber PU, Friess H, Signer C, Stoupis C, Buchler MW. Microcirculation in chronic alcoholic pancreatitis: a laser Doppler flow study. *Pancreas* 1999; **19**: 21-25

7 **Kusterer K**, Poschmann T, Friedemann A, Enghofer M, Zendler S, Usadel KH. Arterial constriction, ischemia-reperfusion, and leukocyte adherence in acute pancreatitis. *Am J Physiol* 1993; **265**: G165-G171

8 **Letko G**, Nosofsky T, Lessel W, Siech M. Transition of rat pancreatic juice edema into acute pancreatitis by single ethanol administration. *Pathol Res Pract* 1991; **187**: 247-250

9 **Anderson MC**. Venous stasis in the transition of edematous pancreatitis to necrosis. *JAMA* 1963; **183**: 534-537

10 **Klar E**, Rattner DW, Compton C, Stanford G, Chernow B, Warshaw AL. Adverse effect of therapeutic vasoconstrictors in experimental acute pancreatitis. *Ann Surg* 1991; **214**: 168-174

11 **Sanfey H**, Cameron JL. Increased capillary permeability: an early lesion in acute pancreatitis. *Surgery* 1984; **96**: 485-491

12 **McKay C**, Imrie CW, Baxter JN. Mononuclear phagocyte activation and acute pancreatitis. *Scand J Gastroenterol* Suppl 1996; **219:** 32-36

13 **Formela LJ**, Galloway SW, Kingsnorth AN. Inflammatory mediators in acute pancreatitis. *Br J Surg* 1995; **82**: 6-13

14 **Frossard JL**, Hadengue A, Pastor CM. New serum markers for the detection of severe acute pancreatitis in humans. *Am J Respir Crit Care Med* 2001; **164**: 162-170

15 **Huch K**, Schmidt J, Schratt W, Sinn HP, Buhr H, Herfarth C, Klar E. Hyperoncotic dextran and systemic aprotinin in necrotizing rodent pancreatitis. *Scand J Gastroenterol* 1995; **30**:812-816

16 **Schoenberg MH**, Buchler M, Younes M, Kirchmayr R, Bruckner UB, Beger HG. Effect of antioxidant treatment in rats with acute hemorrhagic pancreatitis. *Dig Dis Sci* 1994; **39**: 1034-1040

17 **Paszkowski AS,** Rau B, Mayer JM, Moller P, Beger HG. Therapeutic application of caspase 1/interleukin-1beta-converting enzyme inhibitor decreases the death rate in severe acute experimental pancreatitis. Ann Surg 2002; **235:** 68-76

18 **Norman J**. The role of cytokines in the pathogenesis of acute pancreatitis. *Am J Surg* 1998; **175**: 76-83

19 **Steinbrook RA**. Epidural anesthesia and gastrointestinal motility. *Anesth Analg* 1998; **86**: 837-844

20 **Tuman KJ**, McCarthy RJ, March RJ, DeLaria GA, Patel RV, Ivankovich AD. Effects of epidural anesthesia and analgesia on coagulation and outcome after major vascular surgery. *Anesth Analg* 1991; **73**: 696-704

21 **Sielenkamper AW**, Eicker K, Van Aken H. Thoracic epidural anesthesia increases mucosal perfusion in ileum of rats. *Anesthesiology* 2000; 93: 844-851

22 **Ai K**, Kotake Y, Satoh T, Serita R, Takeda J, Morisaki H. Epidural anesthesia retards intestinal acidosis and reduces portal vein endotoxin concentrations during progressive hypoxia in rabbits. *Anesthesiology* 2001; **94**: 263-269

23 **Bernhardt A**, Kortgen A, Niesel HCh, Goertz A. [Using epidural anesthesia in patients with acute pancreatitis--prospective study of 121 patients]. *Anaesthesiol Reanim* 2002; **27**: 16-22

24 **Grouls RJ**, Meert TF, Korsten HH, Hellebrekers LJ, Breimer DD. Epidural and intrathecal n-butyl-p-aminobenzoate solution in the rat. Comparison with bupivacaine. *Anesthesiology* 1997; **86**: 181-187

25 **Aho HJ**, Koskensalo SM, Nevalainen TJ. Experimental pancreatitis in the rat. Sodium taurocholate-induced acute haemorrhagic pancreatitis. *Scand J Gastroenterol* 1980; **15**: 411-416

26 **Frossard JL**, Kwak B, Chanson M, Morel P, Hadengue A, Mach F. Cd40 ligand-deficient mice are protected against cerulein-induced acute pancreatitis and pancreatitis-associated lung injury. *Gastroenterology* 2001; **121**: 184-194

27 **Phillips AR**, Farrant GJ, Abu-Zidan FM, Cooper GJ, Windsor JA. A method using laser Doppler flowmetry to study intestinal and pancreatic perfusion during an acute intestinal ischaemic injury in rats with pancreatitis. *Eur Surg Res* 2001; **33**: 361-369

28 **Hogan QH**, Stekiel TA, Stadnicka A, Bosnjak ZJ, Kampine JP. Region of epidural blockade determines sympathetic and mesenteric capacitance effects in rabbits. *Anesthesiology* 1995; **83**: 604-610

29 **Shibata K**, Taki Y, Futagami A, Yamamoto K, Kobayashi T. Epidural anesthesia modifies cardiovascular responses to severe hypoxia in dogs. *Acta Anaesthesiol Scand* 1995; **39**: 748-753

30 **Yano H**, Takaori M. The microcirculation during enflurane and isoflurane anaesthesia in dogs. *Can J Anaesth* 1994; **41**: 149-155

31 **Buchler M**, Friess H, Uhl W, Beger HG. Clinical relevance of experimental acute pancreatitis. *Eur Surg Res* 1992; **24** Suppl 1: 85-88


**S- Editor** Kumar M and Guo SY **L- Editor** Elsevier HK **E- Editor** Kong LH

PO Box 2345, Beijing 100023, China
www.wjgnet.com
wjg@wjgnet.com

*World J Gastroenterol* 2006 February 14; 12(6): 921-927
***World Journal of Gastroenterology*** ISSN 1007-9327
© 2006 The WJG Press. All rights reserved.

*BASIC RESEARCH*

# Expression, purification and characterization of enterovirus-71 virus-like particles

Yao-Chi Chung, Jen-Huang Huang, Chia-Wei Lai, Heng-Chun Sheng, Shin-Ru Shih, Mei-Shang Ho, Yu-Chen Hu

Yao-Chi Chung, Jen-Huang Huang, Chia-Wei Lai, Heng-Chun Sheng, Yu-Chen Hu, Department of Chemical Engineering, National Tsing Hua University, Hsinchu 300, Taiwan, China
Shin-Ru Shih, School of Medical Technology, Chang Gung University, Taoyuan 333, Taiwan, China
Mei-Shang Ho, Institute of Biomedical Sciences, Academia Sinica, Taipei 11529, Taiwan, China
Supported by the National Science Council, No. 93-2214-E-007-016 and Ministry of Economic Affairs, No. 93-EC-17A-17S1-0009
Correspondence to: Dr. Yu-Chen Hu, Department of Chemical Engineering, National Tsing Hua University, Hsinchu 300, Taiwan, China. yuchen@che.nthu.edu.tw
Telephone: +886-3-571-8245 Fax: +886-3-571-5408
Received: 2005-04-01 Accepted: 2005-07-20

## Abstract

**AIM:** Enterovirus 71 (EV71) has been implicated as the etiological agent responsible for the recent outbreaks of hand, foot and mouth disease associated with severe neurological diseases in the Asia-Pacific region.

**METHODS:** The assembly process was hypothesized to occur via an orchestrated proteolytic processing of the P1 precursor by the viral protease 3CD. To test this hypothesis, we constructed 3 recombinant baculoviruses: Bac-P1 expressing P1; Bac-3CD expressing 3CD; and Bac-P1-3CD co-expressing P1 and 3CD.

**RESULTS:** Both single infection by Bac-P1-3CD and co-infection by Bac-P1 and Bac-3CD resulted in correct cleavage of P1 to yield individual proteins VP0, VP1 and VP3, while the former approach yielded higher VLP production. In the cells, the structural proteins self-assembled into clusters of virus-like particles (VLP) resembling the authentic EV71 particle aggregates. After ultracentrifugation purification, the dispersed VLPs were indistinguishable from the authentic virus in size, appearance, composition and surface epitopes, as determined by SDS-PAGE, Western blot, transmission electron microscopy and immunogold labeling.

**CONCLUSION:** Our data, for the first time, suggest that in insect cells EV71 structural proteins adopt a processing and assembly pathway similar to poliovirus assembly. The preservation of particle morphology and composition suggest that the VLP may be a valuable vaccine candidate to prevent EV71 epidemics.

© 2006 The WJG Press. All rights reserved.

**Key words**: Enterovirus 71; Virus-like particle; VLP; Vaccine; Baculovirus; Insect cell

Chung YC, Huang JH, Lai CW, Sheng HC, Shih SR, Ho MS, Hu YC. Expression, purification and characterization of enterovirus-71 virus-like particles. *World J Gastroenterol* 2006; 12(6): 921-927

http://www.wjgnet.com/1007-9327/12/921.asp

## INTRODUCTION

Enterovirus 71 (EV71), like poliovirus, is one of the 69 enterovirus serotypes belonging to the *Picornaviridae* family. EV71 infection manifests most frequently as hand, foot and mouth disease (HFMD) and children under 5 years of age are particularly susceptible to the most severe forms of EV71-associated neurological disease, including aseptic meningitis, brainstem encephalitis and acute flaccid paralysis indistinguishable from poliomyelitis[1]. The neurovirulence of EV71 first came to people's attention in 1975 in Bulgaria when 44 people died of a polio-like disease[2]. EV71 was further implicated as the causative agent responsible for the epidemics of central nervous system disease occurring in New York, Europe, Australia and Asia[3-6]. Recent HFMD outbreaks also affected thousands of children in Taiwan[7], Japan[8] and Singapore[9], causing the fatality of more than 80 children. Thus EV71 appears to emerge as an increasingly important neurotropic enterovirus in the upcoming era of poliomyelitis eradication. However, no effective antiviral drugs or vaccines are available yet.

EV71 possesses a positive single-stranded RNA genome that consists of a single open reading frame (ORF). The ORF expresses a large polyprotein that can be co- and post-translationally cleaved into P1, P2 and P3 regions[10]. P1 region encodes the four structural proteins VP1, VP2, VP3 and VP4, while P2 and P3 regions encode other nonstructural proteins (*e.g.*, 2A and 3CD) responsible for virus replication and virulence[1]. Based on a model derived from poliovirus, protease 2A autocatalytically cleaves P1 at its N-terminus and liberates P1 from the nascent polyprotein[11], while protease 3CD cleaves P1 precursor into VP1, VP3 and VP0 in trans[12]. These three structural proteins spontaneously assemble into icosahedral

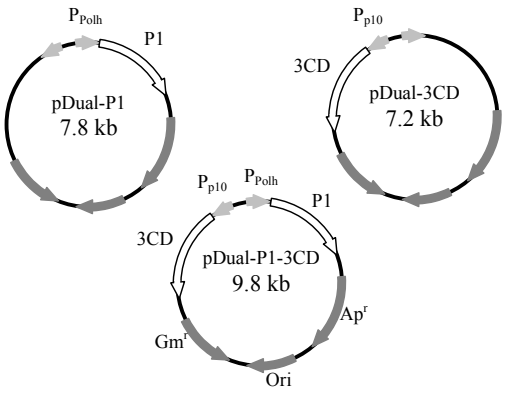


**Figure 1** Construction of three recombinant baculovirus vectors using pFastBac™ DUAL plasmid as the backbone. The gene fragments encoding P1 and 3CD were cloned separately into MCS I and II of pFastBac™ DUAL under the control of polyhedrin ($P_{polh}$) and p10 promoters ($P_{p10}$), respectively. The resultant plasmids were designated pDual-P1 and pDual-3CD, respectively. The P1 and 3CD genes were cloned together into MCS I and II under the control of polyhedrin and p10 promoters. The resultant plasmid was designated pDual-P1-3CD.

procapsid in an ordered manner and proceed through a series of intermediates, followed by the encapsidation of the RNA genome into the provirion[13]. The final encapsidation step involves the cleavage of VP0 into VP2 and VP4, therefore the final mature virion consists of 60 copies each of VP1 and VP3, 58-59 copies of VP2 and VP4 and 2-1 copies of VP0[13].

Besides the mature virions, naturally occurring virus-like particles (VLPs) of poliovirus have been discovered[14]. VLPs are empty particles consisting of viral structural proteins but devoid of viral nucleic acids, hence they are non-infectious. VLPs can generally induce broad and strong immune responses thanks to the preservation of many essential epitopes[15-17], therefore VLPs have captured increasing attention as potential vaccine candidates[17-19]. To date, numerous VLPs of clinically important viruses, including human immunodeficiency virus[20], SARS coronavirus[21] and hepatitis delta virus[22], have been expressed. In addition, recombinant poliovirus VLPs have been produced using the baculovirus/insect cell or vaccinia virus expression system. These particles were produced via the (1) expression of the complete ORF; (2) co-expression of individual VP0, VP1 and VP3 proteins; or (3) co-expression of P1 and 3CD proteins[23-25]. Since EV71 and poliovirus share identical genome organization and similar protein functions, we hypothesized that EV71 assembly occurs in a way similar to poliovirus and have previously demonstrated the formation of EV71 VLP by co-infecting insect cells with two recombinant baculoviruses, Bac-P1 expressing P1 and Bac-3CD expressing 3CD[26]. However, the factors influencing the VLP yield were not investigated, and the VLPs were not purified or characterized. In this study, we extended our previous work by further constructing a new recombinant baculovirus simultaneously expressing P1 and 3CD. The new virus was used for single infection of insect cells, co-expression of P1 and 3CD and synthesis of VLP. The yields of VLP produced via the single infection and co-infection strategies were compared. Finally, the VLPs were purified and characterized.

## MATERIALS AND METHODS

### Cell culture and media

*Spodoptera frugiperda* (Sf-9) insect cells were cultured in spinner flasks (Bellco) at 27 °C using TNM-FH medium supplemented with 100 mL/L fetal bovine serum (FBS, Gibco BRL) as described elsewhere[27].

### Generation of recombinant baculoviruses

The gene fragments coding for P1 and 3CD were amplified by polymerase chain reaction from the full-length cDNA clone of EV71 *neu* strain[28] and subcloned separately into multiple cloning site (MCS) I and II of pFastBac™ DUAL plasmids (Invitrogen) as described previously[26]. The resultant plasmids were designated pDual-P1 and pDual-3CD, respectively. Likewise, the P1 gene fragment was cloned into MCS I under the polyhedrin promoter and the 3CD gene fragment was inserted into MCS II under the p10 promoter. The resultant plasmid carrying two gene cassettes was designated pDual-P1-3CD (Figure 1). The recombinant baculoviruses were subsequently generated using Bac-to-Bac® system (Invitrogen) as described previously[29] and designated Bac-P1, Bac-3CD and Bac-P1-3CD based on the genes they encoded. The recombinant viruses were propagated, amplified, stored and titered according to standard procedures[30].

### SDS-PAGE and Western blot

To confirm the expression of recombinant P1 and VP1, the infected cells were harvested by low-speed centrifugation and then lysed by incubation in the lysis buffer (0.1% Triton X-100 in Tris-buffered saline) at 4 °C for 30 min. The proteins were resolved on 100 g/L gels as described previously[26] and stained by Commassie blue. For Western blot, the proteins were transferred onto nitrocellulose membranes according to standard procedures (Bio-Rad Laboratories). The transferred membrane was blocked with 50 g/L non-fat milk and probed by mouse anti-VP1 monoclonal antibody (MAb). The secondary antibody was goat anti-mouse IgG conjugated with alkaline phosphatase (Kirkegaard and Perry Laboratories). The membranes were developed with BCIP/NBT color developing reagent (Sigma).

### Purification of VLP by ultracentrifugation

EV71 VLPs were produced by infecting Sf-9 cells with Bac-P1-3CD at a multiplicity of infection (MOI) of 10. Approximately 150 mL cells ($1.5\times10^6$ cells/mL) were harvested at 2 d post-infection (dpi) by centrifugation (1 000 r/min for 5 min) and were re-suspended in 10 mL TE buffer (0.01 mol/L Tris-HCl, 0.001 mol/L EDTA, pH 7.4). The cell suspension was supplemented with 1 mL of 10X HO buffer (0.01 mol/L Tris, 0.25 mol/L NaCl, 0.01 mo/L 2-mercaptoethanol) and 100 g/L NP-40, lysed by sonication for 3 min and centrifuged at 13 000 *g* (R20A2 rotor, CR22G, Hitachi) for 30 min. The supernatant was passed through a 0.22-μm filter to remove the debris and then ultracentrifuged at 27 000 *g* (P40ST rotor, CP100MX, Hitachi) for 4 h. The pellets were resuspended in TE buffer, sonicated for 30 s and loaded onto the discontinuous sucrose gradient (15%, 30% and 65%

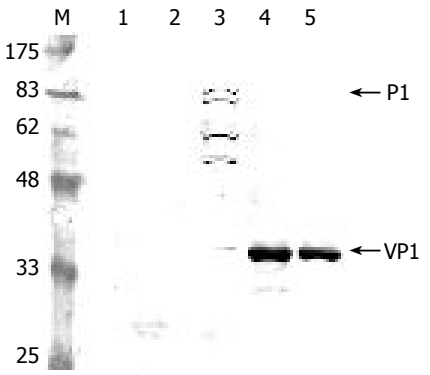


**Figure 2** Western blot analysis of cell lysates infected by different viruses. The Sf-9 cells were infected by the viruses at a total MOI of 10 and harvested at 3 dpi. The proteins were separated by SDS-PAGE, electrotransferred to a nitrocellulose membrane and probed using anti-VP1 MAb as the primary antibody. Lane 1: mock infection; Lane 2: wild-type baculovirus AcMNPV; Lane 3: Bac-P1; Lane 4: Bac-P1-3CD; Lane 5: Bac-P1 and Bac-3CD.

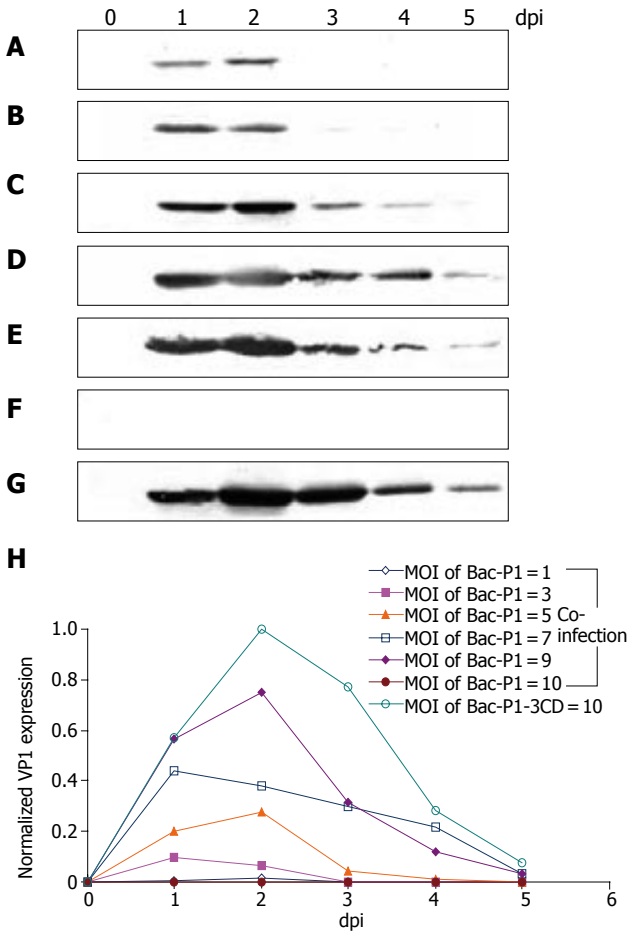


**Figure 3** Time course profiles of VP1 production under various infection conditions as analyzed by Western blot. Insect cells were infected at a total MOI of 10 by single infection with Bac-P1-3CD (G), or co-infection at MOI ratios (Bac-P1/Bac-3CD) of 1/9 (**b**), 3/7 (**B**), 5/5 (**C**), 7/3 (**D**), 9/1 (**E**) and 10/0 (**F**). Lanes 0-5 represent the cell lysates collected at 0, 1, 2, 3, 4, and 5 dpi, respectively. The relative VP1 production levels under different conditions were quantified by scanning densitometry (**H**). The data represent the average values of duplicated experiments.

sucrose dissolved in TE buffer). After ultracentrifugation at 27 000 *g* (P40ST rotor) for 3 h, the milky white band between the interfaces of 15-35% sucrose was collected and layered on top of a 1.33 g $cm^{-3}$ cesium chloride (CsCl) solution. After ultracentrifugation at 34 000 *g* (P40ST rotor) for 24 h, the bands collected from CsCl gradient were dialyzed against phosphate-buffered saline (pH 7.4) and were ultracentrifuged again at 34 000 *g* for 5 h. The pellets were resuspended in 50 μL pure water for SDS-PAGE, Western blot and transmission electron microscopy (TEM) analyses. The purities of the samples and the composition of VLPs were quantified by densitometry using Scion Image Shareware (Scion Corporation).

### *TEM and immunogold labeling*

The VLPs within the insect cells were visualized under a transmission electron microscope (H-7500, Hitachi), prior to which ultrathin sectioning of cells was performed as described previously[26]. The particles after purification were adsorbed onto Formvar-coated copper grids, negatively stained by 20 g/L phosphotungstic acid (PTA) and examined by TEM. For immunogold labeling, purified particles were adhered onto copper grids and probed by mouse anti-VP1 MAb. The secondary antibody was goat anti-mouse IgG conjugated with 5 nm gold particles (Sigma). After washing of the unbound gold particles, the grids were stained by 20 g/L PTA and observed by TEM.

## RESULTS

### *Expression of recombinant proteins in insect cells*

To determine whether the recombinant P1 and 3CD were successfully expressed by Bac-P1-3CD, Sf-9 cells were singly infected by wild-type AcMNPV, Bac-P1, and Bac-P1-3CD (MOI 10), or co-infected by Bac-P1 (MOI 5) and Bac-3CD (MOI 5). The cells were harvested at 3 dpi and lysed for Western blot analysis. As shown in Figure 2, the mock-infected and wild-type AcMNPV-infected cells did not express P1 (lanes 1 and 2), whereas the Bac-P1-infected cells expressed a protein with a molecular mass corresponding to 97 ku, indicating the successful expression of P1 (lane 3). Other P1-associated proteins migrating faster than P1 were also found (lane 3), suggesting a possible degradation of P1 by the cellular proteases, but this non-specific degradation did not yield VP1 (39 ku).

We also noted that no antibody specifically recognizing 3CD was available, hence the 3CD expression was detected indirectly by observing whether P1 was cleaved into VP1 upon co-expression of both proteins. Lanes 4 and 5 depict that either single infection by Bac-P1-3CD (lane 4) or co-infection by Bac-P1 and Bac-3CD (lane 5) led to complete cleavage of P1 into VP1, proving the successful co-expression of functional P1 and 3CD by both approaches.

### *Optimization of VP1 production*

Since P1 relies on 3CD for cleavage and subsequent VLP assembly, delicately controlling the relative expression levels of P1 and 3CD is crucial for optimal VLP production. To address this issue, the cells were co-infected by Bac-P1 and Bac-3CD at MOI ratios of 1/9, 3/7, 5/5, 7/3, 9/1 and 10/0, or singly infected by Bac-P1-3CD at MOI 10 in order to compare and optimize the VP1 yield. Figures (3A-3G) show the time-course profiles

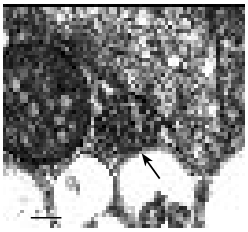

**Figure 4** Electron microscopy examinations of EV71 VLP aggregates formed in cytoplasm of the Bac-P1-3CD-infected insect cells (100 000 X magnification). The cells were infected at MOI 10, harvested at 3 dpi and ultrathin sectioned for TEM. The arrowhead indicates the VLP aggregate. Bar:100 nm.

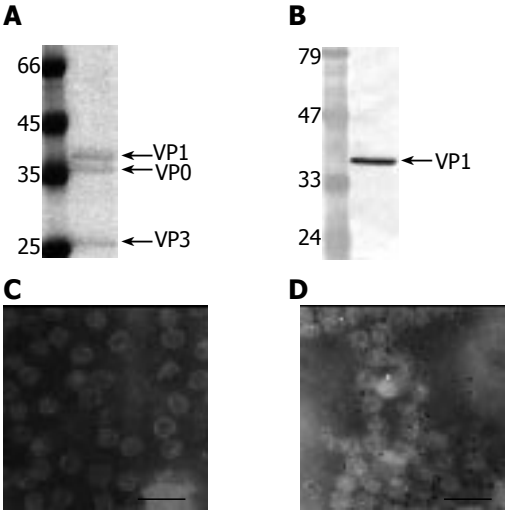


**Figure 5** Purification and characterization of EV71 VLP (100 000 X magnification,). The VLPs were produced by infecting 150 mL Sf-9 cells ($1.5\times10^6$ cells/mL) with Bac-P1-3CD at MOI 10, harvested at 2 dpi and purified by ultracentrifugation. The purified VLPs were characterized by SDS-PAGE (**A**), Western blot (**B**), TEM examination (**C**) and immunogold labeling (**D**). The PAGE gel was stained by Commassie blue and scanned for densitometry analysis. The primary antibody used in the Western blot and immunogold labeling was anti-VP1 MAb. The size of the gold particles was 5 nm. Bar: 100 nm.

of VP1 production, in which lanes 0-5 represent the samples harvested at 0, 1, 2, 3, 4 and 5 dpi, respectively. As shown, both single infection and co-infection approaches resulted in similar expression kinetics (except MOI 10/0), that is, the VP1 concentration rapidly culminated at 1-2 dpi, declined thereafter and virtually vanished at 5 dpi. The concentration peaked slightly earlier compared to those of many other proteins whose maximum concentration occurred at 3 dpi[27,31] probably because of proteolytic degradation by cellular proteases (data not shown).

The production levels using different MOI combinations were also compared by scanning densitometry, by which all band intensities were normalized against the strongest band intensity (lane 2, Figure 5G). Figure 5H reveals that in the case of co-infection VP1 concentration increased with the MOI of Bac-P1 provided that the total MOI was fixed at 10. However, the maximum VP1 yield obtained from single infection (by Bac-P1-3CD at MOI 10) was the highest, being ≈30% and ≈120% greater than those obtained from co-infection at MOI 9/1 and 7/3, respectively.

### *Formation of intracellular virus-like particle aggregates*

Since single infection with Bac-P1-3CD yielded the highest VP1 production, the formation of VLPs by single infection strategy was further examined. The cells were singly infected by Bac-P1-3CD at MOI 10 and subjected to ultrathin sectioning and TEM examination. As shown in Figure 4, clusters of virus-like particles were observed in the cytoplasm. These particles measured 25-27 nm in diameter and appeared icosahedral, thus resembling the authentic enterovirus in size and appearance. Such VLP aggregates were not observed in Sf-9 cells infected by Bac-P1 alone (data not shown), indicating that the particles were not the assembly products of individual structural proteins degraded from P1 precursor.

### *Purification and characterization of EV 71 VLP*

The subsequent VLP production was performed by infecting insect cells with Bac-P1-3CD (MOI 10). The particles were released from the infected cells, purified by ultracentrifugation and analyzed by SDS-PAGE (Figure 5A) and Western blot (Figure 5B). We observed that the purified sample contained three major proteins whose molecular masses corresponded to those of VP1 (39 ku), VP0 (36 ku) and VP3 (26 ku), and the purity of the sample was greater than 90% (Figure 5A). The molar concentrations of the three proteins as determined by scanning densitometry were roughly equal, agreeing with the notion that the molar ratios of VP0, VP1 and VP3 are identical in the enterovirus provirions[13]. Because no antibodies specifically recognizing VP0 and VP3 were available, the Western blot was performed using anti-VP1 antibody only, which further confirmed that the 39 ku protein was VP1. The purified particles were also subjected to TEM examination (Figure 5C), which showed that particles with size and morphology similar to those of the particles observed *in vivo* except the purified VLPs were dispersed. The immunogold labeling using anti-VP1 antibody further revealed gold particles surrounding the distinct particles (Figure 5D), indicating the exposure of VP1 on the outer surface. All these data confirmed that the Bac-P1-3CD infection successfully resulted in the formation of VLP comprising VP0, VP1 and VP3 and these particles could be purified by ultracentrifugation to near homogeneity.

The purified VLPs were also used as the standard to measure the specific yields of VLP. Approximately 10 mg of VLP was expressed per $10^9$ Bac-P1-3CD-infected cells at MOI 10. This high expression level may contribute to future mass production and downstream purification.

## DISCUSSION

The assembly pathway of EV71 has not been definitely identified, but the assembly model of poliovirus suggests that concerted cleavage of P1 by protease 3CD is required for capsid assembly. In this study, 3 recombinant baculoviruses were employed to express P1 and 3CD simultaneously in order to mimic the natural assembly process. By either single infection with Bac-P1-3CD or co-infection with Pac-P1 and Bac-3CD, successful processing

of P1 into VP1 (Figure 1) was demonstrated, proving the successful expression of both P1 and functional 3CD. Alternative approach by co-expression of individual VP1, VP2, VP3 and VP4 proteins has been tested for VLP assembly, yet the yield was very low (personal communication). The comparison of these approaches suggests that VLP synthesis from the P1 precursor is a more favorable route, which agrees with the assembly pathway of poliovirus VLP[24].

The co-infection experiments further suggested that the amount of P1 required was larger than that of 3CD for VLP assembly as the co-infection at MOI 9/1 yielded considerably larger amounts of VP1 than MOI 5/5 or 1/9 (Figure 3). Intriguingly, we observed that single infection by Bac-P1-3CD was superior to co-infection by Bac-P1 and Bac-3CD with regard to VP1 production (Figure 3H). Since we lacked proper antibodies to detect 3CD, the relative expression levels of P1 and 3CD in the cells singly infected by Bac-P1-3CD remained unclear. However, since P1 expression was driven by polyhedrin promoter which was stronger than p10 promoter regulating the 3CD expression, one may surmise that differential expression of P1 and 3CD arose, namely, the P1 expression exceeded the 3CD expression. Another reason that may account for the higher production by single infection methodology is the VLP-producing cell population distribution as a result of the co-infection approach, whereby only the cells that were co-infected could produce VLP. Using the co-infection methodology, the probability of a cell to be infected by one or two types of viruses and the number of virus entering any given cells follow the modified Poisson distribution as predicted previously[32]. Hence, a population of cells that were singly infected by Bac-P1 or Bac-3CD arose, and no P1 processing or VLP assembly occurred in these cells. Even for the cells that were co-infected by both viruses, the number of infecting Bac-P1 and Bac-3CD within one cell might vary[32]. In cells where the number of Bac-P1 infection far more exceeded that of Bac-3CD infection, insufficient expression of 3CD and inadequate P1 cleavage could occur. On the contrary, in cells where the Bac-3CD infection considerably outnumbered the Bac-P1 infection, a drought in P1 supply could occur and lead to inadequate VLP assembly. Such heterogeneity could decrease the P1 processing and VLP assembly in many cells. In contrast, the infection of Bac-P1-3CD alone resulted in P1 processing in all cells, leading to a higher VP1 yield.

Despite the lower yield, the significance of co-infection strategy should not be ignored because it offers a new dimension to manipulate the composition of VLPs. For instance, the cells may be co-infected with Bac-P1-3CD and a new recombinant baculovirus expressing VP1 derived from a different EV71 strain (e.g., the prototype BrCr strain). The phenotypic mixing may allow the incorporation of VP1 from BrCr strain into the VLP, thus generating chimeric, multivalent VLPs and broadening the spectrum of protection.

In addition to the higher expression level, single infection strategy resulted in the formation of VLP morphologically indistinguishable from the authentic viruses. Within the cells, clusters of virus-like particles resembling those observed in EV71-infected human rhabdomyosarcoma (RD) cells[26] and in enterovirus-infected skeletal muscle cells[33] were observed. The *in vivo* formation of particle aggregates was not previously reported by other researchers studying the poliovirus VLPs[23,25], but was recently noted in BHK-38 cells infected by foot-and-mouth disease virus[34], a relatively genetically distant picornavirus. To date, the biological significance of the particle aggregation remains to be explored, but the resemblance in particle morphology and the aggregation patterns between the VLP and the authentic enterovirus suggests that EV71 VLP adopts an assembly pathway in insect cells in a way similar to the authentic viruses do in their natural host cells. Despite the aggregation within cells, the VLP could be dispersed in solution and purified through CsCl gradient ultracentrifugation to near homogeneity. The purified VLPs comprised VP0, VP3 and VP1 of roughly equal molar ratios, a result consistent with previous findings that poliovirus provirions are composed of 60 copies each of VP1, VP3 and VP0[13]. This implied the similarity between the VLP and the authentic virus in composition. Notably, in insect cells VP0 did not appear to undergo further cleavage into VP2 and VP4, a maturation process associated with the acquisition of infectivity and the increase in particle stability[35]. The lack of further processing is reasonable as the natural maturation process takes place after the RNA encapsidation, yet in this expression system, no RNA packaging into the central cavity occurred.

Nonetheless, after purification, the size and morphology of VLPs appeared indistinguishable from those of poliovirus VLP. More importantly, the immunogold labeling confirmed the presence of VP1 epitopes on the VLP surface. These data suggest that the VLPs contain the important antigenic sites essential for eliciting the immune responses. This is particularly important because neutralizing epitopes are most densely clustered on VP1 and many of them consist of amino acids from different domains or from different polypeptides[36,37], that is, many of them are conformation-dependent. In this regard, the use of VLP as a vaccine candidate against EV71 infection may be particularly promising. In recent years, VLP-based vaccines have been demonstrated to not only elicit neutralizing antibodies, but also provoke potent cytotoxic and helper T-lymphocyte responses and have been shown to confer protection from virus challenge in the animal models[38-40]. Furthermore, papillomavirus-like particles have been shown to induce acute activation of dendritic cells[16]. Other VLPs that have been evaluated in pre-clinical studies for their potentials as vaccines include JC virus, human immunodeficiency virus, rotavirus and parvovirus[41]. Moreover, the humoral, mucosal and cellular immune responses to Norwalk VLP in humans have been reported[42], while VLP vaccines against human papillomavirus have entered into phase II clinical trials and promising data have been presented[43]. All these further justify the development of VLP vaccines.

Since EV71 has caused seasonal morbidity and mortality in children with increasing frequency in recent years, vaccine development has become a top priority among all control strategies. Although other vaccine types,

such as inactivated virus and VP1 subunit vaccines, have been tested[44], only the inactivated virus elicited strong immune responses, again confirming the importance of preserving epitope conformation. However, further assessment of safety and efficacy of the inactivated virus vaccine is required. In this study, we have successfully demonstrated the formation and purification of EV71 VLP via co-expression of P1 and 3CD and a reasonable production yield (≈10 mg/$10^9$ cells) was achieved, thus offering an attractive alternative to the inactivated virus vaccine. At present, the immunological evaluation has been impeded due to the difficulty in obtaining sufficient amounts of pure VLP because the recovery yield of VLP by ultracentrifugation was very low. The poor recovery yield may be attributed to the impaired VLP stability as empty capsids are less stable than mature virions[45]. The particle stability may be enhanced by the addition of a stabilizer (e.g., pirodavir, disoxaril or R 78206) that binds the pocket underneath the canyon of the particle[46]. The feasibility of enhancing VLP integrity by stabilizers is being evaluated. Furthermore, the development of a more efficient chromatography-based purification scheme is necessary for process scale-up and is underway.

## REFERENCES


1 **McMinn PC.** An overview of the evolution of enterovirus 71 and its clinical and public health significance. *FEMS Microbiol Rev* 2002; **26**: 91-107

2 **Chumakov M**, Voroshilova M, Shindarov L, Lavrova I, Gracheva L, Koroleva G, Vasilenko S, Brodvarova I, Nikolova M, Gyurova S, Gacheva M, Mitov G, Ninov N, Tsylka E, Robinson I, Frolova M, Bashkirtsev V, Martiyanova L, Rodin V. Enterovirus 71 isolated from cases of epidemic poliomyelitis-like disease in Bulgaria. *Arch Virol* 1979; **60**: 329-340

3 **Blomberg J**, Lycke E, Ahlfors K, Johnsson T, Wolontis S, von Zeipel G. Letter: New enterovirus type associated with epidemic of aseptic meningitis and-or hand, foot, and mouth disease. *Lancet* 1974; **2**: 112

4 **Gilbert GL,** Dickson KE, Waters MJ, Kennett ML, Land SA, Sneddon M. Outbreak of enterovirus 71 infection in Victoria, Australia, with a high incidence of neurologic involvement. *Pediatr Infect Dis J* 1988; 7: 484-488

5 **Nagy G**, Takatsy S, Kukan E, Mihaly I, Domok I. Virological diagnosis of enterovirus type 71 infections: experiences gained during an epidemic of acute CNS diseases in Hungary in 1978. *Arch Virol* 1982; **71**: 217-227

6 **Samuda GM**, Chang WK, Yeung CY, Tang PS. Monoplegia caused by Enterovirus 71: an outbreak in Hong Kong. *Pediatr Infect Dis J* 1987; **6**: 206-208

7 **Ho M,** Chen ER, Hsu KH, Twu SJ, Chen KT, Tsai SF, Wang JR, Shih SR. An epidemic of enterovirus 71 infection in Taiwan. Taiwan Enterovirus Epidemic Working Group. *N Engl J Med* 1999; **341:** 929-935

8 **Fujimoto T**, Chikahira M, Yoshida S, Ebira H, Hasegawa A, Totsuka A, Nishio O. Outbreak of central nervous system disease associated with hand, foot, and mouth disease in Japan during the summer of 2000: detection and molecular epidemiology of enterovirus 71. *Microbiol Immunol* 2002; **46**: 621-627

9 **Singh S**, Chow VT, Phoon MC, Chan KP, Poh CL. Direct detection of enterovirus 71 (EV71) in clinical specimens from a hand, foot, and mouth disease outbreak in Singapore by reverse transcription-PCR with universal enterovirus and EV71-specific primers. *J Clin Microbiol* 2002; **40**: 2823-2827

10 **Brown BA**, Pallansch MA. Complete nucleotide sequence of enterovirus 71 is distinct from poliovirus. *Virus Res* 1995; **39**: 195-205

11 **Toyoda H**, Nicklin MJ, Murray MG, Anderson CW, Dunn JJ, Studier FW, Wimmer E. A second virus-encoded proteinase involved in proteolytic processing of poliovirus polyprotein. *Cell* 1986; **45**: 761-770

12 **Ypma-Wong MF,** Dewalt PG, Johnson VH, Lamb JG, Semler BL. Protein 3CD is the major poliovirus proteinase responsible for cleavage of the P1 capsid precursor. *Virology* 1988; **166**: 265-270

13 **Putnak JR**, Phillips BA. Picornaviral structure and assembly. *Microbiol Rev* 1981; **45**: 287-315

14 **Hummeler K**, Anderson TF, Brown RA. Identification of poliovirus particles of different antigenicity by specific agglutination as seen in the electron microscope. *Virology* 1962; **16**: 84-90

15 **Casal JI**. Use of parvovirus-like particles for vaccination and induction of multiple immune responses. *Biotechnol Appl Biochem* 1999; **29** ( Pt 2): 141-150

16 **Lenz P**, Day PM, Pang YY, Frye SA, Jensen PN, Lowy DR, Schiller JT. Papillomavirus-like particles induce acute activation of dendritic cells. *J Immunol*. 2001; **166**: 5346-5355

17 **Roy P**. Genetically engineered particulate virus-like structures and their use as vaccine delivery systems. *Intervirology* 1996; **39**: 62-71

18 **Gilbert SC**. Virus-like particles as vaccine adjuvants. *Mol Biotechnol* 2001; **19**: 169-177

19 **Schiller JT**, Lowy DR. Papillomavirus-like particle based vaccines: cervical cancer and beyond. *Expert Opin Biol Ther* 2001; **1**: 571-581

20 **Luo L**, Li Y, Cannon PM, Kim S, Kang CY. Chimeric gag-V3 virus-like particles of human immunodeficiency virus induce virus-neutralizing antibodies. *Proc Natl Acad Sci U S A* 1992; **89**: 10527-10531

21 **Ho Y**, Lin PH, Liu CY, Lee SP, Chao YC. Assembly of human severe acute respiratory syndrome coronavirus-like particles. *Biochem Biophys Res Commun* 2004; **318**: 833-838

22 **Wang KC**, Wu JC, Chung YC, Ho YC, Chang MD, Hu YC. Baculovirus as a highly efficient gene delivery vector for the expression of hepatitis delta virus antigens in mammalian cells. *Biotechnol Bioeng* 2005; **89**: 464-473

23 **Ansardi DC**, Porter DC, Morrow CD. Coinfection with recombinant vaccinia viruses expressing poliovirus P1 and P3 proteins results in polyprotein processing and formation of empty capsid structures. *J Virol* 1991; **65**: 2088-2092

24 **Brautigam S**, Snezhkov E, Bishop DH. Formation of poliovirus-like particles by recombinant baculoviruses expressing the individual VP0, VP3, and VP1 proteins by comparison to particles derived from the expressed poliovirus polyprotein. *Virology* 1993; **192**: 512-524

25 **Urakawa T**, Ferguson M, Minor PD, Cooper J, Sullivan M, Almond JW, Bishop DH. Synthesis of immunogenic, but non-infectious, poliovirus particles in insect cells by a baculovirus expression vector. *J Gen Virol* 1989; **70 ( Pt 6)**: 1453-1463

26 **Hu YC**, Hsu JT, Huang JH, Ho MS, Ho YC. Formation of enterovirus-like particle aggregates by recombinant baculoviruses co-expressing P1 and 3CD in insect cells. *Biotechnol Lett* 2003; **25**: 919-925

27 **Chung YC**, Liu HJ, Hu YC. Facile monitoring of avian reovirus sB expression and purification processes by tagged green fluorescent protein. *Enzyme Microb. Technol*. 2004; **35**: 494-500

28 **Lin YC**, Wu CN, Shih SR, Ho MS. Characterization of a Vero cell-adapted virulent strain of enterovirus 71 suitable for use as a vaccine candidate. *Vaccine* 2002; **20**: 2485-2493

29 **Hu YC**, Tsai CT, Chung YC, Lu JT, Hsu JTA. Generation of chimeric baculovirus with histidine-tags displayed on the envelope and its purification using immobilized metal affinity chromatography. *Enzyme Microb Technol* 2003; **33**: 445-452

30 **Hu YC**, Liu HJ, Chung YC. High level expression of the key antigenic protein, sC, from avian reovirus into insect cells and its purification by immobilized metal affinity chromatography. *Biotechnol Lett* 2002; **24**: 1017-1022

31 **Hu YC**, Bentley WE. Effect of MOI ratio on the composition and yield of chimeric infectious bursal disease virus-like particles by baculovirus co-infection: deterministic predictions and experimental results. *Biotechnol Bioeng* 2001; **75**: 104-119

32 **Arbustini E**, Grasso M, Porcu E, Bellini O, Diegoli M, Fasani

R, Banchieri N, Pilotto A, Morbini P, Dal Bello B, Campana C, Gavazzi A, Vigano M. Enteroviral RNA and virus-like particles in the skeletal muscle of patients with idiopathic dilated cardiomyopathy. *Am J Cardiol* 1997; **80**: 1188-1193

33 **Monaghan P**, Cook H, Jackson T, Ryan M, Wileman T. The ultrastructure of the developing replication site in foot-and-mouth disease virus-infected BHK-38 cells. *J Gen Virol* 2004; **85**: 933-946

34 **Arnold E**, Luo M, Vriend G, Rossmann MG, Palmenberg AC, Parks GD, Nicklin MJ, Wimmer E. Implications of the picornavirus capsid structure for polyprotein processing. *Proc Natl Acad Sci U S A* 1987; **84**: 21-25

35 **Mateu MG**. Antibody recognition of picornaviruses and escape from neutralization: a structural view. *Virus Res* 1995; **38**: 1-24

36 **Minor PD**, Ferguson M, Evans DM, Almond JW, Icenogle JP. Antigenic structure of polioviruses of serotypes 1, 2 and 3. *J Gen Virol* 1986; **67** ( Pt 7): 1283-1291

37 **Breitburd F**, Kirnbauer R, Hubbert NL, Nonnenmacher B, Trin-Dinh-Desmarquet C, Orth G, Schiller JT, Lowy DR. Immunization with viruslike particles from cottontail rabbit papillomavirus (CRPV) can protect against experimental CRPV infection. *J Virol* 1995; **69**: 3959-3963

38 **Suzich JA**, Ghim SJ, Palmer-Hill FJ, White WI, Tamura JK, Bell JA, Newsome JA, Jenson AB, Schlegel R. Systemic immunization with papillomavirus L1 protein completely prevents the development of viral mucosal papillomas. *Proc Natl Acad Sci U S A* 1995; **92**: 11553-11557

39 **Yao Q**, Bu Z, Vzorov A, Yang C, Compans RW. Virus-like particle and DNA-based candidate AIDS vaccines. *Vaccine* 2003; **21**: 638-643

40 **Garcea RL**, Gissmann L. Virus-like particles as vaccines and vessels for the delivery of small molecules. *Curr Opin Biotechnol* 2004; **15**: 513-517

41 **Tacket CO**, Sztein MB, Losonsky GA, Wasserman SS, Estes MK. Humoral, mucosal, and cellular immune responses to oral Norwalk virus-like particles in volunteers. *Clin Immunol* 2003; **108**: 241-247

42 **Koutsky LA,** Ault KA, Wheeler CM, Brown DR, Barr E, Alvarez FB, Chiacchierini LM, Jansen KU. A controlled trial of a human papillomavirus type 16 vaccine. *N Engl J Med* 2002; **347**: 1645-1651

43 **Wu CN**, Lin YC, Fann C, Liao NS, Shih SR, Ho MS. Protection against lethal enterovirus 71 infection in newborn mice by passive immunization with subunit VP1 vaccines and inactivated virus. *Vaccine* 2001; **20**: 895-904

44 **Rombaut B**, Vrijsen R, Boeye A. New evidence for the precursor role of 14S subunits in poliovirus morphogenesis. *Virology* 1990; **177**: 411-414

45 **Rombaut B**, Andries K, Boeye A. A comparison of WIN 51711 and R 78206 as stabilizers of poliovirus virions and procapsids. *J Gen Virol* 1991; **72** ( Pt 9): 2153-2157

46 **Rombaut B,** Foriers A, Boeye A. In vitro assembly of poliovirus 14 S subunits: identification of the assembly promoting activity of infected cell extracts. *Virology* 1991; **180:** 781-787

**S- Editor** Kumar M and Guo SY **L- Editor** Elsevier HK **E- Editor** Kong LH

PO Box 2345, Beijing 100023, China
www.wjgnet.com
wjg@wjgnet.com

*World J Gastroenterol* 2006 February 14; 12(6): 928-934
***World Journal of Gastroenterology*** ISSN 1007-9327
© 2006 The WJG Press. All rights reserved.

*CLINICAL RESEARCH*

# Cyclooxygenase-2 and epithelial growth factor receptor up-regulation during progression of Barrett's esophagus to adenocarcinoma

Yan Li, John M Wo, Mukunda B Ray, Whitney Jones, Ruifeng R Su, Susan Ellis, Robert C G Martin

Yan Li, Ruifeng R Su, Susan Ellis, Robert C G Martin, Division of Surgical Oncology, University of Louisville School of Medicine, Louisville, KY 40202, United States
John M Wo, Whitney Jones, Division of Gastroenterology/ Hepatology, University of Louisville School of Medicine, Louisville, KY 40202, United States
Mukunda B Ray, Department of Anatomical Pathology, University of Louisville School of Medicine, Louisville, KY 40202, United States
Supported by the University of Louisville Hospital and the Society for Surgery of the Alimentary Tract Career Development Award
Correspondence to: Robert C G Martin, MD, Department of Surgery, Division of Surgical Oncology, J. Graham Brown Cancer Center, University of Louisville School of Medicine, 315 E. Broadway - #312, Louisville, KY 40202
United States. robert.martin@louisville.edu
Telephone: +502-629-3355 Fax: +502-629-3030
Received: 2005-05-08 Accepted: 2005-07-05

## Abstract

**AIM:** To investigate the expression of cyclooxygenase-2 (COX-2) and epithelial growth factor receptor (EGFR) throughout the progression of Barrett's esophagus (BE).

**METHODS:** COX-2 and EGFR protein expressions were detected by using immunohistochemical method. A detailed cytomorphological changes were determined. Areas of COX-2 and EGFR expression were quantified by using computer Imaging System.

**RESULTS:** The expressions of both COX-2 and EGFR increased along with the progression from BE to esophagus adenocarcinoma (EAC). A positive correlation was found between COX-2 expression and EGFR expression.

**CONCLUSION:** COX-2 and EGFR may be cooperative in the stepwise progression from BE to EAC, thereby leading to carcinogenesis.

© 2006 The WJG Press. All rights reserved.

**Key words:** Cycloxygenase -2 (COX-2); Epithelial growth factor receptor (EGFR); Barrett's esophagus; Carcinogenesis

Li Y, Wo JM, Ray MB, Jones W, Su RR, Ellis S, Martin RCG. Cyclooxygenase-2 and epithelial growth factor receptor up-regulation during progression of Barrett's esophagus to adenocarcinoma. *World J Gastroenterol* 2006; 12(6): 928-934

http://www.wjgnet.com/1007-9327/12/928.asp

## INTRODUCTION

Esophageal adenocarcinoma (EAC) is one of the most rapidly increasing cancers over the past two decades in Caucasian males in the United States[1,2]. After being diagnosed with adenocarcinoma, patients have only a 13-15% 5-year survival rate[3]. Most of the EAC are developed from Barrett's esophagus (BE), a pre-malignant disease characterized by replacement of the normal esophageal squamous epithelium with a specialized intestinal metaplasia (SIM)[4]. The risk of EAC in BE patients has been estimated to be about 30 -125 times higher than the general population[2,5].

The mechanisms of the evolution from BE to EAC are largely unknown[6,7]. During the neoplastic transformation, aberrations in the cell cycle lead to uncontrolled cellular replication, a molecular mechanism is believed to be involved in all carcinogenesis[8]. Epidermal growth factor receptor (EGFR) family of receptor tyrosine kinases lies at the head of a complex signal transduction cascade that modulates cell proliferation, differentiation, adhesion and migration[9]. EGFR is a transmembrane receptor composed of an extracellular ligand-binding domain and a cytoplasmic region with enzymatic activity. This structure enables signals to be transmitted across the plasma membrane activating gene expression and inducing cellular responses, such as proliferation and differentiation. Over-expression of EGFR has been shown to occur in various malignancies, including esophageal adenocarcinoma[10].

Another important enzyme involved in tumor growth is cycloxygenase-2 (COX-2)[11]. There are two isoforms of COX enzyme. COX-1 is constitutively expressed in most tissues; however, COX-2 has a markedly different expression pattern. Normally, COX-2 is undetectable in most tissues, but can be expressed at high levels after induction with a variety of substances, including inflammatory mediators and mitogens[12-14]. Epidemiological studies have shown that intake of aspirin, a nonsteroidal anti-inflammatory drug (NSAID) known as COX enzymes blocker, is associated with an up to 90% decreased risk of developing esophageal

cancer[15,16]. Experimental studies also have indicated that over-expression of COX-2 is associated with decreased apoptosis and cell-cell adhesion, and with increased proliferation and differentiation[17,18].

Recently, experimental investigations have suggested a close relationship between COX-2 and EGFR. Expression of EGFR was markedly increased in the COX-2-transfected cells , and inhibition of COX-2 could suppress the induction of EGFR in these cells[19]. It has also been demonstrated that activation of EGFR can induce COX-2 expression and prostaglandin production[20]. Furthermore, a combination of an EGFR inhibitor with a nonselective COX-1/COX-2 inhibitor was shown to prevent the development of intestinal cancer in nude mice[21]. Taken together, these data link COX and EGFR, and provide a theoretical basis whereby the COX-2 and EGFR signaling pathway may have additive effects of tumor growth. Some studies on expression of COX-2[18] and EGFR[22] in the human Barrett's esophagus specimens have been reported. However, to our knowledge, a detailed morphologic description of the esophageal epithelium expressing both COX-2 and EGFR in the BE metaplasia to dysplasia to adenocarcinoma sequence has not yet been performed.

In the present study, we therefore investigated the expressions of both COX-2 and EGFR in biopsy tissues from different histologic stages of BE by using immunohistochemical assay, and addressed the morphological features of Barrett's epithelium with over-expressed protein levels of COX-2 and EGFR in the histologic stages of metaplasia and dysplasia. Furthermore, we set forth to determine the correlation between COX-2 and EGFR in progression from the metaplasia to dysplasia to adenocarcinoma sequence.

## MATERIALS AND METHODS

### Case selection and review

The study samples were collected retrospectively from 104 patients who had undergone esophageal biopsy between 1996 and 2004. All of these patients were recruited from the Barrett's Esophagus registry at the University of Louisville with established diagnoses of SIM, indefinite/low-grade dysplasia (I/LGD), high-grade dysplasia (HGD), and EAC. No preoperative radio- or chemotherapy had been performed. None of the patients had received NSAIDs therapy. A microscope examination confirmed the diagnoses of SIM, LGD, HGD and EAC on these esophageal tissues reviewed by two pathologists independently, blinded to the subject's clinical history. Alcian-blue staining was used to identify any presence of SIM. Hematoxylin-eosin staining was used to identify any presence of dysplasia and EAC. A control group consisted of 30 subjects with nondetectable Barrett's (NB), defined by endoscopic findings of columnar-lined esophagus (CLE), but no pathologic evidence of SIM despite alcian-blue staining on all of the four-quadrant biopsies. This study was approved by the Institutional Review Board for Human Study at the University of Louisville.

### Immunohistochemica assay for COX-2 and EGFR

COX-2 and EGFR protein expressions were determined by using an immunohistochemical assay. Staining was carried out on the paraffin-embedded tissues using the DAKO EnVision™+System Kit (DAKO Corporation, Carpinteria, CA) according to the manufacturer's instructions. In brief, the sections were deparaffinized and hydrated. The slides were washed with TRIS-buffer, and peroxidase blocking was performed for 5 min. After rewashing, the slides were incubated separately with the monoclonal mouse COX-2 antibody (1:200) or EGFR antibody (1:200) (SantaCruz Biotechnology Inc, CA) for 30 min at room temperature. The chromogenic substrate diaminobenzidine was added as a visualization reagent. Finally, the slides were counterstained with haematoxylin. A negative control was included in each run.

### Cytomorphology associated with localization of COX-2 and EGFR

Microscopic evaluation of the morphological features of epithelium was performed at high-power fields (X 400 magnification) on the COX-2 and EGFR staining sections. Two cytomorphological features were chosen as the criteria of assessment based on observed morphological differences among SIM, I/LGD, HGD and EAC along with NB columnar epithelium: (1) ordering of nuclei; and (2) the presence of basally located nuclei with an apical cytoplasmic layer. We considered the normal cell phenotype (NCP) when the epithelial cells were arranged in a single layer with their long axes orientated towards the center of the lumen, and had a basally located nucleus with a thick apical layer of cytoplasm, whereas the abnormal cell phenotype (ACP) included multiple cell layers, displayed and enlarged nucleus and less cytoplasm. Every slide was examined throughout to identify the NCP cell and ACP cell with COX-2 staining and EGFR staining. Then, the COX-2-stained and the EGFR-stained epithelial cells were categorized to NCP cells and ACP cells. The other cells were ignored during the evaluation.

### Computer image analysis

A computer image analysis was performed to quantify the expressions of COX-2 and EGFR in totally 104 subjects diagnosed with SIM, I/LGD, HGD and EAC, and in 30 controls. The imaging fields were chosen randomly from various section levels to ensure objectivity of sampling. Five imaging fields were scanned for each specimen sample. All digital images were acquired with the microscope at 40x magnification using the Spot camera via the MetaMorph® Imaging System (Universal Imaging Corporation., Downingtown, PA) and stored as JPG data files (the resolutions were fixed as 200 pixels/inch). The acquired color images from the immunohistochemical staining were defined a standard threshold according to the software specification. The computer program then quantified the threshold area represented by color images. COX-2 and EGFR protein expressions were defined by the percentages of threshold area in acquired color images.

### Statistical analysis

Spearman rank correlation coefficient (R) was used to analyze the correlation between COX-2 and EGFR expressions with the various histologic stages of Barrett's

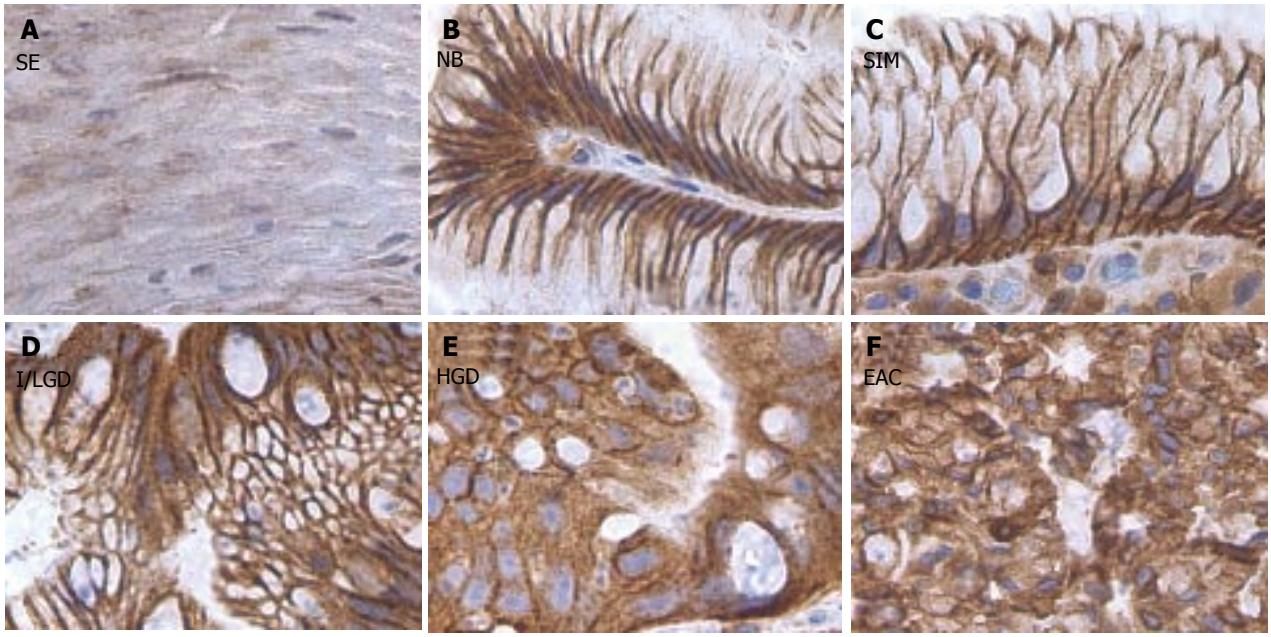


**Figure 1** COX-2 staining in the sections from different stages of BE along with the sections from normal squamous and CLE nondetectable BE. **A:** Squamous epithelium (SE); **B:** Nondetectable BE in CLE (NB); **C:** Specialized intestinal metaplasia (SIM); **D:** Indeterminate/low-grade dysplasia (I/LGD); **E:** high-grade dysplasia (HGD); **F:** Esophageal adenocarcinoma (EAC). Strong COX-2 staining was detected in both NCP cells and ACP cells in the histological stages of SIM, I/LGD, HGD and EAC. A weak COX-2 staining was observed in the normal squamous epithelium.

**Table 1 Demographics of 104 study subjects with Barrett's esophagus and 30 control subjects**

| | NB | SIM | I/LDG | HDG | EAC |
|---|---|---|---|---|---|
| Subjects | 30 | 37 | 36 | 16 | 15 |
| Gender (male:female) | 28:2 | 34:3 | 30:6 | 14:2 | 14:1 |
| Mean age (yr ) | 60 | 55 | 61 | 68 | 66 |
| Short-segment CLE | 27 | 21 | 7 | 1 | 0 |
| Long-segment CLE | 3 | 16 | 29 | 15 | 15 |

SIM: Specialized intestinal metaplasia; I/LGD: Indeterminate/low-grade dysplasia; HGD: High-grade dysplasia; EAC: Esophageal adenocarcinoma; NB: Nondetectable Barrett's; CLE: Columnar-lined esophagus.

esophagus. Multiple analysis of variance (MANOVA) was used to determine the differences between COX-2 and EGFR expressions, if any, between the different histologic stages of carcinogenesis. $P$ values less than 0.05 were considered statistically significant.

## RESULTS

One hundred and four subjects (92 males, 12 females) with Barrett's esophagus were enrolled in this study. The study population consisted of 37 subjects with a diagnosis of SIM without dysplasia, 36 with I/LGD, 16 with HGD, and 15 with EAC. The control group consisted of 30 NB subjects. Patients identified as having no Barrett's were mostly those with a short segment of CLE whereas those identified with SIM, I/LDG, HDG or EAC were mostly found to have a long segment of CLE (Table 1).

### *Cytomorphological features associated with localization of COX-2 and EGFR*

A very strong COX-2 staining in all Barrett's epithelium compared to a weak staining in normal squamous epithelium and CLE without Barrett's epithelium was observed. In particular, in the regions with COX-2-positive staining, the epithelial cells presented cytomorphological features of both NCP cells and ACP cells in the histological stages of SIM, I/LGD, HGD and EAC (Figure 1). A positive EGFR staining was presented in all Barrett's epithelium, but not as strong as that seen in the COX-2 staining. In contrast to COX-2 staining, the regions of positive EGFR expression exhibited ACP cells while those regions with weak or no EGFR staining exhibited NCP cells (Figure 2).

### *Expression of COX-2 in the metaplasia to dysplasia to adenocarcinoma sequence*

We observed significant increases in COX-2 expression in specimens with SIM (7.8±0.8), I/LGD (10.0±0.9), HGD (14.2±1.8) and EAC (16.0±2.2) as compared with the control specimens (6.9±1) ($P<0.05$). Furthermore, COX-2 expression appeared to increase with the histological severity of BE; there was a significant positive correlation between COX-2 expression and histopathologic changes from I/LGD to EAC ($r=0.97$, $P<0.001$) (Figure 3).

### *Expression of EGFR in the metaplasia–dysplasia–adenocarcinoma sequence*

We found significant increases in EGFR expression in specimens with SIM (2.1±0.5), I/LGD (2.7±0.6), HGD (3.9±0.7) and EAC (5.2±0.9) as compared with the control specimens (0.8±0.4) ($P<0.05$). Furthermore, EGFR expression appeared to increase with the histological severity of BE; there was a significant positive

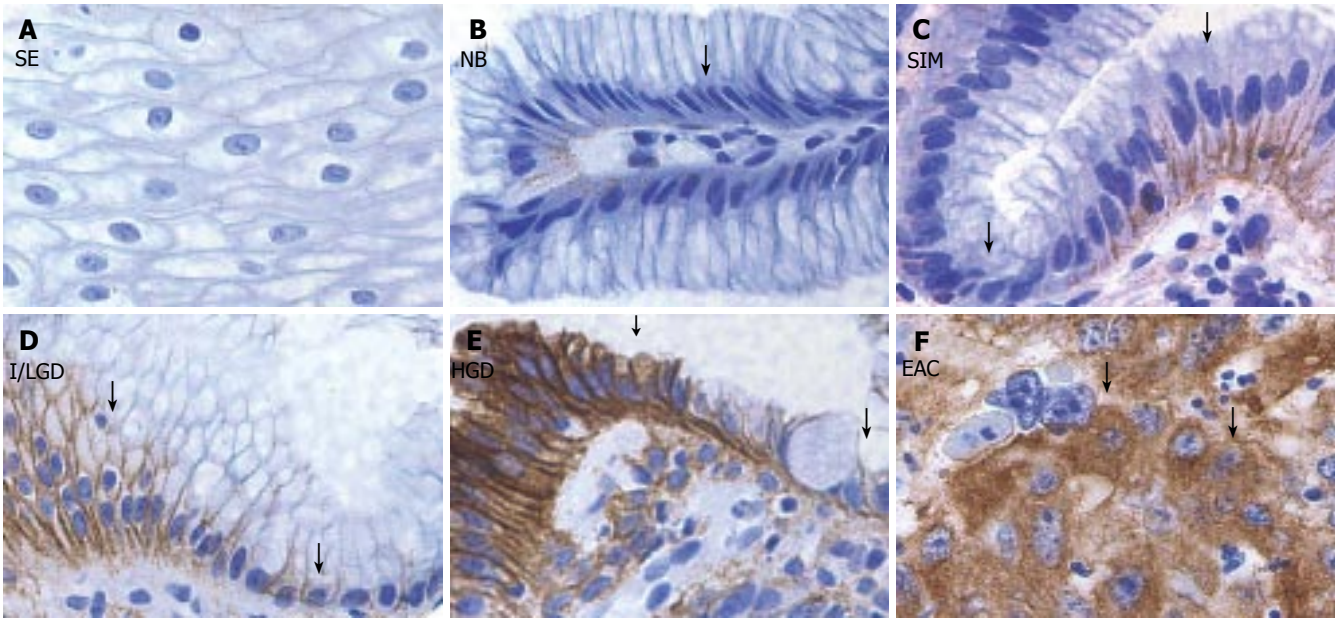


**Figure 2** EGFR staining in the sections from different stages of BE along with the sections from normal squamous and CLE nondetectable BE. **A:** Squamous epithelium (SE); **B:** Nondetectable BE in CLE (NB); **C:** Specialized intestinal metaplasia (SIM); **D:** Indeterminate/low-grade dysplasia (I/LGD); **E:** high-grade dysplasia (HGD); **F:** Esophageal adenocarcinoma (EAC). Strong EGFR staining was detected in ACP cells (arrowhead) in the histological stages of SIM, I/LGD, HGD and EAC. A weak EGFR staining was found in NCP cells (arrow) and in the normal squamous epithelium.

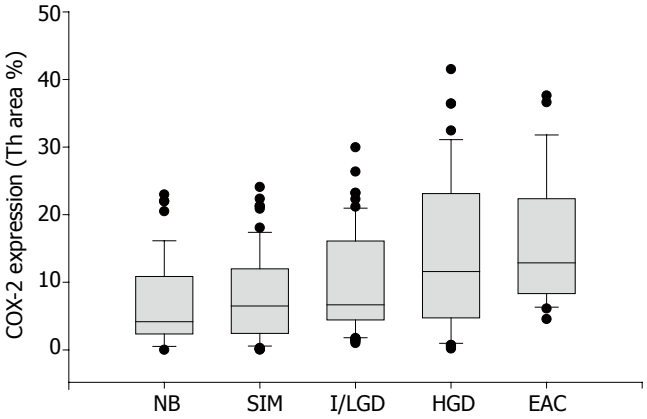


**Figure 3** COX-2 expression and pathological severity of BE. COX-2 expression is plotted against the 4 stages of Barrett's esophagus. The line enclosed within the box represents the median value; the small circles indicate outlying data points. COX-2 expression in specimens with SIM, I/LGD, HGD and EAC was significantly increased in comparison with that in NB ($P<0.01$). A significant positive correlation between COX-2 expression and histopathologic changes from SIM to EAC was observed ($r=0.97$, $P<0.001$).

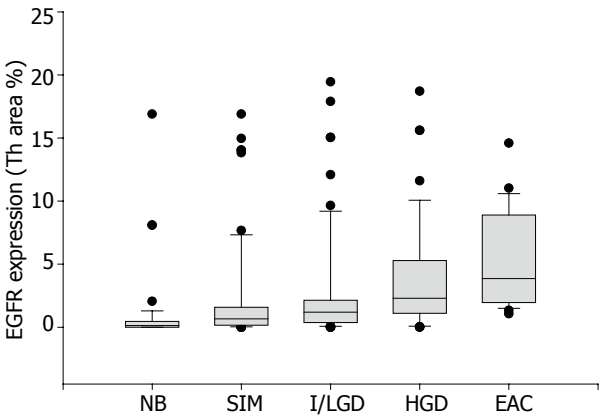


**Figure 4** EGFR expression and pathological severity of BE. EGFR expression is plotted against the 4 stages of Barrett's esophagus. The line enclosed within the box represents the median value; the small circles indicate outlying data points. EGFR expression in specimens with SIM, I/LGD, HGD and EAC was significantly increased in comparison with that in NB ($P<0.01$). A significant positive correlation between EGFR expression and histopathologic changes from SIM to EAC was found($r=0.97$, $P<0.001$).

correlation between EGFR expression and histopathologic changes from I/LGD to EAC ($r=0.97$, $P<0.001$) (Figure 4).

### *Correlation between COX-2 and EGFR in metaplasia–dysplasia–adenocarcinoma sequence*

The data from computer quantification of COX-2 expression and EGFR expression in all immunohistochemically stained sections were used to determine the correlation between COX-2 and EGFR in the metaplasia-dysplasia- adenocarcinoma sequence. A significant positive correlation between COX-2 expression and EGFR expression was determined in the BE tissues ($r=0.94$, $P<0.001$) (Figure 5).

## DISCUSSION

Our results showed a detailed information on localization of COX-2 and EGFR protein within the metaplastic cells, dysplastic cells and cancer cells. We demonstrated a significant increase in both COX-2 and EGFR expressions in the metaplasia-dysplasia-adenocarcinoma sequence. In particular, weak COX-2 and EGFR stainings were found in the normal squamous epithelium and NB epithelium, while strong COX-2 and EGFR stainings were found in the region with histological changes of metaplasia, dysplasia and EAC. To our best of knowledge, this is the first study to examine the relationship between COX-2 and EGFR in respect to the histologic progression from BE

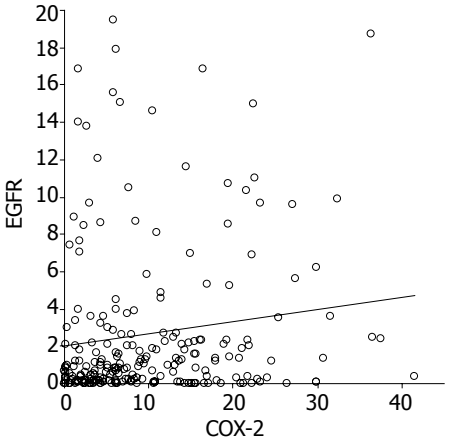


**Figure 5** Relationship between COX-2 expression and EGFR expression in 104 patients. A significant positive correlation between COX-2 expression and EGFR expression was found ($r = 0.94$, $P < 0.001$).

to EAC. Since both COX-2 and EGFR expression levels increase dramatically in BE, each of these changes could enhance the tumorigenic potential of BE[10,11,18,22].

This study focused on the morphological features of Barrett's epithelium with the expression of COX-2 and EGFR for the following reasons. First, evaluation from BE to EAC is primarily based on the cytomorphological characteristics[1,7,23,24]. Neoplasia develops in a series of steps through the development of a morphologically changed cell population. It is widely accepted that COX-2 and EGFR play important roles during carcinogenesis, and the over-expression of COX-2 and EGFR would be expected to predispose the epithelium to tumorigenic morphological change. Second, up-regulations of COX-2 and EGFR have been reported in BE and EAC, but no evidence has been provided for the joint signaling of COX-2 and EGFR in the induction of Barrett's epithelium to adenocarcinoma transition. This induction remains an integral process occurring during critical phase of tumor progression. Third, although COX-2 and EGFR play different biological roles in tumor formation, targeting both COX-2 and EGFR to abrogate both pathways and their downstream targets achieved significant antitumor and antiangiogenic effects in the *in vivo* and *in vitro* studies[21,25]. Therefore, the two proteins might be cooperatively carcinogenic, which intensify the transformation effects on Barrett's metaplasia to dysplasia to adenocarcinoma sequence.

The exact function of COX-2 in tumor development and progression *in vivo* is not known as yet. One possibility follows that over-expression of COX-2 leads to high levels of prostaglandins synthesis in the tissues. Prostaglandins produced by COX-2 may subsequently facilitate tumor progression by acting as growth factors, differentiation factors, immunosuppressors and angiogenic agents[26,27]. Other possibilities from recent studies indicate that reactive oxygen species (ROS) are generated during the conversion from prostaglandins G2 to prostaglandins H2[28,29], this enhanced level of ROS parallels the levels of COX-2 mRNA. The COX-2-derived oxidative DNA damage may contribute to the accumulation of genetic damage, and the accumulation of genetic and epigenetic aberrations produces one or more clones with tumorigenic potential. In addition, the COX-2 enzyme itself may promote tumor development and progression by a prostaglandins-independent pathway. This is supported by the evidences that NSAIDs suppressed proliferative activity and inhibited the growth in colon cancer cells without repressing prostaglandins synthesis[30]. Over-expression of COX-2 can also up-regulate anti-apoptotic oncoprotein such as BCL-2 and multiple proliferation-promoting cyclins and cyclin-dependent kinases, and down-regulate some tumor suppressor proteins[17,31]. The postulation for the involvement of COX-2 over-expression related to the progression in metaplasia to dysplasia to adenocarcinoma sequence is based on extensive studies of the relationship between COX-2 and tumor development and progression in multiple organ system.

Our data demonstrated a strong immunoreactivity for COX-2 protein within metaplastic cells, dysplastic, and malignant cells when compared to normal squamous cells and NB columnar cells. The cytomorphological features of COX-2 distribution in all epithelium may reflect two aspects of the effect of COX in contribution to the development of tumor. COX-2 is an important factor to maintain the microenvironment for tumor growth, and COX-2 may not be the critical factor in contribution to the phenotype changes of pre-malignant cells. COX-2 is undetectable in most tissues in the physiological condition[13,14]; the animals lacking COX-2 and prostaglandins synthesis show no innate gastrointestinal pathology[32]. These features of COX-2 do not confirm COX-2 expression as a central event in carcinogenesis. On the other hand, it is also possible that duodenal-gastro reflux and/or rapid growth and invasion of cancer cells in BE would stimulate local inflammation to inflammatory mediators and mitogens[12,13], which, in turn, would induce COX-2 synthesis. Nevertheless, the high level of COX-2 synthesis would prolong the survival of these abnormal cells and increase the chance for tumorigenesis.

EGFR signaling module plays a fundamental role in the morphogenesis of a diverse spectrum of organisms, and has been highly conserved through the course of evolution. In humans, the EGFR family, which consists of the EGFR itself and the receptors known as HER 2-4, and more than 30 ligands lie at the head of a complex, multilayered signal-transduction network[33]. The aberrant activity of the members in this family has been shown to play a key role in the development and growth of tumor cells[9]. The EGFR family is over-expressed in various types of human neoplasms, such as esophagus, thyroid, breast, testis, bladder, melanoma, pancreas, colon, cervical carcinomas, renal carcinoma, prostate and liver cancer[10]. The underlying mechanism for EGFR involvement in carcinogenesis is likely to reduce the requirement for exogenously supplied growth factors to maintain tumorigenic cells proliferation. Over-expression of EGFR can hypersensitize the cells to low concentration of growth factors to maintain their viability, and to facilitate their phenotype transformation mediated by these growth factors[34,35]. The aberrant activity of the EGFR might regulate the expression of specific oncogenes or tumor suppressor genes involved in the intracellular signal transduction pathway to synthesize endogenously produced growth factors[36]. Several stud-

ies have also supported the notion that the endogenous growth factors might function via an intracrine, juxtacrine, autocrine or paracrine mechanisms to control cell proliferation[34-36].

The results obtained from this study for EGFR staining showed a significant effect of EGFR in contribution to the cytomorphological changes. A large amount of EGFR protein was expressed in the epithelial cells displaying multiple cell layers, enlarged nucleus and less cytoplasm in SIM, I/LGD, HGD and EAC. This over-expression was consistent across the BE progression, thereby indicating an important role of EGFR in the initiation of Barrett's cells transition to adenocarcinoma. The phenotypic effects of abnormal function of EGFR protein are far more dramatic. Recent studies have indicated that animals lacking EGFR have abnormal eyes and epidermal tissues and die due to defects in the development of epithelial organ[37,38]. Therefore, EGFR may play a key role in the morphogenesis of metaplasia, dysplasia and adenocarcinoma. In our study, the immunoreactivity of EGFR was observed in the same increasing trend with the metaplasia to dysplasia to adenocarcinoma sequence as that seen in COX-2 immunoreactivity, thus suggesting a cooperative effect of these two proteins.

In summary, our study demonstrates a positive relationship between expression of COX-2 and EGFR in the progression from metaplasia to dysplasia to adenocarcinoma in subjects with BE. This suggests that both COX-2 and EGFR may increase the likelihood of Barrett's cells to undergo abnormal cell cycling or gene expression. Further studies are needed to correlate the COX-2 and EGFR expression pattern with clinical outcome. Animal models and tissue culture are also required to determine the exact mechanism of COX-2 and EGFR action in the metaplasia to dysplasia to adenocarcinoma sequence.

## REFERENCES


1 **Blot WJ,** Devesa SS, Kneller RW, Fraumeni JF Jr. Rising incidence of adenocarcinoma of the esophagus and gastric cardia. *JAMA* 1991; **265:** 1287-1289

2 **Pera M,** Cameron AJ, Trastek VF, Carpenter HA, Zinsmeister AR. Increasing incidence of adenocarcinoma of the esophagus and esophagogastric junction. *Gastroenterology* 1993; **104:** 510-513

3 **Farrow DC,** Vaughan TL. Determinants of survival following the diagnosis of esophageal adenocarcinoma (United States). *Cancer Causes Control* 1996; **7**: 322-327

4 **Isolauri J,** Luostarinen M, Isolauri E, Reinikainen P, Viljakka M, Keyrilainen O. Natural course of gastroesophageal reflux disease: 17-22 year follow-up of 60 patients. *Am J Gastroenterol* 1997; **92:** 37-41

5 **Altorki NK,** Oliveria S, Schrump DS. Epidemiology and molecular biology of Barrett's adenocarcinoma. *Semin Surg Oncol* 1997; **13**: 270-280

6 **Geboes K.** Barrett's esophagus: the metaplasia-dysplasia-carcinoma sequence: morphological aspects. *Acta Gastroenterol Belg* 2000; **63**: 13-17

7 **Jankowski JA,** Wright NA, Meltzer SJ, Triadafilopoulos G, Geboes K, Casson AG, Kerr D, Young LS. Molecular evolution of the metaplasia-dysplasia-adenocarcinoma sequence in the esophagus. *Am J Pathol* 1999; **154:** 965-973

8 **Hanahan D**, Weinberg RA. The hallmarks of cancer. *Cell* 2000; **100**: 57-70

9 **Yarden Y**. The EGFR family and its ligands in human cancer. signalling mechanisms and therapeutic opportunities. *Eur J Cancer* 2001; **37** Suppl 4: S3-S8

10 **Salomon DS,** Brandt R, Ciardiello F, Normanno N. Epidermal growth factor-related peptides and their receptors in human malignancies. *Crit Rev Oncol Hematol* 1995; **19:** 183-232

11 **Gately S**, Li WW. Multiple roles of COX-2 in tumor angiogenesis: a target for antiangiogenic therapy. *Semin Oncol* 2004; **31**: 2-11

12 **Evett GE,** Xie W, Chipman JG, Robertson DL, Simmons DL. Prostaglandin G/H synthase isoenzyme 2 expression in fibroblasts: regulation by dexamethasone, mitogens, and oncogenes. *Arch Biochem Biophys* 1993; **306:** 169-177

13 **Lee SH,** Soyoola E, Chanmugam P, Hart S, Sun W, Zhong H, Liou S, Simmons D, Hwang D. Selective expression of mitogen-inducible cyclooxygenase in macrophages stimulated with lipopolysaccharide. *J Biol Chem* 1992; **267:** 25934-25938

14 **Masferrer JL,** Zweifel BS, Manning PT, Hauser SD, Leahy KM, Smith WG, Isakson PC, Seibert K. Selective inhibition of inducible cyclooxygenase 2 in vivo is antiinflammatory and nonulcerogenic. P*roc Natl Acad Sci U S A*. 1994; **91**: 3228-3232

15 **Funkhouser EM,** Sharp GB. Aspirin and reduced risk of esophageal carcinoma. *Cancer* 1995; **76**: 1116-1119

16 **Thun MJ,** Namboodiri MM, Calle EE, Flanders WD, Heath CW Jr. Aspirin use and risk of fatal cancer. *Cancer Res* 1993; **53**: 1322-1327

17 **Tsujii M**, DuBois RN. Alterations in cellular adhesion and apoptosis in epithelial cells overexpressing prostaglandin endoperoxide synthase 2. *Cell* 1995; **83**: 493-501

18 **Zimmermann KC**, Sarbia M, Weber AA, Borchard F, Gabbert HE, Schror K. Cyclooxygenase-2 expression in human esophageal carcinoma. *Cancer Res* 1999; **59**:198-204

19 **Yoshimoto T,** Takahashi Y, Kinoshita T, Sakashita T, Inoue H, Tanabe T. Growth stimulation and epidermal growth factor receptor induction in cyclooxygenase-overexpressing human colon carcinoma cells. *Adv Exp Med Biol* 2002; **507**: 403-407

20 **Ranelletti FO,** Almadori G, Rocca B, Ferrandina G, Ciabattoni G, Habib A, Galli J, Maggiano N, Gessi M, Lauriola L. Prognostic significance of cyclooxygenase-2 in laryngeal squamous cell carcinoma. *Int J Cancer* 2001; **95:** 343-349

21 **Tortora G,** Caputo R, Damiano V, Melisi D, Bianco R, Fontanini G, Veneziani BM, De Placido S, Bianco AR, Ciardiello F. Combination of a selective cyclooxygenase-2 inhibitor with epidermal growth factor receptor tyrosine kinase inhibitor ZD1839 and protein kinase A antisense causes cooperative antitumor and antiangiogenic effect. *Clin Cancer Res* 2003; **9:** 1566-1572

22 **Jankowski J,** Hopwood D, Pringle R, Wormsley KG. Increased expression of epidermal growth factor receptors in Barrett's esophagus associated with alkaline reflux: a putative model for carcinogenesis. *Am J Gastroenterol* 1993; **88:** 402-408

23 **Reid BJ,** Haggitt RC, Rubin CE, Roth G, Surawicz CM, Van Belle G, Lewin K, Weinstein WM, Antonioli DA, Goldman H. Observer variation in the diagnosis of dysplasia in Barrett's esophagus. *Hum Pathol* 1988; **19:** 166-178

24 **Haggitt RC**. Barrett's esophagus, dysplasia, and adenocarcinoma. *Hum Pathol* 1994; **25**: 982-993

25 **Chen Z,** Zhang X, Li M, Wang Z, Wieand HS, Grandis JR, Shin DM. Simultaneously targeting epidermal growth factor receptor tyrosine kinase and cyclooxygenase-2, an efficient approach to inhibition of squamous cell carcinoma of the head and neck. *Clin Cancer Res* 2004; **10:** 5930-5939

26 **Marnett LJ**. Aspirin and the potential role of prostaglandins in colon cancer. *Cancer Res* 1992; **52**: 5575-5589

27 **Hla T,** Ristimaki A, Appleby S, Barriocanal JG. Cyclooxygenase gene expression in inflammation and angiogenesis. *Ann N Y Acad Sci* 1993; **696:** 197-204

28 **Chung HY,** Kim HJ, Kim JW, Yu BP. The inflammation hypothesis of aging: molecular modulation by calorie restriction. *Ann N Y Acad Sci* 2001; **928:** 327-335

29 **Vane JR**, Bakhle YS, Botting RM. Cyclooxygenases 1 and 2. *Annu Rev Pharmacol Toxicol* 1998; **38**: 97-120

30 **Hanif R,** Pittas A, Feng Y, Koutsos MI, Qiao L, Staiano-Coico L, Shiff SI, Rigas B. Effects of nonsteroidal anti-inflammatory

drugs on proliferation and on induction of apoptosis in colon cancer cells by a prostaglandin-independent pathway. *Biochem Pharmacol* 1996; **52:** 237-245

31 **Goldberg Y,** Nassif II, Pittas A, Tsai LL, Dynlacht BD, Rigas B, Shiff SJ. The anti-proliferative effect of sulindac and sulindac sulfide on HT-29 colon cancer cells: alterations in tumor suppressor and cell cycle-regulatory proteins. *Oncogene* 1996; **12:** 893-901

32 **Morham SG,** Langenbach R, Loftin CD, Tiano HF, Vouloumanos N, Jennette JC, Mahler JF, Kluckman KD, Ledford A, Lee CA, Smithies O. Prostaglandin synthase 2 gene disruption causes severe renal pathology in the mouse. *Cell* 1995; **83:** 473-482

33 **Ullrich A**, Schlessinger J. Signal transduction by receptors with tyrosine kinase activity. *Cell* 1990; **61**: 203-212

34 **Logan A**. Intracrine regulation at the nucleus--a further mechanism of growth factor activity? *J Endocrinol* 1990; **125**: 339-343

35 **Sporn MB,** Roberts AB. Autocrine secretion--10 years later. *Ann Intern Med* 1992; **117**: 408-414

36 **Aaronson SA**. Growth factors and cancer. *Science* 1991; **254**: 1146-1153

37 **Sibilia M**, Wagner EF. Strain-dependent epithelial defects in mice lacking the EGF receptor. *Science* 1995; **269**: 234-238

38 **Threadgill DW,** Dlugosz AA, Hansen LA, Tennenbaum T, Lichti U, Yee D, LaMantia C, Mourton T, Herrup K, Harris RC. Targeted disruption of mouse EGF receptor: effect of genetic background on mutant phenotype. *Science* 1995; **269:** 230-234

**S- Editor** Kumar M and Guo SY **L- Editor** Elsevier HK **E- Editor** Kong LH

PO Box 2345, Beijing 100023, China
www.wjgnet.com
wjg@wjgnet.com

World J Gastroenterol 2006 February 14; 12(6): 935-939
World Journal of Gastroenterology ISSN 1007-9327
© 2006 The WJG Press. All rights reserved.

CLINICAL RESEARCH

# Low central venous pressure reduces blood loss in hepatectomy

Wei-Dong Wang, Li-Jian Liang, Xiong-Qing Huang, Xiao-Yu Yin

Wei-Dong Wang, Department of General Surgery, The First People's Hospital of Shun De, Foshan, 528300, Guangdong Province, China
Li-Jian Liang, Xiao-Yu Yin, Department of Hepatobiliary Surgery, The First Affiliated Hospital, Sun Yat-Sen University, Guangzhou 510080, Guangdong Province, China
Xiong-Qing Huang, Department of Anaesthesia, The First Affiliated Hospital, Sun Yat-Sen University, Guangzhou 510080, Guangdong Province, China
Correspondence to: Li-Jian Liang, Department of Hepatobiliary Surgery, The First Affiliated Hospital, Sun Yat-Sen University, Guangzhou 510080, Guangdong Province, China. lianglj@medmail.com.cn
Telephone: +86-757-22318706 Fax: +86-757-22223899
Received: 2005-05-12 Accepted: 2005-06-6

## Abstract

**AIM:** To investigate the effect of low central venous pressure (LCVP) on blood loss during hepatectomy for hepatocellular carcinoma (HCC).

**METHODS:** By the method of sealed envelope, 50 HCC patients were randomized into LCVP group ($n=25$) and control group ($n=25$). In LCVP group, CVP was maintained at 2-4 mmHg and systolic blood pressure (SBP) above 90 mmHg by manipulation of the patient's posture and administration of drugs during hepatectomy, while in control group hepatectomy was performed routinely without lowering CVP. The patients' preoperative conditions, volume of blood loss during hepatectomy, volume of blood transfusion, length of hospital stay, changes in hepatic and renal functions were compared between the two groups.

**RESULTS:** There were no significant differences in patients' preoperative conditions, maximal tumor dimension, pattern of hepatectomy, duration of vascular occlusion, operation time, weight of resected liver tissues, incidence of post-operative complications, hepatic and renal functions between the two groups. LCVP group had a markedly lower volume of total intraoperative blood loss and blood loss during hepatectomy than the control group, being 903.9±180.8 mL *vs* 2 329.4±2 538.4 ($W=495.5$, $P<0.01$) and 672.4±429.9 mL *vs* 1 662.6±1 932.1 ($W=543.5$, $P<0.01$). There were no remarkable differences in the pre-resection and post-resection blood losses between the two groups. The length of hospital stay was significantly shortened in LCVP group as compared with the control group, being 16.3±6.8 d *vs* 21.5±8.6 d ($W=532.5$, $P<0.05$).

**CONCLUSION:** LCVP is easily achievable in technique. Maintenance of CVP⩽4 mmHg can help reduce blood loss during hepatectomy, shorten the length of hospital stay, and has no detrimental effects on hepatic or renal function.

© 2006 The WJG Press. All rights reserved.

**Key words:** Hepatectomy; Hepatocellular carcinoma; Central venous pressure; Blood loss

Wang WD, Liang LJ, Huang XQ, Yin XY. Low central venous pressure reduces blood loss in hepatectomy. *World J Gastroenterol* 2006; 12(6): 935-939

http://www.wjgnet.com/1007-9327/12/935.asp

## INTRODUCTION

Hepatectomy remains as the treatment of choice for hepatocellular carcinoma (HCC). Intra-operative blood loss is one of the major causes for post-operative morbidity and mortality. Various techniques, such as Pringle's maneuver and unilateral hepatic hilum occlusion, have been used to control bleeding from hepatic arterial and portal venous systems during hepatectomy in clinical settings. However, for excision of HCC adjacent to major blood vessels, hepatic system could be the major source of hemorrhage, especially after the application of Pringle's maneuver. Hence, effective control of hepatic venous hemorrhage is crucial to minimize intraoperative blood loss. This prospective randomized clinical trial aims at evaluating the role of low central venous pressure (LCVP) in reducing blood loss during hepatectomy for HCC.

## MATERIALS AND METHODS

### *Patients'data and grouping*

From June 2002 to December 2003, a total of 50 consecutive patients with HCC (40 men and 10 women) underwent hepatectomy by the same group of surgeons at our hospital. By the sealed envelope method, the patients were blindly randomized into LCVP group ($n=25$) and control group ($n=27$) at the beginning of the operation. Two patients in the control group were excluded from the study because hepatectomy was given up due to cardiac arrest in one and unclear tumor demarcation in the other. Eventually, there were 25 patients in each group. The demographic data of the patients are shown in Table 1,

**Table 1 Comparison of patient's clinical data between two groups**

| Groups | Gender (male/female)[1] | Age (yr)[2] | Body weight (kg)[3] | Liver cirrhosis (*n*)[4] | Liver function (Child-Pugh class)[5] | | |
|---|---|---|---|---|---|---|---|
| | | | | | A | B | C |
| LCVP | 19/6 | 45.33±14.59 | 60.11±12.14 | 14 | 21 | 3 | 1 |
| Control | 21/4 | 46.00±12.14 | 59.91±10.84 | 15 | 21 | 4 | 0 |

[1]$\chi^2$=0.500, [2]$t$=0.174, [3]$t$=0.055, [4]$\chi^2$=0.082, [5]$\chi^2$=1.143.

**Table 2 Comparison of blood routine examination, hepatic and renal functions, and coagulation function between two groups**

| Groups | Blood routine examination | | | Hepatic function | | | Coagulation function | Renal function | |
|---|---|---|---|---|---|---|---|---|---|
| | Hb(g/L) | RBC($\times 10^{12}$/L) | HCT | ALT(μ/L) | TBIL(μmol/L) | ALB(g/L) | PT(s) | BUN[a](mmol/L) | Cr(μmol/L) |
| LCVP | 134.08±19.17 | 4.632±0.83 | 0.41±0.058 | 51.24±29.91 | 29.04±42.71 | 41.29±6.13 | 12.56±1.12 | 4.75±1.24 | 69.04±15.72 |
| Control | 136.48±13.51 | 4.58±0.55 | 0.41±0.039 | 61.36±47.51 | 22.64±11.27 | 41.12±4.79 | 12.53±1.16 | 5.48±1.12 | 70.76±17.99 |
| $t$ | 0.512 | 0.292 | 0.233 | 0.901 | 0.724 | 573.00 | 0.087 | 2.096 | 0.360 |

[a]$P$<0.05, BUN values in both groups were within normal range (2.5-6.4 mmol/L).

and the preoperative laboratory findings are demonstrated and listed in Table 2.

### *Intraoperative management*

In the LCVP group, patient's right internal jugular vein was cannulated by a dual-channel catheter following anesthesia, with one channel being connected to the transducer for continuously monitoring CVPs. Arterial pressure was measured by puncture of radial artery. Systolic blood pressure (SBP) was maintained above 90 mmHg by intravenous infusion of dopamine (4-6 μg/kg). During hepatectomy, CVP was maintained at 2-4 mmHg by adopting Trendelenburg's posture (with head 15° lower than low extremities), limiting the volume of infusion and intravenously administering nitroglycerine (0.5-2 mg/time), and furosemide (10-20 mg) was used if necessary. From the beginning of anesthesia to the completion of liver resection, the infusion was maintained at a speed of <75 mL/h, urine output >25 mL/h, and SBP >90 mmHg. If hypotension occurred, the dose of dopamine and the speed and volume of infusion were adjusted. If hemoglobin (Hb) was <80 g/L during the operation, packed red cells were transfused. After liver resection and hemostasis were completed, the blood volume was restored with crystalloid and colloid solutions. Post-operative Hb value should be kept at above 100 g/L. In the control group, patients were managed in the same way as those in LCVP group, except for manipulation of patient's posture and administration of nitroglycerine and furosemide to lower CVP.

### *Hepatectomic technique*

The liver was completely separated. The extent of hepatectomy and whether or not applying hepatic blood inflow occlusion were determined based on the tumor situation and severity of liver cirrhosis. For the patients with severe cirrhosis or peripheral tumors, hepatic blood inflow occlusion was not used. For patients with tumor located at one lobe of the liver, unilateral hepatic hilum occlusion was employed. In hepatic parenchymal transection, method of blunt division but not cavitron ultrasonic surgical aspirator (CUSA) was used. The ductal structures were first ligated and then divided, with reinforced suture for larger blood vessels. The cutting surface of the liver was sprayed with biological glue. The patterns of hepatectomy between the two groups were compared as shown in Table 3.

### *Measurement of blood loss during hepatectomy*

Total intra-operative blood loss consisted of the following three parts: (1) from the start of the operation to complete separation of the liver (pre-hepatectomic blood loss); (2) during division of hepatic parenchyma (intra-hepatectomic blood loss); (3) from completion of hepatic parenchymal division to the closure of the abdominal wall (post-hepatectomic blood loss). Operation was continued to the next step only after complete hemostasis was achieved. The blood-collection bottle was changed in each step and the volume of the collected blood was measured. All blood-stained gauzes were harvested and weighed. The difference between the weight of the blood-stained gauzes and their initial weight was considered as the weight of blood in the gauze, which was then converted into the volume of blood (the blood specific gravity: 1.054-1.062 g/mL in men with an average of 1.058 g/mL; 1.048-1.062 g/mL in women with an average of 1.055 g/mL).

### *Evaluation parameters*

The following pre-, intra-, and post-operative data were collected: (1) patient's gender, age, body weight, red blood cell (RBC) count, hematocrit (HCT), hemoglobin (Hb), alanine aminotransferase (ALT), aspartate aminotransferase (AST), total bilirubin (TBIL), serum albumin (ALB), blood urea nitrogen (BUN), creatinine (Cr), prothrombin

**Table 3 Comparison of operative pattern between two groups**

| Groups | Types of hepatectomy[1] | | | | Types of vascular occlusions (n)[2] | | time (min)[3] | Maximal tumor dimension (cm)[4] | Weight of the resected liver tissues (g) |
|---|---|---|---|---|---|---|---|---|---|
| | Right | Left | ≥2 hepatic segments | Single hepatic segments | Unilateral | Portal hepatitis | | | |
| LCVP | 5 | 3 | 13 | 4 | 4 | 7 | 20.00±12.17 | 10.7±4.9 | 633.80±567.38 |
| Control | 4 | 5 | 10 | 6 | 2 | 11 | 17.27±6.56 | 9.88±4.2 | 603.20±497.62 |

[1]$\chi^2$=1.402, [2]$\chi^2$=1.709, [3]$t$=0.621, [4]$t$=0.633, [5]$t$=0.203.

**Table 4 Comparison of intra-operative blood loss between two groups**

| Group | Pre-hepatectomy | Intra-hepatectomy | Post-hepatectomy[2] | Total |
|---|---|---|---|---|
| LCVP | 318.2±605.6 | 672.4±429.9[b] | 42±35.4 | 903.9±180.8[d] |
| Control | 603.4±973.7 | 1 662.6±1 932.1 | 63.4±52.9 | 2 329.4±2 538.4 |
| $W$[1] | 495 | 543.5 | 538 | 495.5 |

[1]Rank sum test; [2]$P$=0.05, [b]$P$<0.01, [d]$P$<0.01 *vs* control.

time (PT), presence or absence of liver cirrhosis and liver function grading; (2) pre-hepatectomic, intra-hepatectomic and post-hepatectomic blood loss and total intra-operative blood loss; (3) operation time, pattern of hepatic hilum occlusion and duration, maximal tumor dimension, weight of the excised liver tissue and extent of hepatectomy, transfusion volume of packed RBCs and fresh frozen plasma (FFP); (4) liver and renal functions on post-operative d 1, 3, and 7; (5) post-operative morbidity and length of hospital stay.

### Statistical analysis

The results were expressed as mean±SD. SPSS software package version 10.0 was used to run the statistical analysis. For continuous variables, Student's $t$ test, rank test or ANOVA was employed to compare the inter-group difference, and $\chi^2$ test was adopted for categorical variables. Statistical significance was considered at two-tailed $P<0.05$.

## RESULTS

### Patient's general clinical data

There were no significant differences in gender, age, body weight, severity of liver cirrhosis and grades of liver function between LCVP and control groups (Table 1).

### Preoperative laboratory data

Table 2 shows that preoperative RBC count, HCT, Hb, ALT, AST, TBIL, ALB, PT and Cr in LCVP group was not markedly different from those in the control group. Preoperative BUN in both the groups was within the normal range, being higher in control group than in LCVP group ($P<0.05$).

### Operative pattern

All patients had large tumors. There were no remarkable differences in patterns of operation, modes of hepatic blood inflow occlusion and duration, maximal tumor dimension, weight of the excised hepatic tissue between the two groups (Table 3).

### Operative time, intra-hepatectomic blood loss, blood transfusion, post-operative complications and length of hospital stay

Total intra-operative blood loss and intra-hepatectomy blood loss were dramatically less in LCVP group than in the control group ($P<0.01$, Table 4). There were no significant differences in pre- and post-hepatectomic blood losses between the two groups (Table 4). Eight of twenty-five patients in LCVP group and 14 of 25 patients in control group needed blood transfusion, with a significantly lower volume of transfusion in LCVP than in the control group ($P<0.05$, Table 5). There was no significant difference in operative time between the two groups (Table 5). Post-operative complications included biliary fistula, gastrointestinal bleeding, pleural effusion and subphrenic fluid collection, with an incidence of 20% (5/25) in LCVP group and 24% (6/25) in control group ($P>0.05$). LCVP group had a remarkably shorter hospital stay than the control group, being 16.3±6.8 d *vs* 21.5±8.6 d ($P<0.05$).

### Post-operative hepatic and renal functions

There were no significant differences in ALT, TBIL, and Cr on post-operative d 1, 3, and 7 between the two groups (Table 6, $P>0.05$). BUN was significantly higher in control group than in the LCVP group, but it was within the normal range in both groups (Table 6, $P>0.05$).

## DISCUSSION

Blood loss during hepatectomy has an adverse effect on the post-operative outcome and increases post-operative morbidity. Intra- or post-operative massive blood transfusion carries risks of causing infectious diseases,

**Table 5 Comparison of operation time and incidence of post-operative complications**

| Groups | Operation time (min)[1] | Intra- and post-operative transfusion (mL) | | Incidence of post-operative complications ($n$)[4] |
|---|---|---|---|---|
| | | Packed RBC[2] | FFP[3] | |
| LCVP | 229.60±67.33 | 525.00±237.57[a] | 437.50±250.36[c] | 5 |
| Control | 246.00±112.36 | 1 285.71±1 162.13 | 1 057.14±658.33 | 6 |

[1]$t$=0.626; [2]$W$=63.00, [3]$t$=2.537, [4]$\chi^2$=9.778, [a]$P$<0.05, [c]$P$<0.05 *vs* control.

**Table 6 Comparison of post-operative hepatic and renal functions between two groups**

| Parameters | Postoperative day | LCVP | Control |
|---|---|---|---|
| ALT (μ/L)[1] | 1 | 561.00±409.23 | 700.76±610.77 |
| | 3 | 286.4±204.09 | 396.60±423.86 |
| | 7 | 104.60±56.18 | 173.04±268.17 |
| TBIL (μmol/L)[2] | 1 | 29.04±42.71 | 22.64±11.27 |
| | 3 | 39.34±47.08 | 40.46±28.33 |
| | 7 | 23.69±26.40 | 28.95±30.82 |
| BUN (mmol/L)[3] | 1 | 4.75±1.24 | 5.48±1.12 |
| | 3 | 4.87±2.59 | 5.72±1.84 |
| | 7 | 5.10±1.75 | 6.03±2.23 |
| Cr (μmol/L)[4] | 1 | 69.04±15.72 | 70.76±17.99 |
| | 3 | 58.04±15.68 | 65.28±17.67 |
| | 7 | 59.12±11.57 | 60.96±15.60 |

[1]$F$=72.955, [2]$F$=0.185, [3]$F$=0.860, [4]$F$=6.462.

coagulatory disorder, acute respiratory distress syndrome, multiple organ failure, and also promotes tumor recurrence due to its inhibitory effects on immunologic function[1,2]. Hence, various methods, including Pringle's maneuver, unilateral hepatic hilum occlusion and normothermic total hepatic vascular exclusion[3], have been adopted to reduce intra-operative blood loss. In recent years, application of CUSA in liver resection under hepatic hilum occlusion has been reported to significantly lessen the intra-operative blood loss[4]. Some studies reported that LCVP during liver resection could significantly cut down the intra-operative blood loss, decrease the incidence of post-operative complications and shorten the hospital stay[5,6]. Under hepatic hilum occlusion, blood loss during liver resection mainly derives from hepatic vein and hepatic short vein. Hepatic sinusoidal pressure is directly related to CVP. With lowering of the pressure in inferior vena cava, the hepatic venous pressure and then hepatic sinusoidal pressure would decline. Blood loss during liver resection is proportional to the pressure gradient of vascular walls and the diameter of the injured vessels. Though total hepatic vascular exclusion or clamping inferior vena cava can reduce blood loss from hepatic venous system during hepatectomy[7], they are associated with remarkable injury and technically difficult.

LCVP in hepatectomy was generally referred to as CVP lower than 5 mmHg[6]. Maintenance of LCVP should not lower the arterial pressure. In the present study, by maintaining CVP below 5 mmHg during liver resection with manipulation of patient's posture, administration of drugs and control of infusion speed, the arterial pressure was effectively sustained and blood loss was markedly cut down. Our results suggested that Trendelenburg's posture was helpful to prevent LCVP-induced air embolism. With the maintenance of the arterial pressure, the perfusion of organs was ensured. The post-operative evaluation showed that LCVP would not deteriorate hepatic and renal functions. LCVP group had shorter hospital stay than the control group. It is suggested that LCVP was helpful for post-operative recovery. The LCVP technique was not complicated and achievable even in middle-class hospitals. Hence, it is of clinical value.

Many studies reported that various methods reduced intra-operative transfusion volume[8]. However, transfusion volume sometimes could not correctly reflect intra-operative blood loss, since the former was related to the patient's preoperative conditions, tolerance to ischemia, control of intraoperative infusion volume and speed, and anesthetist's mastery of indication for transfusion. Intra-operative blood loss included bleeding not only from hepatic parenchymal division, but also from dissection of perihepatic ligaments, separation of tumors from adjacent tissues, the cutting surface of liver after resection and the accidental tumor rupture. The latter was also affected by the surgeon's experiences and techniques, and patient's coagulation function. Hence, strictly speaking, only bleeding from hepatic parenchymal division accounts for the real blood loss of hepatectomy. In the present study, we have divided the procedure of hepatectomy into three steps, i.e.,: pre-, intra-, and post-hepatectomic, and blood loss in each step was completely collected and accurately measured. Our results showed that total intra-operative blood loss was markedly less in LCVP group than that in the control group. There were no significant differences in pre-hepatectomic and post-hepatectomic blood losses between the two groups, but intra-hepatectomic blood loss was remarkably lower in LCVP group than in the control group.

It suggested that lowering CVP during hepatectomy could effectively reduce blood loss. Additionally, transfusion volume was markedly cut down in LCVP as compared with the control group. It indicated that decline in intra-hepatectomic blood loss could reduce the transfusion volume, which is helpful for the recovery of patient's immunological function and prevention of tumor recurrence. The present study is a prospective randomized clinical trial. The number of cases is not big enough, and the effect of decline in intra-operative blood loss on prognosis still awaits further observations.

## REFERENCES

1 **Yamamoto J**, Kosuge T, Takayama T, Shimada K, Yamasaki S,

Ozaki H, Yamaguchi N, Mizuno S, Makuuchi M. Perioperative blood transfusion promotes recurrence of hepatocellular carcinoma after hepatectomy. *Surgery* 1994; **115**: 303-309

2 **Li CH**, Chau GY, Lui WY, Tsay SH, King KL, Hsia CY, Wu CW. Risk factors associated with intra-operative major blood loss in patients with hepatocellular carcinoma who underwent hepatic resection. *J Chin Med Assoc* 2003; **66**: 669-675

3 **Lai J M**, Liang L J, Li D M. Application of hepatovascular occlusion in hepatocellular carcinoma recection. *Chin J Bases Clin General Surg* 1999; **6**: 217-219

4 **Wu W**, Lin XB, Qian JM, Ji ZL, Jiang Z. Ultrasonic aspiration hepatectomy for 136 patients with hepatocellular carcinoma. *World J Gastroenterol* 2002; **8**: 763-765

5 **Johnson M**, Mannar R, Wu AV. Correlation between blood loss and inferior vena caval pressure during liver resection. *Br J Surg* 1998; **85**: 188-190

6 **Smyrniotis V**, Kostopanagiotou G, Theodoraki K, Tsantoulas D, Contis JC. The role of central venous pressure and type of vascular control in blood loss during major liver resections. *Am J Surg* 2004; **187**: 398-402

7 **Otsubo T**, Takasaki K, Yamamoto M, Katsuragawa H, Katagiri S, Yoshitoshi K, Hamano M, Ariizumi S, Kotera Y. Bleeding during hepatectomy can be reduced by clamping the inferior vena cava below the liver. *Surgery* 2004; **135**: 67-73

8 **Peng SY**, Liu YB, Xu B, Cai XJ, Mu YP, Wu YL, Cao LP, Fang HQ, Wang JW, Li HJ, Li JT, Wang XB, Deng GL. Role and significance of extrahepatic control of hepatic vein and inferior vena cava in difficult hepatectomies for patients with liver tumors. *Zhonghua Waike Zazhi* 2004; **42**: 260-264

**S- Editor** Ma JY **L- Editor** Elsevier HK **E- Editor** Kong LH

PO Box 2345, Beijing 100023, China
www.wjgnet.com
wjg@wjgnet.com

*World J Gastroenterol* 2006 February 14; 12(6): 940-944
***World Journal of Gastroenterology*** ISSN 1007-9327
© 2006 The WJG Press. All rights reserved.

*RAPID COMMUNICATION*

# Removal selectivity of Prometheus: A new extracorporeal liver support device

Kinan Rifai, Thomas Ernst, Ulrich Kretschmer, Hermann Haller, Michael Peter Manns, Danilo Fliser

Kinan Rifai, Thomas Ernst, Michael Peter Manns, Division of Gastroenterology, Hepatology and Endocrinology, Department of Internal Medicine, Medical School Hannover, Germany
Ulrich Kretschmer, Hermann Haller, Danilo Fliser, Division of Nephrology, Department of Internal Medicine, Medical School Hannover, Germany
Supported by the Fresenius Medical Care
Correspondence to: Dr. Kinan Rifai, Division of Gastroenterology, Hepatology and Endocrinology, Department of Internal Medicine, Medical School Hannover, Carl Neuberg Strasse 1, Hannover 30625, Germany. rifai.k@gmx.de
Telephone: +49-511-532-3305 Fax: +49-511-532-4896
Received: 2004-11-17 Accepted: 2004-12-20

## Abstract

**AIM:** To evaluate whether treatment with the Prometheus® system significantly affects cytokines, coagulation factors and other plasma proteins.

**METHODS:** We studied nine patients with acute-on-chronic liver failure and accompanying renal failure. Prometheus® therapy was performed on 2 consecutive days for up to 6 h in all patients. Several biochemical parameters and blood counts were assessed at regular time points during Prometheus® treatment.

**RESULTS:** We observed a significant decrease of both protein-bound (e.g. bile acids) and water-soluble (e.g. ammonia) substances after Prometheus® therapy. Even though leukocytes increased during treatment ($P<0.01$), we found no significant changes of C-reactive protein, interleukin-6, and tumor necrosis factor-α plasma levels (all $P>0.5$). Further, antithrombin 3, factor II and factor V plasma levels did not decrease during Prometheus® therapy (all $P>0.5$), and the INR remained unchanged ($P=0.4$). Plasma levels of total protein, albumin, and fibrinogen were also not altered during Prometheus® treatment (all $P>0.5$). Finally, platelet count did not change significantly during therapy ($P=0.6$).

**CONCLUSION:** Despite significant removal of protein-bound and water-soluble substances, Prometheus® therapy did not affect the level of cytokines, coagulation factors or other plasma proteins. Thus, the filters and adsorbers used in the system are highly effective and specific for water-soluble substances and toxins bound to the albumin fraction.

**Key words:** Prometheus; Albumin dialysis; Extracorporeal system; Tumor necrosis factor-α; Interleukin-6; Coagulation factors; Fibrinogen

Rifai K, Ernst T, Kretschmer U, Haller H, Manns MP, Fliser D. Removal selectivity of Prometheus: A new extracorporeal liver support device. *World J Gastroenterol* 2006; 12(6): 940-944

http://www.wjgnet.com/1007-9327/12/940.asp

## INTRODUCTION

Extracorporeal liver support devices have recently gained much interest. Prometheus® is a newly designed system for extracorporeal treatment of liver failure. It is based upon a recently developed method of albumin dialysis, i.e. fractionated plasma separation and adsorption[1]. First, an albumin-permeable membrane (AlbuFlow, cut-off 250 ku) separates the albumin fraction together with all albumin-bound substances in a secondary circuit. There, direct purification of the plasma is performed by one or two adsorbers (Prometh01 and Prometh02) in order to remove albumin-bound toxins. In parallel, a conventional high-flux dialysis is performed to remove the water-soluble substances.

Results from past studies have documented that extracorporeal liver support devices can remove cytokines and other important plasma proteins[2,3]. Theoretically, removal of these substances may influence spontaneous liver regeneration, similarly as has been proposed for interleukin-6 (IL-6) and tumor necrosis factor-α (TNF-α)[4]. Furthermore, development of thrombopenia with an increased risk of bleeding was documented in several patients undergoing albumin dialysis using the MARS system[5]. Until now, there are not sufficient controlled studies available that have evaluated whether treatment with the Prometheus® device may result in an unspecific removal of cytokines or leads to a decrease of coagulation factors or platelets. In addition, albumin or other plasma proteins may be lost during Prometheus® as a result of removal or after clotting in the secondary circuit. Therefore, we performed a prospective clinical study in patients with liver failure and assessed the course of different cytokines, coagulation factors, protein fractions, and thrombocytes during treatment with Prometheus®.

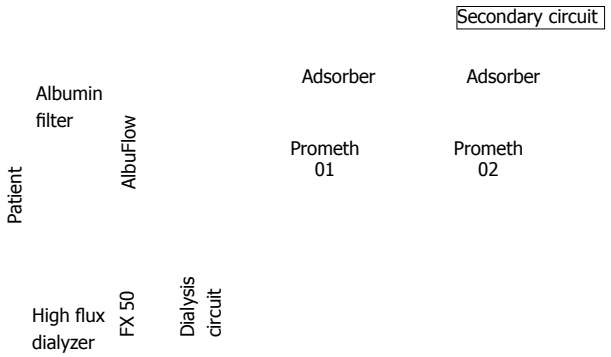


**Figure 1** The albumin fraction of the patient's blood is filtered through an albumin-permeable membrane (AlbuFlow®) into a secondary circuit. There, the separated albumin fraction is purified by direct adsorption of albumin-bound toxins using one or two adsorbers (Prometh01® and Prometh02®). The plasma is then pumped back into the primary circuit where a conventional high-flux dialysis (FX 50) is performed.

## MATERIALS AND METHODS

### Patients

The study was approved by the Ethics Committee of the Hannover Medical School. The Declaration of Helsinki and the rules from Good Clinical Practice were followed. Written informed consent was obtained from all patients or next of kin. Nine patients (four males) with liver failure (five with end-stage cirrhosis, two with acute alcoholic hepatitis, two with liver failure late after liver transplantation) and concomitant renal failure were included in the trial. Their mean age was 52 ± 8 years, and the average APACHE II score was 16.8 ± 3.2. Seven patients (78%) had the highest stage of cirrhosis (C Child-Pugh score) with an average of 11.3 ± 1.7 points. Six patients (67%) were treated in the intensive care unit. All patients were already undergoing hemodialysis and had a functionable double-lumen catheter in place.

### Prometheus® device

Blood coming from the patient by a double-lumen dialysis catheter is pumped into the extracorporeal circuit. There, it passes through an albumin-permeable filter, which is made of polysulfone (AlbuFlow®). The filter has a sieving coefficient that is specially designed. It allows large molecules up to the size of albumin (68 ku) to pass into the secondary circuit. The cut-off is at about 250 ku. Larger molecules cannot pass through the filter. The secondary circuit is filled with isotonic sodium chloride solution. It is driven by a separate plasma pump. By recirculation of the albumin-rich plasma, the filtration and adsorption capacities are enhanced. One or two adsorbers are used to directly purify the filtered albumin-rich plasma: a neutral resin adsorber (Prometh01®) for direct adsorption of the albumin-bound toxins and an anion exchanger (Prometh02®) with chloride used as counterion. The content of the adsorber consists of spherical adsorber particles with 300-1 000 μm in diameter. The adsorbers consist of styrene-divinylbenzene copolymer. Their cylindrical housing has a central inlet and outlet closed at both ends by sieves with a mesh size of 100 μm. The sieves circumvent a passage of the particles through the inlets. Even in case of leakage, they are held back in the secondary circuit by the albumin filter membrane. After the purification of the fractionated plasma in the secondary circuit, the purified plasma is returned to the primary circuit, i.e. into the blood side of the albumin filter. Here the blood is guided through a high-flux hemodialyzer (FX 50®). There, water-soluble substances are removed by diffusion.

A modified hemodialysis unit (4008 H) is used to integrate the two parts of the Prometheus® system (Fresenius Medical Care AG, Bad Homburg, Germany): a "standard" extracorporeal blood circuit connected to the double-lumen dialysis catheter and a secondary circuit containing the separated plasma (Figure 1). Both circuits are separately monitored by different hardware and software allowing the user to perform hemodialysis with simultaneous albumin detoxification or conventional hemodialysis alone.

### Treatments

Instead of their regular hemodialysis sessions, all patients underwent two Prometheus® treatments for at least 4 h on two consecutive days. In 5/9 patients (56%), the device was equipped with two adsorbers (Prometh01® and Prometh02®), while the other four patients (44%) were treated only with Prometh01®. The average treatment time was 5.1 ± 1.1 h, and mean blood flow rate was 193 ± 10 mL/min. The total processed volume within each treatment was 58 ± 14 L. Anticoagulation during therapy consisted of unfractionated heparin administered as a bolus. Because of the increased risk of bleeding in liver patients, heparin administration was restricted to low doses. The activated coagulation time was used to control anticoagulation. It was targeted between 120 and 150. Blood samples for measurement of cytokines (TNF-α and IL-6), platelets, coagulation factors (antithrombin 3, factors II and V) and plasma proteins (total protein, albumin, and fibrinogen) were taken before the start of Prometheus therapy, after 30 min, 2, and 5 h of treatment as well as 24 h after the end of the treatment.

### Measurements

Plasma concentration of C-reactive protein was measured with a clinically validated nephelometric assay (Dade Behring, Germany); the normal range is below 5 mg/L. Plasma concentrations of inflammatory cytokines, e.g. IL-6 and TNF-α, were measured with an ELISA (R&D Systems, USA). The intra-assay coefficients of variation for these tests ranged between 4.9% and 6.8%, respectively. The other biochemical parameters were measured by certified routine analytical methods.

### Statistical analysis

The SPSS program was used for statistical analysis (version 12.0, SPSS, Chicago, USA). All data are presented as mean ± SD. Pre- and post-treatment values were compared using two-tailed *t*-test for paired data. Correlations were assessed with Pearson's correlation analysis. A $P < 0.05$ was considered as statistically significant.

## RESULTS

A significant decrease of both protein-bound substances (e.g., bile acids; $P<0.01$) and water-soluble substances (e.g., urea; $P<0.001$) was observed under Prometheus® therapy (Figure 2A). Even though leukocytes increased from $15.1\times10^3$ to $22.7\times10^3/\mu L$ ($P<0.01$), there were no significant changes of plasma concentrations of C-reactive protein ($P=0.7$), TNF-α ($P=1.0$; Figure 2B) or IL-6 ($P=0.9$; Figure 2B). TNF-α and IL-6 were correlated with each other ($P<0.03$). Furthermore, they were positively associated with body temperature (TNF-α: $P<0.03$; IL-6: $P<0.001$), but not with C-reactive protein (both $P>0.2$). All these parameters were already increased in our patients before Prometheus® therapy.

Platelet count and coagulation factors such as antithrombin 3, factors II and V were substantially decreased in our patients before the start of Prometheus® therapy. However, there was no decrease of platelets during treatment ($P=0.6$). Furthermore, the coagulation factors and INR did not significantly change under Prometheus® treatment (all $P>0.4$; Figure 2C). All coagulation factors were highly associated with each other (all $P<0.001$) and with C-reactive protein (all $P<0.01$). A strong positive association was found between factors II and factor V on one hand and leukocyte count on the other hand (both $P<0.001$).

Plasma levels of total protein, albumin, and fibrinogen were reduced in liver patients before the start of Prometheus® therapy. Even though we had two episodes of clotting of the secondary, i.e. albumin-filled circuit occurred, we observed no significant alterations of total protein, albumin, and fibrinogen during treatment (all $P>0.5$; Figure 2D).

In one patient with hepatitis C cirrhosis and hepatorenal syndrome, we found a marked increase of TNF-α (from 17 to 12 420 ng/L) and IL-6 (from 49 to 15 732 ng/L) already after the 2nd h of treatment on the 1st day of Prometheus® therapy. In parallel, leukocytes decreased from $8.1\times10^3$ to $1.6\times10^3/\mu L$. No specific clinical problems were recorded at that time, so that the Prometheus® treatment was completed. When treatment was stopped, mean arterial pressure was 52 mmHg, whereas body temperature was 38.9 °C and leukocytes $4.4\times10^3/\mu L$. At this time point, we later measured already decreasing TNF-α plasma levels (1 012 ng/L), whereas IL-6 was still increasing (76 250 ng/L). This episode turned out to be a catheter-related bacteremia, and the catheter was removed immediately. After the catheter had been changed, no clinical problems were observed during Prometheus® therapy on the next day. Plasma levels of TNF-α after the second treatment decreased to 49 ng/L and that of IL-6 to 108 ng/L.

## DISCUSSION

Removal selectivity of extracorporeal blood purification devices is a key to assess their specificity and efficacy. Therefore, it is crucial to evaluate whether particular substances are removed or not. With Prometheus® both protein-bound and water-soluble substances that accumulate in liver failure are removed in a single step, i.e. during a single passage of the blood through the extracorporeal circuit. The system is based upon the FSPA method, and in contrast to the MARS system, Prometheus® allows direct purification of the albumin fraction in the secondary circuit[1]. Furthermore, a high-flux dialyzer is incorporated in the Prometheus® system as well.

We were able to show that Prometheus® significantly removed protein-bound (e.g., bile acids) and water-soluble substances (e.g., urea), but we did not observe (unspecific) removal of cytokines such as TNF-α and IL-6. In contrast, it has been shown that both cytokines are removed during MARS treatment[2,3]. This could be of considerable clinical importance, since these pro-inflammatory cytokines are postulated to play a major role also in the process of liver regeneration[4]. Thus, while cytokine removal may have beneficial effects in clinical conditions where activation of pro-inflammatory cytokines is part of the pathophysiological basis of the syndrome, e.g. systemic inflammatory response syndrome (SIRS)[7], it could be potentially even harmful in liver patients by impeding liver regeneration[8]. Since large prospective controlled trials on survival are lacking, it remains to be elucidated whether (unspecific) cytokine removal in liver patients is beneficial or whether these patients benefit more if pro-regenerative cytokines such as TNF-α and IL-6 remain in the body.

Another point of interest in our study was the influence of Prometheus® therapy on coagulation factors and platelets. Usually, patients with liver failure present with moderate to severe coagulopathy. In order to prevent bleeding complications in these patients, the coagulation status should not be further worsened by a removal, activation or consumption of coagulation factors. In none of our patients we observed a decrease of platelets, and coagulation factors such as antithrombin 3, factor II or factor V remained stable throughout the therapy without substitution. This is in contrast to data obtained with the MARS system; it may induce thrombopenia in a significant number of patients with a subsequently elevated risk of bleeding complications[5].

An important point in the evaluation of extracorporeal liver support systems is the possible loss of plasma proteins during treatment. This may result from an unspecific removal, from adsorption on the adsorber, or by a clotting of the secondary circuit that is filled with the patients' albumin. Even though two episodes of clotting of the secondary circuit occurred in our study, no significant loss of plasma total protein or albumin developed. Furthermore, the selectivity of protein removal was confirmed by measurement of serum fibrinogen concentrations. Fibrinogen molecules are much larger than albumin and should be held in patients' blood if the sieving coefficient of the membrane used for plasma separation remains unaltered. As expected, fibrinogen levels in our patients remained stable throughout the whole study period.

In conclusion, our data document that the extracorporeal liver support device Prometheus® provides selective removal of protein-bound and water-soluble substances, whereas measured cytokines, coagulation factors or plasma protein fractions as well as platelets remain unaltered. In this aspect the system seems to offer an advantage over the MARS system.

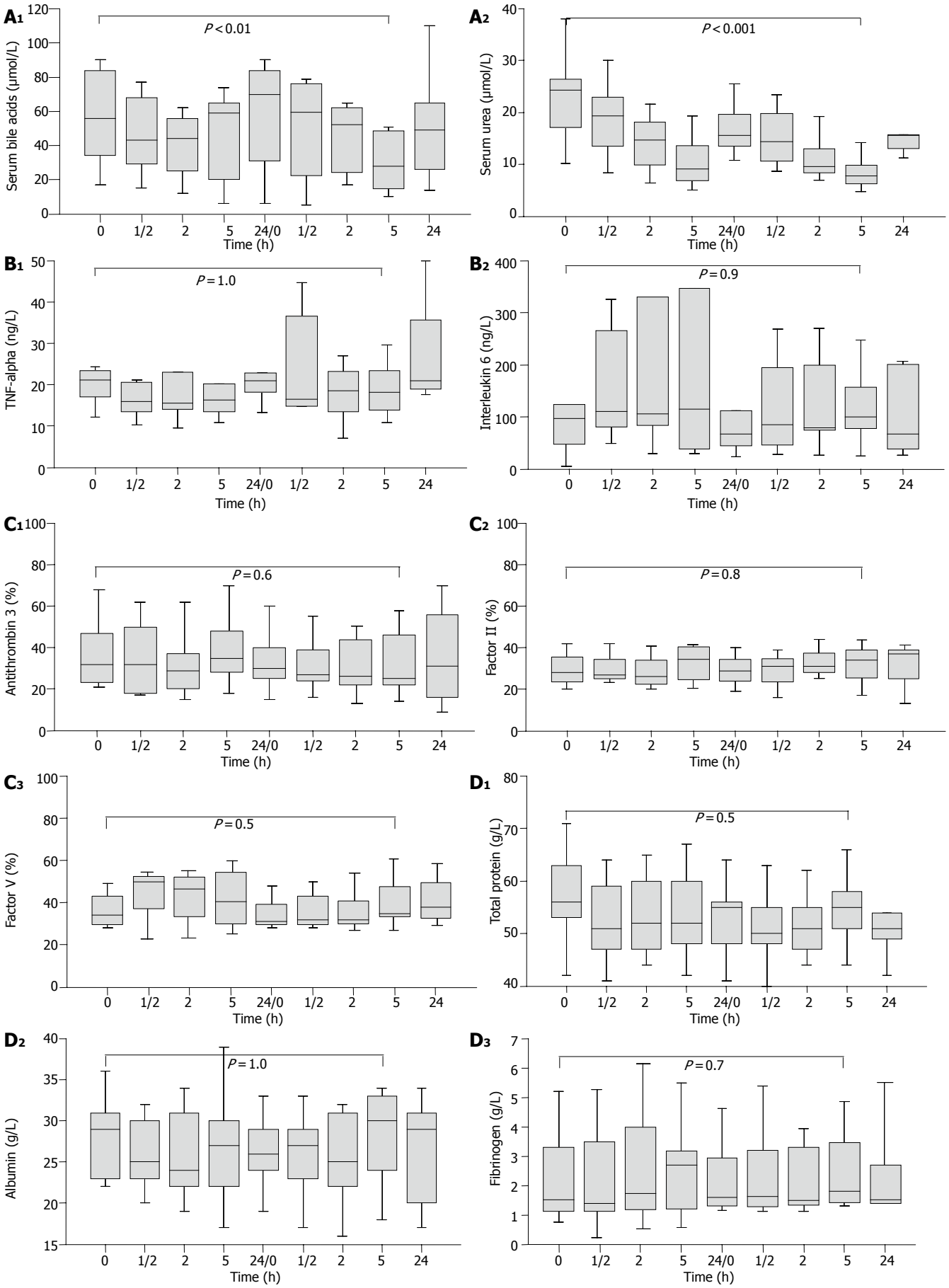


**Figure 2** (**A1-A2**) Course of plasma bile acids and urea concentrations before, during and after 2 d of Prometheus® therapy. Data are presented as median, quartiles, and minimum/maximum values. (**B1-B2**) Course of plasma TNF-α and IL-6 concentrations before, during and after 2 d of Prometheus® therapy. Data are presented as median, quartiles, and minimum/maximum values. (**C1-C3**) Course of antithrombin 3, factors II and V levels before, during and after 2 d of Prometheus® therapy. Data are presented as median, quartiles, and minimum/maximum values. (**D1-D3**) Course of plasma total protein, albumin, and fibrinogen before, during, and after 2 d of Prometheus® therapy. Data are presented as median, quartiles, and minimum/maximum values.

## REFERENCES


1 **Falkenhagen D**, Strobl W, Vogt G, Schrefl A, Linsberger I, Gerner FJ, Schoenhofen M. Fractionated plasma separation and adsorption system: a novel system for blood purification to remove albumin bound substances. *Artif Organs* 1999; **23:** 81-86

2 **Stange J**, Hassanein TI, Mehta R, Mitzner SR, Bartlett RH. The molecular adsorbents recycling system as a liver support system based on albumin dialysis: a summary of preclinical investigations, prospective, randomized, controlled clinical trial, and clinical experience from 19 centers. *Artif Organs* 2002; **26:** 103-110

3 **Guo LM**, Liu JY, Xu DZ, Li BS, Han H, Wang LH, Zhang WY, Lu LH, Guo X, Sun FX, Zhang HY, Liu XD, Zhang JP, Yao Y, He ZP, Wang MM. Application of Molecular Adsorbents Recirculating System to remove NO and cytokines in severe liver failure patients with multiple organ dysfunction syndrome. *Liver Int* 2003; **23** Suppl 3: 16-20

4 **Fausto N**. Liver regeneration. *J Hepatol* 2000; **32:** 19-31

5 **Jalan R**, Sen S, Williams R. Prospects for extracorporeal liver support. *Gut* 2004; **53:** 890-898

6 **Stange J**, Mitzner S, Ramlow W, Gliesche T, Hickstein H, Schmidt R. A new procedure for the removal of protein bound drugs and toxins. *ASAIO J* 1993; **39:** M621-M625

7 **Rodriguez-Gaspar M**, Santolaria F, Jarque-Lopez A, Gonzalez-Reimers E, Milena A, de la Vega MJ, Rodriguez-Rodriguez E, Gomez-Sirvent JL. Prognostic value of cytokines in SIRS general medical patients. *Cytokine* 2001; **15:** 232-236

8 **Mullin EJ**, Metcalfe MS, Maddern GJ. Artificial liver support: potential to retard regeneration? *Arch Surg* 2004; **139:** 670-677


**S- Editor** Guo SY **L- Editor** Elsevier HK **E- Editor** Kong LH

PO Box 2345, Beijing 100023, China
www.wjgnet.com
wjg@wjgnet.com

*World J Gastroenterol* 2006 February 14; 12(6): 945-950
***World Journal of Gastroenterology*** ISSN 1007-9327
© 2006 The WJG Press. All rights reserved.

*RAPID COMMUNICATION*

# Randomized controlled trial of consensus interferon with or without zinc for chronic hepatitis C patients with genotype 2

Hideyuki Suzuki, Ken Sato, Hitoshi Takagi, Daisuke Kanda, Naondo Sohara, Satoru Kakizaki, Hiroaki Nakajima, Toshiyuki Otsuka, Takeaki Nagamine, Masatomo Mori

Hideyuki Suzuki, Ken Sato, Hitoshi Takagi, Daisuke Kanda, Naondo Sohara, Satoru Kakizaki, Hiroaki Nakajima, Toshiyuki Otsuka, Takeaki Nagamine, Masatomo Mori, Department of Medicine and Molecular Science, Gunma University Graduate School of Medicine, 3-39-15 Showa, Maebashi, Gunma 371-8511, Japan
Supported by the grant center of Excellence, Biomedical research using accelerator technology, Gunma, Japan
Correspondence to: Ken Sato, MD, PhD, Department of Medicine and Molecular Science, Gunma University Graduate School of Medicine, 3-39-15 Showa, Maebashi, Gunma 371-8511, Japan. satoken@showa.gunma-u.ac.jp
Telephone: +81-27-220-8127 Fax: +81-27-220-8136
Received: 2005-07-21 Accepted: 2005-08-26

## Abstract

**AIM:** The beneficial effect of zinc supplementation on the efficacy of interferon as a treatment for chronic hepatitis C had been demonstrated in hepatitis virus genotype 1b of high viral load. This study focused on patients with genotype 2, which is more sensitive to interferon than genotype 1b, and used consensus interferon (CIFN) with or without zinc.

**METHODS:** We randomized 83 patients with chronic hepatitis C to CIFN at 18 MIU six times/wk for 4 wk, followed by CIFN at 18 MIU six times/wk for another 20 wk, in combination with polaprezinc 300 mg (regimen A, $n=41$) or as monotherapy (regimen B, $n=42$). Thirty-one patients in regimen A and 33 patients in regimen B completed the clinical trial; the remaining patients withdrew because of side effects or a transfer to another hospital.

**RESULTS:** Sustained biochemical response, defined as a normal aminotransferase level at the end of the 6-mo post-treatment observation, was 68% and 69%, and sustained virological response, defined as undetectable HCV-RNA at the end of the 6-mo post-treatment observation, was 54% and 67% for regimens A and B, respectively.

**CONCLUSION:** CIFN treatment combined with zinc did not enhance the effect of CIFN as shown by biochemical, virological criteria. No side effects related to polaprezinc were noted.

© 2006 The WJG Press. All rights reserved.

**Keywords**: Randomized controlled trial; Consensus interferon; Zinc; Chronic hepatitis C; Genotype 2

Suzuki H, Sato K, Takagi H, Kanda D, Sohara N, Kakizaki S, Nakajima H, Otsuka T, Nagamine T, Mori M. Randomized controlled trial of consensus interferon with or without zinc for chronic hepatitis C patients with genotype 2. *World J Gastroenterol* 2006; 12(6): 945-950

http://www.wjgnet.com/1007-9327/12/945.asp

## INTRODUCTION

Interferon (IFN) is an effective treatment for chronic hepatitis C and is the only method of treatment that eliminates hepatitis C virus (HCV)[1,2]. The incidence of hepatocellular carcinoma (HCC) decreases if liver function improves, even if the virus is not eradicated after IFN treatment[3-6], or if HCV RNA becomes undetectable during IFN treatment[7]. IFN treatment for chronic hepatitis C plays a pivotal role in the prevention of HCC.

HCV-RNA clearance rates are reported to be approximately 30-40% in patients treated with IFN alone[8-10]. However, better results have been reported when IFN-α is used in combination with ribavirin in both naïve patients[11,12] and in those who failed to respond to, or relapsed after, IFN-α monotherapy[13,14]. However, IFN plus ribavirin treatment for 24 wk causes more frequent side effects leading to dose reduction or discontinuation of treatment in 28% of cases compared that in 21% of cases in IFN alone treatment[11]. Furthermore, in Japan, the use of ribavirin is restricted to naïve patients with chronic hepatitis C who have high viral loads greater than 100 KIU/mL.

Consensus IFN (CIFN) is a genetically engineered novel type I IFN molecule derived from commonly observed amino acids of several natural IFN subtypes [15]. CIFN has demonstrated higher *in vitro* antiviral effects on an equal mass basis, than IFN- 2α or 2β[16,17]. In Japan, 9-18 MIU CIFN treatment for 6 mo is reported to be well tolerated and 18 MIU CIFN is considered to be the maximum tolerable dose in patients with chronic hepatitis C and is superior in efficacy, without additional toxicity, to 9 MIU CIFN in high-titer chronic hepatitis C patients[18].

Serum zinc levels are low in patients with chronic liver disease because of a trace element metabolism disorder[19]. Previously, we have demonstrated that zinc supplementa-

tion in chronic hepatitis C patients with genotype 1b of high viral load enhanced the response to IFN-α monotherapy[20]. Although zinc has diverse biological properties including antiviral, anti-inflammatory, and antioxidant functions[21-24], the mechanism responsible for the beneficial effect of zinc during treatment with IFN remains to be elucidated. Treatment efficacy depends on the genotype, HCV load, and staging; HCV genotypes 2a and 2b are more sensitive to IFN than genotype 1a or 1b[1,25,26].

We planned a randomized controlled study for the treatment of genotypes 2a and 2b hepatitis C to determine whether zinc supplementation could also enhance the efficacy of IFN in chronic hepatitis C patients as well as genotype 1b. We used CIFN instead of IFN plus ribavirin for the following reasons. (1) Naïve chronic hepatitis C patients with low viral load could not be treated by the standard treatment, IFN-α 2b plus ribavirin or pegylated-IFN plus ribavirin, under the current health insurance regulations in Japan, due to high sensitivity of HCV with low viral load to IFN. (2) Even with high viral loads, HCV genotype 2a/2b can be expected to be relatively sensitive to IFN monotherapy without ribavirin. (3) CIFN has fewer restrictions or contraindications, and is less expensive than the combination of IFN-α 2b and ribavirin.

## MATERIALS AND METHODS

### Patient selection criteria

Patients with chronic HCV infection who had never received IFN therapy were eligible for this study. The patients were continuously positive for HCV-RNA genotype 2 using the amplicor HCV monitor assay and were diagnosed with chronic active hepatitis from a liver biopsy. The eligibility criteria included histological evidence of chronic hepatitis, as judged on a liver biopsy performed no longer than 6 mo prior to enrolment, and confirmation of HCV infection by polymerase chain reaction (PCR) analysis. Liver-biopsy specimens were assessed independently by two pathologists who were blinded to the patients' clinical details. Pathological diagnosis was made using the classification established by Desmet *et al*[27]. The exclusion criteria included: age lower than 18 years or older than 65 years, pregnancy or lack of appropriate contraceptive measures in women of child bearing age, previous treatment with antiviral or immunosuppressive drugs, current or previous drug addiction, alcoholism, positive HbsAg or HIV test, histological evidence of liver cirrhosis, concomitant metabolic, autoimmune or neoplastic liver diseases, severe concomitant diseases other than liver disease, history of depression or psychiatric diseases.

### Study design

This was a randomized, open-label, controlled study conducted between December 2001 and December 2003. The study was approved by the Ethical Committee of Gunma University. Eighty-three patients gave written informed consent and were randomly assigned to two groups: patients in regimen A received CIFN with polaprezinc and patients in regimen B received CIFN alone. All patients were given CIFN subcutaneously every day for 4 wk and then thrice a wk for 20 wk at a dose of 18 mega units (MU). Forty-one patients in regimen A were given 75 mg of oral polaprezinc twice daily (Plomac; Zeria Pharmaceutical Co., Tokyo, Japan) with CIFN for 24 wk, and zinc administration was discontinued simultaneously with discontinuation of CIFN, for a total of 24 wk. Forty-three patients in regimen B were given CIFN according to the protocol for 24 wk. Serum HCV-RNA was measured before treatment and every mo for one year during and after CIFN therapy. Patient adherence to the protocol and compliance with treatment were encouraged by regular hospital visits.

### Endpoints and definitions

Two endpoints were selected for comparing the efficacy of regimen A with the standard regimen B. The first endpoint involved serum HCV-RNA levels. 'Sustained virological response (SVR)' was defined as undetectable HCV-RNA at the end of the 6-mo post-treatment observation. 'End-of treatment virological response (EVR)' was defined as undetectable HCV-RNA at the end of the treatment. 'Non virological response (NVR)' was defined as detectable HCV-RNA at the end of the 6-mo post-treatment observation. The second endpoint was serum alanine aminotransferase (ALT) levels. Normalization of serum ALT at the end of treatment and at the end of the 6-mo post-treatment observation was defined as 'end-of treatment biochemical response (EBR)' and 'sustained biochemical response (SBR)', respectively. 'Non biochemical response (NBR)' was defined as elevation of serum ALT at the end of the 6-mo post-treatment observation.

### Assessment of safety

We evaluated all adverse events, subjective and objective symptoms, and laboratory test results for safety. All adverse events were checked by the patients using questionnaires, double-checked, and recorded by the investigators. All adverse events were graded for severity based on the World Health Organization (WHO) criteria and the guideline to grading severity of adverse events determined by the Japanese Ministry of Health and Welfare. Global safety assessments were made at the end of post-treatment observation using the following classifications: no abnormality, abnormality requiring no symptomatic treatments, abnormality requiring symptomatic treatments, abnormality requiring study withdrawal, and non-evaluable.

### Statistical analysis

Results were expressed as mean±SD of the mean on an intention to treat or per-protocol basis. Statistically significant differences in outcomes between the two regimens were assessed using both parametric and non-parametric tests including the Student's *t*-test for paired and unpaired observations, and Fisher' s exact test as appropriate.

A logistic multiple regression model was used to examine the relationship between baseline clinical characteristics and the binary outcome of response to CIFN therapy. Each variable was transformed into categorical data consisting of two simple ordinal numbers for the logistic multiple regression model. Variable selection was an important step in characterizing prognostic relations and identifying variables most strongly related to

**Table 1 Characteristics of participating patients**

| | Regimen A IFN + zinc) | Regimen B (CIFN) | *P* |
|---|---|---|---|
| Number of entry | 41 | 42 | |
| Male/Female | 28/13 | 21/21 | NS |
| Age (yr) | 60±8.5 | 55±21 | NS |
| Body mass index | 23±2.4 | 24±3.7 | NS |
| Pre-treatment zinc concentration (μg/dl) | 77.8±13.6 | 82.5±16.4 | NS |
| Pre-treatment ALT (IU/l) | 113±75 | 101±96 | NS |
| Pre-treatment leukocyte counts ($x10^3mm^{-3}$) | 5.1±1.3 | 5.0±1.4 | NS |
| Pre-treatment platelet counts ($x10^3mm^{-3}$) | 19±5 | 17±5 | NS |
| Pre-treatment HCV-RNA genotype (2A/2B) | 31/10 | 31/11 | NS |
| Pre-treatment HCV-RNA titer (KIU/mL) | 484±1075 | 304±318 | NS |
| 0<pretreatment HCV-RNA<100 | 11 | 16 | NS |
| 100≤pretreatment HCV-RNA<400 | 15 | 14 | NS |
| 400≤pretreatment HCV-RNA<700 | 6 | 2 | NS |
| 700≤pretreatment HCV-RNA | 9 | 9 | NS |
| Histological findings (staging) | 1.8±1 | 1.3±0.8 | NS |
| Histological findings (grading) | 1.6±0.7 | 1.3±0.9 | NS |

Mean±SD; NS: not significant

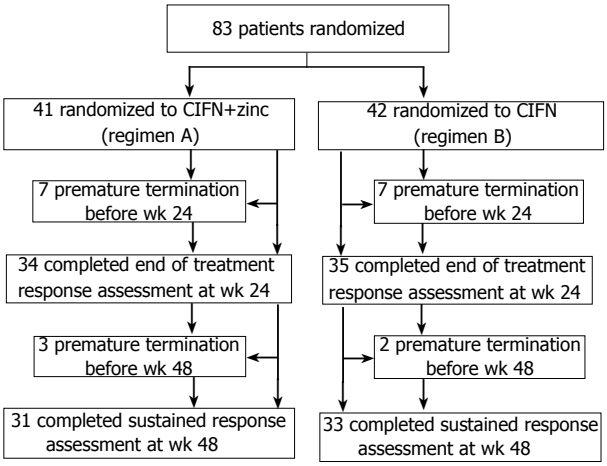


**Figure 1** Trial profile.

the outcome. We selected, as candidate predictors of SVR, age, sex, weight, body mass index (BMI), pretreatment platelet counts, pretreatment ALT, pretreatment γGTP levels, liver histology (staging and grading), pretreatment HCV-RNA viral load, wk of HCV-RNA clearance (less than 1, 4, 8, and 12 wk) and zinc supplementation. Thus, variables ($P<0.2$) on univariate analysis, that is, zinc supplementation, BMI, staging, pretreatment HCV-RNA viral load (less than 400 KIU/mL), wk of HCV-RNA clearance (less than 8 wk) and pretreatment ALT were included in a logistic multiple regression model. Differences with a $P<0.05$ were considered significant.

## RESULTS

Eighty-three patients were enrolled into the trial; 41 were randomized to regimen A and 42 to regimen B. The pretreatment clinical characteristics of the patients assigned to the two regimens were similar (Table 1).

**Table 2 Effect on viremia and serum transaminases**

| | Regimen A (CIFN + zinc) | Regimen B (CIFN) | *P* |
|---|---|---|---|
| ALT (U/l): | | | |
| Wk 0 | 113±75 | 101±96 | NS |
| Wk 24 | 46±51 | 40±30 | NS |
| Wk 48 | 26±17 | 22±12 | NS |
| Biochemical response (by intention to treat): | | | |
| Wk 24 (EBR) | 46% | 50% | NS |
| Wk 48 (SBR) | 68% | 69% | NS |
| Virological response (by intention to treat): | | | |
| Wk 24 (EVR) | 68% | 76% | NS |
| Wk 48 (SVR) | 54% | 67% | NS |

Mean±SD; EBR: End-of treatment biochemical response; SBR: Sustained biochemical response; EVR: End-of treatment virological response; SVR: Sustained virological response; NS: not significant

### *Follow-up and protocol compliance*

The progression of randomized patients through the trial is summarized in Figure 1. Seven patients in regimen A withdrew prematurely from the study before wk 24 due to intolerance to IFN in five patients, and personal problems or low compliance in the other two patients. Seven patients in regimen B also withdrew prematurely from the study before wk 24 due to intolerance to IFN in six patients, and low compliance in the other patient. Three more patients, all in regimen A, withdrew prematurely from the study before wk 48 because of job transfer or personal problems. Two patients in regimen B withdrew prematurely due to personal problems.

### *Effect of treatment on viremia and serum transaminase*

There were 28/41 (68%) end-of treatment virological responders for regimen A and 32/42 (76%) for regimen B when analyzed on an intention to treat basis; the corresponding values were 28/31 (90%) and 32/33 (97%), respectively, when analyzed on a per-protocol basis (Table 2). There were 22/41 (54%) sustained virological responders for regimen A and 28/42 (67%) responders for regimen B when analyzed on an intention to treat basis; the corresponding values were 22/31 (71%) and 28/33 (85%), respectively, when analyzed on a per-protocol basis. There were 19/41 (46%) end-of treatment biochemical responders for regimen A and 21/42 (50%) responders for regimen B when analyzed on an intention to treat basis; the corresponding values were 19/31 (61%) and 21/33 (64%), respectively, when analyzed on a per-protocol basis. There were 28/41 (68%) sustained biochemical responders for regimen A and 29/42 (69%) responders for regimen B when analyzed on an intention to treat basis; the corresponding values were 28/31 (90%) and 29/33 (88%), respectively, when analyzed on a per-protocol basis. There were no significant differences between the two regimens in these four responses.

### *Factors contributing to sustained virological response*

Variables that correlated with sustained virological response were analyzed by both univariate and multivariate analyses. In univariate analysis, the sustained virological response

**Table 3 Logistic regression model of predictors of response to CIFN treatment**

| Variables | Odds ratio (95% Confidence Interval) | |
|---|---|---|
| Zinc supplementation (regimen B *vs.* A) | 0.254 (0.033-1.948) | 0.1873 |
| BMI (<23.4 *vs.* ≥23.4) | 1.245 (0.162-9.579) | 0.8330 |
| Staging (0-1 *vs.* 2-3) | 0.213 (0.024-1.877) | 0.1635 |
| pretreatment HCV-RNA (<400 *vs.* ≥400) | 0.104 (0.011-0.951) | 0.0450 |
| Week of HCV-RNA clearance (<8 *vs.* ≥8) | 0.106(0.005-2.399) | 0.1584 |
| pretreatment ALT (<107 *vs.* ≥107) | 13.709 (0.960-195.749) | 0.1873 |

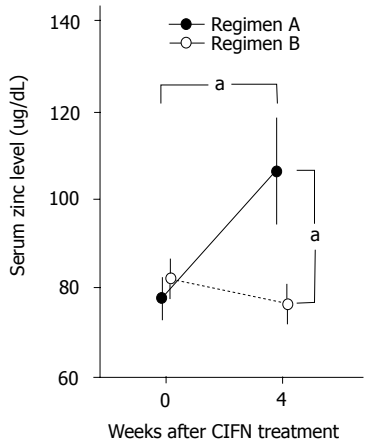


**Figure 2** Serum zinc concentrations (mean±SD) at wk 0 (baseline) and after 4 wk of CIFN treatment in patients with regimen A (closed circles) and regimen B (open circles). Serum zinc levels at wk 4 were significantly higher in regimen A patients than those in regimen B patients ($^aP<0.05$). Serum zinc levels at wk 4 were significantly higher than those recorded at wk 0 (baseline) in regimen A patients ($^aP<0.05$).

**Table 4 Incidence of selected adverse events (>10% frequency)**

| Adverse event | RegimenA (CIFN+zinc) | Regimen B (CIFN) |
|---|---|---|
| *n* | 41 | 42 |
| Fever | 41 (100%) | 42 (100%) |
| Headache | 17 (41.5%) | 16 (38.1%) |
| Malaise | 15 (36.6%) | 12 (28.6%) |
| Anorexia | 14 (34.1%) | 19 (45.2%) |
| Arthralgia | 14 (34.1%) | 13 (31.0%) |
| Insomnia | 11 (26.8%) | 11 (26.2%) |
| Stomach discomfort | 7 (17.1%) | 5 (11.9%) |
| Alopecia | 6 (14.6%) | 6 (14.3%) |
| depression | 6 (14.6%) | 5 (11.9%) |
| Nausea | 6 (14.6%) | 5 (11.9%) |
| Myalgia | 5 (12.2%) | 6 (14.3%) |
| Rash | 5 (12.2%) | 4 (9.5%) |

**Table 5 Incidence of selected laboratory abnormalities (>10% frequency)**

| Laboratory abnormality | Regimen A (CIFN+zinc) | Regimen B (CIFN) |
|---|---|---|
| *n* | 41 | 42 |
| Thrombocytopenia | 31 (78%) | 29 (69%) |
| Leucopenia | 24 (59%) | 30(71%) |
| Increase in AST | 20 (49%) | 18 (43%) |
| Increase in ALT | 18 (44%) | 16 (38%) |
| Increase in γ-GTP | 12 (29%) | 12 (29%) |
| Decrease in hemoglobin | 7 (17%) | 9 (21%) |
| Increase in ZTT | 7 (17%) | 7 (17%) |

correlated significantly with liver histology (staging) and pretreatment HCV-RNA viral load. In multivariate analysis, only pretreatment HCV-RNA less than 400 KIU/mL was associated with a sustained virological response (Table 3). The other factors, including zinc supplementation, BMI, staging, wk of HCV-RNA clearance, and pretreatment ALT level, did not influence sustained virological response.

### *Serum zinc concentrations*

Serum zinc concentrations at 4 wk after the commencement of polaprezinc treatment were elevated and significantly higher than pretreatment levels in regimen A patients (Figure 2). Serum zinc concentrations in patients of regimen A were significantly higher than those of regimen B patients at 4 wk after the start of administration of polaprezinc (Figure 2).

### *Adverse effects*

Each of the serious adverse events including depression, thrombocytopenia, leukopenia, and severe elevations in γGTP was observed in one patient in regimen A. In addition, regimen B was also associated with serious adverse events such as depression in one patient, and severe leukopenia in two patients. Frequent adverse events and laboratory abnormalities recorded during the study are summarized in Tables 4 and 5. The type and frequency of the adverse events, and laboratory abnormalities were similar in both regimens. Five (12.2%) patients and six (14.3%) patients dropped out of the study due to the adverse events before wk 24 in regimen A and regimen B, respectively. There were no significant differences of grading severity of adverse effects as well as incidence of them in the global safety assessment of the two regimens (data not shown).

## DISCUSSION

The metabolism of trace elements is impaired in chronic liver disease[19]. Zinc deficiency in chronic hepatitis C is improved by IFN treatment[28]. Zinc supplementation enhances the response to IFN-α treatment in patients with genotype 1b chronic hepatitis C[20]. Conversely, zinc supplementation did not enhance the response to CIFN treatment in patients with chronic hepatitis C with genotype 2 in this trial. The reasons for the lack of synergy between zinc and IFN are unclear, however, there are several possible reasons that are worthy of consideration. The viral genotype 2 in both regimens may account for the virological response, differing from the previous study that involved patients with genotype Ib. It is also possible

that the relatively higher response rate achieved with CIFN in both regimens in this trial compared with the previous study with IFN-α could have masked any differences in efficacy. In addition, individual differences in serum zinc concentration increases, as a result of zinc administration, may alter the virological response because the extent of the increases in serum zinc concentration varied in regimen A. Furthermore, differences in the type of IFN may affect the virological response, given that natural IFN-α was used in the previous study.

The overall therapeutic efficacy (60% SVR) of CIFN in our study was similar to that (50% SVR) of low-titer or genotype 2 group in a previous report from Japan[18]. Recent reports showed that pegylated-IFN plus ribavirin[29] had excellent treatment efficacy (100% SVR) in chronic hepatitis C patients with genotype 2[30]. SVR rates of IFN-α 2b plus ribavirin for chronic hepatitis C patients with genotypes except 1[11] or CIFN plus ribavirin for chronic hepatitis C patients with genotypes 2/3 were reported to be from 60% to 70%[31]. Given the overall 60% SVR in our study, CIFN without ribavirin can be considered as a good candidate for patients in whom ribavirin is contraindicated.

Interestingly, the cases of undetectable HCV-RNA titer at 1 wk, but not 4 or 12 wk after the start of treatment, showed 95% and 100% of sustained virological response rate in regimens A and B, respectively. Although only a pretreatment HCV-RNA less than 400 KIU/mL was considered to be a predictive factor for sustained virological response, based on a logistic multiple regression model in our trial, earlier responses at 1 wk after the start of treatment may also be a good predictor of sustained virological response.

The type and frequency of adverse events, and laboratory abnormalities were similar in both regimens. Overall, adverse events and laboratory abnormalities were similar to those in previous reports in Japan[18]. Although 18 MIU CIFN was relatively well tolerated in our trial, there were a few cases of serious adverse events. Twelve MIU and nine MIU CIFN, which are now available in Japan, may allow us to reduce the incidence of serious adverse events.

In conclusion, our study does not support the use of zinc as an adjunct to CIFN for the treatment of chronic hepatitis C with genotype 2, because combination treatment was not superior to CIFN monotherapy in achieving a sustained virological response. High viral loads of over 400 KIU/mL may indicate a low probability of sustained virological response for CIFN treatment, regardless of zinc supplementation.

## REFERENCES


1 **Davis GL**, Balart LA, Schiff ER, Lindsay K, Bodenheimer HC Jr, Perrillo RP, Carey W, Jacobson IM, Payne J, Dienstag JL. Treatment of chronic hepatitis C with recombinant interferon alfa. A multicenter randomized, controlled trial. Hepatitis Interventional Therapy Group. *N Engl J Med* 1989; **321:** 1501-1506

2 **Di Bisceglie AM**, Martin P, Kassianides C, Lisker-Melman M, Murray L, Waggoner J, Goodman Z, Banks SM, Hoofnagle JH. Recombinant interferon alfa therapy for chronic hepatitis C. A randomized, double-blind, placebo-controlled trial. *N Engl J Med* 1989; **321:** 1506-1510

3 **Kasahara A**, Hayashi N, Mochizuki K, Takayanagi M, Yoshioka K, Kakumu S, Iijima A, Urushihara A, Kiyosawa K, Okuda M, Hino K, Okita K. Risk factors for hepatocellular carcinoma and its incidence after interferon treatment in patients with chronic hepatitis C. Osaka Liver Disease Study Group. *Hepatology* 1998; **27:** 1394-1402

4 **Yoshida H**, Shiratori Y, Moriyama M, Arakawa Y, Ide T, Sata M, Inoue O, Yano M, Tanaka M, Fujiyama S, Nishiguchi S, Kuroki T, Imazeki F, Yokosuka O, Kinoyama S, Yamada G, Omata M. Interferon therapy reduces the risk for hepatocellular carcinoma: national surveillance program of cirrhotic and noncirrhotic patients with chronic hepatitis C in Japan. IHIT Study Group. Inhibition of Hepatocarcinogenesis by Interferon Therapy. *Ann Intern Med* 1999; **131:** 174-181

5 **Ikeda K**, Saitoh S, Arase Y, Chayama K, Suzuki Y, Kobayashi M, Tsubota A, Nakamura I, Murashima N, Kumada H, Kawanishi M. Effect of interferon therapy on hepatocellular carcinogenesis in patients with chronic hepatitis type C: A long-term observation study of 1,643 patients using statistical bias correction with proportional hazard analysis. *Hepatology* 1999; **29:** 1124-1130

6 **Okanoue T**, Itoh Y, Minami M, Sakamoto S, Yasui K, Sakamoto M, Nishioji K, Murakami Y, Kashima K. Interferon therapy lowers the rate of progression to hepatocellular carcinoma in chronic hepatitis C but not significantly in an advanced stage: a retrospective study in 1148 patients. Viral Hepatitis Therapy Study Group. *J Hepatol* 1999; **30:** 653-659

7 **Okanoue T**, Itoh Y, Kirishima T, Daimon Y, Toyama T, Morita A, Nakajima T, Minami M. Transient biochemical response in interferon therapy decreases the development of hepatocellular carcinoma for five years and improves the long-term survival of chronic hepatitis C patients. *Hepatol Res* 2002; **23:** 62-77

8 **Poynard T**, Leroy V, Cohard M, Thevenot T, Mathurin P, Opolon P, Zarski JP. Meta-analysis of interferon randomized trials in the treatment of viral hepatitis C: effects of dose and duration. *Hepatology* 1996; **24:** 778-789

9 **Carithers RL Jr**, Emerson SS. Therapy of hepatitis C: meta-analysis of interferon alfa-2b trials. *Hepatology* 1997; **26**: 83S-88S

10 **Orito E**, Mizokami M, Nakano T, Terashima H, Nojiri O, Sakakibara K, Mizuno M, Ogino M, Nakamura M, Matsumoto Y. Serum hepatitis C virus RNA level as a predictor of subsequent response to interferon-alpha therapy in Japanese patients with chronic hepatitis C. *J Med Virol* 1994; **44:** 410-414

11 **McHutchison JG**, Gordon SC, Schiff ER, Shiffman ML, Lee WM, Rustgi VK, Goodman ZD, Ling MH, Cort S, Albrecht JK. Interferon alfa-2b alone or in combination with ribavirin as initial treatment for chronic hepatitis C. Hepatitis Interventional Therapy Group. *N Engl J Med* 1998; **339:** 1485-1492

12 **Poynard T**, Marcellin P, Lee SS, Niederau C, Minuk GS, Ideo G, Bain V, Heathcote J, Zeuzem S, Trepo C, Albrecht J. Randomised trial of interferon alpha2b plus ribavirin for 48 weeks or for 24 weeks versus interferon alpha2b plus placebo for 48 weeks for treatment of chronic infection with hepatitis C virus. International Hepatitis Interventional Therapy Group (IHIT) *Lancet* 1998; **352:** 1426-1432

13 **Davis GL**, Esteban-Mur R, Rustgi V, Hoefs J, Gordon SC, Trepo C, Shiffman ML, Zeuzem S, Craxi A, Ling MH, Albrecht J. Interferon alfa-2b alone or in combination with ribavirin for the treatment of relapse of chronic hepatitis C. International Hepatitis Interventional Therapy Group. *N Engl J Med* 1998; **339:** 1493-1499

14 **Barbaro G**, Di Lorenzo G, Belloni G, Ferrari L, Paiano A, Del Poggio P, Bacca D, Fruttaldo L, Mongio F, Francavilla R, Scotto G, Grisorio B, Calleri G, Annese M, Barelli A, Rocchetto P, Rizzo G, Gualandi G, Poltronieri I, Barbarini G. Interferon alpha-2B and ribavirin in combination for patients with chronic hepatitis C who failed to respond to, or relapsed after, interferon alpha therapy: a randomized trial. *Am J Med* 1999; **107:** 112-118

15 **Blatt LM**, Davis JM, Klein SB, Taylor MW. The biologic activity and molecular characterization of a novel synthetic interferon-alpha species, consensus interferon. *J Interferon Cytokine*

*Res* 1996; **16**: 489-499
16 **Alton K** , Stabinshy Y, Richards R, *et al*. Production, characterization and biological effects of recombinant DNA derived human interferon-α and interferon-γ analogs. In: The Biology of the Interferon System. *Amsterdam: Elsevier Science*, 1983: 119-128
17 **Ozes ON**, Reiter Z, Klein S, Blatt LM, Taylor MW. A comparison of interferon-Con1 with natural recombinant interferons-alpha: antiviral, antiproliferative, and natural killer-inducing activities. *J Interferon Res* 1992; **12**: 55-59
18 **Suzuki H**, Tango T. A multicenter, randomized, controlled clinical trial of interferon alfacon-1 in comparison with lymphoblastoid interferon-alpha in patients with high-titer chronic hepatitis C virus infection. *Hepatol Res* 2002; **22**: 1-12
19 **Loguercio C**, De Girolamo V, Federico A, Feng SL, Cataldi V, Del Vecchio Blanco C, Gialanella G. Trace elements and chronic liver diseases. *J Trace Elem Med Biol* 1997; **11:** 158-161
20 **Takagi H**, Nagamine T, Abe T, Takayama H, Sato K, Otsuka T, Kakizaki S, Hashimoto Y, Matsumoto T, Kojima A, Takezawa J, Suzuki K, Sato S, Mori M. Zinc supplementation enhances the response to interferon therapy in patients with chronic hepatitis C. *J Viral Hepat* 2001; **8:** 367-371
21 **Novick SG**, Godfrey JC, Pollack RL, Wilder HR. Zinc-induced suppression of inflammation in the respiratory tract, caused by infection with human rhinovirus and other irritants. *Med Hypotheses* 1997; **49**: 347-357
22 **Kumel G**, Schrader S, Zentgraf H, Brendel M. [Therapy of banal HSV lesions: molecular mechanisms of the antiviral activity of zinc sulfate]. *Hautarzt* 1991; **42**: 439-445
23 **Powell SR**. The antioxidant properties of zinc. *J Nutr* 2000; **130**: 1447S-1454S
24 **Prasad AS**. Zinc and immunity. *Mol Cell Biochem* 1998; **188**: 63-69
25 **Tsubota A**, Chayama K, Ikeda K, Yasuji A, Koida I, Saitoh S, Hashimoto M, Iwasaki S, Kobayashi M, Hiromitsu K. Factors predictive of response to interferon-alpha therapy in hepatitis C virus infection. *Hepatology* 1994; **19:** 1088-1094
26 **Martinot-Peignoux M**, Marcellin P, Pouteau M, Castelnau C, Boyer N, Poliquin M, Degott C, Descombes I, Le Breton V, Milotova V. Pretreatment serum hepatitis C virus RNA levels and hepatitis C virus genotype are the main and independent prognostic factors of sustained response to interferon alfa therapy in chronic hepatitis C. *Hepatology* 1995; **22:** 1050-1056
27 **Desmet VJ**, Gerber M, Hoofnagle JH, Manns M, Scheuer PJ. Classification of chronic hepatitis: diagnosis, grading and staging. *Hepatology* 1994; **19**: 1513-1520
28 **Nagamine T**, Takagi H, Hashimoto Y, Takayama H, Shimoda R, Nomura N, Suzuki K, Mori M, Nakajima K. The possible role of zinc and metallothionein in the liver on the therapeutic effect of IFN-alpha to hepatitis C patients. *Biol Trace Elem Res* 1997; **58:** 65-76
29 **Zeuzem S**, Hultcrantz R, Bourliere M, Goeser T, Marcellin P, Sanchez-Tapias J, Sarrazin C, Harvey J, Brass C, Albrecht J. Peginterferon alfa-2b plus ribavirin for treatment of chronic hepatitis C in previously untreated patients infected with HCV genotypes 2 or 3. *J Hepatol* 2004; **40:** 993-999
30 **Seeff LB**, Hoofnagle JH. National Institutes of Health Consensus Development Conference: management of hepatitis C: 2002. *Hepatology* 2002; **36**: S1- S2
31 **Fattovich G**, Zagni I, Minola E, Felder M, Rovere P, Carlotto A, Suppressa S, Miracolo A, Paternoster C, Rizzo C, Rossini A, Benedetti P, Capanni M, Ferrara C, Costa P, Bertin T, Pantalena M, Lomonaco L, Scattolini C, Mazzella G, Giusti M, Boccia S, Milani S, Marin R, Lisa Ribero M, Tagger A. A randomized trial of consensus interferon in combination with ribavirin as initial treatment for chronic hepatitis C. *J Hepatol* 2003; **39:** 843-849

**S- Editor** Guo SY **L- Editor** Elsevier HK **E- Editor** Bai SH

PO Box 2345, Beijing 100023, China
www.wjgnet.com
wjg@wjgnet.com

*World J Gastroenterol* 2006 February 14; 12(6): 951-955
***World Journal of Gastroenterology*** ISSN 1007-9327
© 2006 The WJG Press. All rights reserved.

*RAPID COMMUNICATION*

# Absence of *MutY* homologue mutation in patients with multiple sporadic adenomatous polyps in Korea

Hansoo Kim, Hyo-Jong Kim, Sung-Gil Chi, Sang-Kil Lee, Gwang-Ro Joo, Seok-Ho Dong, Byung-Ho Kim, Young-Woon Chang, Jung-Il Lee, Rin Chang

Hansoo Kim, Hyo-Jong Kim, Sang-Kil Lee, Gwang-Ro Joo, Seok-Ho Dong, Byung-Ho Kim, Young-Woon Chang, Jung-Il Lee, Rin Chang, Department of Internal Medicine, College of Medicine, Kyung Hee University, Seoul, Korea
Sung-Gil Chi, Department of Bioscience, College of Life Sciences, Korea University, Seoul, Korea
Correspondence to: Dr. Hyo-Jong Kim, Department of Medicine, Kyung Hee University School of Medicine, #1 Hoegi-Dong, Dongdaemun-Gu, Seoul 130-702, Korea. hjkim@khmc.or.kr
Telephone: +82-2-958-8200 Fax: +82-2-968-1848
Received: 2005-03-17 Accepted: 2005-06-18

## Abstract

**AIM**: Recently, germ-line mutation in the base excision repair gene *MYH* has been identified to cause a novel autosomal recessive form of familial adenomatous polyposis (FAP). Interestingly, a striking evidence for *MYH* mutations within different ethnic groups has been demonstrated. In this study, we screened 30 patients with multiple adenomatous polyps for *MYH* mutations to assess its prevalence and ethnic specificity in Korea.

**METHODS**: Thirty patients (21 men and 9 women; mean age 62.3 years) with multiple adenomatous polyps were examined for *MYH* mutations. The mean number of adenomas per patient was 10.0. Sixteen exonic regions and their intronic sequences were amplified by PCR and subjected to SSCP and DNA sequencing analyses.

**RESULTS**: None of the patients was identified to carry any truncating or sequence alterations in *MYH*. Our screening for the mutational regions, which were recognized from Caucasian patients or affected Indian families, also failed to detect sequence substitutions.

**CONCLUSION**: Mutation in *MYH* may be rarely involved in the pathogenesis of multiple sporadic colorectal adenomas in Korean population, although a large-scale analysis will be required to clarify the presence of specific *MYH* variants in a subset of patients and their role in the predisposition of multiple colorectal adenomas in Korean population.

© 2006 The WJG Press. All rights reserved.

**Key words**: MY; Multiple adenomatous polyps; Germ-line mutation; Familial adenomatous polyposis; Ethnic difference

Kim H, Kim HJ, Chi SG, Lee SK, Joo GR, Dong SH, Kim BH, Chang YW, Lee JI, Chang R. Absence of *MutY* homologue mutation in patients with multiple sporadic adenomatous polyps in Korea. *World J Gastroenterol* 2006; 12(6): 951-955

http://www.wjgnet.com/1007-9327/12/951.asp

## INTRODUCTION

It has been well established that genetic factors play a pivotal role in up to 35% of all colorectal cancers (CRC)[1-3]. Familial adenomatous polyposis (FAP) is an autosomal dominant disorder with an increased predisposition to multiple colorectal adenomatous polyps, and thence to CRCs[4]. Classic FAP is caused by inherited mutations in the adenomatous polyposis coli (*APC*) gene, which encodes a protein that plays a critical role in the regulation of colonic cell growth[5,6]. Attenuated FAP (AFAP) is associated with smaller numbers of adenomas and is caused by mutations in the extreme of 5' or 3' ends of *APC* or in the alternatively spliced region of exon 9[4,5].

Somatic mutations of *APC* consist of the substitution of a thymine-adenine pair for a guanine-cytosine pair (G:C→T:A), which is a typical change caused by oxidative damage to DNA[7-11]. Oxidative DNA damage produces the stable 8-oxo-7, 8-dihydro2'deoxyguanosine (8-oxoG)[9]. It is highly mutagenic because it tends to mispair with adenine residues, leading to an increased frequency of spontaneous G:C→T:A transversion mutations in repair-deficient bacteria and yeast cells[10-13].

Recently, Al-Tassan *et al*[14] reported a novel autosomal recessive form of FAP. They found that three of seven siblings from a single British Caucasian family were all compound heterozygous for two non-conservative missense variants, Y165C and G382D, in the base excision repair gene *MutY* homologue (*MYH*). This finding first implicated a defect in the base excision repair mechanism in inherited predisposition to colorectal tumors in human beings.

Base excision repair (BER) is cell's mechanism of protection against oxidative DNA damage[15]. The BER pathway repairs mutations caused by reactive oxygen species that are generated during aerobic metabolism[16]. Three main components of BER have been identified in human. *MutT* homologue (*MTH*) removes oxidized base from 8-oxoG:C pairs to reduce the chances of incorporation of

**Table 1 Characteristics of patients**

| Characteristics | Patient with CRC and adenomatous polyp ($n$ = 10) | Patient with adenomatous polyp only ($n$ = 20) |
|---|---|---|
| Sex | 3 males : 1 females | 15 males : 5 females |
| Age (yr) | Mean 45.9 (range: 21 ~ 78) | Mean 51.8 (range: 44 ~ 69) |
| Number of adenomatous polyps | Mean 9 (range: 1 ~ 10) | Mean 7 (range: 3 ~ 100) |
| Family history of adenomatous polyps | 0 | 0 |

CRC: colorectal cancer.

8-oxoG during DNA replication, and 8-oxoG glycosylase (OGG) initiates base-excision of 8-oxoG from 8-oxoG:C pairs[17]. Adenine-specific DNA glycosylase *MYH* removes adenine mispaired with 8-oxoG in 8-oxoG:A pairs. [18-20]

The prevalence of *MYH* mutations has been determined in patients with multiple colorectal polyps in Caucasian populations. However, to our knowledge, a few studies have been carried out regarding the prevalence of *MYH* mutations in Asian patients with multiple colorectal adenomatous polyps. In the present study, we therefore explored the possible implication of germ-line mutations of *MYH* in the development of multiple sporadic colorectal adenomatous polyps in Korean population.

## METHODS

### Specimens

Thirty patients (21 men and 9 women; mean age, 62.3 years) with multiple sporadic colorectal adenomatous polyps were recruited from Kyung Hee University, Medical Center, Seoul, Korea. All patients were Korean and none had a family history of vertical transmission of colorectal cancer or adenomatous polyps. Five individuals who did not have any recognizable diseases were selected as healthy controls. Informed consent was taken from all patients. Ten milliliters of blood were obtained from all the patients and healthy controls for extraction of genomic DNA. The characteristics of patients are summarized in Table 1.

**Table 2 Primer sequences of oligonucleotide primers used for PCR-SSCP analysis of *MYH***

| Exon | Primers | Sequences (5′ to 3′) | Length (bp) |
|---|---|---|---|
| 1 | M1S | CAGAGCGCAGAGGCTTTGAACA | 240 |
| | M1AS | CTGAACGGAAGTTCGACCCATC | |
| 2 | M2S | AATTTGGCCTCATTGTGACTGA | 221 |
| | M2AS | AATCTGCCTTTCATGGCCAATG | |
| 3 | M3S | CACAGGCTGCTGTGTCCCAAGA | 259 |
| | M3AS | CCCACCCACTGTCCCTGCTCCT | |
| 4+5 | M45S | AACTCCTCATCTGGGGTTGCAT | 296 |
| | M45AS | GGTCTGACCCATGACCCTTCCC | |
| 6+7 | M67S | ACCACCTTCACCCTTGACCTTG | 268 |
| | M67AS | ACCCAAGACTCCTGGGTTCCTA | |
| 8 | M8S | GGAACCCAGGAGTCTTGGGTGT | 222 |
| | M8AS | AAGGAGGCTGGGCACGCACAAA | |
| 9 | M9S | TTTGTGCGTGCCCAGCCTGGTT | 223 |
| | M9AS | TGCTGTGAAGCAGAGCTCCAAA | |
| 10 | M10S | AAAGGAGCTCTGCTTCACAGCA | 227 |
| | M10AS | CACTCCTTAGGACTTCTCACTG | |
| 11 | M11S | GTAAGCCTACTGGGGAAGGGG | 222 |
| | M11AS | GCAGAATCTTACTCAGGTTAG | |
| 12 | M12S | GCCCTCTTGGCTTGAGTAGGGT | 278 |
| | M12AS | TCTCTTGTTACTCATGCCACTG | |
| 13 | M13S | AGGGAATCGGCAGCTGAGGCCT | 226 |
| | M13AS | AAAAGCCAACATCCTTGGCTAT | |
| 14 | M14S | TATATCCACAGGCCTATTTGAA | 256 |
| | M14AS | ATATTCATGTAGAACATGTAGG | |
| 15 | M15S | GACATGAAGTTAAGGGCAGAAC | 212 |
| | M15AS | TGTTCACCCAGACATTCGTTAG | |
| 16 | M16S | AACTACAAGGCCTCCCTCCTTCCA | 270 |
| | M16AS | AACAACAGGATTCTCAGGGAATG | |

### PCR amplification of MYH gene

Genomic DNA was prepared from venous blood samples using QIAGEN Genomic-tip system (Qiagen, Hilden, Germany) according to the manufacturer's instructions. The concentration of extracted DNA was determined by a spectrophotometric measurement (Schimadzu Scientific Instruments, Inc., Concord, CA). Exons 1-16 of *MYH* and their flanking intronic sequences were amplified by PCR with 14 primer sets which cover the entire coding region of *MYH*. Primer sequences used for PCR amplification are shown in Table 2. PCR was performed with 200 ng genomic DNA as template for 38 cycles at 95℃ (1 min), 58-62℃ (30 s), and 72℃ (30 s) in 1.5 mmol/L $MgCl_2$-containing reaction buffer (PCR buffer II, Perkin Elmer-Cetus, Concord, CA). Ten microliters of PCR products were electrophoresed on 20 g/L agarose gel containing ethidium bromide, visualized under ultraviolet light, and photographed.

### Single strand conformation polymorphism analysis

To identify sequence alterations in the *MYH* gene, we performed nonisotopic PCR-SSCP analysis as described previously[14]. Briefly, 20 μL of the PCR products was mixed with 5 μL of 0.5 mol/L NaOH, 10 mmol/L EDTA and 10 μL of denaturing loading buffer (950 mL/L formamide, 20 mmol/L EDTA, 0.5 g/L bromophenol blue, and 0.5 g/L xylene cyanol). After heating at 95℃ for 5 min, the samples were rapidly loaded in wells pre-cooled to 4℃ and run simultaneously on two 80 g/L non-denaturing polyacrylamide gels with or without 100 g/L glycerol. These two gels were run at 18-20℃ and then repeated at 6-10℃ in a buffer-jacketed gel apparatus (DGGE-II; Aladin Enterprises, Inc., San Francisco, CA). Following an 8 h run at 400 volts, the gels were stained with ethidium bromide and photographed under ultraviolet light.

### Automated DNA sequencing

PCR amplification products were purified using the PCR purification kit (Quiagen). DNA sequencing was carried out using ABI PRISM 377 automated DNA sequencer (Applied Biosystems, Foster City, CA) according to the

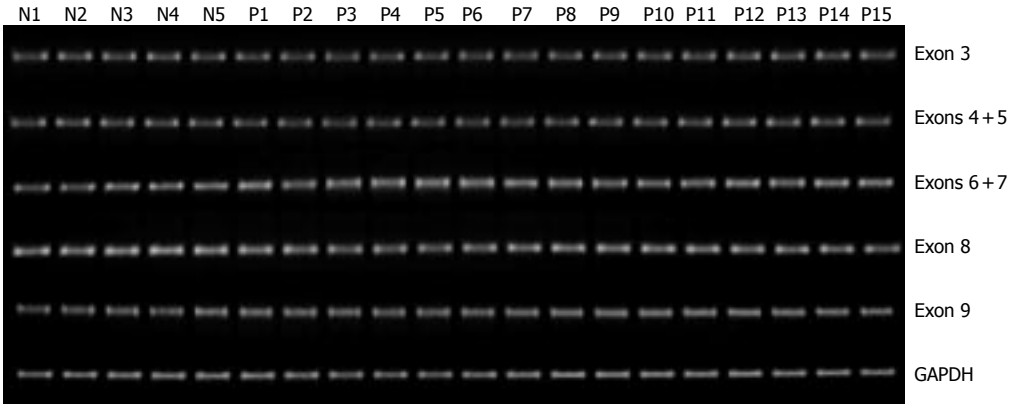


**Figure 1** Genomic status of MYH in patients with multiple colorectal adenomas determined by quantitative DNA-PCR analysis. Representative examples for exons 3-9 amplification are shown. Two hundred nanograms of DNA obtained from 30 patients and 5 healthy controls were used as templates for PCR amplification of 16 exonic regions using 14 intronic primer sets. GAPDH was used as an internal control for PCR. Ten microliters of PCR product was resolved on 20 g/L agarose gel and visualized by ethidium bromide staining. No significant reduction of gene levels was identified in samples from patients as compared with normal controls. Lanes N1-N5: Normal controls; Lanes P1-P15: Patients.

manufacturer's instructions. Sequencing was carried out in both directions to confirm the findings.

## RESULTS

To explore the presence of germ-line alterations of *MYH*, we, using quantitative genomic PCR analysis, initially evaluated genomic status of *MYH*. Blood DNA samples from 30 patients with multiple sporadic colorectal adenomatous polyps and 5 healthy individuals were subjected to PCR amplification of *MYH*. All of the 16 exons and flanking intronic sequences of the gene were amplified as 14 fragments using intron-specific primer sets, and their levels in the patients were compared with those in healthy controls. As shown in Figure 1, genomic levels of *MYH*, which were evaluated for 14 separate gene regions, showed no detectable difference between patients and healty individuals, and none of the patients was found to have structural alteration within these protein-encoding regions of the gene. Although systemic analysis for the genomic status was not carried out in this study, the results suggested that our patients did not harbor germ-line deletion or structural abnormalities of the gene, which could result in loss or significant reduction of MYH protein function.

Using PCR-SSCP and DNA sequencing analyses, we next screened for mutations and sequence variants across the entire coding region of the *MYH* gene. To detect the *MYH* variants, such as Y165C, G382D, Y90X and E466X, which are commonly observed in Caucasian patients or affected Indian families, we performed comprehensive SSCP assay under four different running conditions[14]. However, we could not observe any truncating *MYH* mutations in patient or control samples. Neither did we identify any likely pathogenic mutations and sequence variants in the patient samples. Representative examples of SSCP analysis are shown in Figure 2.

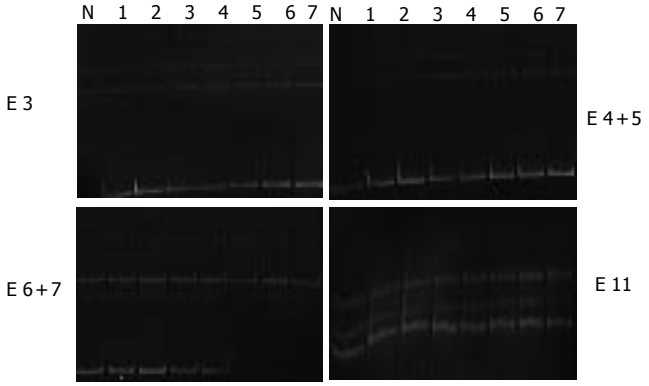


**Figure 2** Non-isotopic PCR-SSCP analysis of MYH. For detection of sequence alterations, all of the 16 exons and flanking intronic sequences were amplified by PCR as 14 separate fragments, and 20 μL of PCR product was subjected to non-isotopic SSCP analysis. Genomic DNA isolated from the healthy controls was used as normal controls. None of patient samples showed abnormal migration shift of single strand DNA molecules. Lane N: Normal control; Lanes 1-7: Patients; Lane E: Exons.

## DISCUSSION

Germ-line mutation of the *MYH* gene has been known to predispose persons in a variety of European populations to recessive inheritance of multiple colorectal adenomatous polyposis and classic FAP[4, 22]. In addition, all patients with bialleic *MYH* mutations have an increased predisposition to CRCs.

*MYH* mutation presents with a distinguished genetic pathway in developing colorectal tumors. Many questions regarding its role in pathogenesis of multiple colorectal adenomatous polyps and CRCs still remain open. For example, it has not been identified why germ-line *MYH* mutations are associated with tumors of gastrointestinal tract, or why *MYH* polyposis differs in its phenotype and inheritance from classical FAP[21].

It is difficult to distinguish between patients with *APC* mutations and those with *MYH* germ-line mutation on the basis of clinical features or pathological findings. *MYH* mutations seem to be a more common cause of the multiple adenoma phenotypes than are *APC* mutations[23-26]. They are, however, a less common cause of classic colorectal adenomatous polyposis.

Jones *et al*[4] could not identify any pathogenic variants in BER genes *OGG1* or *MTH1* in cases with colorectal tumors. Thus, there is a possibility that these genes are less frequently mutated than *MYH*. It is also possible that those mutations do not predispose to tumors in humans due to unknown mechanism. However, further studies are required to determine whether *OGG1* or *MTH1* are involved in CRC predisposition.

On the basis of previous studies, genetic analysis of *MYH* mutation should be considered for patients with a phenotype resembling FAP or AFAP, when no clear evidence of vertical transmission is noted. However, whether it is worthwhile to perform genetic testing in the family of patients with *MYH* mutations is a question that still remains unclear.

In the present study, we failed to detect any truncating or sequence alterations of the *MYH* gene in Korean patients with multiple colorectal adenomas. Although patient numbers enrolled in this study are too small to exclude the association of *MYH* mutations with development of multiple colonic adenoma in Korean population, our data suggests the presence of ethnic difference in contribution of *MYH* mutations to disease development between the Korean patients and the white patients. Previous studies identified four British families that were either homozygous for Y165C or compound heterozygous for Y165C/G382D, three Indian families that were homozygous for E466X, and a single Pakistani family that was homozygous for Y90X[4]. Specific *MYH* mutations appear to be identified in different ethnic groups. A question still remains as to how frequently MYH mutations contribute to the phenotype of apparently sporadic AFAP/FAP. Further studies of patients from distinct geographical and ethnic groups will help to define the possible ethnic differences in actual mutations.

In conclusion, our observations suggest that *MYH* mutations are not common in patients with multiple colorectal adenomas in Korean population. Considering that number and histology of colorectal polyps are the cornerstones of detection of many CRC predisposition conditions, further larger-scale evaluation including the histologic analyses of the polyps, is required to determine whether *MYH* polymorphisms play a role in predisposition of a subset of multiple sporadic colorectal adenomas in Korean population.

## REFERENCES


1 **Cannon-Albright LA**, Skolnick MH, Bishop DT, Lee RG, Burt RW. Common inheritance of susceptibility to colonic adenomatous polyps and associated colorectal cancers. *N Engl J Med* 1988; **319**: 533-537

2 **Houlston RS**, Collins A, Slack J, Morton NE. Dominant genes for colorectal cancer are not rare. *Ann Hum Genet* 1992; **56 ( Pt 2):** 99-103

3 **Lichtenstein P**, Holm NV, Verkasalo PK, Iliadou A, Kaprio J, Koskenvuo M, Pukkala E, Skytthe A, Hemminki K. Environmental and heritable factors in the causation of cancer--analyses of cohorts of twins from Sweden, Denmark, and Finland. *N Engl J Med* 2000; **343**: 78-85

4 **Jones S**, Emmerson P, Maynard J, Best JM, Jordan S, Williams GT, Sampson JR, Cheadle JP. Biallelic germline mutations in MYH predispose to multiple colorectal adenoma and somatic G:C-->T:A mutations. *Hum Mol Genet* 2002; **23**: 2961-2967

5 **Fearnhead NS**, Britton MP, Bodmer WF. The ABC of *APC*. *Hum Mol Genet* 2001; **10**: 721-733

6 **Fearnhead NS**. Familial adenomatous polyposis and *MYH*. *Lancet* 2003; **362**: 5-6

7 **Halliwell B**. Mechanisms involved in the generation of free radicals. *Pathol Biol (Paris)* 1996; **44**: 6-13

8 **Wang D**, Kreutzer DA, Essigmann JM. Mutagenicity and repair of oxidative DNA damage: insights from studies using defined lesions. *Mutat Res* 1998; **400**: 99-115

9 **Shibutani S**, Takeshita M, Grollman AP. Insertion of specific bases during DNA synthesis past the oxidation-damaged base 8-oxodG. *Nature* 1991; **349**: 431-434

10 **Nghiem Y**, Cabrera M, Cupples CG, Miller JH. The mutY gene: a mutator locus in Escherichia coli that generates G.C---T.A transversions. *Proc Natl Acad Sci U S A* 1988; **85**: 2709-2713

11 **Michaels ML**, Miller JH. The GO system protects organisms from the mutagenic effect of the spontaneous lesion 8-hydroxyguanine (7,8-dihydro-8-oxoguanine). *J Bacteriol* 1992; 1**74**: 6321-6325

12 **Moriya M**, Grollman AP. Mutations in the mutY gene of Escherichia coli enhance the frequency of targeted G:C-->T:a transversions induced by a single 8-oxoguanine residue in single-stranded DNA. *Mol Gen Genet* 1993; **239**: 72-76

13 **Thomas D**, Scot AD, Barbey R, Padula M, Boiteux S. Inactivation of OGG1 increases the incidence of G . C-->T . A transversions in Saccharomyces cerevisiae: evidence for endogenous oxidative damage to DNA in eukaryotic cells. *Mol Gen Genet* 1997; **254**: 171-178

14 **Al-Tassan N**, Chmiel NH, Maynard J, Fleming N, Livingston AL, Williams GT, Hodges AK, Davies DR, David SS, Sampson JR, Cheadle JP. Inherited variants of MYH associated with somatic G:C-->T:A mutations in colorectal tumors. *Nat Genet* 2002; **30**: 227-232

15 **Lindahl T**. Instability and decay of the primary structure of DNA. *Nature* 1993; **362**: 709-715

16 **Sakumi K**, Furuichi M, Tsuzuki T, Kakuma T, Kawabata S, Maki H, Sekiguchi M. Cloning and expression of cDNA for a human enzyme that hydrolyzes 8-oxo-dGTP, a mutagenic substrate for DNA synthesis. *J Biol Chem* 1993; **268**: 23524-23530

17 **Roldan-Arjona T,** Wei YF, Carter KC, Klungland A, Anselmino C, Wang RP, Augustus M, Lindahl T. Molecular cloning and functional expression of a human cDNA encoding the antimutator enzyme 8-hydroxyguanine-DNA glycosylase. *Proc Natl Acad Sci U S A* 1997; **94:** 8016-8020

18 **McGoldrick JP**, Yeh YC, Solomon M, Essigmann JM, Lu AL. Characterization of a mammalian homolog of the Escherichia coli MutY mismatch repair protein. *Mol Cell Biol* 1995; **15**: 989-996

19 **Ohtsubo T**, Nishioka K, Imaiso Y, Iwai S, Shimokawa H, Oda H, Fujiwara T, Nakabeppu Y. Identification of human MutY homolog (hMYH) as a repair enzyme for 2-hydroxyadenine in DNA and detection of multiple forms of hMYH located in nuclei and mitochondria. *Nucleic Acids Res* 2000; **28**: 1355-1364

20 **Takao M**, Zhang QM, Yonei S, Yasui A. Differential subcellular localization of human *MutY* homolog (*hMYH*) and the functional activity of adenine:8-oxoguanine DNA glycosylase. *Nucleic Acids Res* 1999; **27**: 3638-3644

21 **Lipton L**, Halford SE, Johnson V, Novelli MR, Jones A, Cummings C, Barclay E, Sieber O, Sadat A, Bisgaard ML, Hodgson SV, Aaltonen LA, Thomas HJ, Tomlinson IP. Carcinogenesis in MYH-associated polyposis follows a distinct genetic pathway. *Cancer Res* 2003; **63**: 7595-7599

22 **Sieber OM**, Lipton L, Crabtree M, Heinimann K, Fidalgo P, Phillips RK, Bisgaard ML, Orntoft TF, Aaltonen LA, Hodgson SV, Thomas HJ, Tomlinson IP. Multiple colorectal adenomas, classic adenomatous polyposis, and germ-line mutations in MYH. *N Engl J Med* 2003; **348**: 791-799

23 **Kohno T**, Shinmura K, Tosaka M, Tani M, Kim SR, Sugimura H, Nohmi T, Kasai H, Yokota J. Genetic polymorphisms and alternative splicing of the hOGG1 gene, that is involved in the repair of 8-hydroxyguanine in damaged DNA. *Oncogene* 1998; **16**: 3219-3225

24 **Wikman H**, Risch A, Klimek F, Schmezer P, Spiegelhalder B, Dienemann H, Kayser K, Schulz V, Drings P, Bartsch H. hOGG1 polymorphism and loss of heterozygosity (LOH): significance for lung cancer susceptibility in a caucasian population. *Int J Cancer* 2000; **88**: 932-937

25 **Hanaoka T**, Sugimura H, Nagura K, Ihara M, Li XJ, Hamada GS, Nishimoto I, Kowalski LP, Yokota J, Tsugane S. hOGG1 exon7 polymorphism and gastric cancer in case-control studies of Japanese Brazilians and non-Japanese Brazilians. *Cancer Lett* 2001; **170**: 53-61

26 **Lamlum H**, Al Tassan N, Jaeger E, Frayling I, Sieber O, Reza FB, Eckert M, Rowan A, Barclay E, Atkin W, Williams C, Gilbert J, Cheadle J, Bell J, Houlston R, Bodmer W, Sampson J, Tomlinson I. Germline APC variants in patients with multiple colorectal adenomas, with evidence for the particular importance of E1317Q. *Hum Mol Genet* 2000; **9**: 2215-2221

**S- Editor** Kumar M and Guo SY **L- Editor** Elsevier HK **E- Editor** Bi L

PO Box 2345, Beijing 100023, China
www.wjgnet.com
wjg@wjgnet.com

*World J Gastroenterol* 2006 February 14; 12(6): 956-960
***World Journal of Gastroenterology*** ISSN 1007-9327
© 2006 The WJG Press. All rights reserved.

*RAPID COMMUNICATION*

# Risk factors of acute cholecystitis after endoscopic common bile duct stone removal

Jun Kyu Lee, Ji Kon Ryu, Joo Kyung Park, Won Jae Yoon, Sang Hyub Lee, Kwang Hyuck Lee, Yong-Tae Kim, Yong Bum Yoon

Jun Kyu Lee, Ji Kon Ryu, Joo Kyung Park, Won Jae Yoon, Sang Hyub Lee, Kwang Hyuck Lee, Yong-Tae Kim, Yong Bum Yoon, Department of Internal Medicine, Seoul National University College of Medicine, Seoul, Korea
Correspondence to: Ji-Kon Ryu, MD, Department of Internal Medicine, Seoul National University College of Medicine, 28 Yongon-dong, Chongno-gu, 110-744 Seoul, Korea. jkryu@snu.ac.kr
Telephone: +82-2-2072-1962 Fax: +82-2-743-6701
Received: 2005-04-21 Accepted: 2005-08-26

## Abstract

**AIM:** To evaluate the risk factors of acute cholecystitis after endoscopic common bile duct (CBD) stone removal.

**METHODS:** A total 100 of patients who underwent endoscopic CBD stone removal with gallbladder (GB) *in situ* without subsequent cholecystectomy from January 2000 to July 2004 were evaluated retrospectively. The following factors were considered while evaluating risk factors for the development of acute cholecystitis: age, gender, serum bilirubin level, GB wall thickening, cystic duct patency, presence of a GB stone, CBD diameter, residual stone, lithotripsy, juxtapapillary diverticulum, presence of liver cirrhosis or diabetes mellitus, a presenting illness of cholangitis or pancreatitis, and procedure-related complications.

**RESULTS:** During a mean 18-mo follow-up, 28 (28%) patients developed biliary symptoms; 17 (17%) acute cholecystitis and 13 (13%) CBD stone recurrence. Of patients with acute cholecystitis, 15 (88.2%) received laparoscopic cholecystectomy and 2 (11.8%) open cholecystectomy. All recurrent CBD stones were successfully removed endoscopically. The mean time elapse to acute cholecystitis was 10.2 mo (1-37 mo) and that to recurrent CBD stone was 18.4 mo. Of the 17 patients who received cholecystectomy, 2 (11.8%) developed recurrent CBD stones after cholecystectomy. By multivariate analysis, a serum total bilirubin level of <1.3 mg/dL and a CBD diameter of <11 mm at the time of stone removal were found to predict the development of acute cholecystitis.

**CONCLUSION:** After CBD stone removal, there is no need for routine prophylactic cholecystectomy. However, patients without a dilated bile duct (<11 mm) and jaundice (<1.3 mg/dL) at the time of CBD stone removal have a higher risk of acute cholecystitis and are possible candidates for prophylactic cholecystectomy.

© 2006 The WJG Press. All rights reserved.

**Key words:** Sphincterotomy; Choledocholithiasis; Acute cholecystitis; Cholecystectomy

Lee JK, Ryu JK, Park JK, Yoon WJ, Lee SH, Lee KH, Kim YT, Yoon YB. Risk factors of acute cholecystitis after endoscopic common bile duct stone removal. *World J Gastroenterol* 2006; 12(6): 956-960

http://www.wjgnet.com/1007-9327/12/956.asp

## INTRODUCTION

Endoscopic sphincterotomy is the treatment of choice for patients with common bile duct (CBD) stones. The high success rate and safety of this modality have been well established by a number of studies[1-5]. Because gallstones may pass from the gallbladder (GB) into the CBD, calculous GB is considered to be one of the risk factors for the recurrence of bile duct stones after sphincterotomy[4,6]. Some studies have compared the results of the wait-and-see policy and prophylactic cholecystectomy to prevent biliary complications but arrived at contradictory results[7-9]. Thus, it still remains controversial as to whether subsequent laparoscopic cholecystectomy is indicated in patients with concurrent GB stones. Most studies have focused on the identification of predictors of CBD stone recurrence, which can be treated again endoscopically without surgery; however, the development of acute cholecystitis is a definite indication of cholecystectomy. So the risk factors of subsequent acute cholecystitis are more important than those of recurrent CBD stones in terms of the decision concerning prophylactic cholecystectomy. However, few studies have identified the risk factors of acute cholecystitis after endoscopic CBD stone removal in patients with GB *in situ*. The aims of this study were to assess the risks of biliary symptom recurrence and to identify the risk factors of acute cholecystitis in patients with GB *in situ* who have received endoscopic CBD stone removal.

## MATERIALS AND METHODS

### Patients

The medical records of patients with GB *in situ* who

**Table 1 Baseline characteristics and CBD stone recurrence**

| | Cholecystectomy due to acute cholecystitis | |
|---|---|---|
| | Yes ($n$=17) | No ($n$=83) |
| Mean age±SD | 58.9±16.3 | 65.4±12.0 |
| Gender (M/F) | 8/9 | 54/29 |
| Recurrence of CBD stone | 2/17 (11.8%) | 11/83 (13.2%) |

underwent endoscopic CBD stone removal for the first time in our hospital from January 2000 to July 2004 were reviewed. Patients were excluded if another neoplasm or acute cholecystitis was diagnosed at the time of CBD stone removal, and if they had undergone prophylactic cholecystectomy after CBD stone removal.

The diagnosis of CBD stone was made by either ultrasonography (USG) or computed tomography (CT) before endoscopic retrograde cholangiopancreatography (ERCP) in the majority of patients, but a definite diagnosis was defined as visible CBD stones on ERCP. The presence of GB stone was evaluated using USG, CT, and ERCP and the wall thickness of GB was evaluated using either USG or CT. Patients with no visible stone on all imaging modalities were allocated to the no GB stone group. The patients who required treatment for a CBD stone 6 mo after complete endoscopic stone removal were defined as having CBD stone recurrence. Radiological data were analyzed using a digitalized picture archiving communication system (PACS). Patient records were checked in each case to ascertain whether cholecystectomy due to acute cholecystitis was done or not after endoscopic CBD stone removal, and telephone calls were made to determine this in the few patients lost during follow-up.

### Endoscopy protocol

Duodenal endoscopic intubation (TJF-240, Olympus, Tokyo, Japan) was performed under midazolam sedation. Sphincterotomy was performed in all the patients using a standard sphincterotome and/or a needle knife. After visualizing a CBD stone by cholangiography under fluoroscopic guidance, stones were extracted using a stone basket, balloon catheter, or a mechanical lithotripter according to stone size.

### Statistical analysis

Data were analyzed using a statistical software package (SPSS, version 12.0; SPSS Inc.). Differences between the groups were analyzed using the $\chi^2$ test. Logistic regression analysis was used to estimate odds ratios. The cumulative rate of acute cholecystitis requiring cholecystectomy was calculated using the Kaplan-Meier method.

## RESULTS

### Patient population

During the study, a total of 1 986 patients underwent ERCP at our hospital. The diagnosis of a CBD stone was made for 452 (22.8%) patients, and endoscopic CBD stone removal was performed successfully in 414 (91.6%) patients. Of these, 198 (47.8%) had a GB *in situ* at the time of endoscopic CBD stone removal. Forty-seven (23.7%) patients had a previous history of endoscopic CBD stone removal more than once, and 38 patients (19.1%) received subsequent cholecystectomy for the management of acute cholecystitis. Another 3 (1.5%) patients who experienced incidental cholecystectomy during cancer surgery (2 for gastric cancer and 1 for hepatoma) and 12 (6.0%) patients with inadequate medical information were omitted from the analysis. The total number of study subjects subjected to analysis was 100. No prophylactic cholecystectomy was planned during the follow-up for these patients.

### Recurrence of biliary complications after endoscopic CBD stone removal

During a mean 18-mo follow-up, 28 (28%) patients developed biliary symptoms; 17 (17%) with acute cholecystitis and 13 (13%) with CBD stone recurrence. No difference was observed between those who received cholecystectomy and those who did not receive cholecystectomy in terms of mean age or gender (Table 1). The mean time elapsed between original CBD stone removal and acute cholecystitis was 10.2 mo (1-37 mo). Of the 17 patients who received cholecystectomy, 2 patients (11.8%) developed recurrent CBD stones after cholecystectomy. The CBD stone recurrence rate in patients without acute cholecystitis was 13.2% (11/83). All cases of CBD stone recurrence were managed by endoscopic stone removal without surgery. The mean time elapsed (±SD) from endoscopic CBD stone removal to the development of acute cholecystitis was 10.2 (±10.6) mo with a range of 1-37 mo. All the patients in whom acute cholecystitis developed received emergency or elective cholecystectomy. Laparoscopic cholecystectomy was performed for all the patients initially and in 2 of the 17 patients (11.8%) the operation was converted to open cholecystectomy. The mean follow-up time (±SD) of the patients in whom acute cholecystitis did not occur was 18.4 mo (±9.8) and the range was 4-44 mo.

### Risk factors for acute cholecystitis after endoscopic CBD stone removal

The results of univariate analysis of potential risk factors for the development of acute cholecystitis after endoscopic CBD stone removal are shown in Table 1. Of the 15 variables, total bilirubin <1.3 mg/dL, the presence of a GB stone and a CBD diameter <11 mm were found to be significant by univariate analysis ($P$=0.01, 0.02, and 0.03, respectively). However, multiple logistic regression analysis with forward selection and backward elimination identified only total bilirubin <1.3 mg/dL and CBD diameter <11 mm, and both variables reached statistical significance (Tables 2 and 3). Cumulative rates of acute cholecystitis requiring cholecystectomy, according to these two variables were calculated by the Kaplan-Meier method as shown in Figures 1 and 2.

## DISCUSSION

The present study found that the overall recurrence rate of CBD stone after endoscopic CBD stone removal was 13%

**Table 2 Univariate analysis of potential risk factors for the development of acute cholecystitis after endoscopic CBD stone removal**

| Variable | *n* | Acute cholecystitis (%) | OR[1] | 95%CI[2] | *P* value |
|---|---|---|---|---|---|
| Gender | | | | | |
| Male | 62 | 8 (12.9) | 1 | | |
| Female | 38 | 9 (23.7) | 2.10 | 0.73-6.01 | 0.13 |
| Age | | | | | |
| ⩾60 yr | 74 | 11 (14.9) | 1 | | |
| <60 yr | 26 | 6 (23.1) | 1.72 | 0.56-5.24 | 0.25 |
| Total bilirubin | | | | | |
| ⩾1.3 mg/dL | 67 | 7 (10.6) | 1 | | |
| <1.3 mg/dL | 33 | 10 (31.3) | 3.83 | 1.29-11.31 | 0.01 |
| GB wall thickening | | | | | |
| No | 77 | 13 (16.9) | 1 | | |
| Yes | 23 | 4 (17.4) | 1.04 | 0.30-3.56 | 0.59 |
| Patency of cystic duct | | | | | |
| No | 45 | 8 (17.8) | 1 | | |
| Yes | 55 | 9 (16.4) | 0.91 | 0.32-2.58 | 0.53 |
| Presence of GB stone | | | | | |
| No | 48 | 4 (8.3) | 1 | | |
| Yes | 52 | 13 (25.0) | 3.67 | 1.10-12.18 | 0.02 |
| CBD diameter | | | | | |
| ⩾11.5 mm | 88 | 12 (13.6) | 1 | | |
| <11.5 mm | 12 | 5 (41.7) | 4.52 | 1.23-16.59 | 0.03 |
| Residual stone | | | | | |
| No | 91 | 15 (16.5) | 1 | | |
| Yes | 9 | 2 (22.2) | 1.45 | 0.27-7.66 | 0.48 |
| Lithotripsy | | | | | |
| Yes | 13 | 0 (0) | 1 | | |
| No | 87 | 17 (19.5) | 1.24 | 1.12-1.38 | 0.11 |
| Diverticulum | | | | | |
| No | 57 | 11 (19.3) | 1 | | |
| Yes | 43 | 6 (14.0) | 0.68 | 0.23-2.01 | 0.34 |
| Liver cirrhosis | | | | | |
| No | 92 | 15 (16.3) | 1 | | |
| Yes | 8 | 2 (25.0) | 1.71 | 0.32-9.30 | 0.41 |
| Diabetes mellitus | | | | | |
| No | 88 | 16 (18.2) | 1 | | |
| Yes | 12 | 1 (8.3) | 0.41 | 0.05-3.40 | 0.35 |
| Cholangitis at ERCP | | | | | |
| No | 71 | 14 (19.7) | 1 | | |
| Yes | 29 | 3 (10.3) | 0.47 | 0.12-1.78 | 0.20 |
| Pancreatitis at ERCP | | | | | |
| No | 88 | 15 (17.1) | 1 | | |
| Yes | 12 | 2 (16.7) | 0.97 | 0.19-4.90 | 0.67 |
| Complication after ERCP | | | | | |
| No | 95 | 16 (16.8) | 1 | | |
| Yes | 5 | 1 (20.0) | 1.23 | 0.13-11.79 | 0.61 |

[1]Odds ratio; [2]confidence interval.

**Table 3 Multivariate analysis of potential risk factors for the development of acute cholecystitis after endoscopic CBD stone removal**

| Variable | OR[1] | 95%CI[2] | *P* value |
|---|---|---|---|
| Total bilirubin | | | |
| <1.3 mg/dL | 4.62 | 1.39-15.33 | 0.01 |
| ⩾1.3 mg/dL | 1 | | |
| CBD diameter | | | |
| <11.5 mm | 5.10 | 1.19-21.80 | 0.03 |
| ⩾11.5 mm | 1 | | |
| Presence of GB stone | | | |
| Yes | 2.98 | 0.83-10.63 | 0.09 |
| No | 1 | | |

[1]Odds ratio; [2]confidence interval.

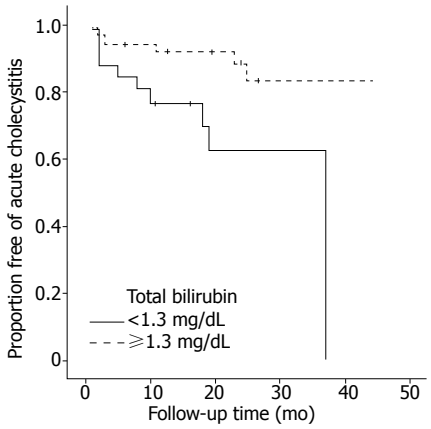


**Figure 1** Kaplan–Meier's curve comparing two total bilirubin levels in relation to the development of acute cholecystitis. Patients with a total bilirubin of <1.3 mg/dL developed acute cholecystitis more frequently than patients with a level of ⩾1.3 mg/dL ($P$=0.01, log-rank test).

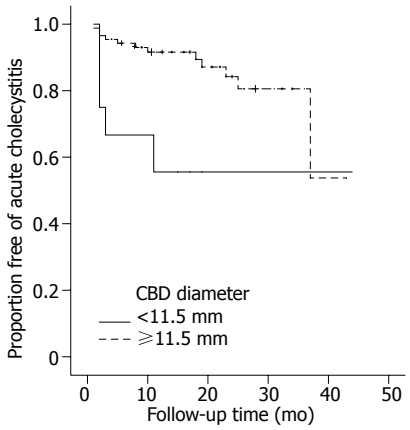


**Figure 2** Kaplan–Meier's curve comparing two CBD diameters in relation to acute cholecystitis development. Patients with CBD diameters <11 mm developed acute cholecystitis more frequently than patients with CBD diameters of ⩾11 mm ($P$=0.03, log-rank test).

(13/100), and that the frequency of acute cholecystitis after endoscopic CBD stone removal was 17% (17/100). Because two patients in whom acute cholecystitis developed also experienced CBD stone recurrence and there was no case of cholangitis or CBD stricture, the overall recurrence rate of biliary-related events during follow-up after endoscopic CBD stone removal was 28% (28/100), which is similar to the rates of 5-24% reported previously[1,2,4,6,8-28].

The advisability of prophylactic cholecystectomy to prevent biliary complications after endoscopic CBD stone removal remains a matter of debate; even

recent prospective[7] and large scale cohort studies[9] produced contrary conclusions concerning prophylactic cholecystectomy *vs* the wait-and-see approach. Moreover, because no consensus has been reached, the decision as to whether to operate or not is made empirically on a case-by-case basis[8,13,17-19]. However, two important points should not be missed. The first is that, as presented by previous studies and ours, the occurrence of acute cholecystitis requiring cholecystectomy is not uncommon and the second is that morbidities such as bile duct injury and mortality caused by laparoscopic cholecystectomy are not negligible[29-31]. Recurrent CBD stones can be retreated endoscopically without surgery but the development of acute cholecystitis is a definite indication for cholecystectomy. Thus the risk factors of subsequent acute cholecystitis are more important than that of recurrent CBD stones with respect to decisions concerning prophylactic cholecystectomy. In the present study, the development of acute cholecystitis (17%) was more common than that of CBD stone (13%) recurrence after CBD stone removal. We believed that if the risk factors of acute cholecystitis in patients who receive an endoscopic CBD stone removal could be identified, we might be able to identify the indicators of prophylactic cholecystectomy, as has been mentioned by earlier investigators[13]. Some studies have compared the results of prophylactic cholecystectomy and non-surgical treatment[7,9,17]. However, as far as we know, few studies have addressed the risk factors of acute cholecystitis after endoscopic CBD stone removal in patients with GB *in situ*, and thus our report might be the first to focus on this subject.

After conducting univariate and multivariate analyses to identify potential risk factors, we concluded that the occurrence of acute cholecystitis after endoscopic CBD stone removal was significantly more frequent in patients with a serum total bilirubin level of <1.3 mg/dL and a CBD diameter of <11 mm at the time of ERCP. Interestingly, a dilated CBD was identified as a risk factor of bile duct stone recurrence after endoscopic papillotomy by previous studies[4,6]. However, our results should be interpreted from a different point of view because the pathogenesis of CBD stone recurrence and the development of acute cholecystitis differ. In East Asia the number of primary CBD stone cases is relatively high compared with the number of secondary CBD stones originating from a GB stone as compared with the situation in the West, although the number of secondary CBD stone cases is increasing over the recent years due to the Westernization of diet[32-34]. In patients with GB or CBD stones, the differentiation of primary and secondary CBD stones is practically impossible because GB stones cannot be sampled for chemical analysis endoscopically, even though they are visualized by ERCP. However, considering the fact that patients with a dilated bile duct tend to form new stones in the bile duct and the cystic duct seldom passes large stones, large CBD stones with a dilated CBD are likely to be primary CBD stones[4,26,35,36]. On the other hand, small CBD stones in association with a non-dilated CBD are more likely to originate from the GB. If cholecystectomy is not performed in such patients, acute cholecystitis development due to cystic duct obstruction by a gallstone is a risk during the process of passage[37,38]. The same assumption can be applied to patients with a low total bilirubin level who were found to develop acute cholecystitis more frequently. Of the 17 patients with cholecystectomy, 2 patients (11.8%) developed recurrent CBD stones after cholecystectomy. Thus cholecystectomy did not reduce CBD stone recurrence in our study, which suggests that most CBD stones may have been secondary rather than primary stones in our patients.

According to our data, 4 of 48 patients who were classified as acalculous at the time of ERCP developed acute cholecystitis during follow-up. A review of our operative records revealed that 2 of 4 patients had calculous cholecystitis and that the remaining 2 had no evidence of a GB stone. However, for the two acalculous cholecystitis patients, the possibility of calculous cholecystitis with a previously passed be excluded, because none of them had the well-known predisposing factors of acalculous cholecystitis, i.e., severe illness or old age[39,40].

In conclusion, the present study shows that a serum bilirubin level of <1.3 mg/dL and a CBD diameter of <11 mm at the time of endoscopic CBD stone removal are risk factors for the development of acute cholecystitis requiring cholecystectomy. Although our results are limited due to the retrospective nature of our study, we suggest that prophylactic cholecystectomy should be reserved for patients who have the risk factors of acute cholecystitis. Prospective randomized studies are needed to more definitively establish the risk factors of acute cholecystitis after endoscopic CBD stone removal.

## REFERENCES


1 **Davidson BR**, Neoptolemos JP, Carr-Locke DL. Endoscopic sphincterotomy for common bile duct calculi in patients with gall bladder in situ considered unfit for surgery. *Gut* 1988; **29**: 114-120

2 **Escourrou J,** Cordova JA, Lazorthes F, Frexinos J, Ribet A. Early and late complications after endoscopic sphincterotomy for biliary lithiasis with and without the gall bladder 'in situ'. *Gut* 1984; **25:** 598-602

3 **Kawai K**, Akasaka Y, Murakami K, Tada M, Koli Y. Endoscopic sphincterotomy of the ampulla of Vater. *Gastrointest Endosc* 1974; **20**: 148-151

4 **Pereira-Lima JC**, Jakobs R, Winter UH, Benz C, Martin WR, Adamek HE, Riemann JF. Long-term results (7 to 10 years) of endoscopic papillotomy for choledocholithiasis. Multivariate analysis of prognostic factors for the recurrence of biliary symptoms. *Gastrointest Endosc* 1998; **48**: 457-464

5 **Tanaka M**, Takahata S, Konomi H, Matsunaga H, Yokohata K, Takeda T, Utsunomiya N, Ikeda S. Long-term consequence of endoscopic sphincterotomy for bile duct stones. *Gastrointest Endosc* 1998; **48**: 465-469

6 **Ando T**, Tsuyuguchi T, Okugawa T, Saito M, Ishihara T, Yamaguchi T, Saisho H. Risk factors for recurrent bile duct stones after endoscopic papillotomy. *Gut* 2003; **52**: 116-121

7 **Boerma D,** Rauws EA, Keulemans YC, Janssen IM, Bolwerk CJ, Timmer R, Boerma EJ, Obertop H, Huibregtse K, Gouma DJ. Wait-and-see policy or laparoscopic cholecystectomy after endoscopic sphincterotomy for bile-duct stones: a randomised trial. *Lancet* 2002; **360:** 761-765

8 **Kwon SK**, Lee BS, Kim NJ, Lee HY, Chae HB, Youn SJ, Park SM. Is cholecystectomy necessary after ERCP for bile duct stones in patients with gallbladder in situ? *Korean J Intern Med* 2001; **16**: 254-259

9 **Schreurs WH**, Vles WJ, Stuifbergen WH, Oostvogel HJ.

Endoscopic management of common bile duct stones leaving the gallbladder in situ. A cohort study with long-term follow-up. *Dig Surg* 2004; **21**: 60-64; discussion 65

10 **Lai KH,** Lin LF, Lo GH, Cheng JS, Huang RL, Lin CK, Huang JS, Hsu PI, Peng NJ, Ger LP. Does cholecystectomy after endoscopic sphincterotomy prevent the recurrence of biliary complications? *Gastrointest Endosc* 1999; **49:** 483-487

11 **Costamagna G**, Tringali A, Shah SK, Mutignani M, Zuccala G, Perri V. Long-term follow-up of patients after endoscopic sphincterotomy for choledocholithiasis, and risk factors for recurrence. *Endoscopy* 2002; **34**: 273-279

12 **Wojtun S**, Gil J, Gietka W, Gil M. Endoscopic sphincterotomy for choledocholithiasis: a prospective single-center study on the short-term and long-term treatment results in 483 patients. *Endoscopy* 1997; **29**: 258-265

13 **Hammarstrom LE,** Holmin T, Stridbeck H. Endoscopic treatment of bile duct calculi in patients with gallbladder in situ: long-term outcome and factors. *Scand J Gastroenterol* 1996; **31:** 294-301

14 **Kim DI**, Kim MH, Lee SK, Seo DW, Choi WB, Lee SS, Park HJ, Joo YH, Yoo KS, Kim HJ, Min YI. Risk factors for recurrence of primary bile duct stones after endoscopic biliary sphincterotomy. *Gastrointest Endosc* 2001; **54**: 42-48

15 **Targarona EM**, Ayuso RM, Bordas JM, Ros E, Pros I, Martinez J, Teres J, Trias M. Randomised trial of endoscopic sphincterotomy with gallbladder left in situ versus open surgery for common bileduct calculi in high-risk patients. *Lancet* 1996; **347**: 926-929

16 **Lai KH**, Peng NJ, Lo GH, Cheng JS, Huang RL, Lin CK, Huang JS, Chiang HT, Ger LP. Prediction of recurrent choledocholithiasis by quantitative cholescintigraphy in patients after endoscopic sphincterotomy. *Gut* 1997; **41**: 399-403

17 **Keulemans YC**, Rauws EA, Huibregtse K, Gouma DJ. Current management of the gallbladder after endoscopic sphincterotomy for common bile duct stones. *Gastrointest Endosc* 1997; **46**: 514-519

18 **Hill J**, Martin DF, Tweedle DE. Risks of leaving the gallbladder in situ after endoscopic sphincterotomy for bile duct stones. *Br J Surg* 1991; **78**: 554-557

19 **Welbourn CR**, Beckly DE, Eyre-Brook IA. Endoscopic sphincterotomy without cholecystectomy for gall stone pancreatitis. *Gut* 1995; **37**: 119-120

20 **Riemann JF**, Lux G, Forster P, Altendorf A. Long-term results after endoscopic papillotomy. *Endoscopy* 1983; **15** Suppl 1: 165-168

21 **Rosch W**, Riemann JF, Lux G, Lindner HG. Long-term follow-up after endoscopic sphincterotomy. *Endoscopy* 1981; **13**: 152-153

22 **Jacobsen O**, Matzen P. Long-term follow-up study of patients after endoscopic sphincterotomy for choledocholithiasis. *Scand J Gastroenterol* 1987; **22**: 903-906

23 **Seifert E**. Long-term follow-up after endoscopic sphincterotomy (EST). *Endoscopy* 1988; **20** Suppl 1: 232-235

24 **Ikeda S**, Tanaka M, Matsumoto S, Yoshimoto H, Itoh H. Endoscopic sphincterotomy: long-term results in 408 patients with complete follow-up. *Endoscopy* 1988; **20**: 13-17

25 **Ingoldby CJ**, el-Saadi J, Hall RI, Denyer ME. Late results of endoscopic sphincterotomy for bile duct stones in elderly patients with gall bladders in situ. *Gut* 1989; **30**: 1129-1131

26 **Hawes RH**, Cotton PB, Vallon AG. Follow-up 6 to 11 years after duodenoscopic sphincterotomy for stones in patients with prior cholecystectomy. *Gastroenterology* 1990; **98**: 1008-1012

27 **Bergman JJ**, van der Mey S, Rauws EA, Tijssen JG, Gouma DJ, Tytgat GN, Huibregtse K. Long-term follow-up after endoscopic sphincterotomy for bile duct stones in patients younger than 60 years of age. *Gastrointest Endosc* 1996; **44**: 643-649

28 **Prat F**, Malak NA, Pelletier G, Buffet C, Fritsch J, Choury AD, Altman C, Liguory C, Etienne JP. Biliary symptoms and complications more than 8 years after endoscopic sphincterotomy for choledocholithiasis. *Gastroenterology* 1996; **110**: 894-899

29 **Steiner CA**, Bass EB, Talamini MA, Pitt HA, Steinberg EP. Surgical rates and operative mortality for open and laparoscopic cholecystectomy in Maryland. *N Engl J Med* 1994; **330**: 403-408

30 **Richardson MC**, Bell G, Fullarton GM. Incidence and nature of bile duct injuries following laparoscopic cholecystectomy: an audit of 5913 cases. West of Scotland Laparoscopic Cholecystectomy Audit Group. *Br J Surg* 1996; **83**: 1356-1360

31 **Kimura T**, Suzuki K, Umehara Y, Kawabe A, Wada H. Features and management of bile leaks after laparoscopic cholecystectomy. *J Hepatobiliary Pancreat Surg* 2005; **12**: 61-64

32 **Nakayama F**, Miyake H. Changing state of gallstone disease in Japan. Composition of the stones and treatment of the condition. *Am J Surg* 1970; **120**: 794-799

33 **Su CH**, Lui WY, P'eng FK. Relative prevalence of gallstone diseases in Taiwan. A nationwide cooperative study. *Dig Dis Sci* 1992; **37**: 764-768

34 **Park YH**, Park SJ, Jang JY, Ahn YJ, Park YC, Yoon YB, Kim SW. Changing patterns of gallstone disease in Korea. *World J Surg* 2004; **28**: 206-210

35 **Cotton PB**. Is your sphincterotomy really safe--and necessary? *Gastrointest Endosc* 1996; **44**: 752-755

36 **Uchiyama K**, Onishi H, Tani M, Kinoshita H, Kawai M, Ueno M, Yamaue H. Long-term prognosis after treatment of patients with choledocholithiasis. *Ann Surg* 2003; **238**: 97-102

37 **Glenn F**. Acute cholecystitis. *Surg Gynecol Obstet* 1976; **143**: 56-60

38 **Roslyn JJ**, DenBesten L, Thompson JE Jr, Silverman BF. Roles of lithogenic bile and cystic duct occlusion in the pathogenesis of acute cholecystitis. *Am J Surg* 1980; **140**: 126-130

39 **Barie PS**, Fischer E. Acute acalculous cholecystitis. *J Am Coll Surg* 1995; **180**: 232-244

40 **Wiboltt KS**, Jeffrey RB Jr. Acalculous cholecystitis in patients undergoing bone marrow transplantation. *Eur J Surg* 1997; **163**: 519-524

**S- Editor** Guo SY **L- Editor** Elsevier HK **E- Editor** Kong LH

PO Box 2345, Beijing 100023, China
www.wjgnet.com
wjg@wjgnet.com

World J Gastroenterol 2006 February 14; 12(6): 961-965
World Journal of Gastroenterology ISSN 1007-9327
© 2006 The WJG Press. All rights reserved.

RAPID COMMUNICATION

# Effect of interferon alpha and ribavirin treatment on serum levels of transforming growth factor-β1, vascular endothelial growth factor, and basic fibroblast growth factor in patients with chronic hepatitis C

Ewa Janczewska-Kazek, Bogdan Marek, Dariusz Kajdaniuk, Halina Borgiel-Marek

Ewa Janczewska-Kazek, Department of Infectious Diseases, Medical University of Silesia, Chorzow, Poland
Bogdan Marek, Dariusz Kajdaniuk, Department of Pathophysiology, Medical University of Silesia, Zabrze, Poland
Halina Borgiel-Marek, Medical University of Silesia, Katowice, Poland
Co-first-authors: Ewa Janczewska-Kazek and Bogdan Marek
Correspondence to: Ewa Janczewska-Kazek MD, PhD, Department of Infectious Diseases, Medical University of Silesia, Zjednoczenia 10, 41-500 Chorzow, Poland. e.janczewska@neostrada.pl
Telephone: +48-322417192
Received: 2005-04-02 Accepted: 2005-10-20

## Abstract

**AIM:** To assess the role of transforming growth factor-β1 (TGF-β1), vascular endothelial growth factor (VEGF) and basic fibroblast growth factor (bFGF) in the pathogenesis of fibrosis associated with chronic hepatitis C (CHC) and to evaluate the influence of the antiviral therapy on above parameter levels depending on the treatment results (complete response or no response).

**METHODS:** Study group included 100 patients with CHC, in whom fibrosis in liver specimens was assessed (Scheuer fibrosis score: 1-4 points). Control group included 30 subjects with antibodies anti-HCV present and persistently normal ALT level, without fibrosis (Scheuer fibrosis score: 0 points). Concentration of studied parameters was assayed in the serum by immunoenzymatic method before and after the therapy with interferon alpha-2b and ribavirin.

**RESULTS:** TGF-β1 levels were significantly higher in the study group compared to the control group (35.89 *vs* 32.37 ng/mL; $P=0.023$). Such differences were not found in VEGF and bFGF levels. In patients showing complete response (negative HCV RNA and normal ALT level), significant increase in VEGF (112.8 *vs* 315.03 pg/mL; $P<0.05$) and bFGF (2.51 *vs* 15.79 pg/mL; $P=0.04$) levels were found. Significant decrease in TGF-β1 level was observed both in responders (37.44 *vs* 30.02 ng/mL; $P=0.05$), and in non-responders (38.22 *vs* 30.43 ng/mL; $P=0.043$). bFGF levels before the treatment were significantly lower (2.51 *vs* 5.94 pg/mL; $P=0.04$), and after the treatment significantly higher (15.79 *vs* 4.35 pg/mL; $P=0.01$) in patients with complete response than in those with no response.

**CONCLUSION:** Among the analyzed parameters TGF-β1 seems to play the most important role in the pathogenesis of fibrosis in CHC. Levels of this factor are significantly lower in subjects who do not have fibrosis developed in them. Good therapeutic effect in CHC patients is associated with significant changes in TGF-β1, VEGF, and bFGF levels. bFGF seems to have the highest usefulness in the prognosis of treatment efficacy.

© 2006 The WJG Press. All rights reserved.

**Key words:** Liver fibrosis; HCV; Interferon; Ribavirin; Growth factor

Janczewska-Kazek E, Marek B, Kajdaniuk D, Borgiel-Marek H. Effect of interferon alpha and ribavirin treatment on serum levels of transforming growth factor-β1, vascular endothelial growth factor, and basic fibroblast growth factor in patients with chronic hepatitis C. *World J Gastroenterol* 2006; 12(6): 961-965

http://www.wjgnet.com/1007-9327/12/961.asp

## INTRODUCTION

Hepatitis C virus (HCV) is among the main causes of chronic liver diseases. Consequences of chronic HCV infection and high treatment costs make it a significant worldwide epidemiological, clinical, and social problem.

No pathological fibrosis is found during the initial stages of the disease, however in course of its development, the process increases, and the final stage is cirrhosis[1]. Fibrosis as an after-effect of chronic liver inflammation is compared to wound healing[2,3]. It is supposed that growth factors taking part in classical reaction of wound healing may play an important role in similar repair process occurring in the liver. Nature of fibrogenesis is excessive deposition of collagen and other extracellular matrix (ECM) components in the organ parenchyma. ECM protein synthesis takes place mainly in hepatic stellate cells[2-4]. Inhibition and regression of fibrosis is connected with the limitation of excessive

ECM protein production and degradation of components already produced[5,6]. Growth factors may be detected in blood that is circulated. There are premises that they could serve as markers of fibrosis and inflammatory activity, and could be useful in non-invasive hepatological diagnostics, especially in those situations when there are contraindications for liver biopsy[2].

Among several known isomeric forms of transforming growth factor-β (TGF-β), the most significant role in pathogenesis of liver fibrosis is played by TGF-β1. Main source of TGF-β1 in the liver are activated stellate cells and Kupffer cells. The role of this factor in fibrosis development has been studied for several years[5-10]. Results of those studies confirm the existence of a connection between the factor's concentration in the blood and progression of liver lesions[8-10], as well as reduction of those concentrations following treatment leading to the decrease of fibrosis stage[10].

Vascular endothelial growth factor (VEGF) stimulates angiogenesis both in regular conditions and in neoplastic processes[11-15]. It has been verified to be closely involved in the development of hepatocellular carcinoma and hepatic metastases[15].

Basic fibroblast growth factor (bFGF, FGF-2) is found in almost all tissues of mesoderm and endoderm origins. Studies conducted on animal models show participation of the cytokine in regeneration of tissues, angiogenesis and in wound healing process[16,17]. A role played by bFGF in the processes of liver regeneration and fibrosis is not known. However, mentioned actions of the factor towards other tissues suggest possibility of its influence on fibrosis[18].

The only way of liver fibrosis prevention known so far is effective causal treatment of hepatitis[19]. Preferred treatment for patients with CHC is a combined therapy with interferon alpha and ribavirin. In antiviral treatment recombined interferons alpha (alpha 2a and alpha 2b) are used, recently usage of pegylated interferons has become a standard. Ribavirin is an analog of guanosine. Apart from producing a virostatic effect, the drug shows probably also immunomodulative activity. Aim of CHC treatment is inhibition of HCV replication shown by the disappearance of HCV RNA in peripheral blood, which may lead to the decrease of inflammatory activity and stage of fibrosis found in histopathological examination.

We undertook this study to assess the role of TGF-β1, VEGF, and bFGF in the pathogenesis of liver fibrosis, evaluate effect of antiviral treatment on concentration of these factors depending on the effect of the treatment (full response or lack of response), and define a biochemical marker useful for prognosis of antiviral treatment efficacy.

## MATERIALS AND METHODS

### Patients

Ethical approval for the study was obtained from the Bioethical Committee of Medical University of Silesia. All serum and tissue samples were taken with patients' informed consent.

Study group included 100 patients (48 females and 52 males), aged between 19 and 64 (average 42 ± 3 years) with chronic hepatitis C (CHC).

The diagnosis of CHC was confirmed by the presence of serum HCV-RNA assayed with reverse transcription polymerase chain reaction (RT-PCR) method (Amplicor v.2 Roche Diagnostic test) and persistently elevated alanine aminotransferase (ALT) level for at least 6 mo. All studied patients had liver biopsy performed with Hepafix kit (B. Braun, Melsungen AG, Germany). Grade of inflammatory activity and stage of fibrosis were assessed according to Scheuer numeric scale[20]. Patients with pathologically confirmed cirrhosis met the criteria for the A class in Child-Pugh scale.

Control group included 30 patients with present anti-HCV antibodies and normal ALT activity, with no or minimal necroinflammatory activity and no pathological fibrosis found in liver specimen pathological examination.

### Methods

All patients starting the therapy and those belonging to the control group had blood collected in the beginning of the study. Blood samples were also taken from the study group subjects after the completion of therapy. Obtained serum was frozen at -70 °C until assay.

TGF-β1, VEGF, and bFGF concentrations were measured by immunoenzymatic method (Quantikine Immunoassay, R&D Systems Inc, Minneapolis, USA).

In therapy of CHC patients interferon alpha 2b and ribavirin were used (Rebetron™, Schering-Plough). Interferon alpha was administered at 3 MU dose thrice a week, ribavirin at a dose of 1 200 mg/d for patients ⩾ 75 kg of body weight, or at a dose of 1 000 mg/day for patients with body weight lower than 75 kg. Treatment was continued for 48 wk.

Serum levels of TGF-β1, VEGF, and bFGF were measured before and after the treatment.

In this study, comparison was made between the two groups of patients - those with complete sustained response to applied antiviral treatment (undetectable HCV RNA and normalization of ALT activity 6 mo after the end of therapy) and lack of this response (continuous elevated aminotransferase activity and presence of HCV RNA after conclusion of therapy).

### Statistical analysis

Values were expressed as the mean ± SE. Hypothesis of studied parameters, mean values equality between the compared groups were assessed using Student's *t* test for related and unrelated variables preceded with Fisher's test for variance homogeneity and Mann-Whitney *U* test. $P < 0.05$ was considered statistically significant.

## RESULTS

General characteristics of patients with CHC and subjects belonging to the control group are presented in Table 1.

Figure 1 shows the results of TGF-β1 assays in compared groups. In group of patients with CHC, there was significantly higher serum concentration of the factor compared to control group (35.89 ± 1.28 *vs* 32.37 ± 1.41 ng/mL; $P = 0.023$).

VEGF serum levels in compared groups are demonstrated in Figure 2. No significant differences of

**Table 1 Characteristics of patients**

| | *n* | Male/female | Age (yr) | ALT (U/L) | AST (U/L) | Alkaline phosphatase (U/L) | Bilirubin (μmol/L) |
|---|---|---|---|---|---|---|---|
| CHC | 100 | 52/48 | 42.08±3 | 108.7±10.12 | 75.6±8.76 | 141.7±6.78 | 18.9±2.42 |
| Control | 30 | 16/14 | 40.79±2 | 21.3±1.92 | 18.5±1.73 | 136.4±6.56 | 13.8±1.76 |

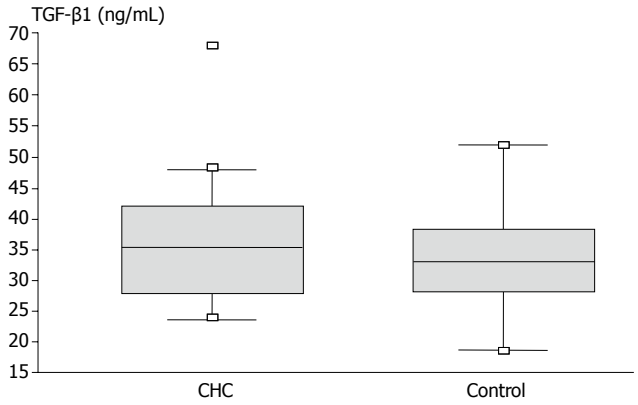


**Figure 1** Serum levels of TGF-β1 (ng/mL) in CHC group and control group. The box represents the interquartile range. The whiskers indicate the highest and lowest values. The line across the box indicates the median value.

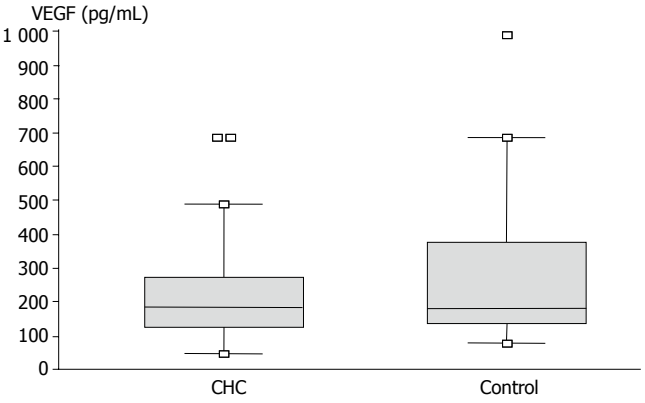


**Figure 2** Serum levels of VEGF (pg/mL) in CHC group and control group. The box represents the interquartile range. The whiskers indicate the highest and lowest values. The line across the box indicates the median value.

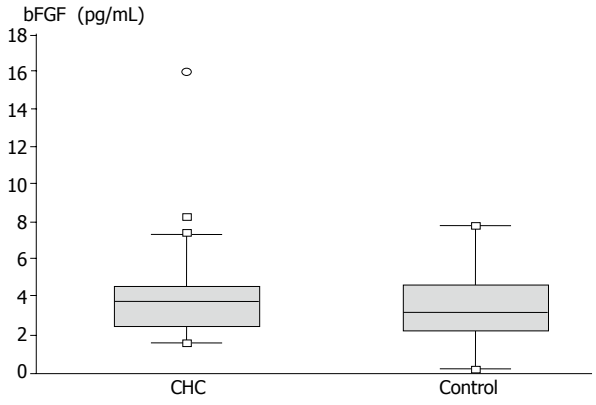


**Figure 3** Serum levels of bFGF (pg/mL) in CHC group and control group. The box represents the interquartile range. The whiskers indicate the highest and lowest values. The line across the box indicates the median value.

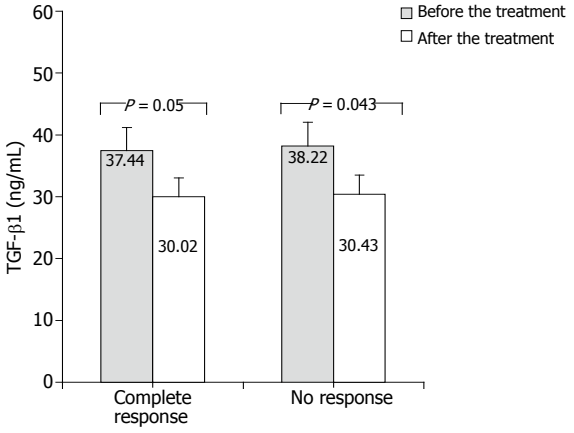


**Figure 4** Comparison of TGF-β1 levels (mean and SE) before and after the antiviral therapy of CHC patients depending on treatment efficacy.

this growth factor concentration were found between the hepatitis C group and control (231.84±24.55 *vs* 262.89±33.99 pg/mL). Figure 3 presents bFGF concentration. No significant differences were found between CHC group and control (4.35±0.58 *vs* 3.30±0.39 pg/mL).

In Figure 4, TGF-β1 concentrations measured before and after antiviral treatment are compared. In both groups – responders and non-responders – significant decrease in serum TGF-β1 concentration was found following antiviral treatment. TGF-β1 level in responders decreases from 37.44±4.31 to 30.02±4.16 ng/mL ($P=0.05$) and in non-responders from 38.22±3.93 to 30.34±3.7 ng/mL ($P=0.043$). Figure 5 shows changes of VEGF concentration following treatment with interferon and ribavirin. In group of responders, significant increase of this factor concentration in blood was found (112.8±10.2 *vs* 315.03±29.3 pg/mL; $P<0.05$), unlike the group of non-responders. In Figure 6, concentrations of bFGF in treated patients are shown. Significant increase of the concentration was demonstrated in patients with complete response to therapy (2.51±0.29 *vs* 15.79±1.8 pg/mL; $P=0.04$). The concentration did not change significantly in the group of non-responders.

bFGF levels before the treatment were significantly lower (2.51 *vs* 5.94 pg/mL; $P=0.04$), and after the treatment significantly higher (15.79 *vs* 4.35 pg/mL; $P=0.01$) in patients with complete response than in those with no response.

## DISCUSSION

Process of liver fibrosis has been recently a subject of numerous studies. Attempts are made to recognize

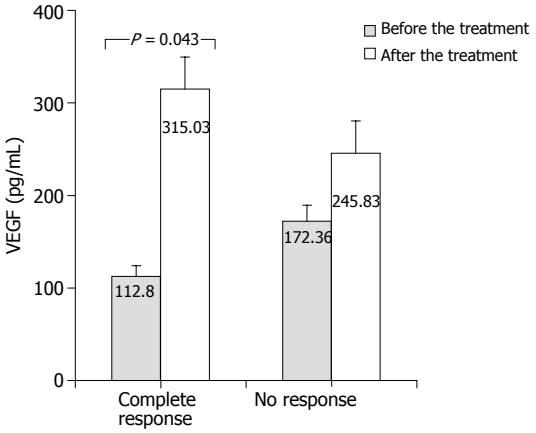


**Figure 5** Comparison of VEGF levels (mean and SE) before and after the antiviral therapy of CHC patients depending on treatment efficacy.

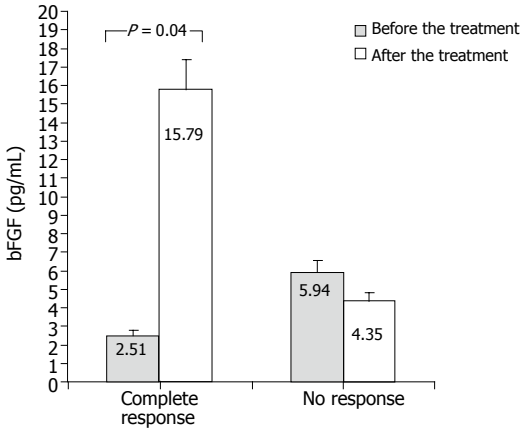


**Figure 6** Comparison of bFGF levels (mean and SE) before and after the antiviral therapy of CHC patients depending on treatment efficacy.

accompanying pathogenetic phenomena and define factors influencing its progression. Reports were published concerning the possibility of fibrosis stage decrease following effective causal treatment, for example, following treatment of CHC with interferon and ribavirin[6,10,21,22]. Some authors have reported even cases of regression of cirrhosis that has been considered irreversible so far[2,6,10,19,23-26]. This study made an attempt to define the role that may be played by chosen growth factors in processes occurring in course of chronic hepatitis.

TGF-β1 is the growth factor of the best known and confirmed pro-fibrogenic activity. In our study it was demonstrated that TGF-β1 concentration in patients with fibrosis in course of CHC was indeed higher compared to the patients in whom there was no fibrosis development. Tsushima *et al* noted significant decrease of TGF-β1 concentration in serum, and inhibited expression of TGF-β1 mRNA in hepatic tissue following antiviral treatment, regardless of the clinical result (both for responders and non-responders)[10]. Similar observations have been made during our study. For both groups of patients significant decrease of the factor concentration was noted, regardless of the final result of treatment. This could suggest existence of direct, inhibitory influence of interferon alpha and/or ribavirin on the expression of TGF-β1 that is independent of the influence of the drug on HCV replication.

VEGF, as a factor specifically inducing proliferation of vascular endothelium cells, plays an important role in angiogenesis, and seems to play on indirect role in regeneration processes. One of the repair processes in which VEGF plays its role is probably "wound healing" process taking place in liver, and being a consequence of chronic inflammatory condition. Studies including analyses of VEGF participation in the development of hepatocellular carcinoma were performed[11-15], but only single attempts to assess its blood concentration and hepatic expression in hepatitis have been reported. Akiyoshi *et al*[27] found significant increase of VEGF concentration in the serum of patients with acute hepatitis of typical course, but in cases of fulminant hepatitis those concentrations were lower than in control group and increased in patients who recovered. Low VEGF concentrations were noted by the authors in cases of cirrhosis, but they did not show significant differences compared to control group in cases of chronic hepatitis. Jinno *et al* obtained different results. In their study VEGF concentrations appeared to be significantly higher in cases of chronic hepatitis and cirrhosis compared to healthy individuals[28]. In our study we did not find statistically significant differences of VEGF concentrations in blood between patients with hepatitis C and control group. No papers estimating possible changes in the cytokine concentration following antiviral therapy have been published yet. Our study showed that in patients meeting the criteria of response to this type of treatment there was a significant increase of VEGF serum concentration. The phenomenon was not observed in non-responsive patients. VEGF concentration increase following effective therapy, after which one could expect inhibition of fibrosis, justifies the assumption that stimulation of angiogenesis by this factor may be a key element in regeneration processes accompanying regression of liver fibrosis.

bFGF, a growth factor with well documented participation in classic process of "wound healing", may also play a role in repair processes taking place in liver damaged by inflammatory condition, however, number of published reports on this topic is very low. Jinno *et al* found that bFGF blood concentrations increase with the liver disease progression[18]. In our study bFGF levels were not statistically different in case and control groups. Following treatment with interferon and ribavirin, significant increase of the factor concentration was found in patients, for whom the therapy proved to be effective. Moreover, it was noted that complete therapeutic response occurred in patients whose initial concentration of this cytokine was significantly lower, and significantly higher following the treatment than in non-responders group. As one of the probable bFGF activity courses is stimulation of endothelium cells proliferation[16,17], it may be assumed that increase of the cytokine concentration following effective treatment may be linked with intensification of angiogenesis, just like in the case of VEGF.

Studies showed that antiviral treatment, especially effective one, causes significant changes in concentrations of some growth factors. Studies documenting decrease of fibrosis stage following the therapy and concluded with persistent inhibition of virus replication are increasing. Combination of those facts justifies assumption that those cytokines may play an important role in pathogenesis of changes taking place in liver during chronic inflammatory conditions. Studies documenting participation of the growth factors other than TGF-β1 in those processes are, as for now, very sparse. It seems, however, that the topic deserves interest. Precise knowledge concerning processes leading to the development of fibrosis could contribute to elaboration of methods aimed at prevention of the disease progression and complications.

Among the factors analyzed in our study, TGF-β1 plays the most significant role in pathogenesis of fibrosis in course of CHC. It supports results of other studies.

We have demonstrated that good therapeutic effect in patients with CHC is connected with influence of drugs on TGF-β1, VEGF, and bFGF serum concentration. These findings suggest possible usefulness of these factors in assessment of antiviral treatment efficacy and indication of medication failure. It seems that bFGF shows the best prognostic value regarding final antiviral treatment results.

## REFERENCES


1 **Poynard T,** Ratziu V, Benhamou Y, Opolon P, Cacoub P, Bedossa P**.** Natural history of HCV infection. *Baillieres Best Pract Res Clin Gastroenterol* 2000; **14**: 211-228

2 **Friedman SL.** Liver fibrosis -- from bench to bedside. *J Hepatol* 2003; **38** Suppl 1: S38-53

3 **Albanis E**, Safadi R, Friedman SL. Treatment of hepatic fibrosis: almost there. *Curr Gastroenterol Rep* 2003; **5**: 48-56

4 **Reeves HL,** Friedman SL. Activation of hepatic stellate cells--a key issue in liver fibrosis. *Front Biosci* 2002; **7**: d808-d826

5 **Arthur MJ**. Fibrogenesis II. Metalloproteinases and their inhibitors in liver fibrosis. *Am J Physiol Gastrointest Liver Physiol* 2000; **279**: G245-G249

6 **Bataller R**, Brenner DA. Liver fibrosis. *J Clin Invest* 2005; **115**: 209-218

7 **Taniguchi H**, Kato N, Otsuka M, Goto T, Yoshida H, Shiratori Y, Omata M. Hepatitis C virus core protein upregulates transforming growth factor-beta 1 transcription. *J Med Virol* 2004; **72**: 52-59

8 **Nelson DR**, Gonzalez-Peralta RP, Qian K, Xu Y, Marousis CG, Davis GL, Lau JY. Transforming growth factor-beta 1 in chronic hepatitis C. *J Viral Hepat* 1997; **4**: 29-35

9 **Gressner AM**, Weiskirchen R, Breitkopf K, Dooley S. Roles of TGF-beta in hepatic fibrosis. *Front Biosci* 2002; **7**: d793-d807

10 **Tsushima H**, Kawata S, Tamura S, Ito N, Shirai Y, Kiso S, Doi Y, Yamada A, Oshikawa O, Matsuzawa Y**.** Reduced plasma transforming growth factor-beta1 levels in patients with chronic hepatitis C after interferon-alpha therapy: association with regression of hepatic fibrosis. *J Hepatol* 1999; **30**: 1-7

11 **Deli G**, Jin CH, Mu R, Yang S, Liang Y, Chen D, Makuuchi M. Immunohistochemical assessment of angiogenesis in hepatocellular carcinoma and surrounding cirrhotic liver tissues. *World J Gastroenterol* 2005; **11**: 960-963

12 **Sun XY**, Wu ZD, Liao XF, Yuan JY. Tumor angiogenesis and its clinical significance in pediatric malignant liver tumor. *World J Gastroenterol* 2005; **11**: 741-743

13 **Imura S**, Miyake H, Izumi K, Tashiro S, Uehara H. Correlation of vascular endothelial cell proliferation with microvessel density and expression of vascular endothelial growth factor and basic fibroblast growth factor in hepatocellular carcinoma. *J Med Invest* 2004; **51**: 202-209

14 **Li X**, Feng GS, Zheng CS, Zhuo CK, Liu X. Expression of plasma vascular endothelial growth factor in patients with hepatocellular carcinoma and effect of transcatheter arterial chemoembolization therapy on plasma vascular endothelial growth factor level. *World J Gastroenterol* 2004; **10**: 2878-2882

15 **Shi B**, Wang X, Yang Z. Vascular endothelial growth factors and liver diseases. *Hepatogastroenterology* 2001; **48**: 1145-1148

16 **Wang JK**, Gao G, Goldfarb M. Fibroblast growth factor receptors have different signaling and mitogenic potentials. *Mol Cell Biol* 1994; **14**: 181-188

17 **Gospodarowicz D.** Fibroblast growth factor. Chemical structure and biologic function. *Clin Orthop Relat Res* 1990; **257**: 231-248

18 **Jin-no K**, Tanimizu M, Hyodo I, Kurimoto F, Yamashita T. Plasma level of basic fibroblast growth factor increases with progression of chronic liver disease. *J Gastroenterol* 1997; **32**: 119-121

19 **Arthur MJ.** Reversibility of liver fibrosis and cirrhosis following treatment for hepatitis C. *Gastroenterology* 2002; **122**: 1525-1528

20 **Scheuer PJ.** Classification of chronic viral hepatitis: a need for reassessment. *J Hepatol* 1991; **13**: 372-374

21 **Poynard T**, McHutchison J, Manns M, Trepo C, Lindsay K, Goodman Z, Ling MH, Albrecht J. Impact of pegylated interferon alfa-2b and ribavirin on liver fibrosis in patients with chronic hepatitis C. *Gastroenterology* 2002; **122**: 1303-1313

22 **Poynard T**, Ratziu V, Benmanov Y, Di Martino V, Bedossa P, Opolon P**.** Fibrosis in patients with chronic hepatitis C: detection and significance. *Semin Liver Dis* 2000; **20**: 47-55

23 **Bonis PA**, Friedman SL, Kaplan MM. Is liver fibrosis reversible? *N Engl J Med* 2001; 344: 452-454

24 **Rockey DC.** Antifibrotic therapy in chronic liver disease. *Clin Gastroenterol Hepatol* 2005; **3**: 95-107

25 **Markham CH,** Diamond SG. Further evidence to support disconjugate eye torsion as a predictor of space motion sickness. *Aviat Space Environ Med* 1992; **63:** 118-121

26 **Abergel A,** Darcha C, Chevallier M, Ughetto S, Henquell C, Pol S, de Ledinghen V, Canva V, Bronowicki JP, Tran A, Martineau N, Lafeuille H, Dechelotte P, Bommelaer G, Bonny C. Histological response in patients treated by interferon plus ribavirin for hepatitis C virus-related severe fibrosis. *Eur J Gastroenterol Hepatol* 2004; **16:** 1219-1227

27 **Akiyoshi F**, Sata M, Suzuki H, Uchimura Y, Mitsuyama K, Matsuo K, Tanikawa K. Serum vascular endothelial growth factor levels in various liver diseases. *Dig Dis Sci* 1998; **43:** 41-45

28 **Jinno K**, Tanimizu M, Hyodo I, Nishikawa Y, Hosokawa Y, Doi T, Endo H, Yamashita T, Okada Y. Circulating vascular endothelial growth factor (VEGF) is a possible tumor marker for metastasis in human hepatocellular carcinoma. *J Gastroenterol* 1998; **33**: 376-382


**S- Editor** Guo SY **L- Editor** Elsevier HK **E- Editor** Kong LH

PO Box 2345, Beijing 100023, China
www.wjgnet.com
wjg@wjgnet.com

*World J Gastroenterol* 2006 February 14; 12(6): 966-970
***World Journal of Gastroenterology*** ISSN 1007-9327
© 2006 The WJG Press. All rights reserved.

*RAPID COMMUNICATION*

# Conversion of cadherin isoforms in cultured human gastric carcinoma cells

Bing-Jing Wang, Zhi-Qian Zhang, Yang Ke

Bing-Jing Wang, Zhi-Qian Zhang, Yang Ke, Beijing Institute for Cancer Research and School of Oncology, Peking University, Beijing 100034, China
Supported by the National Natural Science Foundation of China, No.30370555 and No.30270658, National Major Basic Research Development Program No. G2000057002, and "211" project.
Correspondence to: Dr. Zhi-Qian Zhang, Department of Cell Biology, Beijing Institute for Cancer Research, Haidian District, Beijing 100036, China. zqzhang@public3.bta.net.cn
Telephone: +86-10-88196792 Fax: +86-10-88122437
Received: 2005-06-29 Accepted: 2005-08-03

## Abstract

**AIM:** To explore the expression of cadherin isoforms in cultured human gastric carcinoma cells and its regulation.

**METHODS:** The expressions of cell adhesion molecules (including E-cadherin, N-cadherin, α-catenin, β-catenin) and cadherin transcription factors including snail, slug and twist were determined by reverse transcriptase-polymerase chain reaction(RT-PCR), immunoblotting and immunofluorescence in SV40-immortalized human gastric cell line Ges-1 and human gastric cancer cell lines MGC-803, BGC-823 and SGC-7901.

**RESULTS:** All cell lines expressed N-cadherin, but not E-cadherin. N-cadherin immunofluorescence was detected at cell membranous adherents junctions where co-localization with immunofluorescent staining of inner surface adhesion proteins α- and β-catenins was observed. The transformed Ges-1 and gastric cancer cell lines all expressed transcription factors (snail, slug and twist) which inhibited the expression of E-cadherin and triggered epithelial-mesenchymal transformation.

**CONCLUSION:** Cadherin isoforms can change from E-cadherin to N-cadherin in transformed human gastric cancer cells, which is associated with intracellular events of stomach carcinogenesis and high expression of corresponding transcription factors.

© 2006 The WJG Press. All rights reserved.

**Key words:** E-cadherin; N-cadherin; Transcription factor; Gastric cancer

Wang BJ, Zhang ZQ, Ke Y. Conversion of cadherin isoforms in cultured human gastric carcinoma cells. *World J Gastroenterol* 2006; 12(6): 966-970

http://www.wjgnet.com/1007-9327/12/966.asp

## INTRODUCTION

Cadherins are a family of transmembranous glycoproteins responsible for calcium-dependent intercellular adhesion, and play a dual role as adhesion ligands and receptors in cell adherents junctions (AJs). They are divided into more than ten subclasses, which are distinct in immunologenic specificities and tissue distribution. AJs are cell-to-cell adhesion sites where classic cadherins, cytoplasmic catenins (α-, β-, γ-) and actin-based cytoskeleton are assembled. Such protein complex plays a role as a functional unit in mediating cell adhesion and signal transduction and is involved in regulation of cell recognition, migration and cell sorting behavior [2, 3]. E-cadherin and N-cadherin, members of cadherin superfamily, are the most popular adhesion receptors in tissues. E-cadherin is predominantly expressed in epithelia, and loss of E-cadherin expression is a major characteristic of highly invasive and metastatic cancer [4], while re-expression of E-cadherin results in reversion of metastatic phenotypes to benign phenotypes. E-cadherin has been known as a tumor suppressor against invasion and metastasis of tumors [5]. N-cadherin is expressed in mesenchymal cells, but recent study demonstrated that N-cadherin is associated with an increased invasive potential of cancer [6]. Forced expression of N-cadherin exerts a dominant effect over E-cadherin function in breast cancer cells [7].

In early embryonic development, loss of E-cadherin accompanying the acquisition of fibroblastic phenotype occurs through a mechanism called epithelial-mesenchymal transition (EMT). This is an essential event during gastrulation and neural crest formation [8] as well as in early invasion and metastasis of carcinoma cells [9]. Multiple mechanisms can inactivate E-cadherin in cancer cells, such as gene mutation, promoter hypermethylation, chromatin rearrangement, and transcriptional repressors. Several developmentally important genes inducing EMT act as E-cadherin repressors. In vertebrates, snail and its closely related gene slug bind directly to E-boxes in the *E-cadherin* promoter and repress *E-cadherin* expression directly in mouse and human invasive carcinoma cells [10]. A further molecule known to trigger EMT is twist, which is possibly involved in E-cadherin and N-cadherin conversion during

**Table 1 PCR Primers used in experiments**

| Genes | Primers (sense/anti-sense) |
|---|---|
| E-cadherin (361bp) | 5′-TCCATTTCTTGGTCTACGCC-3′<br>5′-TTTGTCCTACCGACTTCCAC-3′ |
| N-cadherin (373bp) | 5′-GTGCCATTAGCCAAGGGAATTCAGC-3′<br>5′- GGAGGATACTCACCTTGTCCTTGCG-3′ |
| Snail(377bp) | 5′-CTGCAGGACTCTAATCCAG-3′<br>5′- CGAGAGACTCCGGTTCCTA-3′ |
| slug(410bp) | 5′-AGCGAACTGGACACACATAC-3′<br>5′-TCTAGACTGGGCATCGCAG-3′ |
| twist(612bp) | 5′-GCAAGCTTAGAGATGATGCAGGACG-3′<br>5′-GACTCGAGGTGGGACGCGGACATGGA-3′ |
| GAPDH (451bp) | 5′-ACCACAGTCCATGCCATCAC-3<br>5′-ATGTCGTTGTCCCACCACCT-3′ |

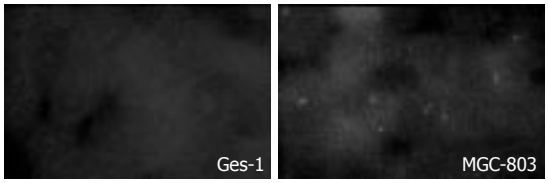


**Figure 1** Expression of E-cadherin in SV40-immortalized Ges-1 and gastric cancer cell lines. Negative staining of E-cadherin in Ges-1 and MGC-803 was shown on immunofluorescent micrographs.

EMT [11]. In the present study, we chose a transformed human gastric cell line as control and three human gastric cancer cell lines to detect the expression of E-cadherin and N-cadherin subtypes and their associated adhesion protein (α- and β-catenins) related to changes of transcription factors (snail, slug and twist), and to analyze the role of snail and other EMT regulators in down-regulating E-cadherin in gastric cancer cells.

## MATERIALS AND METHODS

### *Cell culture*

Human gastric cancer cell lines MGC-803, BGC-823 and SGC-7901 were cultured in RPMI1640 medium (GIBCO/BRL) containing 10% fetal bovine serum. Ges-1, a non-tumorigenic but immortalized human gastric cell line, was obtained by SV40 viral transformation and cultured in RPMI1640 medium supplemented with 15% fetal bovine serum [12].

### *Immunoblotting experiments*

Cells of logarithmic growth potential treated with RIPA lysis buffer (50mmol/L Tris-HCl pH 7.4, 150mmol/L NaCl, 1% NP40, 50mmol/L NaF, 0.1mmol/L $Na_3VO_4$, 1mmol/L phenylmethylsulfonyl fluoride, 10μg/mL leupeptin, 0.1% SDS, 0.5% deoxycholic acid, 50mmol/L HEPES, 10mmol/L EDTA, 50mmol/L sodium pyrophosphate, 50mmol/L ammonium molybdate) were used to determine the total protein concentration according to Bradford protein quantification method. Samples of equal amount were loaded onto 10% SDS-PAGE gel and electrophoretically transferred to PVDF membrane, blocked with 5% non-fat milk/TTBS, reacted with primary antibody, washed with TTBS and labeled with goat and anti-mouse or rabbit secondary antibody. The primary antibodies used were mouse anti-N-cadherin monoclonal antibody, rabbit anti-E-cadherin polyclonal antibody, rabbit anti-α- and β-catenin polyclonal antibody (Sigma). Protein signals were detected using ECL chemiluminescence reagent (Amersham Phamacia).

### *Indirect immunofluorescent staining*

Cells growing on coverslips were fixed in 2% formaldehyde for 3 min and extracted 3 times (10 min each) with 0.5% Triton X-100. The cell samples were incubated with primary antibodies (described above) at 37°C for 1 h, washed with PBS containing 0.5% Triton X-100 and then reacted with FITC- or rhodamine-conjugated secondary antibodies (Jackson ImmunoResearch Laboratories, West Grove, PA) at 37°C for 1 h. After washed, the samples were rinsed in 0.9% NaCl, stained with 1μg/L 4, 6-diamidino-2-phenylindole (DAP; Sigma) and mounted in 60% glycerol/PBS. Olympus BH2 fluorescent microscope equipped with FITC- and rhodamine- channel filter systems was used to observe distribution of different proteins in the same fields. Kodak TMAX-400 black and white films were used for photographs.

### *RT-PCR*

Total RNA was extracted from cells of logarithmic growth potential with Trizol (Invitrogen) as described, then suspended in 50μL RNase-free water and quantified. Reverse-transcription was performed in a final volume of 20μL using superscript III reverse transcriptase (Invitrogen) according to the manufacturer's instructions under the following conditions:1mmol/L dNTP, 50ng Oligo-$dT_{15}$ and 3μg total RNA. The reaction was performed at 50°C for 45 min, followed by inactivation of the enzyme at 70°C for 15 min. The sequences of the specific primers are listed in Table 1. Forty cycles of PCR amplification were performed at 94°C for 1 min, at 58°C for 1 min, at 72°C for 1 min. PCR products were identified by running on 1.2% agarose gel.

## RESULTS

### *E-cadherin expression lost in SV40-immortalized Ges-1 and gastric cancer cell lines*

The three gastric cancer cell lines MGC-803, BGC-823, and SGC-7901 were negative for E-cadherin expression as demonstrated by RT-PCR, immunoblotting and immunofluorescent staining. The SV40-transformed gastric epithelial cell line Ges-1, non-tumorigenic in nude mice with normal cell morphology, was also negative for E-cadherin expression at mRNA and protein levels (Figure 1).

### *N-cadherin expression in SV40-immortalized Ges-1 and gastric cancer cell lines*

In order to understand the formation of adherens junctions in these E-cadherin negative cell lines, N-cadherin expression was detected by RT-PCR, immunoblotting and

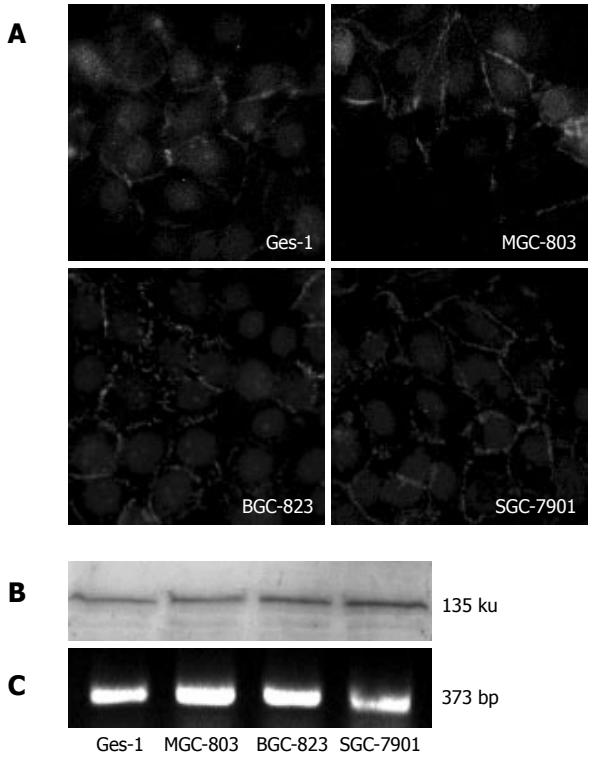


**Figure 2** Expression of N-cadherin in SV40-immortalized Ges-1 and gastric cancer cell lines. **A**: Distribution of N-cadherin fluorescence on cell membranes in Ges-1 and gastric cancer cell lines; **B**: A band of 135 ku N-cadherin protein detected by Western blotting of N-cadherin; **C**: N-cadherin mRNA expression shown by RT-PCR.

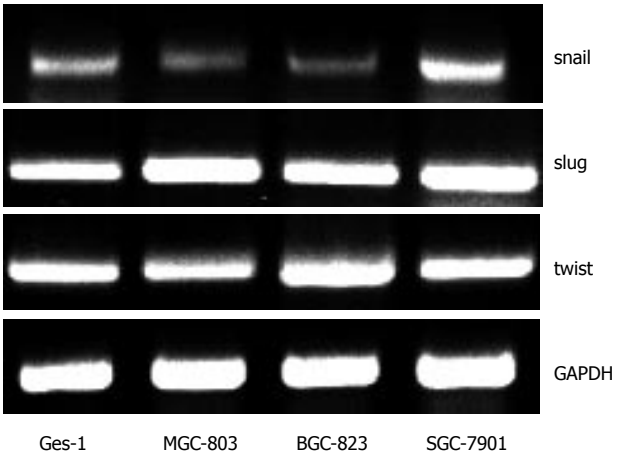


**Figure 4** Expression of E-cadherin transcription repressors (snail, slug) and N-cadherin activator (twist) in Ges-1 and gastric cancer cell lines.

immunofluorescent staining (Figure 2). N-cadherin mRNA was found in all these E-cadherin negative cell lines (SV40-transformed Ges-1, BGC-823, MGC-803, and SGC-7901). In consistence with N-cadherin mRNA expression, a band of 135 ku N-cadherin protein was also shown in these cell lines as detected by Western blotting of N-cadherin. N-cadherin fluorescence was distributed at cell-cell contact membrane regions, suggesting that these cells established adherents junctions through N-cadherin rather than E-cadherin. Alteration of cadherin isoforms from E-cadherin to N-cadherin occurred in the process of carcinogenesis.

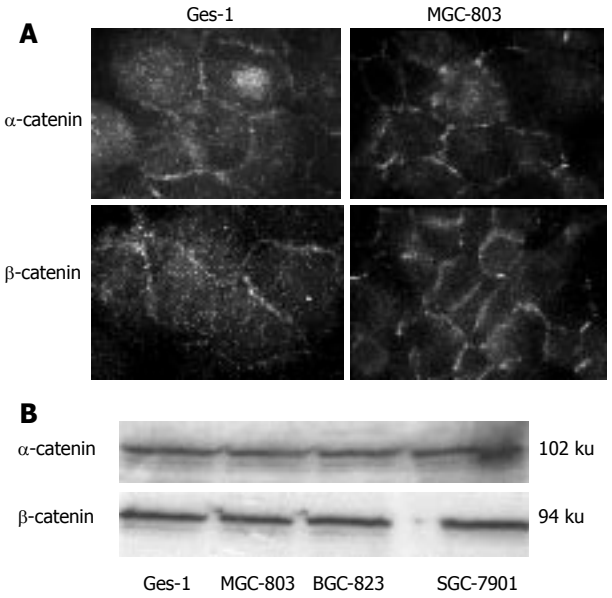


**Figure 3** Expression of α- and β-catenins in Ges-1 and gastric cancer cell lines. **A:** Distribution of α- and β-catenin fluorescence on cell membranes and cell-cell borders in Ges-1 and MGC-803; **B:** Reactive bands at 102 ku and 94 ku of α- and β-catenins in Ges-1 and cancer cell lines.

### *Expression of α- and β-catenins in SV40-immortalized Ges-1 and gastric cancer cell lines*

Immunoblotting of α- and β-catenins showed reactive bands at 102 ku and 94 ku respectively in Ges-1 and gastric cancer cell lines. The fluorescence of α- and β-catenins was found at the cell-cell contact borders irrespective of transformed cells or cancer cells (Figure 3). The colocalization of both cadherin and catenins indicated the formation of cadherin/catenin complex at adherents junctions.

### *Expression of E-cadherin transcription repressor and N-cadherin activator in Ges-1 and gastric cancer cell lines*

The transcription factors (snail, slug and twist) could repress the expression of E-cadherin and induce the expression of N-cadherin. Thus, we examined the expression of these transcription factors in these cell lines with alteration of E-cadherin to N-cadherin by RT-PCR. They were all expressed in Ges-1 and three cancer cell lines, but their expression levels varied (Figure 4).

## DISCUSSION

It is well known that E-cadherin is an adhesion receptor of normal epithelial cells that binds to cytoplasmic adhesion proteins to form E-cadherin/catenin complex as an anchorage site for actin-based cytoskeleton. The E-cadherin/catenin/cytoskeleton complex plays an important role in the maintenance of structural and functional stability of epithelial tissues. Loss of E-cadherin expression or function in epithelial carcinoma has been considered as a primary reason for disruption of cell-cell contacts. However, there is evidence that other cadherins, such as N-cadherin, are up-regulated in cancer cell lines [13]. N-cadherin is present in invasive cancer cell lines and its exogenous expression in tumor cells increases the ability

of invasion and metastasis of tumor cells. Changes in the expression of cadherins occur in the early embryonic development during gastrulation and neural crest formation. The loss of E-cadherin with the acquisition of fibroblastic phenotype occurs through a mechanism called epithelial-mesenchymal transition (EMT) during early invasion and metastasis of carcinoma cells. To investigate the occurrence of cadherin conversion in gastric carcinoma, we determined the expression of E-cadherin and N-cadherin in transformed human gastric cell line and three gastric cancer cell lines. The results demonstrated that three human gastric cancer cell lines were all negative for E-cadherin immunofluorescent staining and immunoblotting, which is in agreement with the reported data, suggesting that E-cadherin expression is inhibited in gastric cancer cells [14]. Meanwhile, our finding is in accordance with the report that loss of E-cadherin is a key step in the progression from benign adenoma to malignant carcinoma *in vivo* [15]. However, in our study, N-cadherin was expressed in all these E-cadherin negative cell lines and N-cadherin fluorescence was distributed at cell-cell contact membrane regions, suggesting that these cells are established at the adherents junctions through N-cadherin rather than E-cadherin. Apparently, alteration of cadherin isoforms from E-cadherin to N-cadherin occurs in the process of carcinogenesis. SV40-transformed gastric epithelial cell line Ges-1 characterized by immortalization *in vitro* and normal cell morphology, was also negative for E-cadherin expression at mRNA and protein levels, suggesting that inhibition of E-cadherin expression may be an early cellular event in the process of cell malignancy.

The interaction between cytoplasmic cadherins and catenins is critical for the formation of stable and functional AJs. The mutation or homozygous deletion of catenin gene leads to loss of cell-cell adhesion. Moreover, β-catenin can act as a transcrption factor in nuclei as an activator of LEF/TCF family of the DNA-binding proteins, which is activated by the Wnt signal pathway [16]. We therefore investigated the expression of α- and β-catenins in the same cell lines. Immunoblotting and immunofluorescence staining showed positive expressions of α- and β-catenins in transformed Ges-1 and three cancer cell lines. Meanwhile, we did not find the relocalization of β-catenin in nuclei, suggesting that cadherin/catenin complex is formed at adherents junctions. In gastric cancer cells, the formation of N-cadherin/catenin complex at AJs after conversion of cadherin isoforms may imply that the mediated adhesion signals are needed for remote metastasis of cancer cell mass.

Multiple mechanisms can inactivate E-cadherin in cancer cells. Recent reports have highlighted the role of EMT regulator, snail, a strong repressor of E-cadherin gene expression in cancer cell lines [17, 18]. Snail is a zinc finger transcription factor which directly represses E-cadherin expression by binding to E-box DNA-binding sequence CAGGTG and is required for mesoderm differentiation and neural crest formation during embryonic development. In human carcinoma and melanoma, the expression of snail correlates with the absence of E-cadherin expression [19-21]. Forced expression of snail in cultured epithelial cells represses the E-cadherin promoter and increases invasion and matrix metalloproteinase-2 expression [22]. Slug, which also represses the E-cadherin promoter, can likewise induce EMT, increase cell motility and invasion and confer tumorigenesis [23]. Twist is originally identified in *Drosophila* as a protein involved in establishing dorso–ventral polarity and in epithelial–mesenchymal transition. Recent findings indicate that twist is both an E-cadherin repressor and an EMT inducer [24]. Furthermore, the findings implicate that twist is involved in tumor cell intravasation and in tumor metastasis. In the present study, strong expressions of snail, slug and twist were observed in the transformed gastric cell line Ges-1 and three gastric carcinoma cell lines. Meanwhile, these cell lines were all negative for E-cadherin expression but positive for N-cadherin expression.

In conclusion, EMT regulators play a critical role in human gastric carcinoma. The transcription factors (snail, slug and twist) are correlated with the alteration of cadherin isoforms in human gastric cancer cells. However, the mechanism of how the transcription factors regulate the alteration of cadherin isoforms remains to be elucidated.

## REFERENCES


1 **Nagafuchi A.** Molecular architecture of adherens junctions. *Curr Opin Cell Biol* 2001; **13**: 600-603

2 **Tepass U**, Truong K, Godt D, Ikura M, Peifer M. Cadherins in embryonic and neural morphogenesis. *Nat Rev Mol Cell Biol* 2000; **1**: 91-100

3 **Beavon IR**. The E-cadherin-catenin complex in tumour metastasis: structure, function and regulation. *Eur J Cancer* 2000; **36**: 1607-1620

4 **Hirohashi S**. Inactivation of the E-cadherin-mediated cell adhesion system in human cancers. *Am J Pathol* 1998; **153**: 333-339

5 **Cavallaro U**, Christofori G. Cell adhesion in tumor invasion and metastasis: loss of the glue is not enough. *Biochim Biophys Acta* 2001; **1552**: 39-45

6 **Nieman MT**, Prudoff RS, Johnson KR, Wheelock MJ. N-cadherin promotes motility in human breast cancer cells regardless of their E-cadherin expression. *J Cell Biol* 1999; **147**: 631-644

7 **Hazan RB**, Phillips GR, Qiao RF, Norton L, Aaronson SA. Exogenous expression of N-cadherin in breast cancer cells induces cell migration, invasion, and metastasis. *J Cell Biol* 2000; **148**: 779-790

8 **Shook D**, Keller R. Mechanisms, mechanics and function of epithelial-mesenchymal transitions in early development. *Mech Dev* 2003; **120**: 1351-1383

9 **Thiery JP**. Epithelial-mesenchymal transitions in tumour progression. *Nat Rev Cancer* 2002; **2**: 442-454

10 **Nieto MA**. The snail superfamily of zinc-finger transcription factors. *Nat Rev Mol Cell Biol* 2002; **3**: 155-166

11 **Oda H**, Tsukita S, Takeichi M. Dynamic behavior of the cadherin-based cell-cell adhesion system during Drosophila gastrulation. *Dev Biol* 1998; **203**: 435-450

12 **Ke Y,** Ning T, Wang B. [Establishment and characterization of a SV40 transformed human fetal gastric epithelial cell line-GES-1]. *Zhonghua Zhongliu Zazhi* 1994; **16**: 7-10

13 **Tomita K**, van Bokhoven A, van Leenders GJ, Ruijter ET, Jansen CF, Bussemakers MJ, Schalken JA. Cadherin switching in human prostate cancer progression. *Cancer Res* 2000; **60**: 3650-3654

14 **Mayer B**, Johnson JP, Leitl F, Jauch KW, Heiss MM, Schildberg FW, Birchmeier W, Funke I. E-cadherin expression in primary and metastatic gastric cancer: down-regulation correlates with cellular dedifferentiation and glandular disintegration. *Cancer*

*Res* 1993; **53**: 1690-1695
15 **Perl AK**, Wilgenbus P, Dahl U, Semb H, Christofori G. A causal role for E-cadherin in the transition from adenoma to carcinoma. *Nature* 1998; **392**: 190-193
16 **Quintanilla RA,** Munoz FJ, Metcalfe MJ, Hitschfeld M, Olivares G, Godoy JA, Inestrosa NC. Trolox and 17beta-estradiol protect against amyloid beta-peptide neurotoxicity by a mechanism that involves modulation of the Wnt signaling pathway. *J Biol Chem* 2005; **280**: 11615-11625
17 **Cano A**, Perez-Moreno MA, Rodrigo I, Locascio A, Blanco MJ, del Barrio MG, Portillo F, Nieto MA. The transcription factor snail controls epithelial-mesenchymal transitions by repressing E-cadherin expression. *Nat Cell Biol* 2000; **2**: 76-83
18 **Bolos V**, Peinado H, Perez-Moreno MA, Fraga MF, Esteller M, Cano A. The transcription factor Slug represses E-cadherin expression and induces epithelial to mesenchymal transitions: a comparison with Snail and E47 repressors. *J Cell Sci* 2003; **116**: 499-511
19 **Blanco MJ**, Moreno-Bueno G, Sarrio D, Locascio A, Cano A, Palacios J, Nieto MA. Correlation of Snail expression with histological grade and lymph node status in breast carcinomas. *Oncogene* 2002; **21**: 3241-3246
20 **Jiao W**, Miyazaki K, Kitajima Y. Inverse correlation between E-cadherin and Snail expression in hepatocellular carcinoma cell lines in vitro and in vivo. *Br J Cancer* 2002; **86**: 98-101
21 **Yokoyama K**, Kamata N, Hayashi E, Hoteiya T, Ueda N, Fujimoto R, Nagayama M. Reverse correlation of E-cadherin and snail expression in oral squamous cell carcinoma cells in vitro. *Oral Oncol* 2001; **37**: 65-71
22 **Yokoyama K**, Kamata N, Fujimoto R, Tsutsumi S, Tomonari M, Taki M, Hosokawa H, Nagayama M. Increased invasion and matrix metalloproteinase-2 expression by Snail-induced mesenchymal transition in squamous cell carcinomas. *Int J Oncol* 2003; **22**: 891-898
23 **Hajra KM,** Chen DY, Fearon ER. The SLUG zinc-finger protein represses E-cadherin in breast cancer. *Cancer Res* 2002; **62**: 1613-1618
24 **Yang J**, Mani SA, Donaher JL, Ramaswamy S, Itzykson RA, Come C, Savagner P, Gitelman I, Richardson A, Weinberg RA. Twist, a master regulator of morphogenesis, plays an essential role in tumor metastasis. *Cell* 2004; **117**: 927-939

**S- Editor** Wang XL and Guo SY **L- Editor** Elsevier HK **E- Editor** Liu WF

PO Box 2345, Beijing 100023, China
www.wjgnet.com
wjg@wjgnet.com

*World J Gastroenterol* 2006 February 14; 12(6): 971-973
***World Journal of Gastroenterology*** ISSN 1007-9327
© 2006 The WJG Press. All rights reserved.

*CASE REPORT*

# A case of an intussuscepted neuroendocrine carcinoma of the appendix

Rachel E Thomas, Karen Maude, Olorunda Rotimi

Rachel E Thomas, Olorunda Rotimi, Department of Histopathology, Algernon Firth Building, Leeds General Infirmary, Great George Street, Leeds LS1 3EX, United Kingdom
Karen Maude, Academic Department of Surgery, Clarendon Wing, Leeds General Infirmary, Great George Street, Leeds LS1 3EX, United Kingdom
Correspondence to: Rachel E Thomas, Department of Histopathology, Algernon-Firth Building, Leeds General Infirmary, Great George Street, Leeds LS2 9NS, United Kingdom. rachelethomas@hotmail.com
Received: 2005-06-16 Accepted: 2005-07-01

## Abstract

We have described a previously unreported entity of an intussuscepted neuroendocrine carcinoma of the appendix. Our patient was a 70-year-old man whose only complaint was insipient weight loss. Colonoscopy showed a malignant cecal "polyp", and an extended right hemicolectomy was performed. We have reviewed the literature on the causes of appendiceal intussusception and their appropriate treatment options, and clarified the classification of neuroendocrine tumors of the gastrointestinal tract.

© 2006 The WJG Press. All rights reserved.

**Key words:** Neuroendocrine carcinoma; Appendix; Intussusception

Thomas RE, Maude K, Rotimi O. A case of an intussuscepted neuroendocrine carcinoma of the appendix. *World J Gastroenterol* 2006; 12(6): 971-973

http://www.wjgnet.com/1007-9327/12/971.asp

## INTRODUCTION

Intussusception of the appendix is a well-recognized, though rare, entity (occurring with an incidence of 0.01% in a large autopsy series[1]). Occasionally it is accompanied by an associated appendiceal abnormality, such as an adenoma, endometriosis, carcinoid tumor or adenocarcinoma. Typically, these cases present as acute appendicitis. Less commonly, they present with chronic episodic abdominal pain, cecal mass or even rectal bleeding, for which the patient may have to undergo an endoscopic examination and the intussuscepted appendix may be interpreted as a cecal polyp. Occasionally, the patient has no gastrointestinal symptoms. Whereas carcinoid tumor (now termed as well-differentiated neuroendocrine tumor) is the commonest tumor of the appendix, neuroendocrine carcinoma of the appendix is a rare entity (occurring in about 0.2% of all appendicectomy specimens[2]). We here present a case of a previously unreported phenomenon of intussusception of the appendix due to a neuroendocrine carcinoma.

## CASE REPORT

A 70-year-old man presented with an 18-mo history of 13 kg weight loss. He was originally referred to the rheumatologists for investigation as he had a past medical history of rheumatoid arthritis. Other past medical history included cholecystectomy and partial gastrectomy with vagotomy for perforated duodenal ulceration. He had no gastrointestinal symptoms.

He underwent an upper gastrointestinal endoscopy with no abnormalities detected. Colonoscopy revealed a lesion in the ascending colon that appeared macroscopically malignant (Figure 1). Two further benign-looking polyps were also identified, one each in the transverse colon and at the hepatic flexure. Biopsies of the ascending colon lesion suggested adenocarcinoma. A CT scan failed to demonstrate the tumor due to extensive fecal loading. There was no evidence of metastatic disease. Pre-operative blood investigations revealed a mild iron-deficiency anemia (hemoglobin 11.9 g/dL) and no other abnormality.

During the operation, a cecal tumor was found and a large lymph node was present in the mesentery. An extended right hemicolectomy was performed and an end-to-end anastomosis fashioned.

The resected specimen showed complete intussusception of the appendix, with invagination of mesoappendix fat seen at the base on the peritoneal surface. The whole of the appendix was involved by the tumor, and measured 4.5 cm in length and 2.5 cm wide at the base (Figure 2). Microscopic examination revealed a well-differentiated neuroendocrine carcinoma with a trabecular and glandular pattern (Figure 3), which was invading into the invaginated serosal fat of the appendix. Immunohistochemistry showed weak positivity with chromogranin (Figure 4) and synaptophysin, and strong membrane and cytoplasmic positivity with the low molecular weight cytokeratin (CK) marker, CAM

**Figure 1** Endoscopic appearance of polypoidal lesion in the cecum.

**Figure 2** Gross specimen of invaginated appendiceal tumor seen on opening cecum.

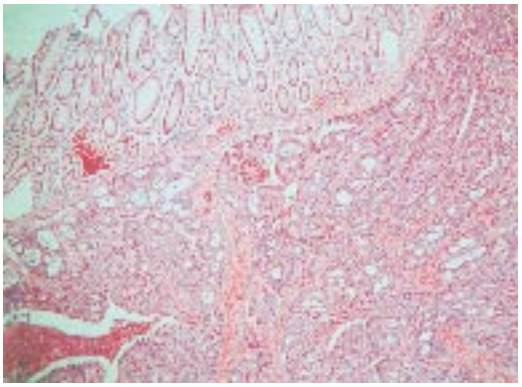

**Figure 3** Well-differentiated neuroendocrine carcinoma, arranged in nests and trabeculae, beneath uninvolved large-intestinal type appendiceal mucosa (top left hand corner) (hematoxylin and eosin; ×16).

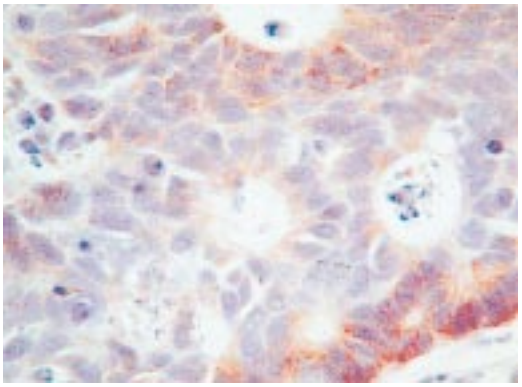

**Figure 4** Chromogranin positive immunohistochemical staining (brown cytoplasmic staining) demonstrating neuroendocrine differentiation of tumor cells (×40, 1:5 000 dilution, DAK-A3 clone, DAKO, Cambridge, UK).

5.2. The tumor cells were negative for CK 20, which is usually positive in primary colorectal adenocarcinoma. The histological pattern and immunoprofile were those of neuroendocrine carcinoma. Lymphovascular invasion was identified and 1 of the 11 dissected lymph nodes contained metastatic carcinoma. The involved node was 2 cm in size and largely necrotic. Five other small polyps were also found within the specimen (2 hyperplastic, 3 adenomatous).

Post-operative recovery was uncomplicated and he was discharged 7 d post-operatively. The case was discussed at the colorectal cancer multidisciplinary (MDT) meeting and consensus was that no further adjuvant treatment was needed. He was to be followed up in the surgical clinic and was well 4 mo post-surgery.

## DISCUSSION

Intussusception of the appendix is rare. In a study by Collins, of 71 000 autopsy appendiceal specimens, prevalence of intussusception was only 0.01%[1]. Clinically it is almost never diagnosed pre-operatively, most commonly mimicking acute appendicitis. It can also present with symptoms of chronic, episodic abdominal pain with or without rectal bleeding, painless rectal bleeding, or may be asymptomatic. Cases can be diagnosed preoperatively by means of radiological examination[3]. At barium enema there is an absence of appendiceal filling together with a cecal-filling defect in the anticipated location of the appendix. Ultrasound scanning may show a "target-like" picture or "concentric ring sign", though neither of these radiological appearances is specific for an intussuscepted appendix[4]. CT scans may reveal a mass lesion within the cecum without a discernable appendix. At colonoscopy, the intussusception may be misinterpreted as a cecal polyp. Therefore, in all the cases of cecal polyp identification, the appendiceal orifice should be routinely searched for and noted to be present.

The mechanism and pathogenesis of intussusception of the appendix has been extensively studied by Fink *et al*[5]. It may be due to anatomical causes, such as a thin mesoappendix, a mobile appendix, or a wide appendicular lumen, or due to an associated appendiceal abnormality. These include intraluminal factors (fecoliths, foreign bodies, parasites) or intramural factors (lymphoid follicle hyperplasia, endometriosis, and tumors).

Tumors of the appendix, with or without intussusception, are uncommon. Mostly they are benign entities, such as mucocoeles, adenomata, and benign carcinoids tumors. Few are malignant, occurring in only about 1% of appendicectomy specimens[6]. In one large series, only 20% of these malignant appendiceal tumors

were neuroendocrine carcinomas[2], the majority being adenocarcinomas. Using the WHO classification of endocrine tumors of the gastroenteropancreatic system (2000)[7], classical benign carcinoid tumors have been incorporated under the heading of neuroendocrine tumors, and are now termed as well-differentiated neuroendocrine tumors. They are considered to be of benign or uncertain malignant potential. Those with malignant features (infiltrative growth pattern, invasion into the muscularis propria, greater than 2 cm in diameter, or with nodal metastases), previously called malignant carcinoids, are now termed as neuroendocrine carcinomas, well- or poorly-differentiated. Until now, no poorly-differentiated neuroendocrine carcinomas of the appendix have been described. Classically, well-differentiated neuroendocrine carcinomas of the appendix have organoid, nesting, trabecular, rosette-like or palisading patterns, suggestive of endocrine differentiation[8]. They are associated with a worse prognosis than the more commonly diagnosed benign carcinoids/well-differentiated neuroendocrine tumors.

It is important that an intussuscepted appendix is managed appropriately. In those cases uninvolved by a concurrent malignant tumor, reduction at laparotomy or laparoscopy with subsequent appendicectomy, or right hemicolectomy is the surgical treatment of choice. These lesions may be misinterpreted as a broad-based cecal polyp during colonoscopy, and subsequent endoscopic resection may result in unexpected complications, such as perforation and peritonitis[9]. Therefore, wide-stalked cecal polyps, where the appendiceal orifice cannot be visualized, should be approached with caution endoscopically. However, in the circumstances when a malignant tumor of the appendix is also present, right hemicolectomy or ileocecal resection with lymph node dissection should be performed[1]. Though a diagnosis of appendiceal intussusception had not been pre-operatively made in our patient, he underwent the correct treatment of an extended right hemicolectomy, because of the pre-operative diagnosis of a presumed malignant cecal polyp.

## REFERENCES


1 **Takahashi M**, Sawada T, Fukuda T, Furugori T, Kuwano H. Complete appendiceal intussusception induced by primary appendiceal adenocarcinoma in tubular adenoma: a case report. *Jpn J Clin Oncol* 2003; **33**: 413-415

2 **McCusker ME**, Cote TR, Clegg LX, Sobin LH. Primary malignant neoplasms of the appendix: a population-based study from the surveillance, epidemiology and end-results program, 1973-1998. *Cancer* 2002; **94**: 3307-3312

3 **Jevon GP**, Daya D, Qizilbash AH. Intussusception of the appendix. A report of four cases and review of the literature. *Arch Pathol Lab Med* 1992; **116**: 960-964

4 **Weissberg DL**, Scheible W, Leopold GR. Ultrasonographic appearance of adult intussusception. *Radiology* 1977; **124**: 791-792

5 **Fink VH**, Santos AL, Goldberg SL. Intussusception of the appendix. Case reports and review of the literature. *Am J Gastroenterol* 1964; **42**: 431-441

6 **Connor SJ,** Hanna GB, Frizelle FA. Appendiceal tumors: retrospective clinicopathologic analysis of appendiceal tumors from 7,970 appendectomies. *Dis Colon Rectum* 1998; **41**: 75-80

7 **Kloppel G,** Perren A, Heitz PU. The gastroenteropancreatic neuroendocrine cell system and its tumors: the WHO classification. *Ann N Y Acad Sci* 2004; **1014**: 13-27

8 **Bernick PE**, Klimstra DS, Shia J, Minsky B, Saltz L, Shi W, Thaler H, Guillem J, Paty P, Cohen AM, Wong WD. Neuroendocrine carcinomas of the colon and rectum. *Dis Colon Rectum* 2004; **47**: 163-169

9 **Fazio RA**, Wickremesinghe PC, Arsura EL, Rando J. Endoscopic removal of an intussuscepted appendix mimicking a polyp--an endoscopic hazard. *Am J Gastroenterol* 1982; **77**: 556-558


**S- Editor** Guo SY **L- Editor** Elsevier HK **E- Editor** Liu WF

PO Box 2345, Beijing 100023, China
www.wjgnet.com
wjg@wjgnet.com

*World J Gastroenterol* 2006 February 14; 12(6): 974-976
***World Journal of Gastroenterology*** ISSN 1007-9327
© 2006 The WJG Press. All rights reserved.

*CASE REPORT*

# Subfulminant hepatitis B after infliximab in Crohn's disease: Need for HBV-screening?

Gunda Millonig, Michaela Kern, Othmar Ludwiczek, Karin Nachbaur, Wolfgang Vogel

Gunda Millonig, Michaela Kern, Othmar Ludwiczek, Karin Nachbaur, Wolfgang Vogel, Department of Gastroenterology and Hepatology, Medical University of Innsbruck, Anichstrasse 35, 6020 Innsbruck, Austria
Supported by the "Verein zur Förderung der Wissenschaft in Gastroenterologie und Hepatologie"
Correspondence to: Gunda Millonig, MD, Department of Gastroenterology and Hepatology, Medical University of Innsbruck, Anichstrasse 35, 6020 Innsbruck, Austria. gunda.millonig@uibk.ac.at
Telephone: +43-512-504-23401 Fax: +43-512-504-24052
Received: 2005-04-30 Accepted: 2005-06-09

## Abstract

Infections are a major adverse effect during the treatment with anti-TNF-α. While exclusion of any bacterial infection and screening for tuberculosis are mandatory before initiating a therapy with anti-TNF-α-antibodies, there are no guidelines whether to screen for or how to deal with chronic viral infections such as hepatitis B. In this case report, we have described a patient with Crohn's disease who developed subfulminant hepatitis B after the fourth infusion of infliximab due to an unrecognized HBs-antigen carrier state. He recovered completely after lamivudine therapy was started, but this severe adverse event could have been prevented if screening for HBV and pre-emptive therapy with lamivudine would have been started prior to infliximab. We therefore strongly argue in favor of extended screening recommendations for infectious diseases including viral infections before considering a therapy with infliximab.

© 2006 The WJG Press. All rights reserved.

**Key words:** Hepatitis B; TNF alpha; Lamivudine

Millonig G, Kern M, Ludwiczek O, Nachbaur K, Vogel W. Subfulminant hepatitis B after infliximab in Crohn's disease: Need for HBV-screening? *World J Gastroenterol* 2006; 12(6): 974-976

http://www.wjgnet.com/1007-9327/12/974.asp

## INTRODUCTION

Infliximab has become the standard therapy for refractory, steroid-dependent or fistulizing Crohn's disease[4,14,19]. The association between the use of this monoclonal chimeric mouse antibody, and increased risk of severe bacterial infections[16] and reactivation of tuberculosis[6] has received much attention. The influence of infliximab on viral infections, however, has not been extensively investigated, and data that are available on reactivation of chronic viral infections such as hepatitis B and C and EBV are conflicting. Reijasse *et al*[15] studied the viral kinetics of EBV in patients receiving immunosuppressive drugs including infliximab and found no increased viral load in them compared to the control group. Several case studies and investigations of small patient cohorts have reported that Crohn's disease in patients with documented pre-existing chronic hepatitis B or C was successfully treated with infliximab, without the drug causing any deterioration of the liver disease[11,13,21]. In contrast to these publications, in their prospective study of Crohn's patients with coexisting chronic HBV-infection treated with infliximab, Esteve *et al*[1] observed two severe hepatitis flare-ups during treatment with this drug. Ostuni *et al*[12] reported on a patient with reactivated hepatitis B after therapy with infliximab and methotrexate. Michel *et al*[8] observed fulminant hepatic failure in a patient with inactive chronic hepatitis B after being treated with infliximab but without signs of HBV-reactivation and therefore of unknown etiology.

Several authors have recommended pre-emptive treatment with lamivudine of HBV-carriers with Crohn's disease before starting infliximab-therapy[1,8].

FDA-recommendations released in December 2004 also alert physicians to the danger of primary hepatotoxicity or reactivation of chronic viral hepatitis caused by the administration of infliximab.

## CASE REPORT

We report here on a 50-year-old patient in whom Crohn's disease with terminal ileitis was diagnosed in January 2001. Initially he received a course of mesalamine. This, proving to be ineffective, was followed by a course of systemic steroids together with mesalamine. Steroid withdrawal was difficult, but in June 2003 steroids were discontinued and the patient was in complete remission until February 2004 when he had a relapse with abdominal pain and loose and bloody stools. Treatment was restarted with budesonide 3 mg t.i.d. and azathioprine 150 mg. Budesonide failed to improve the symptoms and steroid-therapy was switched

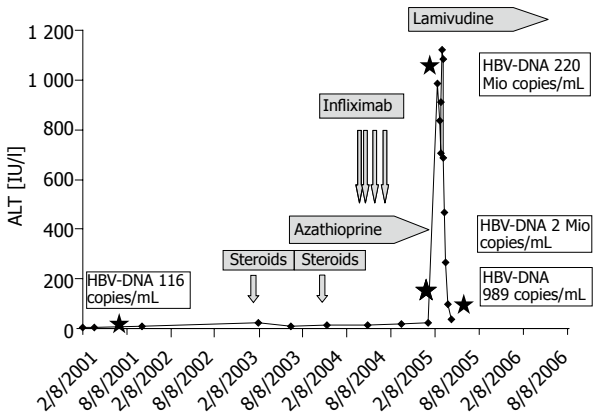


**Figure 1** ALT remained within the normal range during therapy with prednisolone, azathioprine and during the infusions with infliximab. Only after the fourth infusion of infliximab, the patient developed a fulminant hepatitis with ALT up to 1 100 IU/L. HBV-DNA ( ) quantification showed 220 mio copies/mL. Lamivudine (150 mg/d) was started and led to a rapid decrease in transaminases and HBV-DNA.

to systemic steroids (methylprednisolone 40 mg) again. Abdominal pain and bloody stools improved under this regimen but tapering of steroids was followed by an immediate relapse despite azathioprine 2 mg/kg for several months. Endoscopy showed ulcerating inflammation in the terminal ileum and capsule endoscopy revealed involvement of the distal jejunum. Bowel surgery was discussed with the patient, but he wished to try every possible medical treatment before going for surgery. We therefore re-assessed the situation and decided to add infliximab 5 mg/kg (total amount 400 mg) because of steroid-dependent disease. Tuberculosis was excluded by tuberculin-testing and chest X-ray. Blood tests showed mild leukocytosis (14 g/L), all other results including renal and liver function tests, c-reactive protein, iron metabolism, and vitamins were within normal ranges. There was no history of any other disease before the diagnosis of Crohn's disease, besides a mild reactive depression for which the patient has been on mirtazapine for more than a year. Transaminases were documented to be within normal ranges since 2001.

Infliximab was administered successfully at week 0, 2, and 6 followed by complete remission and rapid tapering of steroids. Basis therapy consisted at this time of azathioprine 150 mg, mirtazapine 30 mg, pantoprazole 40 mg and brotizolam 0.25 mg at night. The infusion at wk 6 was followed by 3 d of flu-like symptoms. One month after the third infliximab infusion, the patient came to the outpatient clinic because of abdominal discomfort and malaise. Blood tests showed signs of acute hepatitis (ALT 983 [normal <50 IU/L], AST 413 [normal <50 IU/L], γGT 109 [normal <66 IU/L], LDH 237 [normal <232 IU/L], bilirubin 2.17 [normal <1.28 mg/dL] and a decreased prothrombin time of 63% [normal >70%]) (course of ALT Figure 1). Liver parenchyma was hyperechogenic in sonography but there were no signs of liver cirrhosis and as expected, there were no signs of mechanical cholestasis. The patient mentioned at this point that he had been immunized against hepatitis A and B six months before by his general practitioner because all other members of his family had undergone hepatitis B and he intended to travel to Southern Europe during the summer holidays. No previous serological examination had been performed before immunization.

Complete work-up was done one week after his admission to the hospital. Hepatitis-serology revealed immunity against hepatitis A and negative serology and PCR for hepatitis C, but circulating HBs-antigen, no HBe-antigen but anti-HBe- and anti-HBc-antibodies, and negative anti-HBc-IgM were detected. Quantification of HBV-DNA showed >220 000 000 copies/mL (38 000 000 IU/mL). Other causes for hepatitis such as EBV, CMV, autoimmune hepatitis and acute Wilson's disease were ruled out. We suspected reactivation of hepatitis B from a previously unknown HBV-carrier state. This was corroborated by serology from a frozen serum sample from a previous visit in 2001 also showing the features of an HBs-antigen carrier but a low viral load with 116 copies/mL (20 IU/mL).

Antiviral therapy (lamivudine 150 mg daily) was started immediately after diagnosis. Despite the therapy, liver synthesis parameters transiently decreased and reached a nadir three weeks after the first manifestation with a prothrombin-time of 42% and bilirubin peak of 35 mg/dL. At the same time, the patient developed mild hepatic encephalopathy with increased sleepiness. One month after the diagnosis, the patient recovered, transaminases decreased and prothrombin-time normalized and HBV-DNA dropped to 2 000 000 copies/mL (340 000 IU/mL). The patient could be discharged and followed up in the outpatient clinic. The most recent visit two months after the acute hepatitis showed normal transaminases and HBV-DNA of 989 copies/mL (170 IU/mL).

## DISCUSSION

While patients undergoing chemotherapy for malignancy have long been screened for chronic hepatitis B and treated prophylactically with lamivudine if positive, this has not been performed on a routine basis in patients with chronic inflammatory bowel disease requiring immunosuppressive regimens including infliximab. Our knowledge about the role of TNF-α in chronic viral hepatitis is sparse but there is evidence that TNF-α synergizes with interferons in suppressing viral replication[2,7,22] and is essential in clearing HBV[17]. A promoting effect for increased HBV-replication during treatment with anti-TNF-antibodies could be explained on this basis. But why HBs-antigen carriers, upon anti-TNF-α treatment, suddenly lose their tolerance against HBV and switch to a cytotoxic T-lymphocytic activation leading to hepatocyte injury and liver failure remains to be elucidated. At present we can only speculate that TNF-α might play an important role in maintaining tolerance in the HBs-antigen carrier state.

Till date there are only three case reports and one report of a small group of HBs-antigen carriers that suffered HBV-reactivation following administration of infliximab. Four patients developed fulminant hepatitis B[1,8,12] while one patient had only moderately elevated transaminases[20] that returned to normal without antiviral therapy. Esteve *et al* reported that two of their patients

showed severe reactivation and one died from hepatic failure, but another patient on lamivudine had no worsening of liver disease during infliximab-therapy[1]. Stable HBV under lamivudine has also been reported by Oniankitan *et al*[11] and Valle Garcia-Sanchez *et al*[21]. Keeping these reports in mind and looking for other factors that might influence the course of HBV, we suggest that (1) the number of infliximab-infusions and (2) concomitant immunomodulatory therapy might influence the course of HBV-reactivation (azathioprine in our case and methotrexate therapy in the other cases with severe hepatitis).

In our patient HBV-reactivation was noted after the third infusion of infliximab. Previous treatment with steroids and azathioprine alone had not induced a flare-up in hepatitis B, although it is known that all types of immunosuppressive therapy can lead to a flare-up in hepatitis B. For steroids this has been documented most frequently in patients with hematological malignancies[18]. Azathioprine and methotrexate have also been linked with HBV-recurrence. But while this occurred on treatment with azathioprine[9], it took place only after the discontinuation of methotrexate[3,5,10].

In conclusion, our report on a patient with Crohn's disease developing subfulminant hepatitis under infliximab treatment due to reactivation of a previously unknown HBs-antigen-carrier state draws attention to the need for screening patients with inflammatory bowel disease for hepatitis B and for antiviral prophylaxis in HBV-positive patients prior to therapy with anti-TNF-α antibodies.

## ACKNOWLEDGMENTS

We thank Anna Schlögl, Gisela Egg, and Barbara Wimmer for technical and Rajam Csordas for editorial assistance.

## REFERENCES

1 **Esteve M,** Saro C, Gonzalez-Huix F, Suarez F, Forne M, Viver JM. Chronic hepatitis B reactivation following infliximab therapy in Crohn's disease patients: need for primary prophylaxis. *Gut* 2004; **53**: 1363-1365

2 **Feduchi E,** Alonso MA, Carrasco L. Human gamma interferon and tumor necrosis factor exert a synergistic blockade on the replication of herpes simplex virus. *J Virol* 1989; **63**: 1354-1359

3 **Flowers MA,** Heathcote J, Wanless IR, Sherman M, Reynolds WJ, Cameron RG, Levy GA, Inman RD. Fulminant hepatitis as a consequence of reactivation of hepatitis B virus infection after discontinuation of low-dose methotrexate therapy. *Ann Intern Med* 1990; **112**: 381-382

4 **Hanauer SB,** Feagan BG, Lichtenstein GR, Mayer LF, Schreiber S, Colombel JF, Rachmilewitz D, Wolf DC, Olson A, Bao W, Rutgeerts P. Maintenance infliximab for Crohn's disease: the ACCENT I randomised trial. *Lancet* 2002; **359**: 1541-1549

5 **Ito S,** Nakazono K, Murasawa A, Mita Y, Hata K, Saito N, Kikuchi M, Yoshida K, Nakano M, Gejyo F. Development of fulminant hepatitis B (precore variant mutant type) after the discontinuation of low-dose methotrexate therapy in a rheumatoid arthritis patient. *Arthritis Rheum* 2001; **44**: 339-342

6 **Keane J,** Gershon S, Wise RP, Mirabile-Levens E, Kasznica J, Schwieterman WD, Siegel JN, Braun MM. Tuberculosis associated with infliximab, a tumor necrosis factor alpha-neutralizing agent. *N Engl J Med* 2001; **345**: 1098-1104

7 **Lucin P,** Jonjic S, Messerle M, Polic B, Hengel H, Koszinowski UH. Late phase inhibition of murine cytomegalovirus replication by synergistic action of interferon-gamma and tumour necrosis factor. *J Gen Virol* 1994; **75 (Pt 1)**: 101-110

8 **Michel M,** Duvoux C, Hezode C, Cherqui D. Fulminant hepatitis after infliximab in a patient with hepatitis B virus treated for an adult onset still's disease. *J Rheumatol* 2003; **30**: 1624-1625

9 **Mok MY**, Ng WL, Yuen MF, Wong RW, Lau CS. Safety of disease modifying anti-rheumatic agents in rheumatoid arthritis patients with chronic viral hepatitis. *Clin Exp Rheumatol* 2000; **18**: 363-368

10 **Narvaez J,** Rodriguez-Moreno J, Martinez-Aguila MD, Clavaguera MT. Severe hepatitis linked to B virus infection after withdrawal of low dose methotrexate therapy. *J Rheumatol* 1998; **25**: 2037-2038

11 **Oniankitan O,** Duvoux C, Challine D, Mallat A, Chevalier X, Pawlotsky JM, Claudepierre P. Infliximab therapy for rheumatic diseases in patients with chronic hepatitis B or C. *J Rheumatol* 2004; **31**: 107-109

12 **Ostuni P,** Botsios C, Punzi L, Sfriso P, Todesco S. Hepatitis B reactivation in a chronic hepatitis B surface antigen carrier with rheumatoid arthritis treated with infliximab and low dose methotrexate. *Ann Rheum Dis* 2003; **62**: 686-687

13 **Peterson JR,** Hsu FC, Simkin PA, Wener MH. Effect of tumour necrosis factor alpha antagonists on serum transaminases and viraemia in patients with rheumatoid arthritis and chronic hepatitis C infection. *Ann Rheum Dis* 2003; **62**: 1078-1082

14 **Present DH,** Rutgeerts P, Targan S, Hanauer SB, Mayer L, van Hogezand RA, Podolsky DK, Sands BE, Braakman T, DeWoody KL, Schaible TF, van Deventer SJ. Infliximab for the treatment of fistulas in patients with Crohn's disease. *N Engl J Med* 1999; **340:** 1398-1405

15 **Reijasse D,** Le Pendeven C, Cosnes J, Dehee A, Gendre JP, Nicolas JC, Beaugerie L. Epstein-Barr virus viral load in Crohn's disease: effect of immunosuppressive therapy. *Inflamm Bowel Dis* 2004; **10**: 85-90

16 **Ricart E,** Panaccione R, Loftus EV, Tremaine WJ, Sandborn WJ. Infliximab for Crohn's disease in clinical practice at the Mayo Clinic: the first 100 patients. *Am J Gastroenterol* 2001; **96**: 722-729

17 **Schlaak JF,** Tully G, Lohr HF, Gerken G, Meyer zum Buschenfelde KH. HBV-specific immune defect in chronic hepatitis B (CHB) is correlated with a dysregulation of pro- and anti-inflammatory cytokines. *Clin Exp Immunol* 1999; **115**: 508-514

18 **Takai S,** Tsurumi H, Ando K, Kasahara S, Sawada M, Yamada T, Hara T, Fukuno K, Takahashi T, Oyama M, Onishi H, Tomita E, Takami T, Imawari M, Moriwaki H. Prevalence of hepatitis B and C virus infection in haematological malignancies and liver injury following chemotherapy. *Eur J Haematol* 2005; **74**: 158-165

19 **Targan SR,** Hanauer SB, van Deventer SJ, Mayer L, Present DH, Braakman T, DeWoody KL, Schaible TF, Rutgeerts PJ. A short-term study of chimeric monoclonal antibody cA2 to tumor necrosis factor alpha for Crohn's disease. Crohn's Disease cA2 Study Group. *N Engl J Med* 1997; **337**: 1029-1035

20 **Ueno Y,** Tanaka S, Shimamoto M, Miyanaka Y, Hiyama T, Ito M, Kitadai Y, Yoshihara M, Sumii M, Chayama K. Infliximab therapy for Crohn's disease in a patient with chronic hepatitis B. *Dig Dis Sci* 2005; **50**: 163-166

21 **del Valle Garcia-Sanchez M,** Gomez-Camacho F, Poyato-Gonzalez A, Iglesias-Flores EM, de Dios-Vega JF, Sancho-Zapatero R. Infliximab therapy in a patient with Crohn's disease and chronic hepatitis B virus infection. *Inflamm Bowel Dis* 2004; **10:** 701-702

22 **Wong GH,** Goeddel DV. Tumour necrosis factors alpha and beta inhibit virus replication and synergize with interferons. *Nature* 1986; **323**: 819-822

**S- Editor** Guo SY **L- Editor** Elsevier HK **E- Editor** Kong LH

PO Box 2345, Beijing 100023, China
www.wjgnet.com
wjg@wjgnet.com

*World J Gastroenterol* 2006 February 14; 12(6): 977-978
***World Journal of Gastroenterology*** ISSN 1007-9327
© 2006 The WJG Press. All rights reserved.

*CASE REPORT*

# A case of Crohn's disease involving the gallbladder

Akira Andoh, Yoshihiro Endo, Ryoji Kushima, Kazunori Hata, Tomoyuki Tsujikawa, Masaya Sasaki, Eiji Mekata, Toru Tani, Yoshihide Fujiyama

Akira Andoh, Yoshihiro Endo, Ryoji Kushima, Kazunori Hata, Tomoyuki Tsujikawa, Masaya Sasaki, Eiji Mekata, Toru Tani, Yoshihide Fujiyama, Department of Internal Medicine, Surgery and Clinical Laboratory Medicine, Shiga University of Medical Science, Seta Tukinowa, Otsu 520-2192, Japan
Correspondence to: Dr Akira Andoh, Department of Internal Medicine, Shiga University of Medical Science, Seta Tukinowa, Otsu 520-2192, Japan. andoh@belle.shiga-med.ac.jp
Telephone: +81-77-5482217
Received: 2005-03-06 Accepted: 2005-07-28

## Abstract

Crohn's disease is well known to affect any part of the gastrointestinal tract including the oral cavity and anus. Various extraintestinal complications have been reported in Crohn's disease, but extraintestinal involvement characterized by granulomatous lesions is uncommon. Here, we have reported a case about the involvement of the gallbladder in Crohn's disease. A 33-year-old woman was diagnosed having panperitonitis due to intestinal perforation and cholecystitis. The patient was moved to the surgical service for an emergency operation. On the resected specimen, there was a broad longitudinal ulcer at the mesenteric side. The mucosa of the gallbladder was nodular and granular, and the wall was thickened. The surface epithelium of the gallbladder was partially eroded and pyloric gland metaplasia was observed focally. Rokitansky-Aschoff sinuses were also present. From the lamina propria to the subserosal layer, there were several well-formed epithelioid cell granulomas, which were the non-caseating sarcoidal type different from the foreign-body and xanthomatous granulomas. Periodic-acid Schiff and acid fast stains revealed no organism within the granulomas. Lymphoid aggregates were present throughout the gallbladder wall. Sections from the resected ileum showed typical features of the Crohn's disease. When cholecystectomy is performed in a patient with Crohn's disease, the possibility of gallbladder involvement should be carefully examined by histopathological tests.

© 2005 The WJG Press. All rights reserved.

**Key words:** IBD; Granuloma; Inflammation

Andoh A, Endo Y, Kushima R, Hata K, Tsujikawa T, Sasaki M, Mekata E, Tani T, Fujiyama Y. A case of Crohn's disease involving the gallbladder. *World J Gastroenterol* 2006; 12(6):977-978

http://www.wjgnet.com/1007-9327/12/977.asp

## INTRODUCTION

Crohn's disease is well known to affect any part of the gastrointestinal tract including the oral cavity and anus. Various extraintestinal complications have been reported in Crohn's disease, but extraintestinal involvement characterized by granulomatous lesions is uncommon. Here, we report a case of the involvement of the gallbladder in Crohn's disease.

## CASE REPORT

The patient was a 33-year-old woman who was admitted to the Shiga University of Medical Science Hospital with complaints of nausea, vomiting, and severe abdominal pain, which had lasted for a couple of hours. Her past history included Crohn's disease (ileocolonic type) and gallbladder stone, which had been diagnosed 2 years ago. She was well controlled with medications (2 250 mg/d 5-aminosalicilate and 2 000 kcal/d elemental diet) in these 2 years. She did not feel any symptoms of gallbladder stone.

At the time of admission, her vital signs were as follows: body temperature 37.4 ℃, blood pressure 92/60 Pa, and pulse 98 beats/min. The laboratory data included a white blood count of 13.1 ($\times 10^3$/mL), and C-reactive protein of 13.6 mg/dL. The values for biochemistry were within the normal range. An abdominal CT scan demonstrated a free-air space located in the dorsal side of the abdomen, ascites, strong contrast enhancement of a thickened ileum, fluid collection in the small intestine, and gallbladder swelling with calcifications (Figure 1). The intra- and extrahepatic bile ducts appeared normal. These findings were suggestive of panperitonitis due to intestinal (ileal) perforation and cholecystitis.

After the admission, the patient was moved to the surgical service for an emergency operation. A perforating hole (diameter 5 mm) was located at the ileum 20 cm oral side from Bauhin's valve, and thus segmental ileotomy (25 cm resection) was performed. On the resected specimen, there was a broad longitudinal ulcer at the mesenteric side. Following an ileotomy, the patient also received a cholecystectomy. The serosal surface of the gallbladder adhered tightly to the greater omentum and duodenal bulbus.

The mucosa was nodular and granular, and the wall was

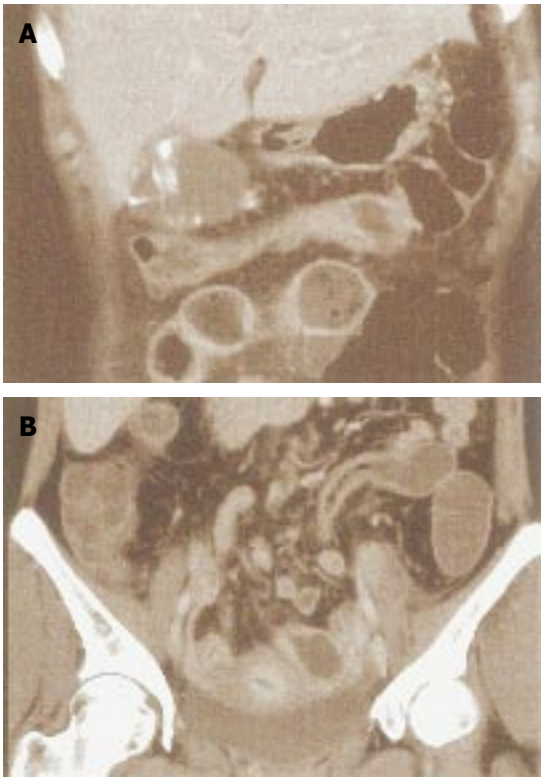


**Figure 1** Abdominal CT scan on admission. CT scan demonstrated gallbladder swelling with thickened wall and stones, ascites, a thickened ileum, and fluid collection in the small intestine.

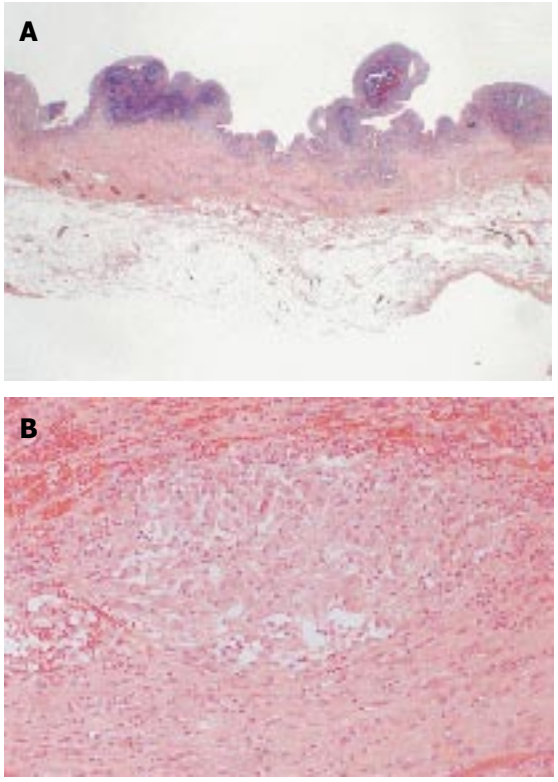


**Figure 2** Histological findings of the gallbladder. **A:** The mucosa was nodular and granular, and the wall was thickened. Erosion and submucosal bleeding were also observed, but there were no obvious ulcers; **B:** There were several well-formed epithelioid cell granulomas, which was non-caseating sarcoidal type, different from the foreign-body and xanthomatous granulomas.

thickened. Erosion and submucosal bleeding were also observed, but there were no obvious ulcers (Figure 2A). The surface epithelium of the gallbladder was partially eroded and pyloric gland metaplasia was observed focally. The lamina propria showed discontinuous chronic active inflammation. The muscular layer was hypertrophied and the subserosal layer was thickened with marked fibrosis. Rokitansky-Aschoff sinuses were also present. From the lamina propria to the subserosal layer, there were several well-formed epithelioid cell granulomas, which were the non-caseating sarcoidal type, different from the foreign-body and xanthomatous granulomas (Figure 2B). Periodic-acid Schiff and acid fast stains revealed no organism within the granulomas. Lymphoid aggregates were present throughout the gallbladder wall. Sections from the resected ileum showed typical features of Crohn's disease.

Her clinical course was good, and she was discharged from the hospital 1 mo after the operation.

## DISCUSSION

A high prevalence of gallstones in Crohn's disease has been reported[1], but gallbladder involvement in Crohn's disease is very rare. Based on our MEDLINE search of the literature, only three case reports were found[2-4]. In all cases including our patient, the pathological examination of the gallbladder revealed transmural inflammation, granulomatous change and lymphoid aggregation, all of which were similar to those seen in the bowel lesions. Duodenal Crohn's disease has been reported to occasionally involve the surrounding organs[2,3], but our case did not present any duodenal lesions, indicating that the gallbladder lesion might not be a consequence of spread by contiguity. When cholecystectomy is performed in a patient with Crohn's disease, the possibility of gallbladder involvement should be carefully examined by histopathological examinations.

## REFERENCES

1 **Lapidus A,** Bangstad M, Astrom M, Muhrbeck O. The prevalence of gallstone disease in a defined cohort of patients with Crohn's disease. *Am J Gastroenterol* 1999; **94:** 1261-1266
2 **McClure J,** Banerjee SS, Schofield PS. Crohn's disease of the gall bladder. *J Clin Pathol* 1984; **37:** 516-518
3 **Post AB,** van Stolk R, Broughan TA, Tuthill RJ. Crohn's disease of the gallbladder. *J Clin Gastroenterol* 1993; **16:** 139-142
4 **Rettally CA,** Trevino HH, Molina K, Kane SV. Crohn's disease involving the gallbladder. case report and review of the literature. *Am J Gastroenterol* 2003; **98:** 509-511

**S- Editor** Xu XQ and Guo SY **L- Editor** Elsevier HK **E- Editor** Bi L

PO Box 2345, Beijing 100023, China
www.wjgnet.com
wjg@wjgnet.com

*World J Gastroenterol* 2006 February 14; 12(6): 979-981
***World Journal of Gastroenterology*** ISSN 1007-9327
© 2006 The WJG Press. All rights reserved.

*CASE REPORT*

# Intestinal Behcet's disease with pyoderma gangrenosum: A case report

Toshio Nakamura, Hiroaki Yagi, Kiyotaka Kurachi, Shohachi Suzuki, Hiroyuki Konno

Toshio Nakamura, Kiyotaka Kurachi, Shohachi Suzuki, Hiroyuki Konno, Second Department of Surgery, Hamamatsu University School of Medicine, Hamamatsu 431-3192, Japan
Hiroaki Yagi, Department of Dermatology, Hamamatsu University School of Medicine, Hamamatsu 431-3192, Japan
Correspondence to: Toshio Nakamura, MD, The Second Department of Surgery, Hamamatsu University School of Medicine, 1-20-1 Handa-yama, Hamamatsu 431-3192, Japan. toshi38@hama-med.ac.jp
Telephone: +81-53-435-2279 Fax: +81-53-435-2273
Received: 2005-06-09 Accepted: 2005-07-08

## Abstract

We report here a very rare case of intestinal Behcet's disease with pyoderma gangrenosum. A 16-year-old woman who was diagnosed with intestinal Behcet's disease by the presence of cutaneous pathergy together with two major criteria (oral and genital aphthoses) and one minor criterion (gastrointestinal manifestations), was referred to our hospital with a left lower leg ulcer and abdominal pain in September 1989. Colonoscopy demonstrated flare-up colitis involving the entire colon. Her lower leg lesion was a painful destructive ulcer with an irregular margin and a ragged overhanging edge. Based on these clinical and laboratory findings, we diagnosed her cutaneous ulcer as pyoderma gangrenosum developing with exacerbated intestinal Behcet's disease. Her cutaneous and intestinal lesions were poorly controlled though she received oral prednisolone treatment for a month. Because of aggravated abdominal symptoms with peritoneal irritation, we performed total colectomy in November 1989. The resected specimen was histologically compatible with intestinal Behcet's disease showing severe inflammation with deep ulcerations and neutrophil accumulation. Subsequently, pyoderma gangrenosum rapidly improved. This clinical course may suggest the close relationship between pyoderma gangrenosum and intestinal Behcet's disease.

© 2006 The WJG Press. All rights reserved.

**Key words**: Behcet's disease; Pyoderma gangrenosum

Nakamura T, Yagi H, Kurachi K, Suzuki S, Konno H. Intestinal Behcet's disease with pyoderma gangrenosum: A case report. *World J Gastroenterol* 2006; 12(6): 979-981

http://www.wjgnet.com/1007-9327/12/979.asp

## INTRODUCTION

Behcet's disease is a multi-system inflammatory disorder of unknown origin, characterized by recurrent oral and genital ulcerations, ocular and cutaneous lesions, arthritis and vascular disease. Cases of Behcet's disease cluster along the ancient Silk Road, which extends from eastern Asia to the Mediterranean basin[1-3]. It is often difficult to distinguish Behcet's disease from other inflammatory bowel diseases. Pyoderma gangrenosum is an idiopathic ulcerative skin disease. Because the histological findings of pyoderma gangrenosum are nonspecific and no laboratory confirmation exists, the diagnosis is based primarily on its clinical manifestations. Though this skin lesion is known to be associated with inflammatory bowel diseases, such as ulcerative colitis and Crohn's disease, pyoderma gangrenosum is very rare in Behcet's disease patients. We present a patient with extensive pyoderma gangrenosum whose skin lesions were resolved after surgical removal of the inflamed intestinal lesions.

## CASE REPORT

A 16-year-old woman was referred to our hospital in September 1989 due to painful ulceration on the left foot and lower abdominal pain. She was diagnosed with intestinal Behcet's disease by the presence of cutaneous pathergy together with two major criteria (oral and genital aphthoses) and one minor criterion (gastrointestinal manifestations) in 1984. Her lower leg lesion was a painful destructive ulcer with an irregular margin and a ragged overhanging edge (Figure 1A). She was negative for repeated bacterial, fungal and viral cultures. Colonoscopy demonstrated flare-up colitis involving the entire colon. Based on these clinical and laboratory findings, her skin lesion was considered pyoderma gangrenosum developing with aggravation of her intestinal Behcet's disease. She was treated with prednisolone (20 mg orally per day) for a month, but the skin lesion was poorly controlled. In November 1989, she complained of severe abdominal pain and melena. Laboratory data showed a white blood cell count of 14900/mm$^3$, serum C-reactive protein of 4.5 mg/dL and hemoglobin of 12.3 g/dL. Because her abdominal symptoms were aggravated with peritoneal irritation, we performed a total colectomy with partial ilealectomy and ileo-rectal anastomosis. The resected specimen revealed severe inflammation with punched-out ulcerations of the colon and ileum (Figure 2A). Microscopic findings showed active colitis with neutrophil

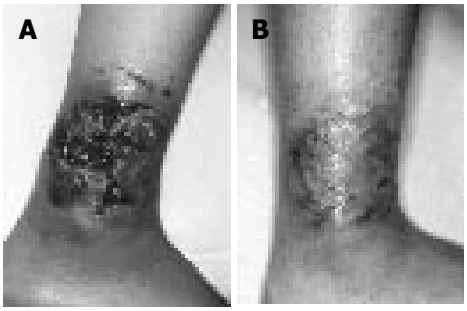


**Figure 1** Painful destructive ulcer of the foot with an irregular margin and a ragged overhanging edge (**A**) and intractable leg ulcer without improvement after oral corticosteroid therapy was cured after total colectomy (**B**).

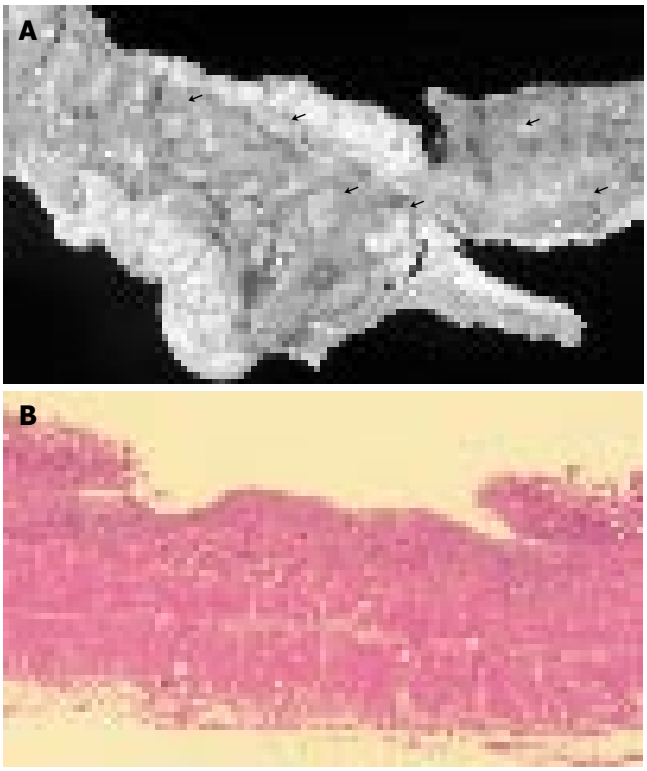


**Figure 2** Severe inflammation and deep ulcerations of specimens from colon and ileum (**A**) and active colitis with neutrophil accumulation around the ulcer beds (**B**) (HE stain, x100).

accumulation around the ulcer beds. Subsequently her abdominal symptoms gradually improved. Surprisingly, intractable ulceration of the left foot disappeared without scarring within two weeks after the surgery (Figure 1B). She was discharged with an uneventful postoperative course. Relapse of pyoderma gangrenosum has not been observed for 10 years after surgery.

## DISCUSSION

Intestinal Behcet's disease has been categorized in a family with inflammatory bowel disease, and causes abdominal pain, diarrhea, melena and even perforation. The ileocecal region is the most commonly affected part of the gastrointestinal tract, but the distal colon may also be involved. It is often difficult to distinguish Behcet's disease from the other inflammatory bowel diseases because of the similar extra-intestinal manifestations including oral aphthosis, uveitis and arthritis. Genital ulceration and positive pathergy test are the extra-intestinal features of Behcet's disease alone, which are not seen in the other inflammatory bowel diseases. Our patient was diagnosed as Behcet's disease by the presence of cutaneous pathergy together with two major criteria (recurrent oral and genital aphthoses) and one minor criterion (gastrointestinal manifestations)[4].

**Table 1 Reported cases of Behcet's disease with pyoderma gangrenosum**

| Author | Year | Age | Gender | Preceding disease | Treatment |
|---|---|---|---|---|---|
| Munro *et al*[5] | 1988 | 43 | Female | Behcet | Thalidomide |
| Lilford *et al*[6] | 1989 | 40 | Female | Behcet | Steroid |
| Rustin *et al*[7] | 1990 | 40 | Male | Behcet | Thalidomide |
| Armas *et al*[8] | 1992 | 52 | Male | Behcet | Steroid |
| Present case | 2003 | 16 | Female | Behcet | Total colectomy |

In Behcet's disease, multiple cutaneous lesions, such as erythema nodosum, folliculitis and pustules are seen, but pyoderma gangrenosum is very rare. Pyoderma gangrenosum in the present case did not respond to oral corticosteroids but was improved soon after the resection of inflamed intestinal lesions. Since the first report by Munro and Cox in 1988[5], four cases of pyoderma gangrenosum associated with Behcet's disease have been reported in English literature[6-8] (Table 1). Behcet's disease always precedes the onset of pyoderma gangrenosum. These patients are treated with corticosteroids, immunosuppressants or thalidomide. It was reported that cases of pyoderma gangrenosum had no improvement after surgical removal of the intestinal lesions[9]. Pyoderma gangrenosum usually responds to systemic corticosteroids and may also be rapidly improved by surgical resection of the associated diseases, such as ulcerative colitis and Crohn's disease. Therefore, the activity of pyoderma gangrenosum is closely related to the activity of associated diseases. In the present case, pyoderma gangrenosum rapidly improved after total colectomy. The skin manifestations of Behcet's disease are classified as neutrophilic vascular reaction[10]. The pathergy test is useful for evaluating skin irritability and is a diagnostic criterion of Behcet's disease. However, this test can also be positive in other diseases such as Sweet's syndrome and pyoderma gangrenosum. Pyoderma gangrenosum is a form of cutaneous vasculitis[11] and accumulation of neutrophils and mononuclear cells is observed at the reaction site. In both Behcet's disease and pyoderma gangrenosum, primary pustular lesions can occur and neither of them has a characteristic histological appearance. They may belong to the category of the neutrophilic dermatoses.

Though the relationship between Behcet's disease and pyoderma gangrenosum is not referred in diagnostic criteria of Behcet's disease, the occurrence of pyoderma gangrenosum may be highly relevant with the pathogenesis of Behcet's disease.

## ACKNOWLEDGEMENTS

We are grateful to Professors Shozo Baba and Keiji Iwatsuki for their excellent comments on the manuscript.

## REFERENCES

1 **Kastner DL**. Intermittent and periodic arthritic syndromes. In: Koopman WJ, ed. Arthritis and allied conditions: a textbook of rheumatology. 13th ed. Vol. 1. Baltimore: Williams & Wilkins, 1997: 1279-1306
2 **Kaklamani VG,** Vaiopoulos G, Kaklamanis PG. Behcet's Disease. *Semin Arthritis Rheum* 1998; **27:** 197-217
3 **Mizuki N,** Inoko H, Ohno S. Pathogenic gene responsible for the predisposition of Behcet's disease. *Int Rev Immunol* 1997; **14:** 33-48
4 Criteria for diagnosis of Behcet's disease. International Study Group for Behcet's Disease. *Lancet* 1990; **335:** 1078-1080
5 **Munro CS,** Cox NH. Pyoderma gangrenosum associated with Behcet's syndrome--response to thalidomide. *Clin Exp Dermatol* 1988; **13:** 408-410
6 **Lilford RJ,** Tindall VR, Batchelor AG. Post-surgical pyoderma gangrenosum of the vaginal vault associated with ulcerative colitis and Behcet's disease; a case report. *Eur J Obstet Gynecol Reprod Biol* 1989; **31:** 93-94
7 **Rustin MH,** Gilkes JJ, Robinson TW. Pyoderma gangrenosum associated with Behcet's disease: treatment with thalidomide. *J Am Acad Dermatol* 1990; **23:** 941-944
8 **Armas JB,** Davies J, Davis M, Lovell C, McHugh N. Atypical Behcet's disease with peripheral erosive arthropathy and pyoderma gangrenosum. *Clin Exp Rheumatol* 1992; **10:** 177-180
9 **Levitt MD**, Ritchie JK, Lennard-Jones JE, Phillips RK. Pyoderma gangrenosum in inflammatory bowel disease. *Br J Surg* 1991; **78:** 676-678
10 **James DW,** Walker JR, Smith MJ. Abnormal polymorphonuclear leucocyte chemotaxis in Behcet's syndrome. *Ann Rheum Dis* 1979; **38:** 219-221
11 **Powell FC,** Schroeter AL, Su WP, Perry HO. Pyoderma gangrenosum: a review of 86 patients. *Q J Med* 1985; **55:** 173-186

**S- Editor** Guo SY **L- Editor** Elsevier HK **E- Editor** Kong LH

PO Box 2345, Beijing 100023, China
www.wjgnet.com
wjg@wjgnet.com

*World J Gastroenterol* 2006 February 14; 12(6): 982-986
***World Journal of Gastroenterology*** ISSN 1007-9327
© 2006 The WJG Press. All rights reserved.

*CASE REPORT*

# Spontaneous rupture of a type IVA choledochal cyst in a young adult during radiological imaging

Ekaterini Stipsanelli, Pipitsa Valsamaki, Spyridon Tsiouris, Angelika Arka, Georgios Papathanasiou, Nikolaos Ptohis, Stephanos Lahanis, Vassilios Papantoniou, Cherry Zerva

Ekaterini Stipsanelli, Pipitsa Valsamaki, Spyridon Tsiouris, Angelika Arka, Georgios Papathanasiou, Vassilios Papantoniou, Cherry Zerva, Department of Nuclear Medicine, 'ALEXANDRA' University Hospital, 80, Vas. Sophia's Ave. & 2, K. Lourou Str., 115 28 Athens, Greece
Nikolaos Ptohis, Department of Radiology, 'ALEXANDRA' University Hospital, 80, Vas. Sophia's Ave. & 2, K. Lourou Str., 115 28 Athens, Greece
Stephanos Lahanis, Department of Radiology, 401 General Military Hospital, Mesogheion Ave. & 3, Kanelopoulou Str., 115 25 Athens, Greece
Correspondence to: Dr Pipitsa Valsamaki, 'ALEXANDRA' University Hospital, Department of Nuclear Medicine, 80, Vas. Sophia's Ave. & 2, K. Lourou Str., 115 28 Athens, Greece. pivals@gmail.com
Telephone: +30-210-33-81-785 Fax: +30-210-77-07-404
Received: 2005-03-23 Accepted: 2005-07-28

## Abstract

A case of a 24-year-old male with jaundice and epigastric pain is reported. The patient underwent a thorough clinical, laboratory, and imaging investigation. Computerized tomography revealed a 9 cm×10 cm choledochal cyst. Magnetic resonance imaging and magnetic cholangiopancreatography were performed, during which he developed an "acute abdomen", with radiological evidence of biliary peritoneal leak. Urgent surgery revealed rupture of the distended malformed common bile duct. A peritoneal drain was instilled and a more definitive surgical procedure was accordingly scheduled. Hepatobiliary scintigraphy following surgery verified these findings, as well as confirmed the adequacy of the urgent surgery. A combination of radiological and nuclear medicine techniques substantially contributes to the diagnosis of choledochal cyst rupture and the adequacy of surgical intervention.

© 2006 The WJG Press. All rights reserved.

**Key words:** Choledochal cyst; Rupture; MRCP; Hepatobiliary scintigraphy

Stipsanelli E, Valsamaki P, Tsiouris S, Arka A, Papathanasiou G, Ptohis N, Lahanis S, Papantoniou V, Zerva C. Spontaneous rupture of a type IVA choledochal cyst in a young adult during radiological imaging. *World J Gastroenterol* 2006; 12(6): 982-986

http://www.wjgnet.com/1007-9327/12/982.asp

## CASE REPORT

A 24-year-old male was admitted to our hospital with jaundice and epigastric pain reflecting low in the back. The body temperature was normal. He was a heavy drinker in the previous 4 years and reported a history of infantile hyperbilirubinemia, which resolved spontaneously. He had positive Murphy and Giordano signs and a palpable epigastric mass. The laboratory examination results above normal range were as follows: WBC: 12 500/μL (neutrophil: 93.6%, lymphocyte: 5.1%), SGOT: 159 IU/L, SGPT: 559 IU/L, γGT: 520 IU/L, ALP: 244 IU/L, LDH: 699 IU/L, CPK: 606 IU/L, bilirubin (total): 7.68 mg/dL, bilirubin (direct): 6.5 mg/dL, and bile in the urine.

Computerized tomography (CT) of the upper abdomen was ordered, and displayed a 9 cm×10 cm cyst in the common bile duct (CBD) region, extending from porta hepatis down to the level of the third portion of the duodenum (Figure 1). Distension of intrahepatic bile ducts with stasis was also observed. The findings were consistent with a choledochal cyst (CC). Further investigation with magnetic resonance imaging (MRI) and MR cholangiopancreatography (MRCP) was considered appropriate. It confirmed the intrahepatic duct distension and the large cyst (Figure 2). It was considered to be a large CC type IVA. During MRI, the patient developed "acute abdomen" symptoms. Spin echo $T_2$-weighed images and MRCP depicted bile leak in the peritoneal cavity (Figure 3).

Immediately after MRCP he underwent urgent abdominal surgery. A 1-cm rupture of the distended CBD was found, with a considerable amount of intraperitoneal bile and focal biliary peritonitis. A Kehr tube was inserted into the CBD at the site of the rupture and the lips of the lesion were appropriately stitched.

In order to verify the adequacy of the urgent surgical intervention, $^{99m}$Tc-mebrofenin hepatobiliary scintigraphy was advocated on the second postoperative day. The study included a 30-min dynamic acquisition, beginning with injection and consisting of 60 30-s images (frames) of the abdomen, followed by planar static images of the upper abdomen at 1½ h and 24 h post-injection. No active leaking in the peritoneal cavity was observed throughout the study. A well-circumscribed fusiform intense tracer

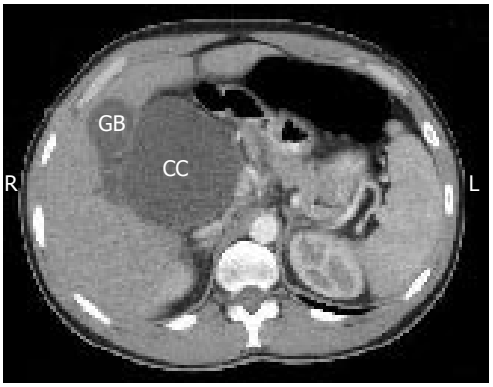


**Figure 1** Upper abdominal CT (after intravenous administration of contrast material) demonstrating the extrahepatic portion of the choledochal cyst (CC). GB: gallbladder.

**Table 1 Classification of choledochal cysts (after Todani *et al*[3])**

| Type | | Characteristics |
|---|---|---|
| I | IA | Dilatation of the common bile duct (CBD), with marked dilatation of part or the entire extrahepatic biliary tree and normal intrahepatic biliary tree |
| | IB | Focal and segmental dilatation of the distal CBD |
| | IC | Fusiform dilatation of the CBD, with diffuse cylindrical dilatation of the common hepatic duct and CBD as well as normal intrahepatic biliary tree |
| II | | Diverticulum of the CBD |
| III | | Choledochocele of the intraduodenal portion of the CBD |
| IV | IVA | Multiple cysts involving both the intrahepatic and extrahepatic bile ducts |
| | IVB | Multiple cysts of the extrahepatic ducts only |
| V | | Caroli's disease |

accumulation was observed in the right hepatic lobe near the hepatic hilum. It appeared early in the dynamic phase (Figure 4) and was most prominent in the 90-min static image while not apparent in the 24-h image (Figure 5). It corresponded to the intrahepatic moiety of the CC. A much fainter bulbous accumulation was displayed in the left hepatic lobe, extending well beyond the liver margins, and corresponded to the large extrahepatic CC moiety. It was apparent earlier in the dynamic study and still visible in the 24-h image (Figures 4 and 5).

## DISCUSSION

Choledochal cysts are congenital abnormalities of the bile ducts of unknown etiology. They comprise cystic dilatations of the extrahepatic and/or intrahepatic biliary tree[1]. They are typically described as a childhood disease. Sixty percent of the patients are diagnosed during the first decade of life. Congenital cysts occur in between 1/100 000 and 1/2 000 000 live births and are more

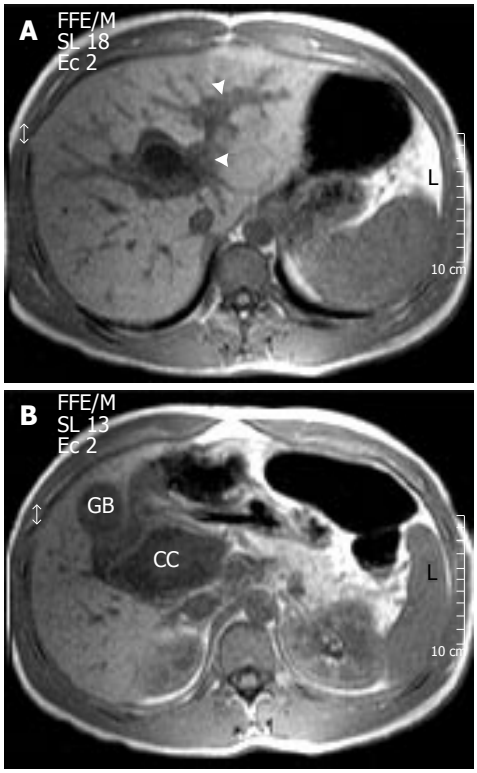


**Figure 2** Significant distension of the intrahepatic bile ducts (arrowhead) in MRI of the upper abdomen (gradient echo $T_1$-weighed acquisition) (**A**). The walls of the choledochal cyst (CC) tend to acquire a concave shape, while its volume appears reduced as compared to the CT findings, both signs are considered as indicative of rupture (**B**). GB: gallbladder.

frequent in females (female-to-male ratio: 3:1 to 4:1). They are usually observed in Asian countries, especially in Japan.

Alonso-Lej *et al*[2] first classified CC into three major types: cystic, diverticular, and choledochocele. Todani *et al*[3] modified the classification system, which currently includes five types based on cholangiographic morphology and number of intrahepatic and extrahepatic bile duct cysts (Table 1). With regard to the shape of extrahepatic and intrahepatic ducts, type IV is further classified into three subtypes: cystic-cystic, cystic-fusiform, and fusiform-fusiform. Cystic-fusiform IVA is the subtype that corresponds to our findings. In this particular subtype, intrahepatic dilatation occurs in both hepatic lobes, with the left being predominantly involved. Yet, in the present case it was the right lobe that was affected.

Ultrasonography is the initial screening examination of choice in suspected CC. Depending on the radiologist's skill it may reveal the type of CC. Nevertheless, inherent limitations (e.g. gas in the bowel, intra-abdominal inflammatory processes, *etc.*) allow for limited anatomic delineation of the non-dilated biliary system[1].

CT imaging can be relied on with a high degree of confidence in confirming an unambiguous diagnosis and providing information regarding CC relationship to the surrounding structures. It usually demonstrates a cyst, which is readily distinguished from the gallbladder as in our case. Depending on patient's age and history, the cystic wall is thickened, especially on the ground of recurrent inflammation and cholangitis.

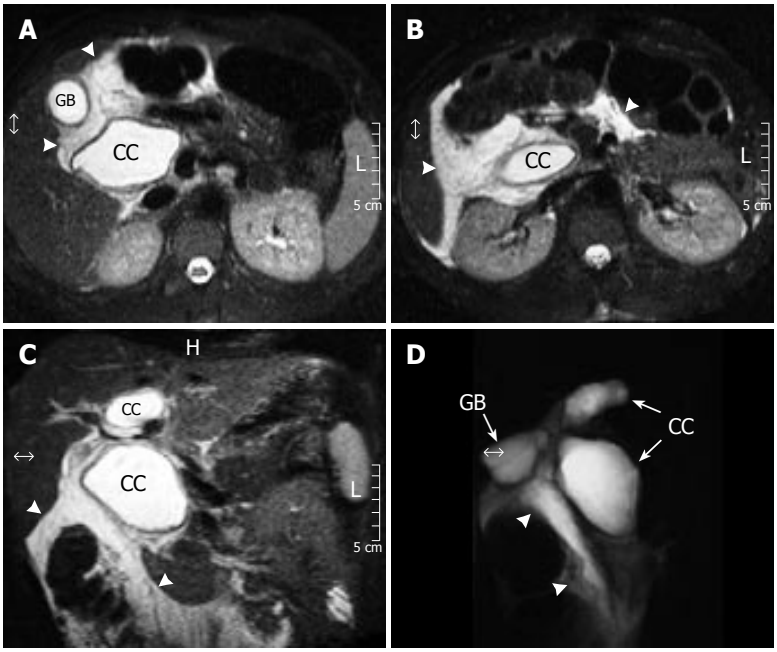


**Figure 3** Abdominal MRI (spin echo $T_2$-weighed, transverse projections - **A** and **B**, coronal projection - **C**) displaying bile leakage into the peritoneal cavity (arrowheads). The study was followed by MRCP (turbo spin echo $T_2$-weighed acquisition - **D**) which imaged the bile leak (arrowheads) and moreover revealed the "egg-timer" bicameral shape of the extrahepatic moiety of the choledochal cyst (CC). GB: gallbladder.

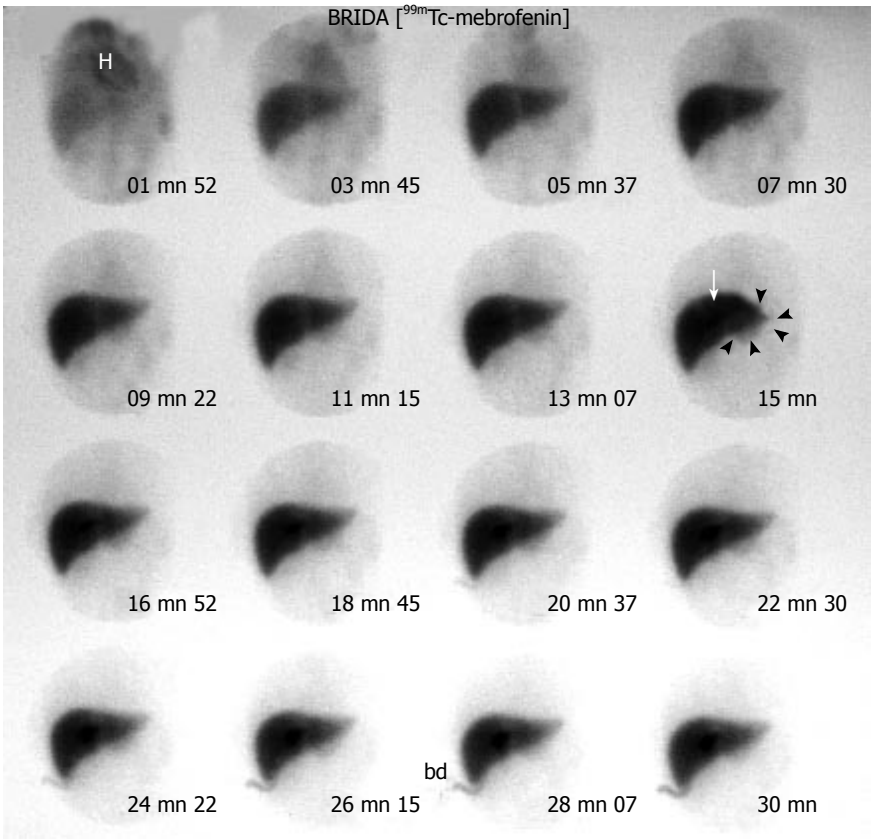


**Figure 4** Postoperative $^{99m}$Tc-mebrofenin dynamic study. A well-circumscribed fusiform tracer accumulation in the right hepatic lobe near the hepatic hilum is clearly visible from the 15$^{th}$ min of the study (arrow), and corresponds to a dilated intrahepatic duct. A much fainter bulbous accumulation is apparent in the area of the left hepatic lobe, extending well beyond the liver margins (arrowheads) and corresponding to the extrahepatic portion of the choledochal cyst. H: heart blood pool; bd: biliary drainage.

MRI with MRCP is the noninvasive imaging modality of choice for the diagnosis of CC. The cysts appear as large fusiform or saccular dilatations producing a specific signal on $T_2$-weighed images. Associated bile duct anomalies can also be demonstrated. On the basis of reported results, MRCP has an estimated diagnostic accuracy of 82-100%[1]. Overall, MRCP is a promising technique that may offer as much as endoscopic retrograde cholangiopancreatography (ERCP).

Hepatobiliary scintigraphy is used in the setting of suspected acute cholecystitis, peritoneal biliary leak, and for the investigation of neonatal jaundice. In addition, it contributes to the diagnosis of CC, although such studies are practically acquired in a limited number of patients. Rajnish *et al*[4] evaluated the efficacy of hepatobiliary scintigraphy in classifying CC patients with confirmed Todani types I and IV cysts and found that it has a good accuracy in the diagnosis, correlating with ERCP or surgical findings in 86% of the cases. The false negative results are mainly attributable to its limitation in identifying

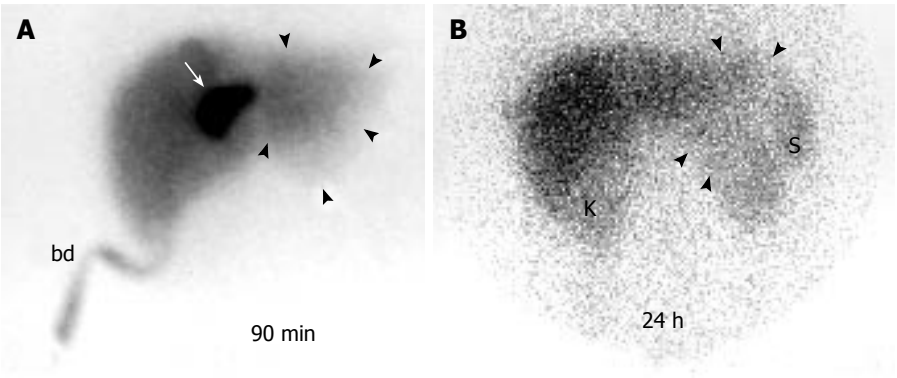


**Figure 5** Planar static scintigraphic images of the upper abdomen. At 90-min post-injection the faint tracer accumulation corresponding to the extrahepatic portion of the choledochal cyst (CC) extends beyond the liver margins (arrowheads), while a fusiform tracer accumulation in a cystic dilated intrahepatic duct is prominent (arrow) (**A**). The latter finding is not visible in the late (24 h) image, nor bowel or peritoneal activity (**B**). bd: biliary drainage; K: kidney; S: spleen.

small intrahepatic dilatations in type IVA. Nevertheless, in our case the fusiform tracer accumulation in the right hepatic lobe corresponds to a dilated intrahepatic duct forming a cyst and its location is uncommon (cysts are usually seen in the left lobe). This intrahepatic cyst was not a continuous extension of the extrahepatic moiety of the CC, but developed secondary to a hepatic hilum ductal stricture, a feature distinguishing CC type IVA from type I[3]. Furthermore, hepatobiliary scintigraphy can provide useful information regarding liver function, biliary patency, and biliary leak in the peritoneum.

Type IVA is observed in 30-40% of CC cases[5]. It is often accompanied with a primary ductal stenosis around the hepatic hilum, which causes either cystic or fusiform dilatation of the intrahepatic duct. The fusiform dilatation imaged in the present case mainly resulted from stricture, whereas cystic dilatation may develop due to primary stricture combined with the weakness of the intrahepatic duct epithelium. The stricture can be radiologically detected and needs cautious surgical exploration[3]. The primary management of type IVA cysts is still controversial. The intrahepatic dilatation tends to gradually reduce in size following sufficient biliary drainage. In addition, lateral hepatic segmentectomy may be necessary, especially in cases of strictures of the upper intrahepatic ducts and when the left hepatic lobe contains gallstones[6]. Patients diagnosed with type IV CC are usually adults, who commonly develop hepatolithiasis[7]. Formation of gallstones leads to the dilatation of the ducts and sometimes is complicated by intrahepatic abscess[8].

Surgical treatment should be recommended to reduce the risk of other serious complications, such as cholangitis, pancreatitis, rupture, portal hypertension, cirrhosis, and cholangiocarcinoma. Pancreatitis develops in 30-70% of adults with CC[9]. Cholangiocarcinoma may evolve in all kinds of cysts, but types I and IV are associated with a higher incidence. In these patients the prognosis is the same as in other cases of cholangiocarcinoma in the general population[10].

On rare occasions, adults may present with an acute abdomen due to CC rupture and biliary peritonitis. The reported incidence ranges between 2-18%[11]. CC perforation is generally spontaneous, although sometimes trauma may be implicated. It is more frequent in children, while in adults it is associated with conditions causing increased intra-abdominal pressure, such as pregnancy[12]. In the present case, no obvious cause of rupture was identified, considering that no kind of abdominal pressure was applied during the MRI/MRCP procedure. We thus believe that rupture was an accidental event. The recommended acute therapy for CC rupture is peritoneal drainage, followed by complete cyst resection, cholecystectomy and Roux-en-Y hepaticojejunostomy reconstruction. Our patient was therefore treated primarily as a surgical emergency with peritoneal drainage and a more definitive surgical procedure was accordingly scheduled.

Controversy exists about the role of hepatic resection in types IV and V cysts due to the difficulty of intrahepatic cyst excision, thus rendering these patients to a more intense long-term follow-up. Alternatively, minimally invasive and laparoscopic treatments have been proposed[9,13,14].

In conclusion, apart from the clinical evidence, the diagnostic algorithm in this case as well as postoperative evaluation comprises information acquired by a combination of imaging modalities, namely CT, MRI/MRCP, and hepatobiliary scintigraphy. The proper handling of such patients relies upon good co-operation between several medical faculties, namely gastroenterology, radiology, nuclear medicine, and surgery, and is essential in order to prevent and treat serious complications.

## ACKNOWLEDGMENTS

The authors thank Dr. Stavroula Lyra, Mr. Alkiviadis Katsoulis, and Mr. Vasilios Makrypoulias, for their technical support.

## REFERENCES

1 **Sawyer MAJ,** Sawyer EM, Patel TH, Varma MK, Allen AW, Murphy TF. Choledochal cyst eMedicine 2004. Available from http://www.emedicine.com/radio/topic161.htm

2 **Alonso-Lej F,** Rever WB Jr, Pessagno DJ. Congenital choledochal cyst, with a report of 2, and an analysis of 94, cases. *Int Abstr Surg* 1959; **108**: 1-30

3 **Todani T,** Watanabe Y, Toki A, Morotomi Y. Classification of congenital biliary cystic disease: special reference to type Ic and IVA cysts with primary ductal stricture. *J Hepatobiliary Pancreat Surg* 2003; **10**: 340-344

4 **Rajnish A,** Gambhir S, Das BK, Saxena R. Classifying choledochal cysts using hepatobiliary scintigraphy. *Clin Nucl Med* 2000; **25**: 996-999

5 **Todani T,** Watanabe Y, Fujii T, Toki A, Uemura S, Koike Y. Congenital choledochal cyst with intrahepatic involvement. *Arch Surg* 1984; **119**: 1038-1043

6 **Lenriot JP,** Gigot JF, Segol P, Fagniez PL, Fingerhut A, Adloff M. Bile duct cysts in adults: a multi-institutional retrospective study. French Associations for Surgical Research. *Ann Surg* 1998; **228**: 159-166
7 **Uno K,** Tsuchida Y, Kawarasaki H, Ohmiya H, Honna T. Development of intrahepatic cholelithiasis long after primary excision of choledochal cysts. *J Am Coll Surg* 1996; **183**: 583-588
8 **Martin LW,** Rowe GA. Portal hypertension secondary to choledochal cyst. *Ann Surg* 1979; **190**: 638-639
9 **Soreide K,** Korner H, Havnen J, Soreide JA. Bile duct cysts in adults. *Br J Surg* 2004; **91**: 1538-1548
10 **Lee KF,** Lai EC, Lai PB. Adult choledochal cyst. *Asian J Surg* 2005; **28**: 29-33
11 **Maheshwari M,** Parekh BR, Lahoti BK. Biliary peritonitis: a rare presentation of perforated choledochal cyst. *Indian Pediatr* 2002; **39**: 588-592
12 **Hewitt PM,** Krige JE, Bornman PC, Terblanche J. Choledochal cyst in pregnancy: a therapeutic dilemma. *J Am Coll Surg* 1995; **181**: 237-240
13 **Ishibashi T,** Kasahara K, Yasuda Y, Nagai H, Makino S, Kanazawa K. Malignant change in the biliary tract after excision of choledochal cyst. *Br J Surg* 1997; **84**: 1687-1691
14 **Kobayashi S,** Asano T, Yamasaki M, Kenmochi T, Nakagohri T, Ochiai T. Risk of bile duct carcinogenesis after excision of extrahepatic bile ducts in pancreaticobiliary maljunction. *Surgery* 1999; **126**: 939-944

**S- Editor** Wang XL and Guo SY **L- Editor** Elsevier HK **E- Editor** Kong LH

PO Box 2345, Beijing 100023, China
www.wjgnet.com
wjg@wjgnet.com

*World J Gastroenterol* 2006 February 14; 12(6): 987-989
***World Journal of Gastroenterology*** ISSN 1007-9327
© 2006 The WJG Press. All rights reserved.

*CASE REPORT*

# Ultrastructure of Kupffer cells and hepatocytes in the Dubin-Johnson syndrome: A case report

Maria Elzbieta Sobaniec-Lotowska, Dariusz Marek Lebensztejn

Maria Elzbieta Sobaniec-Lotowska, Department of Clinical Pathomorphology, Medical University of Bialystok, Poland
Dariusz Marek Lebensztejn, 3rd Department of Pediatrics, Medical University of Bialystok, Poland
Correspondence to: Professor Maria E Sobaniec-Lotowska, Department of Clinical Pathomorphology, Medical University, Waszyngtona 13 Street, Bialystok 15-269, Poland. mariasl@zeus.amb.edu.pl
Telephone: +48-85-7485940 Fax: +48-85-7485990
Received: 2005-08-10 Accepted: 2005-08-26

## Abstract

Ultrastructure of Kupffer cells and hepatocytes in liver bioptate was evaluated in a 17-year-old boy with Dubin –Johnson syndrome (DJS). The liver tissue obtained by needle biopsy was fixed in glutaraldehyde and paraformaldehyde and routinely processed for electron microscopic analysis. The ultrastructural examinations of liver bioptate revealed the accumulation of membrane-bound, electron-dense lysosomal granules within the cytoplasm of hepatocytes, characteristic of DJS. They were located mainly in the vicinity of the biliary pole, and preferentially in the centrilobular region that corresponded to the pigment deposits seen under light microscope. The presence of the granules was accompanied by dilated elements of the granular endoplasmic reticulum and paracrystalline mitochondrial inclusions as well as dilation of the bile canaliculi. The changes in hepatocytes co-existed with marked stimulation and enhanced phagocytic activity of Kupffer cells. This was manifested in the accumulation of pigment deposits within their cytoplasm that corresponded to those observed in hepatocytes. Hyperactive pericentral Kupffer cells which are involved in the response to pigmentary material originating from disintegrated hepatocytes may play an essential role in the development of DJS.

© 2006 The WJG Press. All rights reserved.

**Keywords**: Liver biopsy; Electron microscopic study; Lysosomal granules; Functional hyperbilirubinemia; Dubin–Johnson syndrome

Sobaniec-Lotowska ME, Lebensztejn DM. Ultrastructure of Kupffer cells and hepatocytes in the Dubin-Johnson syndrome: A case report. *World J Gastroenterol* 2006; 12(6): 987-989

http://www.wjgnet.com/1007-9327/12/987.asp

## INTRODUCTION

A rise in serum bilirubin concentration above the norm may be caused by its increased production (hemolytic processes, shunt-bilirubinemia), impairment of its uptake, conjugation and discharge from hepatocytes (congenital non-hemolytic functional hyperbilirubinemia) or excretion of unconjugated and conjugated bilirubin from damaged hepatocytes or biliary canaliculi to the blood. Clinical picture can be similar, as jaundice is the predominant and often isolated symptom in the above pathologies. In doubtful cases, morphological examination of a liver bioptate is a decisive step[1-3].

The main aim of the paper was to demonstrate the ultrastructure of Kupffer cells and hepatocytes in liver biopsy from a patient with Dubin-Johnson syndrome (DJS). To the best of our knowledge, it is the first report on the ultrastructure of Kupffer cells in this disorder.

## CASE REPORT

Our report presents data concerning a 17-year-old boy suffering from hyperbilirubinemia (up to 119.7 μmol/L) with concomitant normal activity of aminotransferases from 6 years of age. He was suspected of congenital functional hyperbilirubinemia. However, since abdominal complaints and hepatomegaly were found to coexist with scleral xanthosis, the boy was sent for further diagnosis to the 3rd Department of Pediatrics, Medical University of Bialystok. On admission, laboratory tests revealed high serum bilirubin concentration (120.55 μmol/L) with the predominance of unconjugated fraction (82.94 μmol/L). However, the activities of aminotransferases (ALT, AST), alkaline phosphatase and GGTP were not increased. Differential diagnosis excluded: hemolytic disorders, infections with hepatotropic viruses (HBV, HCV, CMV, EBV, HSV), metabolic disorders (cystic fibrosis, Wilson's disease, α-1 antitrypsin deficiency, hemochromatosis), hypothyroidism, autoimmune liver diseases, parasitic and epizootic diseases. The ultrasonographic examination of the abdominal cavity confirmed hepatomegaly with no changes in parenchyma echogenicity. Liver biopsy was performed to elucidate the still unclear cause of jaundice.

For ultrastructural analysis, small, fresh tissue blocks (1 $mm^3$) were cut off from the cylinder of liver tissue obtained by needle biopsy. The remaining considerable part of the collected tissue was submitted for examination by the light microscopy.

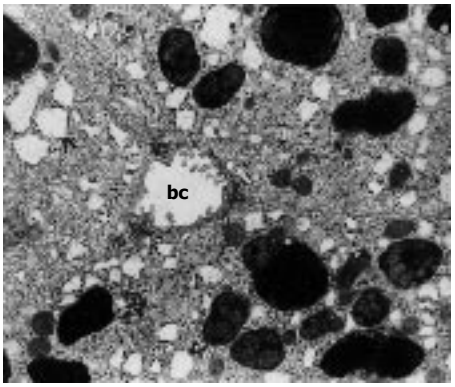


**Figure 1** Several membrane-bound granules – varying in size, content, and electron density – located near the biliary pole of hepatocytes; broadening of granular endoplasmic reticulum (>); dilation of bile canaliculus (cb) with the loss of microvilli (×7 000).

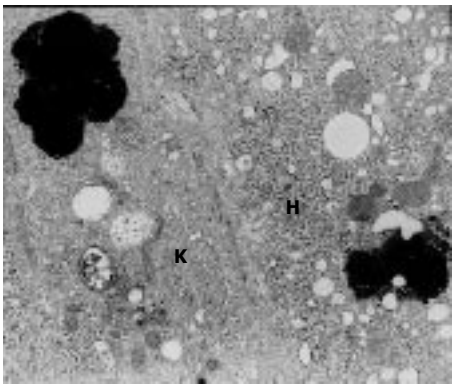


**Figure 2** Fragment of Kupffer cell with phagocytized thick black pigment granules; the cell adheres to a hepatocyte (H) containing a similar pigment deposit (×7 000).

The material for electron microscopic analysis was fixed in 10 g/L glutaraldehyde and 8 g/L paraformaldehyde in 0.1 mol/L cacodylate buffer (pH 7.4). Subsequently, fixation was carried out in osmium tetroxide; then the material was routinely processed for embedding in Epon 812. Ultrathin sections were contrasted with uranyl acetate and lead citrate, and examined using an Opton 900 PC transmission electron microscope (Zeiss, Oberkochen, Germany).

The liver specimen obtained by needle biopsy was grossly dark and greenish, the striking characteristics for DJS. Liver histology showed numerous distinct coarse brownish pigment deposits in the cytoplasm of the hepatocytes.

Ultrastructural examination of these cells showed electron-dense, lysosomal granules, characteristic of DJS, that corresponded to the intracytoplasmic pigment deposits seen in the light microscopic sections. This pigmentary material was frequently surrounded by a single, fine continuous or discontinuous membrane; sometimes no such membrane could be found. The lysosomal pigment granules demonstrated great variability in shape, size, content, and electron density and were located mainly in the vicinity of the biliary pole (Figure 1), and preferentially found in the centrilobular region. Moderately electron-dense finely granular background alternating with denser irregular areas and pleomorphic dark bodies (clearly seen against a finely homogenous granular matrix) characterized these granules. The pleomorphic very dense bodies frequently occupied a considerable part or almost whole lysosomes. Some hepatocytes filled with coarse electron-dense granules were disintegrated. Dilation of bile canaliculi with loss of microvilli typical for DJS was observed (Figure 1). Dilated elements of the granular endoplasmic reticulum (Figure 1), the presence of paracrystalline mitochondrial inclusions, enlarged Golgi complex and dispersed lipid droplets within the cytoplasm of hepatocytes were also noted. The vascular pole of the hepatocytes showed alteration of microvilli including their disintegration; a fine granular material could be occasionally seen in Disse's space. Sometimes this space was discontinued. The basement membrane of some hepatocytes was distinctly outlined, and even thickened.

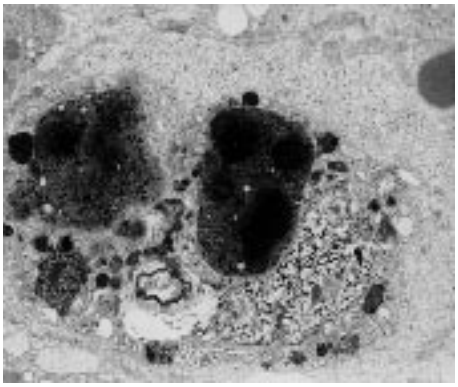

**Figure 3** A hypertrophic, evidently activated Kupffer cell with phagocytized, very thick, black pigment deposits and biliary lamellar material. The cell blocks the sinusoidal vascular lumen. Distinctly dilated Disse's space contains a fine granular material (×4 400).

The ultrastructural examinations of the liver bioptate also showed, especially in the centrilobular region, an increase in hepatic macrophages. Kupffer cells in the lumen of hepatic sinusoidal vessels were frequently hypertrophied and markedly activated, blocking the vascular lumen and demonstrating features of hyperactivity (Figure 3). They contained electron-dense dark pigment granules, varying in shape and size (Figures 2 and 3), often occupying almost whole lysosomes. This material corresponded to the pigment deposits present in hepatocytes (Figure 2). Bile deposits were sometimes observed near the plentiful phagocytized pigment granules (Figure 3).

Since the morphological picture of the liver bioptate was typical of DJS, leaving no doubt, we did not perform very expensive genetic tests (mutation in the ABCC2/MRP2 gene[4]).

## DISCUSSION

Macro- and microscopic, especially ultrastructural, changes observed in the liver bioptate in our patient were characteristic of DJS. The hepatocytes contained numerous electron-dense lysosomal, membrane-bound granules located mainly near the biliary pole that corresponded to

the coarse brownish pigment deposits seen under light microscope. The granules were accompanied by dilated endoplasmic reticulum and paracrystalline inclusions as well as alterations in bile canaliculi of hepatocytes.

However, Kupffer cells demonstrated features of hyper-reactivity. They accumulated pigment granules that corresponded to those observed in hepatocytes.

Morphological abnormalities of hepatocytes observed in the course of our studies were similar to those found by other authors in this syndrome[3,5-7]. It is worth noting that although the pigment granules showed characteristic microscopic features, their exact composition has not been clarified[1,6]. The results of ultrastructural and histochemical studies by Luo *et al*[2] suggest that this deposit material is a lipofuscin–melanin complex.

Up to now, there have been no reports describing the electron microscope picture of Kupffer cells in DJS.

It has been known that Kupffer cells are the largest population of tissue macrophages, predominantly distributed in the lumen of hepatic sinusoids. According to Naito *et al*[8], these cells demonstrate unique differentiation mechanisms, metabolic functions and responsiveness to inflammatory agents. They exhibit endocytic activity against blood-borne material entering the liver as well as phagocytic function in relation to cellular debris[8,9]. Kupffer cells also play an important role in the modulation of drug metabolic enzymes[10], in the carcinogenesis of hepatocellular carcinoma[11] and liver fibrosis[12].

We assume that pigment deposits absorbed by Kupffer cells in the course of DJS may have originated from disintegrating, pigment-load hepatocytes. The present study indicates that it is the process of phagocytosis that plays a significant role in the accumulation of thick black granules within the cytoplasm of these macrophages. This process is strictly connected with the morphological status and function of lysosomes of Kupffer cells. This is confirmed by the fact that the number of lysosomes, both primary and secondary, within the cytoplasm of hyperactivated macrophages was markedly increased in our observations. It can be suggested that in the course of DJS, due to phagocytosis, remnants of pigment-load hepatocytes trapped by the hyperactivated Kupffer cells with the involved macrophage scavenger receptors are shifted to primary lysosomes, i.e. intracytoplasmic reservoirs containing lytic enzymes, which undergo degradation. Then, the lysosomes are transformed into the secondary ones[8].

Unlike in the Gilbert's syndrome, in DJS clinical manifestation of hepatomegaly can be found even in the neonatal-infantile period[3,7,13-14]. In our patient, the cause of hyperbilirubinemia was unknown for many years. DJS was not taken into account because of atypical course of the disease (predominance of unconjugated bilirubin in the blood serum). However, the predominance of non-conjugated bilirubin in the blood serum has been noted in some diagnosed DJS cases[1].

We emphasize that hyperactive pericentral Kupffer cells may play an essential role in the development of the syndrome. They are involved in the response to pigmentary material originating from disintegrated hepatocytes.

## REFERENCES


1 **Berk PD.** Bilirubin metabolism and the hereditary hyperbilirubinemias. *Semin Liver Dis* 1994; **14**: 321-322

2 **Luo Z,** Zhang L, Li Y. [Clinical pathology of Dubin-Johnson syndrome]. *Zhonghua Gan Zang Bing Za Zhi* 2000; **8:** 45-47

3 **Shimizu T,** Tawa T, Maruyama T, Oguchi S, Yamashiro Y, Yabuta K. A case of infantile Dubin-Johnson syndrome with high CT attenuation in the liver. *Pediatr Radiol* 1997; **27**: 345-347

4 **Keitel V,** Kartenbeck J, Nies AT, Spring H, Brom M, Keppler D. Impaired protein maturation of the conjugate export pump multidrug resistance protein 2 as a consequence of a deletion mutation in Dubin-Johnson syndrome. *Hepatology* 2000; **32**: 1317-1328

5 **Baba N,** Ruppert RD. The Dubin-Johnson syndrome: electron microscopic observation of hepatic pigment--a case study. *Am J Clin Pathol* 1972; **57**: 306-310

6 **Cotutiu C,** Moraru I, Ionescu V. Ultrastructural data in a case of Dubin-Johnson syndrome. *Acta Morphol Acad Sci Hung* 1971; **19**: 313-322

7 **Tsai WH,** Teng RJ, Chu JS, Chang MH, Ho MM. Neonatal Dubin-Johnson syndrome. *J Pediatr Gastroenterol Nutr* 1994; **18**: 253-254

8 **Naito M,** Hasegawa G, Ebe Y, Yamamoto T. Differentiation and function of Kupffer cells. *Med Electron Microsc* 2004; **37**: 16-28

9 **Yano H,** Kinoshita S, Kira S. Effects of acute moderate exercise on the phagocytosis of Kupffer cells in rats. *Acta Physiol Scand* 2004; **182**: 151-160

10 **Ding H,** Tong J, Wu SC, Yin DK, Yuan XF, Wu JY, Chen J, Shi GG. Modulation of Kupffer cells on hepatic drug metabolism. *World J Gastroenterol* 2004; **10**: 1325-1328

11 **Liu K,** He X, Lei XZ, Zhao LS, Tang H, Liu L, Lei BJ. Pathomorphological study on location and distribution of Kupffer cells in hepatocellular carcinoma. *World J Gastroenterol* 2003; **9**: 1946-1949

12 **Zhang X**, Yu WP, Gao L, Wei KB, Ju JL, Xu JZ. Effects of lipopolysaccharides stimulated Kupffer cells on activation of rat hepatic stellate cells. *World J Gastroenterol* 2004; **10:** 610-613

13 **Haimi-Cohen Y,** Amir J, Merlob P. Neonatal and infantile Dubin-Johnson syndrome. *Pediatr Radiol* 1998; **28**: 900

14 **Kimura A**, Ushijima K, Kage M, Mahara R, Tohma M, Inokuchi T, Shibao K, Tanaka N, Fujisawa T, Ono E. Neonatal Dubin-Johnson syndrome with severe cholestasis: effective phenobarbital therapy. *Acta Paediatr Scand* 1991; **80:** 381-385


**S- Editor** Guo SY **L- Editor** Elsevier HK **E- Editor** Bai SH

PO Box 2345, Beijing 100023, China
www.wjgnet.com
wjg@wjgnet.com

*World J Gastroenterol* 2006 February 14; 12(6): 990-992
***World Journal of Gastroenterology*** ISSN 1007-9327
© 2006 The WJG Press. All rights reserved.

*CASE REPORT*

# Pyogenic liver abscess associated with large colonic tubulovillous adenoma

Hsueh-Chou Lai, Cho-Yu Chan, Cheng-Yuan Peng, Chih-Bin Chen, Wen-Hsin Huang

Hsueh-Chou Lai, Cheng-Yuan Peng, Chih-Bin Chen, Wen-Hsin Huang, Division of Hepatology and Gastroenterology, Departments of Internal Medicine, China Medical University Hospital, Taichung, Taiwan, China
Cho-Yu Chan, Faculty of Medicine, National Yang-Ming University School of Medicine, Taipei, and Department of Medical Research and Education, Taipei Veterans General Hospital, Taipei, Taiwan, China
Correspondence to: Dr. Cho-Yu Chan, Associate Professor, Faculty of Medicine, National Yang-Ming University School of Medicine, Taipei, Taiwan, China. 155 Li-nong St, Sec, 2, Peitou, Taipei 11221, Taiwan,
China. cychan@ym.edu.tw
Telephone: +886-2-28211699 Fax: +886-2-28202190
Received: 2005-06-07 Accepted: 2005-06-26

## Abstract

Pyogenic liver abscesses usually occur in association with a variety of diseases. Rarely, liver abscess has been reported as the presenting manifestation of colonic tubulovillous adenoma. We report two cases of pyogenic liver abscess without hepatobiliary disease or other obvious etiologies except that one had a history of diabetes mellitus (DM). The pathogen in the patient with DM was *Klebsiella pneumonia* (KP). In both of the patients, ileus developed about two to three weeks after the diagnosis of liver abscess. Colonoscopy revealed large polypoid tumors with pathological findings of tubulovillous adenoma in both cases. Two lessons were learned from these two cases: (1) an underlying cause should be aggressively investigated in patients with cryptogenic liver abscess; (2) DM could be one of the etiologies but not necessarily the only cause of KP liver abscess.

© 2006 The WJG Press. All rights reserved.

**Key words:** Pyogenic liver abscess; *Klebsiella pneumonia*; Colonic tubulovillous adenoma

Lai HC, Chan CY, Peng CY, Chen CB, Huang WH. Pyogenic liver abscess associated with large colonic tubulovillous adenoma. *World J Gastroenterol* 2006; 12(6): 990-992

http://www.wjgnet.com/1007-9327/12/990.asp

## INTRODUCTION

Pyogenic liver abscess is usually related to hepatobiliary tract disease or intra-abdominal infections including cholecystitis, suppurative cholangitis, suppurative pylephlebitis, appendicitis, diverticulitis and peritonitis[1-3]. Recently, colorectal cancer without obvious infection was considered as one of the uncommon etiologies of liver abscess[4,5]. Furthermore, liver abscess was reported as the presenting manifestation of colonic tubulovillous adenoma[6]. However, there are a growing number of reports suggesting a relationship between diabetes mellitus (DM) and *Klebsiella pneumonia* (KP) liver abscess which indicate that a deficiency in the hosts' defense mechanism could be the etiology of this liver infection[7-9]. We hereby report two cases of pyogenic liver abscess both of which were found to have colonic tubulovillous adenoma two to three weeks later after the diagnosis of liver abscess. The association of pyogenic liver abscess and colonic tubulovillous adenoma and the implications of these two cases are discussed.

## CASE REPORT

### CASE 1

A 67-year-old man, who was referred from a local hospital, was admitted to our hospital because of fever, chill, and right upper abdominal pain for seven days. On physical examination, his initial body temperature was 37.9°C and blood pressure was 124/67 mmHg. Light palpation of the abdomen revealed tenderness and mild rebounding pain on epigastric and right upper areas, but no abdominal mass was felt. Significant laboratory data included a leukocyte count of 26,330/μL (normal range = 4000-10,400/μL ), a hemoglobin of 9.5 gm/dL (normal range = 12-16 gm/dL), an aspartate aminotransferase (AST) of 73 IU/L (normal range = 5-34 IU/L), an alanine aminotranferase (ALT) of 79 IU/L (normal range = 0-40 IU/L), a fasting blood sugar of 118 mg/dl (normal range = 70-110 mg/dL), a total bilirubin of 1.03 mg/dL (normal range = 0.2-1.3 mg/dL), a C-Reactive Protein (CRP) of 17.02 mg/dL (normal <0.8 mg/dL), and a carcinoembryonic antigen (CEA) level of 0.33 ng/dL (normal <5 ng/dL).

Abdominal ultrasonography (US) and computed tomography (CT) showed a 4-cm liver abscess in left lobe of liver (Figure 1A). After three sets of blood cultures were completed and broad-spectrum antimicrobial therapy was initiated, CT-guided percutaneous drainage of the liver abscess was performed and pus liked material was aspirated and sent for bacterial culture. However, blood and pus were all negative for bacterial growth. As antimicrobial treatment was continued, the patient's clinical condition improved rapidly and fever subsided four days

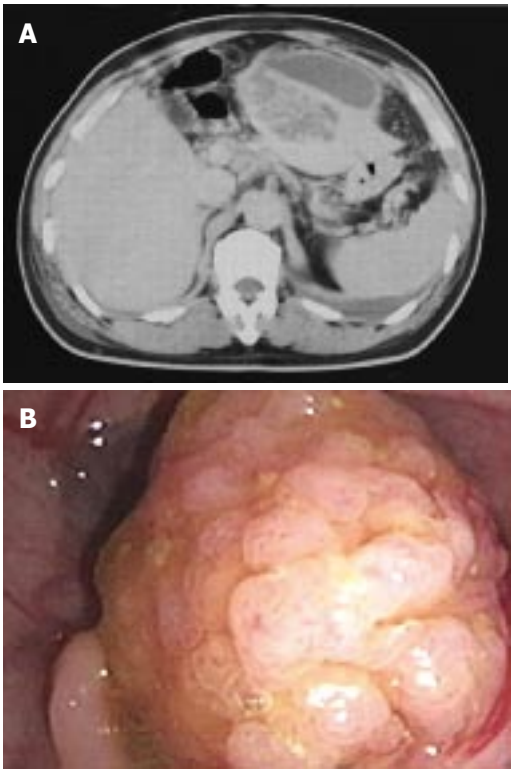


**Figure 1** Case 1. **A**: Enhancement abdominal computed tomography (CT) showed a 4-cm liver abscess in left lobe of the liver; **B**: Colonofibroscopy showed a 3-cm pedunculated polyp in the sigmoid colon.

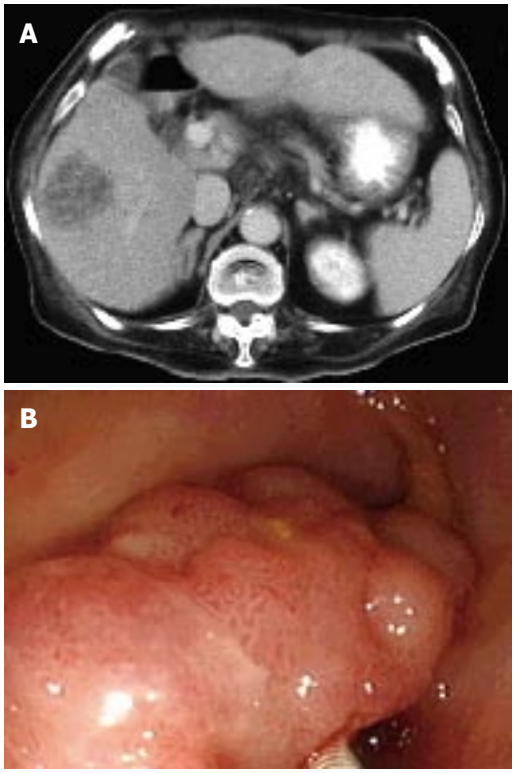


**Figure 2** Case 2. **A**: Enhancement abdominal computed tomography showed a 5-cm liver abscess in right lobe of the liver; **B**: Colonofibroscopy showed a 3-cm polypoid tumor in the sigmoid colon.

later. Then the drainage catheters were removed and the patient was discharged on the 14th d of hospitalization.

One week later, he was admitted again with a chief complaint of abdominal fullness. Physical examination showed a distended abdomen with hypertympanic abdominal sounds on percussion. Plain films of the abdomen disclosed evidence of a paralytic ileus with a suspected obstruction at the level of the sigmoid colon. Colonoscopy was performed which showed a 3-cm pedunculated polyp in the sigmoid colon (Figure 1B). Polypectomy was performed and pathological examination revealed tubulovillous adenoma with mild dysplasia. The patient continued to do well during a follow-up period of 6 mo.

### *CASE 2*

An 84-year-old woman with a history of DM using no regular medication for several years was admitted to the hospital because of fever and right upper abdominal dull pain which was followed by a change of consciousness for the two days preceding admission. On physical examination, her initial body temperature was 37.7°C and blood pressure was 79/30 mmHg. Mild tenderness in the right upper abdomen was noted during performance of light palpation, but no abdominal mass was felt. Significant laboratory data included a leukocyte count of 17,870/μL, a hemoglobin of 12.7 mg/dL, an AST of 59 IU/L, an ALT of 58 IU/L, a fasting blood sugar of 348 mg/dL, a total bilirubin of 2.31 mg/dL, a CRP level of 32.82 mg/dL, and a CEA level of 6.72 ng/dL. Abdominal US and CT showed a 5-cm liver abscess in right lobe of the liver (Figure 2A).

Since the patient could not cooperate for US or CT-guided aspiration, broad-spectrum antimicrobial treatment was started after three sets of blood cultures were performed. The results of blood cultures were positive for *Klebsiella pneumonia* (KP), which was sensitive to the formerly prescribed antibiotics. The patient's clinical condition improved gradually and fever subsided 10 d later. On the 14th d of hospitalization, abdominal fullness developed and the plain film of abdomen showed evidence of ileus with a suspected obstruction at the level of the distal colon. Colonoscopy was performed and showed a 3-cm polypoid tumor in the sigmoid colon (Figure 2B). Polypectomy was not done because of technical difficulty. A biopsy was performed and eight pieces of tissue were taken for pathological examination. The pathological findings were consistent with tubulovillous adenoma. Since ileus resolved spontaneously and the patient's general physical condition was not good, the patient's family refused to have further treatment. Her general condition was **stable** during a follow-up period of two months.

## DISCUSSION

The etiologies and pathogenesis of liver abscesses have changed significantly over the past several decades[1-3,10-11]. Recent reports suggest that pyogenic liver abscess might be a warning indicator of silent colonic cancer[4,5,12-14], therefore, patients with liver abscess but without apparent etiologies, as in Case 1 of this report, should have further examination. In addition, non-growth in cultures of blood samples and abscess aspirate in Case 1 could be due to

the following two possibilities: (1) the patient had been partially treated at an outside hospital; (2) the pathogen of the liver abscess might be an anaerobe that was most probably originated from the colon. Therefore, although a rapid improvement was noted, a complete evaluation of the GI tract should be performed in Case 1 as per the suggestion of Cohen *et al*[4].

Nevertheless, colonoscopy was performed because of ileus and the examination revealed a large colonic tubulovillous adenoma in the sigmoid colon instead of a "silent colonic cancer". Whether colonic adenoma could be an etiology of pyogenic liver abscess remains to be elucidated. In addition to our report, there is only one other report of pyogenic liver abscess as the presentation of colonic villous adenoma[6]. The mechanism for explaining colonic adenoma as an etiology of liver abscess may be the same as that of the colonic cancer, i.e., there are mucosal defects present on the colonic lesions (cancers or adenomas) that allow a route for bacteria invasion into the portal system with subsequent hematogenous spread to the liver.

In recent years, pyogenic liver abscesses have occurred more frequently in immunodeficient patients, including those receiving intensive chemotherapy for hematological or solid malignancies, patients with immunosuppressive therapy after organ transplantation[15] and, especially, patients with DM[8-9]. Case 2 was a DM patient who had a solitary liver abscess caused by KP. As previous reports showed, KP liver abscesses tend to occur in DM patients who did not have any predisposing factors for the development of liver abscess, therefore, the diagnostic procedures and management in Case 2 seemed reasonable. However, the unexpected occurrence of ileus due to a large colonic villous adenoma indicated that the presence of DM could not completely exclude other possible etiologies of liver abscess.

In conclusion, for patients with cryptogenic liver abscess, an underlying cause should be aggressively searched for. DM could be one of the etiologies but not necessarily the only cause of KP liver abscess.

## REFERENCES


1 **Sherman JD,** Robbins SL. Changing trends in the casuistics of hepatic abscess. *Am J Med* 1960; **28:** 943-950

2 **Miedema BW,** Dineen P. The diagnosis and treatment of pyogenic liver abscesses. *Ann Surg* 1984; **200:** 328-335

3 **Stain SC**, Yellin AE, Donovan AJ, Brien HW. Pyogenic liver abscess. Modern treatment. *Arch Surg* 1991; **126:** 991-996

4 **Cohen JL,** Martin FM, Rossi RL, Schoetz DJ Jr. Liver abscess. The need for complete gastrointestinal evaluation. *Arch Surg* 1989; **124:** 561-564

5 **Lonardo A,** Grisendi A, Pulvirenti M, Della Casa G, Melini L, Di Gregorio C, Nasi G, Sarti M, Tamborrino E, Lonardo F. Right colon adenocarcinoma presenting as Bacteroides fragilis liver abscesses. *J Clin Gastroenterol* 1992; **14**: 335-338

6 **Leiba A,** Apter S, Avni I, Osherov A, Thaler M, Grossman E. [Pyogenic liver abscess--an unusual presentation of colonic villous adenoma]. *Harefuah* 2003; **142**: 336-337, 399

7 **Rayfield EJ,** Ault MJ, Keusch GT, Brothers MJ, Nechemias C, Smith H. Infection and diabetes: the case for glucose control. *Am J Med* 1982; **72:** 439-450

8 **Wang JH,** Liu YC, Lee SS, Yen MY, Chen YS, Wang JH, Wann SR, Lin HH. Primary liver abscess due to Klebsiella pneumoniae in Taiwan. *Clin Infect Dis* 1998; **26**: 1434-1438

9 **Yang CC,** Yen CH, Ho MW, Wang JH. Comparison of pyogenic liver abscess caused by non-Klebsiella pneumoniae and Klebsiella pneumoniae. *J Microbiol Immunol Infect* 2004; **37**: 176-184

10 **Gyorffy EJ,** Frey CF, Silva J Jr, McGahan J. Pyogenic liver abscess. Diagnostic and therapeutic strategies. *Ann Surg* 1987; **206**: 699-705

11 **Branum GD,** Tyson GS, Branum MA, Meyers WC. Hepatic abscess. Changes in etiology, diagnosis, and management. *Ann Surg* 1990; **212**: 655-662

12 **Teitz S,** Guidetti-Sharon A, Manor H, Halevy A. Pyogenic liver abscess: warning indicator of silent colonic cancer. Report of a case and review of the literature. *Dis Colon Rectum* 1995; **38**: 1220-1223

13 **Tzur T,** Liberman S, Felzenstein I, Cohen R, Rivkind AI, Almogy G. Liver abscesses caused by Streptococcus milleri: an uncommon presenting sign of silent colonic cancer. *Isr Med Assoc J* 2003; **5**: 206-207

14 **Matsushita M**, Hajiro K, Okazaki K, Takakuwa H, Nishio A. Endophthalmitis with brain, lung, and liver abscesses associated with an occult colon cancer. *Am J Gastroenterol* 2000; **95:** 3664-3665

15 **Marcus SG,** Walsh TJ, Pizzo PA, Danforth DN Jr. Hepatic abscess in cancer patients. Characterization and management. *Arch Surg* 1993; **128**: 1358-1364; discussion 1364


**S- Editor** Pravda J and Guo SY **L- Editor** Elsevier HK **E- Editor** Liu WF

PO Box 2345, Beijing 100023, China
www.wjgnet.com
wjg@wjgnet.com

*World J Gastroenterol* 2006 February 14; 12(6): 993-995
***World Journal of Gastroenterology*** ISSN 1007-9327
© 2006 The WJG Press. All rights reserved.

*CASE REPORT*

# Delayed ischemic gangrene change of distal limb despite optimal decompressed colostomy constructed in obstructed sigmoid colon cancer: A case report

Wen-Shih Huang, Kuang-Wen Liu, Paul Y Lin, Ching-Chuan Hsieh, Jeng-Yi Wang

Wen-Shih Huang, Division of Colon and Rectal Surgery, Department of Surgery, Chang Gung Memorial Hospital, Chiayi, Taiwan; Graduate Institute of Clinical Medicine, Chang Gung University, Taoyuan, Taiwan, China
Kuang-Wen Liu, Department of Surgery, E-Da Hospital/I-Shou University, Kaohsiung, Taiwan, China
Paul Y Lin, Division of Anatomical Pathology, Department of Pathology, Chang Gung Memorial Hospital, Chiayi, Taiwan, China
Ching-Chuan Hsieh, Division of General Surgery, Department of Surgery, Chang Gung Memorial Hospital, Chiayi, Taiwan, China
Jeng-Yi Wang, Division of Colon and Rectal Surgery, Department of Surgery, Chang Gung Memorial Hospital, Chiayi, Taiwan, China
Correspondence to: Prof. Jeng-Yi Wang, Division of Colon and Rectal Surgery, Department of Surgery, Chang Gung Memorial Hospital, Chiayi. 6, Sec. West, Chiapu Road, Putz City, Chiayi County, Taiwan, China. w3625@adm.cgmh.org.tw
Telephone: +886-5-3621000-2000 Fax: +886-5-3623001
Received: 2005-07-14 Accepted: 2005-08-03

## Abstract

Creating blow-hole colostomy for decompression could provide a time-saving and efficient surgical procedure for a severely debilitated case with a completely obstructed colorectal cancer. Complications are reported as prolapse, retraction, and paracolostomal abscess. However, complication with an ischemic distal limb has not been reported. We report a case of critical intra-abdominal disease after decompressed colostomy for relieving malignant sigmoid colon obstruction; a potential fatal condition should be alerted. A 76-year-old male visited our emergency department for symptoms related to obstructed sigmoid colon tumor with foul-odor vomitus containing fecal-like materials. An emergent blow-hole colostomy proximal to an obstructed sigmoid lesion was created, and resolution of complete colon obstruction was pursued. Unfortunately, extensive abdominal painful distention with board-like abdomen and sudden onset of high fever with leukocytopenia developed subsequently. Such surgical abdomen rendered a secondary laparotomy with resection of the sigmoid tumor along with an ischemic colon segment located proximally up to the previously created colostomy. Eventually, the patient had an uneventful postoperative hospital stay. In the present article, we have described an emergent condition of sudden onset of distal limb ischemia after blow-hole colostomy and concluded that despite the decompressed colostomy would resolve acute malignant colon obstruction efficiently; impending ischemic bowel may progress with a possible irreversible peritonitis. Any patient, who undergoes a decompressed colostomy without resection of the obstructed lesion, should be monitored with leukocyte count and abdominal condition survey frequently.

© 2006 The WJG Press. All rights reserved.

**Key words:** Colorectal cancer obstruction; Colostomy; Ischemic colitis; Laparotomy

Huang WS, Liu KW, Lin PY, Hsieh CC, Wang JY. Delayed ischemic gangrene change of distal limb despite optimal decompressed colostomy constructed in obstructed sigmoid colon cancer: A case report. *World J Gastroenterol* 2006; 12(6): 993-995

http://www.wjgnet.com/1007-9327/12/993.asp

## INTRODUCTION

In 8-29% of patients with colorectal cancer, obstruction is the major symptom at presentation, and 85% of patients undergoing emergency colorectal surgery have complete colonic obstruction from colorectal carcinoma[1-4]. Obstructed colorectal cancer often dictates poor cancer-related prognosis and higher mortality or morbidity, because they are more advanced and are associated with a higher incidence of distant metastases[3,5]. One-stage surgery is believed to be the preferred procedure for an obstructive right colon lesion, and staged operation is favored for the management of malignant left-side colonic obstructions[6]. In patients with acute complete colonic obstruction, hemodynamic instability may be debilitated by concomitant medical diseases, and cancer resection may not be possible. Establishing a decompressed colostomy is usually recommended to resolve acute obstructive symptoms prior to cancer resection[7,8].

Obstructive colorectal cancer may be complicated with concomitant proximal ischemic colitis, which would present dramatically with gangrene and/or colonic perforation, if the acute vascular insufficiency is severe[9]. In general, colonic decompression by way of self-expanding metal stent or decompressed colostomy could

deliver intraluminal pressure lower enough than intramural vascular perfusion pressure to avoid hypoperfusive status of the intestine proximal to obstructive lesion. It is common to manifest proximal colon distention in left-sided colorectal cancer obstruction if a competent ileocecal valve exists[10], and impending ischemic change of proximal colon would pursue. No fatal intra-abdominal complication for constructing a blow-hole colostomy, such as a gangrenous distal limb with peritonitis, has been reported.

We here report a case of severe intra-abdominal condition despite that a functional decompressed colostomy was created, a potential fatal situation of which the surgeons should keep in mind when relieving malignant colon obstruction using blow-hole colostomy.

## CASE REPORT

A 76-year-old male patient, who had extensive abdominal distention associated with no stools or flatus passage for 2 d, was referred to our emergency department for sudden onset of vomiting with foul-odor and fecal material-like contents. He had a 4-mo history of gradual body weight loss, abdominal bloat, bowel habit change with decreased stool caliber and poor appetite. Abdominal computerized topography revealed an obstructive sigmoid colon lesion with segmental wall thickening and a stenotic lumen. There was a pill within the distended bowel segment immediately proximal to the stenotic lumen of the obstructed lesion. Sigmoid colon tumor with complete bowel obstruction was diagnosed based on history and image studies. The patient had underlying chronic obstructive pulmonary disease with intermittent consumption of inhalational bronchodilator. Physical examinations reviewed a distended abdomen with silent bowel sound; there was tachypnea with central bronchospasm. Hemogram showed WBC as 11 200/μL with a differential count of segment form, 78.4%; band form, 1%; and lymphocyte, 10.8%. Biochemical analysis showed slightly impaired renal function (BUN: 31 mg/dL, Cr: 2.1 mg/dL), normal electrolyte concentration (Na: 136 meq/L, K: 4.0 meq/L and Cl: 103 meq/L) and suboptimal nutritional status (albumin: 2.6 g/dL). Clinically, the patient complained of serious abdominal painful fullness, fever with chills, and dyspnea. Metal stenting to the colon stenotic lesion was attempted but failed. On account of emergent release of the obstructive bowel pressure, the patient underwent a blow-hole colostomy at proximal transverse colon by mini-laparotomy, which took less than 30 min under general anesthesia. The bowel segment at the operation field was severely distended with edema, however, adequate blood perfusion was observed. There was no ascites. A large amount of liquid yellowish stools with foul smell was drained out from the proximal and distal limbs of the colostomy after it was instituted. The patient sustained a smooth operation course.

A rechecked hemogram at the 2$^{nd}$ post-operation day, which is routinely given to patients undergoing abdominal surgery in our institute as a baseline for follow-up purpose, found rather unremarkable data (WBC as 8 800/μL with slightly elevated segment form of 84%, without band form). Gradual remission of abdominal distention with persistent bowel content drainage was observed within the first three post-operation days; the colostomy would be deemed as a normal physical function. Unfortunately, extensive abdominal painful distention with board-like abdominal appearance, and sudden onset of high fever with a body temperature up to 39.8°C were noted afterwards. At follow-up, hemogram reviewed leukocytopenia with dominant left-shifted differential count (WBC: 1 600/μL, segment: 38%, band: 26%). We found such a surgical abdomen that an emergent operation should be done to explore the etiology.

Emergent laparotomy was done immediately to find marked foul-odor bloody ascites. The distal limb of colostomy extending from the colostomy distally to the obstructed sigmoid colon tumor was found to have severe ischemic gangrenous change. The proximal limb of colostomy was fine. Segmental resection of the lesioned colon, comprising the sigmoid colon cancer with a security of cancer-free distal section margin and a short segment of colon proximal to previously created colostomy, was performed. The blow-hole colostomy was then converted to end-T-colostomy. The patient exerted an uneventful postoperative course and scheduled colostomy reversal was undertaken 6 mo later.

## DISCUSSION

Fine construction of a transverse colostomy by drawing out of a loop of the bowel and securing the mesentery to the skin to decompress obstructions from carcinoma of the rectum was first described in 1797[11]. Intestinal obstruction from malignancy within the colorectum would carry catastrophic complications of perforation, electrolyte imbalance, bowel ischemia, and sepsis caused by bacterial translocation[12]. Moreover, cancer patients, especially those with bowel obstruction, are usually malnourished, older, and dehydrated and may have coexisting disease at the time of presentation[12-14]. Therefore, perioperative management of malignant bowel obstruction, inclusive of surgical planning option to minimize morbidity and mortality is a critical issue.

There are different strategies to decompress colon obstruction with different outcomes, including (1) non-surgical approach as balloon dilation, placement of a plastic non-expandable rectal tube, cryosurgical destruction, electrocoagulation, and laser ablation[15,16] and (2) surgical approach as blow-hole enterostomy, or resection of tumor-bearing colorectal segment with or without colostomy[2,4-8]. Because of the failure of self-expanding metal stent placement in this patient due to severe colon angulations and rather stenotic colon lumen, we recommended a blow-hole proximal transverse colostomy as an emergent procedure for this debilitated patient with severe coexisting medical condition.

To evaluate the surgical planning in malignant large bowel obstruction, it is widely accepted that for malignant colon obstruction from the right colon cancer, resection (right hemicolectomy) should be performed with anastomosis in one stage[5,17,18]. Nevertheless, for obstruction from cancer of left colon or rectum, two types

of surgical approach could be used: (1) primary resection and primary anastomosis or Hartmann's procedure with synchronous treatment of carcinoma and obstruction, and (2) staged resection with the treatment of the obstruction prior to resection[4]. Some surgeons prefer staged resection with fast resolution of the obstruction, and a delayed radical surgery. The main benefits of staged operation are less surgical trauma which is significant in patients whose general condition is precarious, and reduction of the risk of contamination due to unprepared bowel[19]. Poor physical status as this patient, construction of a blow-hole colostomy in a minimal wound (fit to colostomy size) with less time-consumption (less than 30 min) could offer an anticipated decompression effect of the obstruction and prevent further surgical trauma to facilitate scheduled radical resection in the future.

Ischemic episode would take place in malignant large bowel obstruction and present dramatically with gangrene and/or colonic perforation if acute vascular insufficiency is severe[9]. It is postulated that colon distention from malignant colon obstruction reduces the blood supply to the bowel wall and enhances the development of ischemia[10]. Creation of a decompressed colostomy in malignant colon obstruction should rescue impending elevated intra-luminal pressure and possible development of the proximal colitis. But in our case, the cause of gangrenous distal limb might be due to, first, the development of tumor thrombi or septic emboli in the territory of vessels supplying the distal colon, or second, an underlying undetected ischemic change proximal to the cancerous mass which was not observed for the initial limited surgical field by mini-laparotomy. Clinically, the patient sustained sudden onset of high fever, peritoneal signs, and leukocytopenia with dominant left-shifted differential count on the 4$^{th}$ post-operation day, which was in the opposite direction to recovering status. Although, toxic signs presented by this patient alerted us of his deteriorated status, ischemic gangrene change of the distal limb between created stoma and obstructed sigmoid colon cancer was beyond our expectation. Nevertheless, bloody mucoid stools, which are usually in consistent with the clinical features of ischemic colitis, was not identified from the distal stoma ahead of the time in which toxic signs presented.

In conclusion, impending ischemic bowel may progress with a catastrophic peritonitis despite construction of blow-hole colostomy, which rescued malignant sigmoid colon obstruction. Consequently, it is important to monitor leukocyte count change and survey meticulously abdominal condition for patients with decompressed colostomy created without resection of the obstructed lesion.

## REFERENCES


1 **Umpleby HC**, Williamson RC. Survival in acute obstructing colorectal carcinoma. *Dis Colon Rectum* 1984; **27**: 299-304

2 **Yu BM**. Surgical treatment of acute intestinal obstruction caused by large bowel carcinoma. *Zhonghua WaiKe ZaZhi* 1989; **27**: 285-286, 443

3 **Serpell JW**, McDermott FT, Katrivessis H, Hughes ES. Obstructing carcinomas of the colon. *Br J Surg* 1989; **76**: 965-969

4 **De Salvo GL**, Gava C, Pucciarelli S, Lise M. Curative surgery for obstruction from primary left colorectal carcinoma: primary or staged resection? *Cochrane Database Syst Rev* 2004; 2: CD002101

5 **Phillips RK**, Hittinger R, Fry JS, Fielding LP. Malignant large bowel obstruction. *Br J Surg* 1985; **72**: 296-302

6 **Lee YM**, Law WL, Chu KW, Poon RT. Emergency surgery for obstructing colorectal cancers: a comparison between right-sided and left-sided lesions. *J Am Coll Surg* 2001; **192**: 719-725

7 **Poon RT**, Law WL, Chu KW, Wong J. Emergency resection and primary anastomosis for left-sided obstructing colorectal carcinoma in the elderly. *Br J Surg* 1998; **85**: 1539-1542

8 **Lau PW**, Lo CY, Law WL. The role of one-stage surgery in acute left-sided colonic obstruction. *Am J Surg* 1995; **169**: 406-409

9 **Seow-Choen F**, Chua TL, Goh HS. Ischaemic colitis and colorectal cancer: some problems and pitfalls. *Int J Colorectal Dis* 1993; **8**: 210-212

10 **Lichtenstein ME**, Myers WH, Dwyer GF Jr. Perforation of the cecum from obstructing carcinoma of the distal colon. *Am J Surg* 1961; **101**: 26-31

11 **Fine P**. *Am de la Soc de Montpelier* 1797; **6**: 34

12 **Gandrup P**, Lund L, Balslev I. Surgical treatment of acute malignant large bowel obstruction. *Eur J Surg* 1992; **158**: 427-430

13 **Wholey MH**, Levine EA, Ferral H, Castaneda-Zuniga W. Initial clinical experience with colonic stent placement. *Am J Surg* 1998; **175**: 194-197

14 **Mainar A**, Tejero E, Maynar M, Ferral H, Castaneda-Zuniga W. Colorectal obstruction: treatment with metallic stents. *Radiology* 1996; **198:** 761-764

15 **Rupp KD**, Dohmoto M, Meffert R, Holzgreve A, Hohlbach G. Cancer of the rectum--palliative endoscopic treatment. *Eur J Surg Oncol* 1995; **21**: 644-647

16 **Sardi A**, Ojeda H, Barco E. Cryosurgery: adjuvant treatment at the time of resection of a pelvic recurrence in rectal cancer. *Am Surg* 1999; **65**: 1088-1091

17 **Carty NJ**, Corder AP. Which surgeons avoid a stoma in treating left-sided colonic obstruction? Results of a postal questionnaire. *Ann R Coll Surg Engl* 1992; **74**: 391-394

18 **Runkel NS**, Schlag P, Schwarz V, Herfarth C. Outcome after emergency surgery for cancer of the large intestine. *Br J Surg* 1991; **78**: 183-188

19 **Sommeling CA**, Haeck L. Caecostomy in the management of acute left colonic obstruction. *Acta Chir Belg* 1997; **97**: 217-219


**S- Editor** Guo SY **L- Editor** Elsevier HK **E- Editor** Kong LH

PO Box 2345, Beijing 100023, China
www.wjgnet.com
wjg@wjgnet.com

*World J Gastroenterol* 2006 February 14; 12(6): 996
***World Journal of Gastroenterology*** ISSN 1007-9327
© 2006 The WJG Press. All rights reserved.



# Acknowledgments to Reviewers of *World Journal of Gastroenterology*

Many reviewers have contributed their expertise and time to the peer review, a critical process to ensure the quality of *World Journal of Gastroenterology*. The editors and authors of the articles submitted to the journal are grateful to the following reviewers for evaluating the articles (including those were published and those were rejected in this issue) during the last editing period of time.

**Gianfranco D Alpini, Professor**
Internao Medicine and Medical Physiology, Scoh Whot Hospital, 702 SW H.K. dod genloop MRB rm316B, Temple 76504, United States

**Taku Aoki, MD**
Division of Hepato-Biliary-Pancreatic and Transplantation Surgery, Department of Surgery, Graduate School of Medicine, University of Tokyo,7-3-1 Hongo, Bunkyo-ku, Tokyo, 113-8655, Japan

**Mauro Bernardi, Professor**
Internal Medicine,Cardioangiology,Hepatology, University of Bologna, Semeiotica Medica - Policlinico S. Orsola-Malpighi - Via Massarenti, 9, Bologna 40138, Italy

**Xian-Ming Chen, MD**
Center for Basic Research in Digestive Diseases, Division of Gastroenterology and Hepatology, Mayo Clinic College of Medicine, 200 First Street, SW, Rochester, MN 55905, United States

**Jacques Cosnes, Professor**
Department of Gastroenterology, Hospital St. Antoine, Hospital St. Antoine, 184 rue du Faubourg St-Antoine, PARIS 75012, France

**Zong-Jie Cui, PhD, Professor**
Institute of Cell Biology, Beijing Normal University, 19 XinJieKouWaiDaJie, Beijing 100875, China

**Abraham Rami Eliakim, Professor**
Gastroenterology, Rambam Medical Center, Technion School of Medicine, PO Box 9602, Haifa 31096, Israel

**Alfred Gangl, Professor**
Department of Medicine 4, Medical University of Vienna, Allgemeines Krankenhaus, Waehringer Guertel 18-20, Vienna A-1090, Austria

**Axel M Gressner, Professor**
Institut für Klinische Chemie und Pathobiochemie sowie Klinisch-Chemisches Zentrallaboratorium, Universitätsklinikum Aachen, Pauwelsstr. 30, Aachen 52074, Germany

**Mario Guslandi, Professor**
Department of Gastroenterology, S: Raffaele University Hospital, S: Raffaele University Hospitalvia Olgettina 60, Milano 20132,Italy

**Fumio Imazeki, MD**
Department of Medicine and Clinical Oncology, Chiba University, 1-8-1 Inohana, Chuo-ku, Chiba 260-8670, Japan

**Toru Ishikawa, MD**
Department of Gastroenterology, Saiseikai Niigata Second Hospital, Teraji 280-7, Niigata, Niigata 950-1104, Japan

**Masayoshi Ito, MD**
Department of Endoscopy, Yotsuya Medical Cube, 5-5-27-701 Kitashinagawa, Shinagawa-ku, Tokyo 1410001, Japan

**Xiao-Long Ji, Professor**
Institute of Nanomedicine, Chinese Armed Police General Hospital, 69 Yongding Road, Beijing 100039, China

**Richard A Kozarek, MD**
Department of Gastroenterology, Virginia Mason Medical Center, 1100 Ninth Avenue, PO Box 900, Seattle 98111-0900, United States

**SØren MØller, Chief Physician**
Department of Clinical Physiology 239, Hvidovre Hospital, Kettegaard alle 30, DK-2650 Hvidovre, Denmark

**Yoshiharu Motoo, Professor**
Department of Medical Oncology, Kanazawa Medical University, 1-1 Daigaku, Uchinada, Ishikawa 920-0293, Japan

**Chris Jacob Johan Mulder, Professor**
Department of Gastroenterology, VU University Medical Center, PO Box 7057, 1007 MB Amsterdam, The Netherlands

**Gustav Paumgartner, Professor**
University of Munich, Klinikum Grosshadern, Marchioninistr. 15, Munich, D-81377, Germany

**Ian C Roberts-Thomson, Professor**
Department of Gastroenterology and Hepatology, The Queen Elizabeth Hospital, 28 Woodville Road, Woodville South 5011, Australia

**Hidetsugu Saito, Assistant Professor**
Department of Internal Medicine, Keio University, 35 Shinanomachi, Shinjuku-ku, Tokyo 1608582, Japan

**Stuart Sherman, Professor of Medicine and Radiology**
Department of Gastroenterology and Hepatology, Indiana University Medical Center, 550 N. University Blvd, Suite 4100, Indianapolis 46202, United States

**Steven David Wexner, MD, Professor of Surgery**
The Cleveland Clinic Foundation Health Sciences Center of the Ohio State University, and Clinical Professor, Department of Surgery, Division of General Surgery, University of South Florida College of Medicine, 21st Century Oncology Chair in Colorectal Surgery, Chairman Department of Colorectal Surgery, Chief of Staff, Cleveland Clinic Florida, 2950 Cleveland Clinic Boulevard, Weston, Florida 33331, United States

**Jian Wu, Associate Professor of Medicine**
Internal Medicine/Transplant Research Program, University of California, Davis Medical Center, 4635 2nd Ave. Suite 1001, Sacramento CA 95817, United States

**Hiroshi Yoshida, MD**
First Department of Surgery, Nippon Medical School, 1-1-5 Sendagi, Bunkyo-ku, Tokyo 113-8603, Japan

**Kentaro Yoshioka, Associate Professor**
Division of Gastroenterology, Department of I, Fujita Health University School of Medicine, 1-98 Dengakugakubo, Kutsukade, Toyoake 470-1190, Japan

**Yuan Yuan, Professor**
Cancer Institute of China Medical University, 155 North Nanjing Street, Heping District, Shenyang 110001, Liaoning Province, China

PO Box 2345, Beijing 100023, China
www.wjgnet.com
wjg@wjgnet.com

*World J Gastroenterol* 2006 February 14; 12(6): 997
***World Journal of Gastroenterology*** ISSN 1007-9327
© 2006 The WJG Press. All rights reserved.

# Meetings

## MAJOR MEETINGS COMING UP

Digestive Disease Week
107th Annual Meeting of AGA, The American Gastroenterology Association
May 20-25, 2006
Loas Angeles Converntion Center, California
www.ddw.org

## EVENTS AND MEETINGS IN THE UPCOMING 6 MONTHS

10 th World Congress of the International Society for Diseases of the Esophagus (ISDE 2006)
February 22-25, 2006
Adelaide
isde@sapmea.asn.au
www.isde.net

EASL 2006 - The 41st Annual Meeting
April 26-30, 2006
Vienna, Austria

International Gastrointestinal Fellows Initiative
February 22-24, 2006
Banff, Alberta
CAGOffice@cag-acg.org
www.cag-acg.org

Canadian Digestive Disease Week
February 24-27, 2006
Banff, Alberta
CAGOffice@cag-acg.org
www.cag-acg.org

European Multidisciplinary Colorectal Cancer Congress 2006
February 12-14, 2006
Berlin
info@congresscare.com
www.colorectal2006.org

ILTS 12th Annual International Congress
May 3-6, 2006
Milan
www.ilts.org

World Congress on Gastrointestinal Cancer
June 14-17, 2006
Barcelona, Spain
c.chase@imedex.com

5th International Congress of The African Middle East Association of Gastroenterology
February 24-26, 2006
Sharjah
infoevent@infomedweb.com
www.infomedweb.com

Digestive Disease Week 2006
May 20-25, 2006
Los Angeles
www.ddw.org

Annual Postgraduate Course
May 25-26, 2006
Los Angeles, CA
www.asge.org/education

## EVENTS AND MEETINGS IN 2006

10th World Congress of the International Society for Diseases of the Esophagus (ISDE 2006)
February 22-25, 2006
Adelaide
isde@sapmea.asn.au
www.isde.net

10th International Congress of Obesity
September 3-8, 2006
Sydney
enquiries@ico2006.com
www.ico2006.com

EASL 2006 - The 41st Annual Meeting
April 26-30, 2006
Vienna, Austria

International Gastrointestinal Fellows Initiative
February 22-24, 2006
Banff, Alberta
CAGOffice@cag-acg.org
www.cag-acg.org

Canadian Digestive Disease Week
February 24-27, 2006
Banff, Alberta
CAGOffice@cag-acg.org
www.cag-acg.org

Prague Hepatology Meeting 2006
September 14-16, 2006
Prague
veronika.revicka@congressprague.cz
www.czech-hepatology.cz/phm2006

European Multidisciplinary Colorectal Cancer Congress 2006
February 12-14, 2006
Berlin
info@congresscare.com
www.colorectal2006.org

World Congress on Controversies in Obesity, Diabetes and Hypertension (CODHy)
October 25-28, 2006
Berlin
codhy@codhy.com
www.codhy.com

ILTS 12th Annual International Congress
May 3-6, 2006
Milan
www.ilts.org

XXX pan-american congress of digestive diseases
November 25-December 1, 2006
Cancun
amg@gastro.org.mx
www.gastro.org.mx

World Congress on Gastrointestinal Cancer
June 14-17, 2006
Barcelona, Spain
c.chase@imedex.com

5th International Congress of the African Middle East Association of Gastroenterology
February 24-26, 2006
Sharjah
infoevent@infomedweb.com
www.infomedweb.com

7th World Congress of the International Hepato-Pancreato-Biliary Association
September 3-7, 2006
Edinburgh
convention@edinburgh.org
www.edinburgh.org/conference

Digestive Disease Week 2006
May 20-25, 2006
Los Angeles
www.ddw.org

Annual Postgraduate Course
May 25-26, 2006
Los Angeles, CA
www.asge.org/education

71st ACG Annual Scientific Meeting and Postgraduate Course
October 20-25, 2006
Venetian Hotel, Las Vegas, Neveda

AASLD 57th Annual Meeting - The Liver Meeting™
October 27-31, 2006
Boston, MA

PO Box 2345, Beijing 100023, China
www.wjgnet.com
wjg@wjgnet.com

*World J Gastroenterol* 2006 February 14; 12(6): 998-999
***World Journal of Gastroenterology*** ISSN 1007-9327
© 2006 The WJG Press. All rights reserved.

# Instructions to authors

## GENERAL INFORMATION

*World Journal of Gastroenterology* (*WJG, World J Gastroenterol* ISSN 1007-9327 CN 14-1219/R) is a weekly journal of more than 48 000 circulation, published on the 7th, 14th, 21st and 28th of every month.

Original Research, Clinical Trials, Reviews, Comments, and Case Reports in esophageal cancer, gastric cancer, colon cancer, liver cancer, viral liver diseases, *etc.*, from all over the world are welcome on the condition that they have not been published previously and have not been submitted simultaneously elsewhere.

### *Published by*

The WJG Press

## SUBMISSION OF MANUSCRIPTS

Manuscripts should be typed double-spaced on A4 (297mm×210 mm) white paper with outer margins of 2.5 cm. Number all pages consecutively, and start each of the following sections on a new page: Title Page , Abstract, Introduction, Materials and Methods, Results, Discussion, acknowledgements, References, Tables, Figures and Figure Legends. Neither the editors nor the Publisher is responsible for the opinions expressed by contributors. Manuscripts formally accepted for publication become the permanent property of The WJG Press, and may not be reproduced by any means, in whole or in part without the written permission of both the authors and the Publisher. We reserve the right to put onto our website and copy-edit accepted manuscripts. Authors should also follow the guidelines for the care and use of laboratory animals of their institution or national animal welfare committee.

Authors should retain one copy of the text, tables, photographs and illustrations, as rejected manuscripts will not be returned to the author(s) and the editors will not be responsible for the loss or damage to photographs and illustrations in mailing process.

### *Online submission*

Online submission is strongly advised. Manuscripts should be submitted through the Online Submission System at: http://www.wjgnet.com/index.jsp. Authors are highly recommended to consult the ONLINE INSTRUCTIONS TO AUTHORS (http://www.wjgnet.com/wjg/help/instructions.jsp) before attempting to submit online. Authors encountering problems with the Online Submission System may send an email you describing the problem to wjg@wjgnet.com for assistance. If you submit your manuscript online, do not make a postal contribution. A repeated online submission for the same manuscript is strictly prohibited.

### *Postal submission*

Send 3 duplicate hard copies of the full-text manuscript typed double-spaced on A4(297 mm×210 mm) white paper together with any original photographs or illustrations and a 3.5 inch computer diskette or CD-ROM containing an electronic copy of the manuscript including all the figures, graphs and tables in native Microsoft Word format or *.rtf format to:

### Editorial Office

***World Journal of Gastroenterology***
Editorial Department: Apartment 1066, Yishou Garden,
58 North Langxinzhuang Road,
PO Box 2345, Beijing 100023, China
E-mail: wjg@wjgnet.com
http: //www.wjgnet.com

## MANUSCRIPT PREPARATION

All contributions should be written in English. All articles must be submitted using a word-processing software. All submissions must be typed in 1.5 line spacing and in word size 12 with ample margins. The letter font is Tahoma. For authors from China, one copy of the Chinese translation of the manuscript is also required (excluding references). Style should conform to our house format. Required information for each of the manuscript sections is as follows:

### *Title page*

Full manuscript title, running title, all author(s) name(s), affiliations, institution(s) and/or department(s) where the work was accomplished, disclosure of any financial support for the research, and the name, full address, telephone and fax numbers and email address of the corresponding author should be included. Titles should be concise and informative (removing all unnecessary words), emphasize what is new, and avoid abbreviations. A short running title of less than 40 letters should be provided. List the author(s)' name(s) as follows: initial and/or first name, middle name or initial(s) and full family name.

### *Abstract*

An informative, structured abstract of no more than 250 words should accompany each manuscript. Abstracts for original contributions should be structured into the following sections: AIM: Only the purpose should be included. METHODS: The materials, techniques, instruments and equipments, and the experimental procedures should be included. RESULTS: The observatory and experimental results, including data, effects, outcome, *etc.* should be included. Authors should present *P* value where necessary, and the significant data should accompany. CONCLUSION: Accurate view and the value of the results should be included.

The format of structured abstracts is at: http://www.wjgnet.com/wjg/help/11.doc

### *Key words*

Please list 3-10 key words that could reflect content of the study mainly from *Index Medicus*.

### *Text*

For most article types, the main text should be structured into the following sections: INTRODUCTION, MATERIALS AND METHODS, RESULTS and DISCUSSION, and should include in appropriate Figures and Tables. Data should be presented in the body text or in Figures and Tables, but not in both.

### *Illustrations*

Figures should be numbered as 1, 2, 3 and so on, and mentioned clearly in the main text. Provide a brief title for each figure on a separate page. No detailed legend should be involved under the figures. This part should be added into the text where the figures are applicable. Digital images: black and white photographs should be scanned and saved in TIFF format at a resolution of 300 dpi; color images should be saved as CMYK (print files) but not as RGB (screen-viewing files). Place each photograph in a separate file. Print images: supply images of size no smaller than 126 mm×76 mm printed on smooth surface paper; label the image by writing the Figure number and orientation using an arrow. Photomicrographs: indicate the original magnification and stain in the legend. Digital Drawings: supply files in EPS if created by freehand and illustrator, or TIFF from photoshops. EPS files must be accompanied by a version in native file format for editing purposes. Existing line drawings should be scanned at a resolution of 1200 dpi and as close as possible to the size where they will appear when printed. Please use uniform legends for the same subjects. For example: Figure 1 Pathological changes of atrophic gastritis after treatment. A: ...; B: ...; C: ...; D: ...; E: ...; F: ...; G: ...

### *Tables*

Three-line tables should be numbered as 1, 2, 3 and so on, and mentioned clearly in the main text. Provide a brief title for each table. No detailed legend should be included under the tables. This part should be added into the text where the tables are applicable. The information should complement but not duplicate that contained in the text. Use one horizontal line under the title, a second under the column heads, and a third below the Table, above any footnotes. Vertical and italic lines should be omitted.

### *Notes in tables and illustrations*

Data that are not statistically significant should not be noted. $^{a}P<0.05$, $^{b}P<0.01$ should be noted ($P>0.05$ should not be noted). If there are other series of *P* values, $^{c}P<0.05$ and $^{d}P<0.01$ are used. Third series of *P* values can be expressed as $^{e}P<0.05$ and $^{f}P<0.01$. Other notes in tables or under illustrations should be expressed as $^{1}F$, $^{2}F$, $^{3}F$; or some other symbols with a superscript (Arabic numerals) in the upper left corner. In a multi-curve illustration, each curve should be labeled with ●, ○, ■, □, ▲, △, *etc.* in a certain sequence.

### *Acknowledgments*

Brief acknowledgments of persons who have made genuine contributions to the manuscripts and who endorse the data and conclusions are included. Authors are responsible for obtaining written permission to use any copyrighted text and/or illustrations.

## REFERENCES

### *Coding system*

The author should code the references according the citation order in text in Arabic numerals, put references codes in square brackets, superscript it at the end of citation content or the author name of the citation. For those citation content as the narrate part, the coding number and square brackets should be typeset normally. For example, Crohn's disease (CD) is associated with increased intestinal permeability[1,2]. If references are directly cited in the text, they would be put together with the text, for example, from references [19,22-24 ], we know that...

When the authors code the references, please ensure that the order in text is the same as in reference part and also insure the spelling accuracy of the first author's name. Do not code the same citation twice.

### *PMID requirement*

PMID roots in the abstract serial number indexed by PubMed (http://www.ncbi.nlm.nih.gov/entrez/query.fcgi?db=PubMed). The author should supply the PMID for journal citation. For those references that have not been indexed by PubMed, a printed copy of the first page of the full reference should be submitted.

The accuracy of the information of the journal citations is very important. Through reference testing system (http://www.aushome.cn/cgi-bin/index.pl), the authors and editor could check the authors name, title, journal title, publication date, volume number, start page, and end page. We will interlink all references with PubMed in ASP file so that the readers can read the abstract of the citations online immediately.

### *Style for journal references*

Authors: the first author should be typed in bold-faced letter. The surname of all authors should be typed with the initial letter capitalized and followed by their name in abbreviation (For example, Lian-Sheng Ma is abbreviated as Ma LS, Bo-Rong Pan as Pan BR). Title of the cited article and italicized journal title (Journal title should be in its abbreviation form as shown in PubMed), publication date, volume number (in black), start page, and end page [PMID: 11819634]

Note: The author should test the references through reference testing system (http://www.aushome.cn/cgi-bin/index.pl)

### *Style for book references*

Authors: the first author should be typed in bold-faced letter. The surname of all authors should be typed with the initial letter capitalized and followed by their name in abbreviation (For example, Lian-Sheng Ma is abbreviated as Ma LS, Bo-Rong Pan as Pan BR) Book title. Publication number. Publication place: Publication press, Year: start page and end page.

### *Format*

*Standard jounal article (list all authors and include the PubMed ID [PMID] where applicable)*

1 **Das KM,** Farag SA. Current medical therapy of inflammatory bowel disease. *World J Gastroenterol* 2000; 6: 483-489 [PMID: 11819634]

2 **Pan BR**, Hodgson HJF, Kalsi J. Hyperglobulinemia in chronic liver disease: Relationships between *in vitro* immunoglobulin synthesis, short lived suppressor cell activity and serum immunoglobulin levels. *Clin Exp Immunol* 1984; 55: 546-551 [PMID: 6231144]

3 **Lin GZ,** Wang XZ, Wang P, Lin J, Yang FD. Immunologic effect of Jianpi Yishen decoction in treatment of Pixu-diarrhoea. *Shijie Huaren Xiaohua Zazhi* 1999; 7: 285-287

*Books and other monographs (list all authors)*

4 **Sherlock S,** Dooley J. Diseases of the liver and billiary system. 9th ed. Oxford: Blackwell Sci Pub, 1993: 258-296

*Chapter in a book (list all authors)*

5 **Lam SK.** Academic investigator's perspectives of medical treatment for peptic ulcer. In: Swabb EA, Azabo S. Ulcer disease: investigation and basis for therapy. New York: Marcel Dekker, 1991: 431-450

*Electronic journal (list all authors)*

6 **Morse SS.** Factors in the emergence of infectious diseases. Emerg Infect Dis serial online, 1995-01-03, cited 1996-06-05; 1(1):24 screens. Available from: URL: http//www.cdc.gov/ncidod/EID/eid.htm

### *Inappropriate references*

Authors should always cite references that are relevant to their article, and avoid any inappropriate references. Inappropriate references include those that are linked with a hyphen and the difference between the two numbers at two sides of the hyphen is more than 5. For example, [1-6], [2-14] and [1, 3, 4-10, 22] are all considered as inappropriate references. Authors should not cite their own unrelated published articles.

### *Statistical data*

Present as mean ± SD and mean ± SE.

### *Statistical expression*

Express *t* test as *t* (in italics), *F* test as *F* (in italics), chi square test as $\chi^2$ (in Greek), related coefficient as *r* (in italics), degree of freedom as γ (in Greek), sample number as *n* (in italics), and probability as *P* (in italics).

### *Units*

Use SI units. For example: body mass, m (B) = 78 kg; blood pressure, *p*(B)= 16.2/12.3 kPa; incubation time, t (incubation) = 96 h, blood glucose concentration, c (glucose) 6.4 ± 2.1 mmol/L; blood CEA mass concentration, p (CEA) = 8.6 24.5 μg/L; $CO_2$ volume fraction, 50 mL/L $CO_2$ not 5% $CO_2$; likewise for 40 g/L formaldehyde, not 10% formalin; and mass fraction, 8 ng/g, *etc*. Arabic numerals such as 23, 243, 641 should be read 23 243 641.

The format about how to accurately write common units and quantum is at: http://www.wjgnet.com/wjg/help/15.doc

### *Abbreviations*

Standard abbreviations should be defined in the abstract and on first mention in the text. In general, terms should not be abbreviated unless they are used repeatedly and the abbreviation is helpful to the reader. Permissible abbreviations are listed in Units, Symbols and Abbreviations: A Guide for Biological and Medical Editors and Authors (Ed. Baron DN, 1988) published by The Royal Society of Medicine, London. Certain commonly used abbreviations, such as DNA, RNA, HIV, LD50, PCR, HBV, ECG, WBC, RBC, CT, ESR, CSF, IgG, ELISA, PBS, ATP, EDTA, mAb, can be used directly without further mention.

### *Italicis*

Quantities: *t* time or temperature, *c* concentration, *A* area, *l* length, *m* mass, *V* volume.

Genotypes: *gyr*A, *arg* 1, *c myc*, *c fos*, *etc*.

Restriction enzymes: *Eco*RI, *Hin*dI, *Bam*HI, *Kbo* I, *Kpn* I, *etc*.

Biology: *Helicobacter pylori, H pylori, E coli, etc*.

## SUBMISSION OF THE REVISED MANUSCRIPTS AFTER ACCEPTED

Please revise your article according to the revision policies of *WJG*. The revised version including manuscript and high-resolution image figures (if any) should be copied on a floppy or compact disk. Author should send the revised manuscript, along with printed high-resolution color or black and white photos, copyright transfer letter, the final check list for authors, and responses to reviewers by a courier (such as EMS) (submission of revised manuscript by e-mail or on the *WJG* Editorial Office Online System is NOT available at present).

### *Language evaluation*

The language of a manuscript will be graded before sending for revision. (1) Grade A: priority publishing; (2) Grade B: minor language polishing; (3) Grade C: a great deal of language polishing; (4) Grade D: rejected. The revised articles should be in grade B or grade A.

### *Copyright assignment form*

It is the policy of *WJG* to acquire copyright in all contributions. Papers accepted for publication become the copyright of *WJG* and authors will be asked to sign a transfer of copyright form. All authors must read and agree to the conditions outlined in the Copyright Assignment Form (which can be downloaded from http://www.wjgnet.com/wjg/help/9.doc).

### *Final check list for authors*

The format is at: http://www.wjgnet.com/wjg/help/13.doc

### *Responses to reviewers*

Please revise your article according to the comments/suggestions of reviewers. The format for responses to the reviewers' comments is at: http://www.wjgnet.com/wjg/help/10.doc

### *Proof of financial support*

For paper supported by a foundation, authors should provide a copy of the document and serial number of the foundation.

### *Publication fee*

Authors of accepted articles must pay publication fee.

EDITORIAL and LETTERS TO THE EDITOR are free of change.

PO Box 2345, Beijing 100023, China
www.wjgnet.com
wjg@wjgnet.com

*World J Gastroenterol* 2006 February 14; 12(6): 1000
***World Journal of Gastroenterology*** ISSN 1007-9327
© 2006 The WJG Press. All rights reserved.

# ***World Journal of Gastroenterology*** standard of quantities and units

| Number | Nonstandard | Standard | Notice |
|---|---|---|---|
| 1 | 4 days | 4 d | In figures, tables and numerical narration |
| 2 | 4 days | four days | In text narration |
| 3 | day | d | After Arabic numerals |
| 4 | Four d | Four days | At the beginning of a sentence |
| 5 | 2 hours | 2 h | After Arabic numerals |
| 6 | 2 hs | 2 h | After Arabic numerals |
| 7 | hr, hrs, | h | After Arabic numerals |
| 8 | 10 seconds | 10 s | After Arabic numerals |
| 9 | 10 year | 10 years | In text narration |
| 10 | Ten yr | Ten years | At the beginning of a sentence |
| 11 | 0,1,2 years | 0,1,2 yr | In figures and tables |
| 12 | 0,1,2 year | 0,1,2 yr | In figures and tables |
| 13 | 4 weeks | 4 wk | |
| 14 | Four wk | Four weeks | At the beginning of a sentence |
| 15 | 2 months | 2 mo | In figures and tables |
| 16 | Two mo | Two months | At the beginning of a sentence |
| 17 | 10 minutes | 10 min | |
| 18 | Ten min | Ten minutes | At the beginning of a sentence |
| 19 | 50% (*V/V*) | 500 mL/L | |
| 20 | 50% (m/*V*) | 500 g/L | |
| 21 | 1 M | 1 mol/L | |
| 22 | 10 μM | 10 μmol/L | |
| 23 | 1N HCl | 1 mol/L HCl | |
| 24 | 1N $H_2SO_4$ | 0.5 mol/L $H_2SO_4$ | |
| 25 | 4rd edition | 4th edition | |
| 26 | 15 year experience | 15- year experience | |
| 27 | 18.5 kDa | 18.5 ku,18 500u or $M_r$18 500 | |
| 28 | 25 $g.kg^{-1}/d^{-1}$ | 25 g/(kg·d) or 25 g/kg per day | |
| 29 | 6900 | 6 900 | |
| 30 | 1000 rpm | 1 000 r/min | |
| 31 | sec | s | After Arabic numerals |
| 32 | 1 pg $\cdot L^{-1}$ | 1 pg/L | |
| 33 | 10 kilograms | 10 kg | |
| 34 | 13 000 rpm | 13 000 *g* | High speed; *g* should be in italic and suitable conversion. |
| 35 | 1000 *g* | 1 000 r/min | Low speed. *g* cannot be used. |
| 36 | Gene bank | GenBank | International classified genetic materials collection bank |
| 37 | Ten L | Ten liters | At the beginning of a sentence |
| 38 | Ten mL | Ten milliliters | At the beginning of a sentence |
| 39 | umol | μmol | |
| 40 | 30 sec | 30 s | |
| 41 | 1 g/dl | 10 g/L | 10-fold conversion |
| 42 | $OD_{260}$ | $A_{260}$ | "OD" has been abandoned. |
| 43 | One g/L | One microgram per liter | At the beginning of a sentence |
| 44 | *A*260 nm | $A_{260}$ nm | *A* should be in italic. |
| | $^bP<0.05$ | $^aP<0.05$ | In Table, no note is needed if there is no significance instatistics: $^aP<0.05$, $^bP<0.01$ (no note if $P>0.05$). If ther is a second set of *P* value in the same table, $^cP<0.05$ and $^dP<0.01$ are used for a third set: $^eP<0.05$, $^fP<0.01$. |
| 45 | $^*F=9.87$, $^§F=25.9$, $^\#F=67.4$ | $^1F=9.87$, $^2F=25.9$, $^3F=67.4$ | Notices in or under a table |
| 46 | KM | km | kilometer |
| 47 | CM | cm | centimeter |
| 48 | MM | mm | millimeter |
| 49 | Kg, KG | kg | kilogram |
| 50 | Gm, gr | g | gram |
| 51 | nt | N | newton |
| 52 | l | L | liter |
| 53 | db | dB | decibel |
| 54 | rpm | r/min | rotation per minute |
| 55 | bq | Bq | becquerel, a unit symbol |
| 56 | amp | A | ampere |
| 57 | coul | C | coulomb |
| 58 | HZ | Hz | |
| 59 | w | W | watt |
| 60 | KPa | kPa | kilo-pascal |
| 61 | p | Pa | pascal |
| 62 | ev | EV | volt (electronic unit) |
| 63 | Jonle | J | joule |
| 64 | J/mmol | kJ/mol | kilojoule per mole |
| 65 | 10×10×10$cm^3$ | 10 cm×10 cm×10 cm | |
| 66 | N·km | KN·m | moment |
| 67 | *x*±s | mean±SD | In figures, tables or text narration |
| 68 | Mean±SEM | mean±SE | In figures, tables or text narration |
| 69 | *im* | im | intramuscular injection |
| 70 | *iv* | iv | intravenous injection |
| 71 | Wang et al | Wang *et al.* | |
| 72 | EcoRI | *Eco*RI | *Eco* in italic and RI in positive. Restriction endonuclease has its prescript form of writing. |
| 73 | Ecoli | *E.coli* | Bacteria and other biologic terms have their specific expression. |
| 74 | Hp | *H pylori* | |
| 75 | Iga | *Iga* | writing form of genes |
| 76 | *igA* | IgA | writing form of proteins |
| 77 | -70 kDa | ~70 ku | |